NASA Technical Memorandum 81916

NASA-TM-81916 19810006276

NOISE PREDICTION FOR JETSTAR PROP-FAN TEST

F. FARASSAT, R. M. MARTIN, AND G. C. GREENE

DECEMBER 1980

NASA
National Aeronautics and
Space Administration

Langley Research Center
Hampton, Virginia 23665

Errata inserted 6-16-81

ERRATA

NASA Technical Memorandum 81916

NOISE PREDICTION FOR JETSTAR PROP-FAN TEST

F. Farassat, R. M. Martin, and G. C. Greene

December 1980

The speed of sound at two altitudes 6.10 km (20,000 ft) and 7.63 km (25,000 ft) was incorrect in the above report. These errors affect only the calculations for the two altitudes mentioned. Few calculations were performed for these altitudes (flight Mach number of 0.8, microphone 7 only) and the calculations for 9.15 km (30,000 ft) are unaffected. However, the calculations may be corrected easily as follows. The correct speed of sound c is

316.1 m/sec at 6.10 km (20,000 ft)
309.7 m/sec at 7.63 km (25,000 ft)

We define the following two parameters:

$$A = \frac{316.1}{294.9} = 1.07$$

$$B = \frac{309.7}{298.2} = 1.04$$

The tables on pages 13 to 19 are corrected as follows:

Table 2(a):

Multiply forward speed at 6.10 km altitude by A.
Multiply forward speed at 7.63 km altitude by B.

Table 2(b):

Multiply rpm at 6.10 km altitude by A.
Multiple rpm at 7.63 km altitude by B.

Table 2(c) and 2(d):

Multiply hp/blade at 6.10 km altitude by $A^2 = 1.15$.
Multiply hp/blade at 7.63 km altitude by $B^2 = 1.08$.

Table (2e): Unaffected.

Tables 3 and 4: Unaffected.

Table 5(a):

Add $20 \log_{10} A^2 = 1.21$ dB to both thickness and loading noise.

Table 5(b):

Add 20 $\log_{10} B^2$ = 0.66 dB to both thickness and loading noise.

Tables 5(c) to 5(k): Unaffected.

The shapes of the acoustic pressure signatures and spectra are unaffected for these altitudes. The pressure scales in the signatures are corrected as follows:

Multiply pressure scale at 6.10 km altitude by A_2^2 = 1.15.
Multiply pressure scale at 7.63 km altitude by B^2 = 1.08.

The spectra are corrected as follows:

Add 20 log A_2^2 = 1.21 dB to each harmonic at 6.10 km altitude.
Add 20 log B^2 = 0.66 dB to each harmonic at 7.63 km altitude.

NOISE PREDICTION FOR JETSTAR PROP-FAN TEST

F. Farassat, R. M. Martin, and G. C. Greene

SUMMARY

The acoustic calculations reported in this memorandum are for two model prop-fan designs (SR-2 and SR-3 blades) scheduled for test on top of Jetstar aircraft. The predicted acoustic pressure signatures and spectra for selected microphone positions on the fuselage and operating conditions are presented here. The computer program used for these calculations was developed at NASA Langley by Farassat and Nystrom. A detailed presentation of the input data, the acoustic results and the corrections for microphone fuselage reflection are included in this report. The general trend observed in these calculations is that the acoustically optimized model (using SR-3 blades) is substantially quieter than the model with SR-2 blades. This latter design has conventional straight blades.

INTRODUCTION

The acoustic calculations in this report are for two prop-fan models to be tested on a Jetstar aircraft. The models are eight-bladed and are driven by an air turbine. The prop-fan assembly is mounted on the top of the fuselage on a pylon as shown in figure 1.

The calculations reported here were performed using a computer program developed at NASA Langley by F. Farassat and P. A. Nystrom. The relevant theory is explained in references 1 and 2. The input data and the operating conditions are presented in detail in this report. The fuselage reflection corrections are also included.

SYMBOLS

c	speed of sound, m/sec
C	20 log F, fuselage correction in dB to be added to the levels of the harmonics of the acoustic spectra
F	fuselage correction factor for pressure signatures
M	flight Mach number
$\vec{N} = (N_1, N_2, N_3)$	unit outward normal to the fuselage
v_3	forward flight speed, m/sec
r	radiation distance, m (see eq. A-1)
$\vec{x} = (x_1, x_2, x_3)$	microphone position in the frame fixed to the aircraft, m
x	$(x_1^2 + x_2^2 + x_3^2)^{1/2}$, m
θ	The angle between $\vec{N}$ and the radiation vector (see section on Fuselage Correction)
τ	emission time of acoustic signal, sec (see Appendix)
$\Delta\tau$	time of travel of the acoustic signal from prop-fan center to the microphone, sec (see Appendix)

BLADE DESIGNS

Two blade types designated as SR-2 and SR-3 were used in all the calculations. The blade untwisted planforms and the blade form curves are presented in figures 2 and 3. The SR-2 blade has the conventional design with no sweep. The SR-3 blade is the acoustically optimized design. It was shown by wind tunnel tests that this design produces substantially lower noise levels than the conventional straight blade design.

In the planned tests, the prop-fan models have eight blades with a diameter of 0.62 m (2.04 ft). In the acoustic program the blade shapes are modeled precisely from the blue prints supplied by Hamilton Standard. For the method of modeling the three-dimensional blade surfaces, see reference 2.

MICROPHONE POSITIONS

For the specification of the microphone positions, a Cartesian coordinate system fixed to the aircraft is used as follows. The origin of the coordinate system is at the prop-fan center. The x_1-axis is positive downward and directed toward the center of the aircraft fuselage. The positive x_3-axis is in the flight direction and point forward. The x_2-axis is defined such that the $\vec{x}$-frame forms a right-handed coordinate system. This coordinate system is shown in the figure below Table 1.

Table 1 gives the microphone positions in the coordinate frame defined above. The microphone positions are clearly marked in the top view drawing of the Jetstar preceeding each set of calculations for different advance ratios.

Note that the microphone numbers used in this paper may differ from those in other technical documents related to the Jetstar test.

THE EFFECT OF MICROPHONE MOTION

The microphone motion is accounted for by using the moving observer option of Farassat-Nystrom program. In this program, the acoustic pressure signature is calculated for one period of the signal in the moving frame fixed to the aircraft. It is then Fourier analyzed to obtain the acoustic pressure spectrum. The computer program for the acoustic calculations, is based on two solutions of the governing linear wave equation (Ffowcs Williams-Hawkings equation). All the terms in the solution involving the blade

thickness and loading are retained. Thus, no approximation concerning the microphone position (such as being in the far field) is used in these calculations.

THE BLADE LOADING

The blade spanwise distributions for the two-blade designs of the lift coefficient are similar to those supplied by Hamilton Standard for the cruise condition at M = 0.8. Figure 4 presents the spanwise distribution of lift coefficient for the two blade designs. These distributions were scaled up or down to get the correct horsepower absorbed by the prop-fan. The horsepower values were obtained from experimental curves for power coefficient supplied by NASA Lewis Research Center. Table 2 gives the horsepower values (per blade) and other relevant input data for the set of calculations reported here.

The chordwise loading was assumed to be parabolic. The blade loading used in the calculations are quite approximate and they must be considered a source of error.

FLIGHT ALTITUDE AND MACH NUMBER

Three flight altitudes of 9.15 km (30,000 ft), 7.63 km (25,000 ft) and 6.10 km (20,000 ft) were used in the calculations. The forward flight Mach numbers were assumed 0.6, 0.7, and 0.8 at 9.15 km (30,000 ft) altitude. For the other two altitudes, the flight Mach number of 0.8 was used. The most extensive calculations were performed for the altitude of 9.15 km and flight Mach number of 0.8. For comparison, calculations with similar conditions (flight altitude, speed and microphone position) were performed for SR-2 and SR-3 blades. These runs are summarized in Table 3.

Note that for each flight altitude and Mach number, the following advance ratios were used: 2.95, 3.06, 3.25, 3.50, and 4.30. The blade pitch angle at 3/4 radius is 61.3° for SR-3 blade and 60.0° for SR-2 blade.

ACOUSTIC WAVEFORMS AND SPECTRA

The predicted acoustic pressure signatures and spectra are presented in figures 5 to 14. Note that these data are for the free-field condition. The fuselage corrections must be used as discussed in the next section.

The acoustic pressure signatures and spectra each have a run identification on the top right corner of the figures. These should be interpreted as follows:

ABCDEFGHIJ

where

AB = altitude in thousands of feet: 20, 25, 30

CD = flight Mach number: 60 ≡ .6, 70 ≡ .7, 80 ≡ .8

EFG = blade reference angle: 600 ≡ 60.0°, 613 ≡ 61.3°

HIJ = advance ratio: 295 ≡ 2.95, 306 ≡ 3.06, etc.

FUSELAGE CORRECTION

The fuselage correction factor is assumed to be $1+\cos\theta$ where θ is the angle between the normal to the fuselage and the radiation direction. The radiation direction is obtained by assuming that the sources are at the prop-fan center. The motion of the microphones as the sound propagates from the place of emission to the point of reception must be considered in evaluation of the angle θ.

If the microphone position in the frame described above is (x_1, x_2, x_3) and $x = (x_1^2 + x_2^2 + x_3^2)^{1/2}$, then

$$\cos\theta = -\frac{N_1x_1 + N_2x_2}{x^2}\left[\sqrt{M^2x_3^2 + (1-M^2)x^2} - Mx_3\right]$$

where $\vec{N} = (N_1, N_2, N_3)$ is the unit outward normal on the fuselage and M is the flight Mach number. See Appendix for the derivation of this result. The acoustic pressure signatures must be multiplied by the factor $F = 1+\cos\theta$ and the level of each harmonic of the acoustic spectra must be increased by $C = 20 \log F$. The values of these two corrections as a function of Mach number and microphone position are given in Table 4.

ANALYSIS OF THE PREDICTED DATA

The theoretical acoustic pressure spectra are expected to underestimate the measured data by as much as 3 to 5 dB in the first few harmonics. The high frequency end of the spectra is overestimated in those cases where the signatures show small amplitude high frequency oscillations. These oscillations are numerical in origin and are explained in reference 1.

As it can be seen from Table 2, there are many variables in the operating conditions that are changed in these calculations. One can compare the levels of the blade passage frequency for SR-2 and SR-3 blades at similar operating conditions. Some other interesting results can also be obtained from these calculations.

Figure 15 shows the corrected levels of the blade passage frequency as a function of the microphone position directly below the centerline for the two blade designs. Both designs show a directivity pattern which peaks slightly behind the disk plane. However, the peak level of the SR-3 blade is substantially lower than that for the SR-2 blade. This is of the order of 10 dB. This is also true of the overall noise level shown in figure 16.

The advance ratio in both figures 15 and 16 is taken as 3.25. Similar directivity patterns are observed for other advance ratios as seen in figure 17. It is interesting to note that the dominant component of the noise in the peak region of the directivity is due to the blade thickness. Table 5 gives the levels of thickness and loading noise for cases in this report.

Figure 18 shows the change in the levels of the BPF for the SR-3 design as the cruise Mach number increases. This figure is for microphone position 7. Note that the levels are the free-field values. Since for this microphone position, the fuselage correction is about 5 dB for all the test Mach numbers, a similar set of curves but shifted upward will be obtained for corrected levels of BPF. As the cruise Mach number increases, the prop-fan RPM should be increased to keep the advance ratio fixed. This will result in increased relative velocity of the air with respect to the blade across the span of the blade. The local aerodynamic angle of attack remains fixed if the induced effect of the helical vortex sheet behind the propfan is neglected. The propfan power should therefore increase as the cruise Mach number increases (keeping advance ratio and blade pitch angle fixed). This will increase the loading noise. At the same time, the increase in RPM and cruise speed will increase the helical tip speed and therefore will increase the thickness noise. The behavior of the levels of the BPF with the increasing cruise Mach number is therefore expected.

The general trend observed in all the calculations is that the SR-3 design, which is acoustically optimized, is substantially quieter than the conventional straight blade SR-2 design.

CONCLUDING REMARKS

The calculations reported here were performed with two aims in mind. First, they can be used as a test of the prediction theory with no prior knowledge of the experimental data. Second, they can be used as a guide for the selection and calibration of the instruments on the Jetstar prop-fan test aircraft. The two most important sources of error in these calculations are the assumed form of the blade loading distribution and the neglect of nonlinearities in the flow field around the blade.

The error in the blade loading distribution is expected to influence the calculations for SR-2 and SR-3 designs. However, the neglect of nonlinearities will influence the SR-2 calculations to a larger extent than those of the SR-3 blade. Thus, the predictions for the SR-3 blade are expected to agree better with experimental data than those for the SR-2 blade.

APPENDIX

In this Appendix, the derivation of the equation used in the fuselage correction is discussed. Consider the observer at the position (x_1, x_2, x_3). Assume that the source position is at the prop-fan center which is the origin of the moving $\vec{x}$-frame. Let the source emit a signal at the time τ and assume that observer receives the signal the signal at the time $\tau + \Delta\tau$. The observer position at the reception time in the frame fixed to the medium and coinciding with the $\vec{x}$-frame at the time τ is $(x_1, x_2, x_3 + v_3\Delta\tau)$. Here v_3 is the forward speed of the prop-fan. The distance traveled by the signal is given by

$$r^2 = x_1^2 + x_2^2 + (x_3 + v_3\Delta\tau)^2$$

$$= c^2\Delta\tau^2 \qquad \text{(A1)}$$

This equation can be written as

$$r^2 = x_1^2 + x_2^2 + (x_3 + Mr)^2 \qquad \text{(A2)}$$

where $M = v_3/c$ is the flight Mach number. This can be solved for r which is

$$r = \frac{1}{1-M^2}\left[Mx_3 + \sqrt{M^2x_3^2 + (1-M^2)x^2} \right] \qquad \text{(A3)}$$

where $x^2 = x_1^2 + x_2^2 + x_3^2$. The radiation vector $\vec{r}$ is

$$\hat{\vec{r}} = \left(-\frac{x_2}{r}, -\frac{x_2}{r}, -\frac{x_3 + Mr}{r}\right) \qquad \text{(A4)}$$

The fuselage of the aircraft is cylindrical so that $N_3 = 0$ where $\vec{N} = (N_1, N_2, N_3)$ is the unit outward vector to the fuselage. We have

$$\cos = \vec{N} \cdot \vec{\hat{r}}$$

$$= - \frac{N_1 x_1 + N_2 x_2}{r}$$

$$= - \frac{N_1 x_1 + N_2 x_2}{x^2} \left[\sqrt{M^2 x_3^{\,2} + (1-M^2) x^2} - M x_3 \right] \qquad \text{(A5)}$$

Note that $\vec{N}$ must be given in the coordinate frame used for microphone position description.

REFERENCES

1. Nystrom, P. A. and Farassat, F.: A Numerical Technique for Calculation of the Noise of High-Speed Propellers with Advanced Blade Geometry. NASA Technical Paper 1662, July 1980.

2. Farassat, F. and Succi, G. P.: A Review of Propeller Discrete Frequency Noise Prediction Technology with Emphasis on Two Current Methods for Time Domain Calculations. J. Sound and Vibration, vol. 71, no. 3, 1980, p. 399-419.

TABLE 1.- MICROPHONE POSITIONS

Mic. No.	Coordinates (x_1, x_2, x_3) m
1	0.809, 0., 0.660
4	0.809, 0., 0.160
5	0.809, 0., -0.008
7	0.809, 0., -0.252
9	0.809, 0., -0.711
10	0.999, -0.617, -0.252
12	0.848, -0.289, -0.252

Note: Microphone numbers may differ from other related Jetstar documents.

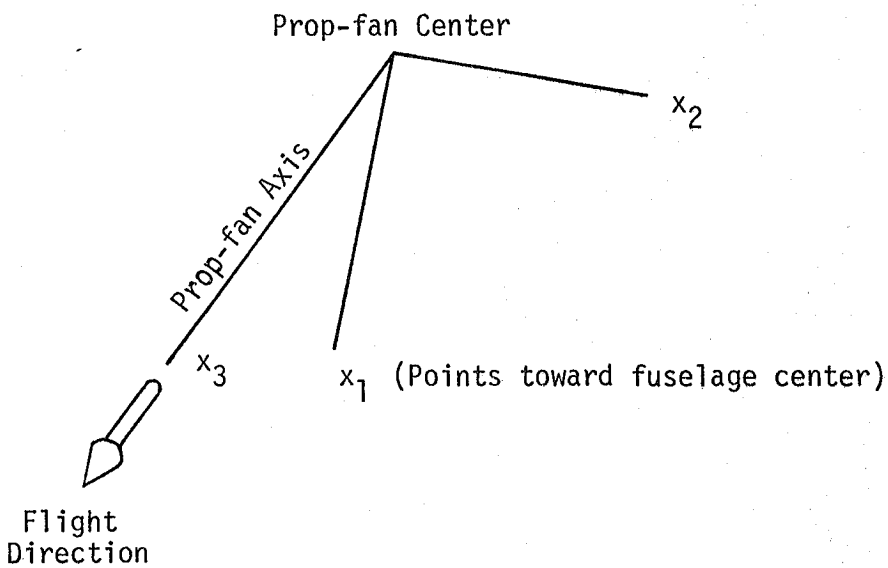

Microphones 10 and 12 are at 0.665 m (26.2 in) and 0.292 m (11.5 in) distance along curved fuselage on the side of prop-fan centerline, respectively.

TABLE 2.- OPERATING CONDITIONS AND HORSEPOWER

OF PROP-FAN USED FOR ACOUSTIC CALCULATIONS

Altitude Km (ft)	Density Kg/m^3	Speed of Sound m/sec	Forward Flight Speed, m/sec		
			M=0.8	M=0.7	M=0.6
6.10 (20,000)	0.651	294.9	235.9	206.4	176.9
7.63 (25,000)	0.548	298.2	238.6	208.7	178.9
9.15 (30,000)	0.457	301.5	241.2	211.1	180.9

(a) Ambient Conditions and Forward Speed.

Altitude Km	M	Advance Ratio				
		4.30	3.50	3.25	3.06	2.95
6.10	0.8	5286.0	6494.2	6993.8	7428.0	7705.0
7.63	0.8	5345.6	6567.4	7072.6	7511.8	7791.9
9.15	0.6	4053.8	4980.4	5363.5	5696.5	5908.9
9.15	0.7	4729.4	5810.4	6257.3	6645.9	6893.7
9.15	0.8	5405.0	6640.4	7151.2	7595.2	7878.4

(b) Prop-fan RPM

Altitude Km	M	Advance Ratio				
		4.30	3.50	3.25	3.06	2.95
6.10	0.8	0	17.04	29.02	41.34	49.59
7.63	0.8	0	14.83	25.27	35.99	43.17
9.15	0.6	0	4.60	7.50	11.01	14.60
9.15	0.7	0	7.93	13.13	19.13	23.63
9.15	0.8	0	12.78	21.78	31.02	37.21

(c) Prop-fan Horsepower/Blade - SR-2 Model

TABLE 2.- CONCLUDED.

Altitude Km	M	Advance Ratio				
		4.30	3.50	3.25	3.06	2.95
6.10	0.8	0	17.42	25.79	34.76	40.96
7.63	0.8	0	15.17	22.46	30.27	35.69
9.15	0.6	0.51	6.00	8.94	11.92	14.13
9.15	0.7	0.50	9.48	13.77	18.84	22.33
9.15	0.8	0	13.08	19.36	26.09	30.74

(d) Prop-fan Horsepower/Blade - SR-3 Model

M	Advance Ratio				
	4.30	3.50	3.25	3.06	2.95
0.6	0.744	0.807	0.835	0.861	0.877
0.7	0.868	0.941	0.975	1.004	1.024
0.8	0.991	1.076	1.114	1.148	1.170

(e) Helical tip Mach number - Both blades
(independent of altitude).

TABLE 3.- MICROPHONE NUMBERS USED IN THE ACOUSTIC CALCULATIONS

Altitude Km	M	Microphone Number (see Table 1)						
		1	4	5	7	9	10	12
6.10	0.8				X			
7.63	0.8				X			
9.15	0.6				X			
9.15	0.7				X			
9.15	0.8	X	X	X	X	X	X	X

Note: For each microphone position marked with X, the advance ratio was varied between 2.95 and 4.30 (see Table 2).

TABLE 4.- FUSELAGE REFLECTION CORRECTION

Mic. No.	M = .6		M = .7		M = .8	
	F	C	F	C	F	C
1	1.392	2.87	1.308	2.33	1.216	1.70
4	1.679	4.50	1.580	3.97	1.456	3.26
5	1.794	5.08	1.707	4.65	1.592	4.04
7	1.951	5.81	1.907	5.61	1.842	5.31
9	1.968	5.88	1.986	5.96	1.997	6.01
10	1.365	2.70	1.341	2.55	1.308	2.33
12	1.778	5.00	1.738	4.80	1.679	4.50

Note: (a) For correction of pressure signatures, multiply theoretical acoustic pressure scale by factor F.

(b) For correction of acoustic spectra, add C dB to all harmonic levels.

(c) The corrections apply to all altitudes.

TABLE 5.- FREE-FIELD OVERALL SOUND PRESSURE LEVELS (dB re: 20 μPa)

FOR THE THICKNESS AND LOADING NOISE COMPONENTS OF THE TWO-BLADE DESIGNS

Noise Component	Blade Type	Advance Ratio				
		4.30	3.50	3.25	3.06	2.96
Thickness	SR-2	124.9	139.7	144.1	146.8	148.2
	SR-3	125.6	137.6	139.9	141.5	142.8
Loading	SR-2	-150.0	140.5	147.1	151.3	153.4
	SR-3	-150.0	136.0	140.4	143.5	145.1

(a) Flight altitude = 6.10 Km (20,000 ft), M=0.8, Microphone 7

Noise Component	Blade Type	Advance Ratio				
		4.30	3.50	3.25	3.06	2.95
Thickness	SR-2	123.7	138.4	142.8	145.5	146.9
	SR-3	124.3	136.3	138.6	140.2	141.5
Loading	SR-2	-150.0	139.1	145.8	150.0	152.1
	SR-3	-150.0	134.7	139.1	142.1	143.8

(b) Flight Altitude = 7.63 Km (25,000 ft), M-0.8, Microphone 7

Noise Component	Blade Type	Advance Ratio				
		4.30	3.50	3.25	3.06	2.95
Thickness	SR-2	79.3	93.7	98.9	103.1	105.8
	SR-3	80.5	94.7	99.8	103.9	106.5
Loading	SR-2	-150.0	104.2	112.1	118.5	122.7
	SR-3	74.7	106.5	113.5	118.9	122.1

(c) Flight Altitude = 9.15 Km (30,000 ft), M=0.6, Microphone 7

TABLE 5.- Continued.

Blade Component	Blade Type	Advance Ratio				
		4.30	3.50	3.25	3.06	2.95
Thickness	SR-2	99.6	114.2	119.9	124.9	128.1
	SR-3	100.6	114.8	120.4	125.2	128.1
Loading	SR-2	-150.0	121.6	129.4	135.5	139.0
	SR-3	87.4	122.2	128.5	133.7	136.6

(d) Flight altitude = 9.15 Km (30,000 ft), M=0.7, Microphone 7

Blade Component	Blade Type	Advance Ratio				
		4.30	3.50	3.25	3.06	2.95
Thickness	SR-2	101.7	111.9	114.0	114.1	112.9
	SR-3	89.4	99.9	104.7	109.0	111.3
Loading	SR-2	-150.0	101.3	109.0	113.9	116.2
	SR-3	-150.0	96.5	103.4	108.6	111.5

(e) Flight altitude = 9.15 Km (30,000 ft), M=0.8, Microphone 1

Noise Component	Blade Type	Advance Ratio				
		4.30	3.50	3.25	3.06	2.95
Thickness	SR-2	132.7	142.1	145.3	146.9	146.3
	SR-3	120.5	128.5	131.6	133.8	134.5
Loading	SR-2	-150.0	118.4	125.6	130.4	132.8
	SR-3	-150.0	120.2	125.8	129.4	131.3

(f) Flight altitude = 9.15 Km (30,000 ft), M=0.8, Microphone 4

TABLE 5.- Continued.

Noise Component	Blade Type	Advance Ratio				
		4.30	3.50	3.25	3.06	2.95
Thickness	SR-2	134.5	144.5	147.0	148.2	149.0
	SR-3	129.0	134.9	134.9	136.1	136.7
Loading	SR-2	-150.0	132.2	136.5	139.1	140.0
	SR-3	-150.0	126.6	130.8	133.3	134.2

(g) Flight altitude = 9.15 Km (30,000 ft), M=0.8, Microphone 5

Noise Component	Blade Type	Advance Ratio				
		4.30	3.50	3.25	3.06	2.95
Thickness	SR-2	122.3	137.3	141.7	144.4	145.5
	SR-3	123.0	135.3	137.4	139.1	140.1
Loading	SR-2	-150.0	137.9	144.6	148.8	150.9
	SR-3	-150.0	133.3	137.8	141.1	142.7

(h) Flight altitude = 9.15 Km (30,000), M=0.8, Microphone 7

Noise Component	Blade Type	Advance Ratio				
		4.30	3.50	3.25	3.06	2.95
Thickness	SR-2	82.1	96.3	101.4	105.7	108.5
	SR-3	84.7	98.6	103.6	107.9	110.7
Loading	SR-2	-150.0	113.1	121.6	127.7	131.2
	SR-3	-150.0	114.8	122.0	127.6	130.8

(i) Flight altitude = 9.15 Km (30,000 ft), M=0.8, Microphone 9

TABLE 5.- CONCLUDED.

Noise Component	Blade Type	Advance Ratio				
		4.30	3.50	3.25	3.06	2.95
Thickness	SR-2	124.9	137.6	141.3	143.0	143.6
	SR-3	123.3	133.5	135.1	136.4	137.7
Loading	SR-2	-150.0	134.8	140.5	144.1	145.8
	SR-3	-150.0	128.0	131.8	134.6	136.1

(j) Flight altitude = 9.15 Km (30,000 ft), M=0.8, Microphone 10

Noise Component	Blade Type	Advance Ratio				
		4.30	3.50	3.25	3.06	2.95
Thickness	SR-2	123.4	137.7	141.6	144.4	145.2
	SR-3	123.4	135.1	137.1	138.5	139.7
Loading	SR-2	-150.0	137.2	143.9	147.8	149.7
	SR-3	-150.0	131.9	136.3	139.4	141.2

(k) Flight altitude = 9.15 Km (30,000 ft), M=0.8, Microphone 12

FIGURES

Figure 1.- The Jetstar prop-fan test bed with pylon assembly on top of fuselage.

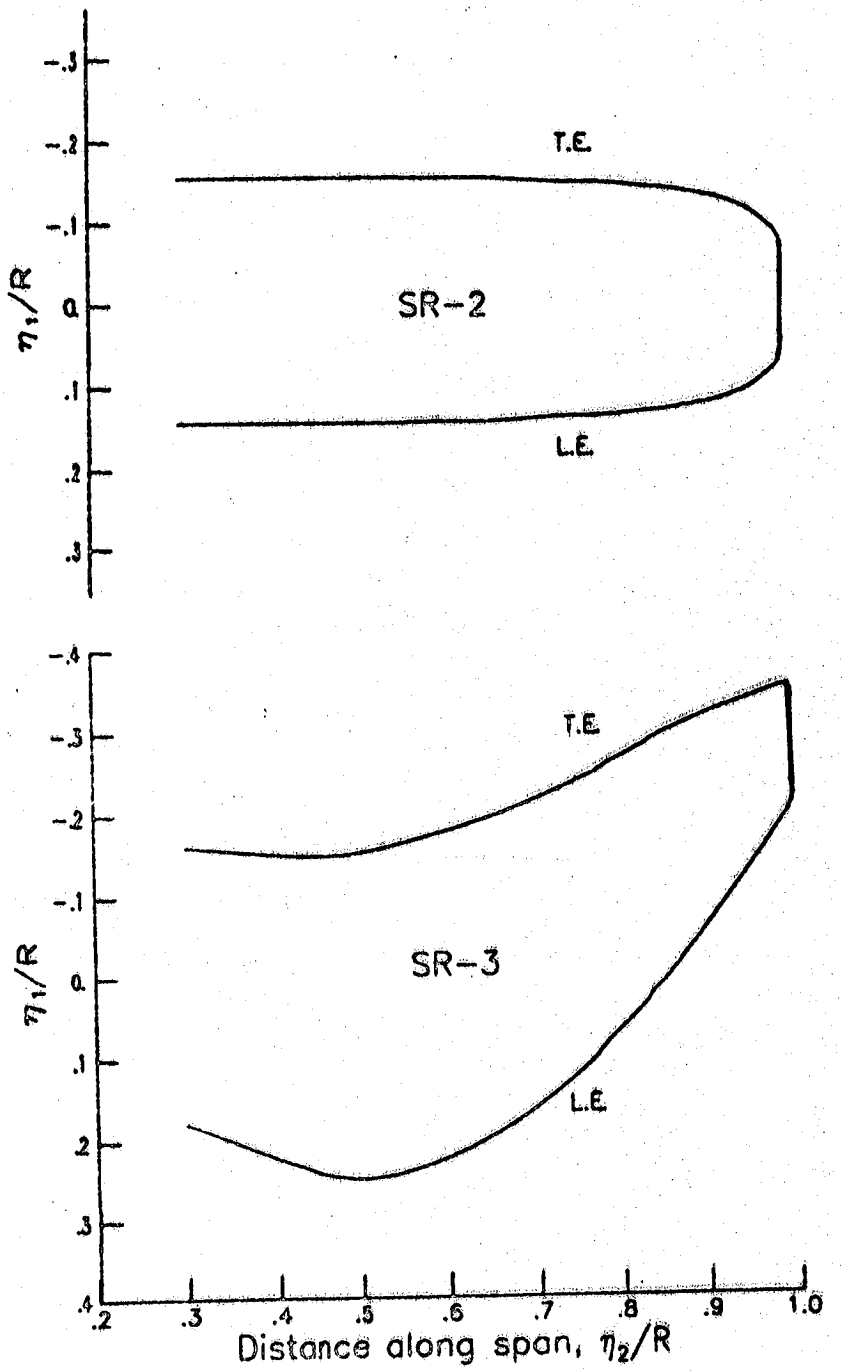

Figure 2.- Planforms of the two-blade designs. Blade radius 0.31 m (1.02 ft). η_1 = distance along the chord from the pitch change axis.

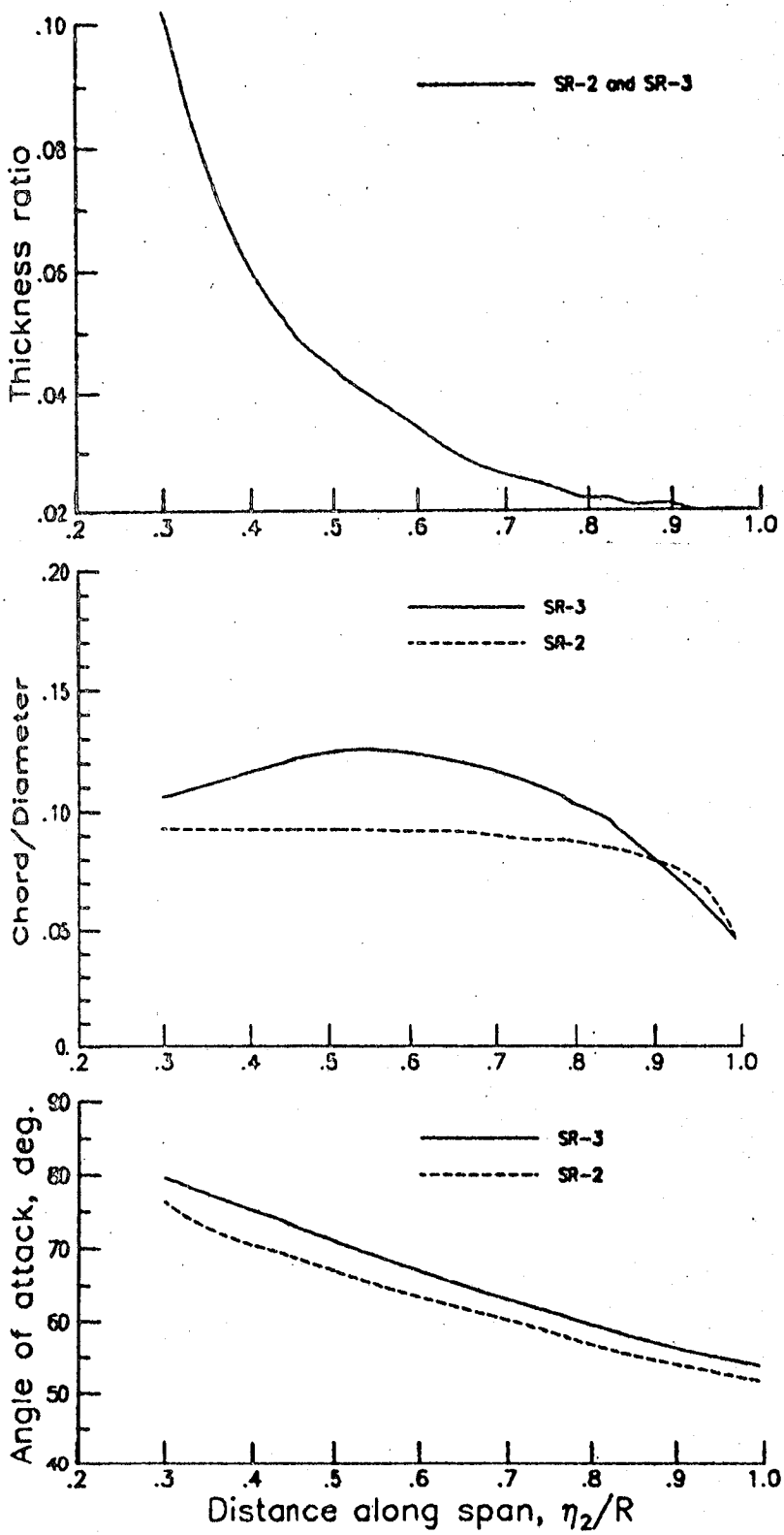

Figure 3.- Blade form curves for the two-blade designs. Blade radius 0.31 m (1.02 ft).

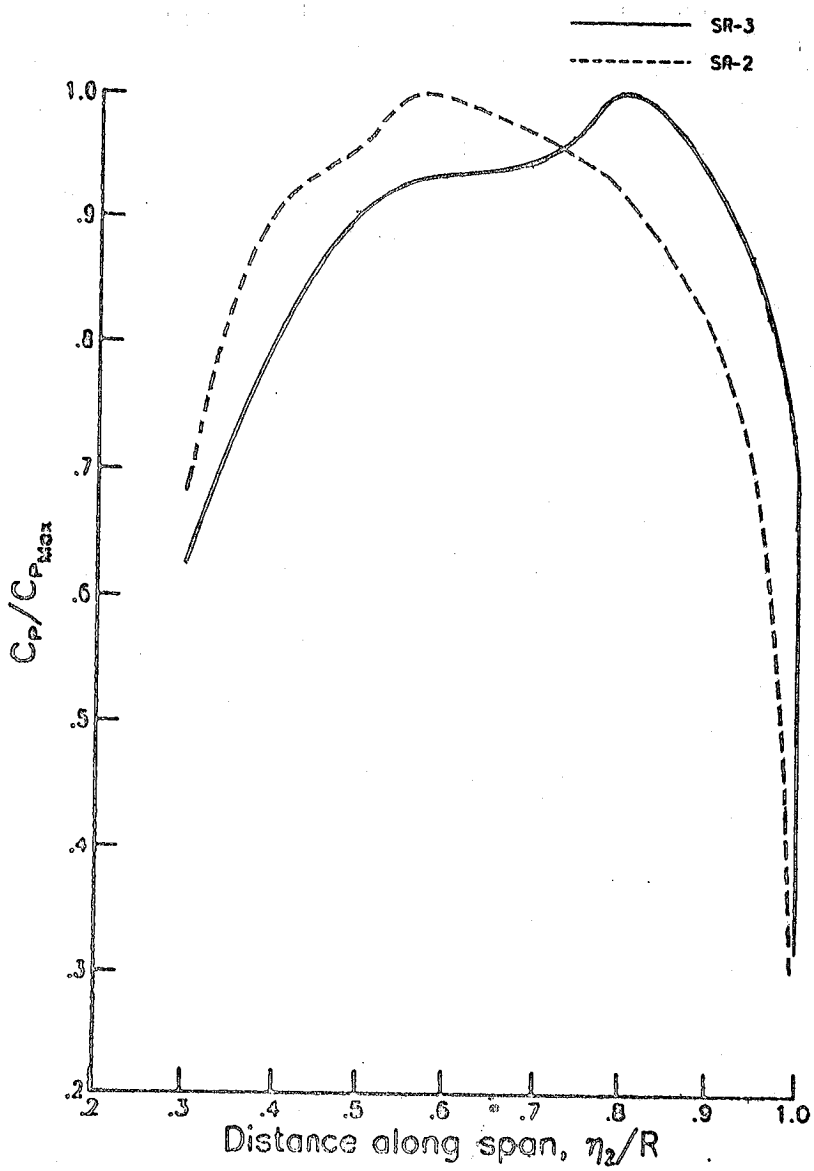

Figure 4.- The radial distribution of the lift coefficient for the two-blade designs.

SR-2 BLADE

FLIGHT ALTITUDE 6.10 km (20,000 ft)

FLIGHT MACH NUMBER 0.8

MICROPHONE 7

(ADVANCE RATIO VARIED)

Figure 5.- Free-field acoustic pressure signatures and spectra for SR-2 blade - Altitude 6.10 Km (20,000 ft), M=0.8, Microphone 7. Note the advance ratio is varied in these calculations.

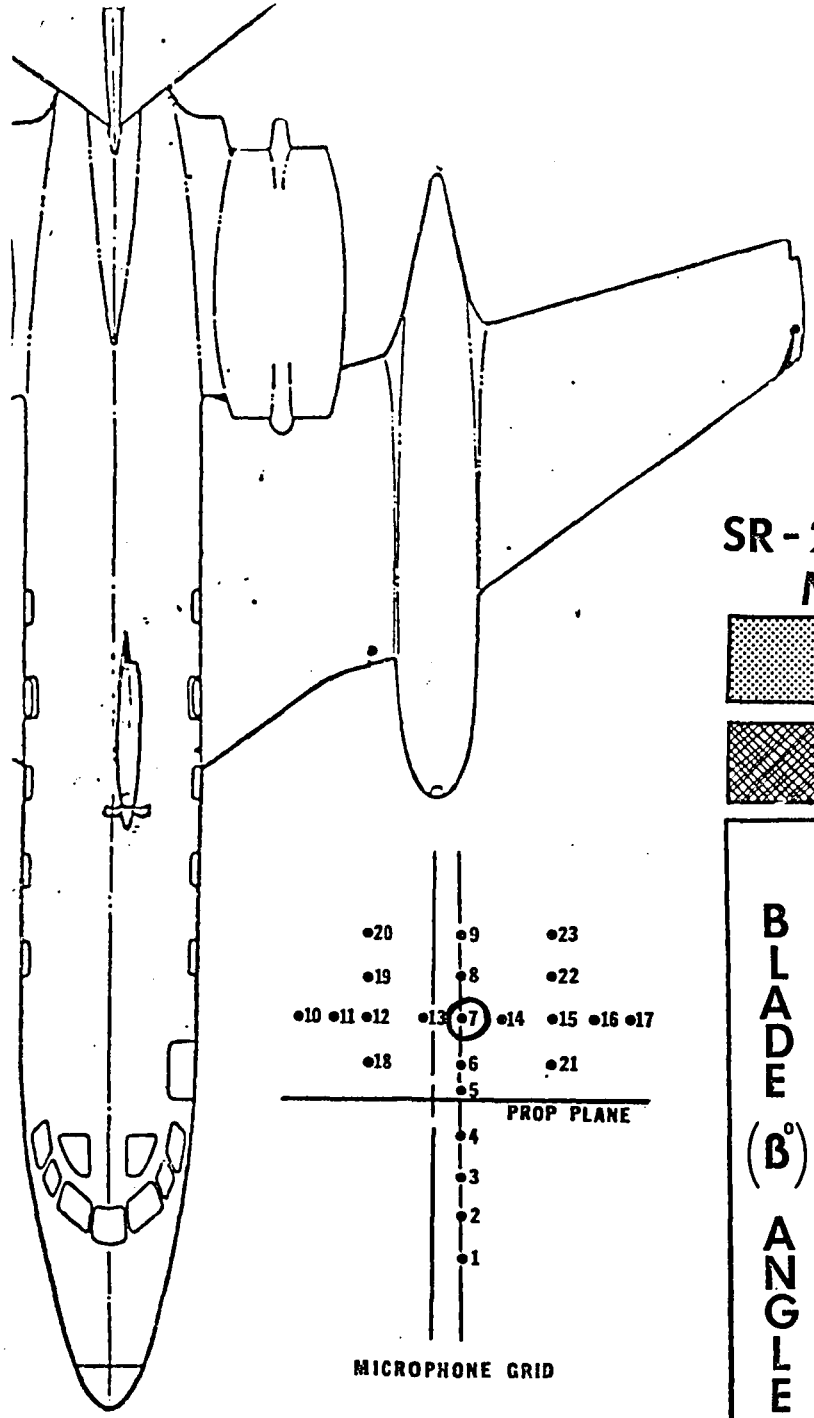

SR-2 TEST MATRIX

EXCEEDS BLEED SYS. POWER CAPACITY

BLADE CRITICAL SPEED

BLADE ANGLE (β°)	ADVANCE RATIO (J)	ALTITUDE (FT) 20,000 MACH # .50	.60	.65	.70	.75	.80	ALTITUDE (FT) 25,000 MACH # .50	.60	.65	.70	.75	.80	ALTITUDE (FT) 30,000 MACH # .50	.60	.65	.70	.75	.80
59.0	4.30																		
	3.50																		
	3.25																		
	3.06																		
	2.90																		
60.0	4.30						X												
	3.50						X												
	3.25						X												
	3.06						X												
	2.95						X												
61.0	4.30																		
	4.07																		
	3.50																		
	3.25																		

Figure 5.- Continued.

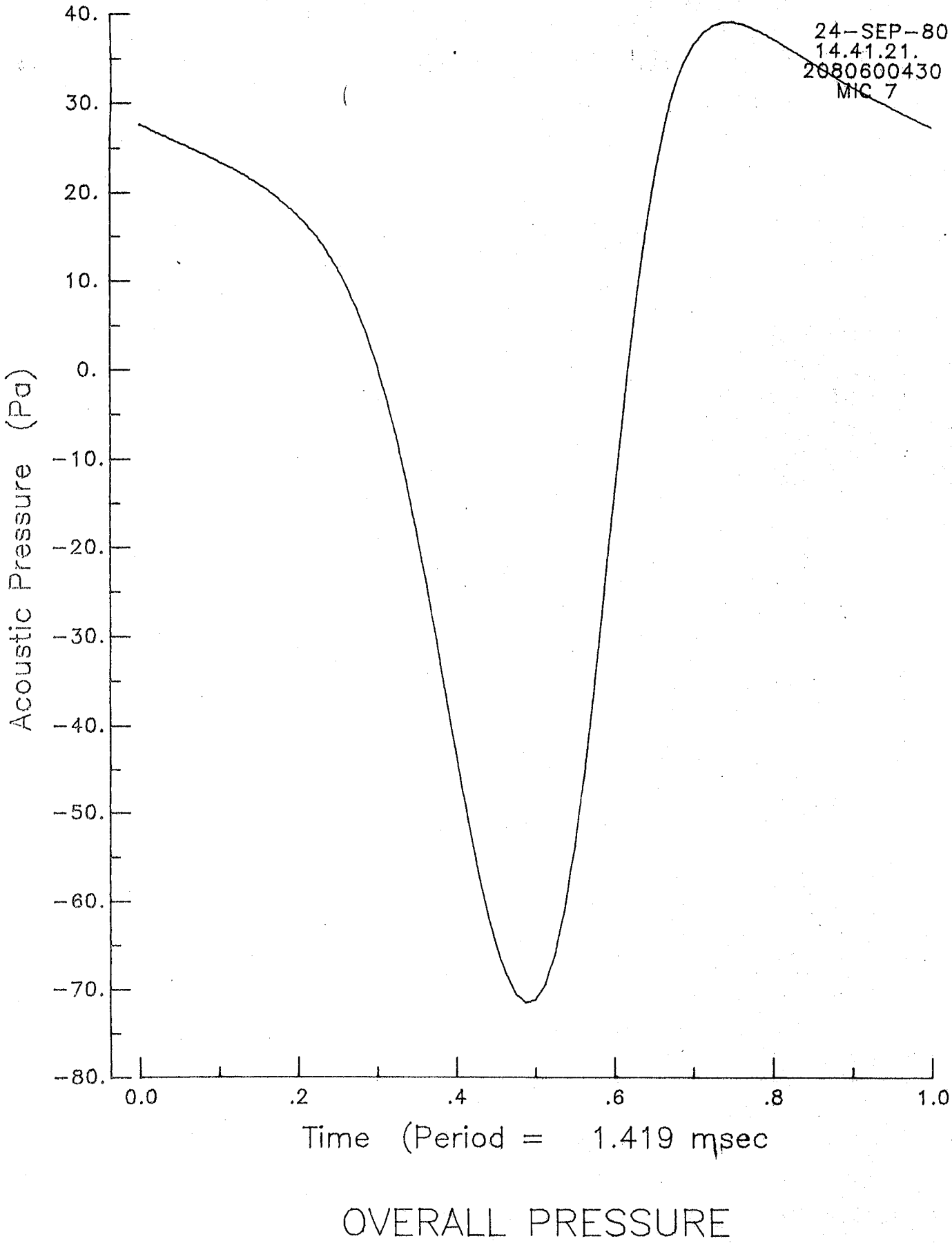

OVERALL PRESSURE

F. Farassat -- P. Nystrom
JIAFS -- NASA/LaRC -- GWU

Figure 5.- Continued.

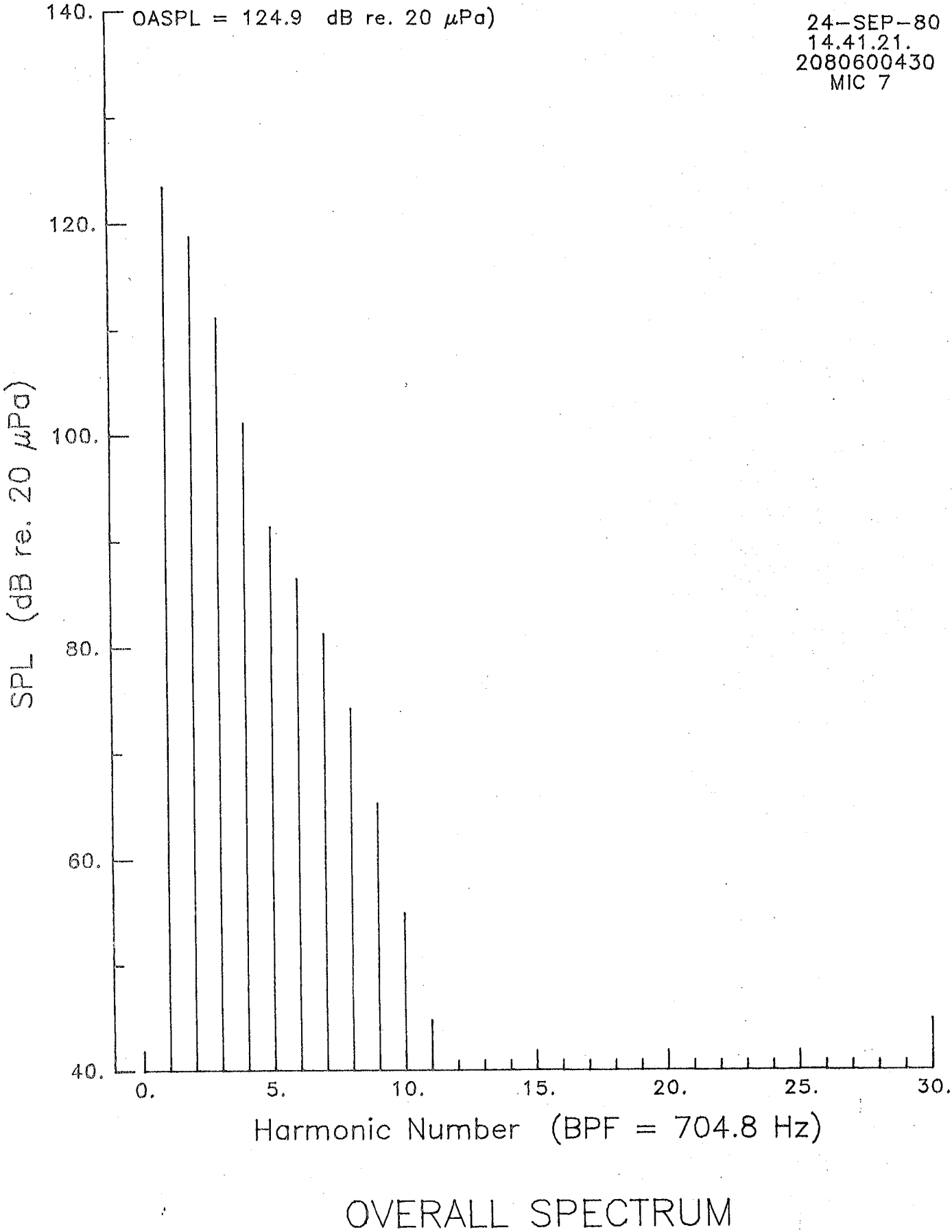

Figure 5.- Continued.

F. Farassat -- P. Nystrom
JIAFS -- NASA/LaRC -- GWU

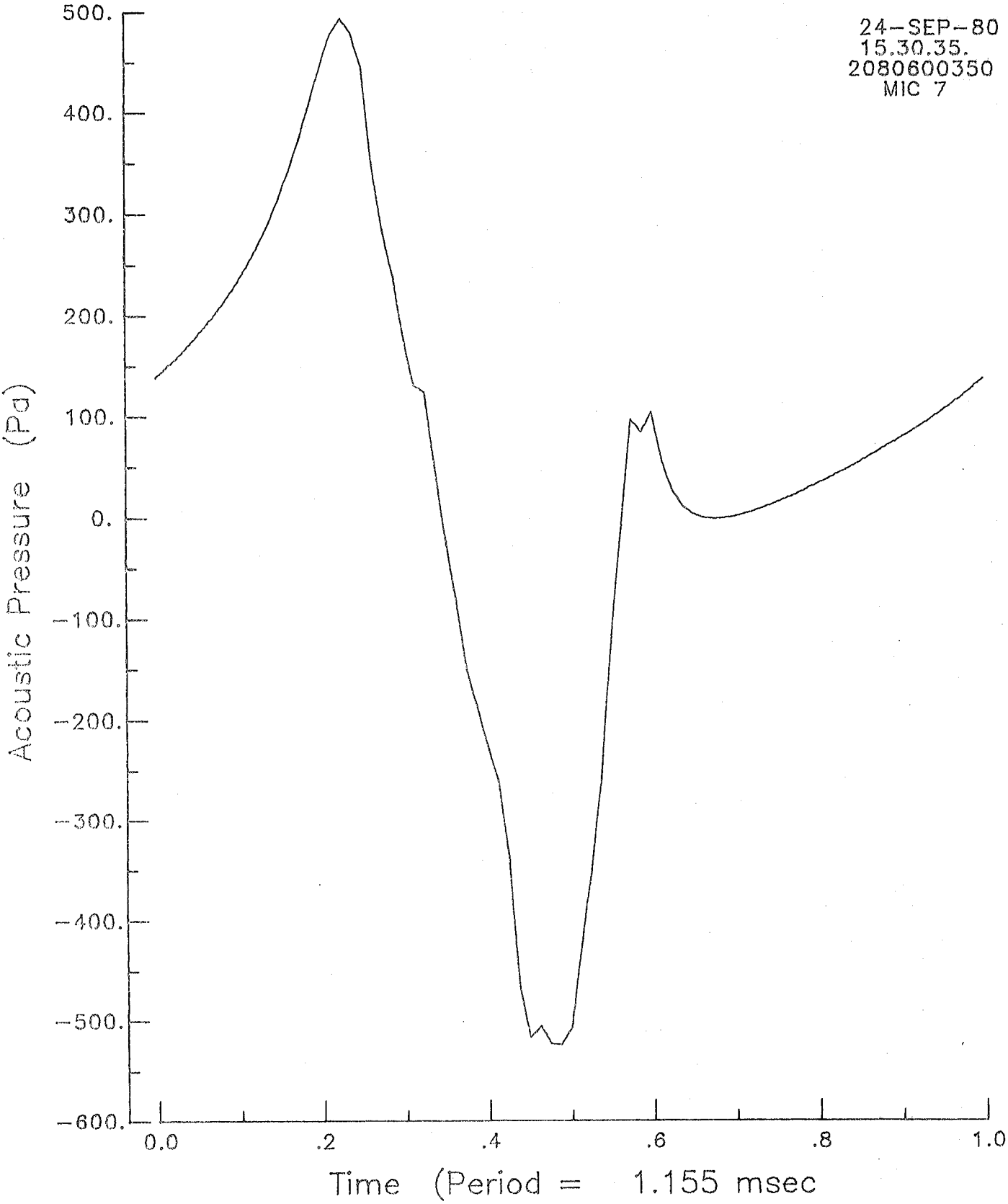

OVERALL PRESSURE

Figure 5.- Continued.

F. Farassat -- P. Nystrom
JIAFS -- NASA/LaRC -- GWU

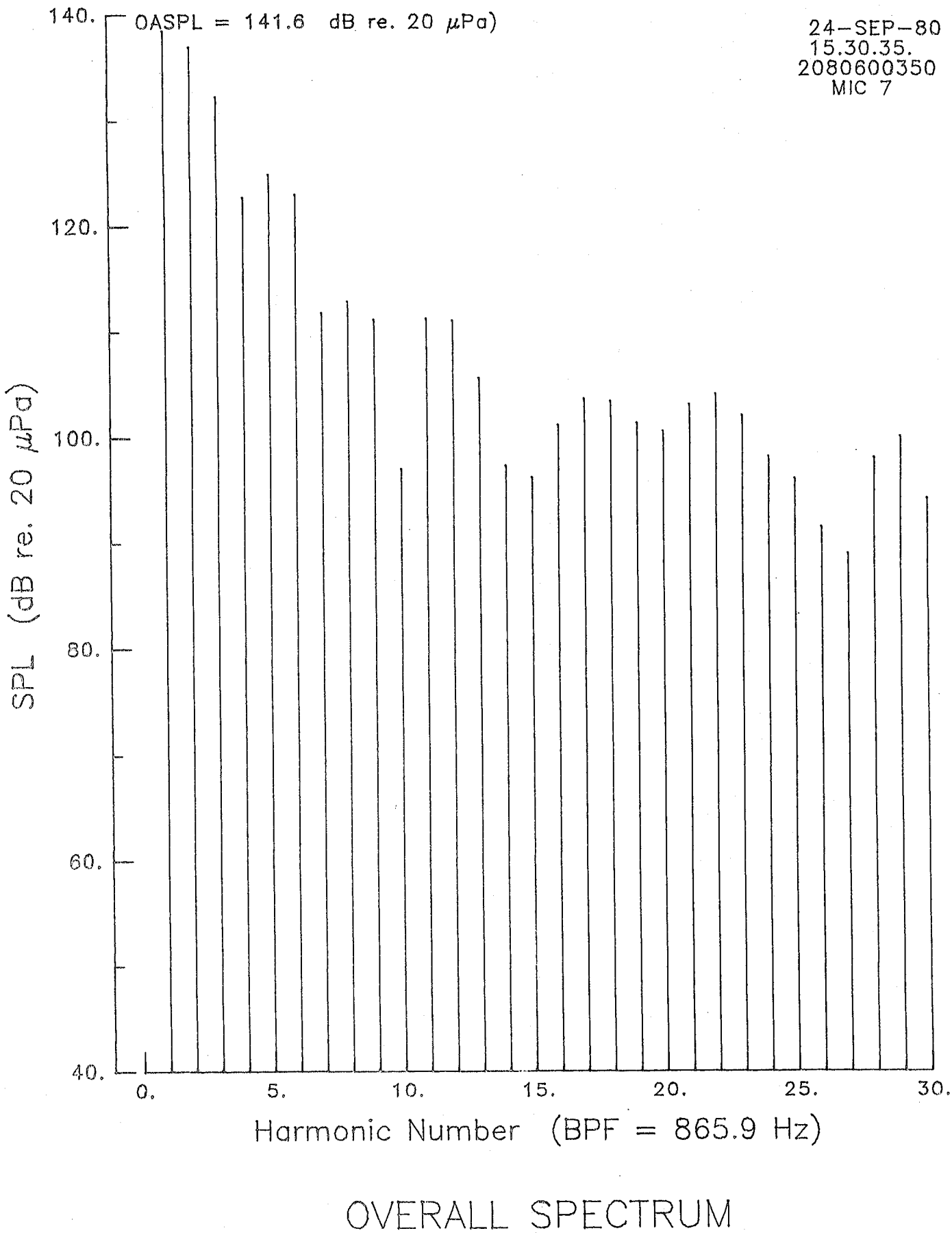

Figure 5.- Continued.

F. Farassat -- P. Nystrom
JIAFS -- NASA/LaRC -- GWU

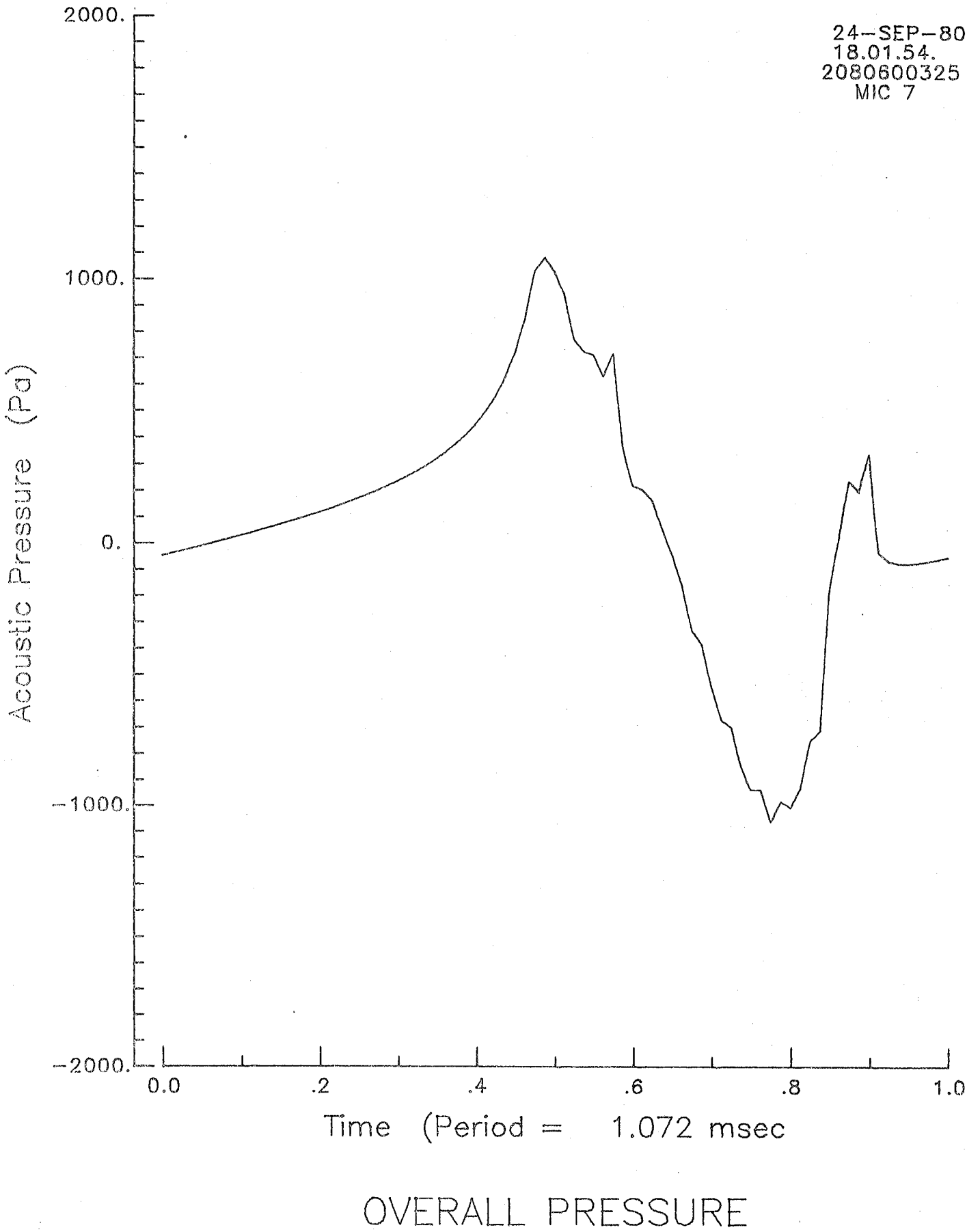

Figure 5.- Continued.

F. Farassat -- P. Nystrom
JIAFS -- NASA/LaRC -- GWU

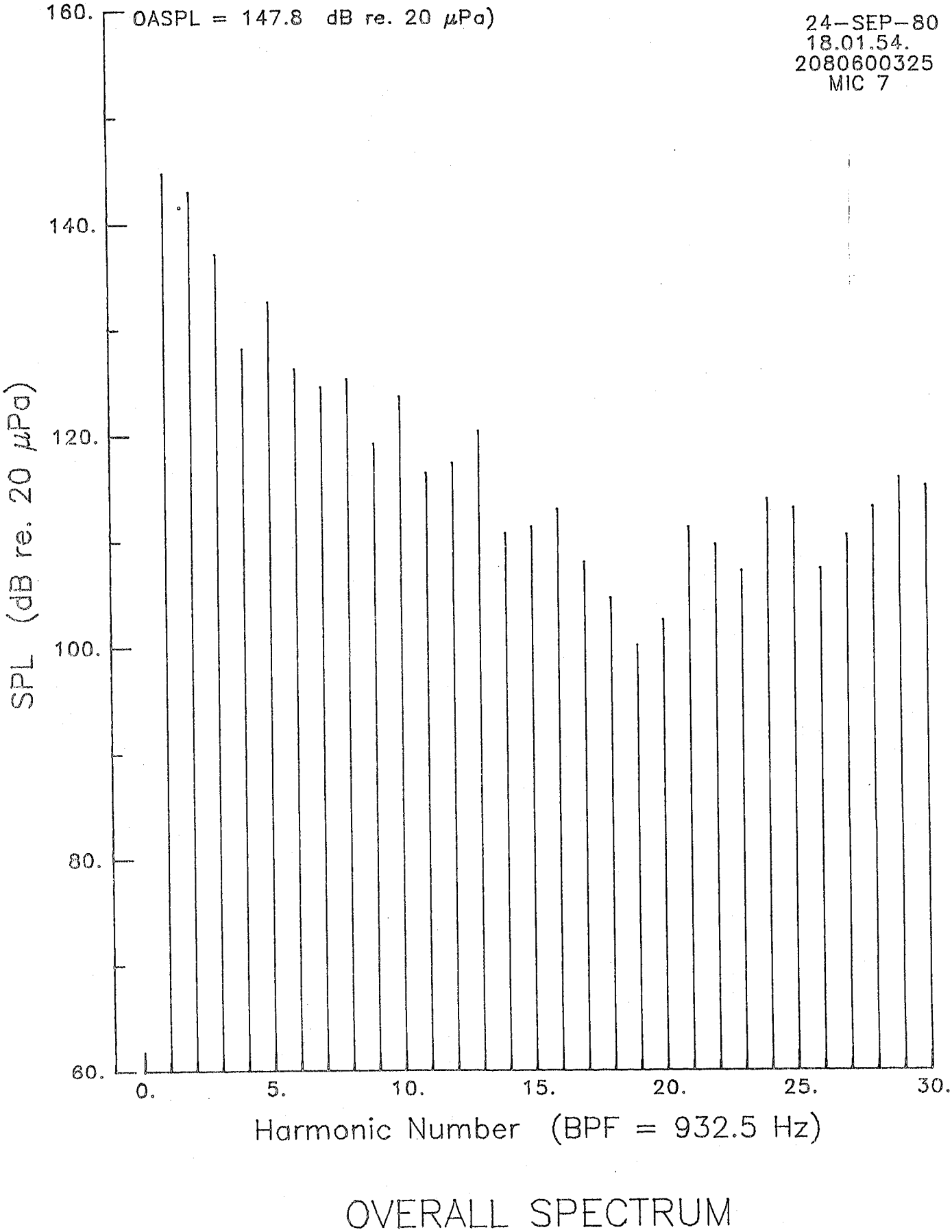

Figure 5.- Continued.

F. Farassat -- P. Nystrom
JIAFS -- NASA/LaRC -- GWU

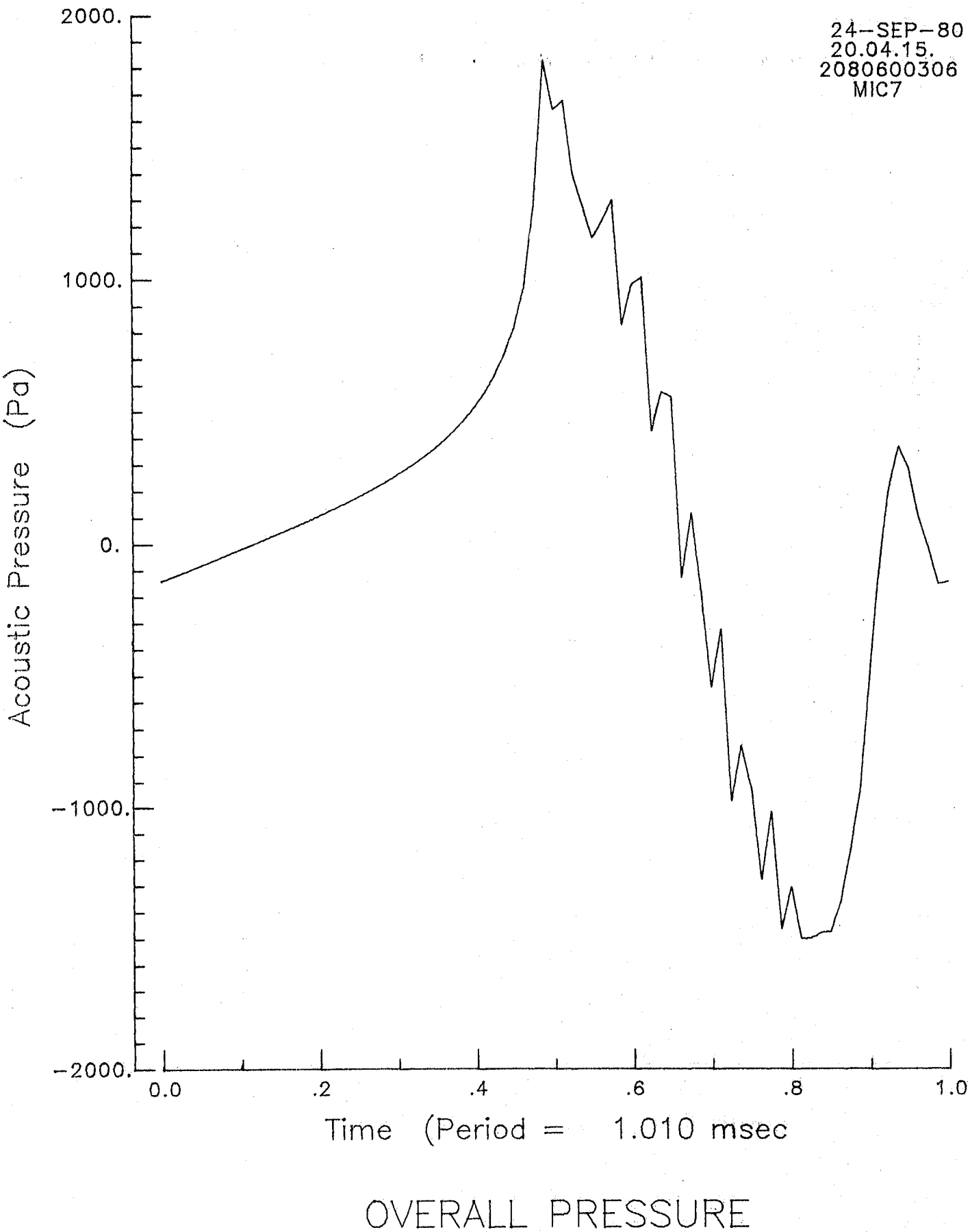

Figure 5.- Continued.

F. Farassat -- P. Nystrom
JIAFS -- NASA/LaRC -- GWU

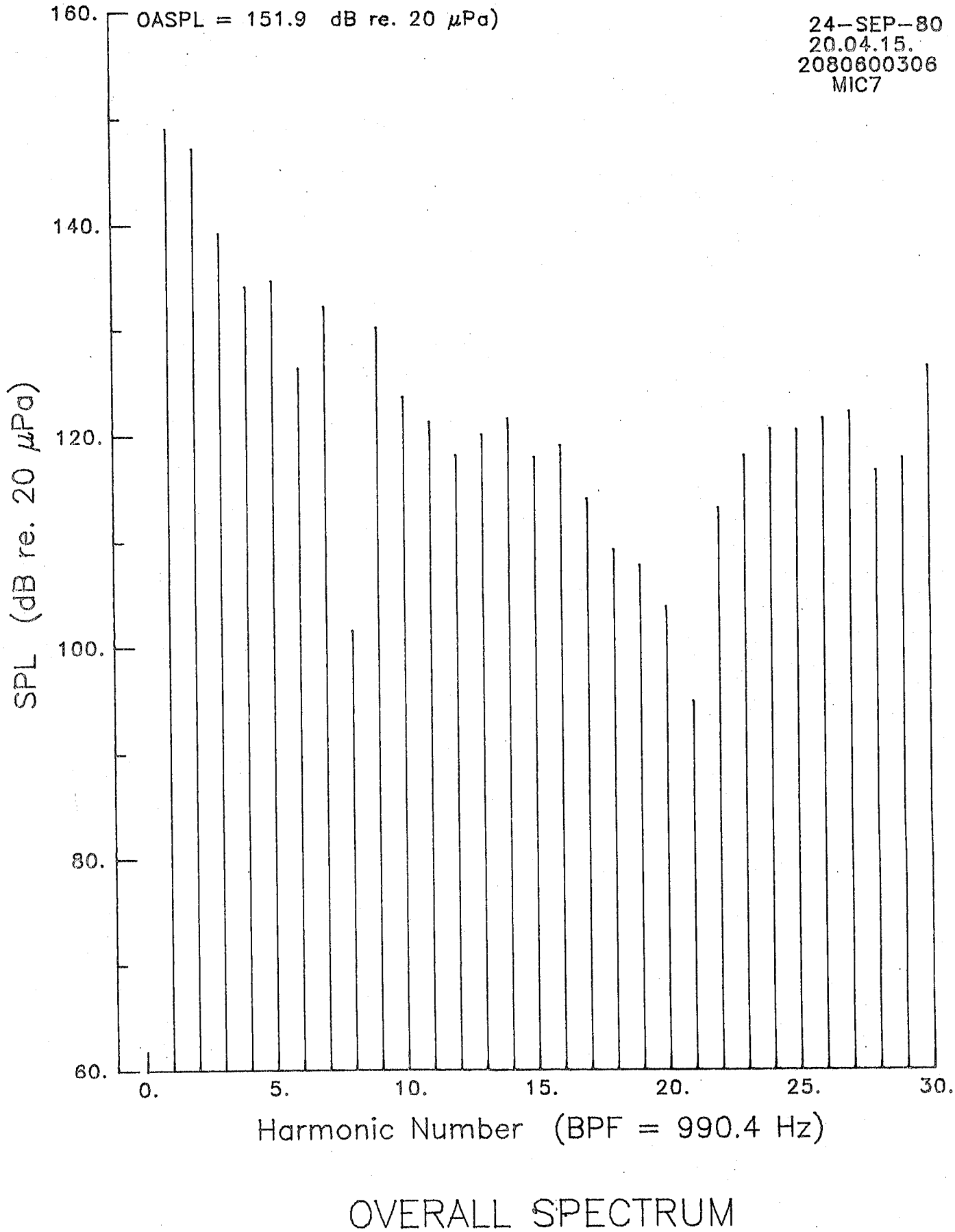

Figure 5.- Continued.

F. Farassat -- P. Nystrom
JIAFS -- NASA/LaRC -- GWU

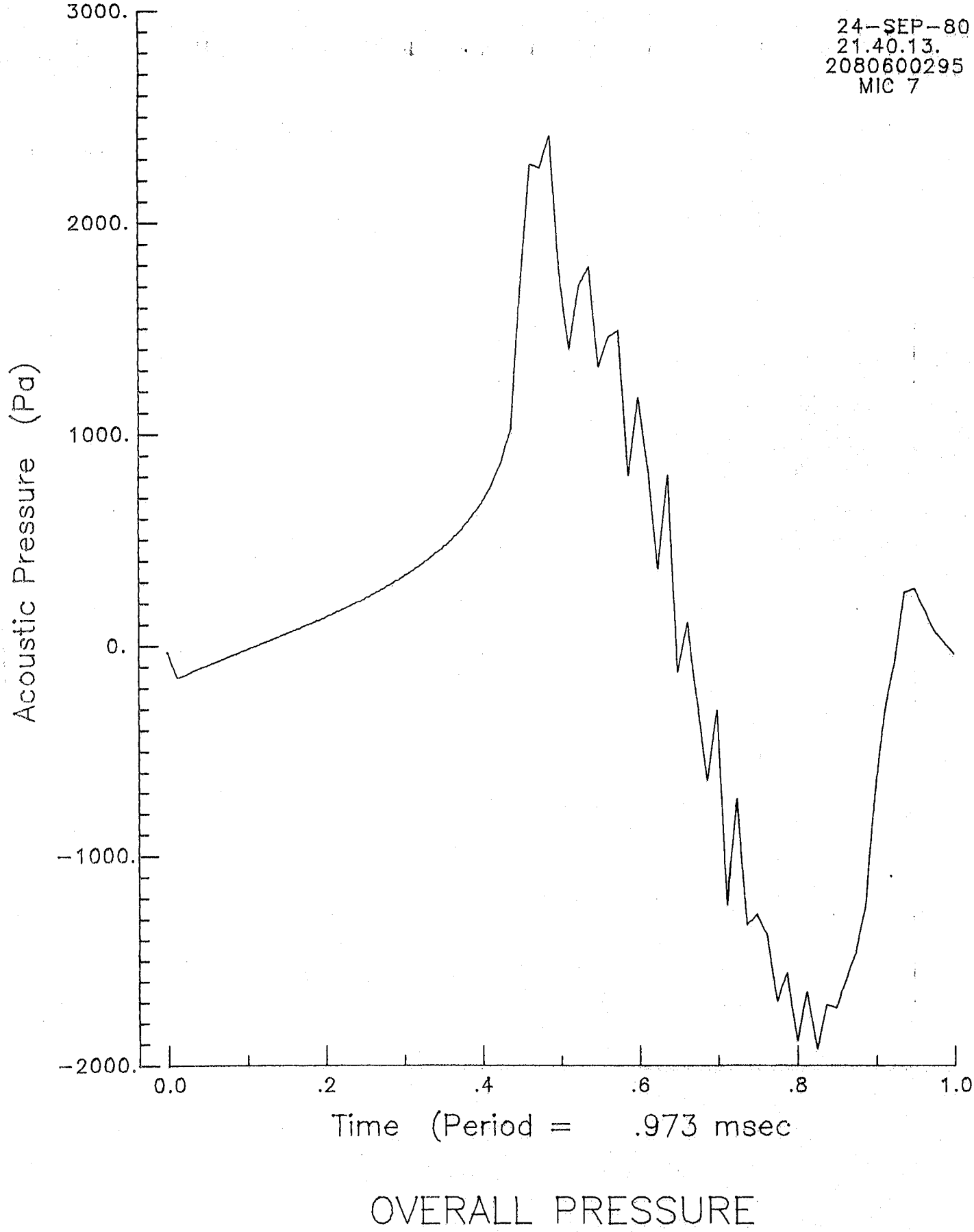

Figure 5.- Continued.

F. Farassat -- P. Nystrom
JIAFS -- NASA/LaRC -- GWU

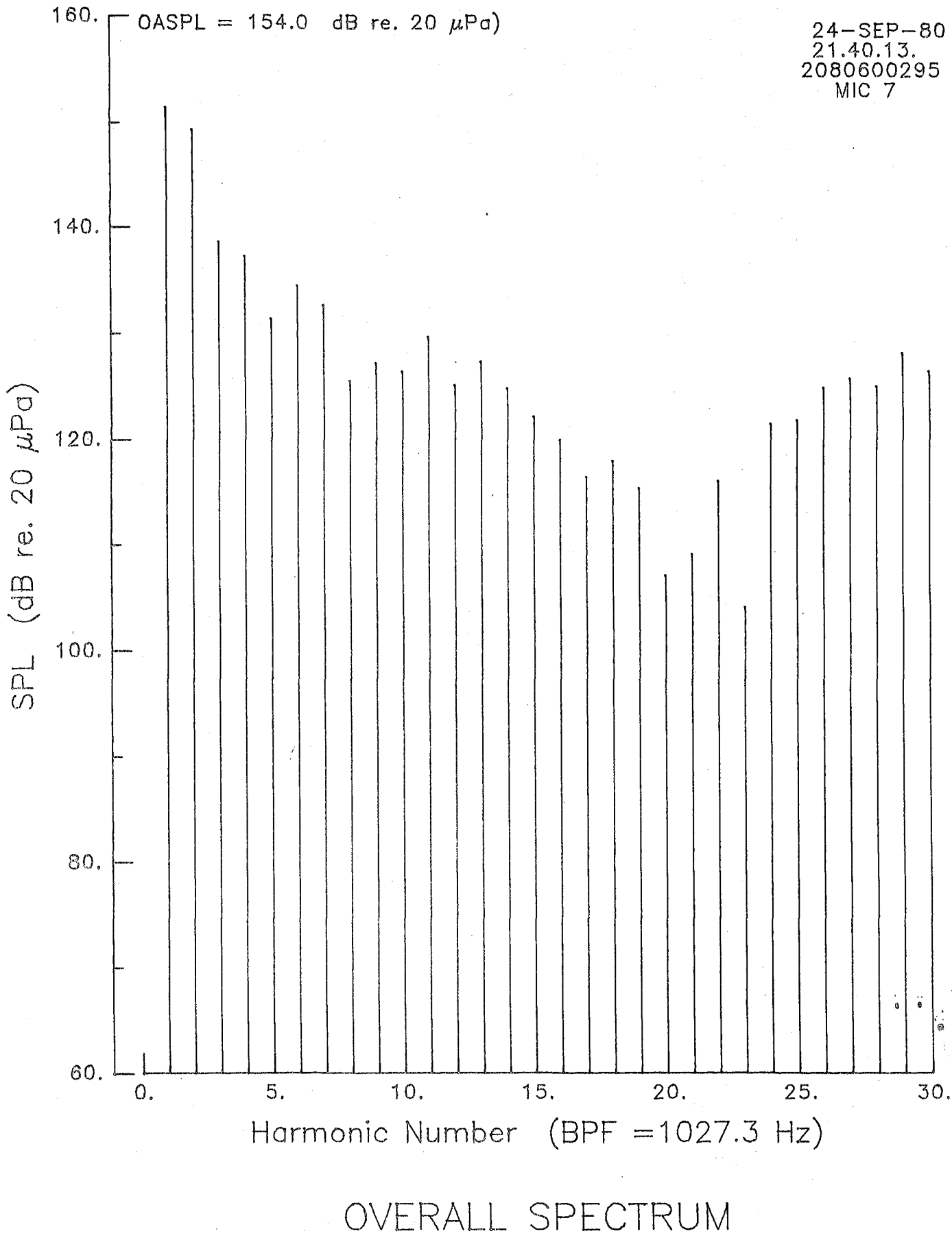

Figure 5.- Concluded.

F. Farassat -- P. Nystrom
JIAFS -- NASA/LaRC -- GWU

SR-2 BLADE

FLIGHT ALTITUDE 7.63 km (25,000 ft)

FLIGHT MACH NUMBER 0.8

MICROPHONE 7

(ADVANCE RATIO VARIED)

Figure 6.- Free-field acoustic pressure signatures and spectra for SR-2 blade - Altitude 7.63 Km (25,000 ft), M=0.8, Microphone 7. Note the advance ratio is varied in these calculations.

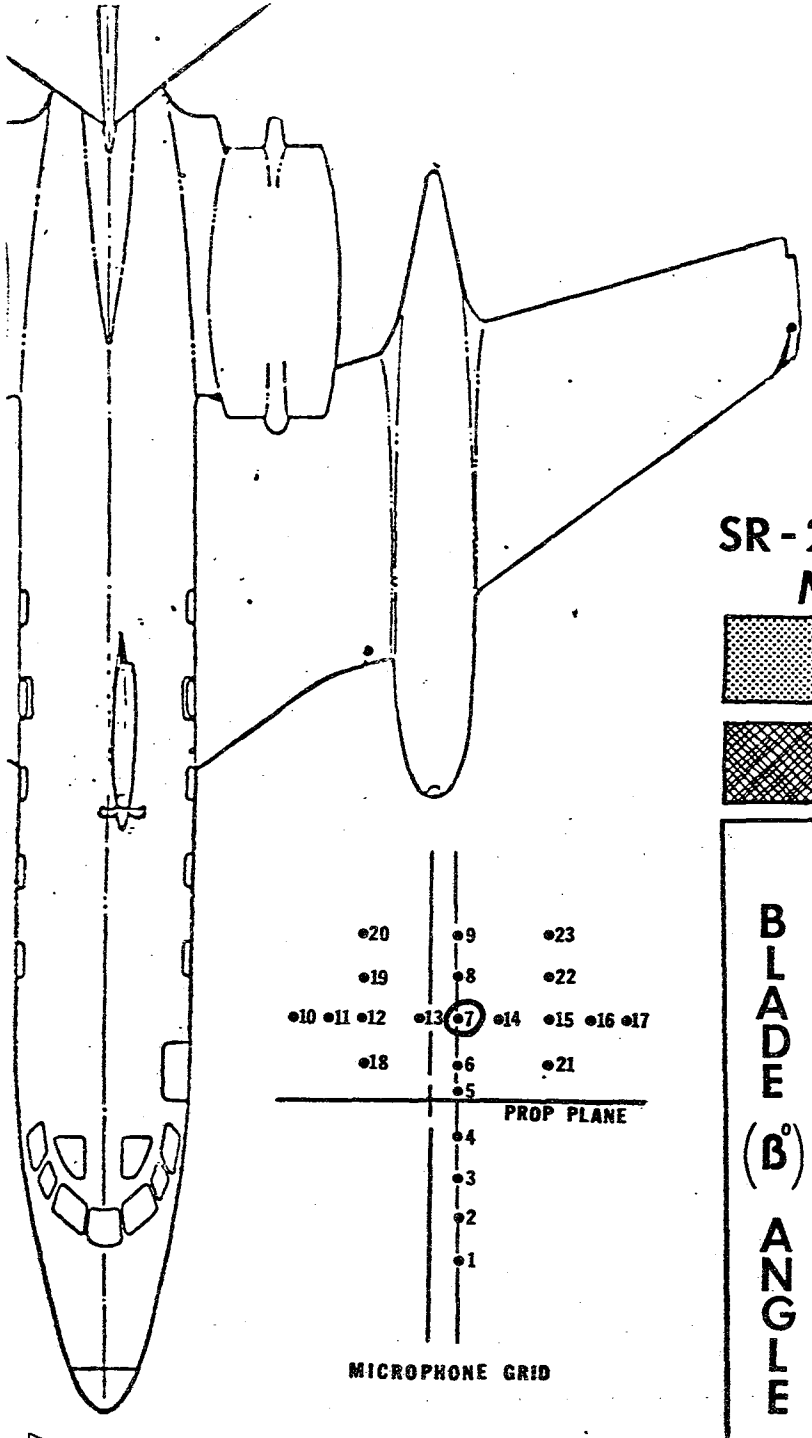

Figure 6.- Continued.

SR-2 TEST MATRIX

EXCEEDS BLEED SYS. POWER CAPACITY

BLADE CRITICAL SPEED

BLADE ANGLE (β°)	ADVANCE RATIO (J)	ALTITUDE (FT) 20,000 — MACH # .50	.60	.65	.70	.75	.80	ALTITUDE (FT) 25,000 — MACH # .50	.60	.65	.70	.75	.80	ALTITUDE (FT) 30,000 — MACH # .50	.60	.65	.70	.75	.80
59.0	4.30																		
	3.50																		
	3.25																		
	3.06																		
	2.90																		
60.0	4.30						X												
	3.50						X												
	3.25						X												
	3.06						X												
	2.95						X												
61.0	4.30																		
	4.07																		
	3.50																		
	3.25																		

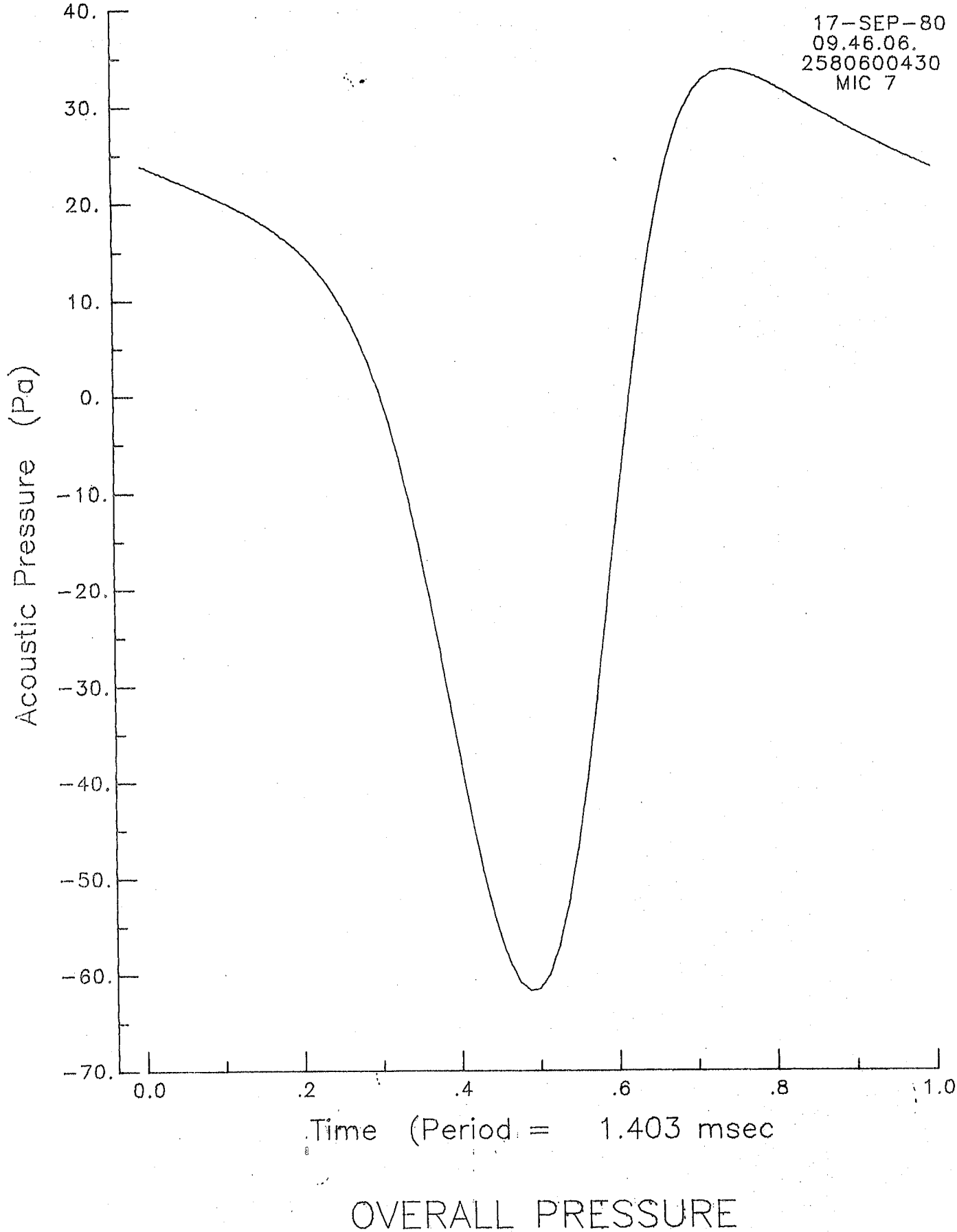

Figure 6.- Continued.

F. Farassat -- P. Nystrom
JIAFS -- NASA/LaRC -- GWU

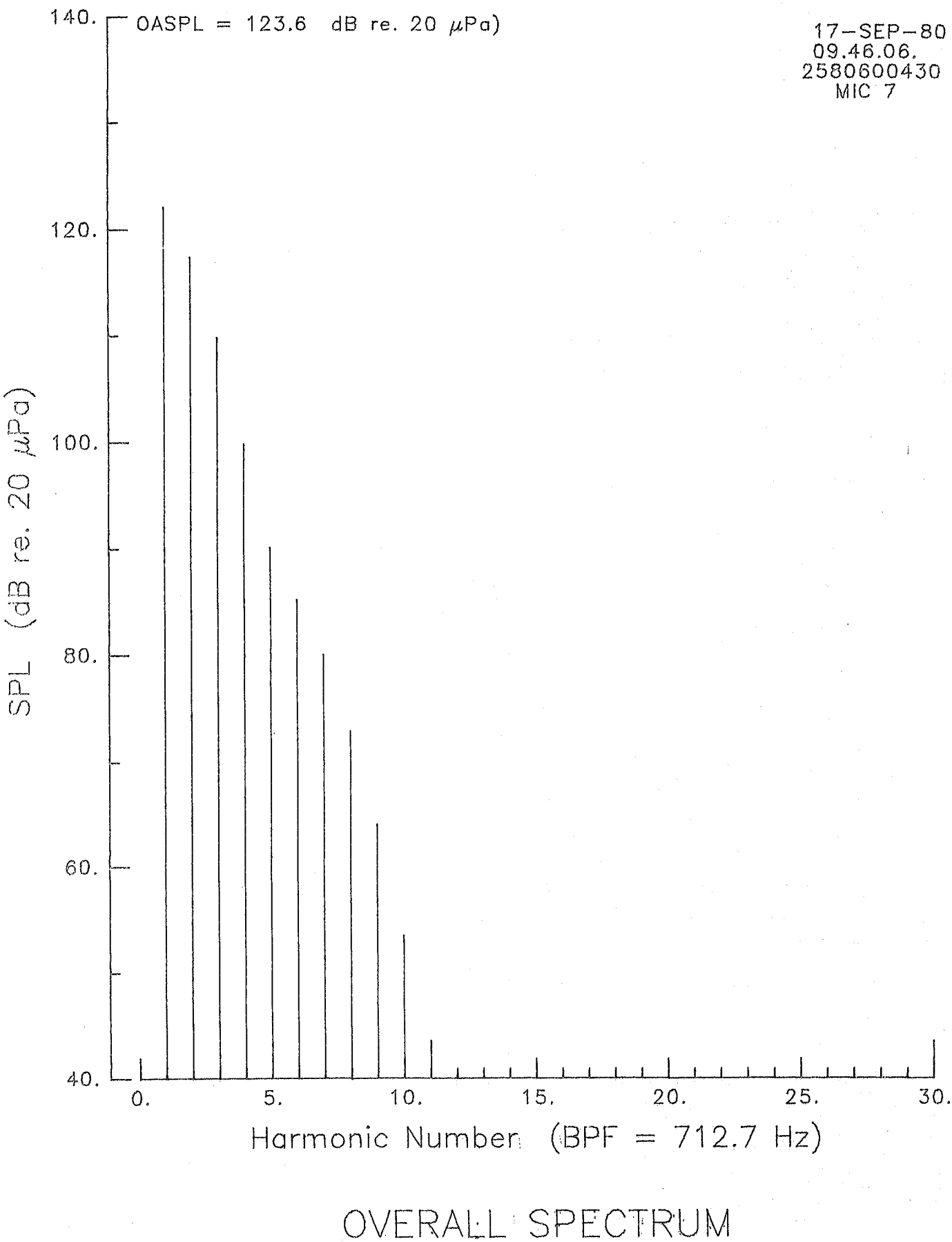

Figure 6.- Continued.

F. Farassat -- P. Nystrom
JIAFS -- NASA/LaRC -- GWU

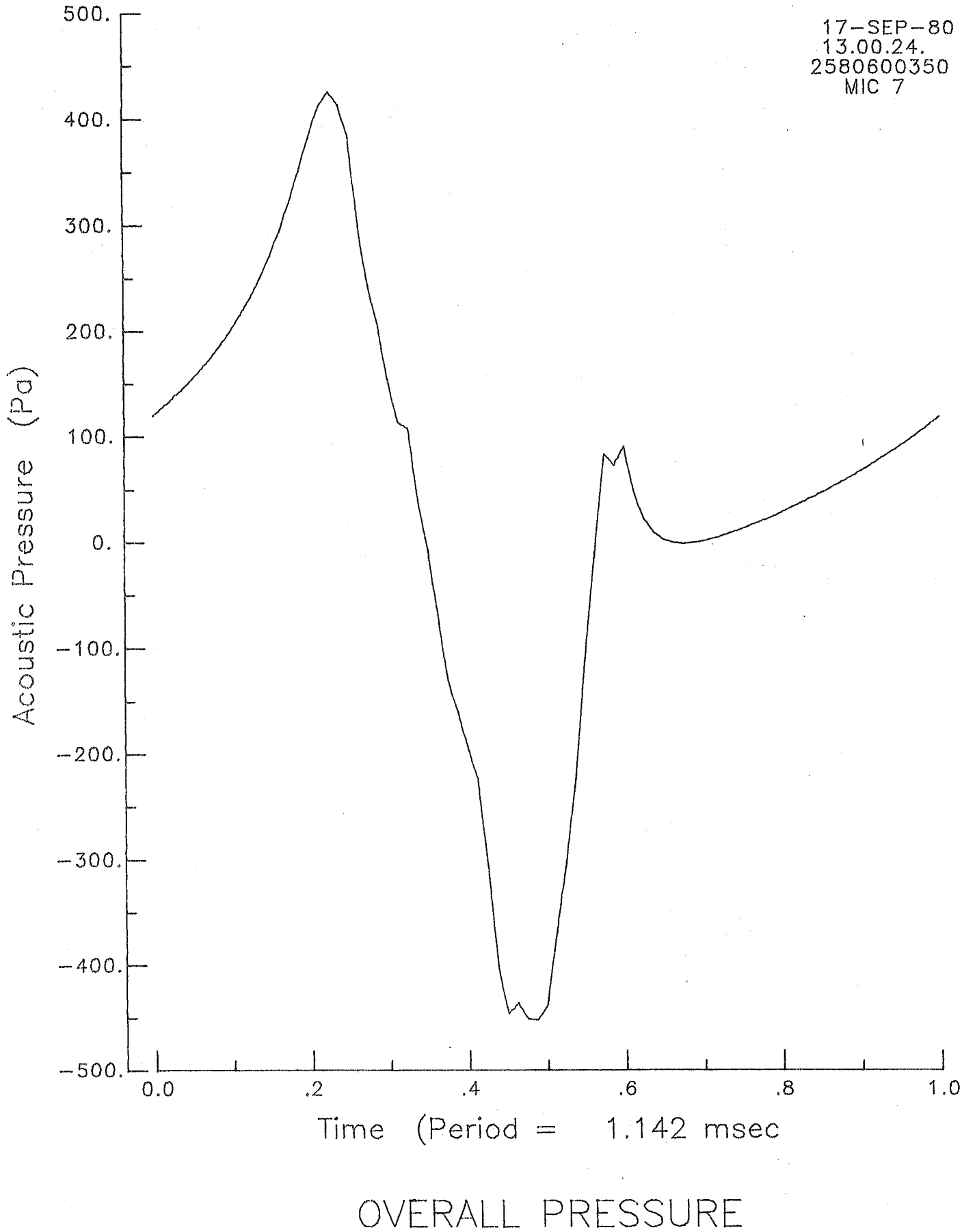

Figure 6.- Continued.

F. Farassat -- P. Nystrom
JIAFS -- NASA/LaRC -- GWU

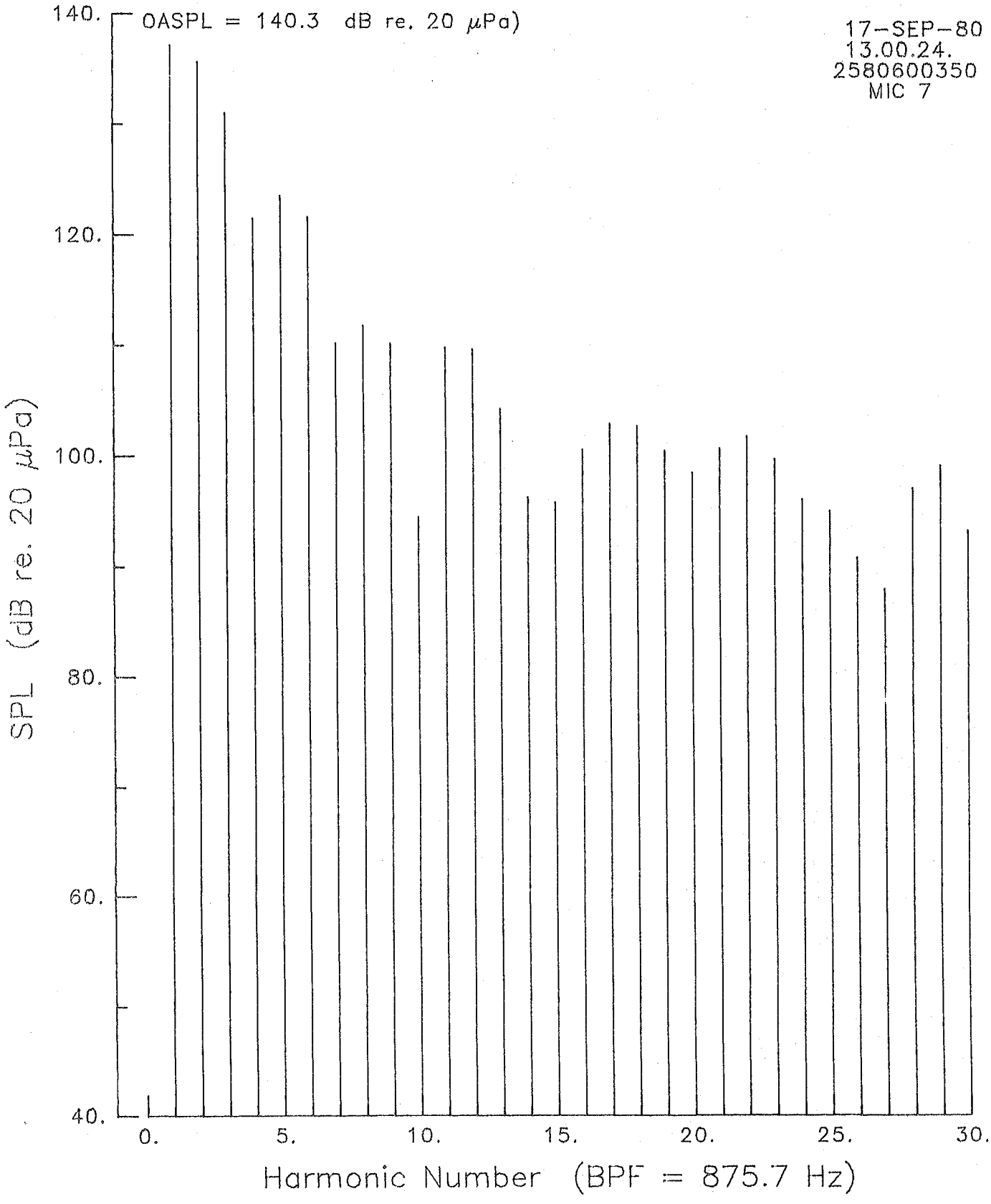

OVERALL SPECTRUM

Figure 6.- Continued.

F. Farassat -- P. Nystrom
JIAFS -- NASA/LaRC -- GWU

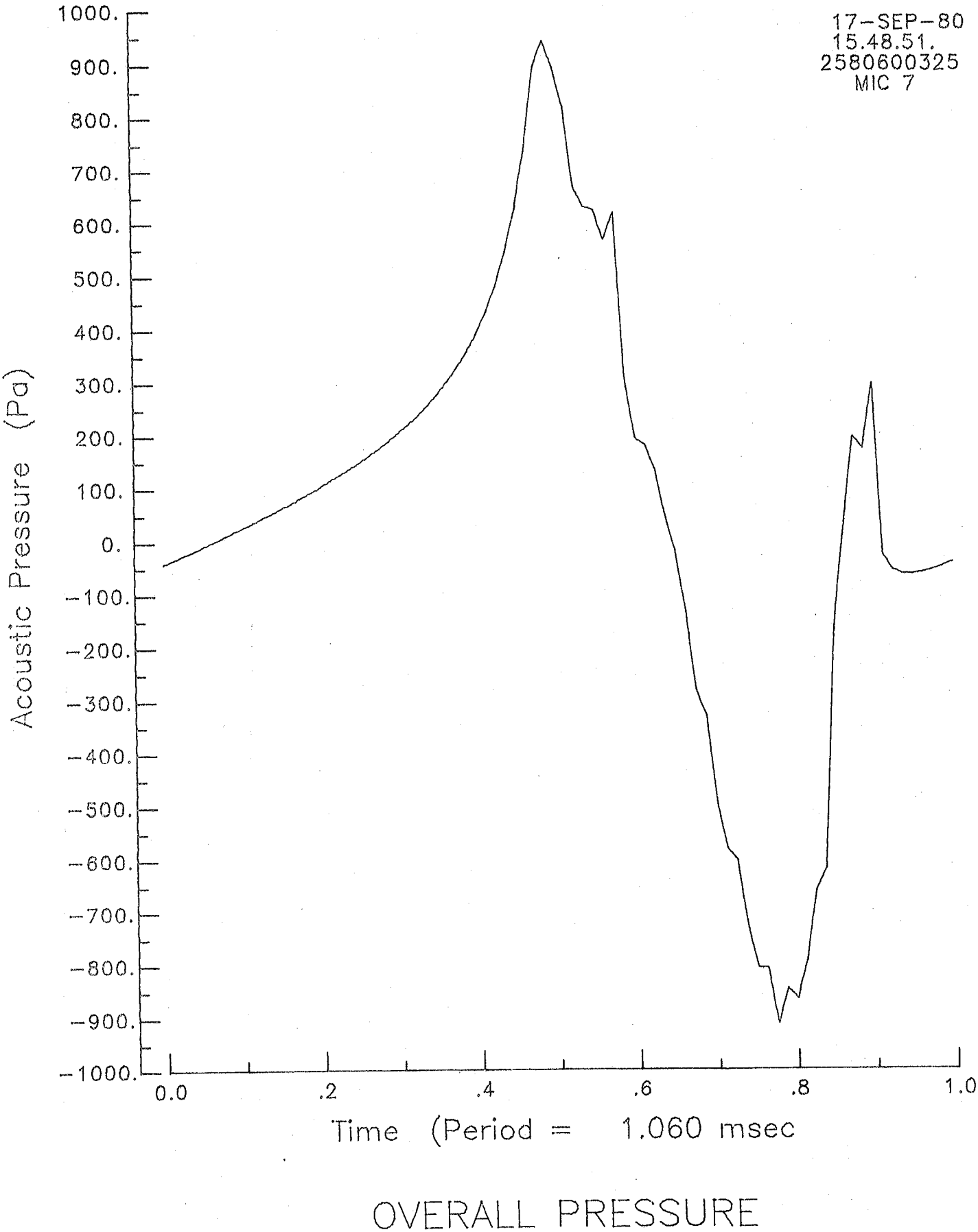

Figure 6.- Continued.

F. Farassat -- P. Nystrom
JIAFS -- NASA/LaRC -- GWU

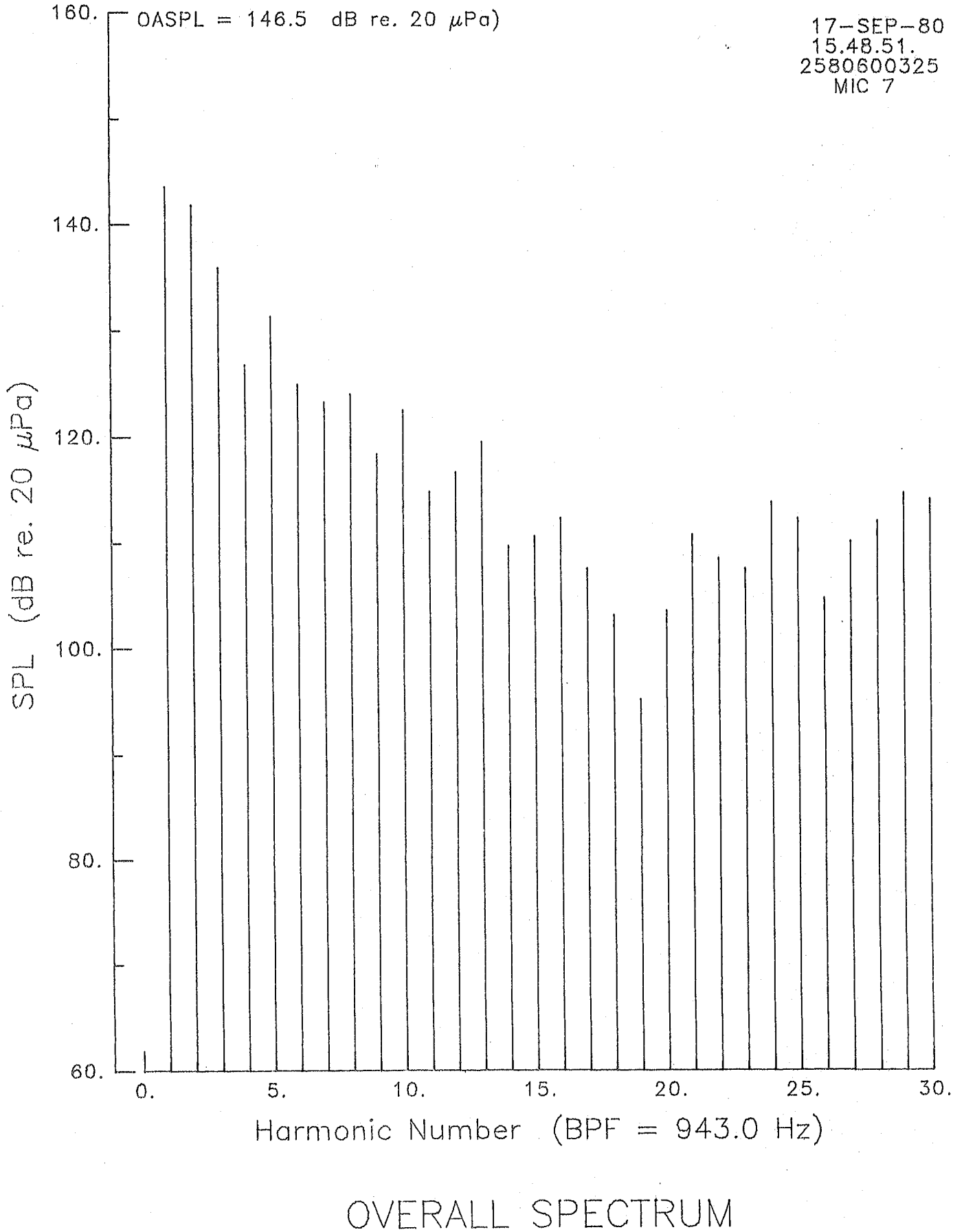

Figure 6.- Continued.

F. Farassat -- P. Nystrom
JIAFS -- NASA/LaRC -- GWU

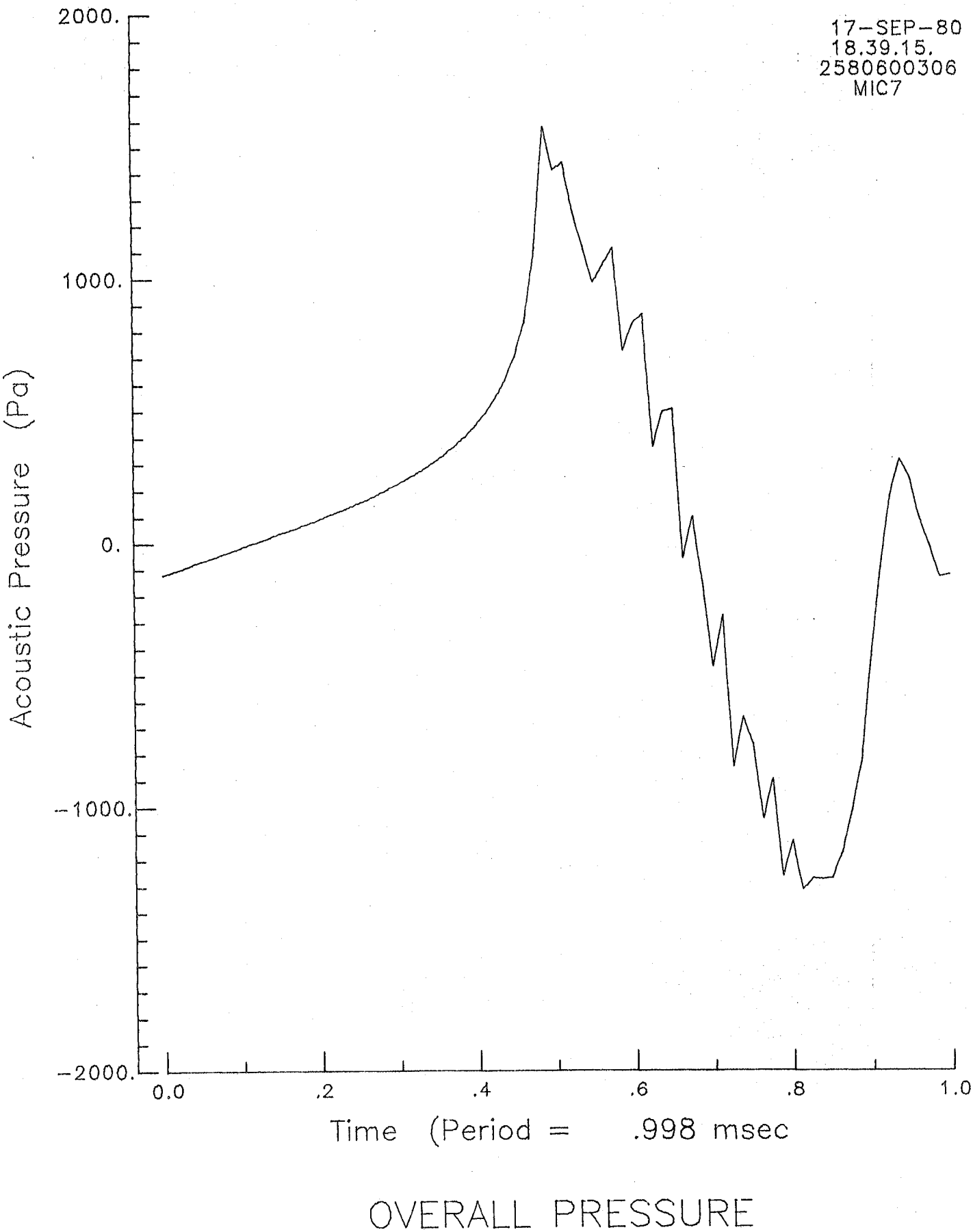

Figure 6.- Continued.

F. Farassat -- P. Nystrom
JIAFS -- NASA/LaRC -- GWU

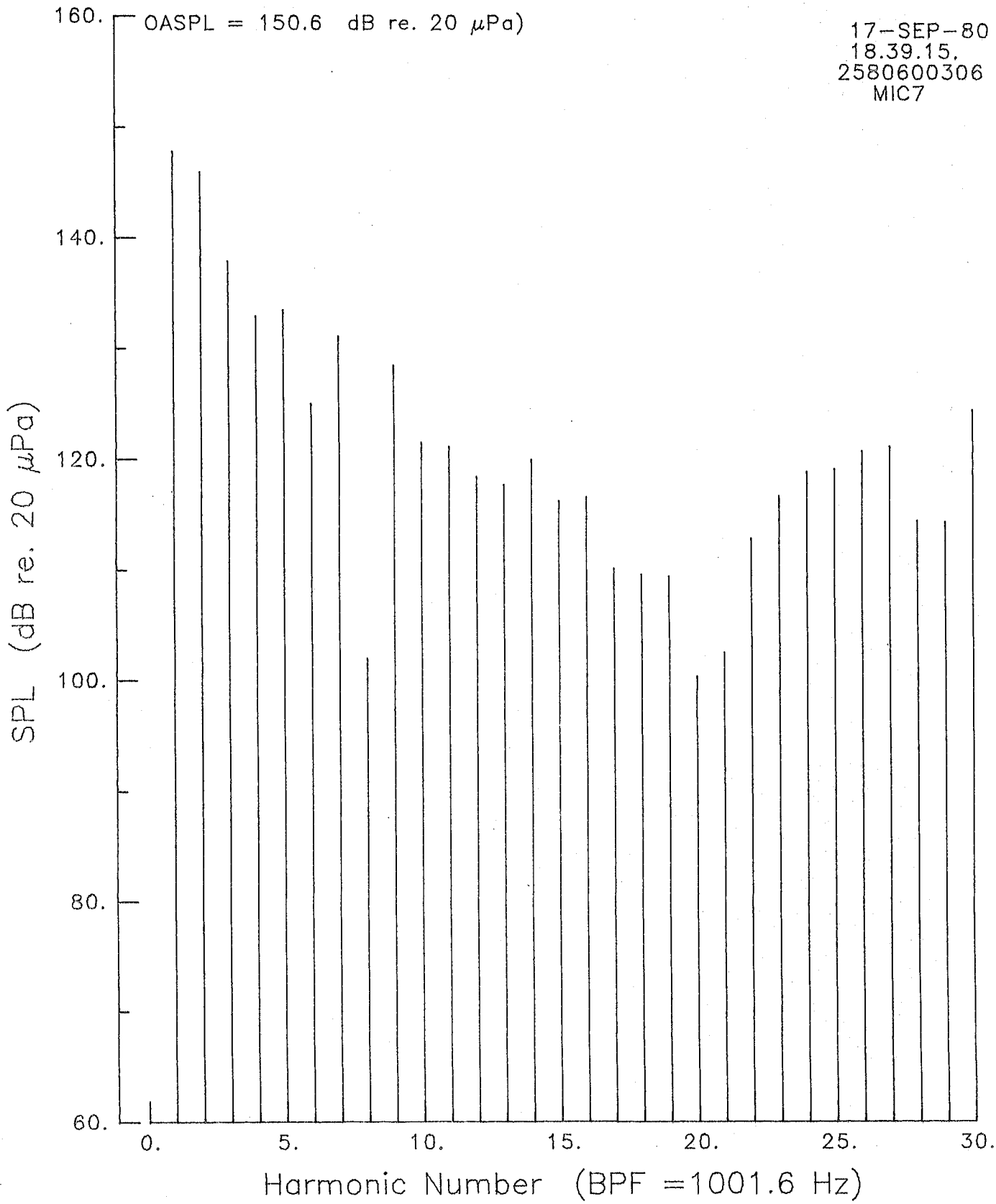

Figure 6.- Continued.

F. Farassat -- P. Nystrom
JIAFS -- NASA/LaRC -- GWU

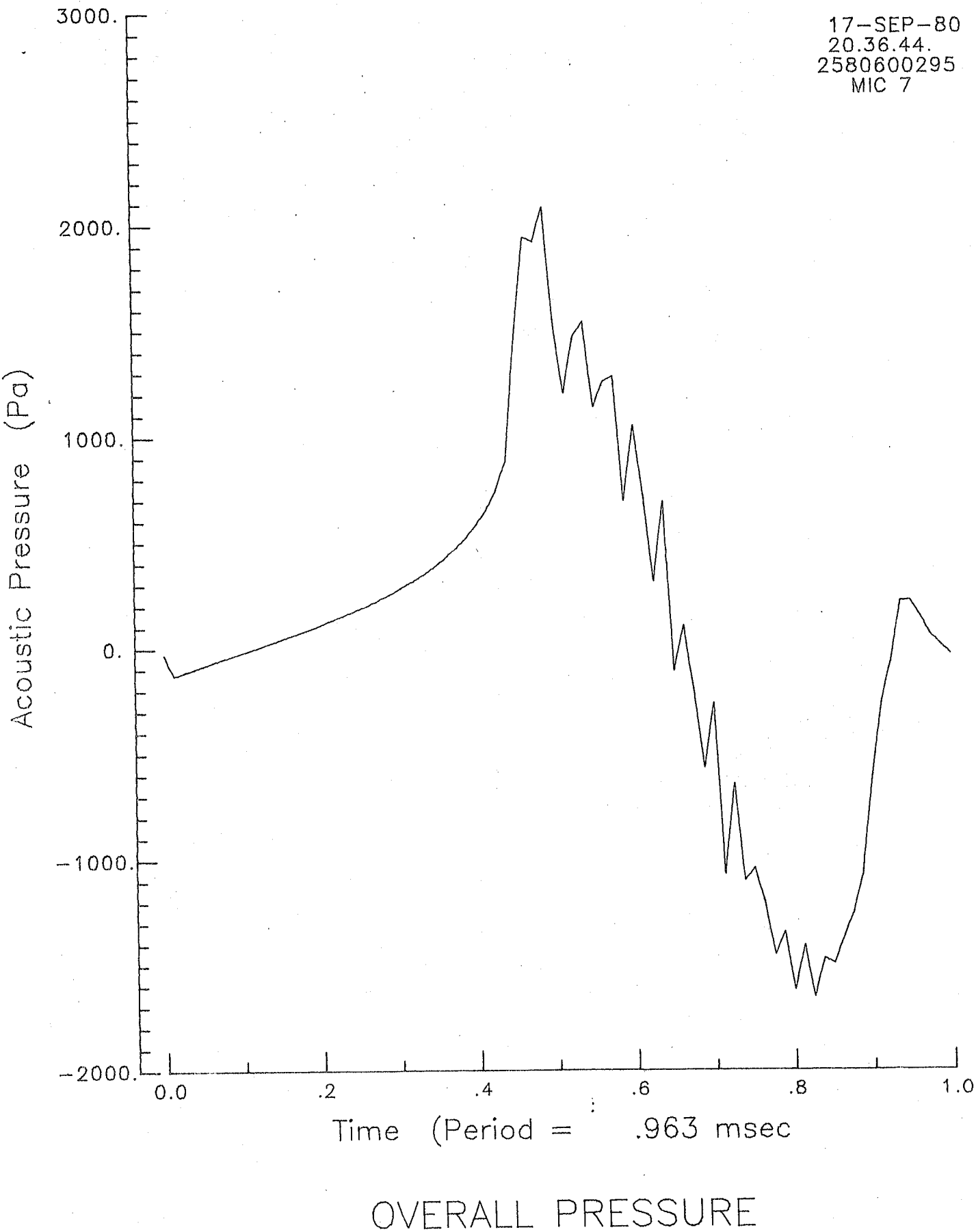

Figure 6.- Continued.

F. Farassat -- P. Nystrom
JIAFS -- NASA/LaRC -- GWU

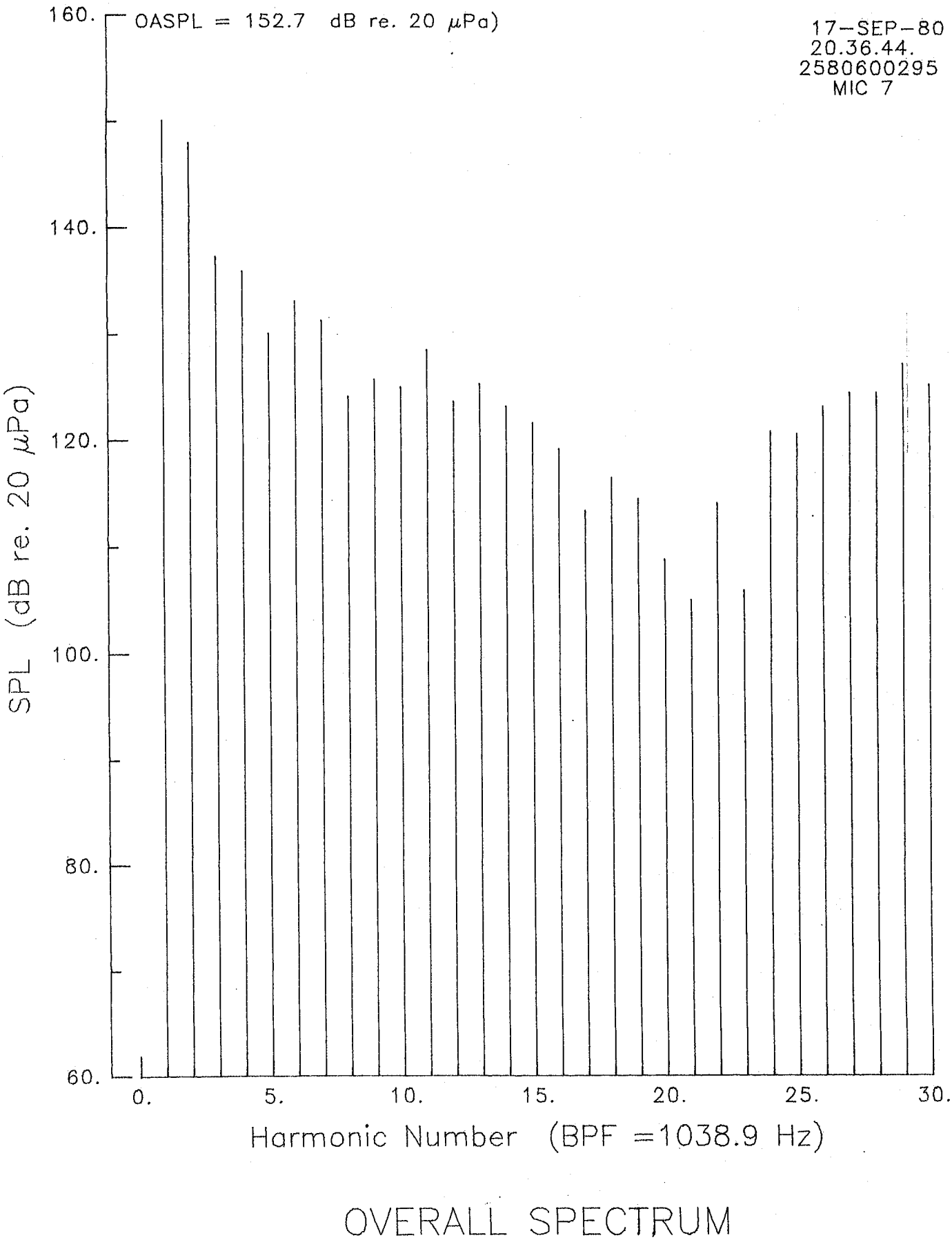

Figure 6.- Concluded.

F. Farassat -- P. Nystrom
JIAFS -- NASA/LaRC -- GWU

SR-2 BLADE

FLIGHT ALTITUDE 9.15 km (30,000 ft)

FLIGHT MACH NUMBER 0.6

MICROPHONE 7

(ADVANCE RATIO VARIED)

Figure 7.- Free-field acoustic pressure signatures and spectra for SR-2 blade - Altitude 9.15 Km (30,000 ft), M=0.6, Microphone 7. Note advance ratio is varied in these calculations.

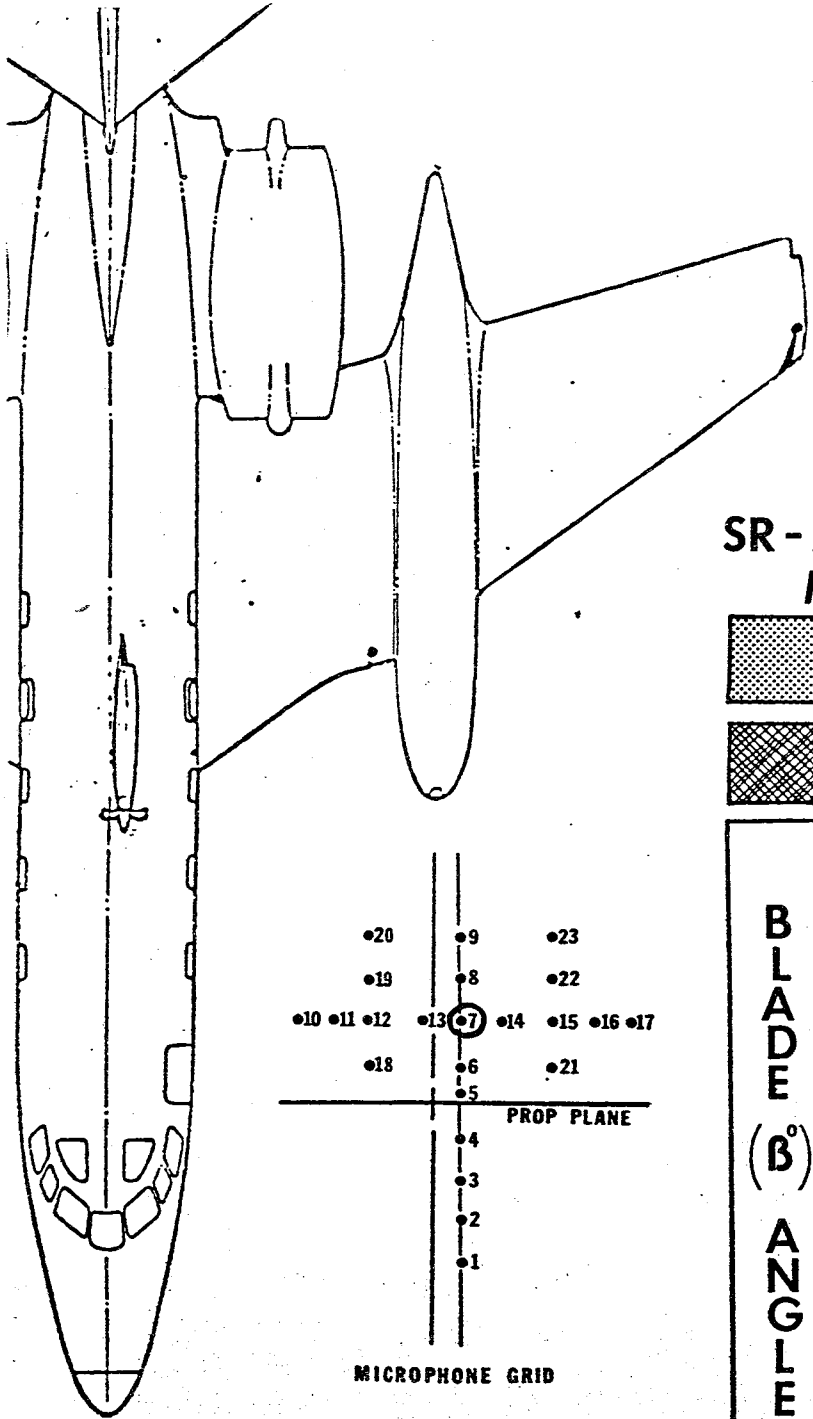

SR-2 TEST MATRIX

EXCEEDS BLEED SYS. POWER CAPACITY

BLADE CRITICAL SPEED

BLADE ANGLE (β°)	ADVANCE RATIO (J)	ALTITUDE (FT) 20,000 — MACH # .50	.60	.65	.70	.75	.80	ALTITUDE (FT) 25,000 — MACH # .50	.60	.65	.70	.75	.80	ALTITUDE (FT) 30,000 — MACH # .50	.60	.65	.70	.75	.80
59.0	4.30																		
	3.50																		
	3.25																		
	3.06																		
	2.90																		
60.0	4.30														X				
	3.50														X				
	3.25														X				
	3.06														X				
	2.95														X				
61.0	4.30																		
	4.07																		
	3.50																		
	3.25																		

Figure 7.- Continued.

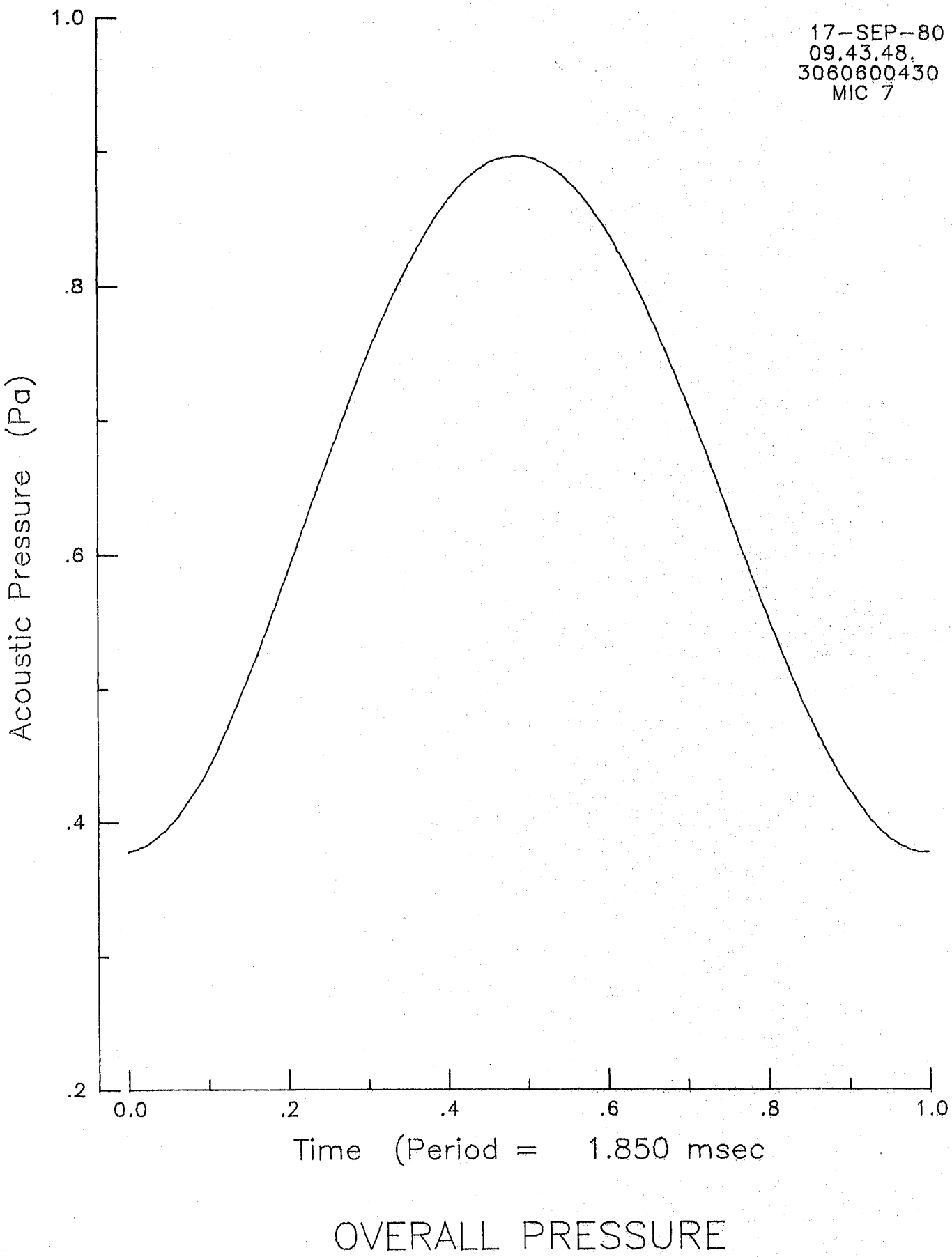

Figure 7.- Continued.

F. Farassat -- P. Nystrom
JIAFS -- NASA/LaRC -- GWU

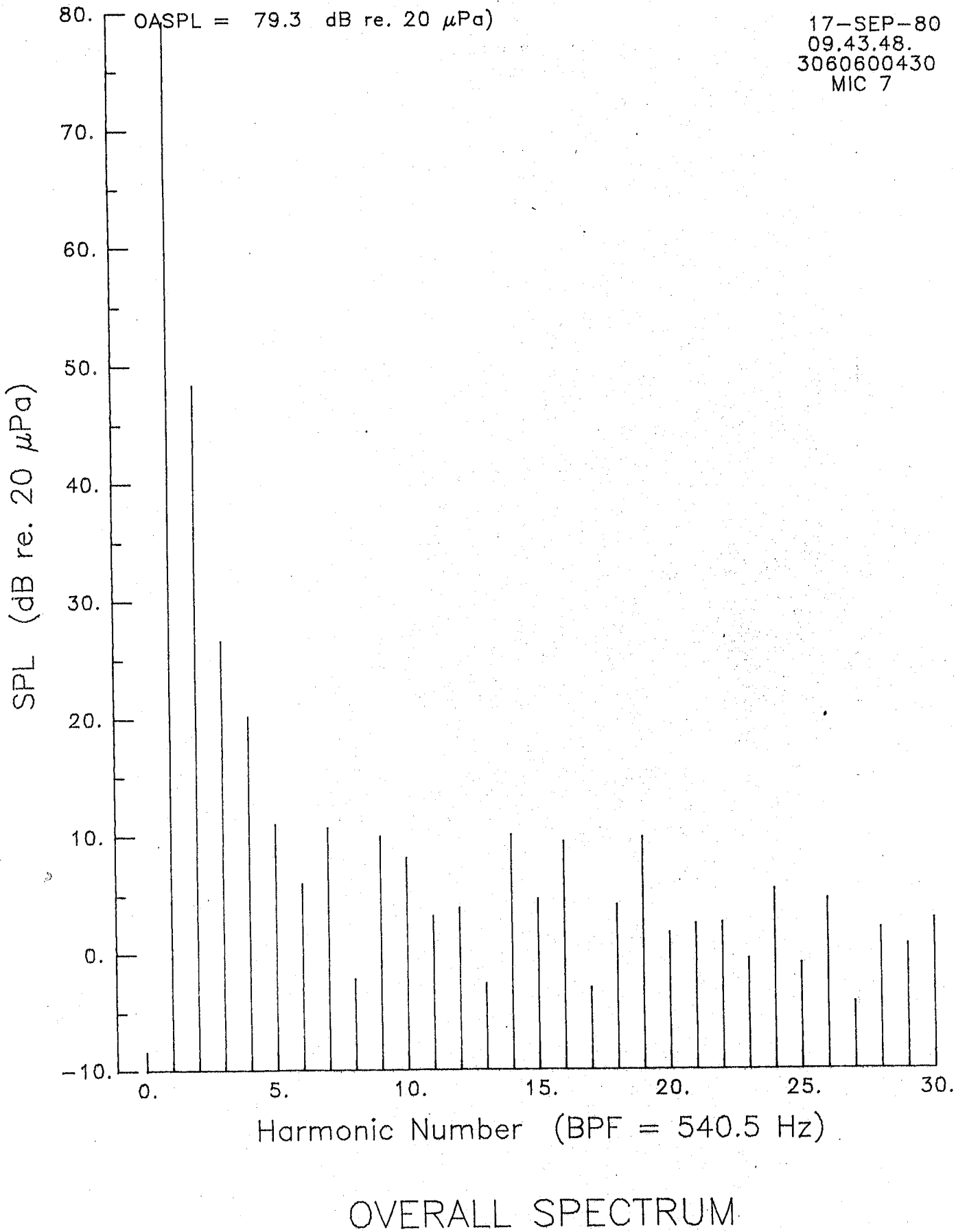

Figure 7.- Continued.

F. Farassat -- P. Nystrom
JIAFS -- NASA/LaRC -- GWU

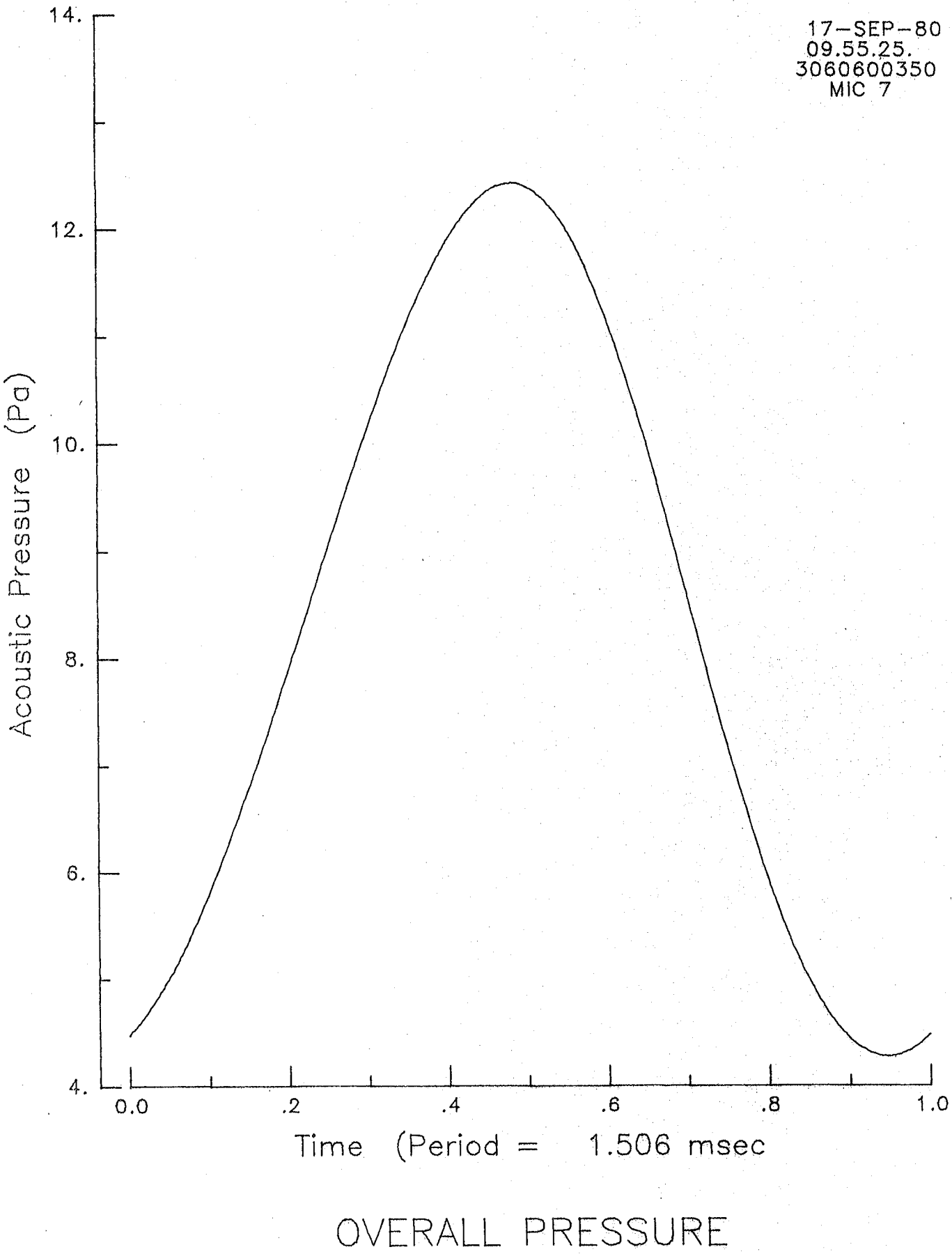

Figure 7.- Continued.

F. Farassat -- P. Nystrom
JIAFS -- NASA/LaRC -- GWU

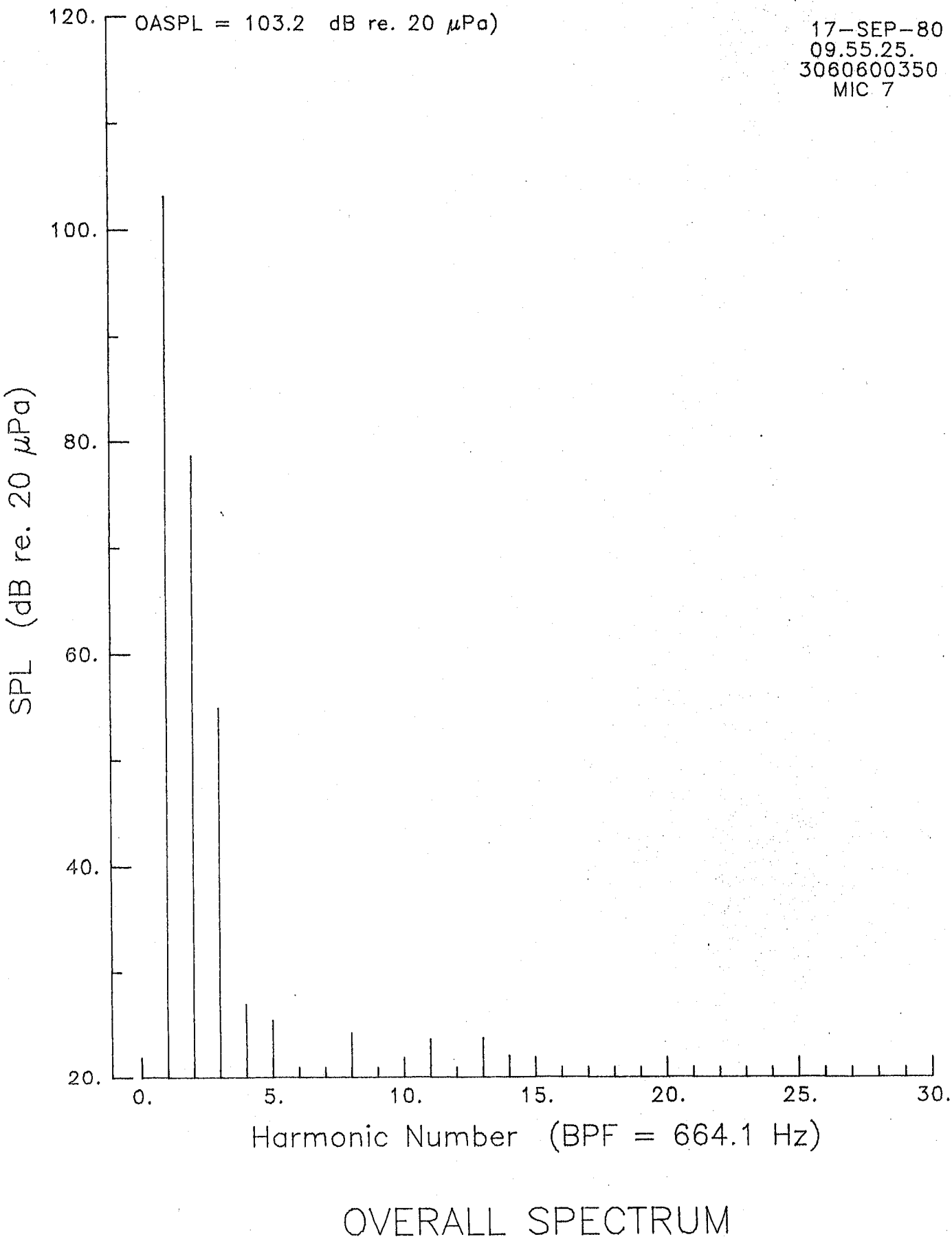

Figure 7.- Continued.

F. Farassat -- P. Nystrom
JIAFS -- NASA/LaRC -- GWU

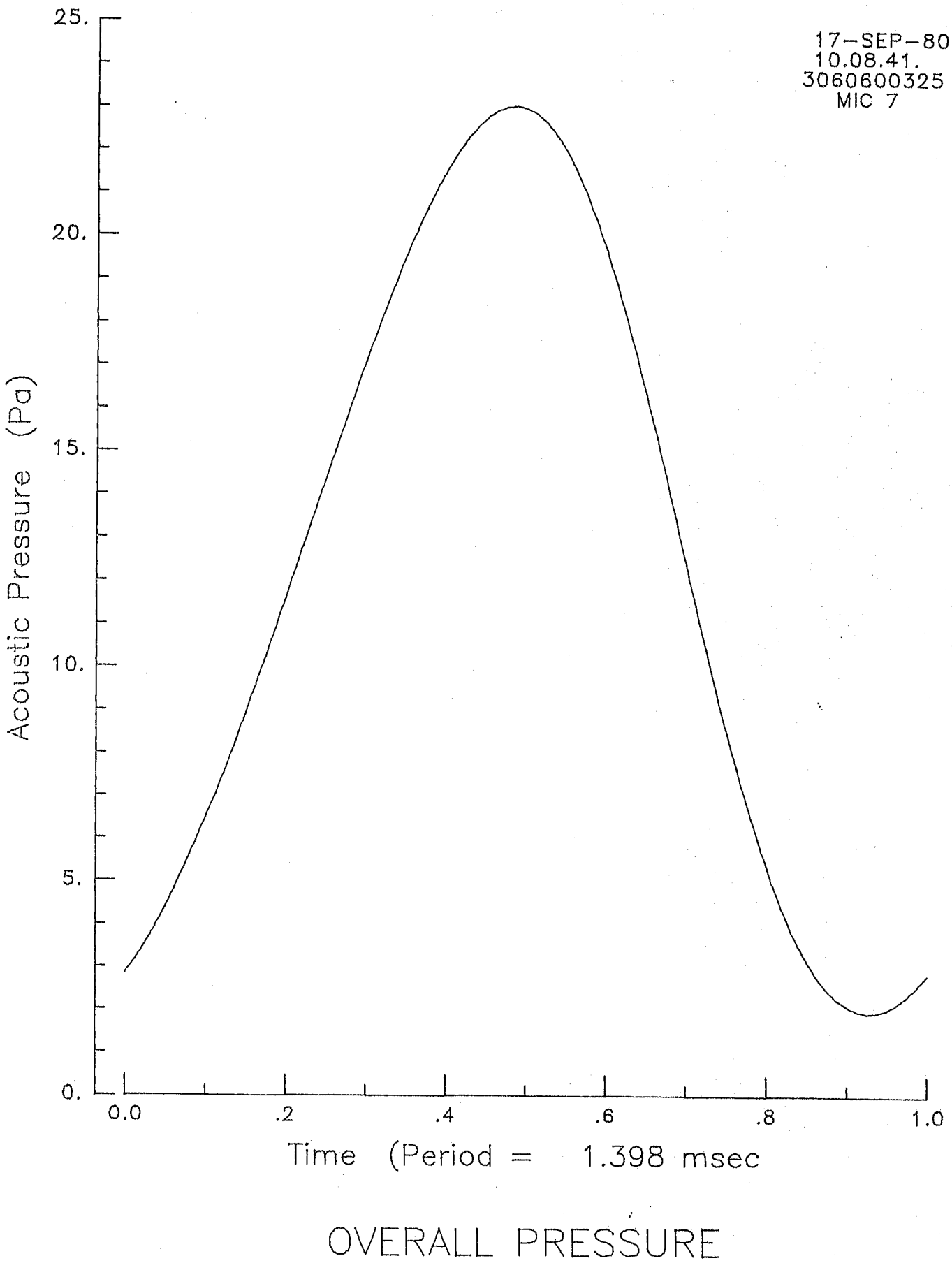

Figure 7.- Continued.

F. Farassat -- P. Nystrom
JIAFS -- NASA/LaRC -- GWU

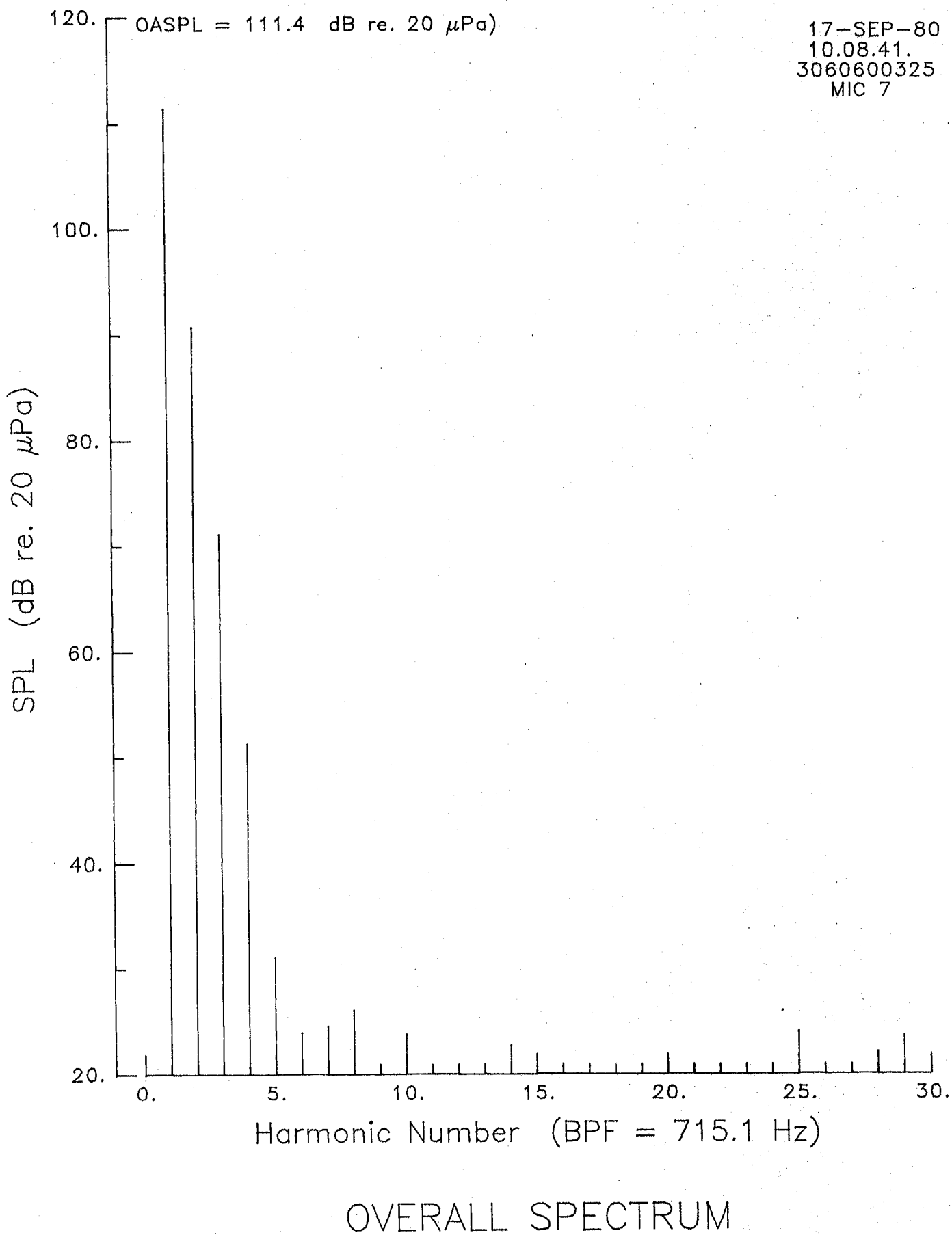

Figure 7.- Continued.

F. Farassat -- P. Nystrom
JIAFS -- NASA/LaRC -- GWU

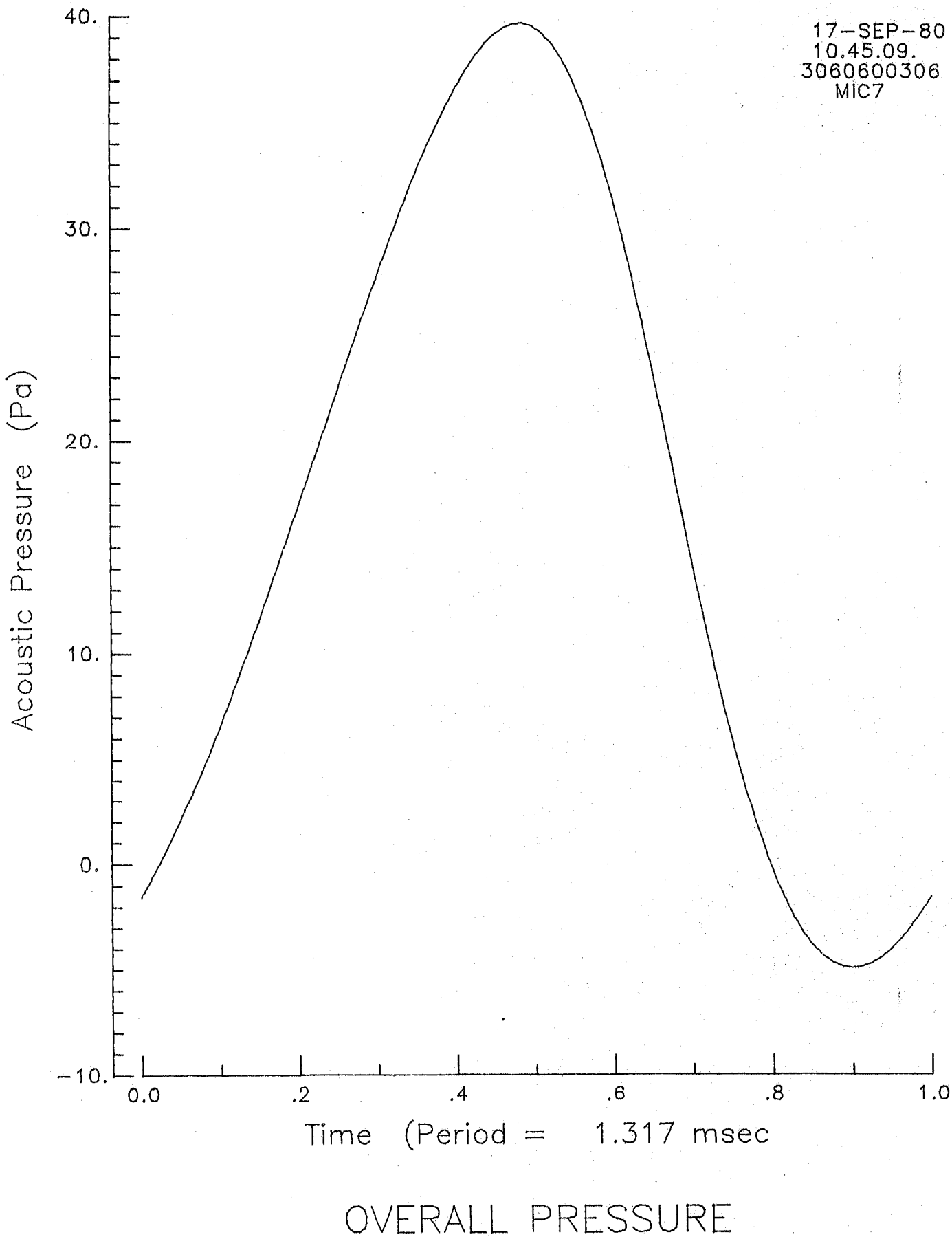

Figure 7.- Continued.

F. Farassat -- P. Nystrom
JIAFS -- NASA/LaRC -- GWU

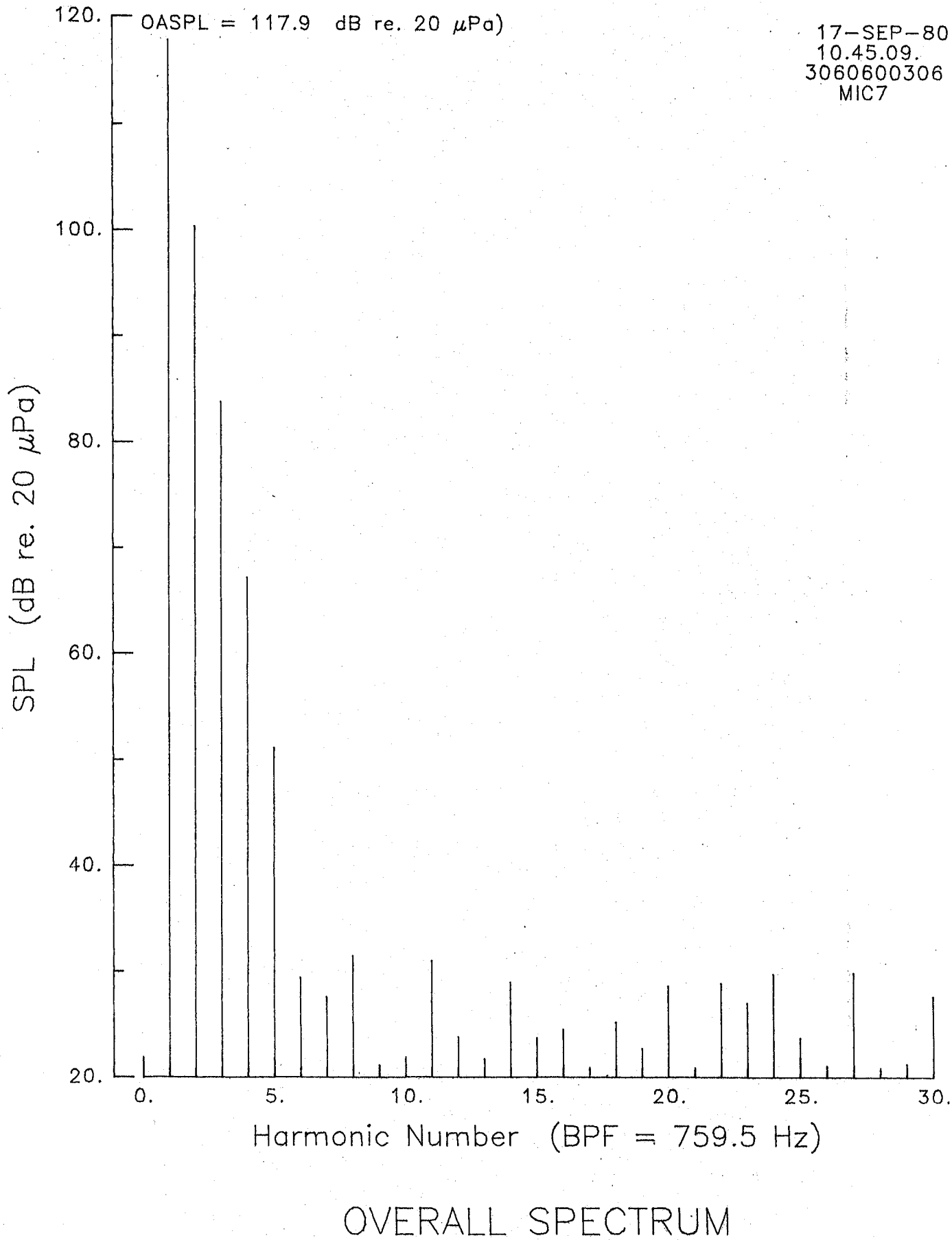

Figure 7.- Continued.

F. Farassat -- P. Nystrom
JIAFS -- NASA/LaRC -- GWU

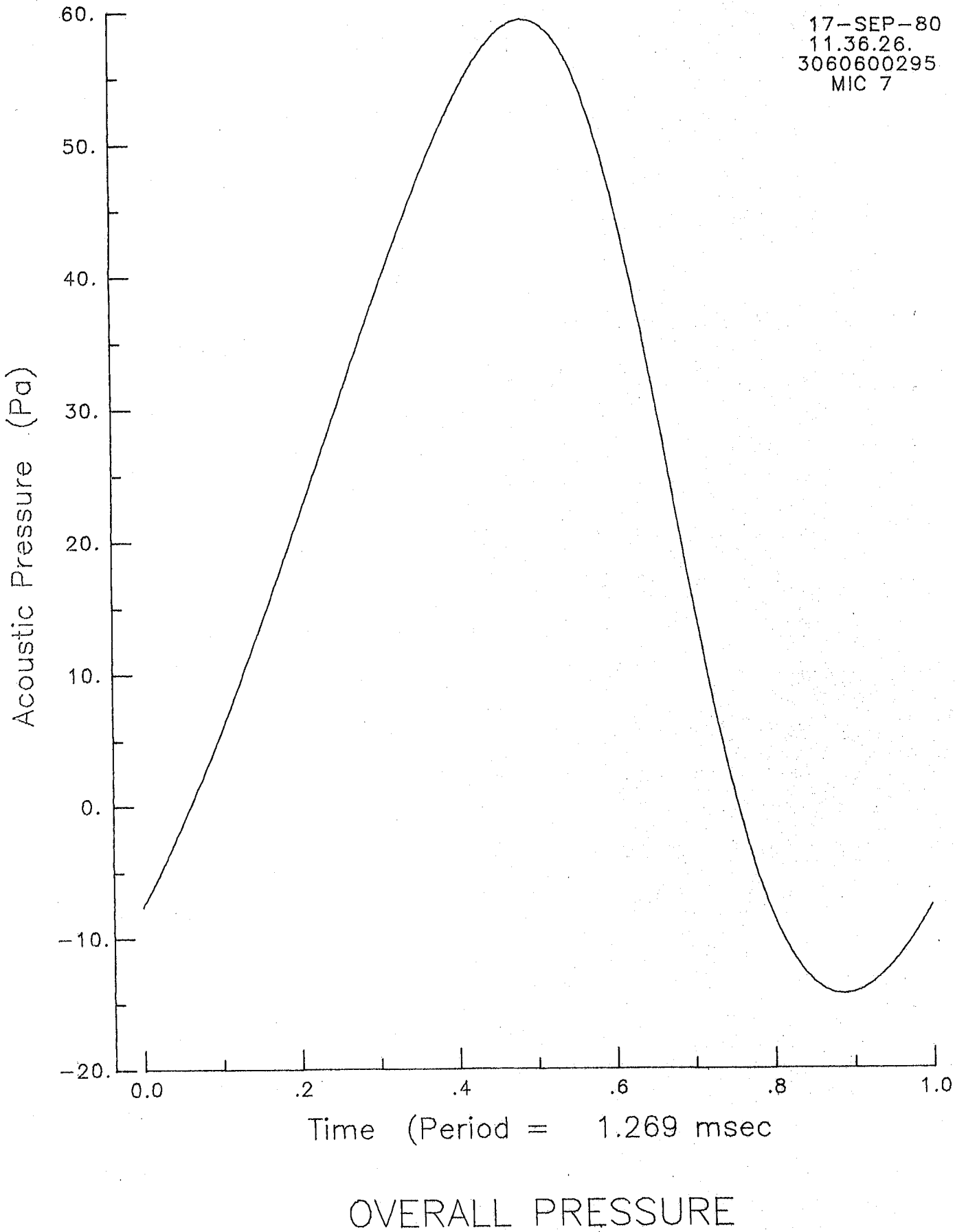

Figure 7.- Continued.

F. Farassat -- P. Nystrom
JIAFS -- NASA/LaRC -- GWU

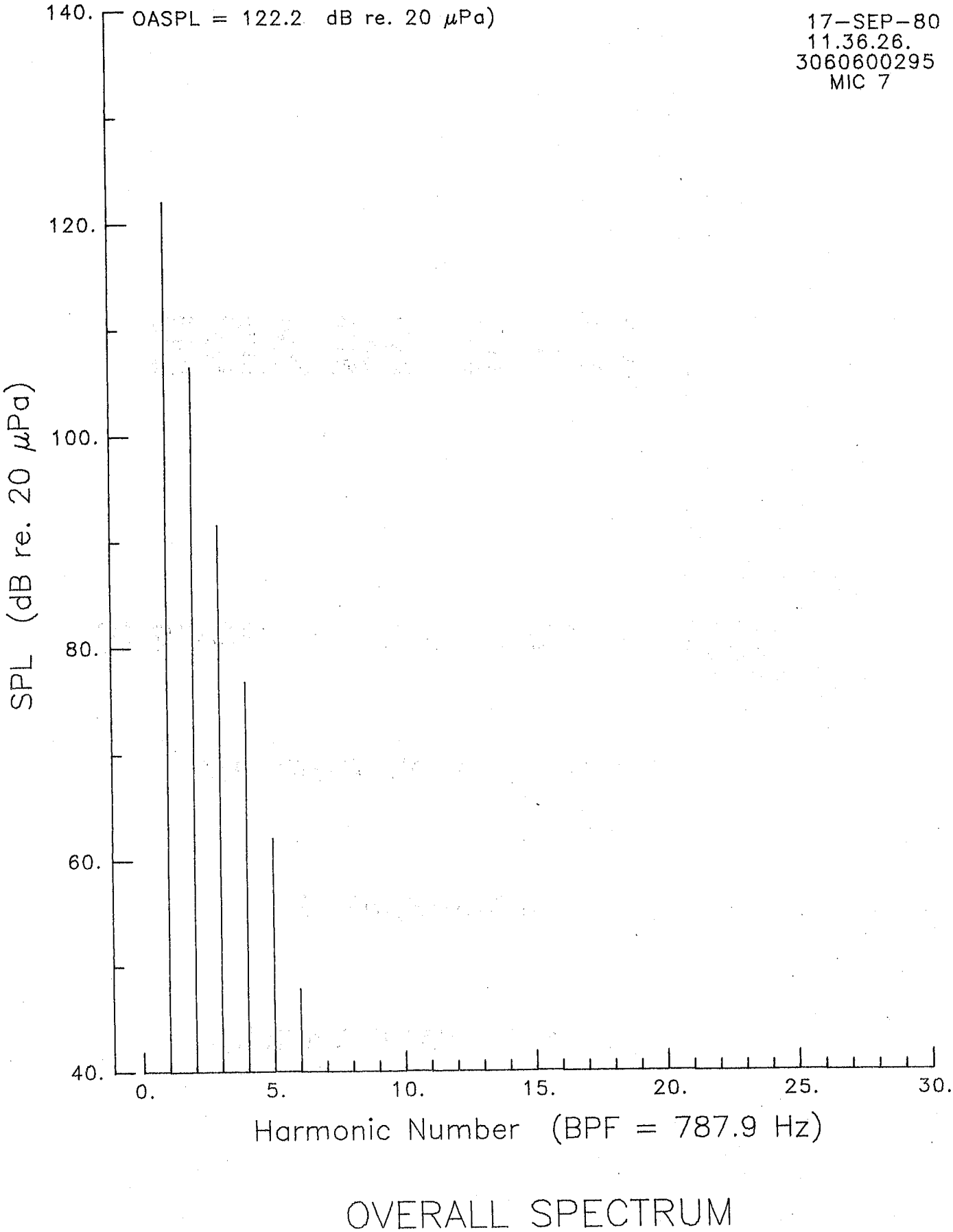

Figure 7.- Concluded.

F. Farassat -- P. Nystrom
JIAFS -- NASA/LaRC -- GWU

SR-2 BLADE

FLIGHT ALTITUDE 9.15 km (30,000 ft)

FLIGHT MACH NUMBER 0.7

MICROPHONE 7

(ADVANCE RATIO VARIED)

Figure 8.- Free-field acoustic pressure signatures and spectra for SR-2 blade - Altitude 9.15 Km (30,000 ft), M=0.7, Microphone 7. Note advance ratio is varied in these calculations.

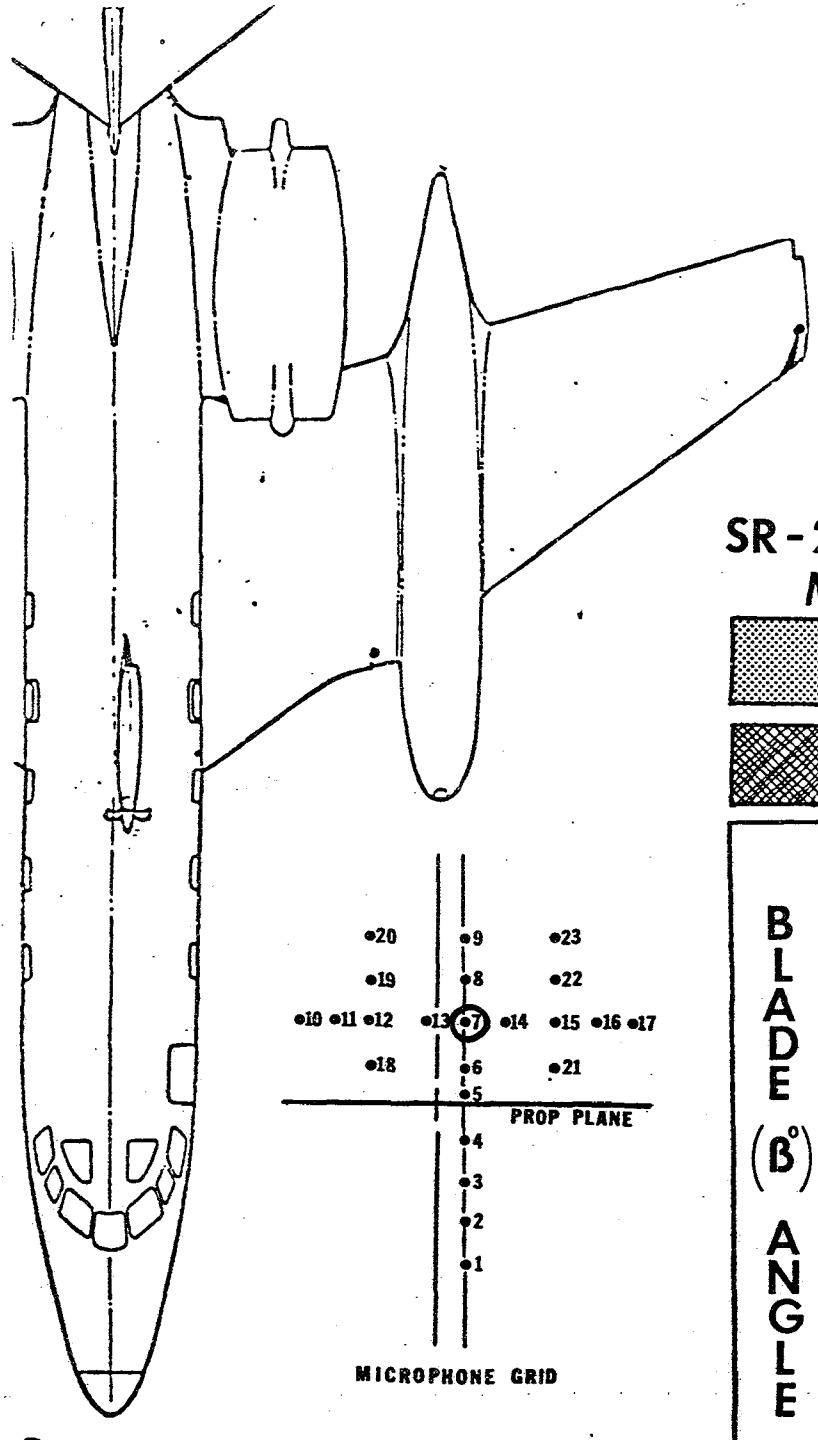

Figure 8.- Continued.

SR-2 TEST MATRIX

EXCEEDS BLEED SYS. POWER CAPACITY

BLADE CRITICAL SPEED

BLADE (β°) ANGLE	ADVANCE RATIO (J)	ALTITUDE (FT) 20,000						25,000						30,000					
		MACH # .50	.60	.65	.70	.75	.80	.50	.60	.65	.70	.75	80	.50	.60	65	.70	.75	.80
59.0	4.30																		
	3.50																		
	3.25																		
	3.06																		
	2.90																		
60.0	4.30																X		
	3.50																X		
	3.25																X		
	3.06																X		
	2.95																X		
61.0	4.30																		
	4.07																		
	3.50																		
	3.25																		

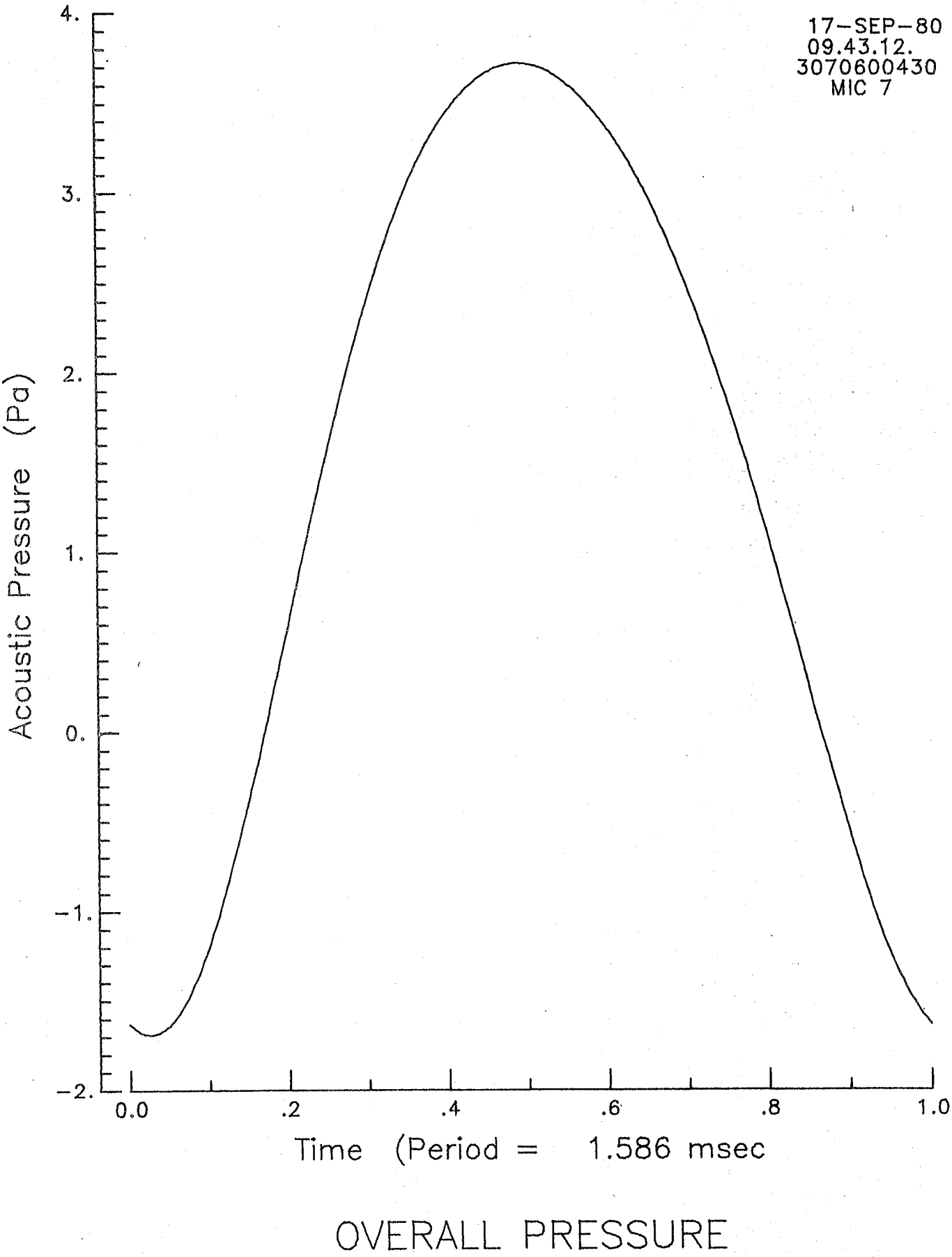

Figure 8.- Continued.

F. Farassat -- P. Nystrom
JIAFS -- NASA/LaRC -- GWU

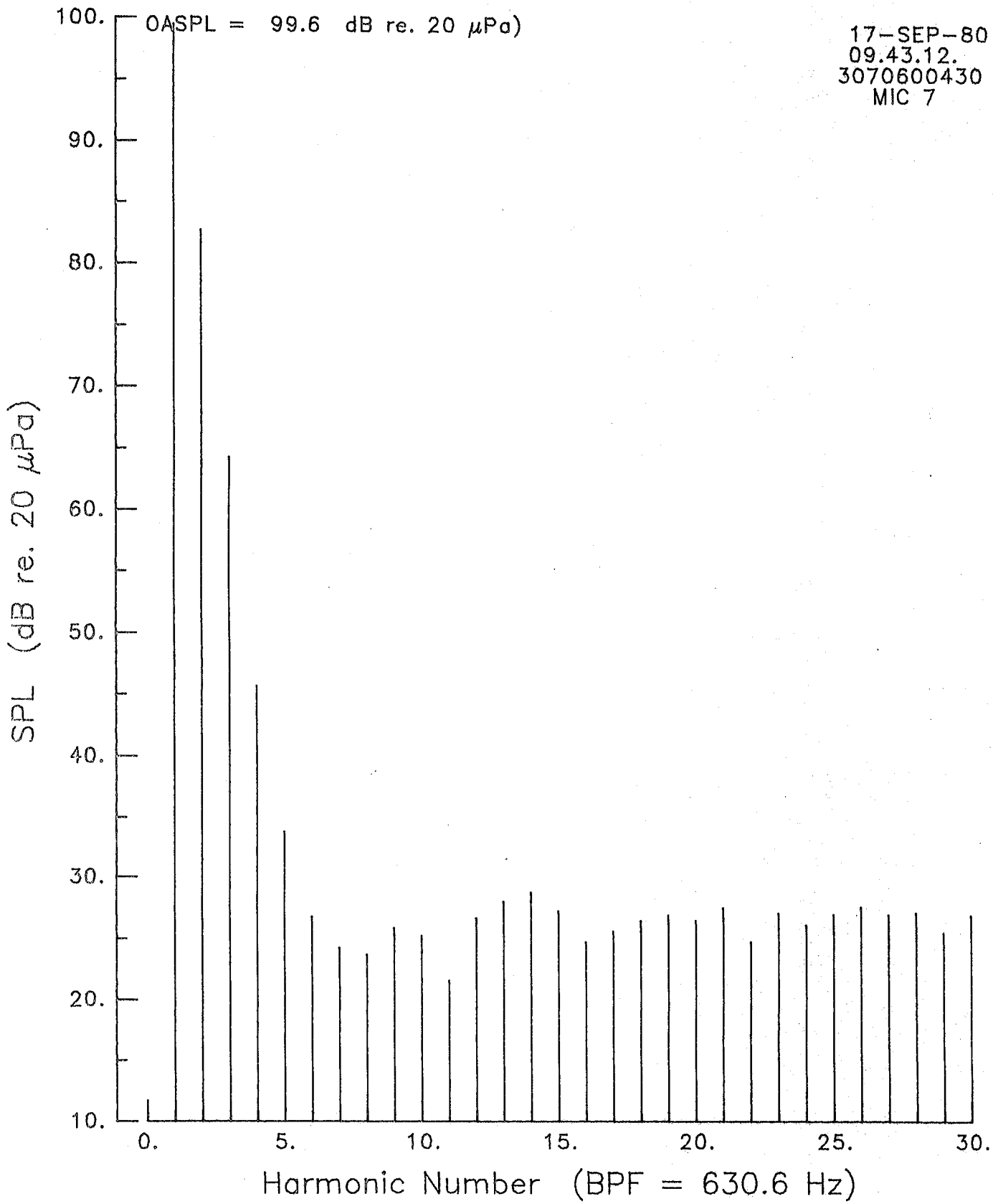

OVERALL SPECTRUM

Figure 8.- Continued.

F. Farassat -- P. Nystrom
JIAFS -- NASA/LaRC -- GWU

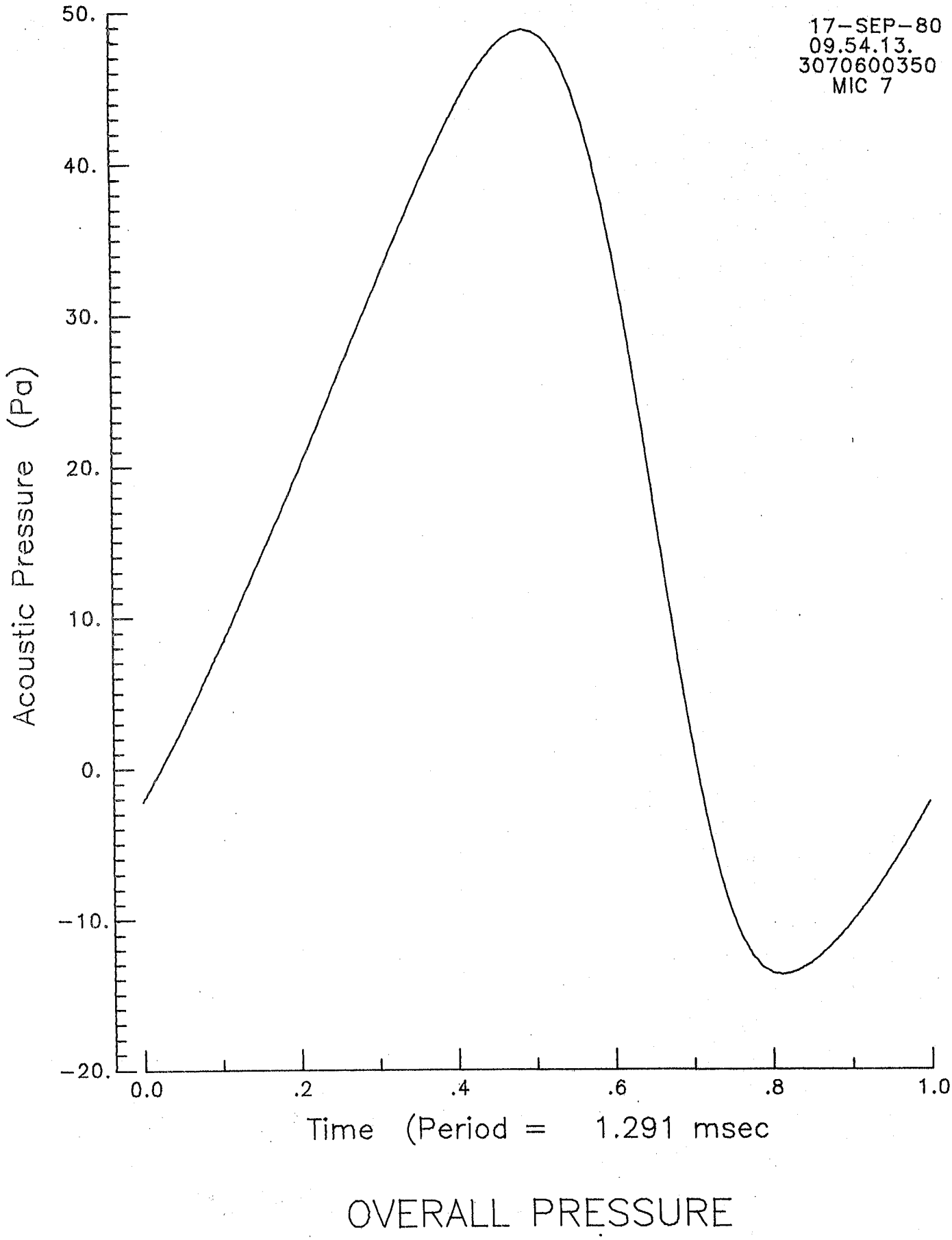

Figure 8.- Continued.

F. Farassat -- P. Nystrom
JIAFS -- NASA/LaRC -- GWU

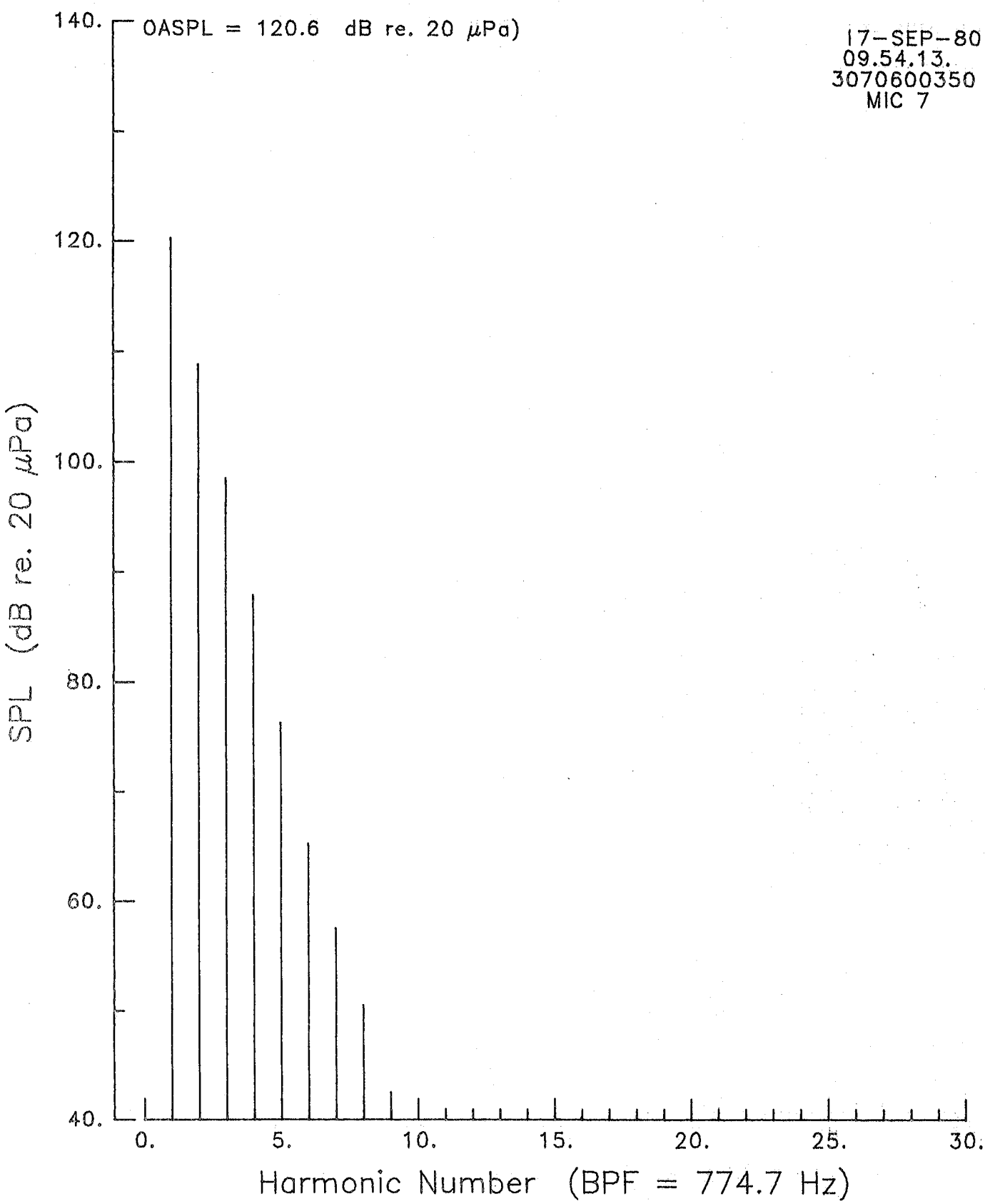

OVERALL SPECTRUM

Figure 8.- Continued.

F. Farassat -- P. Nystrom
JIAFS -- NASA/LaRC -- GWU

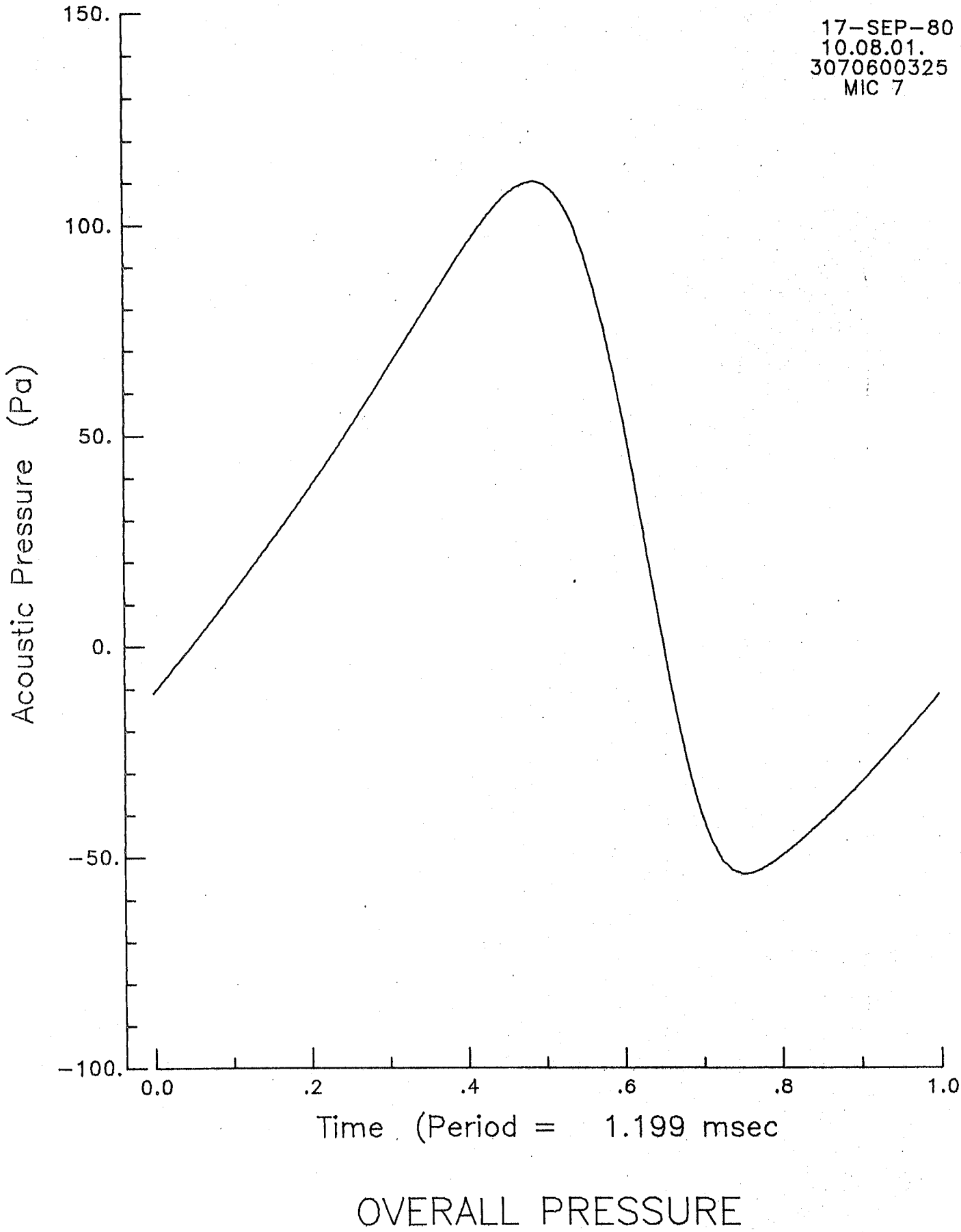

Figure 8.- Continued.

F. Farassat -- P. Nystrom
JIAFS -- NASA/LaRC -- GWU

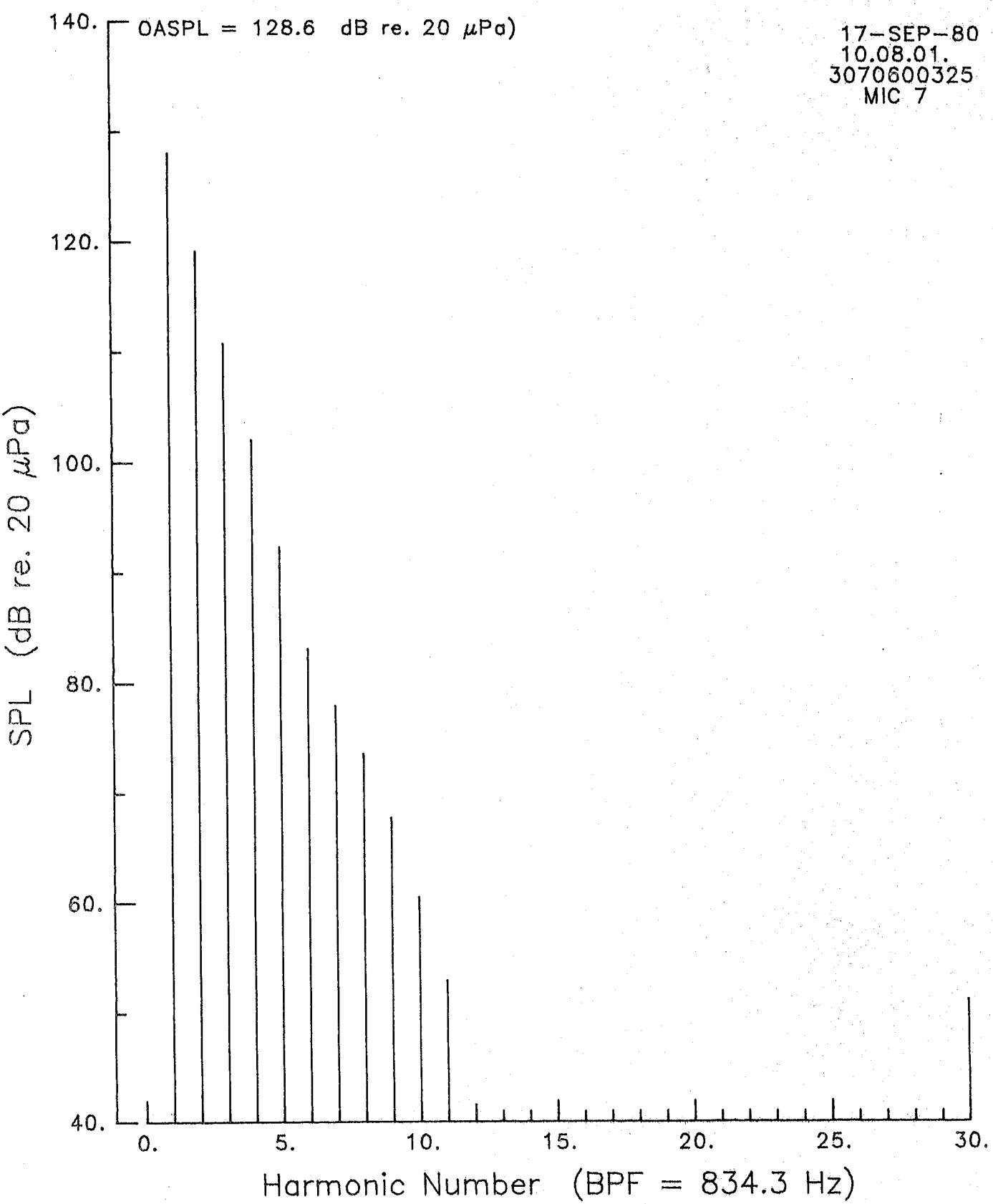

OVERALL SPECTRUM

Figure 8.- Continued.

F. Farassat -- P. Nystrom
JIAFS -- NASA/LaRC -- GWU

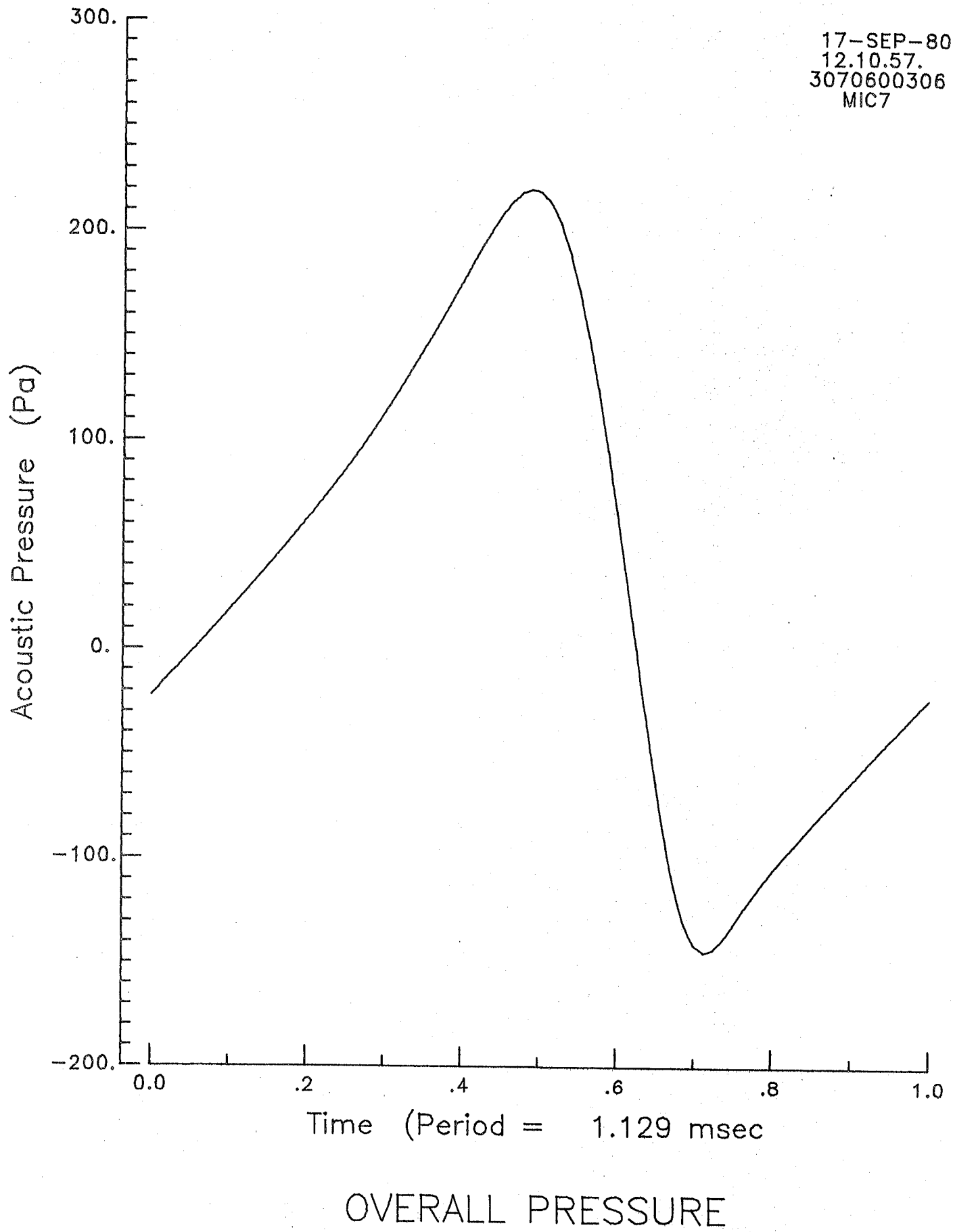

Figure 8.- Continued.

F. Farassat -- P. Nystrom
JIAFS -- NASA/LaRC -- GWU

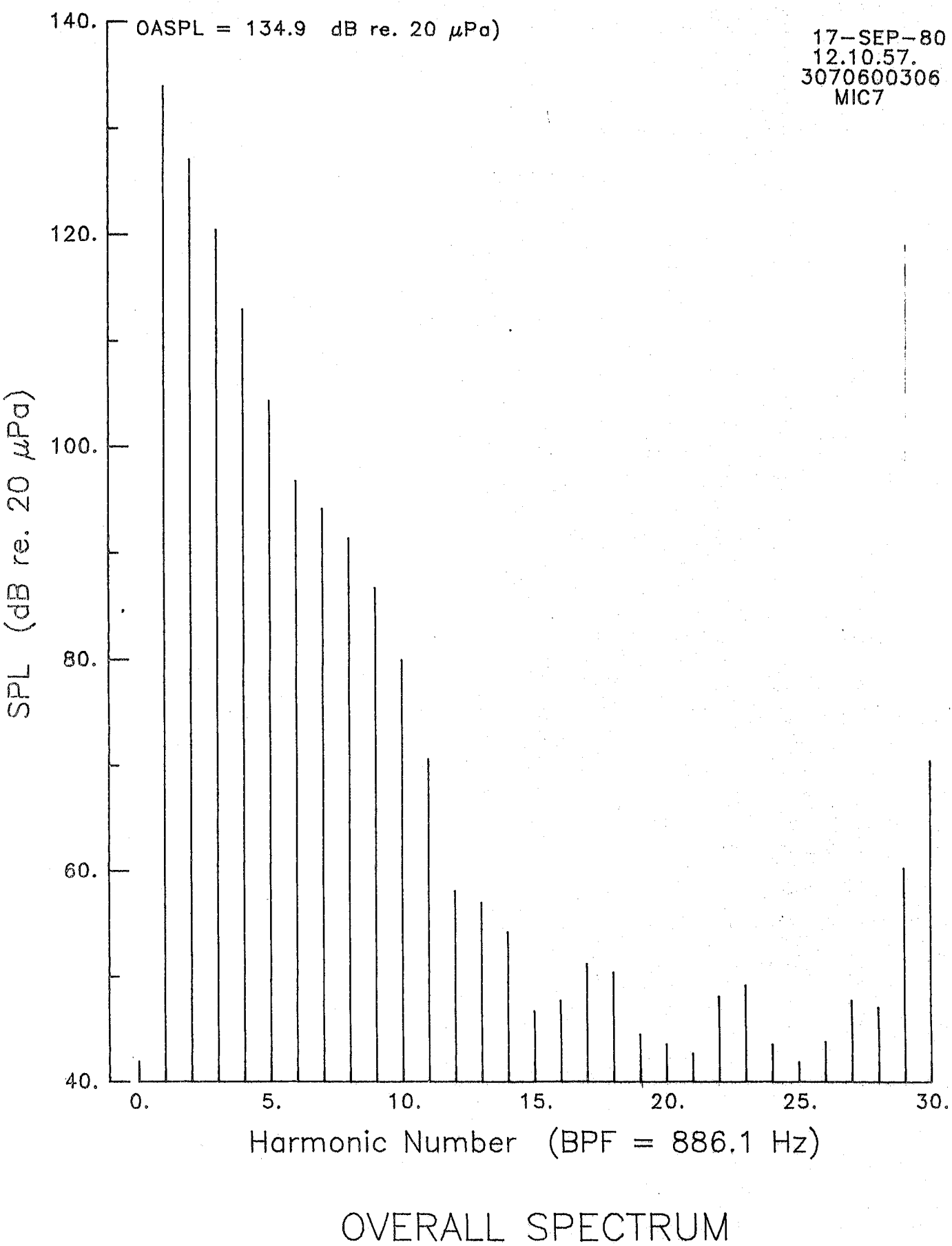

Figure 8.- Continued.

F. Farassat -- P. Nystrom
JIAFS -- NASA/LaRC -- GWU

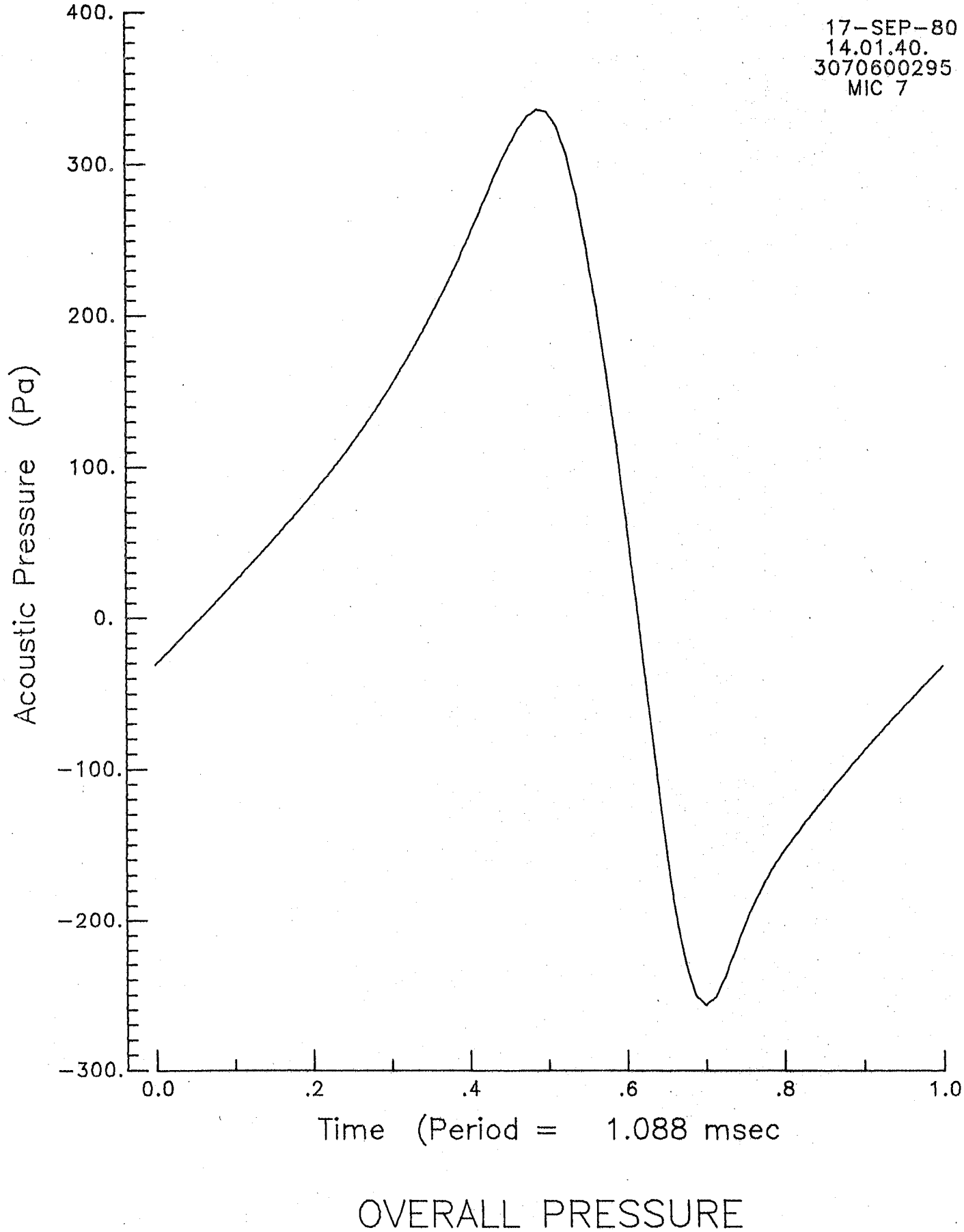

Figure 8.- Continued.

F. Farassat -- P. Nystrom
JIAFS -- NASA/LaRC -- GWU

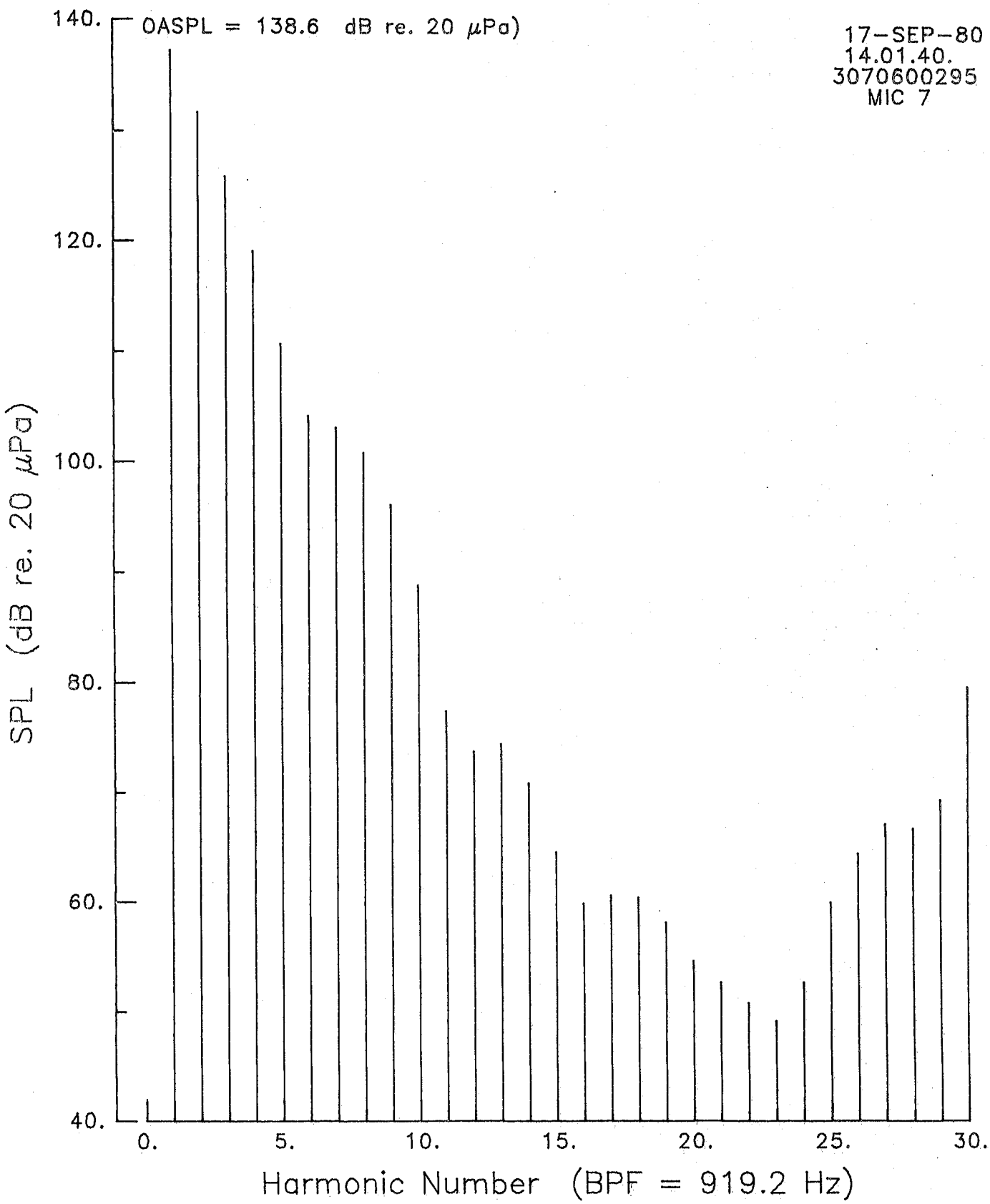

Figure 8.- Concluded.

F. Farassat -- P. Nystrom
JIAFS -- NASA/LaRC -- GWU

SR-2 BLADE

FLIGHT ALTITUDE 9.15 km (30,000 ft)

FLIGHT MACH NUMBER 0.8

MICROPHONES 1, 4, 5, 7, 9, 10, 12

(ADVANCE RATIO VARIED)

Figure 9.- Free-field acoustic pressure signatures and spectra for SR-2 blade - Altitude 9.15 Km (30,000 ft), M=0.8, all microphone positions. Note advance ratio is varied in these calculations for each microphone position. The numbering of this figure is as follows:

Microphone 1 - Figure 9(a)
Microphone 4 - Figure 9(b)
Microphone 5 - Figure 9(c)
Microphone 7 - Figure 9(d)
Microphone 9 - Figure 9(e)
Microphone 10 - Figure 9(f)
Microphone 12 - Figure 9(g)

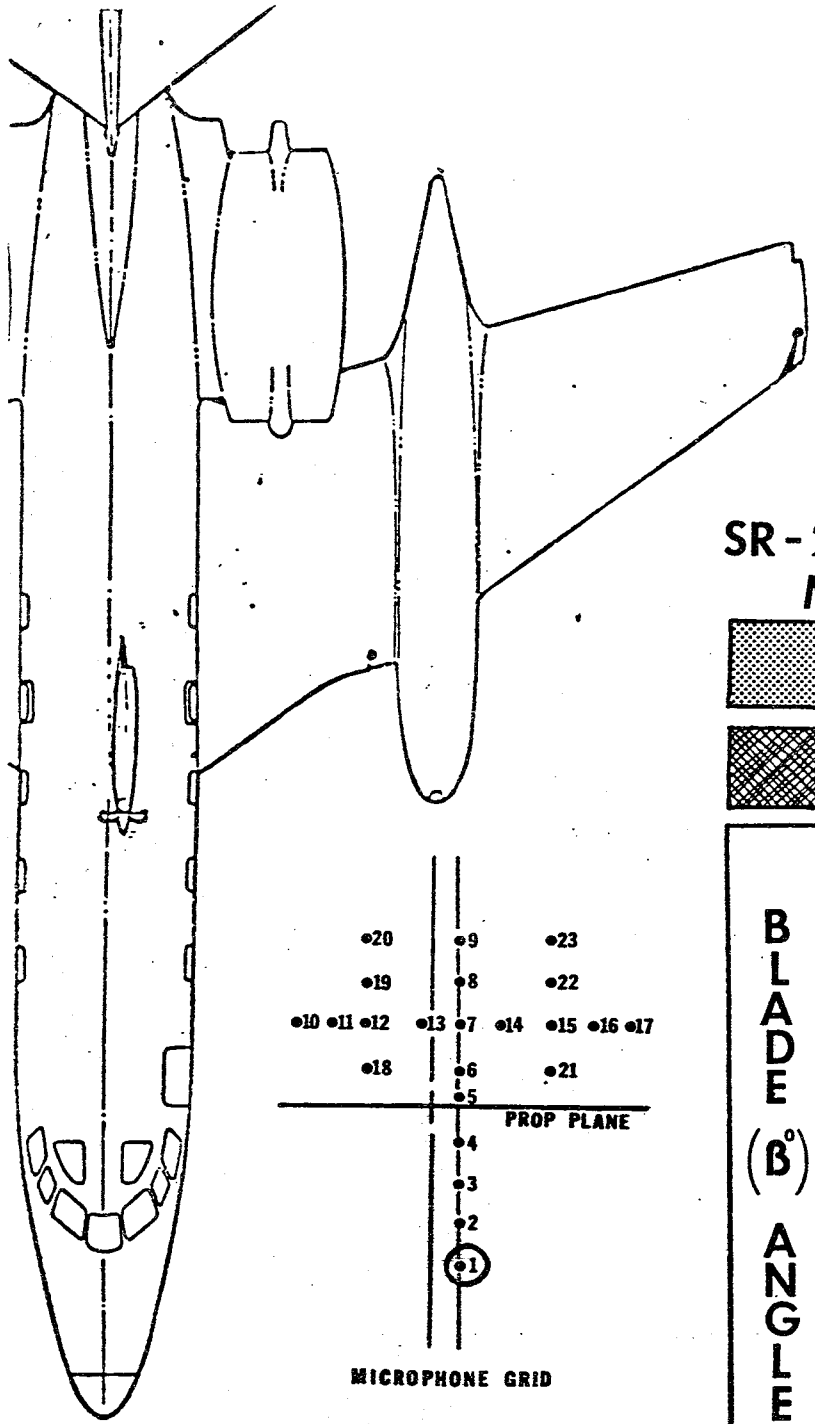

SR-2 TEST MATRIX

EXCEEDS BLEED SYS. POWER CAPACITY

BLADE CRITICAL SPEED

BLADE ANGLE (β°)	ADVANCE RATIO (J)	ALTITUDE (FT) 20,000 / 25,000 / 30,000 — MACH #	.50	.60	.65	.70	.75	.80	.50	.60	.65	.70	.75	.80	.50	.60	.65	.70	.75	.80
59.0	4.30																			
	3.50																			
	3.25																			
	3.06																			
	2.90																			
60.0	4.30																			X
	3.50																			X
	3.25																			X
	3.06																			X
	2.95																			X
61.0	4.30																			
	4.07																			
	3.50																			
	3.25																			

Figure 9(a).-Continued.

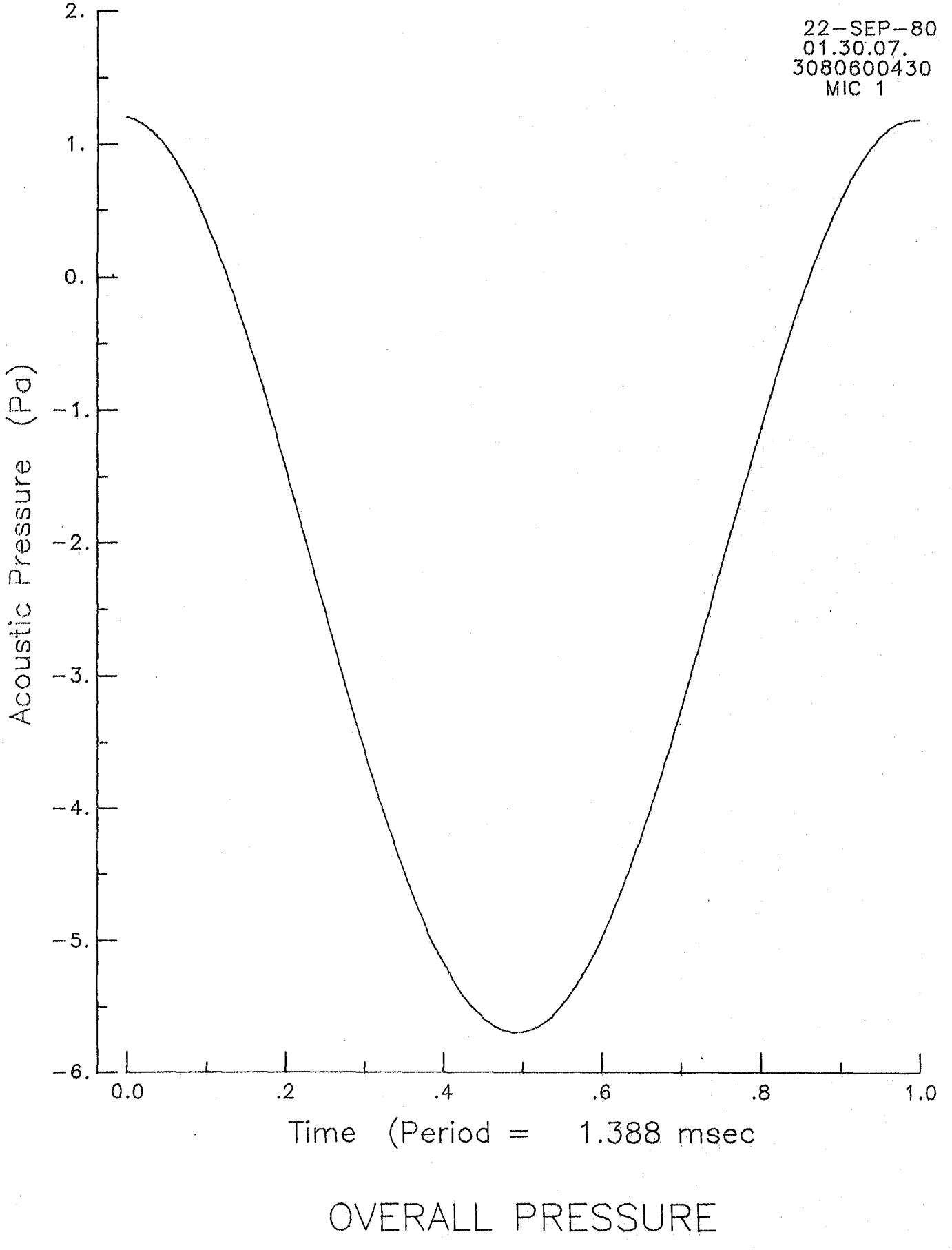

Figure 9(a).- Continued.

F. Farassat -- P. Nystrom
JIAFS -- NASA/LaRC -- GWU

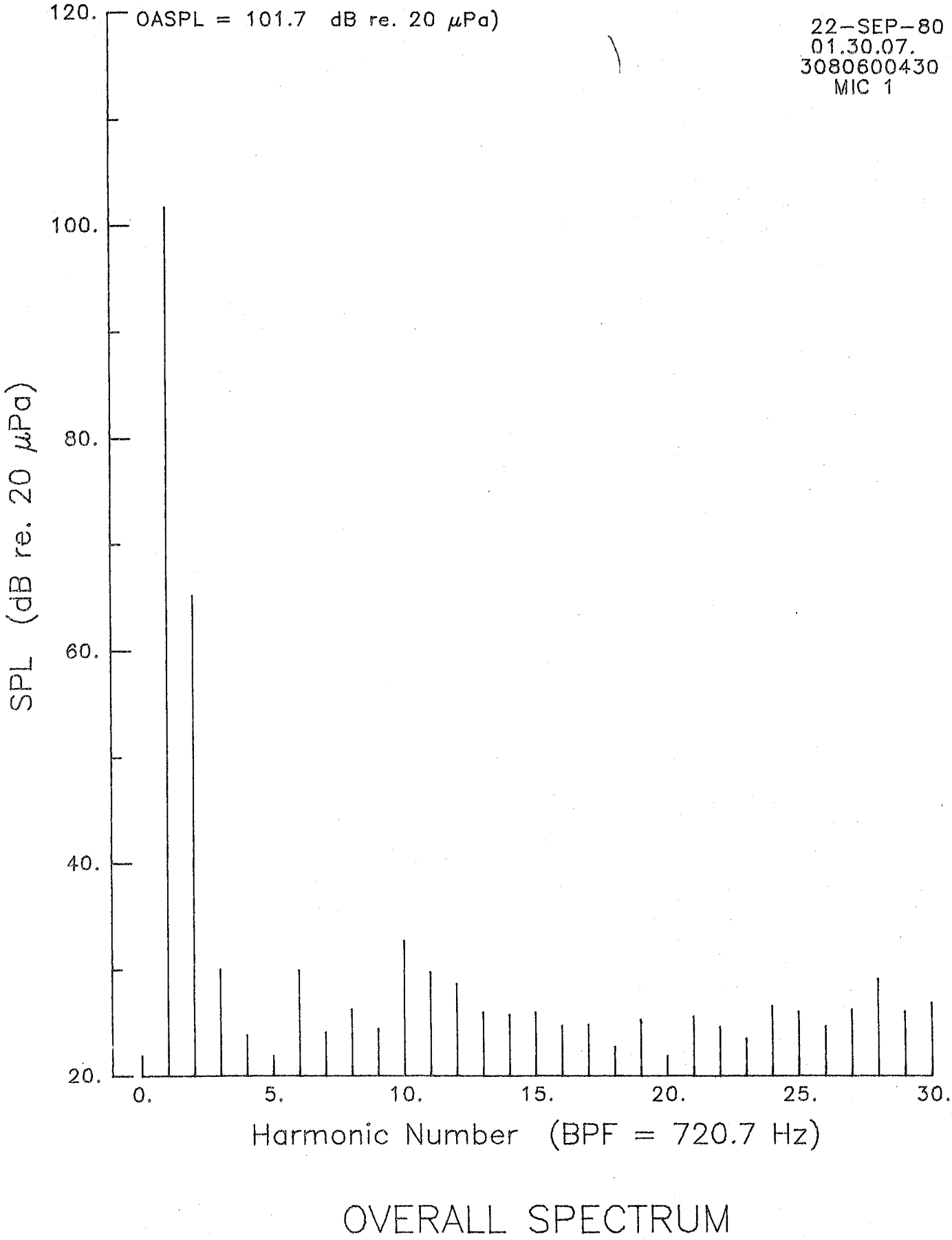

Figure 9(a).- Continued.

F. Farassat -- P. Nystrom
JIAFS -- NASA/LaRC -- GWU

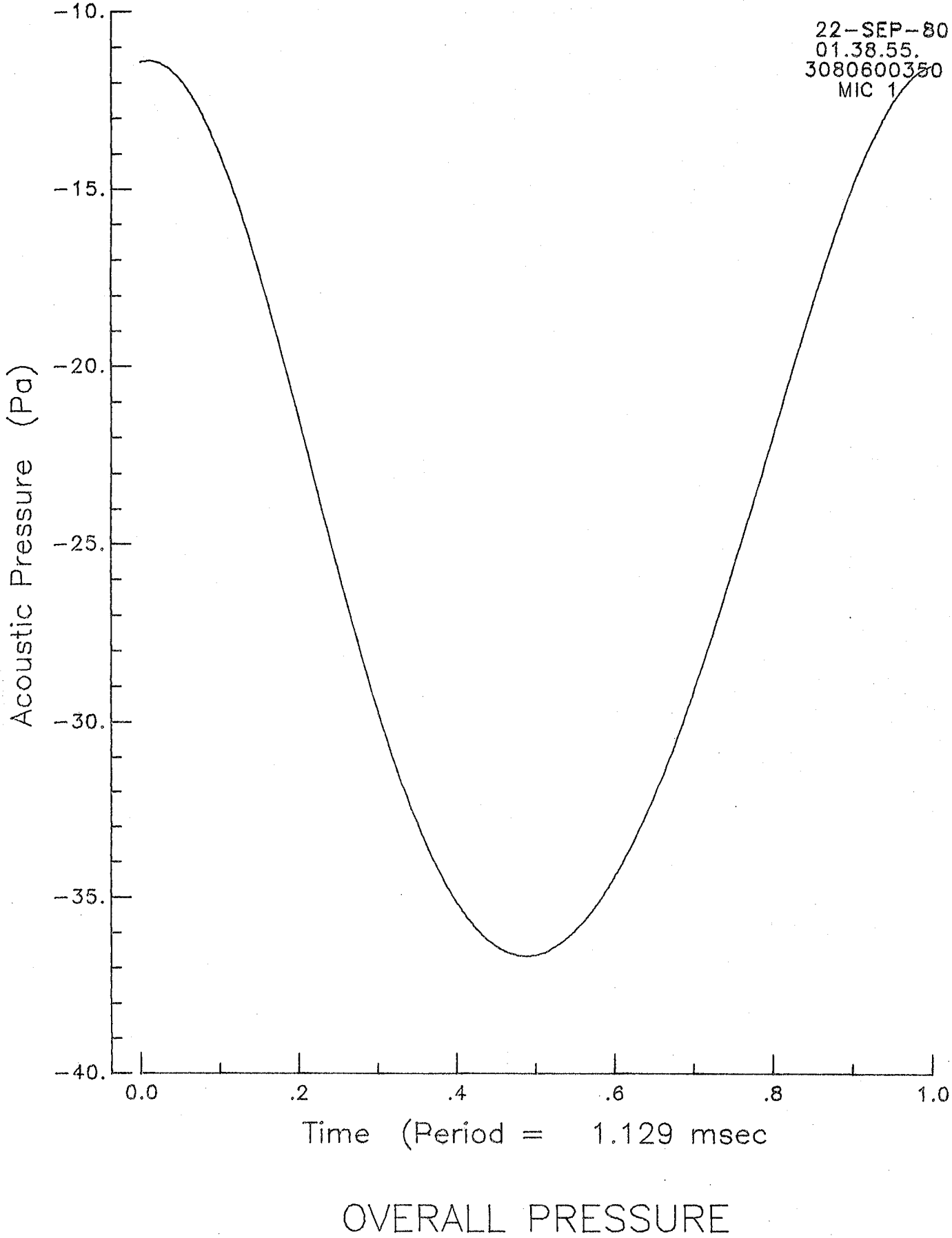

Figure 9(a).- Continued.

F. Farassat -- P. Nystrom
JIAFS -- NASA/LaRC -- GWU

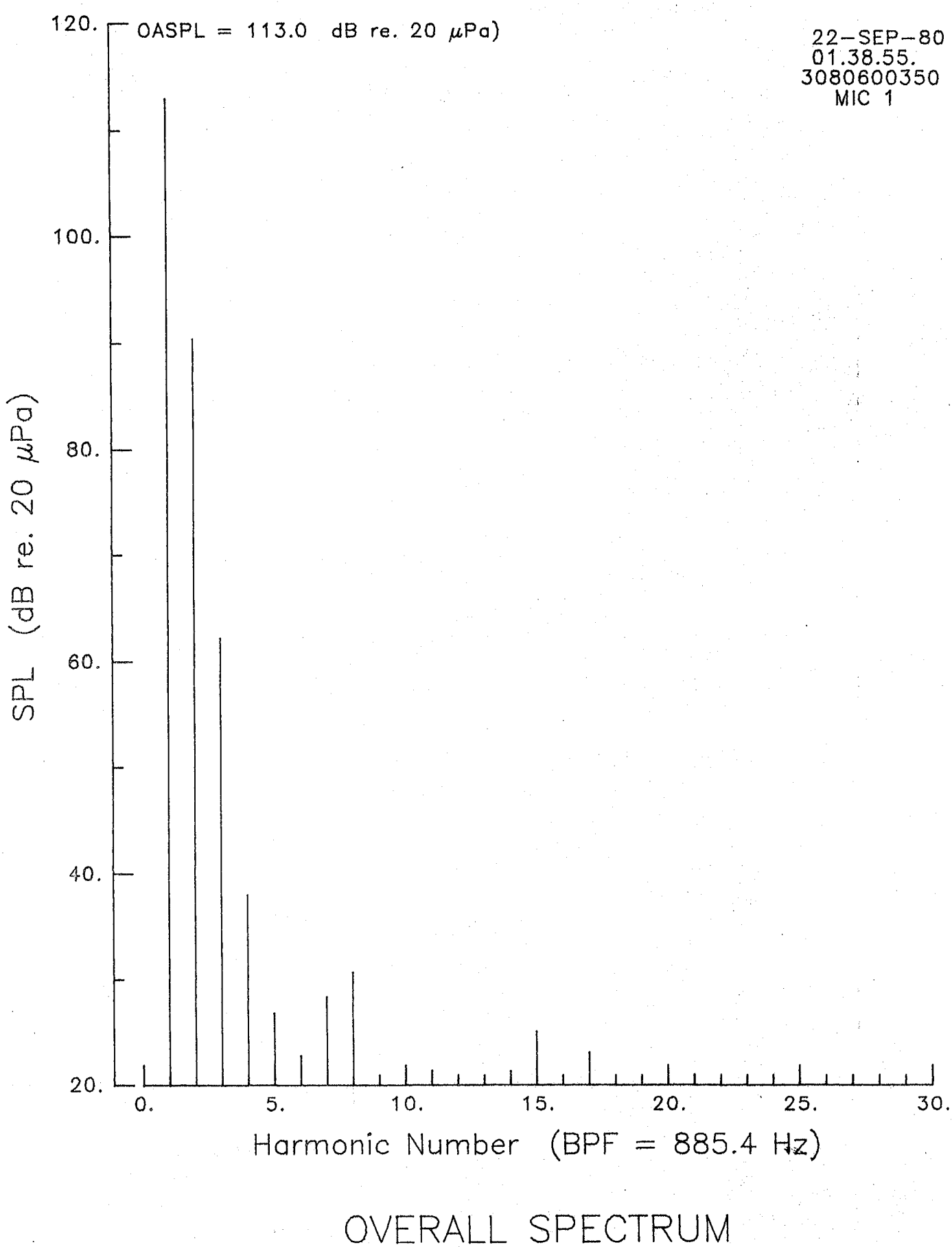

Figure 9(a).- Continued.

F. Farassat -- P. Nystrom
JIAFS -- NASA/LaRC -- GWU

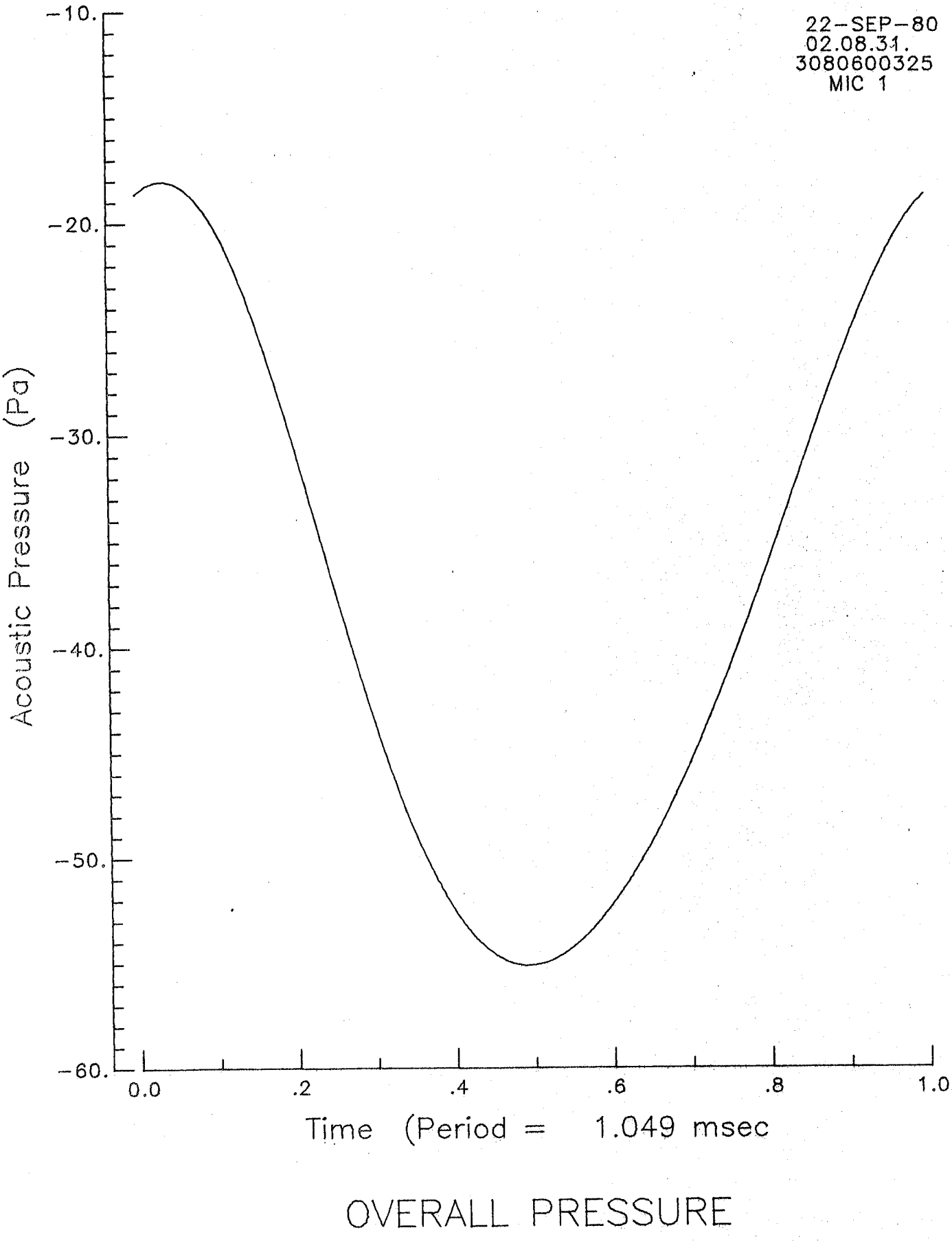

Figure 9(a).- Continued.

F. Farassat -- P. Nystrom
JIAFS -- NASA/LaRC -- GWU

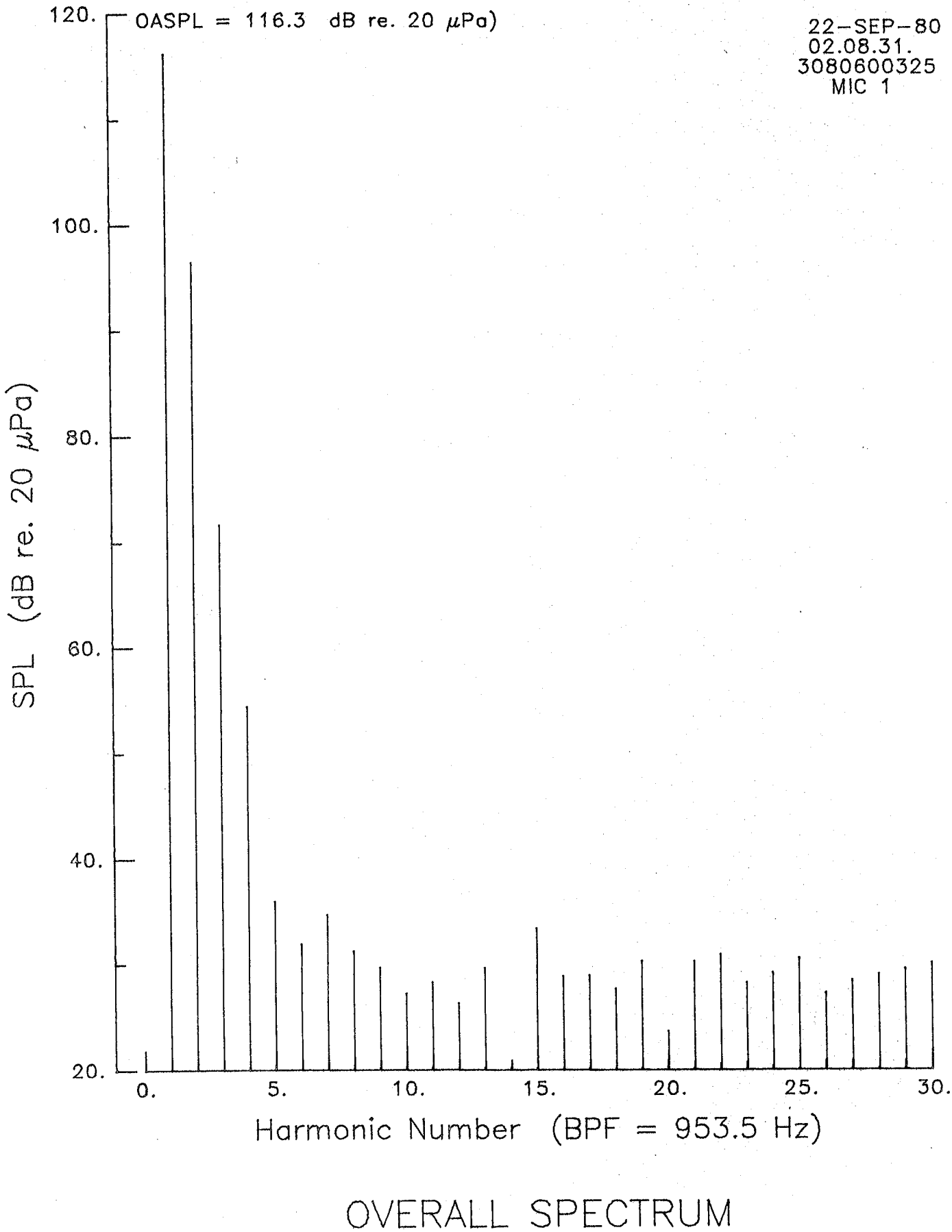

Figure 9(a).- Continued.

F. Farassat -- P. Nystrom
JIAFS -- NASA/LaRC -- GWU

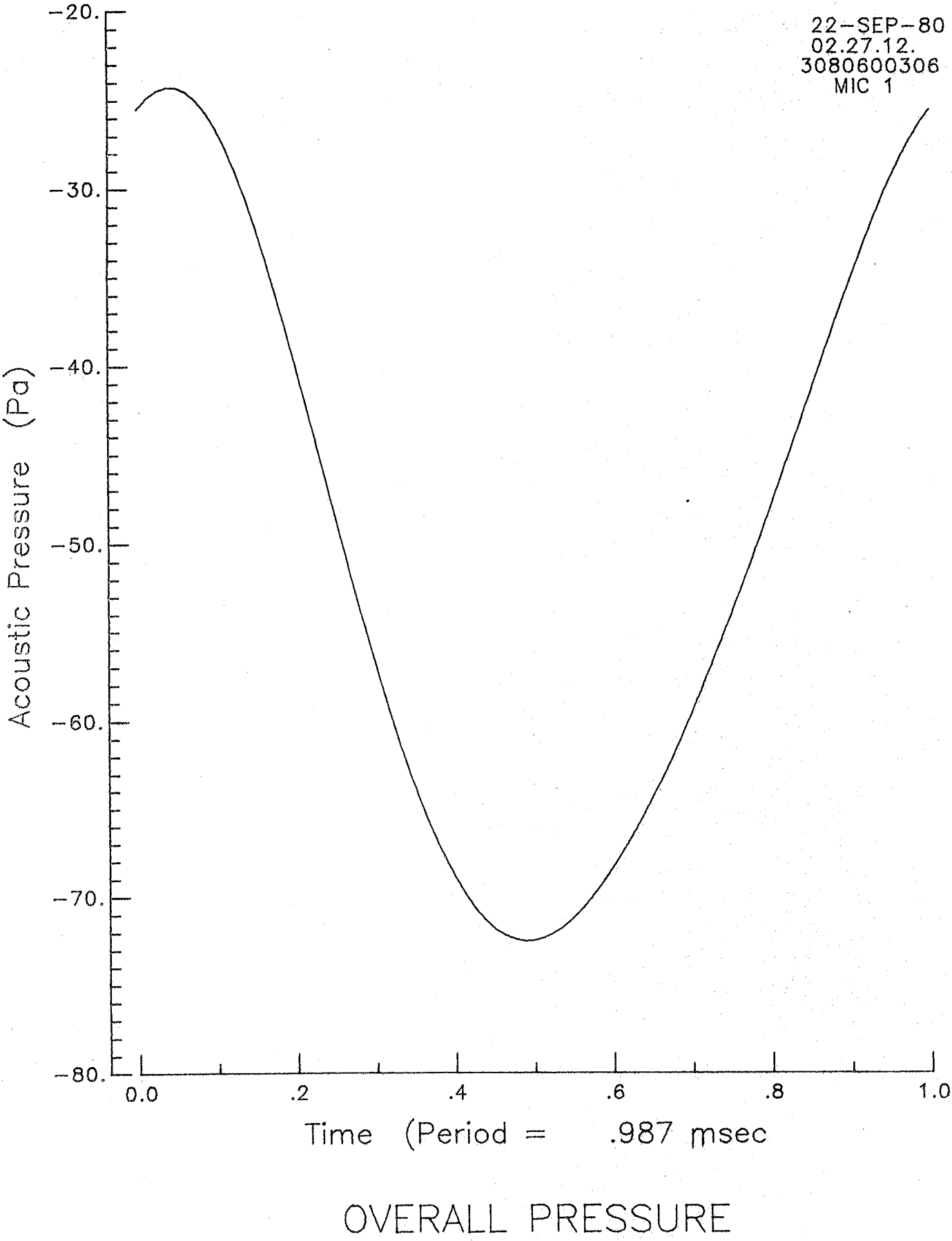

Figure 9(a).- Continued.

F. Farassat -- P. Nystrom
JIAFS -- NASA/LaRC -- GWU

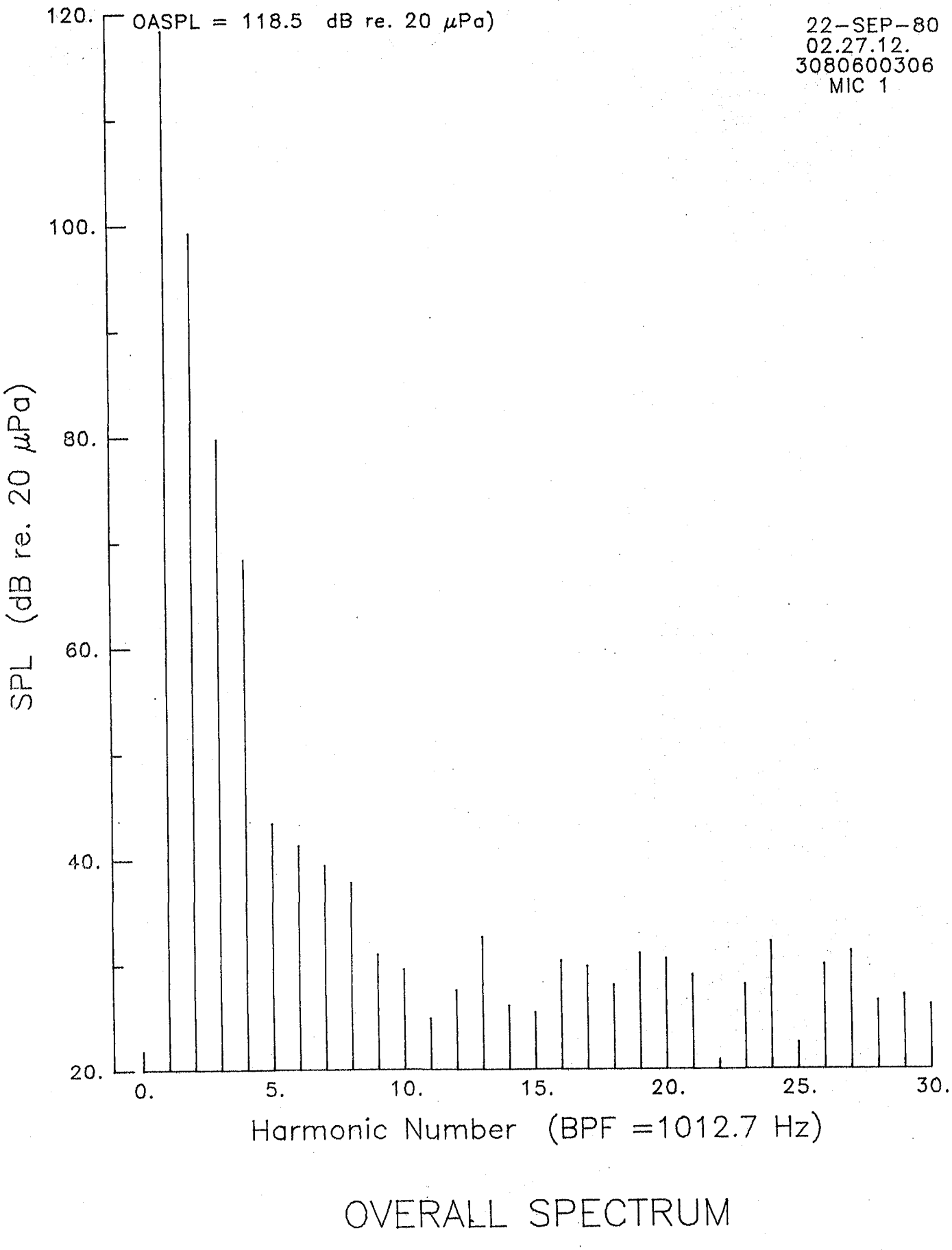

Figure 9(a).- Continued.

F. Farassat -- P. Nystrom
JIAFS -- NASA/LaRC -- GWU

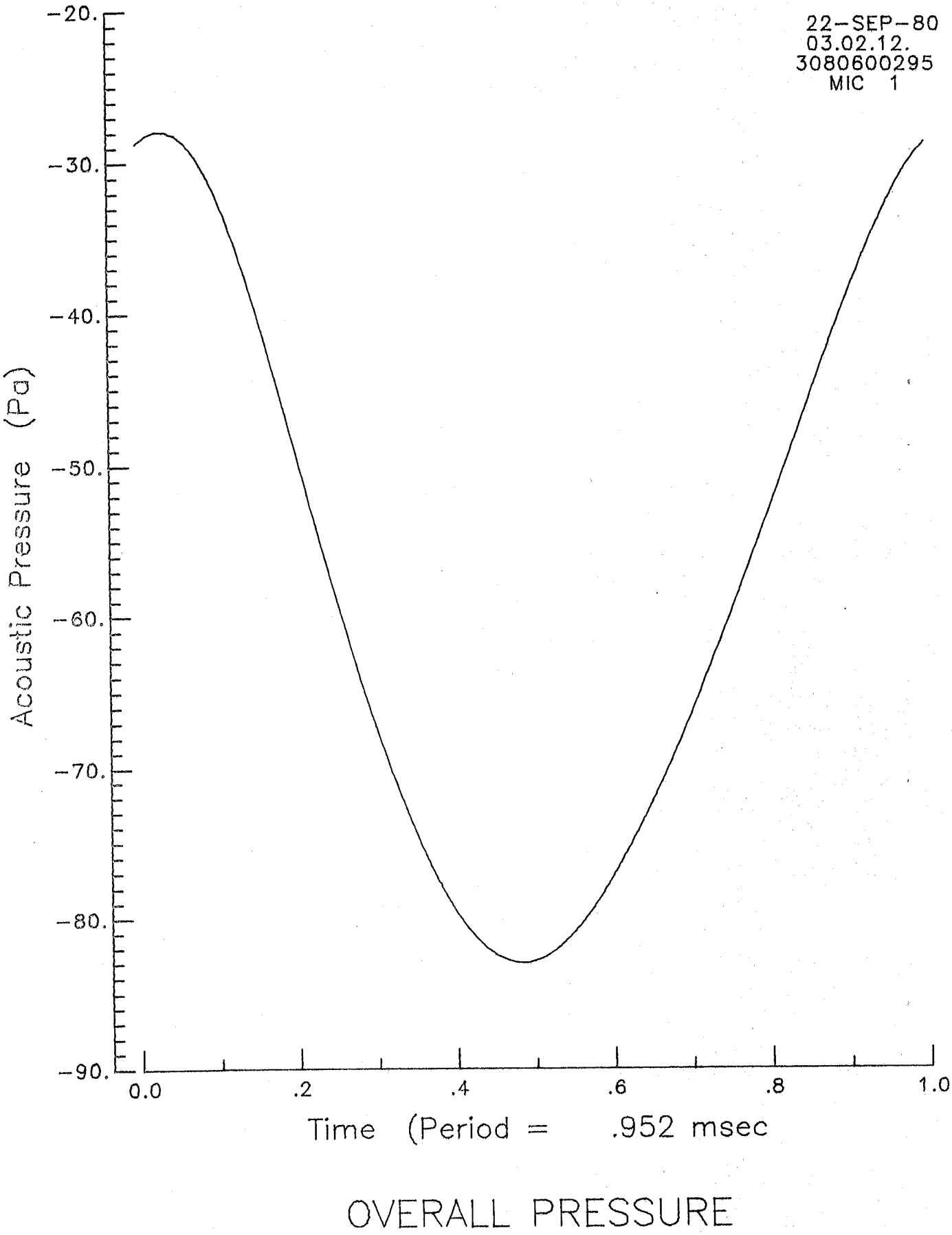

Figure 9(a).- Continued.

F. Farassat -- P. Nystrom
JIAFS -- NASA/LaRC -- GWU

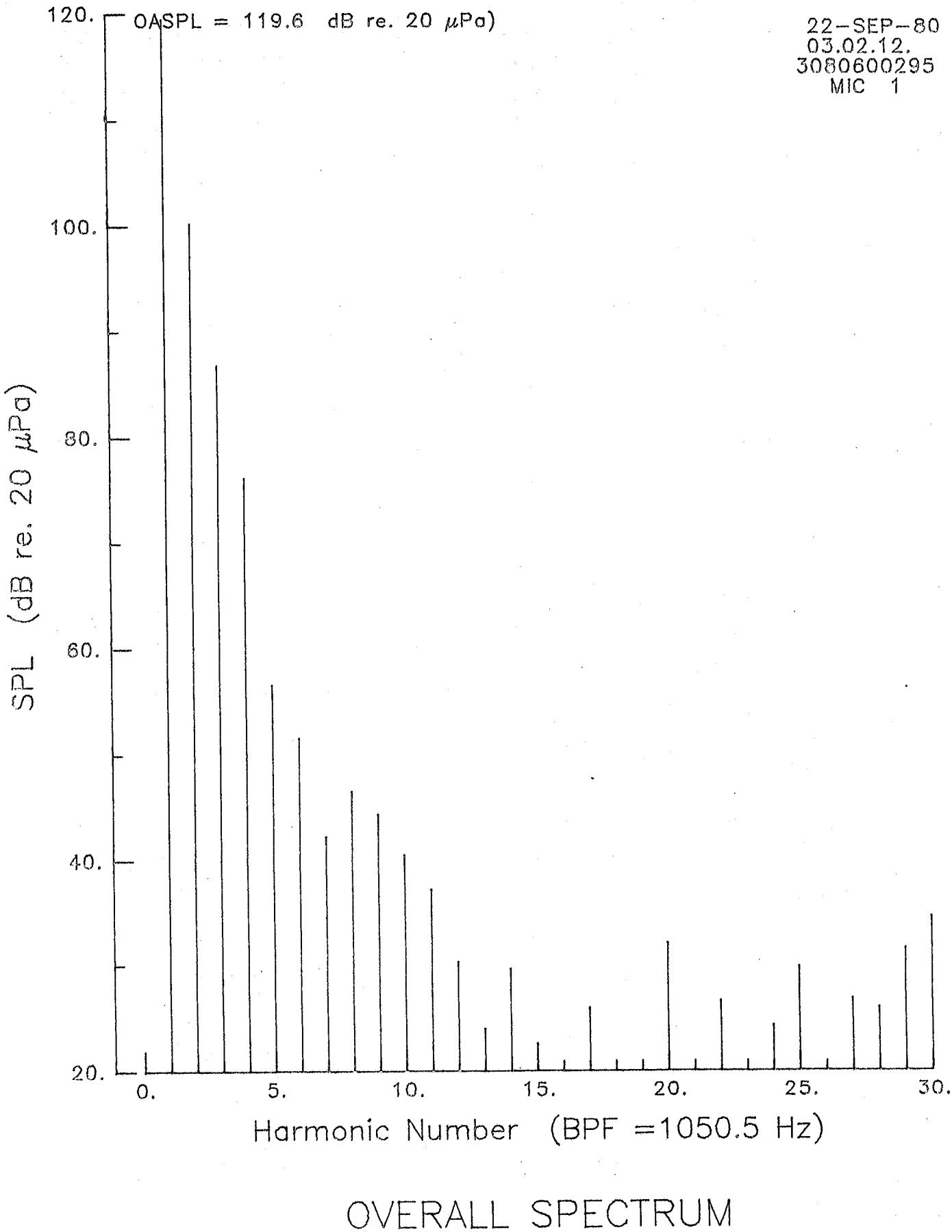

Figure 9(a).- Concluded.

F. Farassat -- P. Nystrom
JIAFS -- NASA/LaRC -- GWU

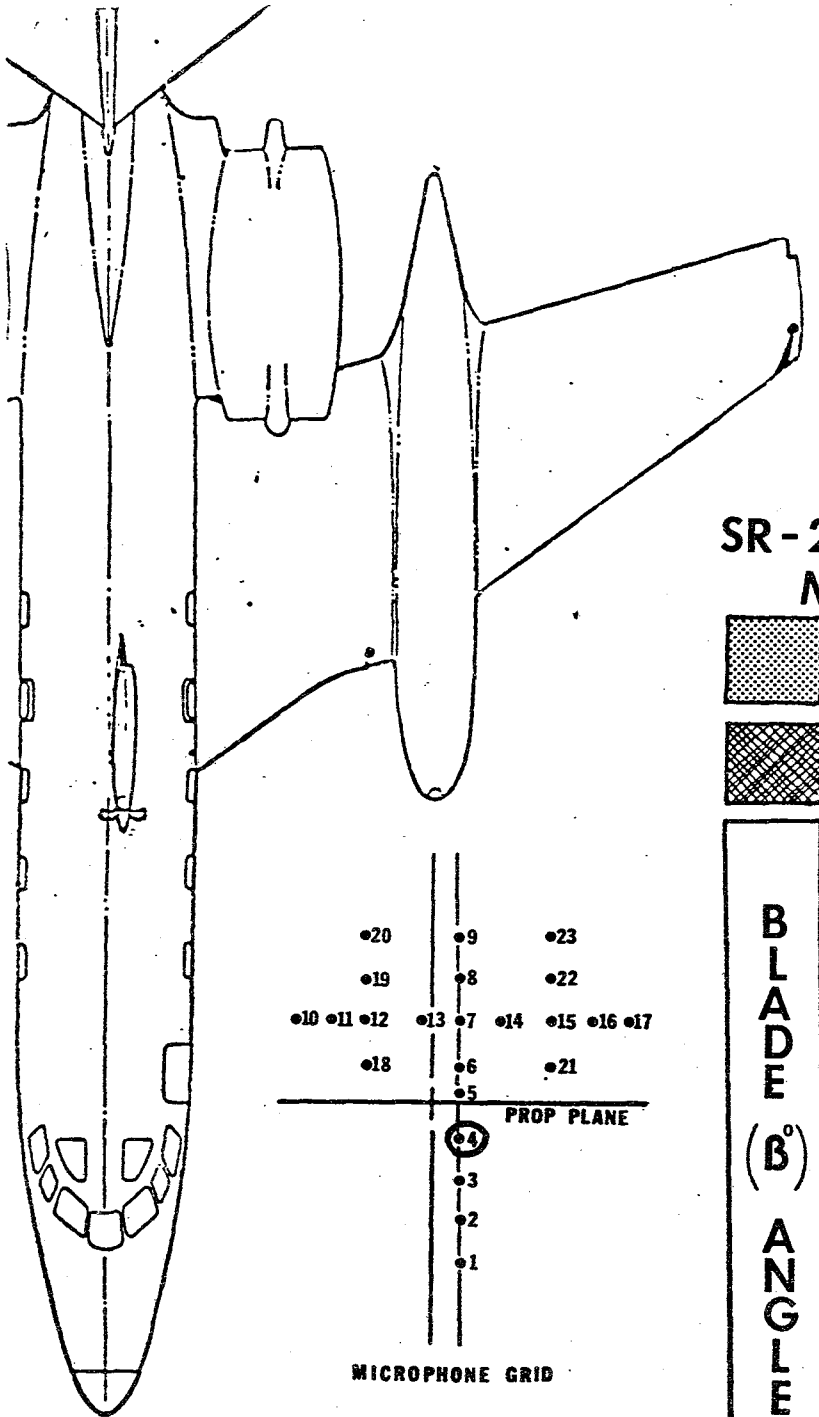

Figure 9(b).- Continued.

SR-2 TEST MATRIX

EXCEEDS BLEED SYS. POWER CAPACITY

BLADE CRITICAL SPEED

BLADE (β°) ANGLE	ADVANCE (J) RATIO	ALTITUDE (FT) 20,000 MACH # .50	.60	.65	.70	.75	.80	ALTITUDE (FT) 25,000 MACH # .50	.60	.65	.70	.75	.80	ALTITUDE (FT) 30,000 MACH # .50	.60	.65	.70	.75	.80
59.0	4.30																		
	3.50																		
	3.25																		
	3.06																		
	2.90																		
60.0	4.30																		X
	3.50																		X
	3.25																		X
	3.06																		X
	2.95																		X
61.0	4.30																		
	4.07																		
	3.50																		
	3.25																		

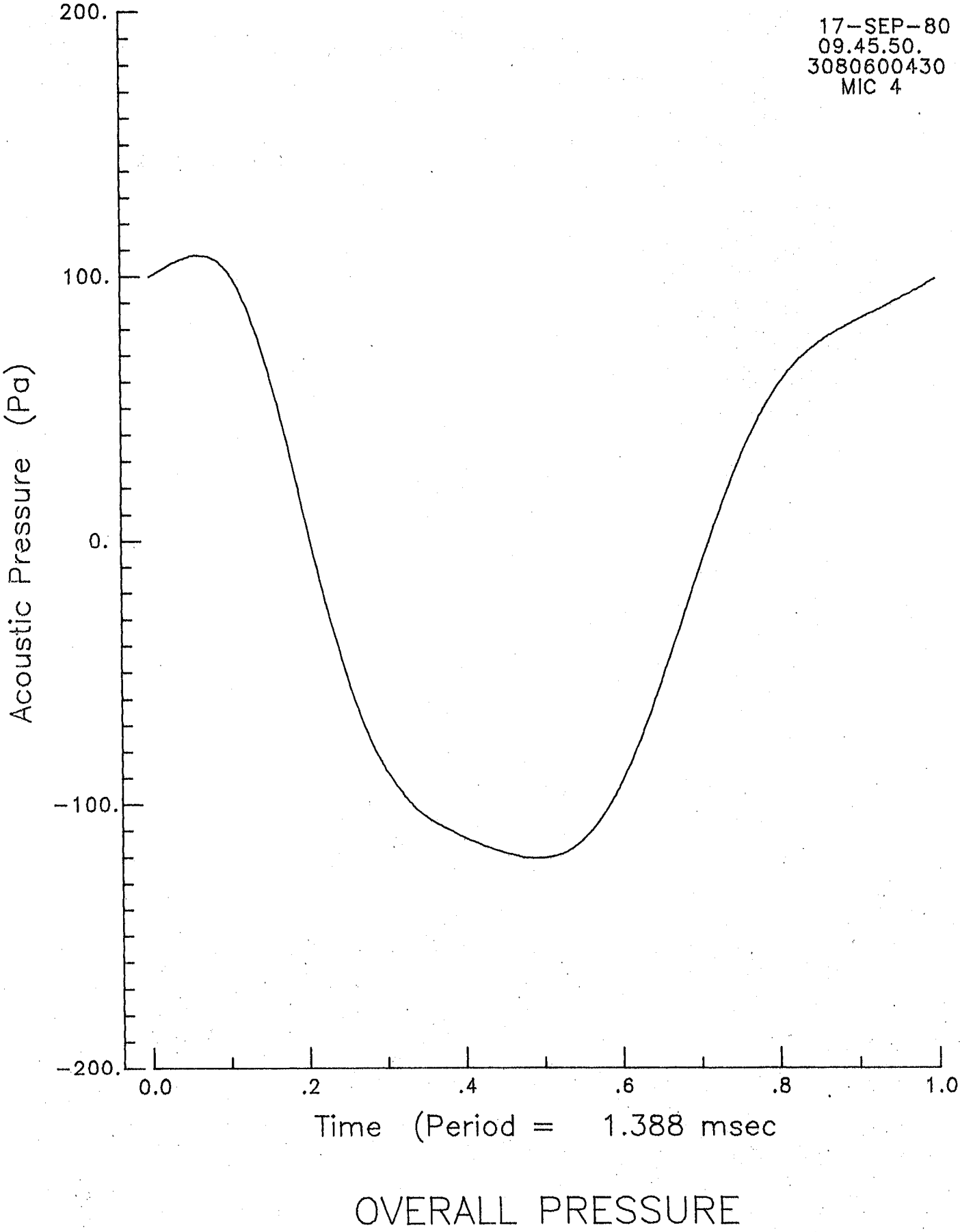

Figure 9(b).- Continued.

F. Farassat -- P. Nystrom
JIAFS -- NASA/LaRC -- GWU

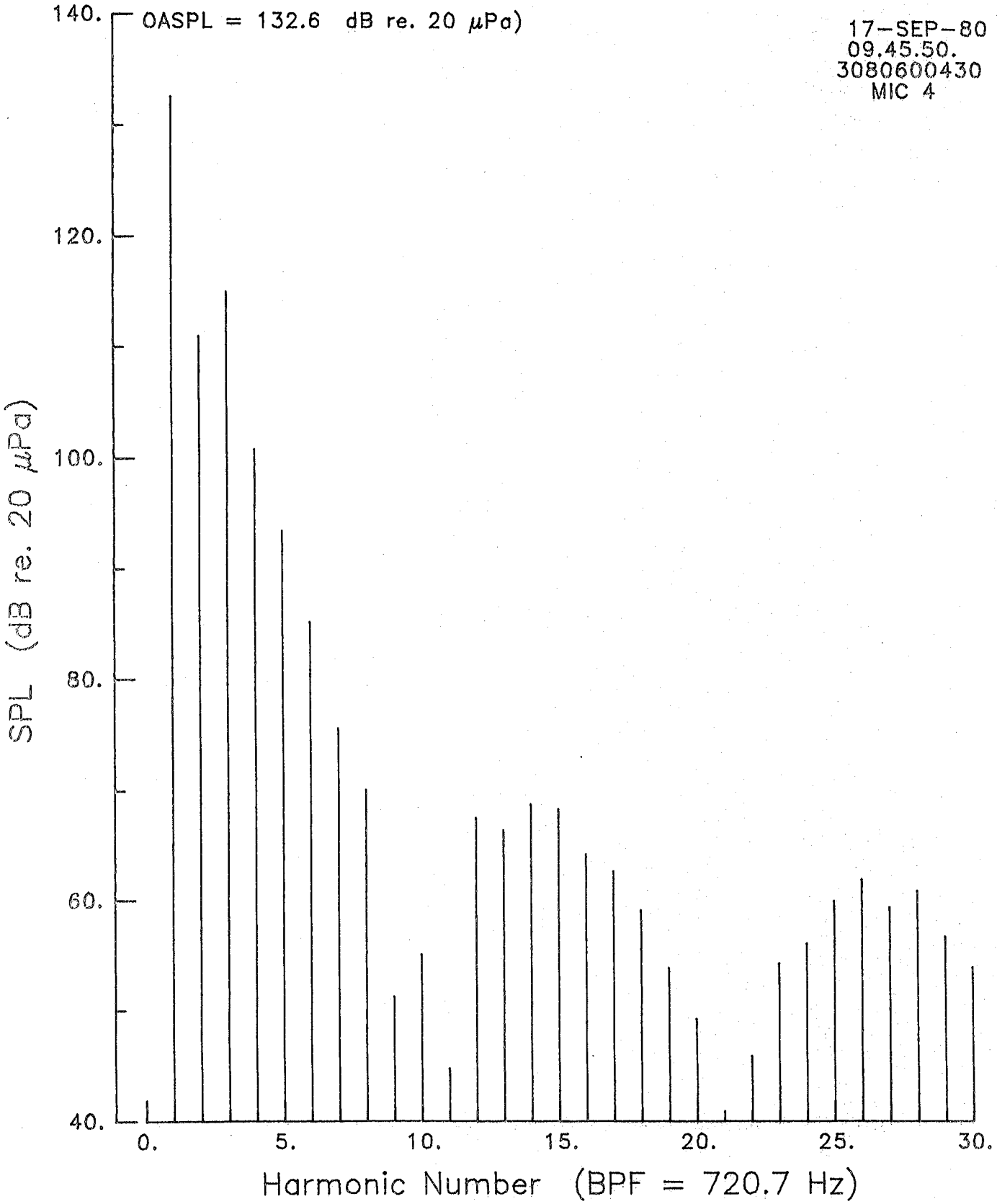

OVERALL SPECTRUM

Figure 9(b).- Continued.

F. Farassat -- P. Nystrom
JIAFS -- NASA/LaRC -- GWU

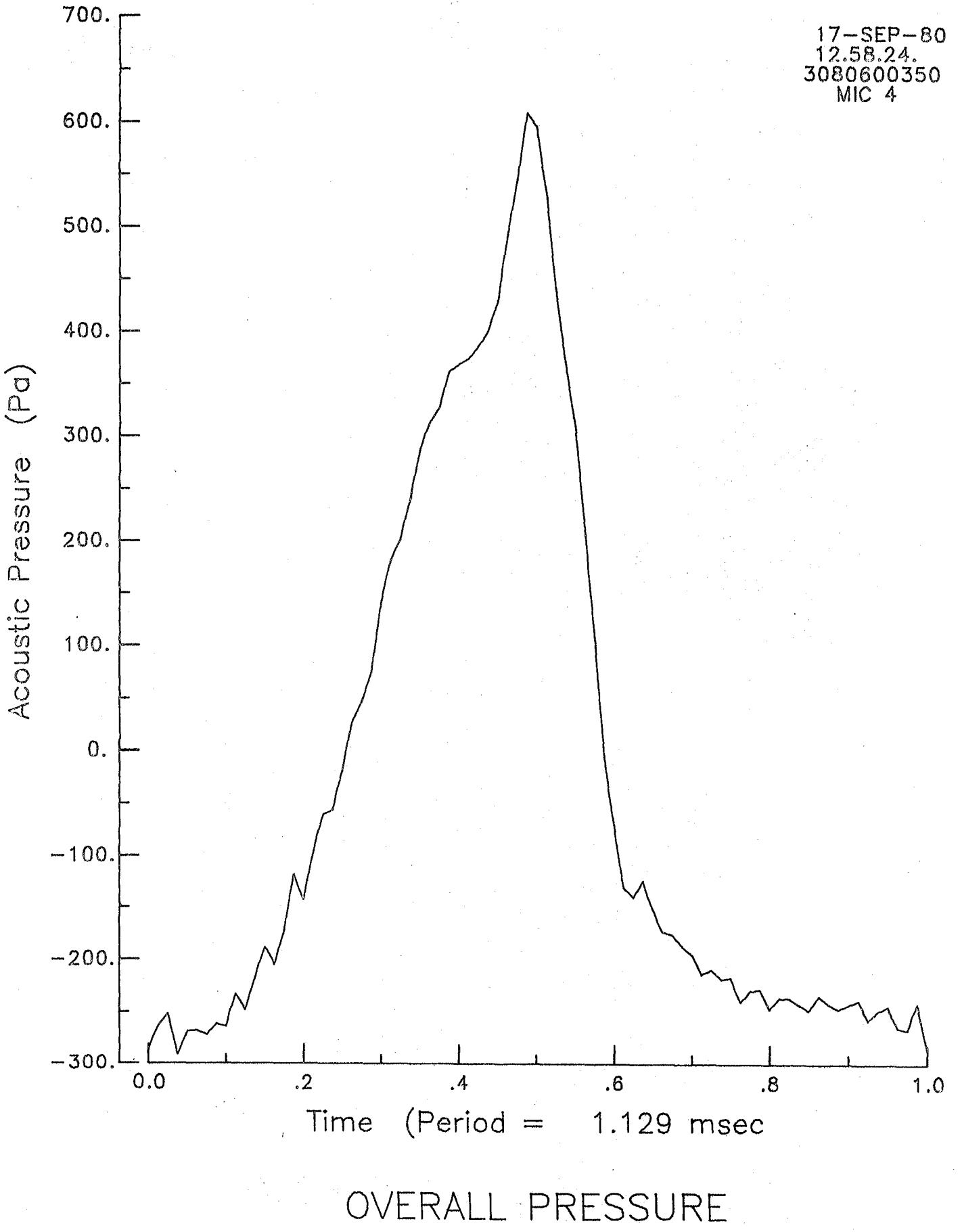

Figure 9(b).- Continued.

F. Farassat -- P. Nystrom
JIAFS -- NASA/LaRC -- GWU

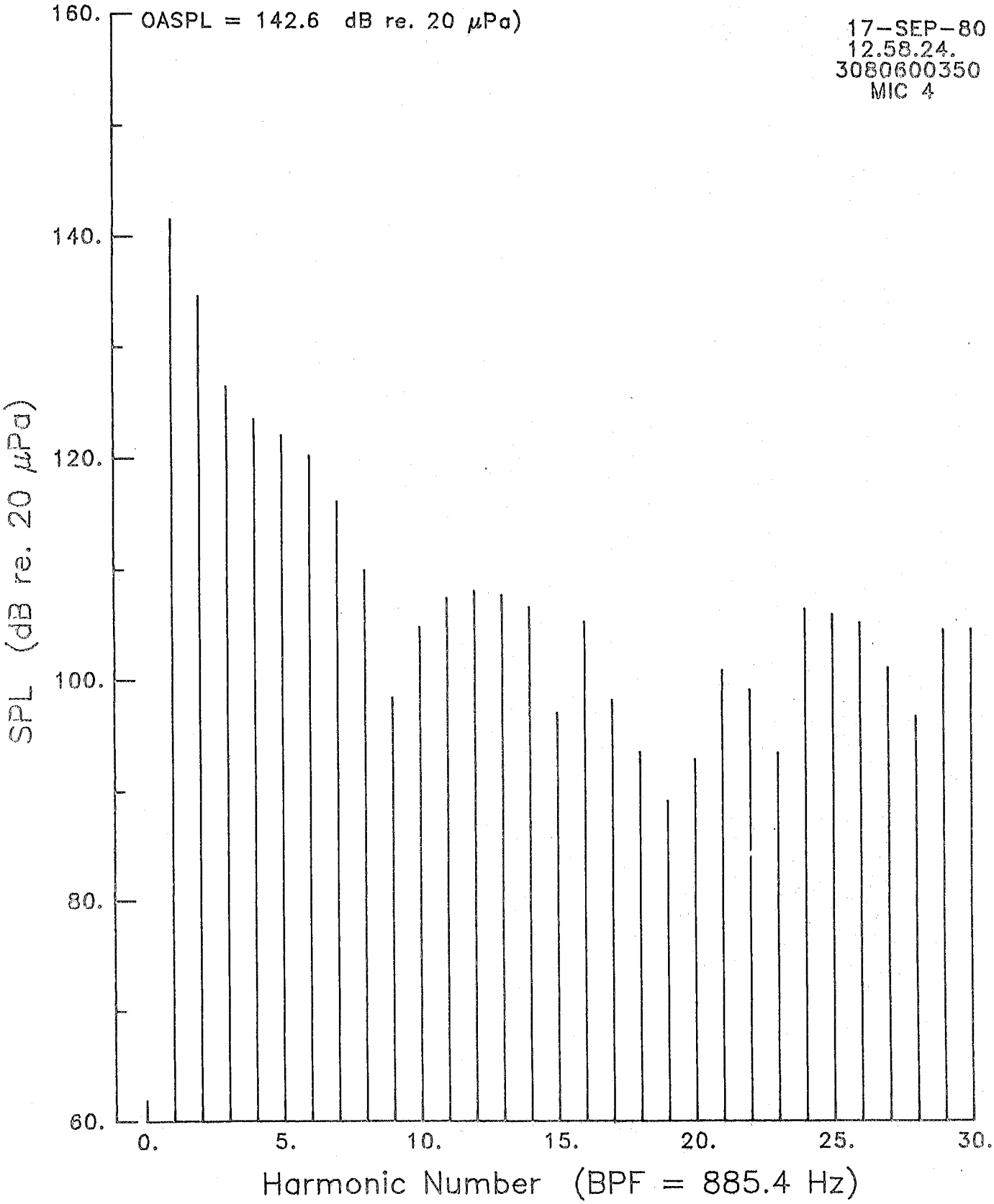

OVERALL SPECTRUM

Figure 9(b).- Continued.

F. Farassat -- P. Nystrom
JIAFS -- NASA/LaRC -- GWU

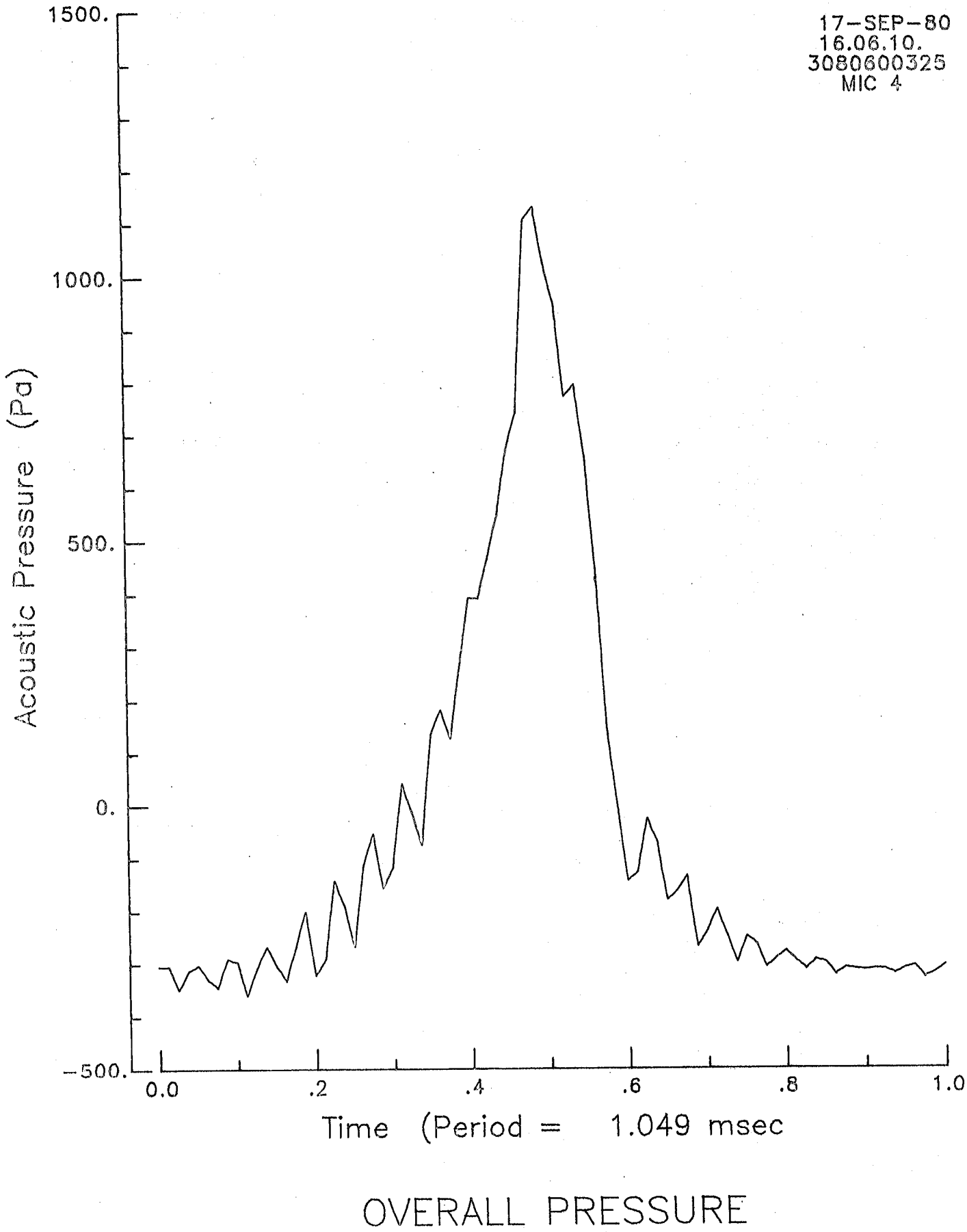

Figure 9(b).- Continued.

F. Farassat -- P. Nystrom
JIAFS -- NASA/LaRC -- GWU

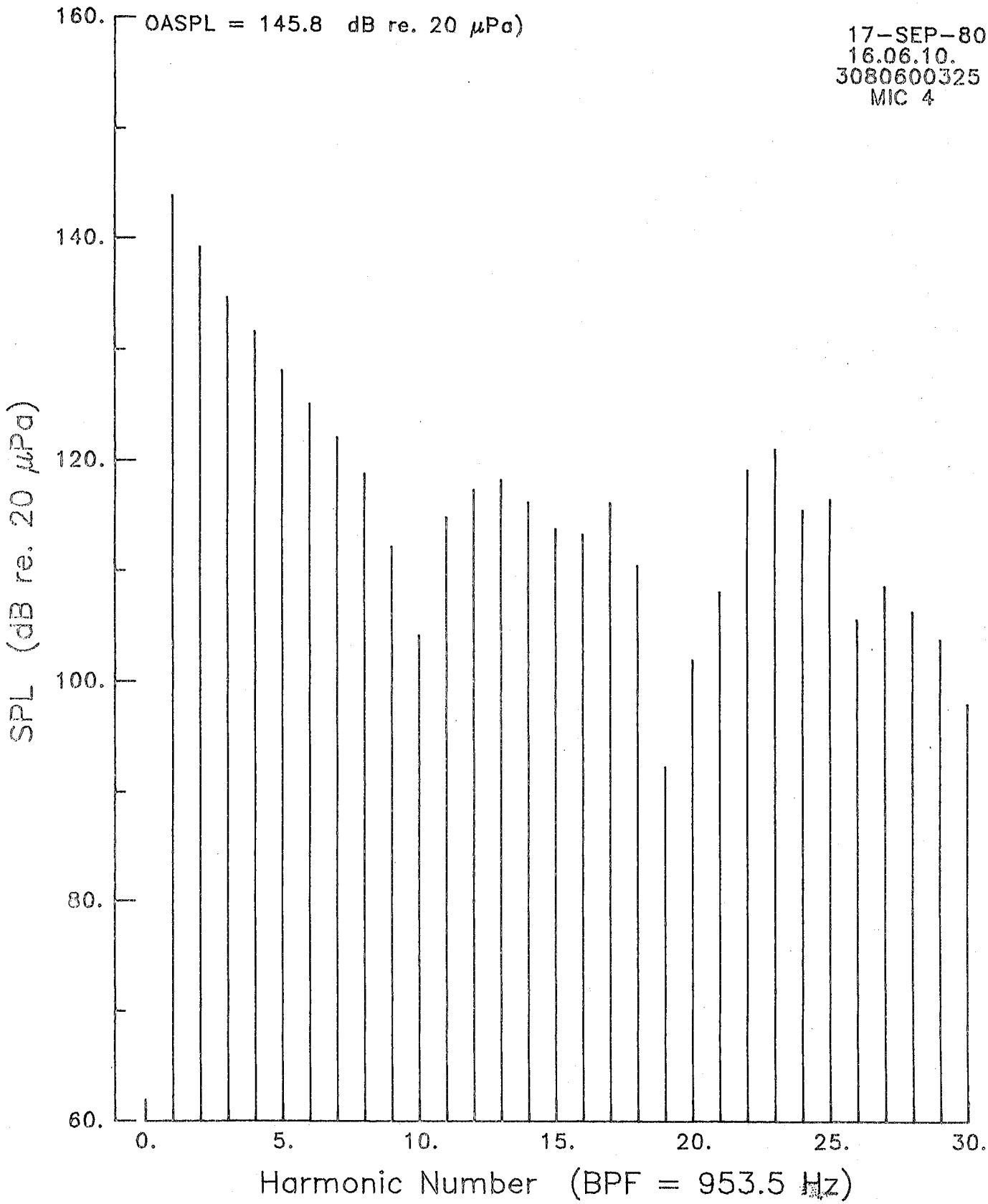

OVERALL SPECTRUM

Figure 9(b).- Continued.

F. Farassat -- P. Nystrom
JIAFS -- NASA/LaRC -- GWU

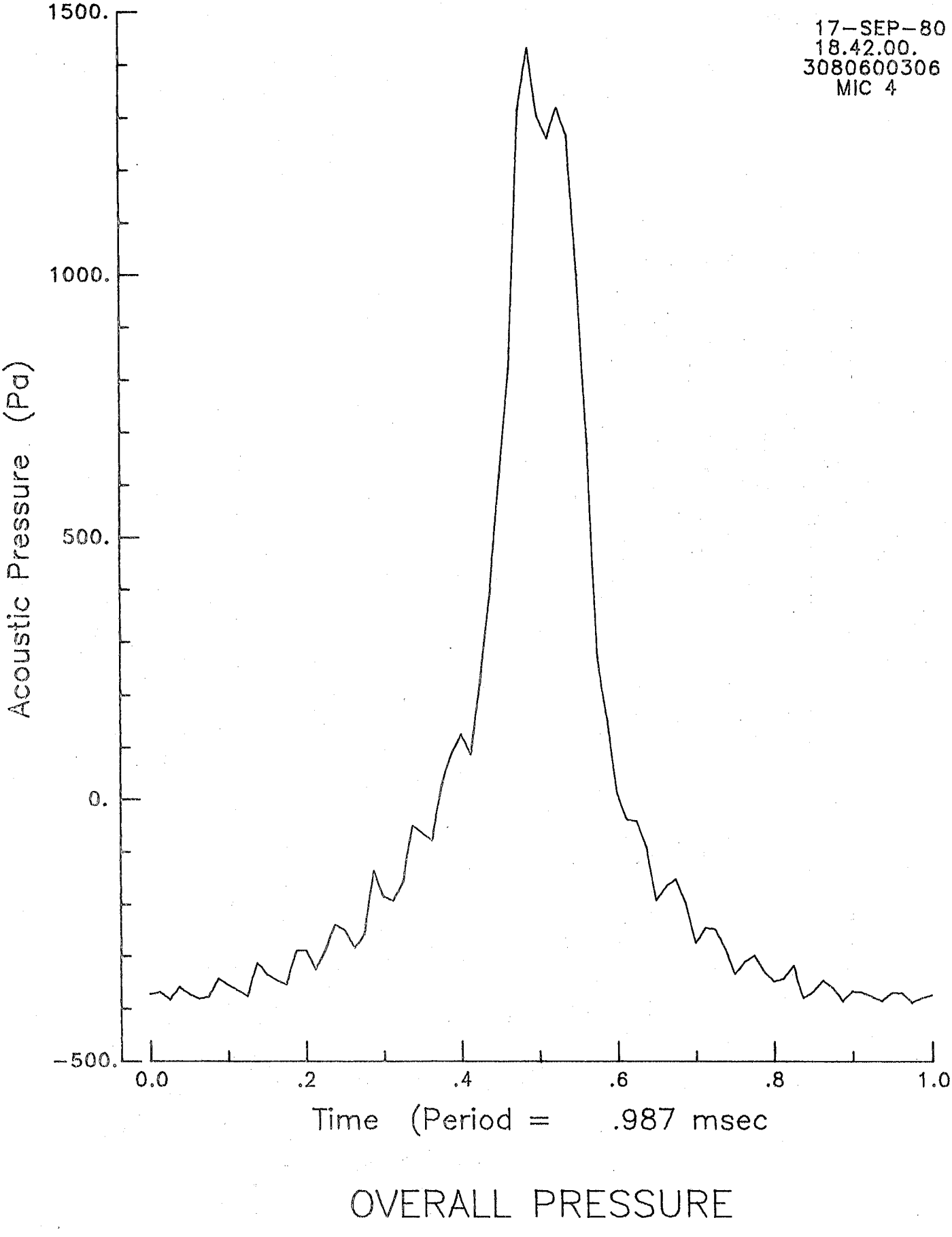

Figure 9(b).- Continued.

F. Farassat -- P. Nystrom
JIAFS -- NASA/LaRC -- GWU

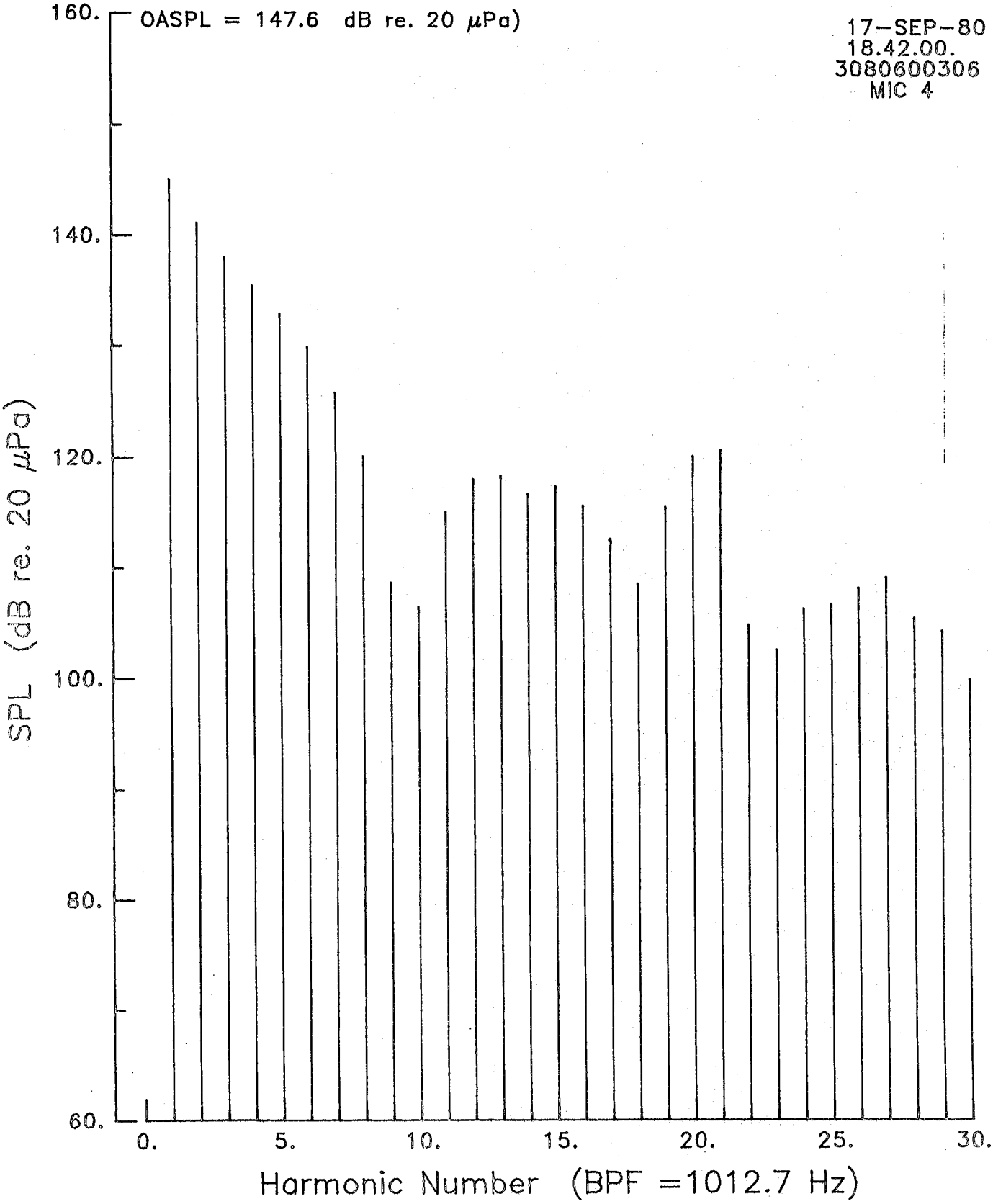

OVERALL SPECTRUM

Figure 9(b).- Continued.

F. Farassat -- P. Nystrom
JIAFS -- NASA/LaRC -- GWU

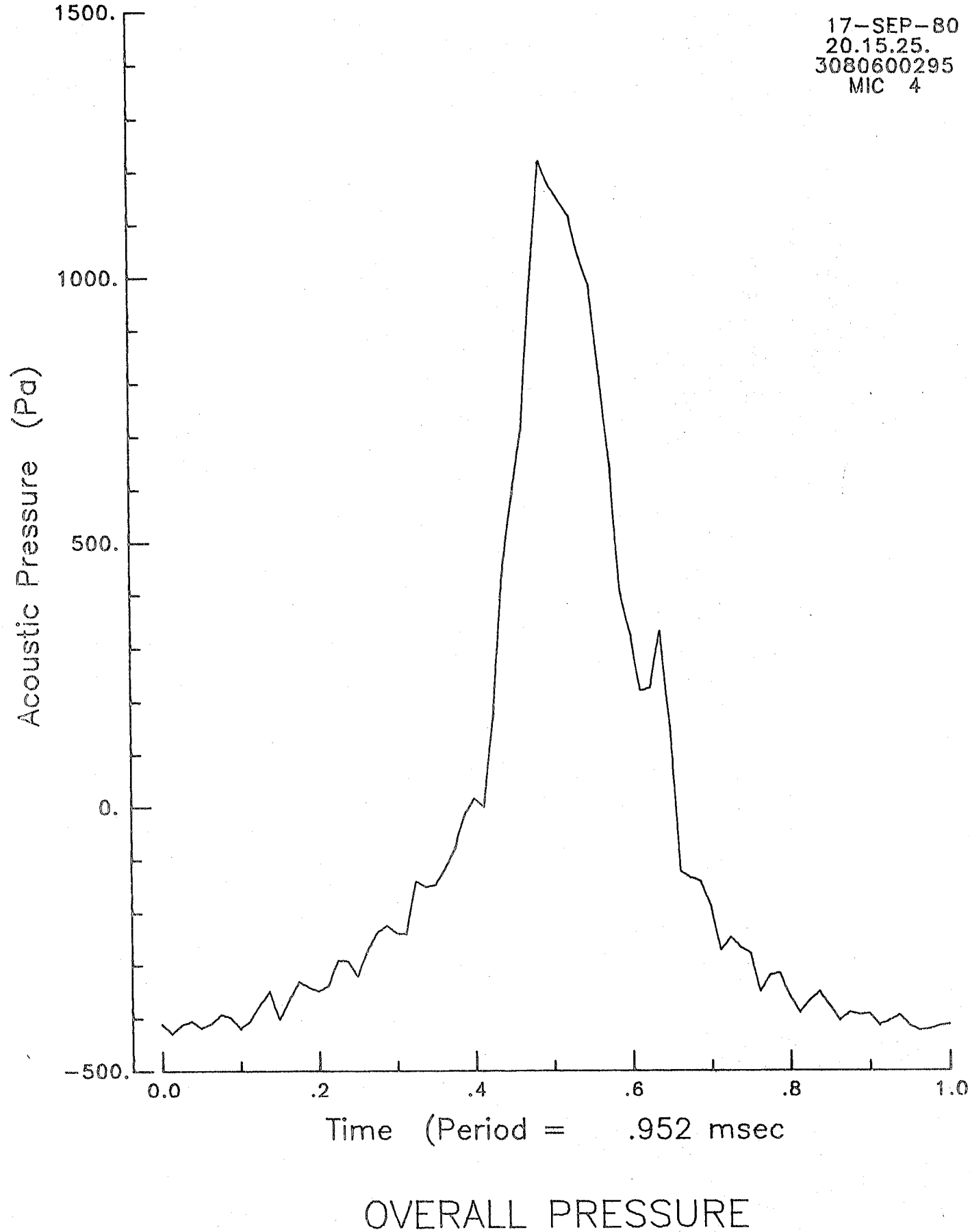

Figure 9(b).- Continued.

F. Farassat -- P. Nystrom
JIAFS -- NASA/LaRC -- GWU

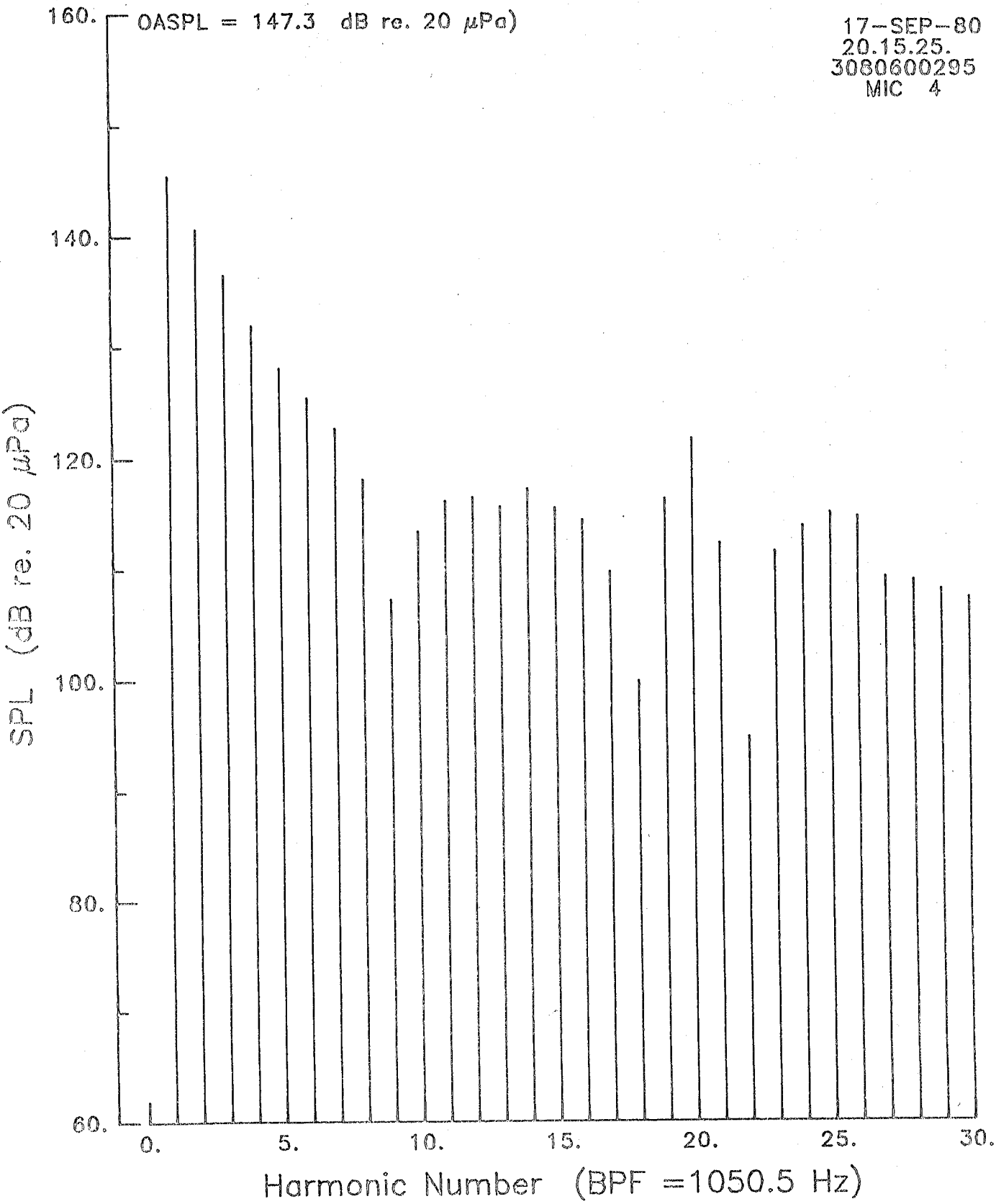

Figure 9(b).- Concluded.

F. Farassat -- P. Nystrom
JIAFS -- NASA/LaRC -- GWU

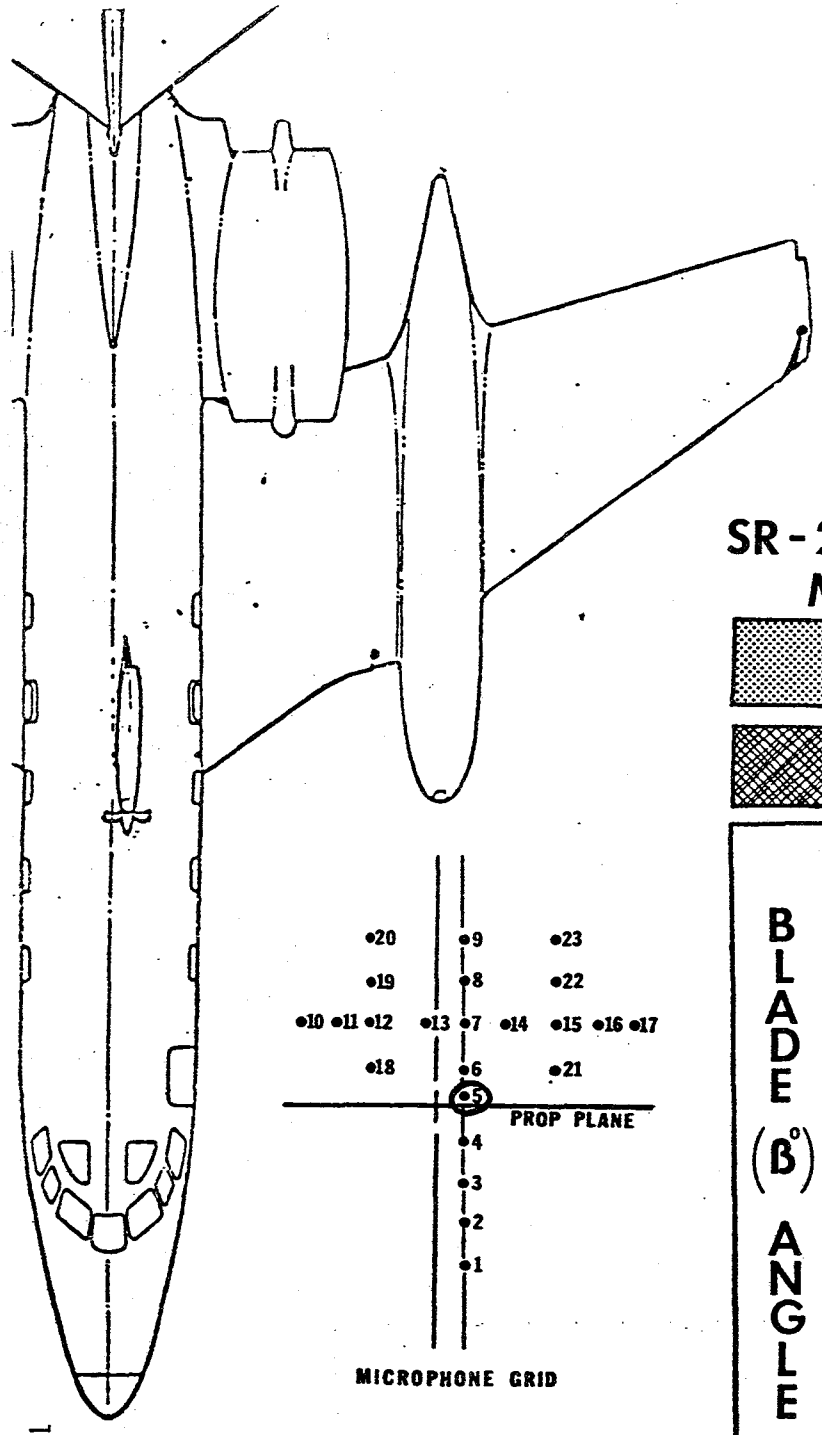

Figure 9(c).- Continued.

SR-2 TEST MATRIX

EXCEEDS BLEED SYS. POWER CAPACITY

BLADE CRITICAL SPEED

BLADE ANGLE (β°)	ADVANCE RATIO (J)	ALTITUDE (FT)	20,000						25,000						30,000					
		MACH #	.50	.60	.65	.70	.75	.80	.50	.60	.65	.70	.75	.80	.50	.60	.65	.70	.75	.80
59.0	4.30																			
	3.50																			
	3.25																			
	3.06																			
	2.90																			
60.0	4.30																			X
	3.50																			X
	3.25																			X
	3.06																			X
	2.95																			X
61.0	4.30																			
	4.07																			
	3.50																			
	3.25																			

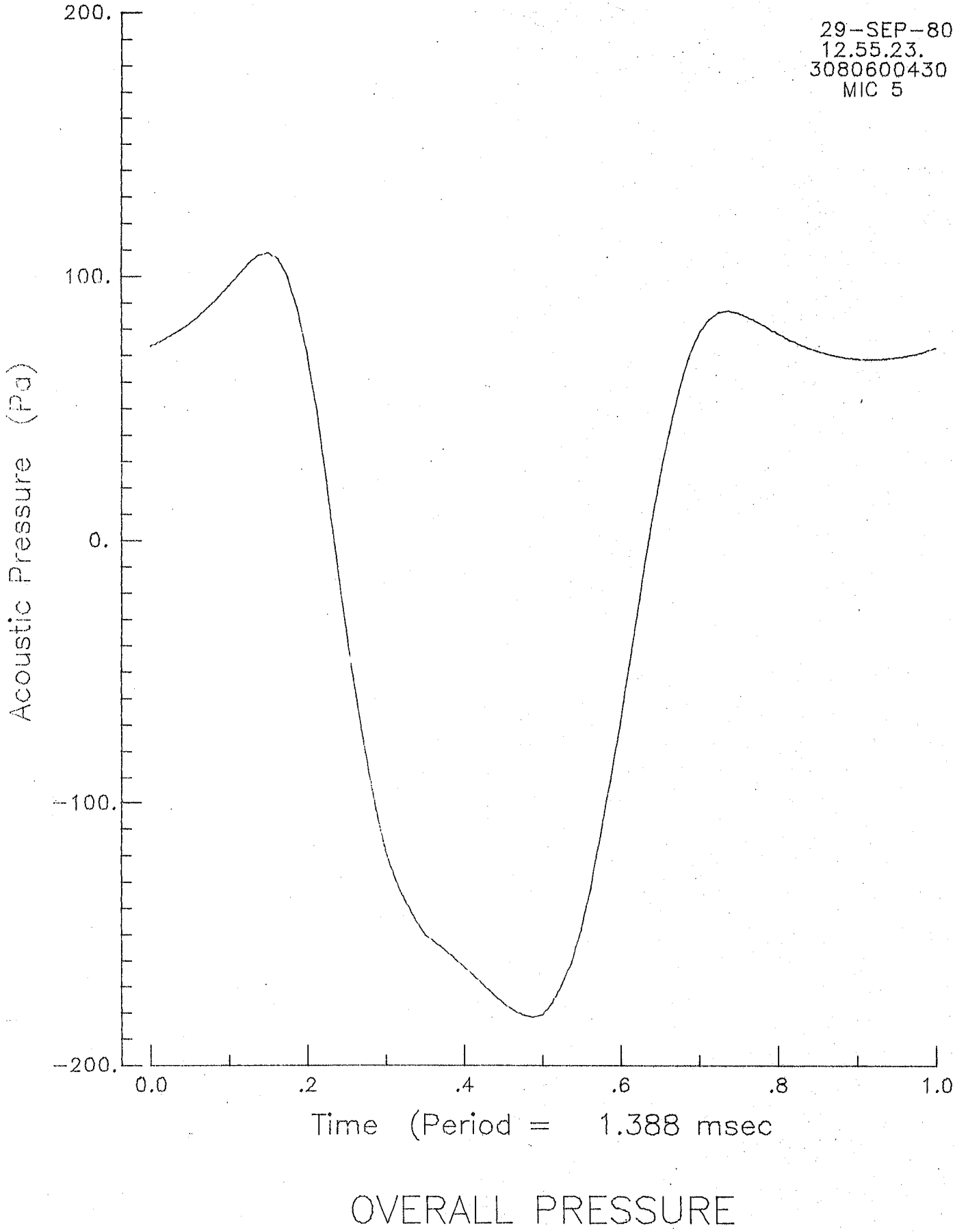

Figure 9(c).- Continued.

F. Farassat -- P. Nystrom
JIAFS -- NASA/LaRC -- GWU

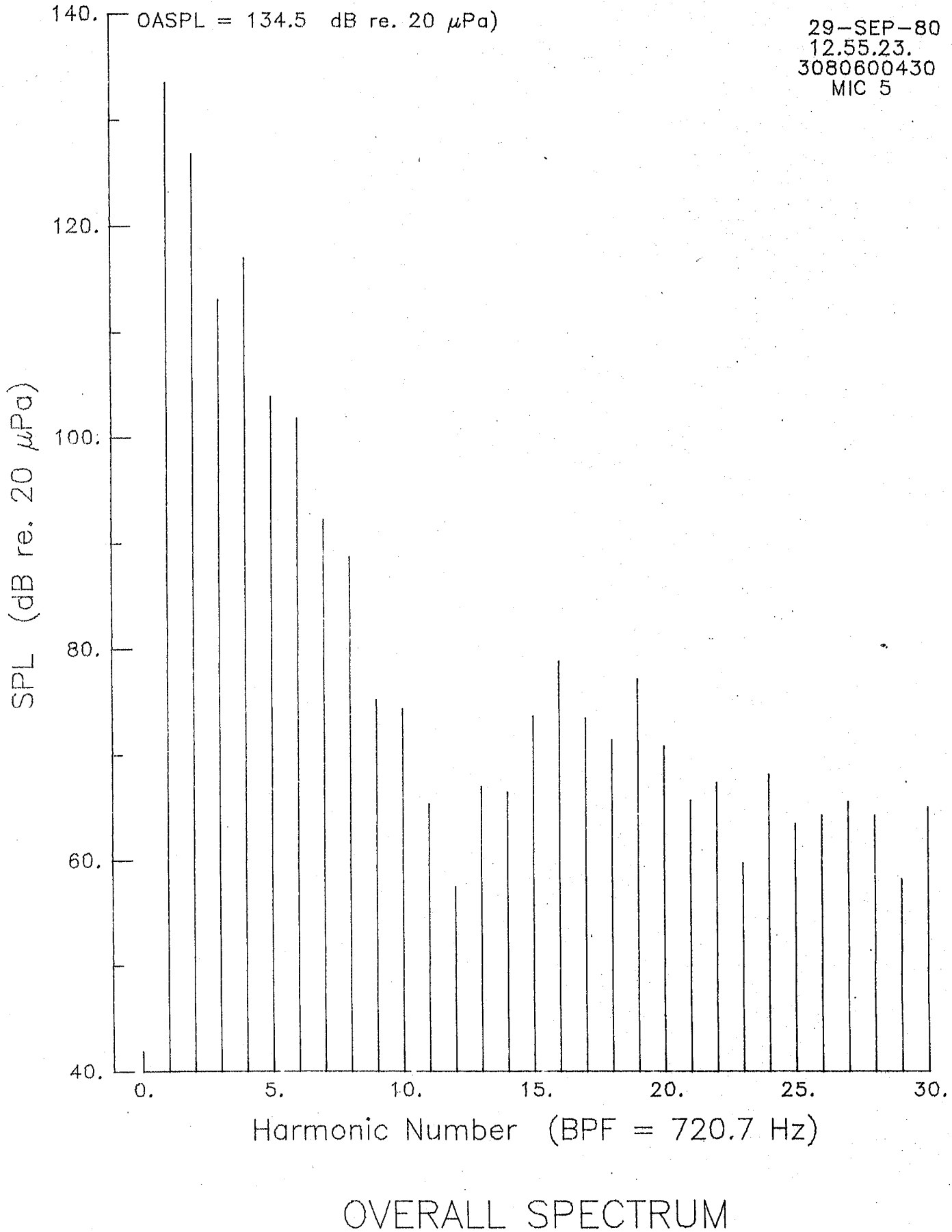

Figure 9(c).- Continued.

F. Farassat -- P. Nystrom
JIAFS -- NASA/LaRC -- GWU

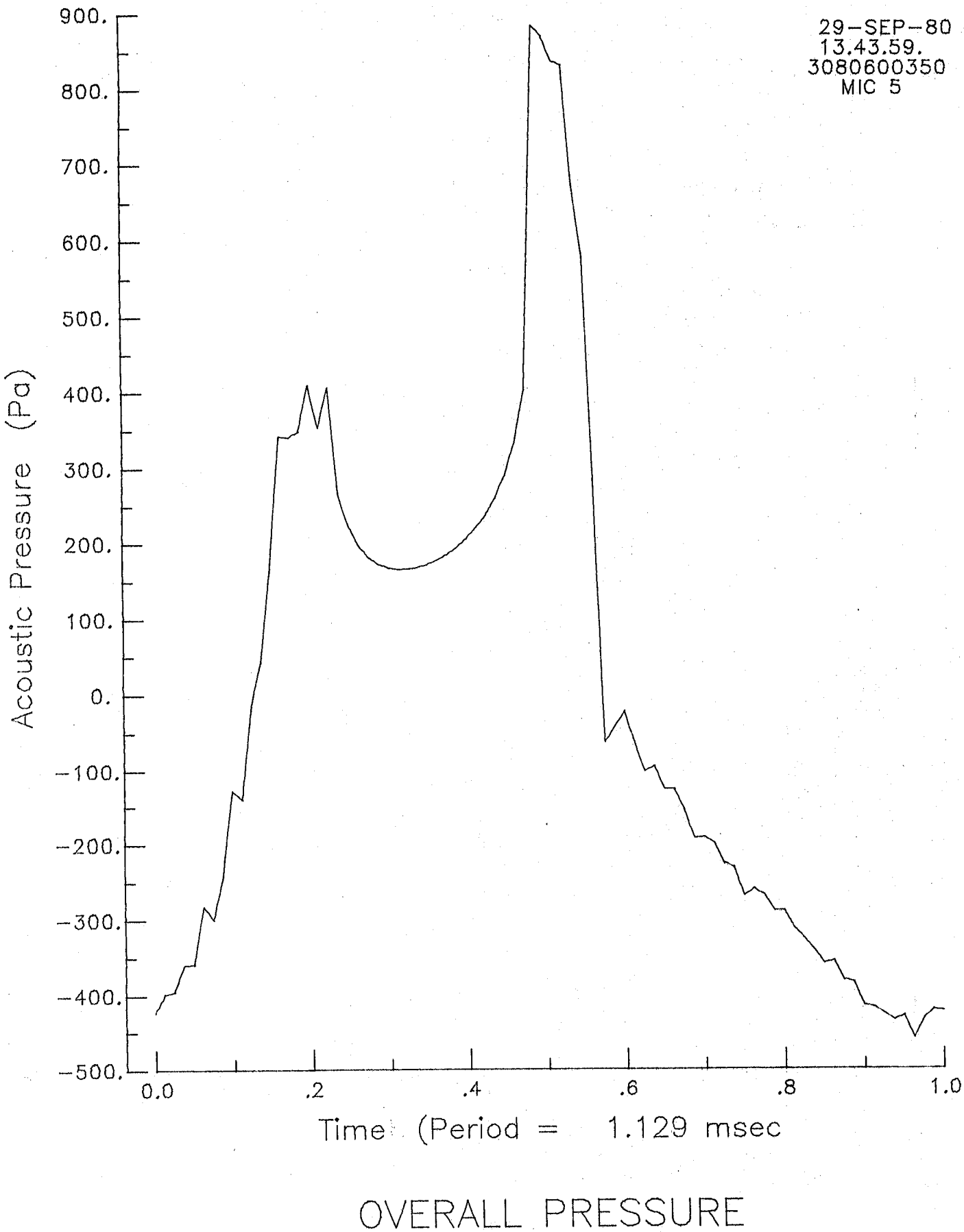

Figure 9(c).- Continued.

F. Farassat -- P. Nystrom
JIAFS -- NASA/LaRC -- GWU

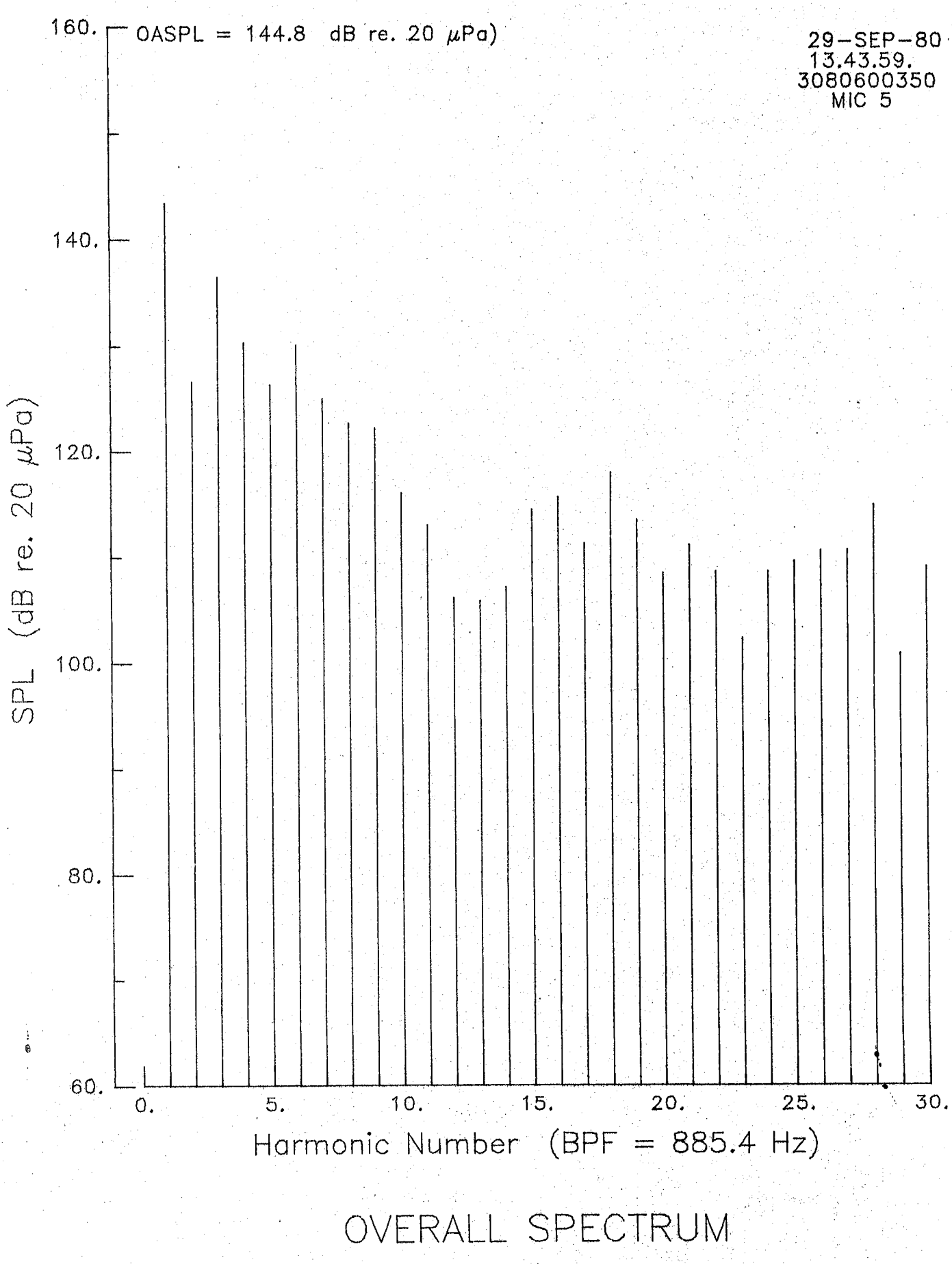

Figure 9(c).- Continued.

F. Farassat -- P. Nystrom
JIAFS -- NASA/LaRC -- GWU

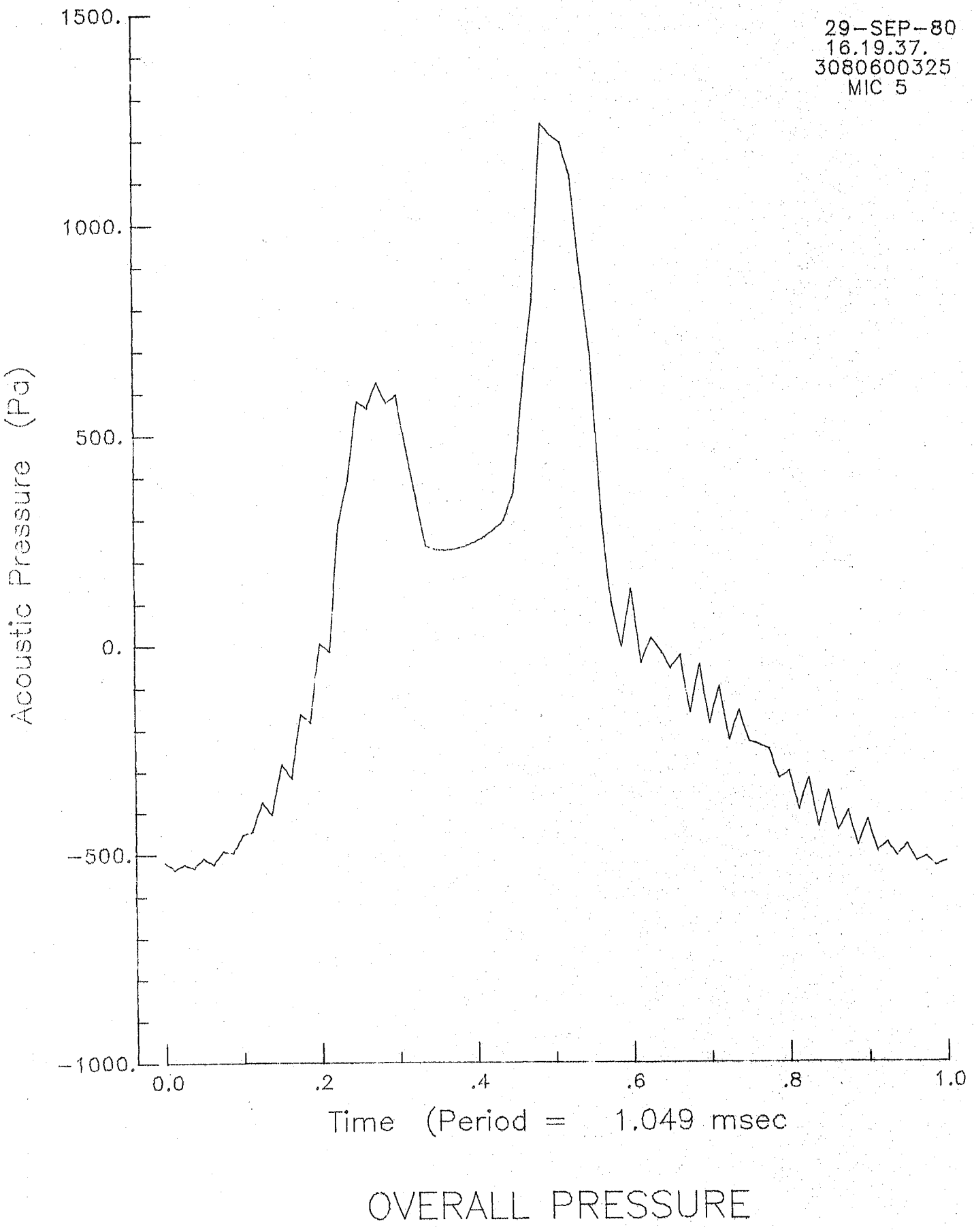

Figure 9(c).- Continued.

F. Farassat -- P. Nystrom
JIAFS -- NASA/LaRC -- GWU

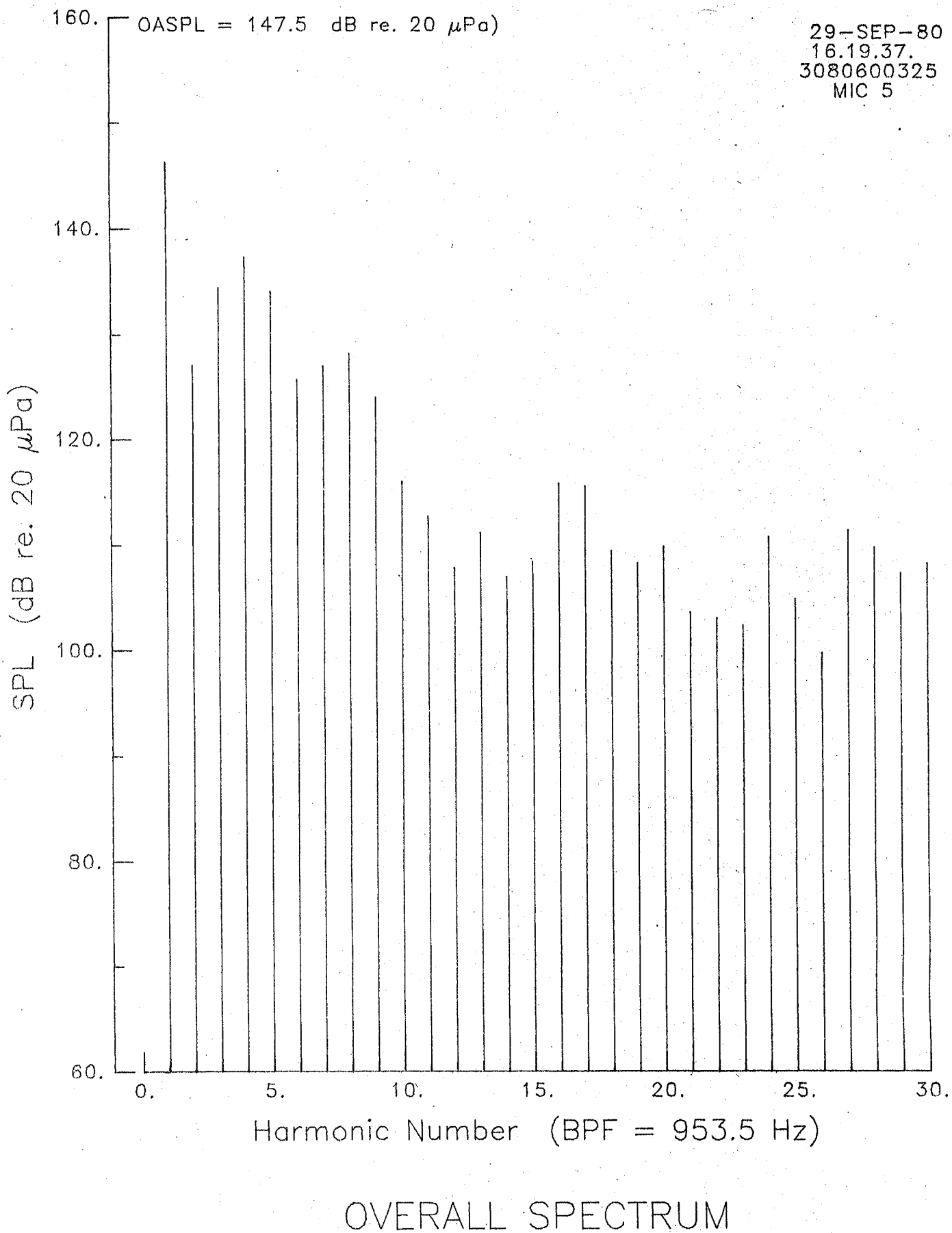

Figure 9(c).- Continued.

F. Farassat -- P. Nystrom
JIAFS -- NASA/LaRC -- GWU

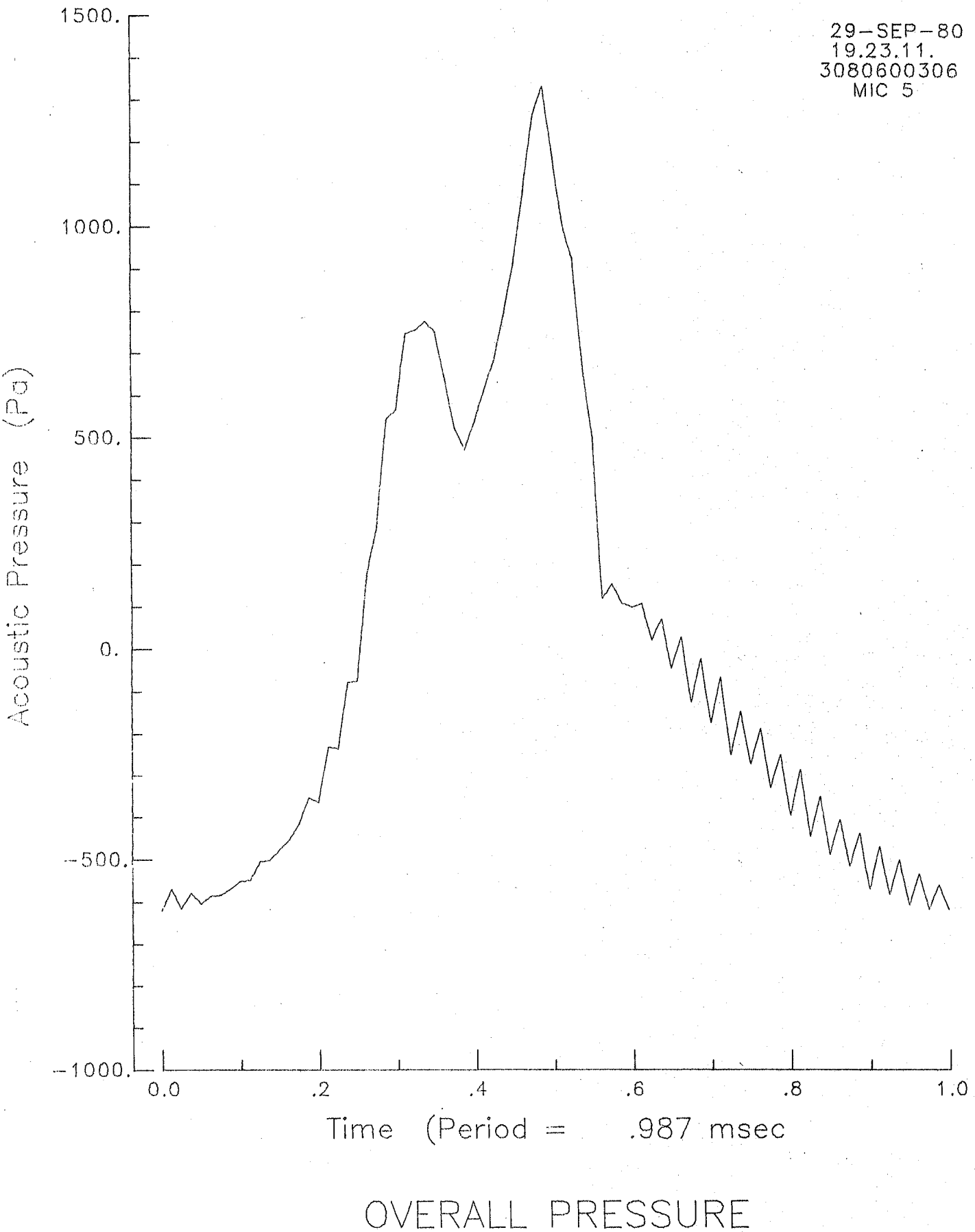

Figure 9(c).- Continued.

F. Farassat -- P. Nystrom
JIAFS -- NASA/LaRC -- GWU

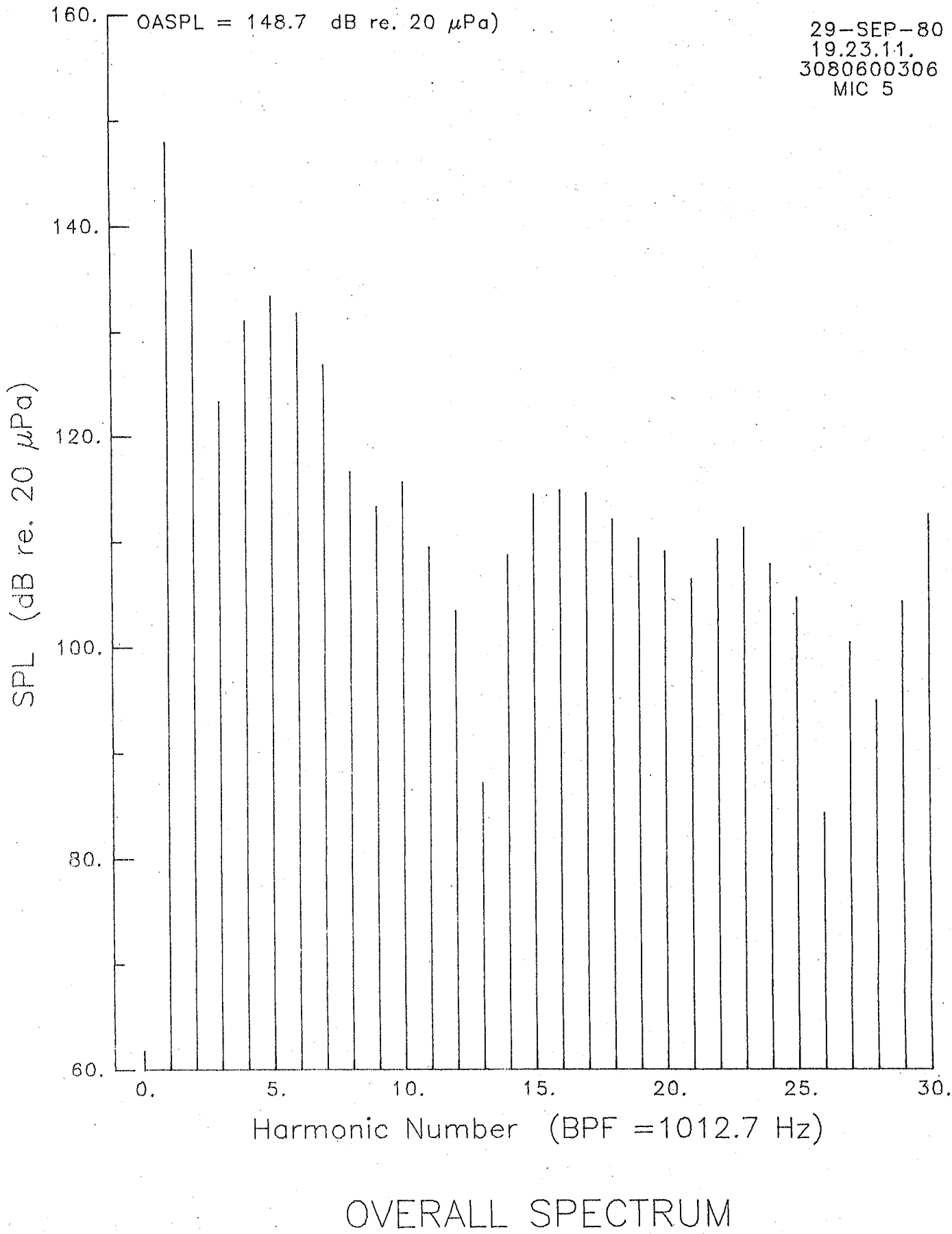

Figure 9(c).- Continued.

F. Farassat -- P. Nystrom
JIAFS -- NASA/LaRC -- GWU

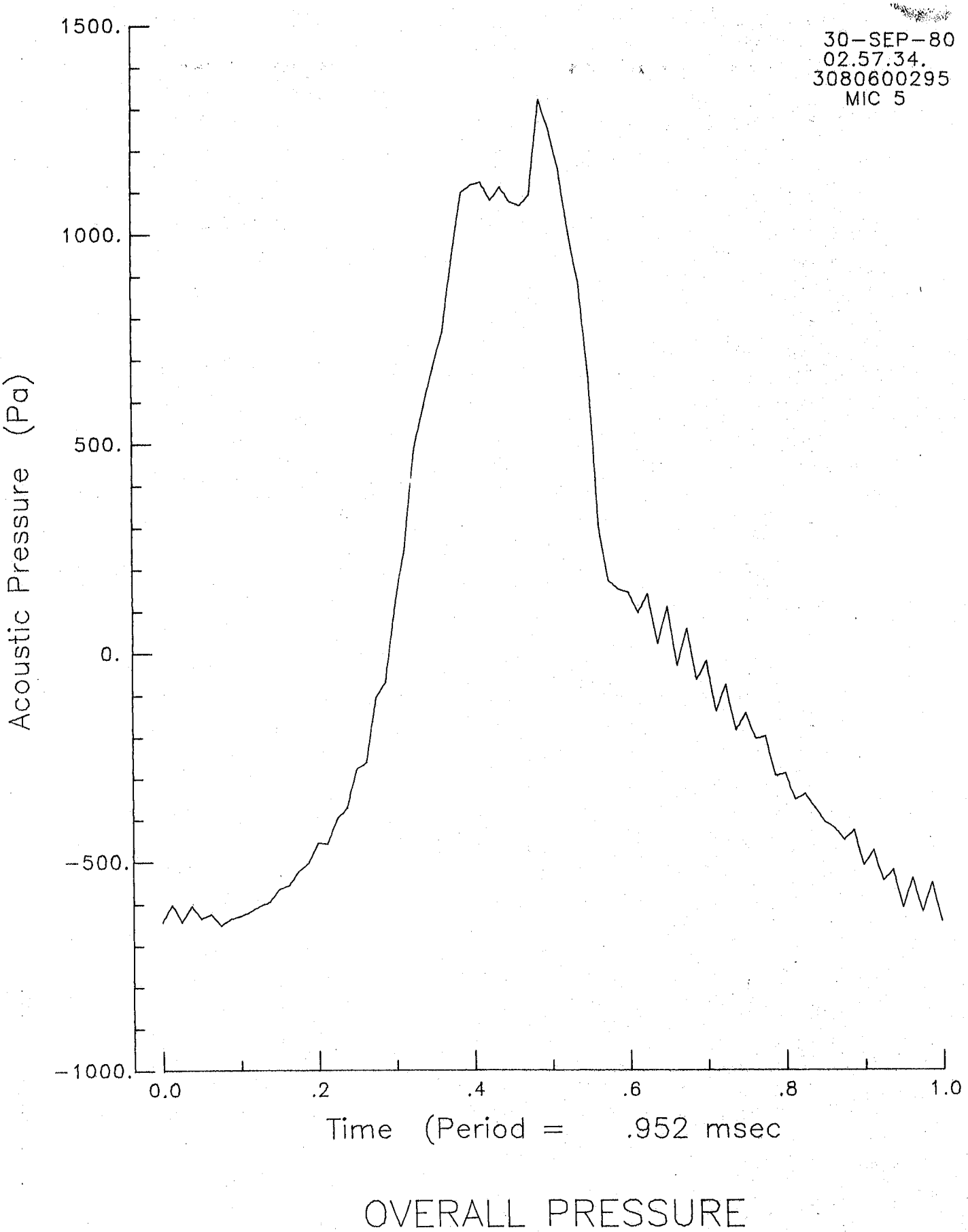

Figure 9(c).- Continued.

F. Farassat -- P. Nystrom
JIAFS -- NASA/LaRC -- GWU

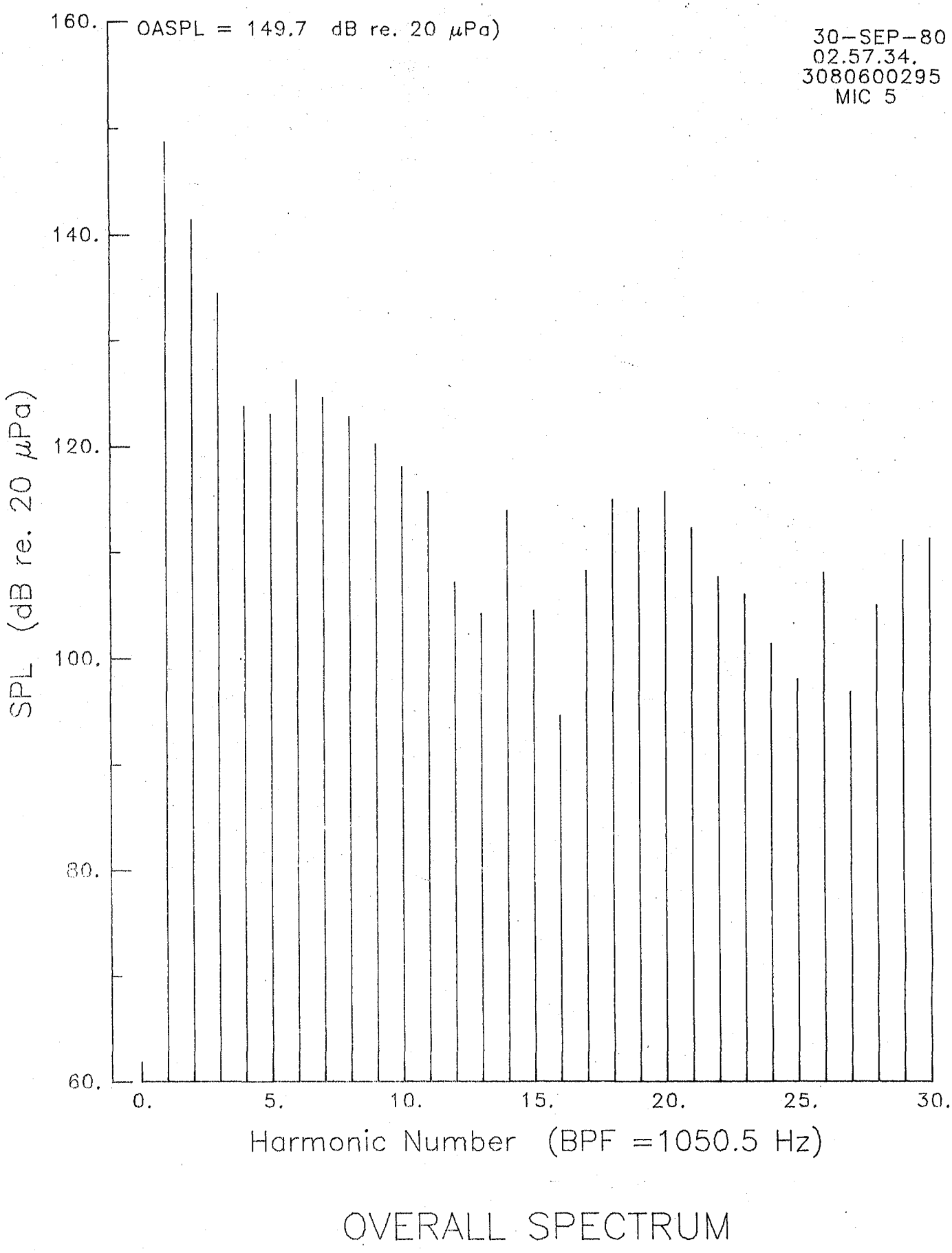

Figure 9(c).- Concluded.

F. Farassat -- P. Nystrom
JIAFS -- NASA/LaRC -- GWU

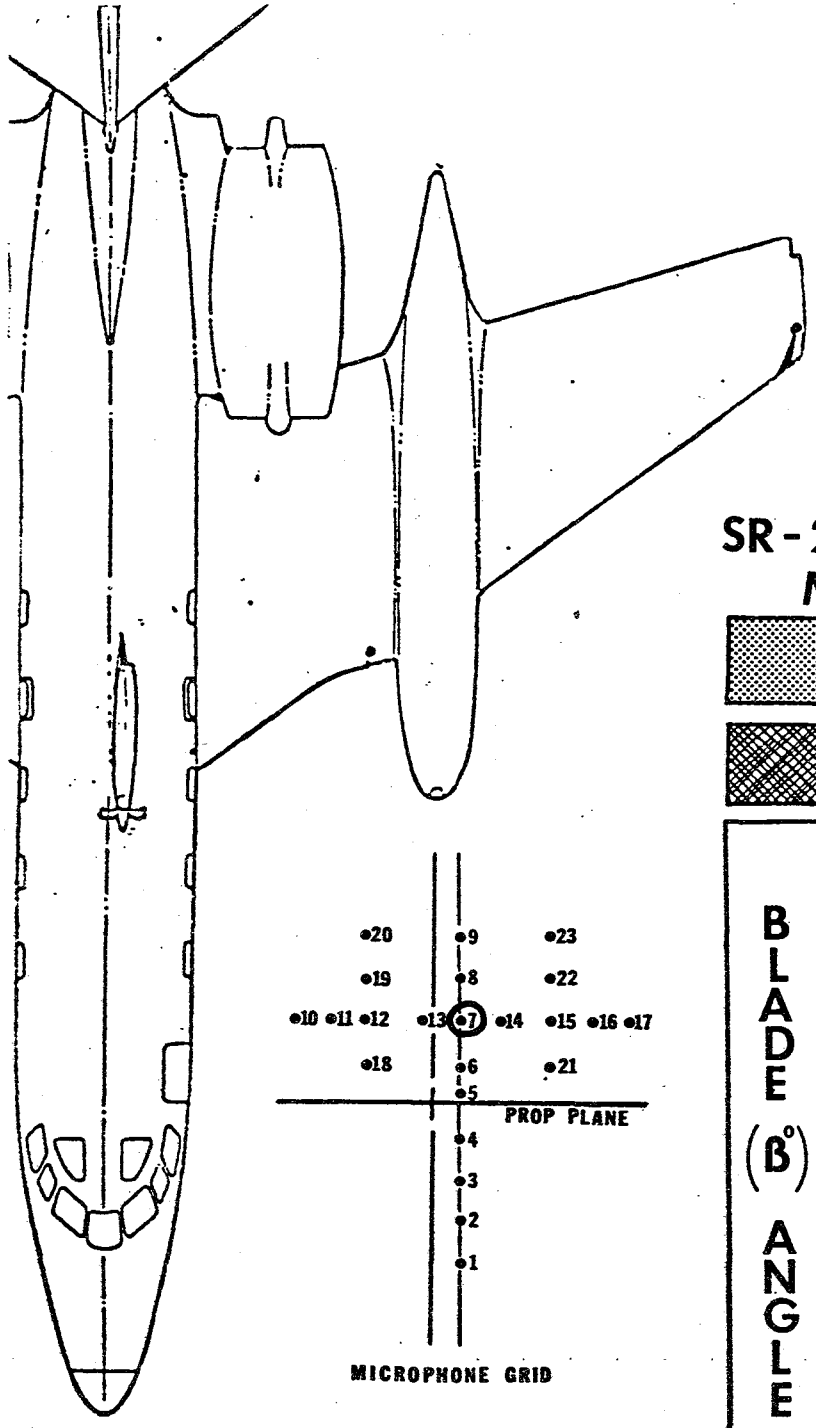

Figure 9(d).- Continued.

SR-2 TEST MATRIX

EXCEEDS BLEED SYS. POWER CAPACITY

BLADE CRITICAL SPEED

BLADE ANGLE (β°)	ADVANCE RATIO (J)	ALTITUDE (FT) 20,000 — MACH # .50	.60	.65	.70	.75	.80	ALTITUDE (FT) 25,000 — MACH # .50	.60	.65	.70	.75	80	ALTITUDE (FT) 30,000 — MACH # .50	.60	66	.70	.75	.80
59.0	4.30																		
	3.50																		
	3.25																		
	3.06																		
	2.90																		
60.0	4.30																		X
	3.50																		X
	3.25																		X
	3.06																		X
	2.95																		X
61.0	4.30																		
	4.07																		
	3.50																		
	3.25																		

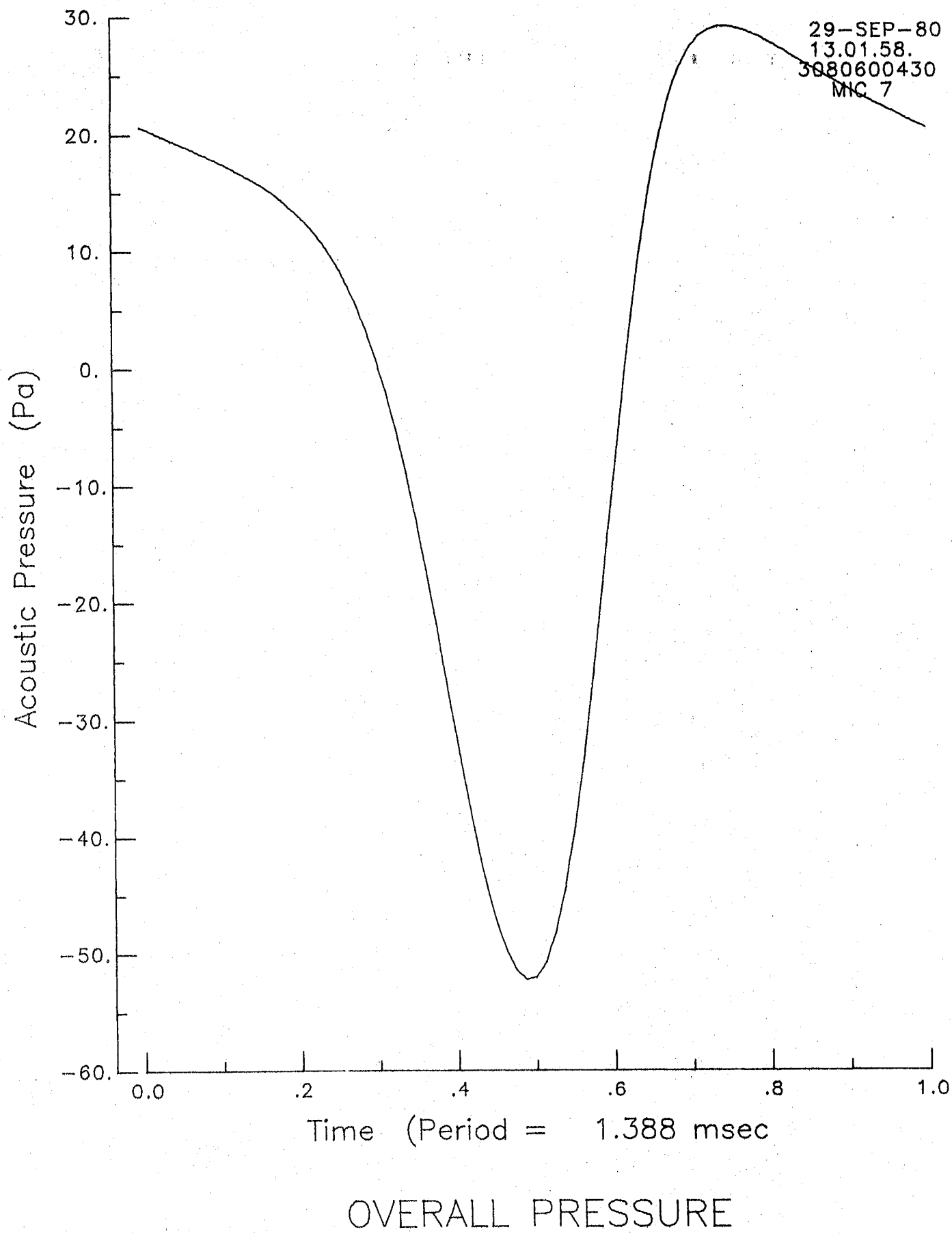

Figure 9(d).- Continued.

F. Farassat -- P. Nystrom
JIAFS -- NASA/LaRC -- GWU

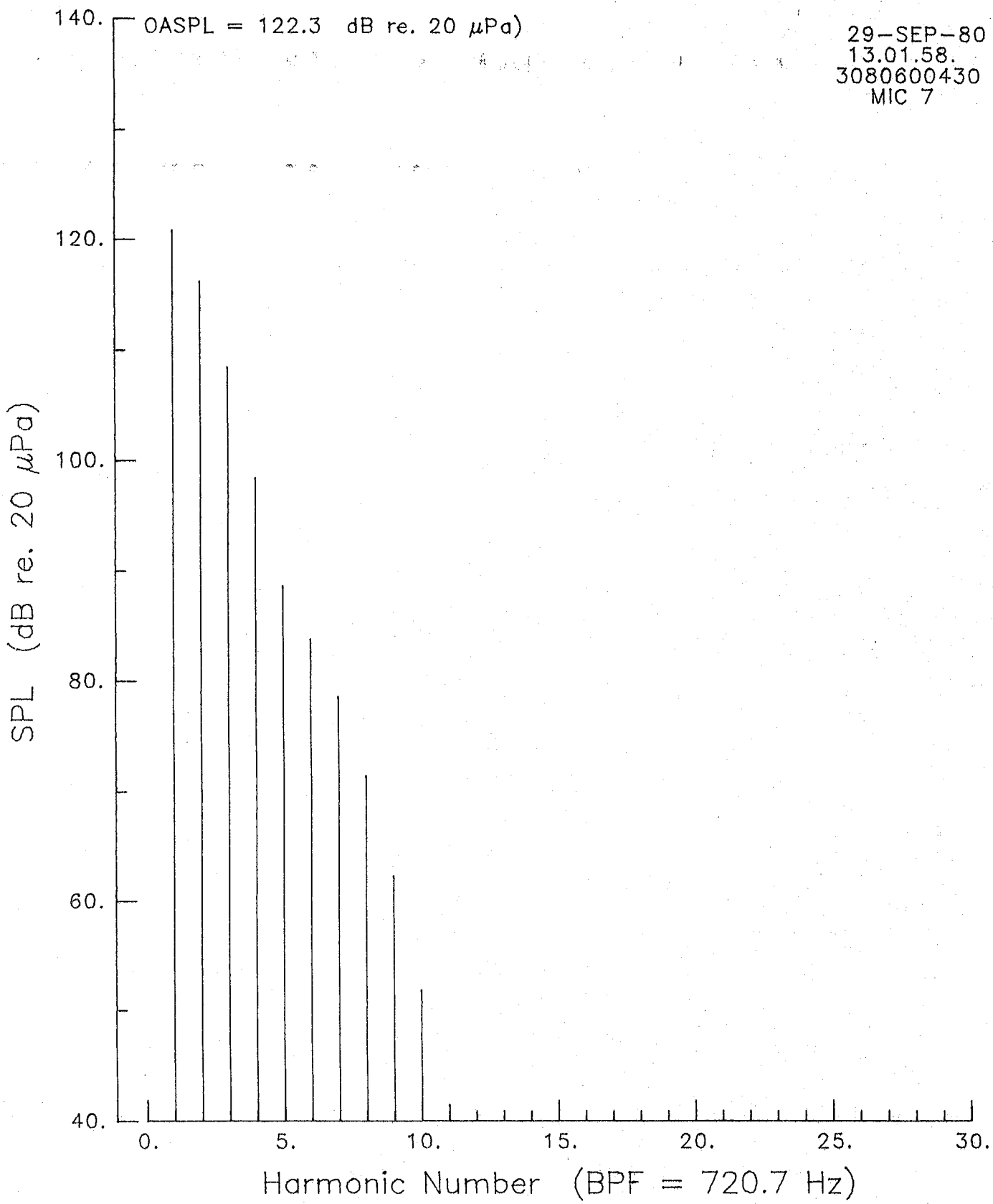

Figure 9(d).- Continued.

F. Farassat -- P. Nystrom
JIAFS -- NASA/LaRC -- GWU

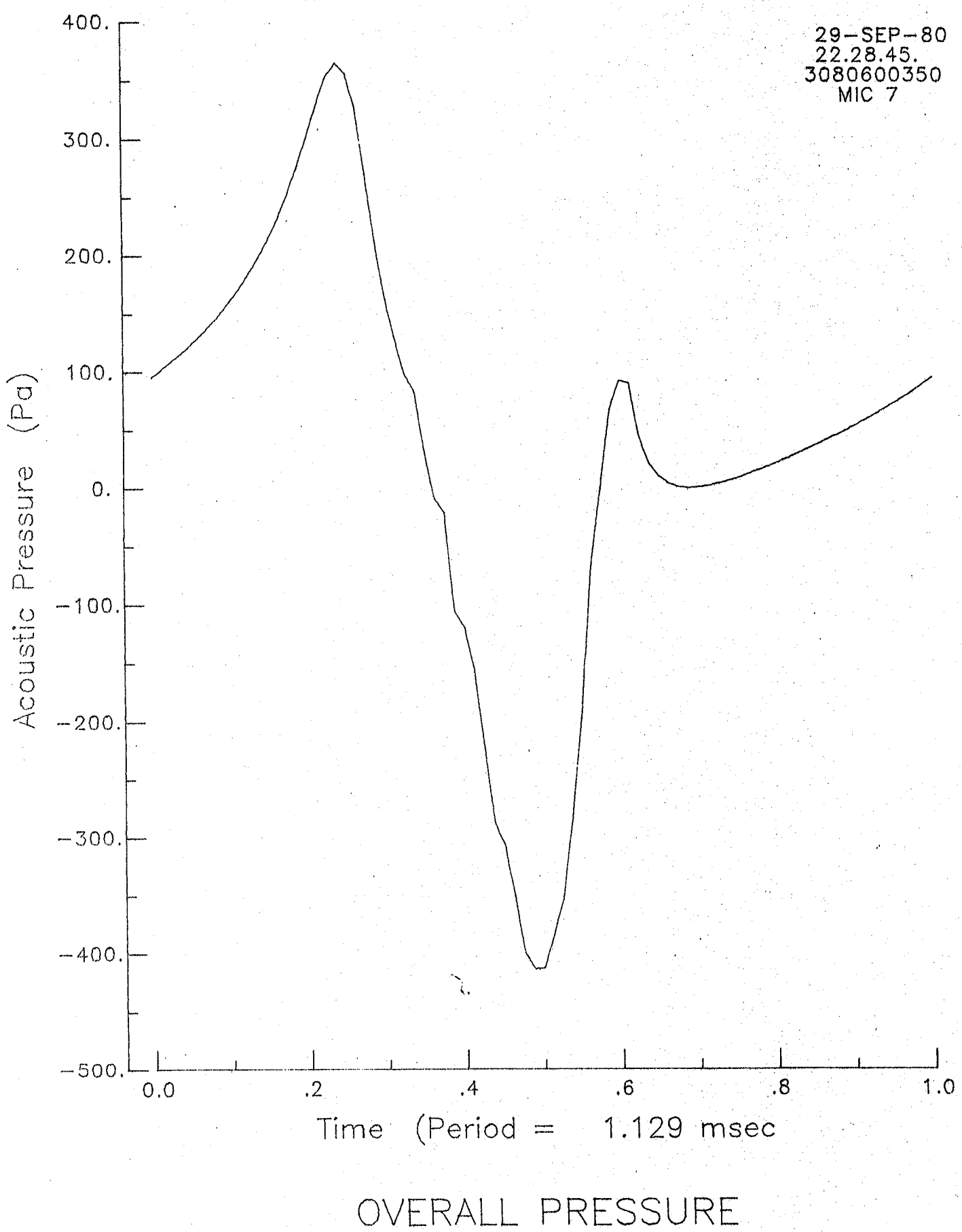

Figure 9(d).- Continued.

F. Farassat -- P. Nystrom
JIAFS -- NASA/LaRC -- GWU

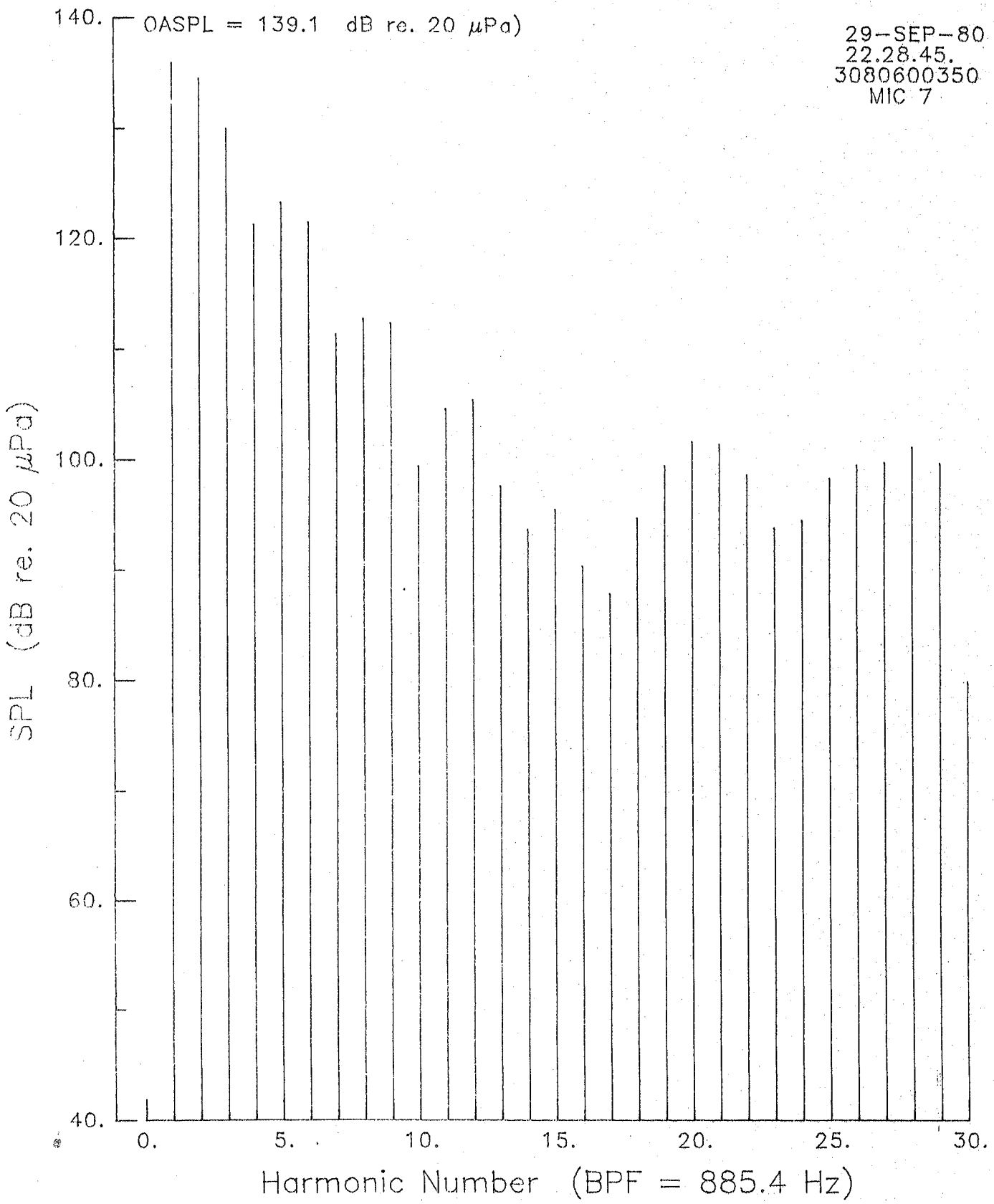

OVERALL SPECTRUM

Figure 9(d).- Continued.

F. Farassat -- P. Nystrom
JIAFS -- NASA/LaRC -- GWU

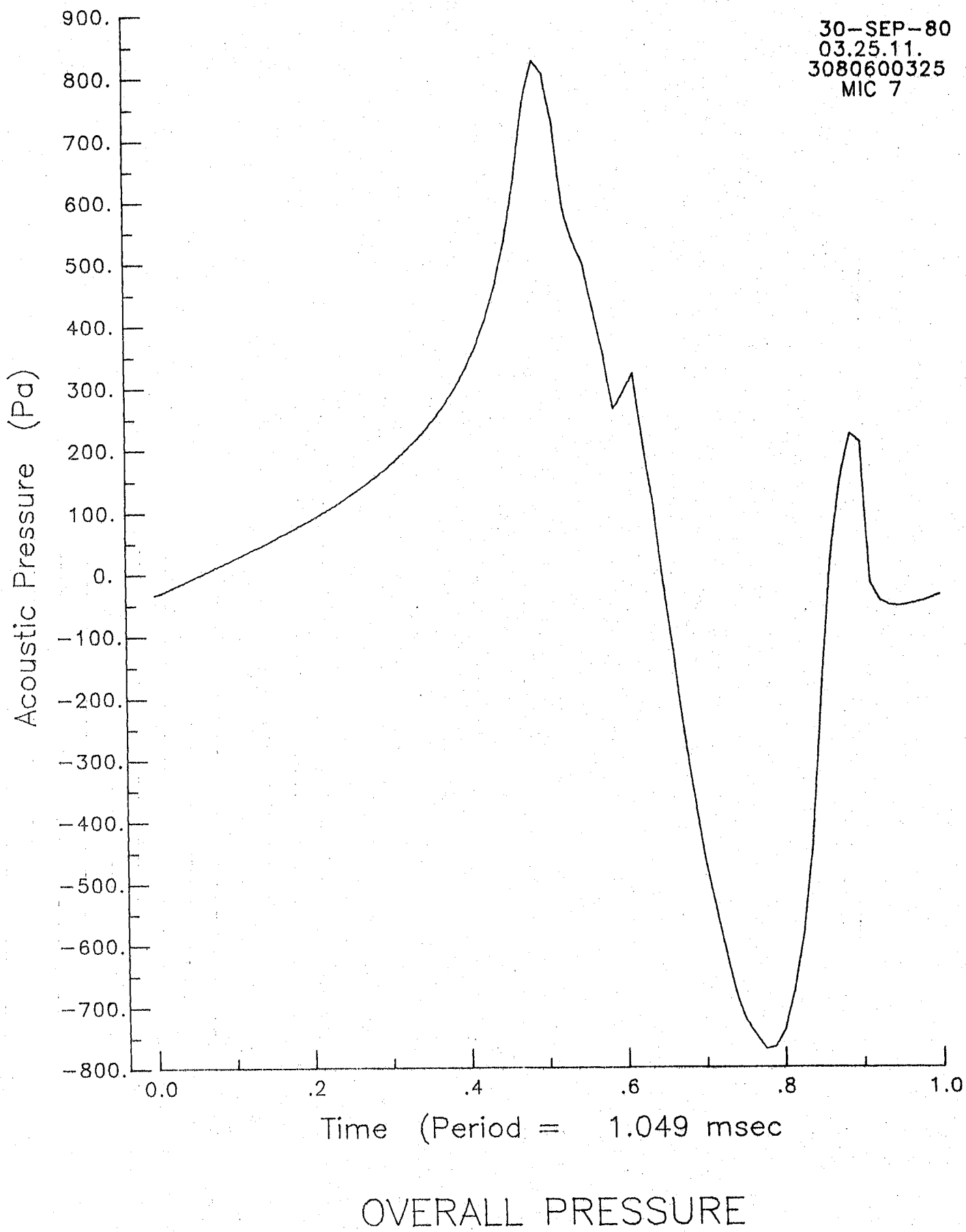

Figure 9(d).- Continued.

F. Farassat -- P. Nystrom
JIAFS -- NASA/LaRC -- GWU

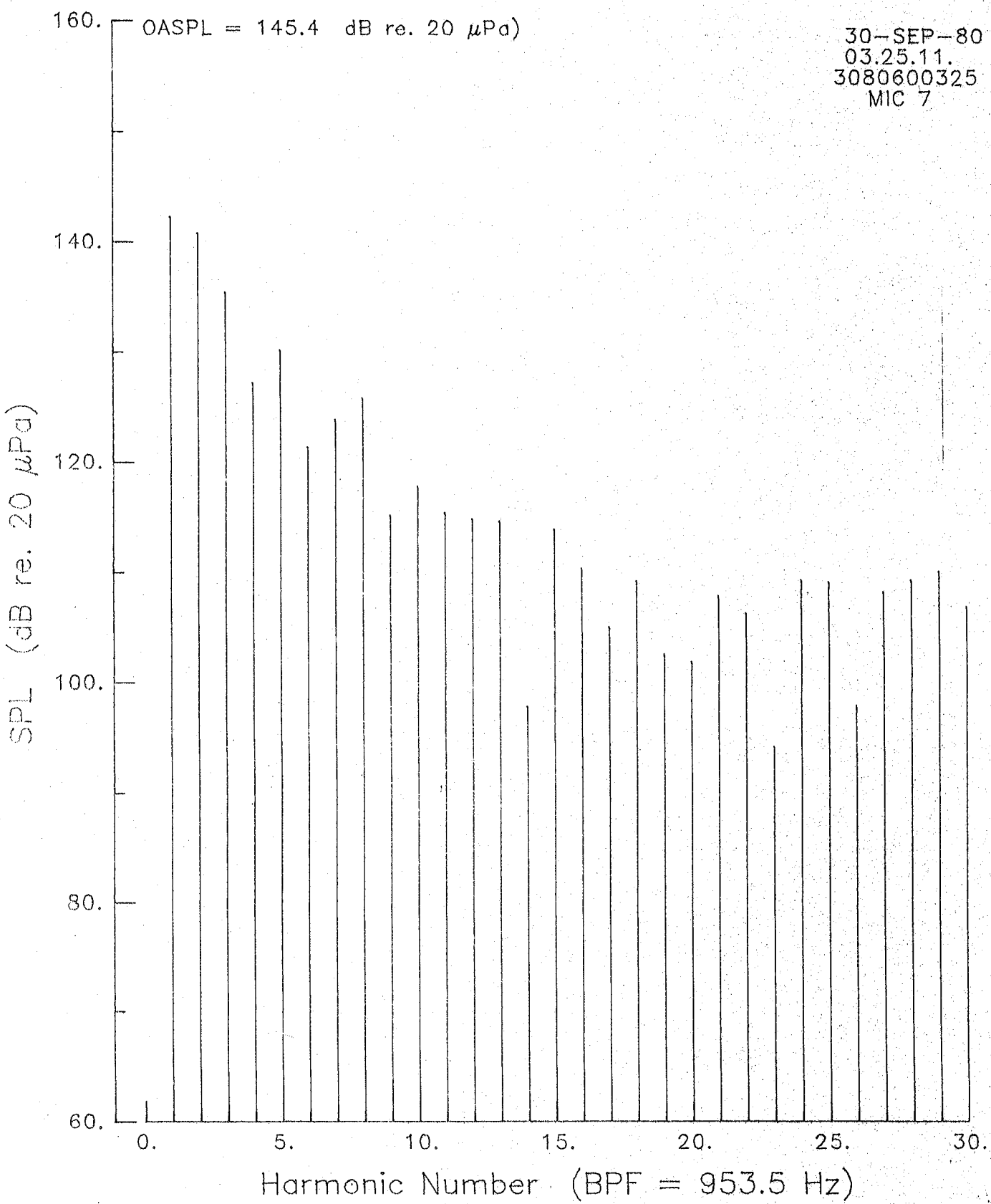

OVERALL SPECTRUM

Figure 9(d).- Continued.

F. Farassat -- P. Nystrom
JIAFS -- NASA/LaRC -- GWU

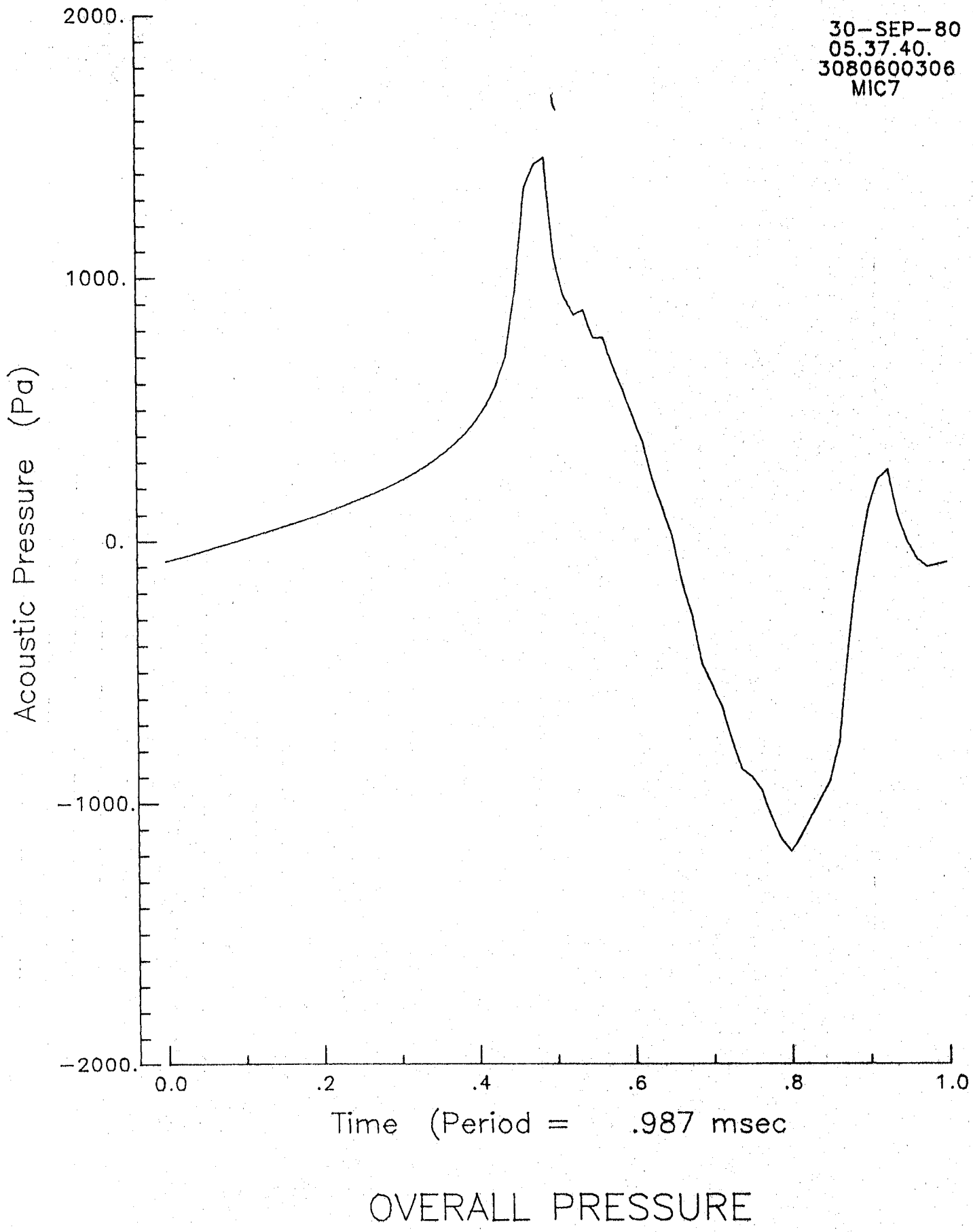

Figure 9(d).- Continued.

F. Farassat -- P. Nystrom
JIAFS -- NASA/LaRC -- GWU

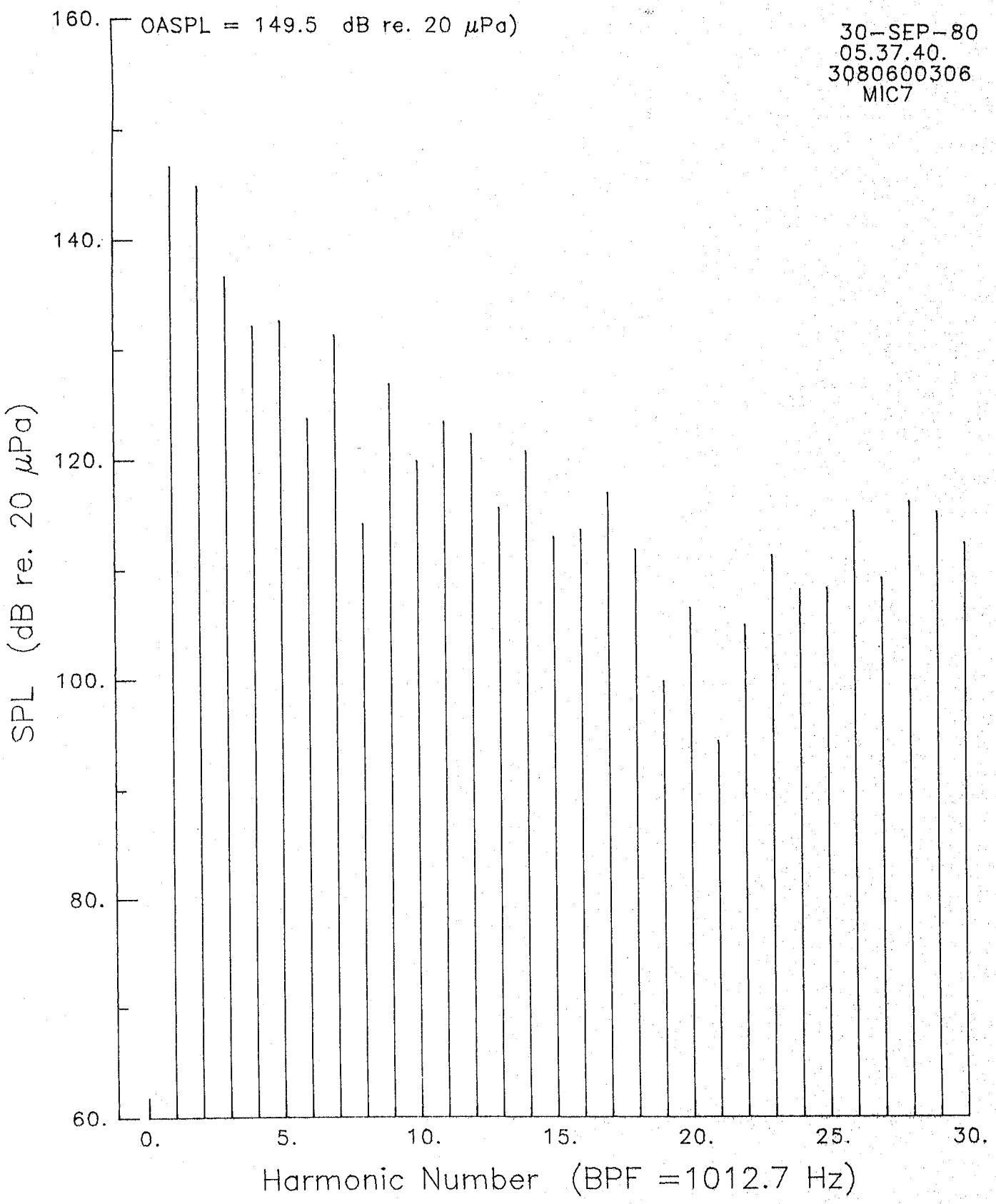

Figure 9(d).- Continued.

F. Farassat -- P. Nystrom
JIAFS -- NASA/LaRC -- GWU

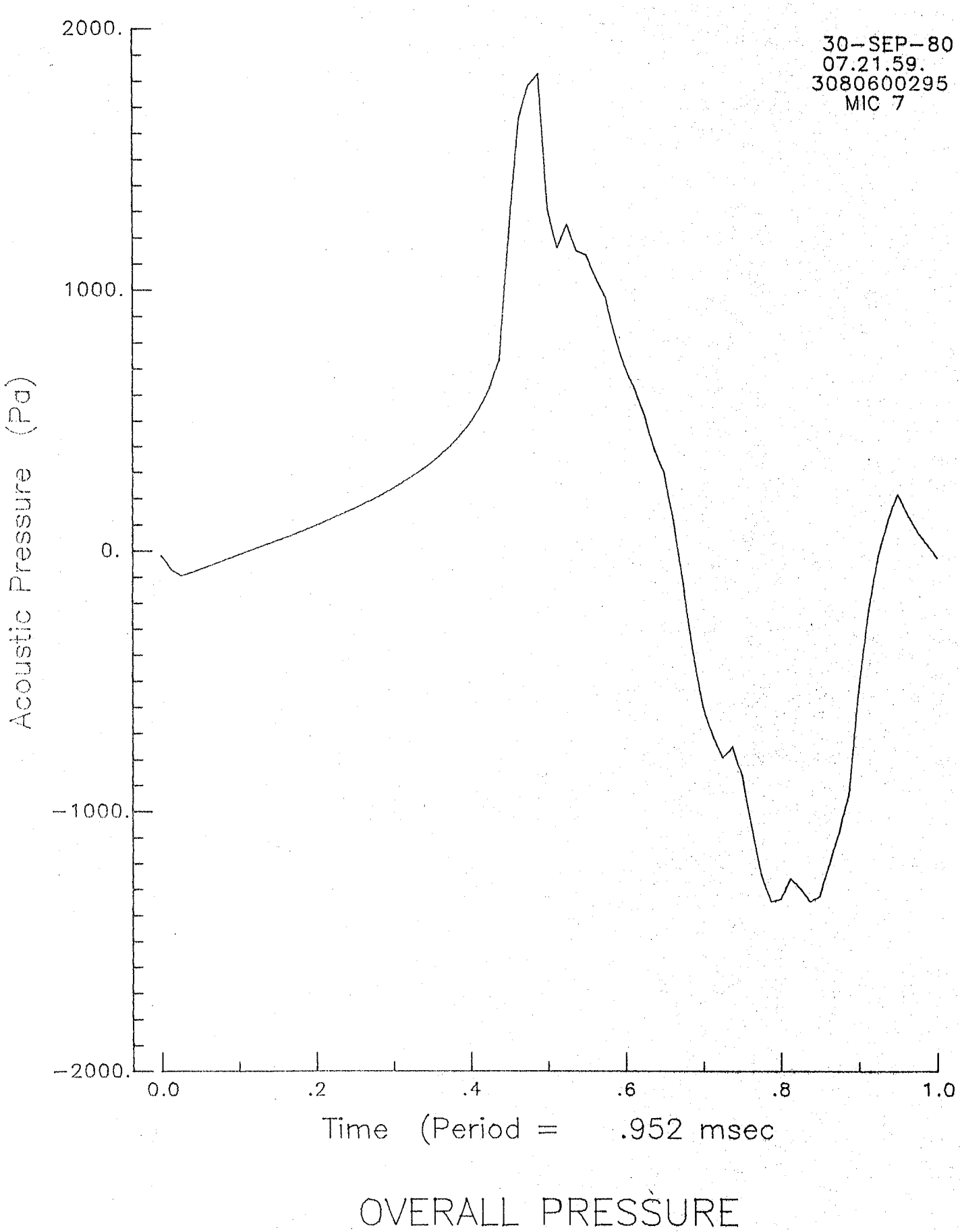

Figure 9(d).- Continued.

F. Farassat -- P. Nystrom
JIAFS -- NASA/LaRC -- GWU

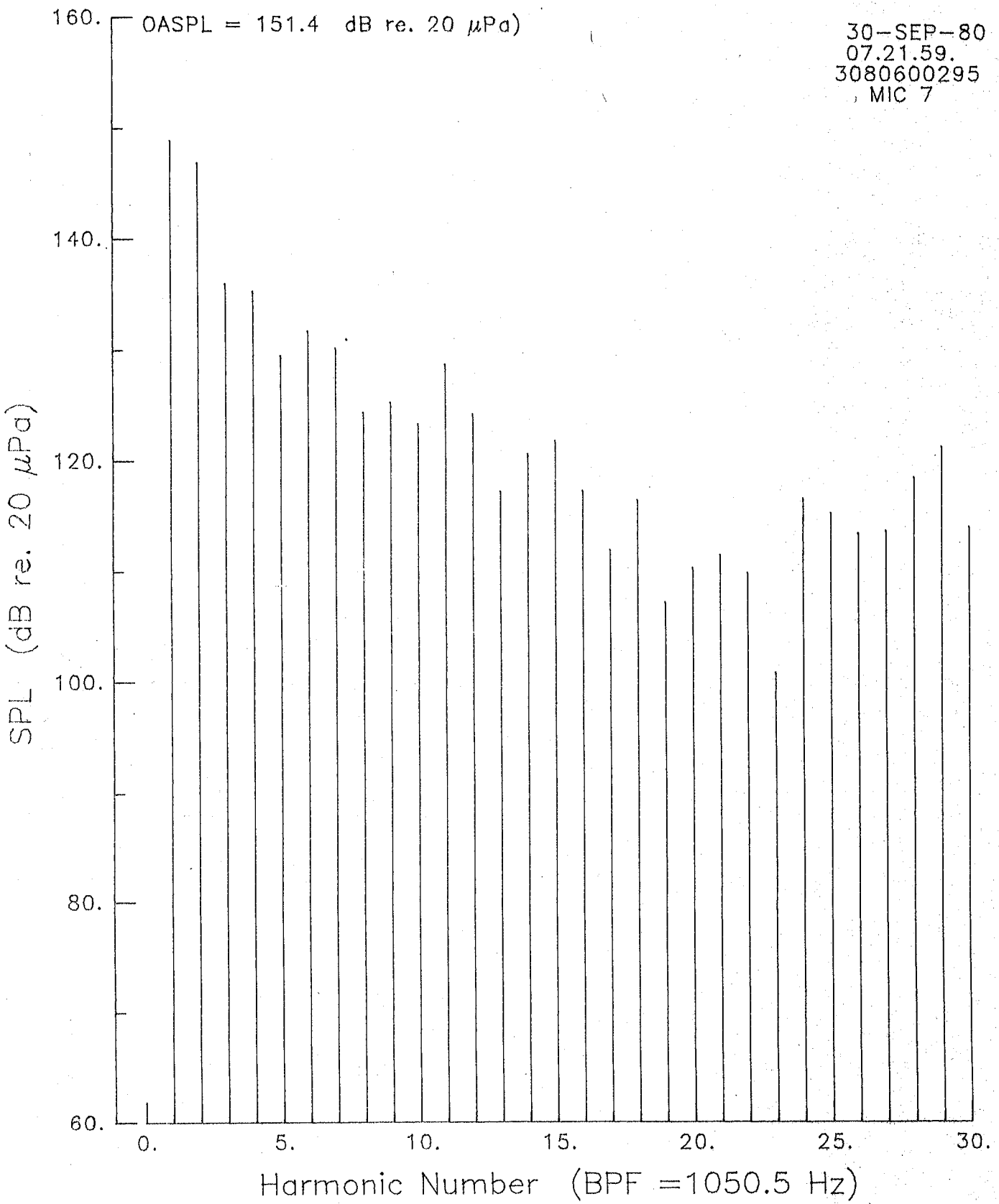

Figure 9(d).- Concluded.

F. Farassat -- P. Nystrom
JIAFS -- NASA/LaRC -- GWU

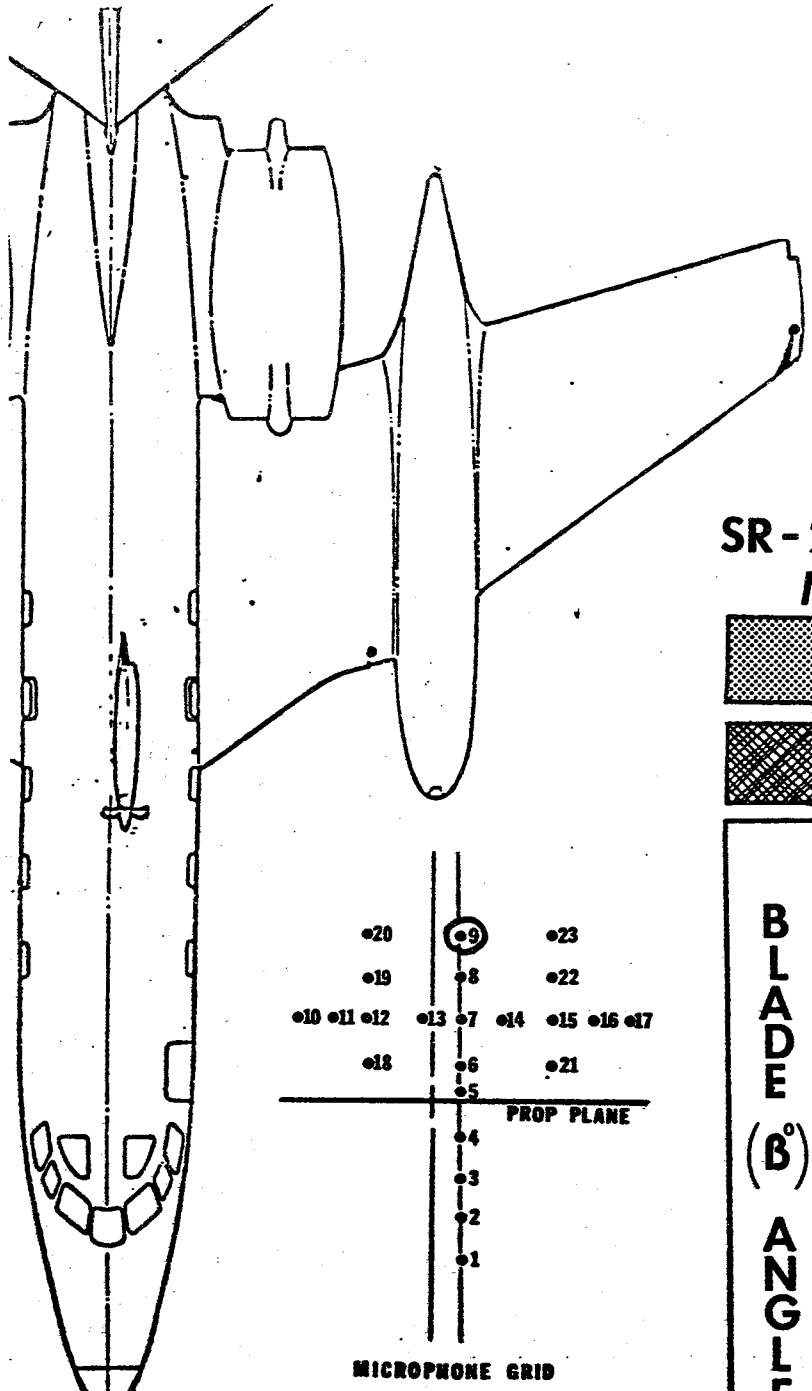

Figure 9(e).- Continued.

SR-2 TEST MATRIX

EXCEEDS BLEED SYS. POWER CAPACITY

BLADE CRITICAL SPEED

BLADE ANGLE (β°)	ADVANCE RATIO (J)	ALTITUDE (FT) 20,000 MACH # .50	.60	.65	.70	.75	.80	ALTITUDE (FT) 25,000 MACH # .50	.60	.65	.70	.75	.80	ALTITUDE (FT) 30,000 MACH # .50	.60	.65	.70	.75	.80
59.0	4.30																		
	3.50																		
	3.25																		
	3.06																		
	2.90																		
60.0	4.30																		X
	3.50																		X
	3.25																		X
	3.06																		X
	2.95																		X
61.0	4.30																		
	4.07																		
	3.50																		
	3.25																		

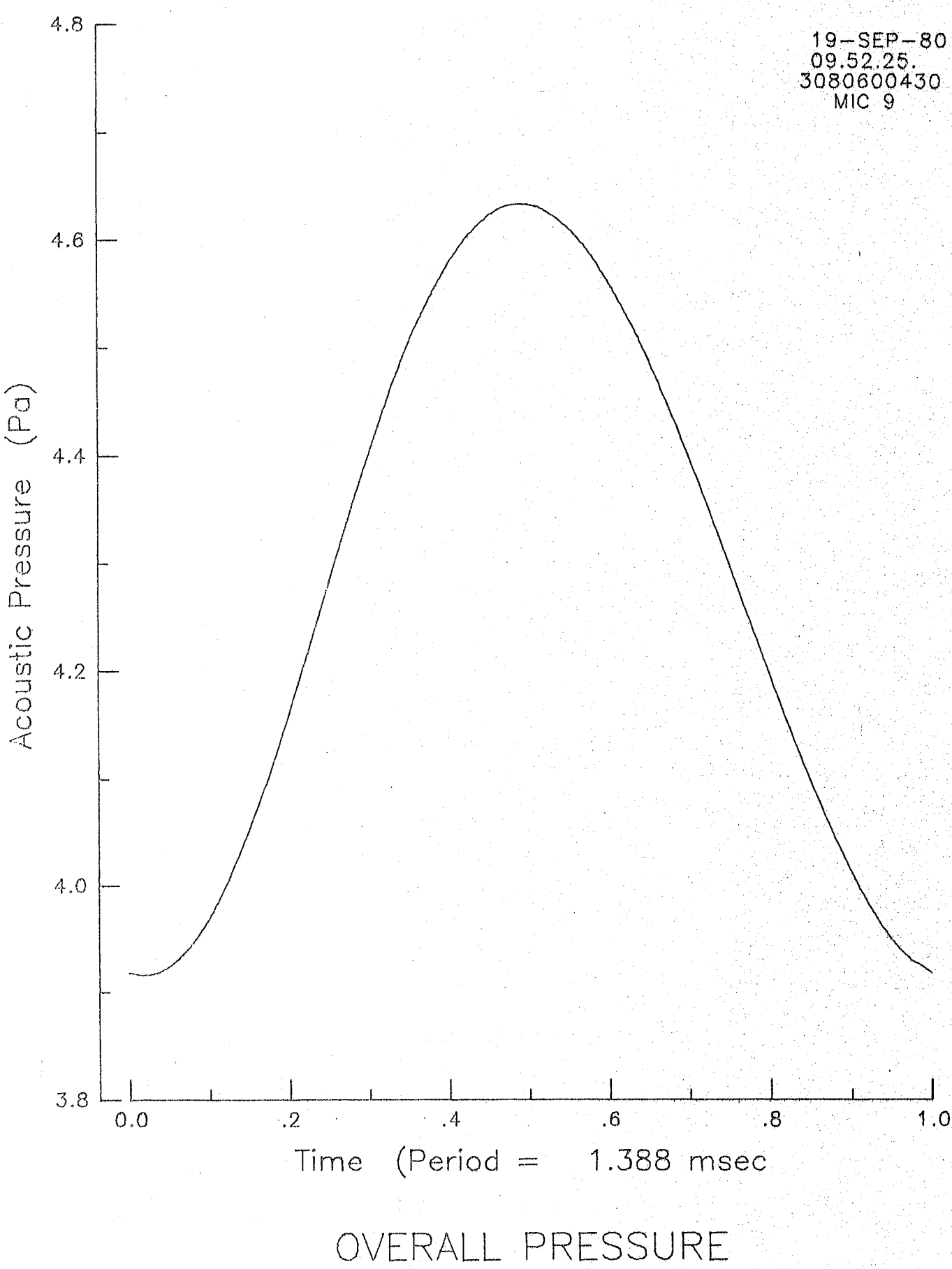

Figure 9(e).- Continued.

F. Farassat -- P. Nystrom
JIAFS -- NASA/LaRC -- GWU

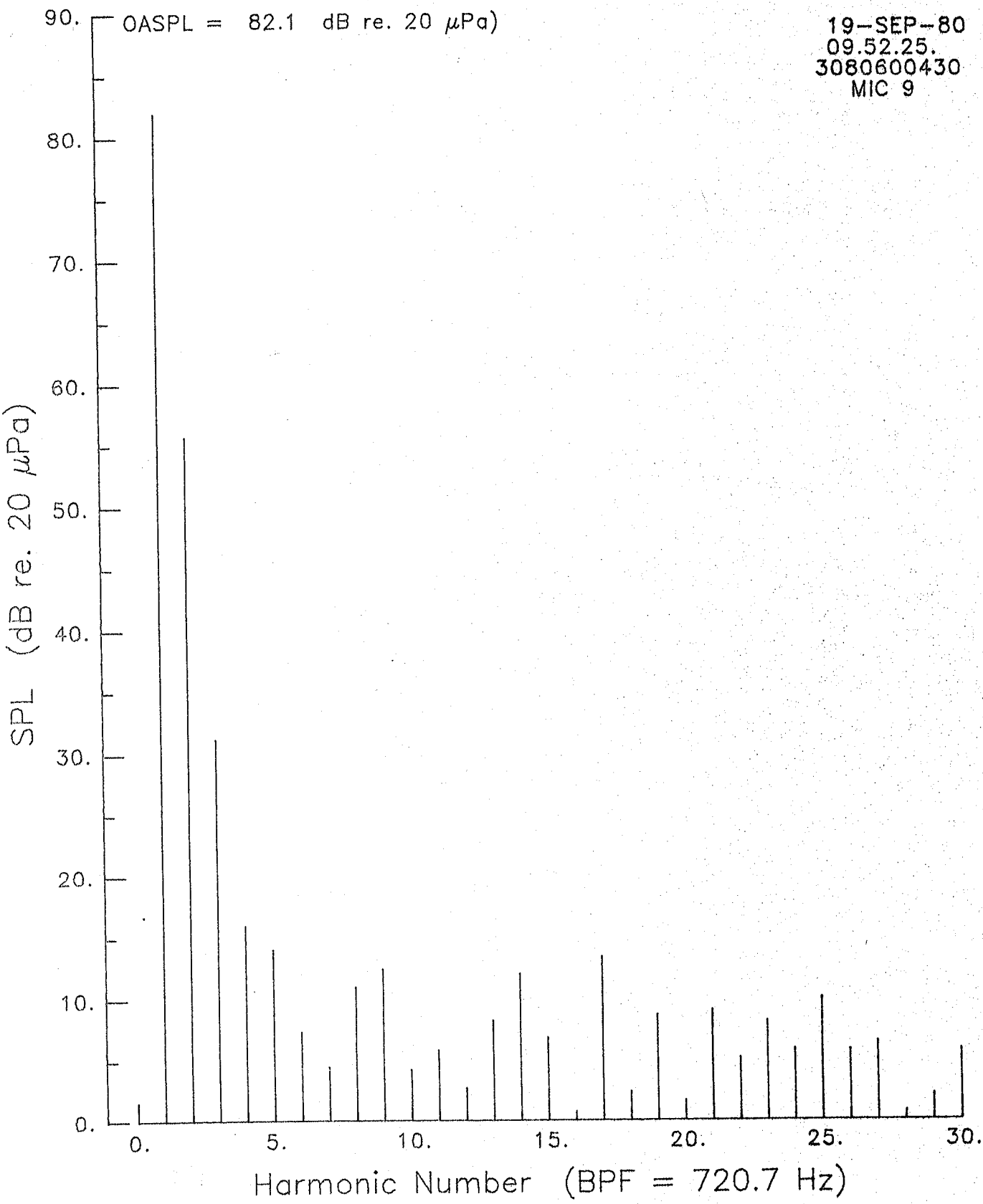

OVERALL SPECTRUM

Figure 9(e).- Continued.

F. Farassat -- P. Nystrom
JIAFS -- NASA/LaRC -- GWU

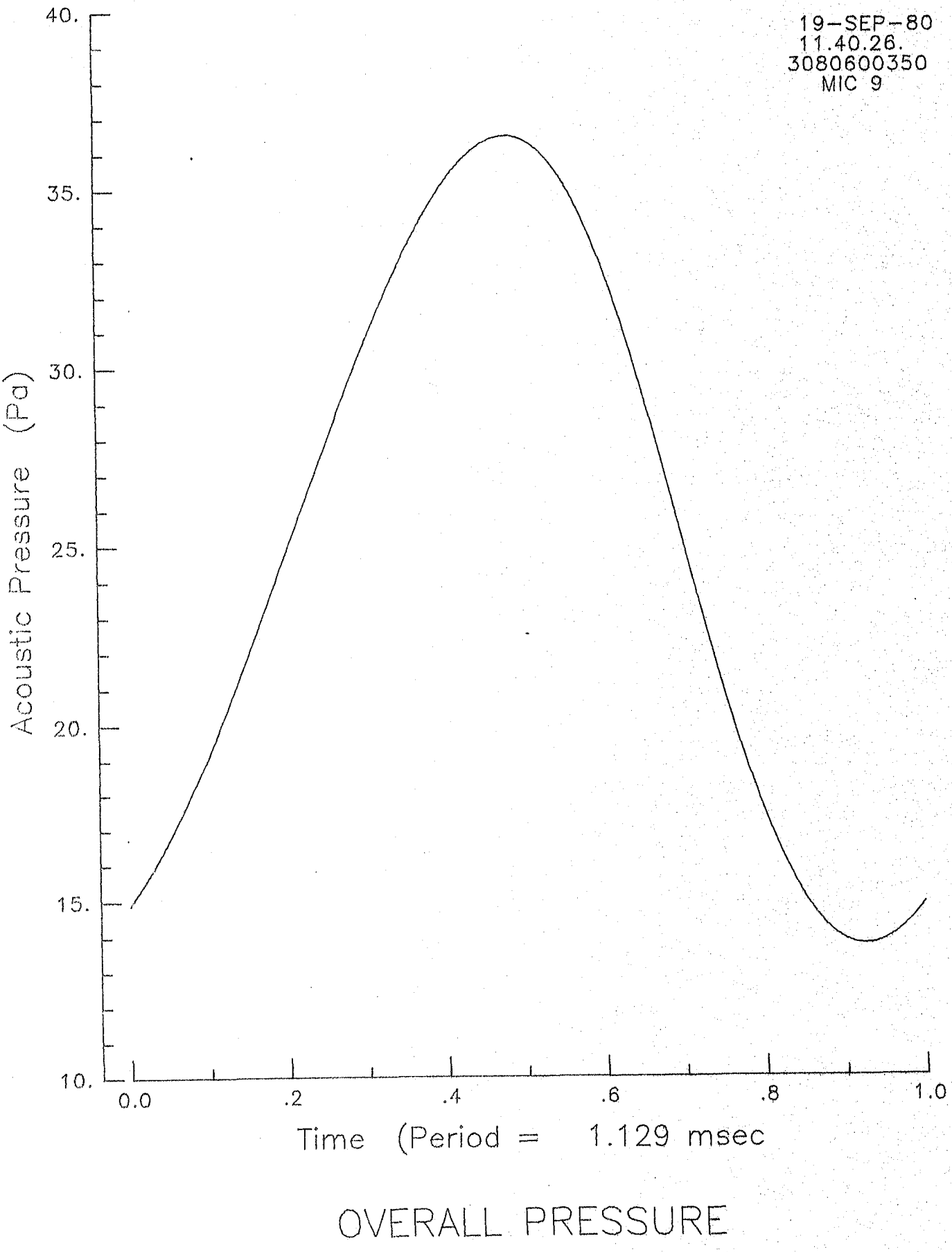

Figure 9(e).- Continued.

F. Farassat -- P. Nystrom
JIAFS -- NASA/LaRC -- GWU

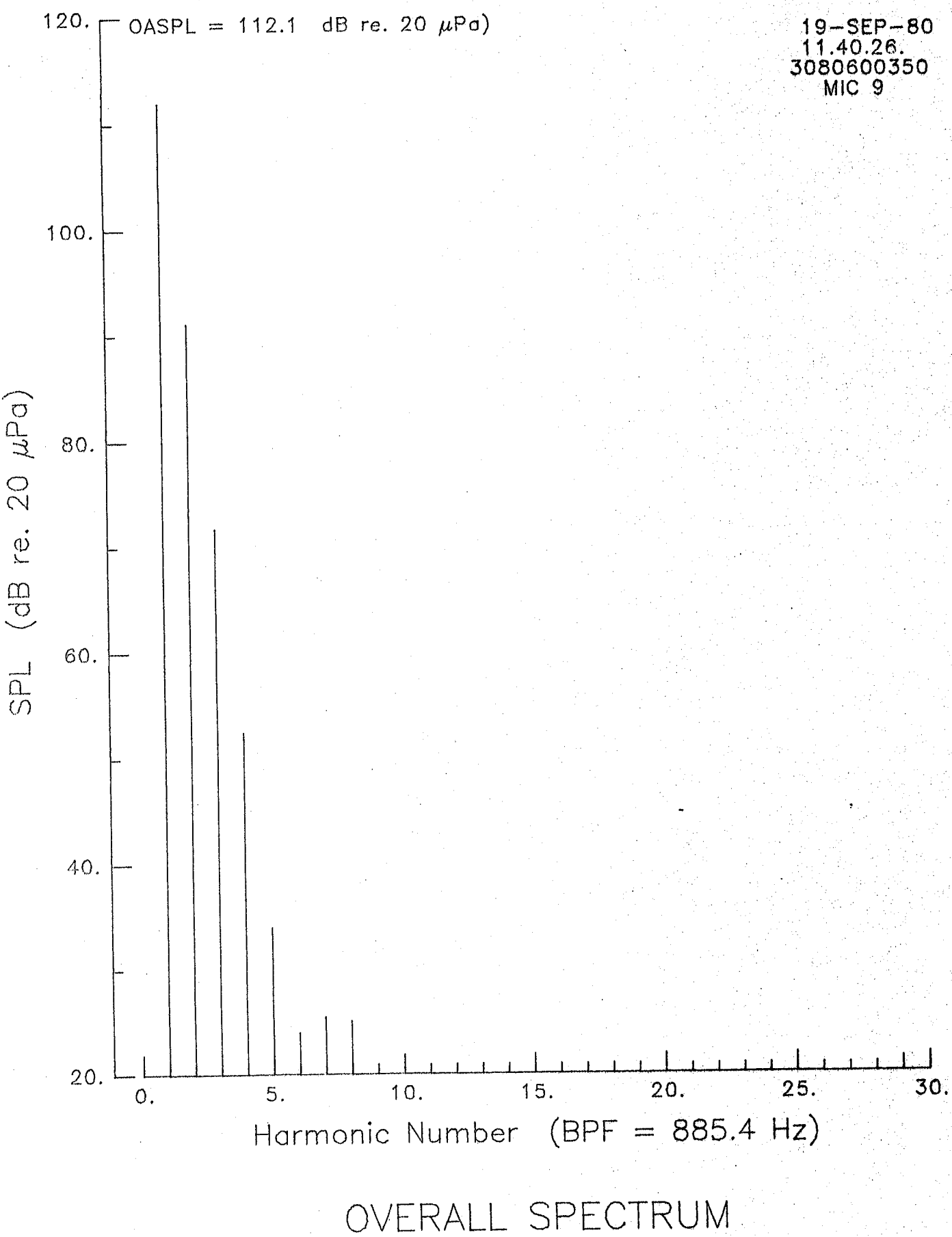

Figure 9(e).- Continued.

F. Farassat -- P. Nystrom
JIAFS -- NASA/LaRC -- GWU

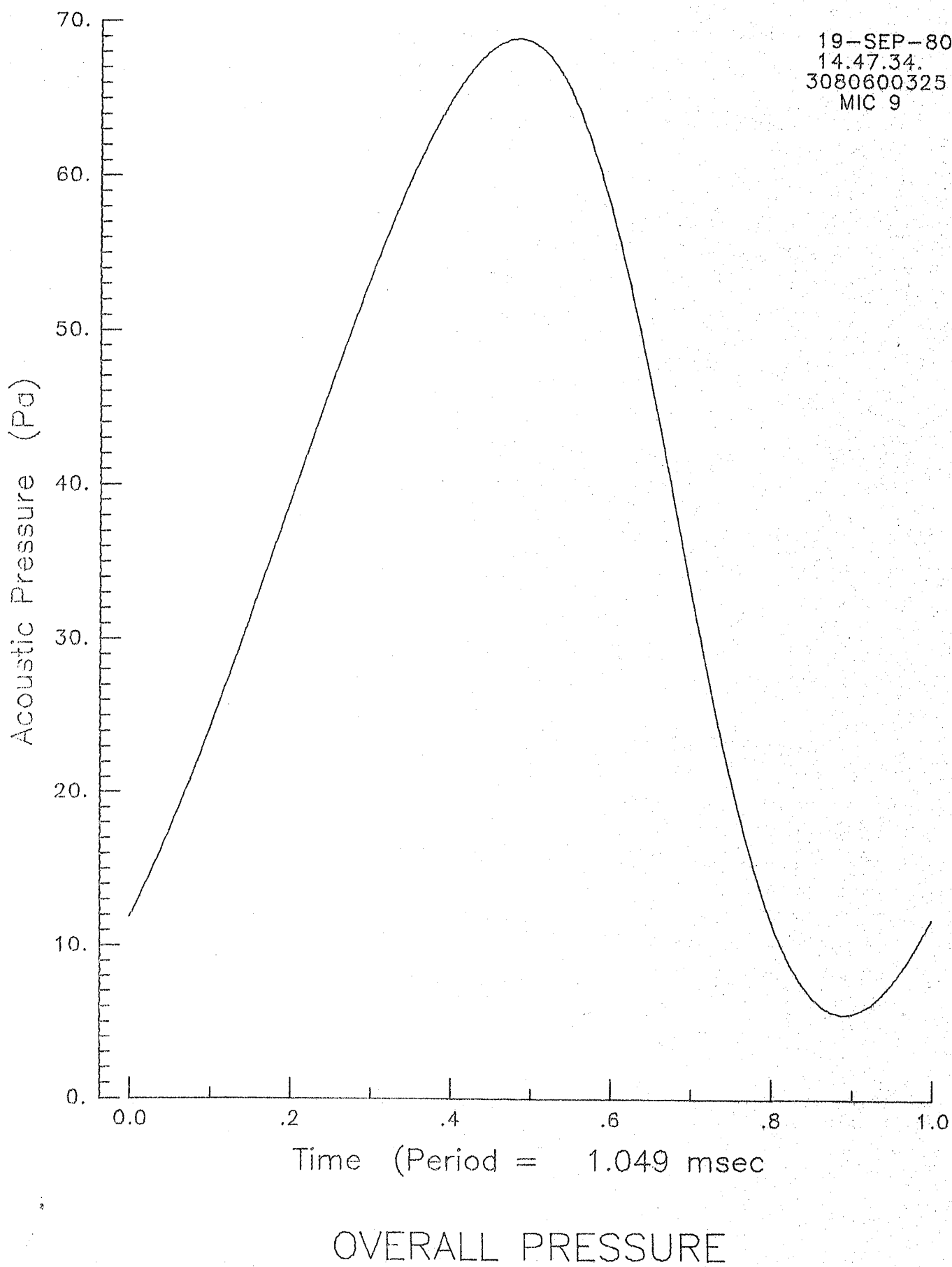

Figure 9(e).- Continued.

F. Farassat -- P. Nystrom
JIAFS -- NASA/LaRC -- GWU

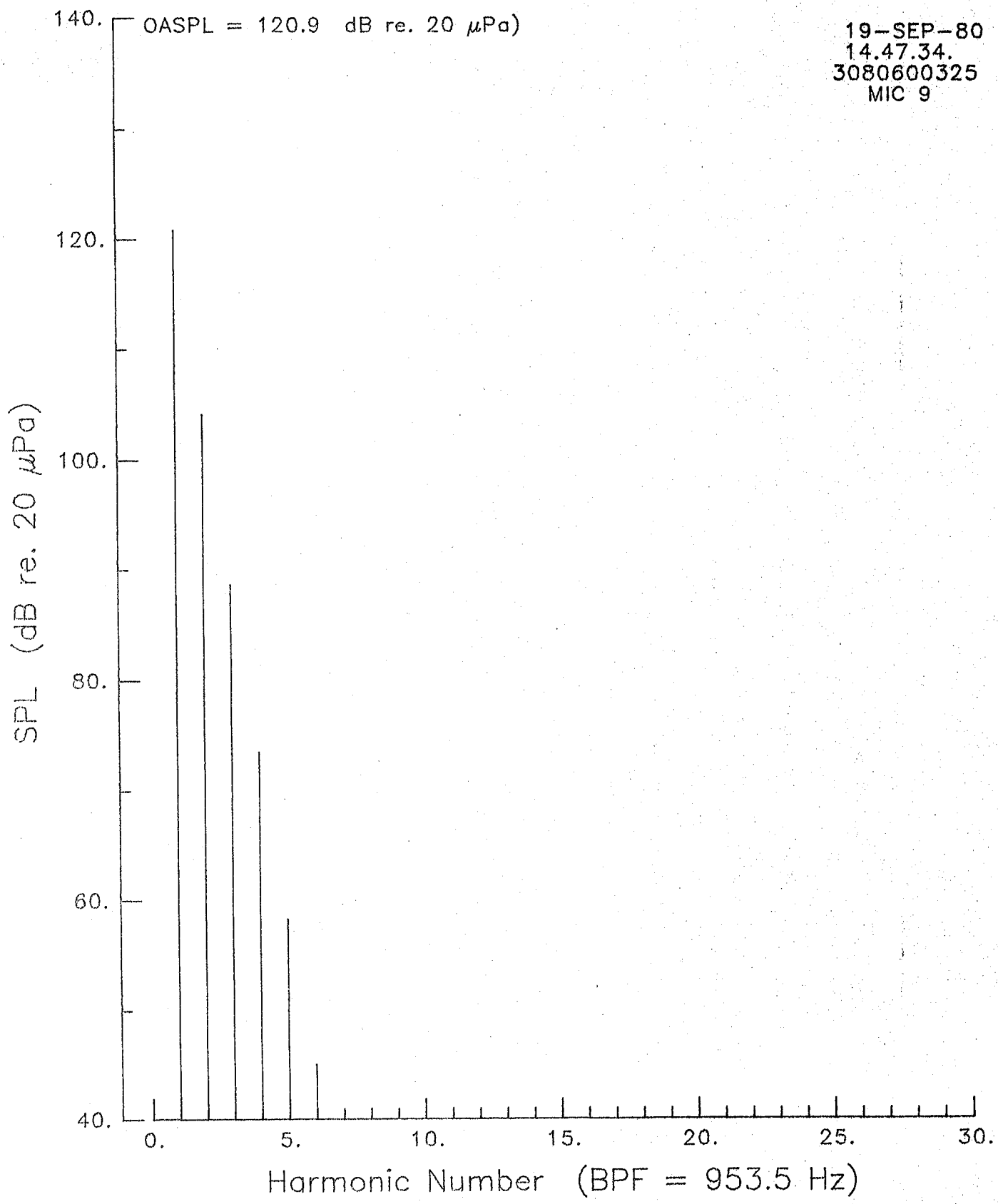

Figure 9(e).- Continued.

F. Farassat -- P. Nystrom
JIAFS -- NASA/LaRC -- GWU

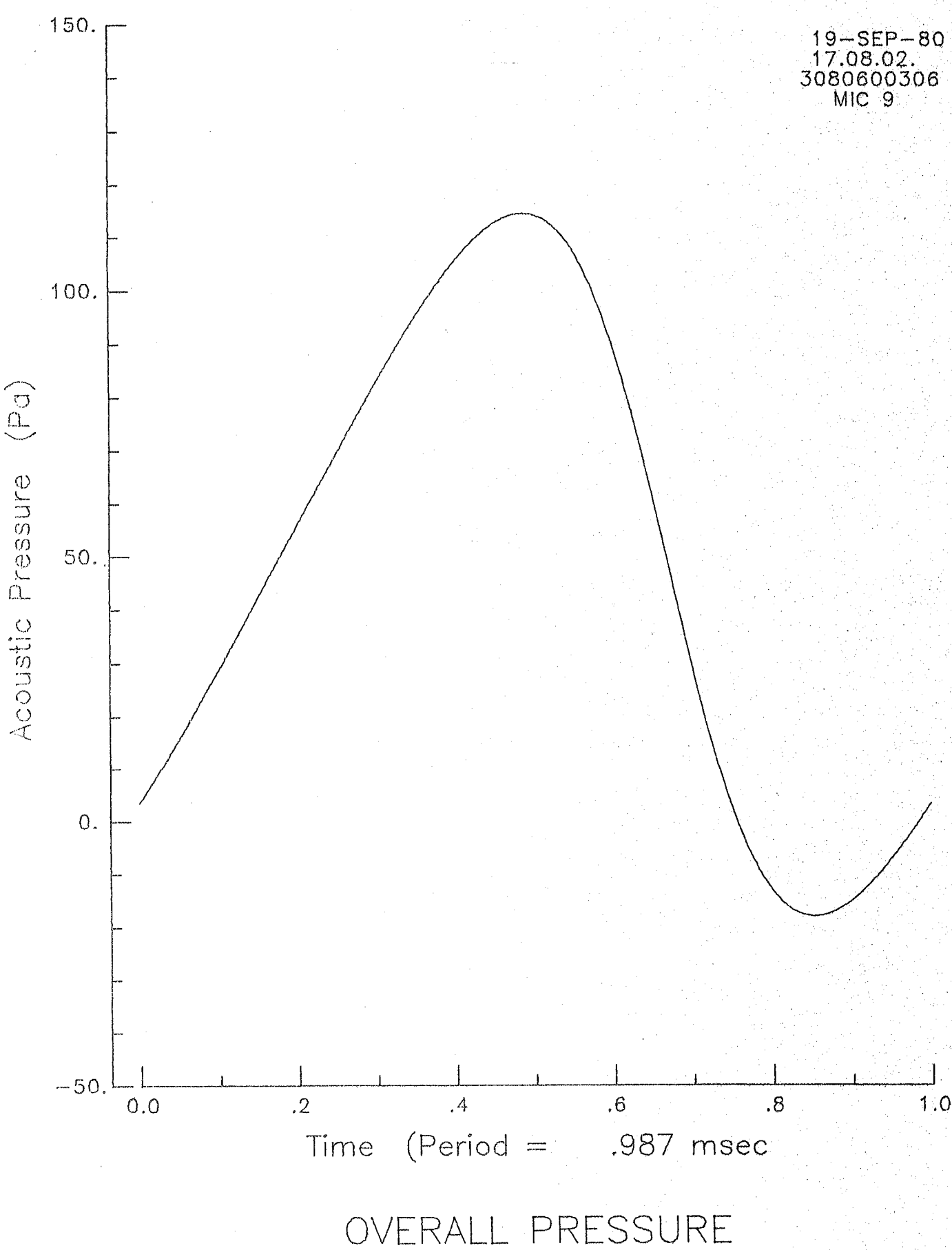

Figure 9(e).- Continued.

F. Farassat -- P. Nystrom
JIAFS -- NASA/LaRC -- GWU

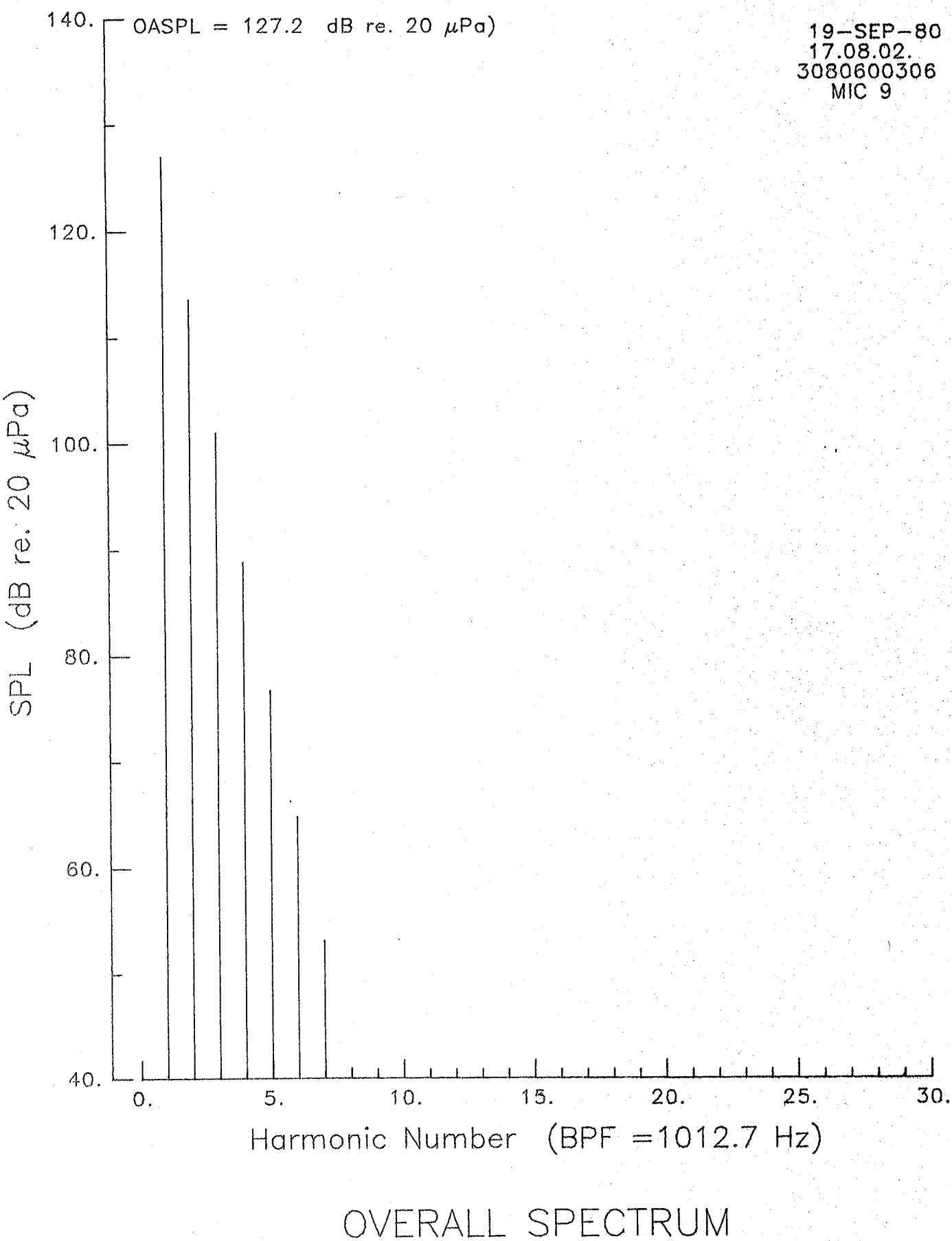

Figure 9(e).- Continued.

F. Farassat -- P. Nystrom
JIAFS -- NASA/LaRC -- GWU

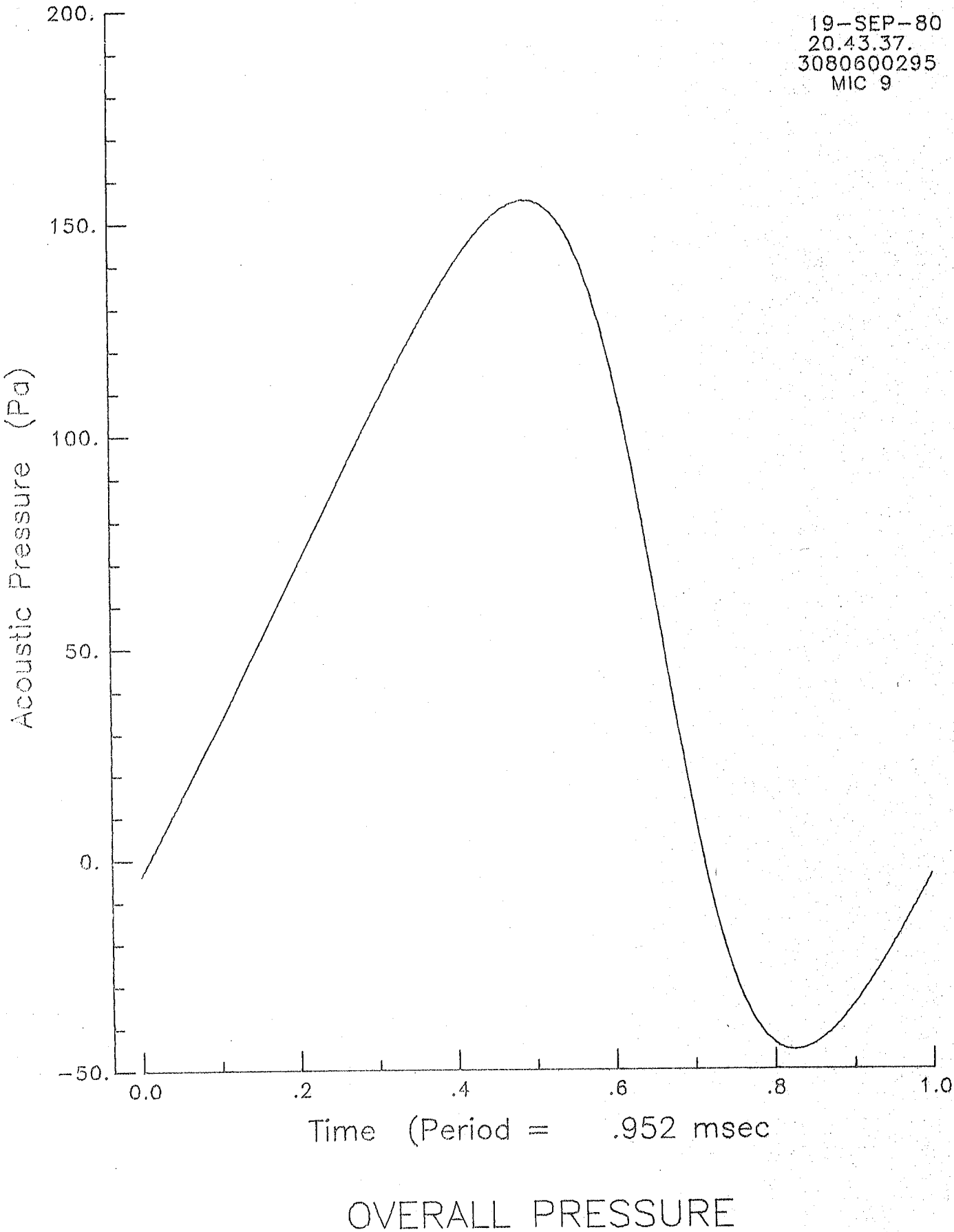

Figure 9(e).- Continued.

F. Farassat -- P. Nystrom
JIAFS -- NASA/LaRC -- GWU

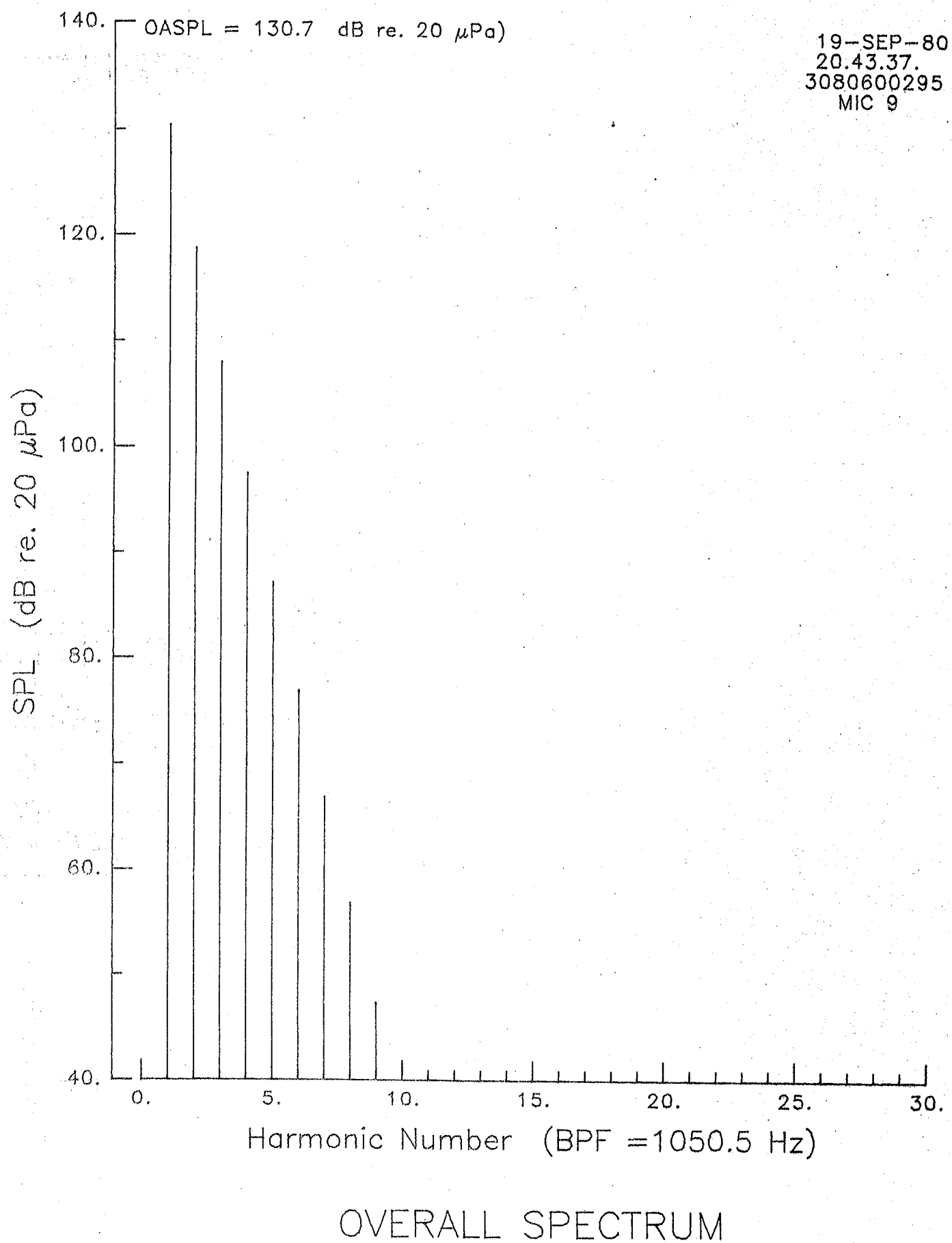

Figure 9(e).- Concluded.

F. Farassat -- P. Nystrom
JIAFS -- NASA/LaRC -- GWU

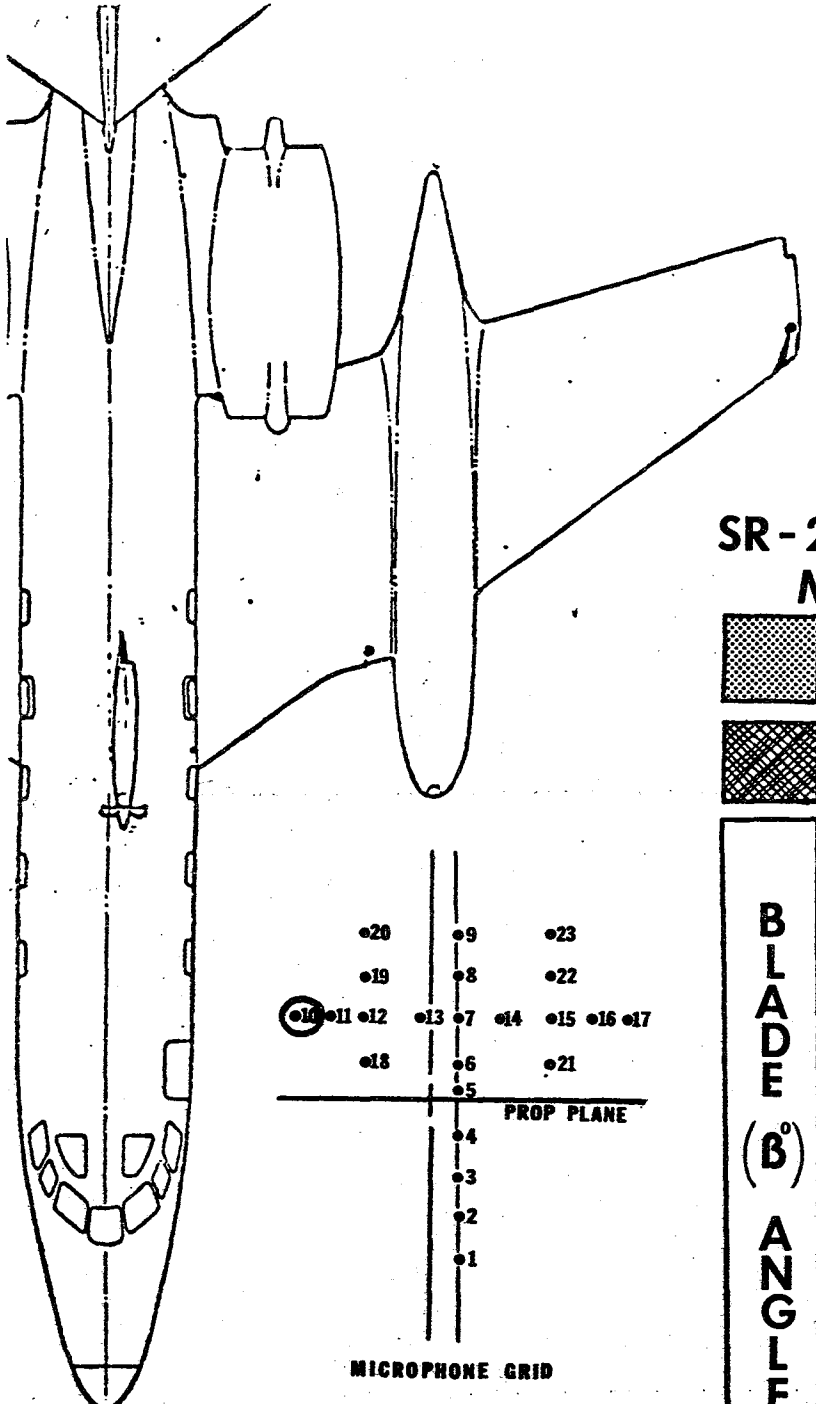

SR-2 TEST MATRIX

EXCEEDS BLEED SYS. POWER CAPACITY

BLADE CRITICAL SPEED

BLADE ANGLE (β°)	ADVANCE RATIO (J)	ALTITUDE (FT) 20,000 — MACH # .50	.60	.65	.70	.75	.80	ALTITUDE (FT) 25,000 — MACH # .50	.60	.65	.70	.75	.80	ALTITUDE (FT) 30,000 — MACH # .50	.60	.65	.70	.75	.80
59.0	4.30																		
	3.50																		
	3.25																		
	3.06																		
	2.90																		
60.0	4.30																		X
	3.50																		X
	3.25																		X
	3.06																		X
	2.95																		X
61.0	4.30																		
	4.07																		
	3.50																		
	3.25																		

Figure 9(f).- Continued.

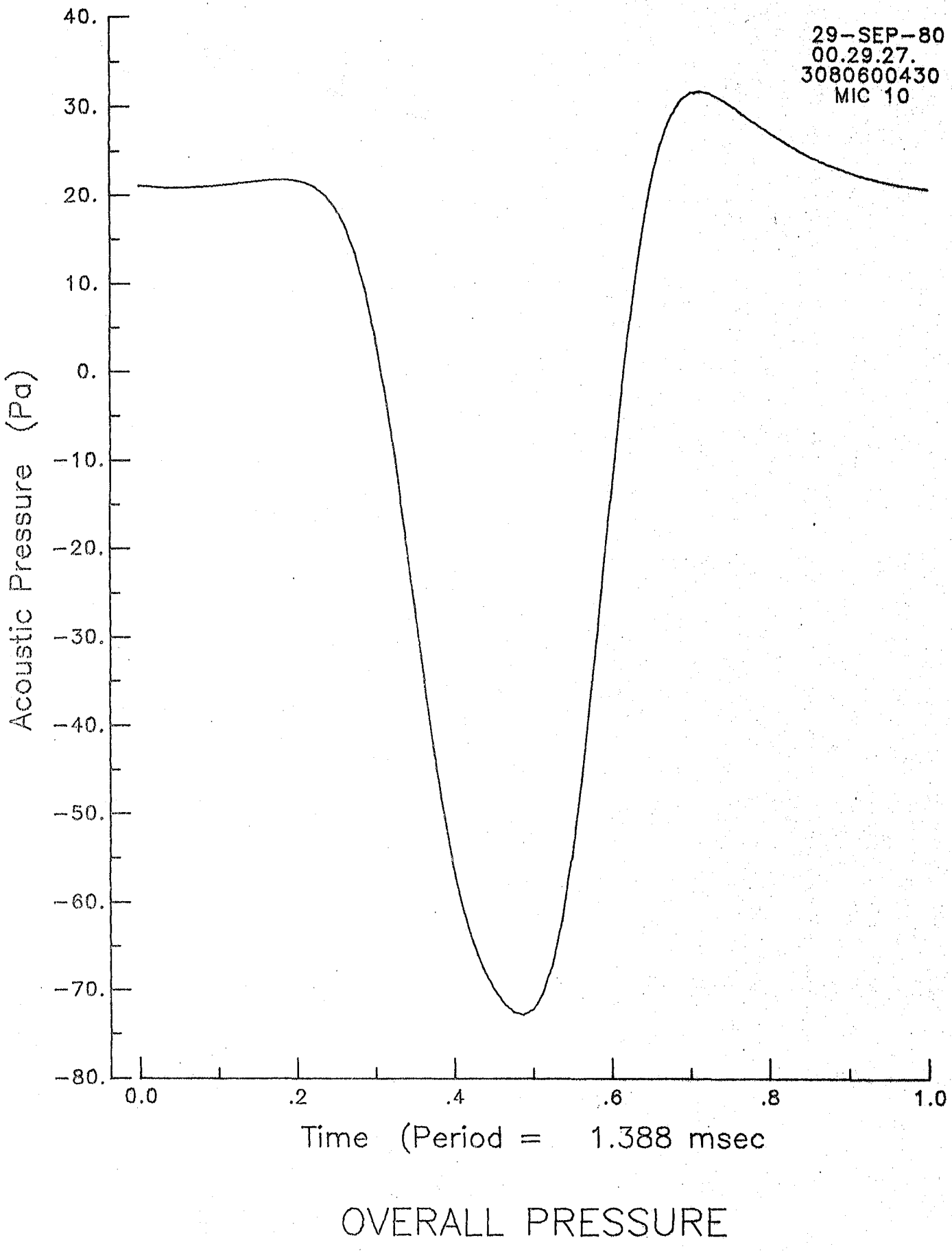

Figure 9(f).- Continued.

F. Farassat -- P. Nystrom
JIAFS -- NASA/LaRC -- GWU

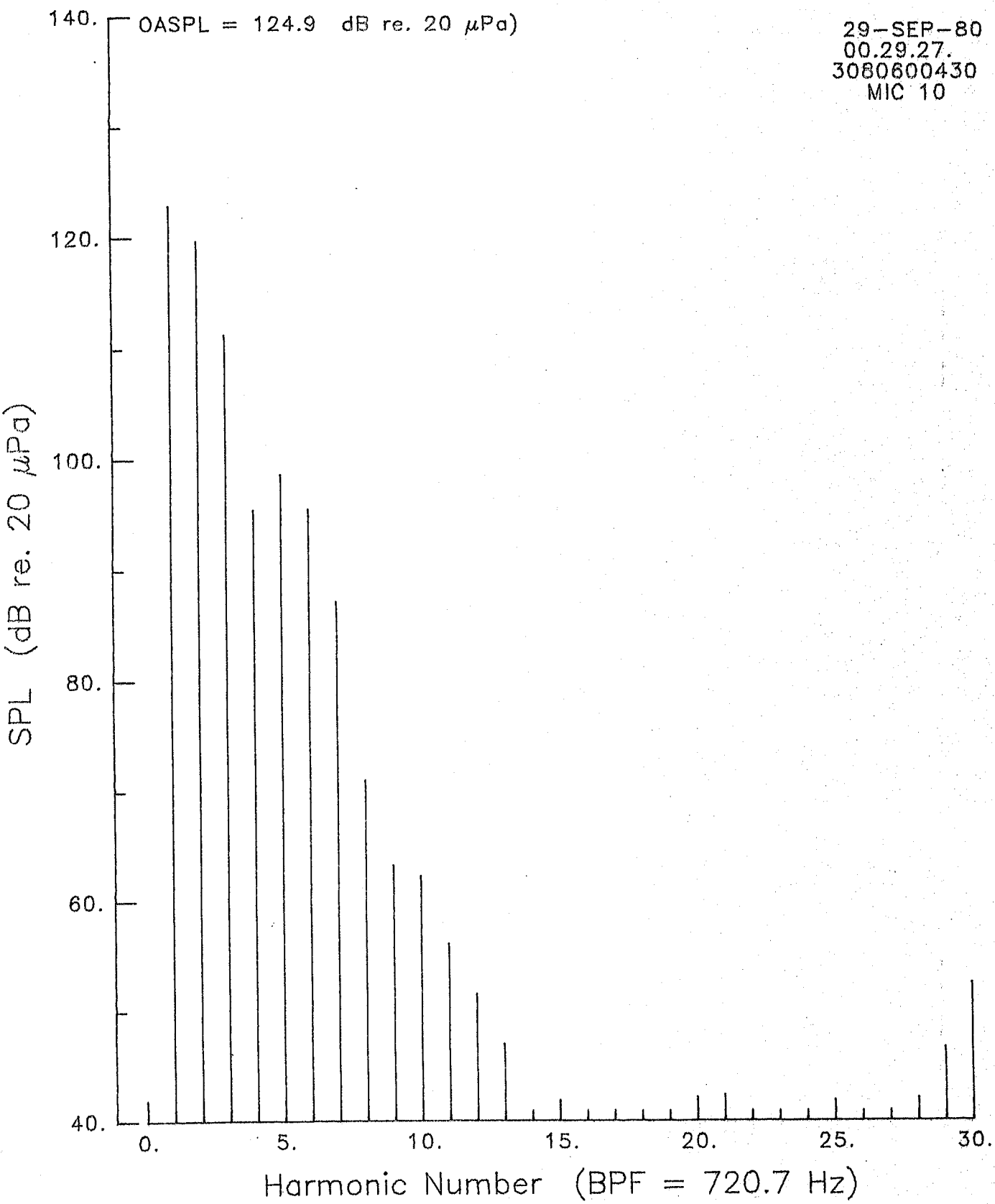

Figure 9(f).- Continued.

F. Farassat -- P. Nystrom
JIAFS -- NASA/LaRC -- GWU

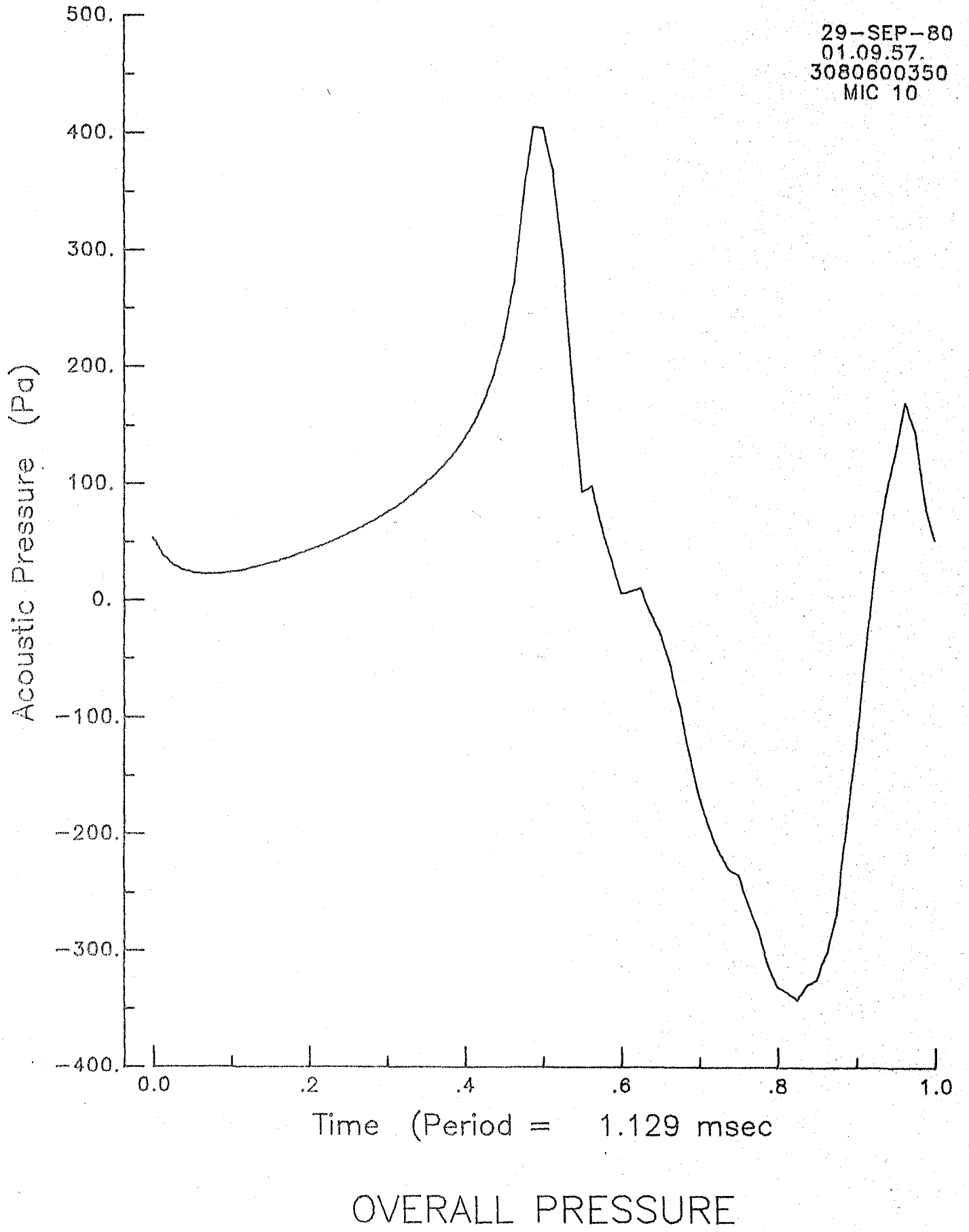

Figure 9(f).- Continued.

F. Farassat -- P. Nystrom
JIAFS -- NASA/LaRC -- GWU

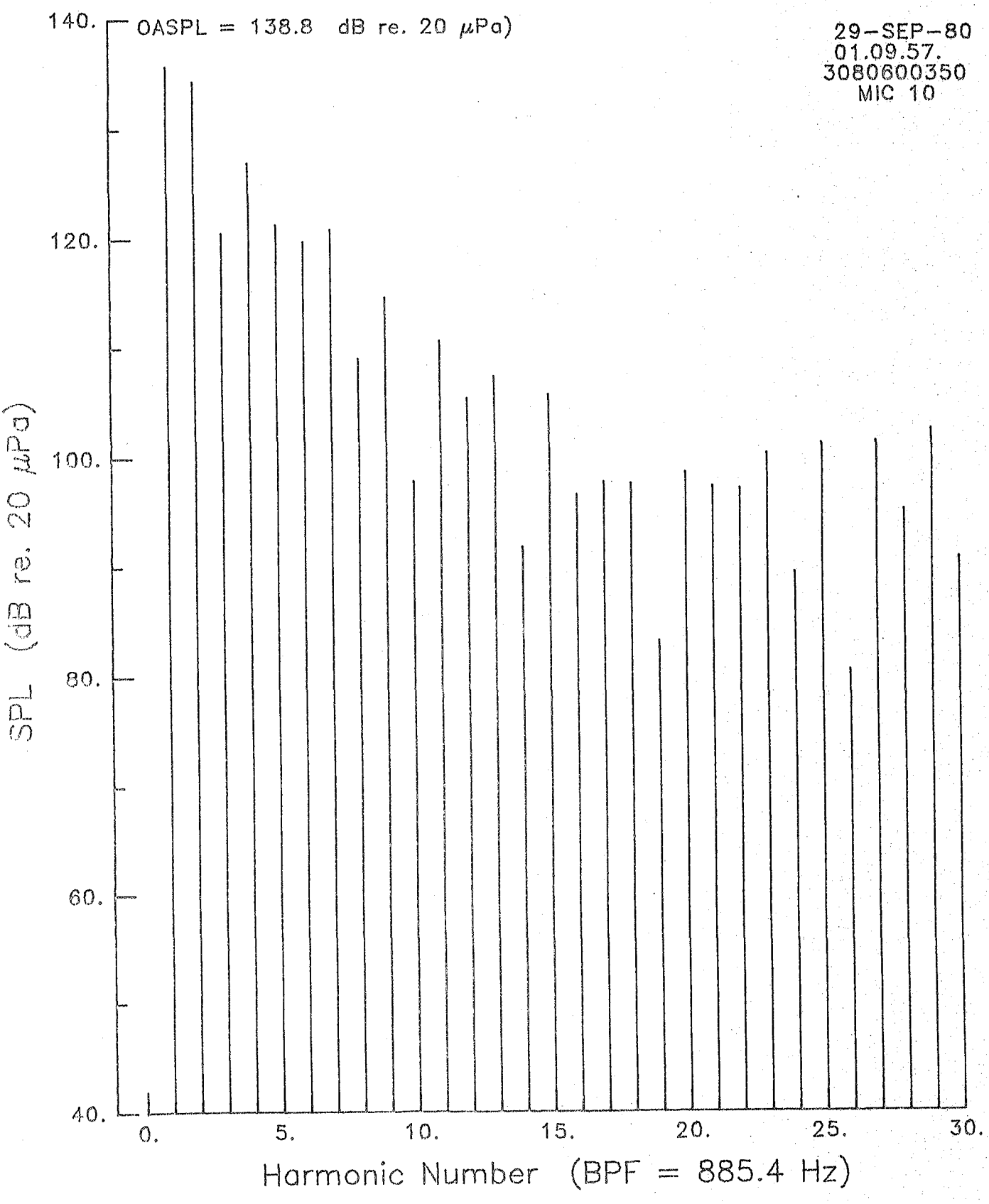

OVERALL SPECTRUM

Figure 9(f).- Continued.

F. Farassat -- P. Nystrom
JIAFS -- NASA/LaRC -- GWU

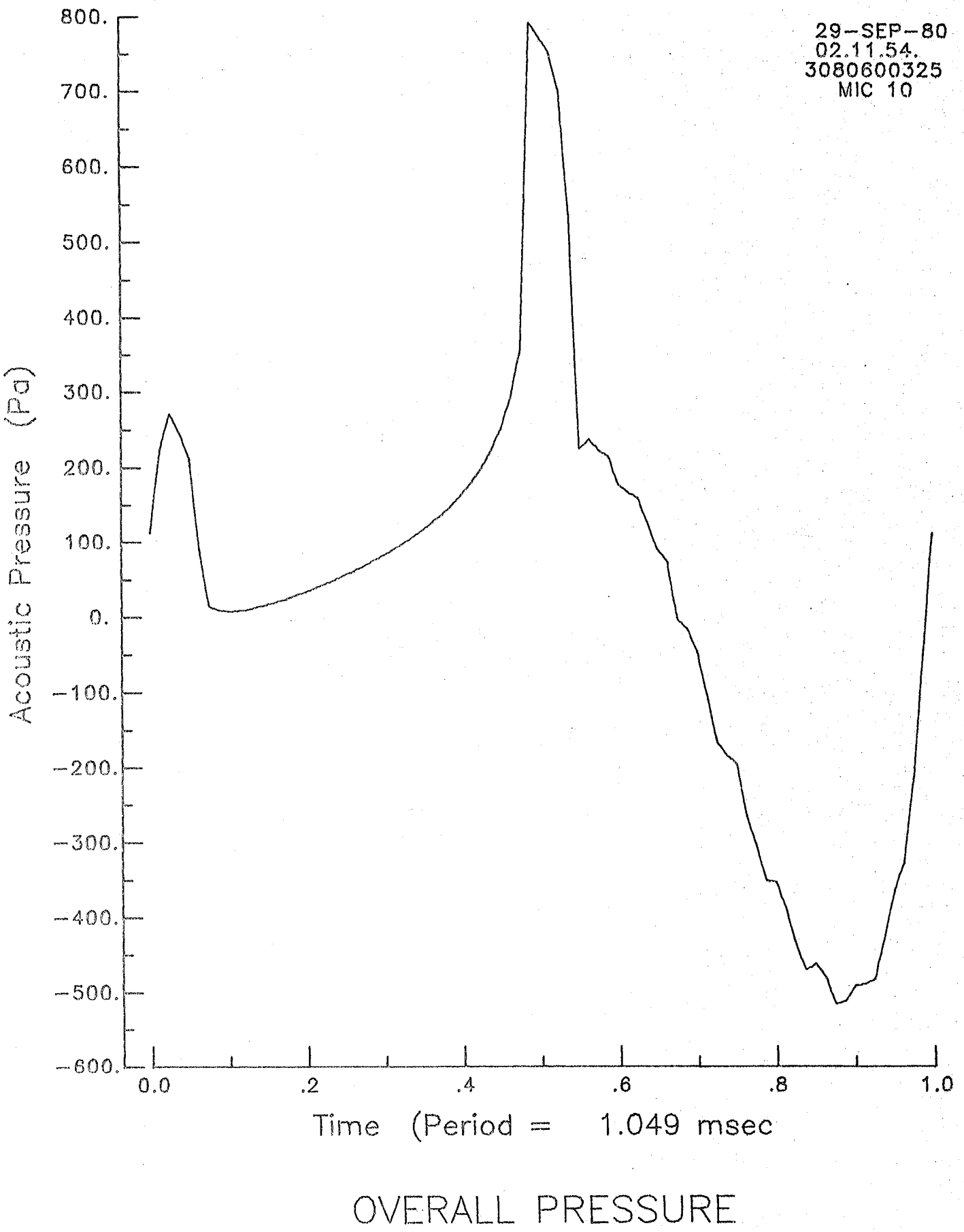

Figure 9(f).- Continued.

F. Farassat -- P. Nystrom
JIAFS -- NASA/LaRC -- GWU

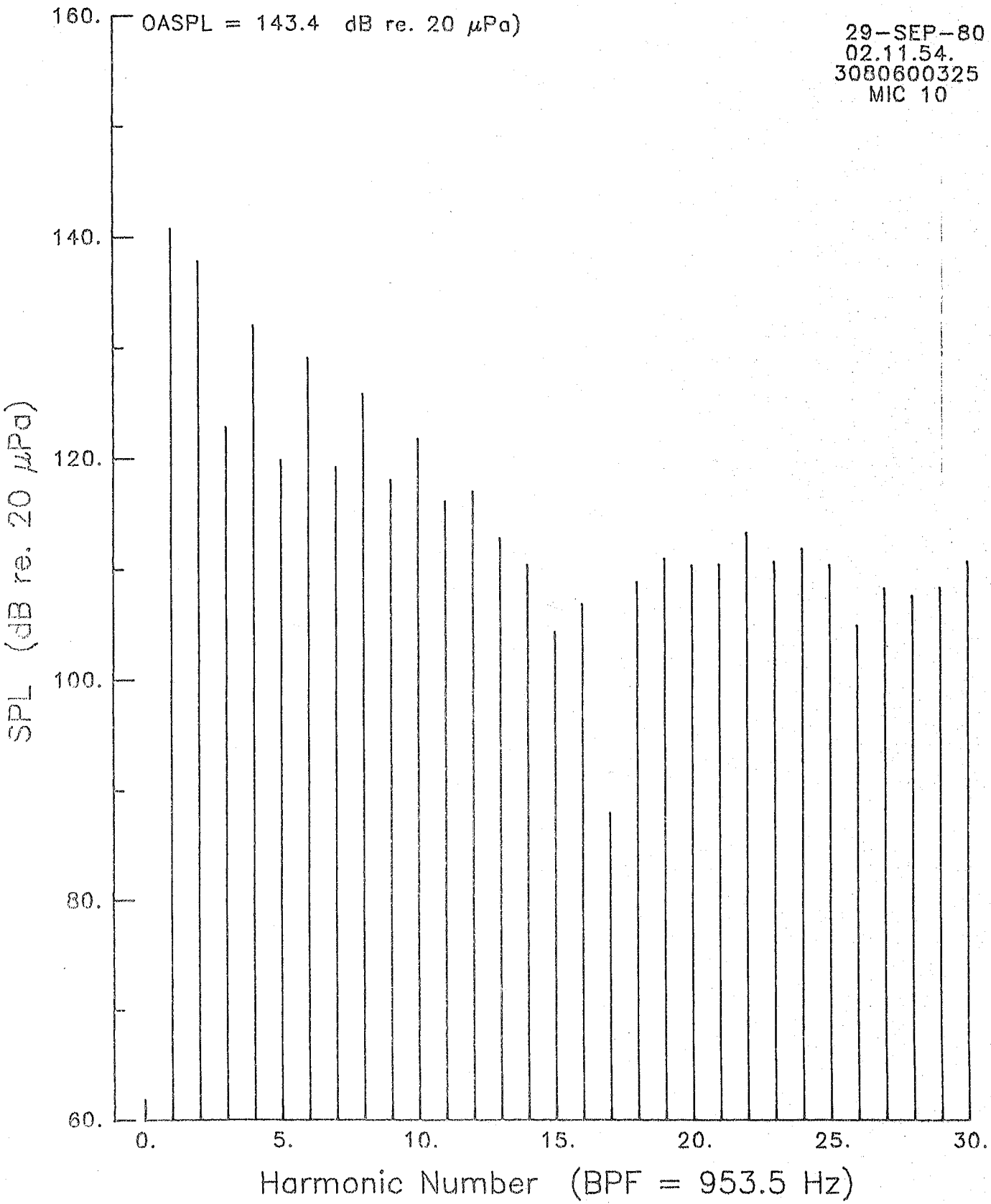

OVERALL SPECTRUM

Figure 9(f).- Continued.

F. Farassat -- P. Nystrom
JIAFS -- NASA/LaRC -- GWU

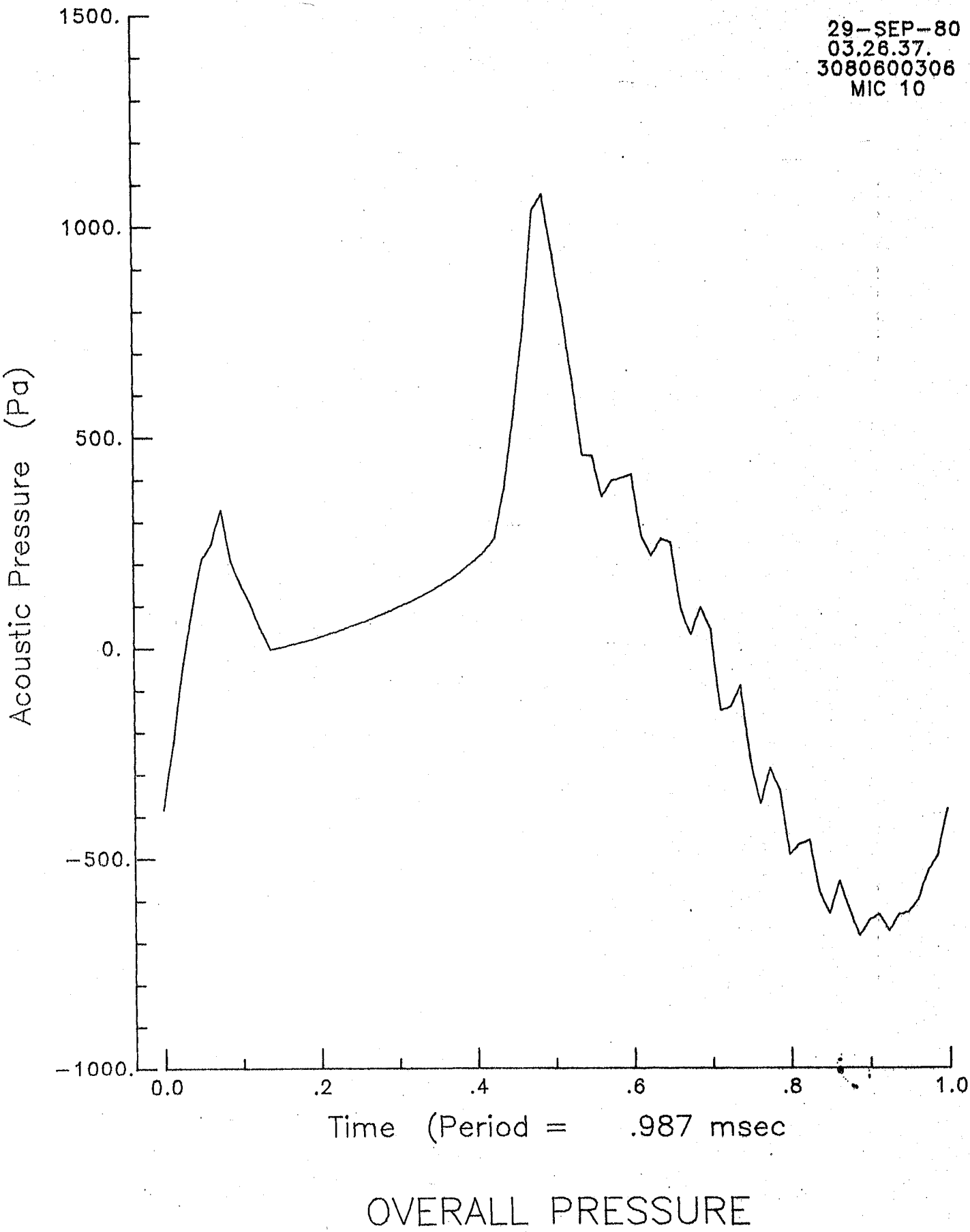

Figure 9(f).- Continued.

F. Farassat -- P. Nystrom
JIAFS -- NASA/LaRC -- GWU

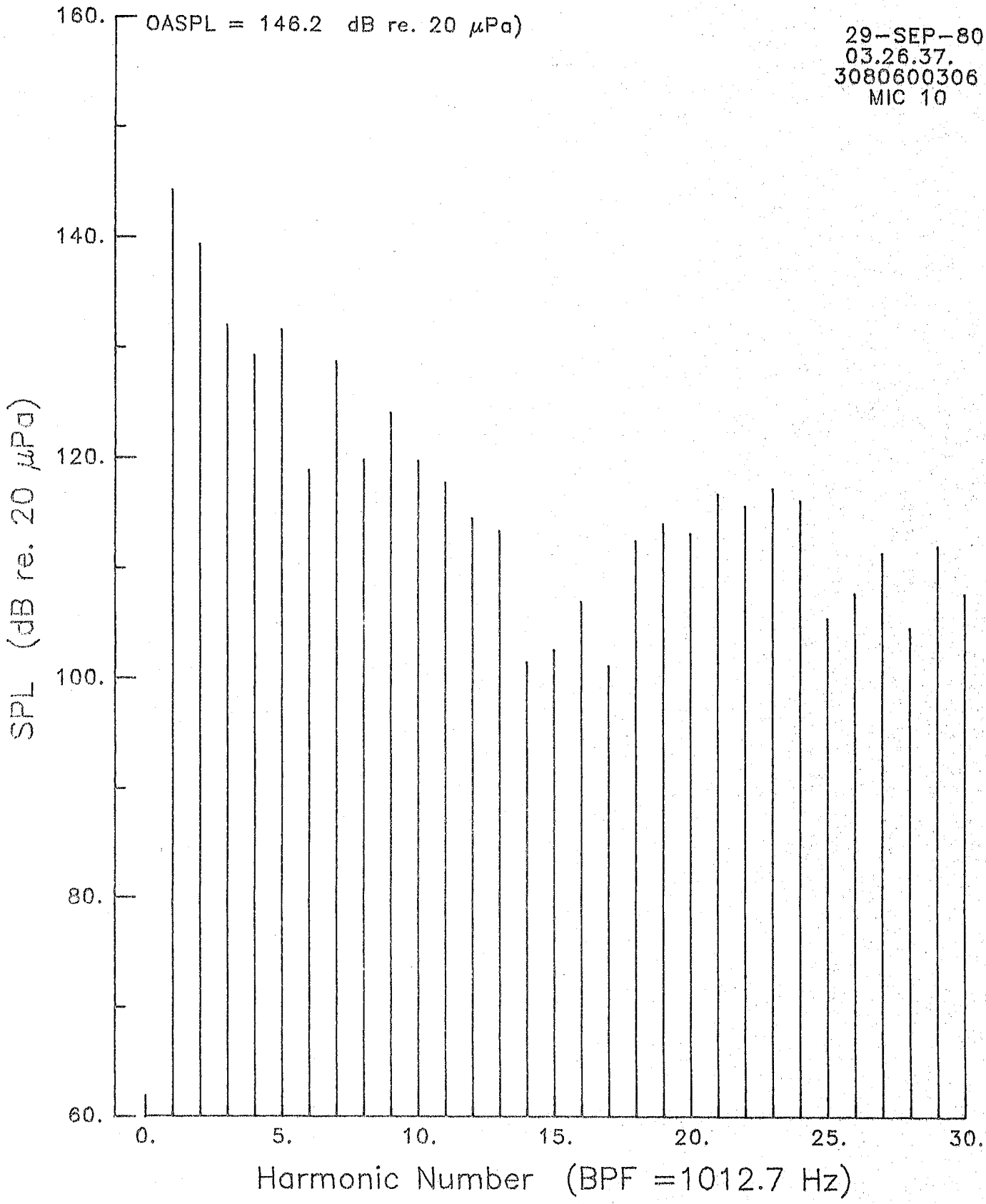

OVERALL SPECTRUM

Figure 9(f).- Continued.

F. Farassat -- P. Nystrom
JIAFS -- NASA/LaRC -- GWU

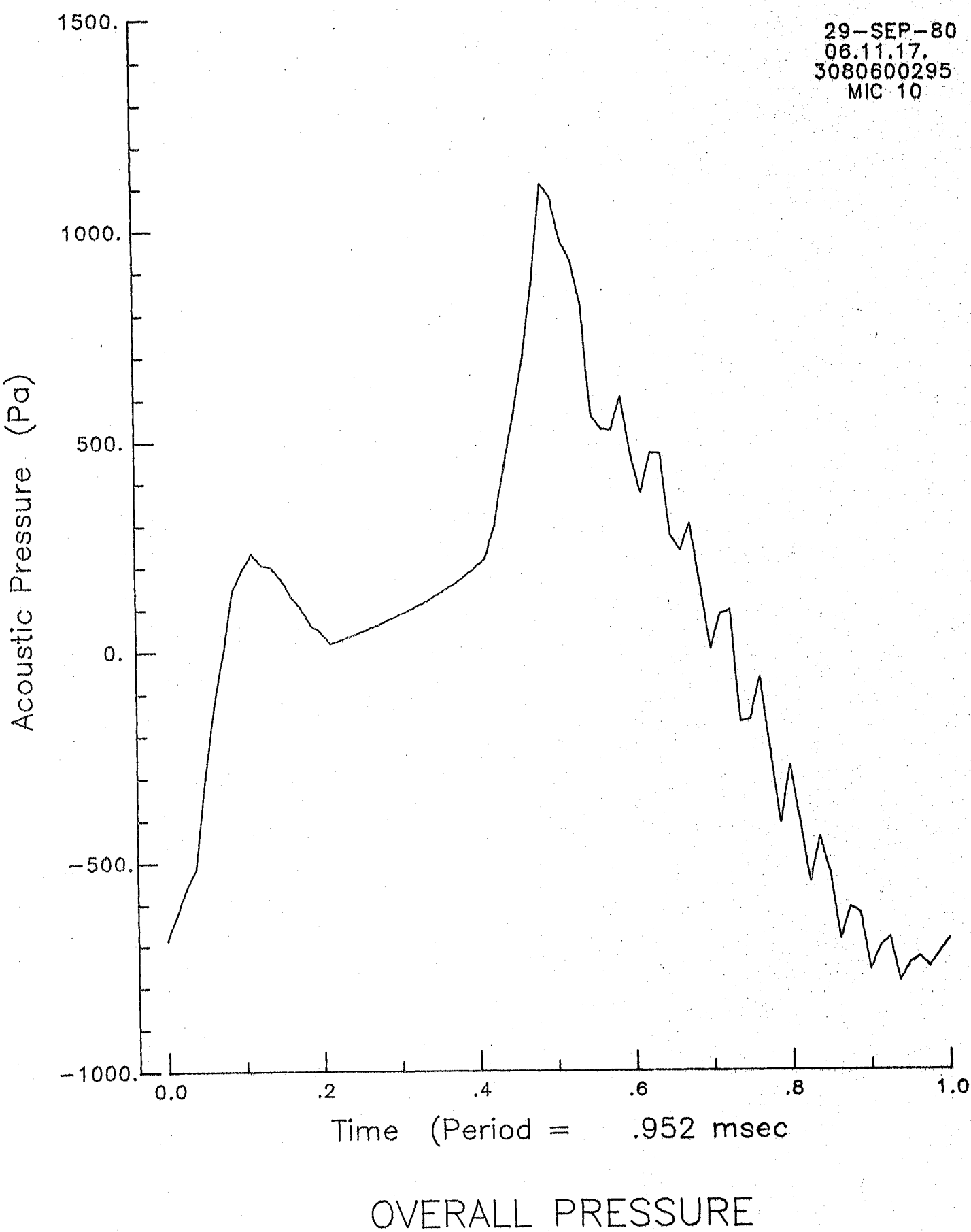

Figure 9(f).- Continued.

F. Farassat -- P. Nystrom
JIAFS -- NASA/LaRC -- GWU

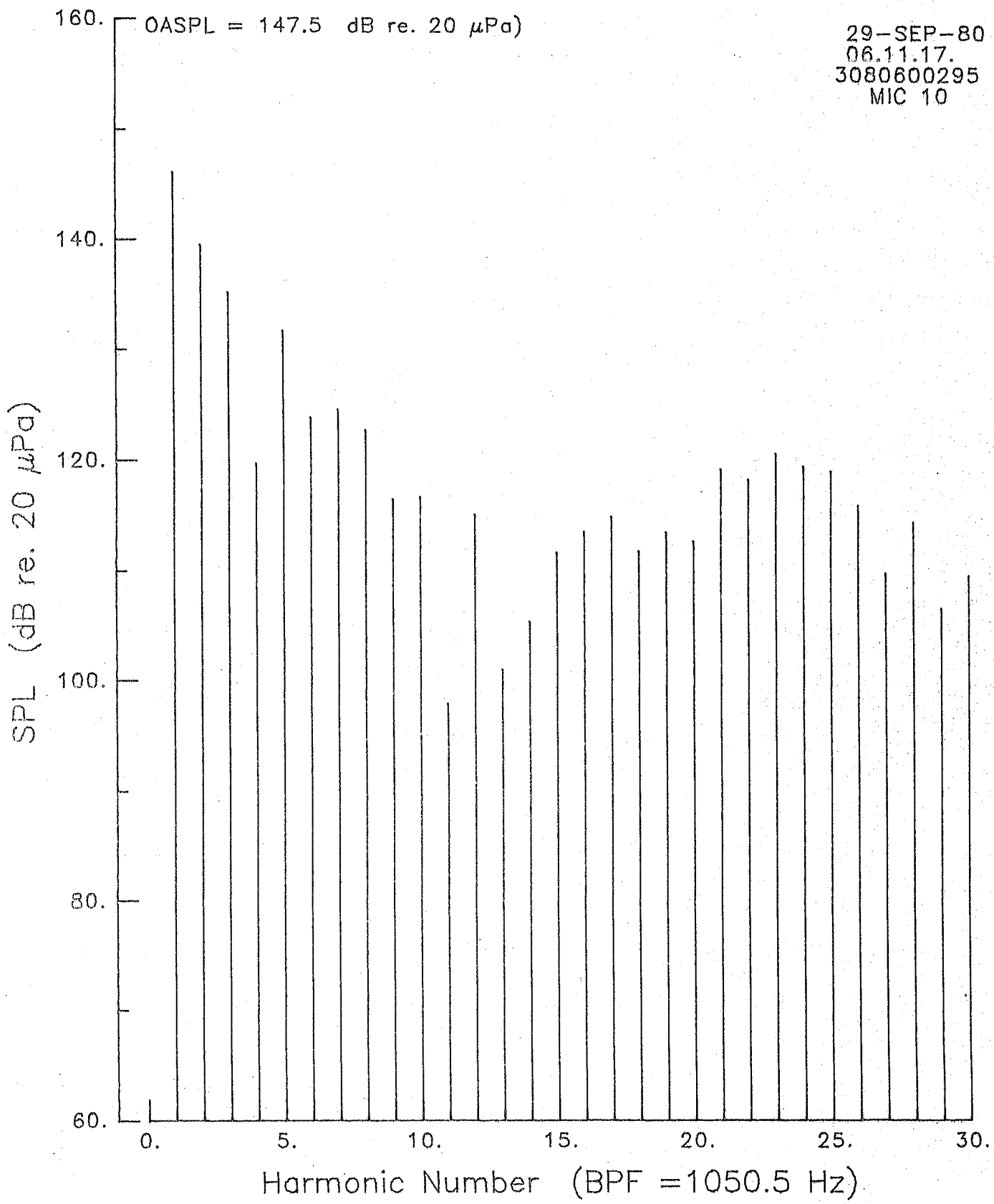

OVERALL SPECTRUM

Figure 9(f).- Concluded.

F. Farassat -- P. Nystrom
JIAFS -- NASA/LaRC -- GWU

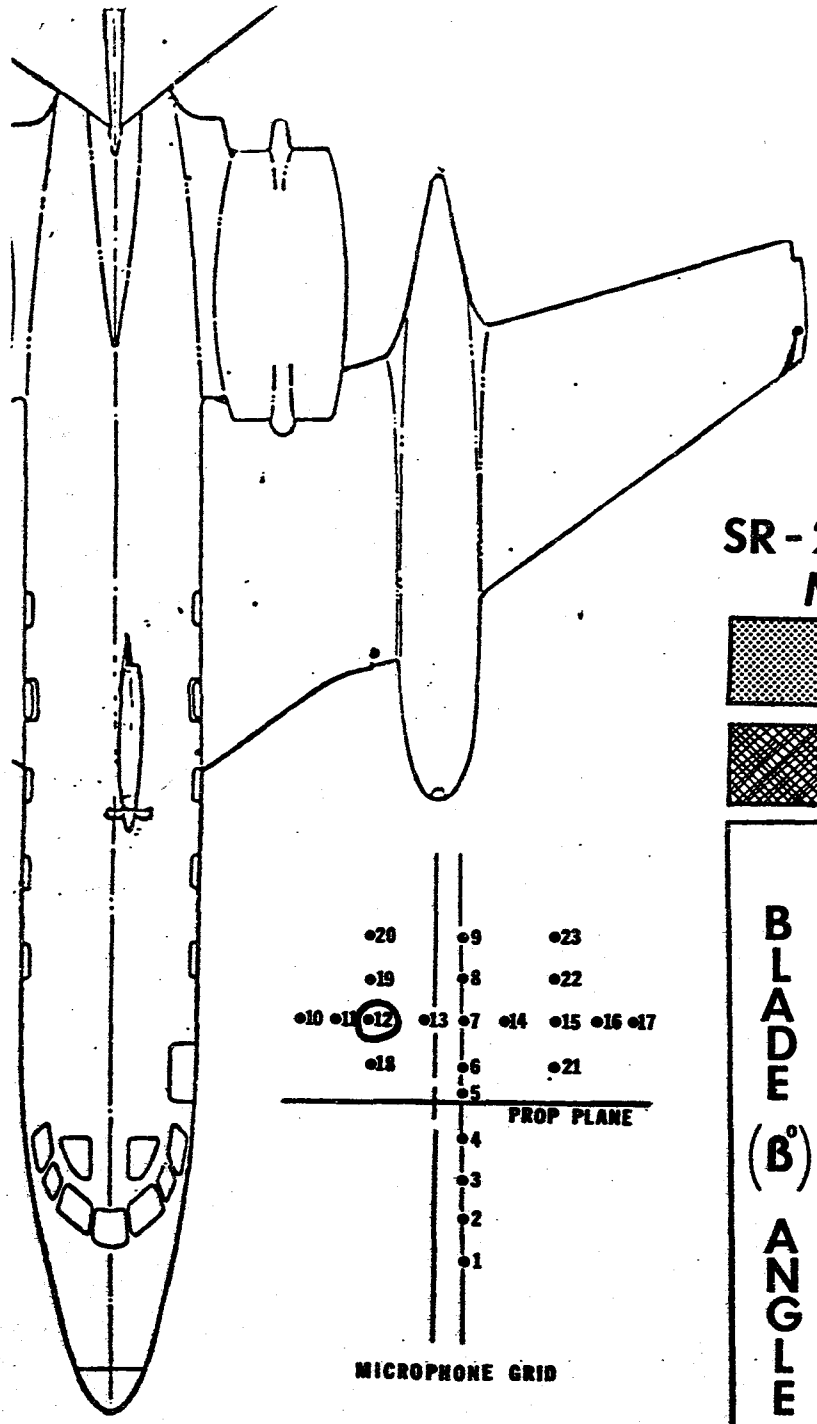

Figure 9(g).- Continued.

SR-2 TEST MATRIX

EXCEEDS BLEED SYS. POWER CAPACITY

BLADE CRITICAL SPEED

BLADE ANGLE (β°)	ADVANCE RATIO (J)	ALTITUDE (FT)	20,000					25,000					30,000				
		MACH #	.50	.60	.65	.70	.75	.80	.50	.60	.65	.70	.75	.80	.50	.60	.65	.70	.75	.80
59.0	4.30																			
	3.50																			
	3.25																			
	3.06																			
	2.90																			
60.0	4.30																			X
	3.50																			X
	3.25																			X
	3.06																			X
	2.95																			X
61.0	4.30																			
	4.07																			
	3.50																			
	3.25																			

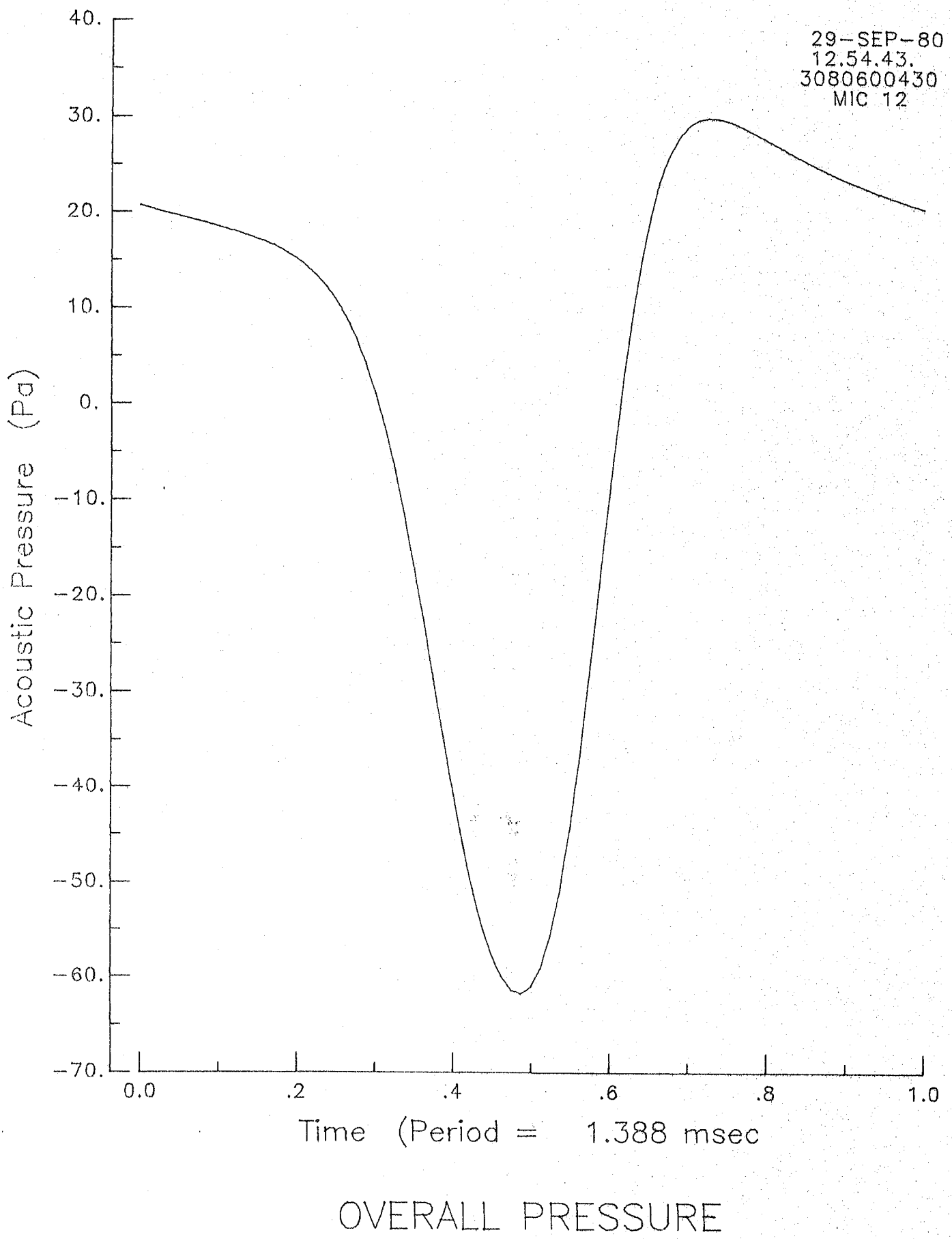

Figure 9(g).- Continued.

F. Farassat -- P. Nystrom
JIAFS -- NASA/LaRC -- GWU

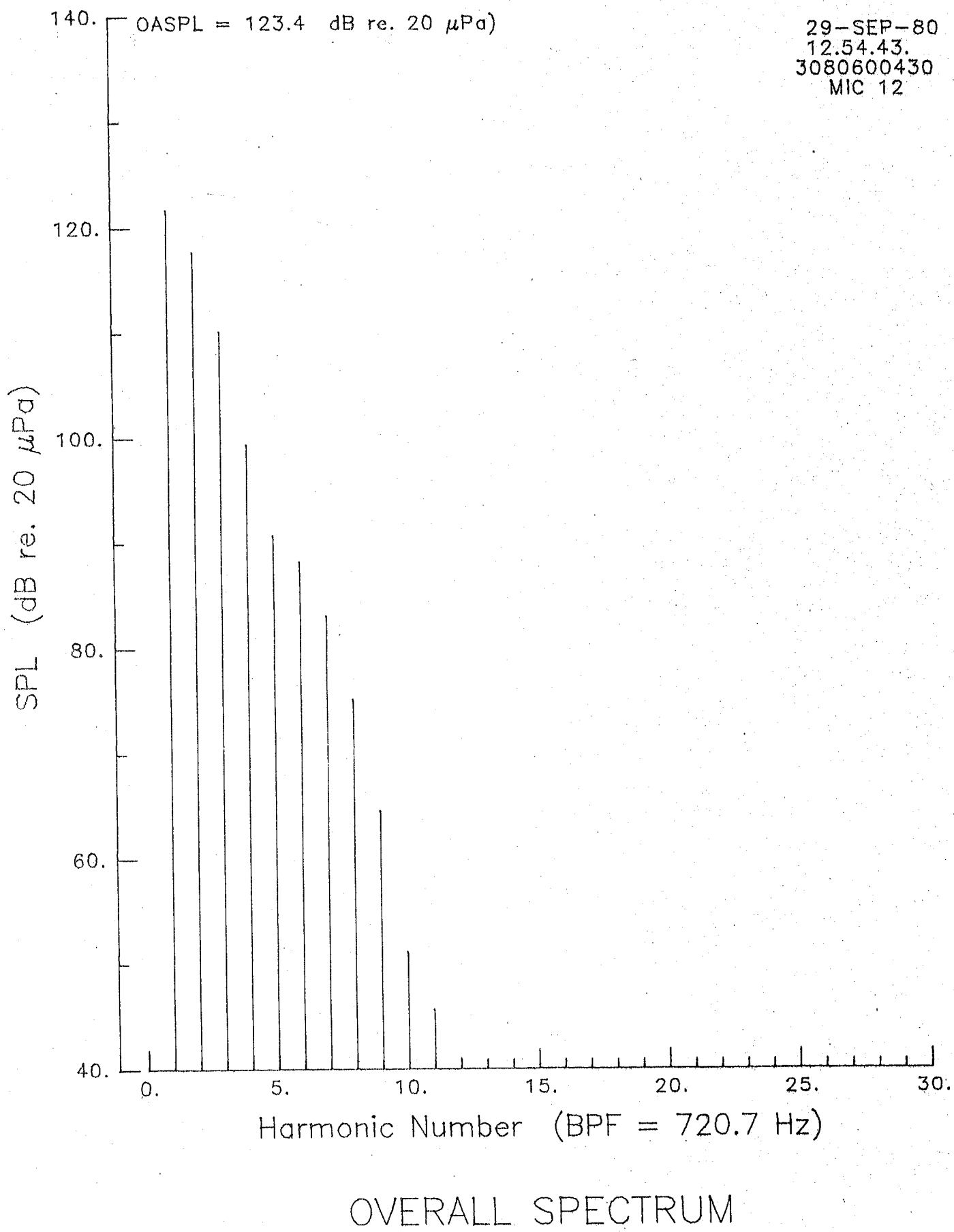

Figure 9(g).- Continued.

F. Farassat -- P. Nystrom
JIAFS -- NASA/LaRC -- GWU

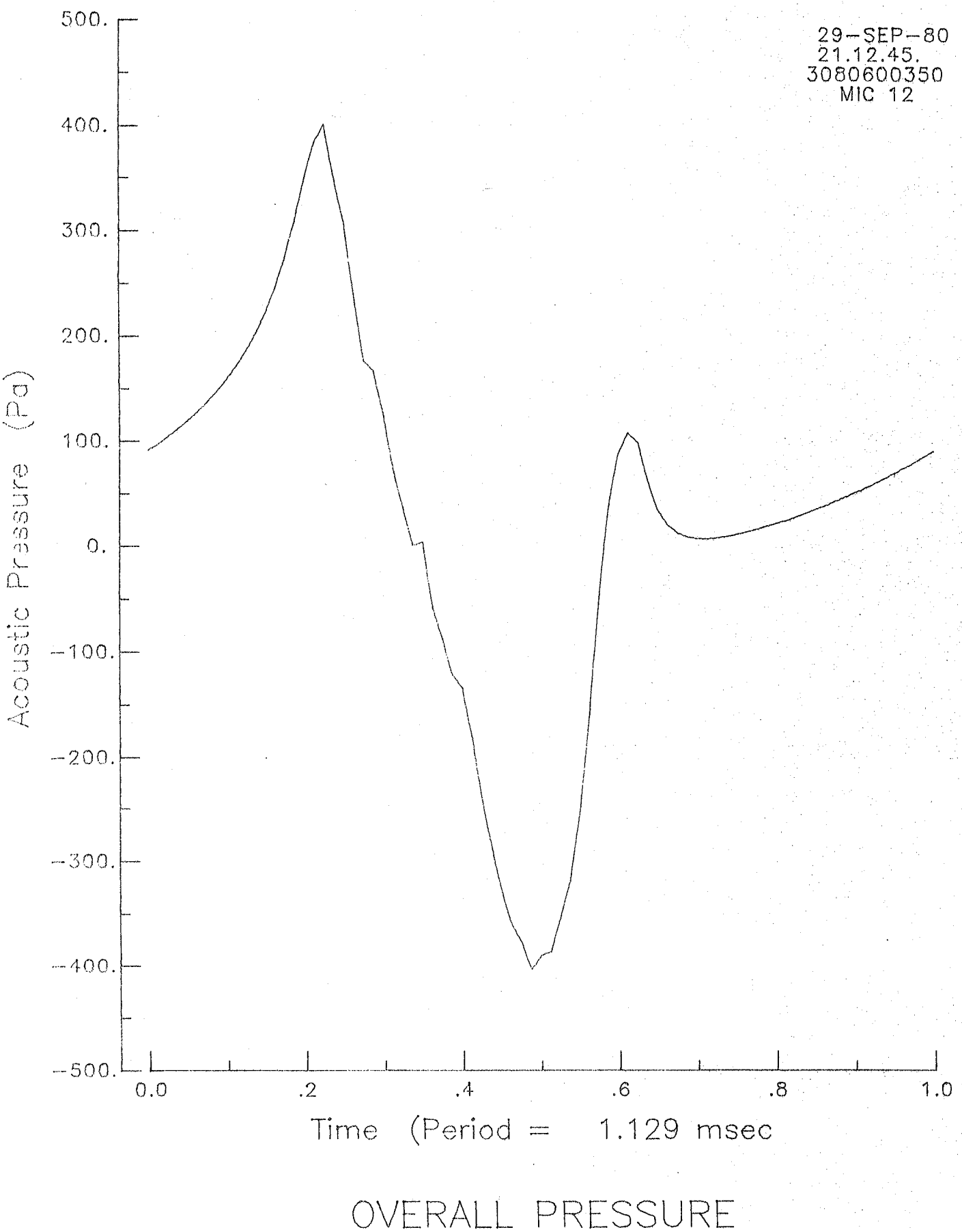

Figure 9(g).- Continued.

F. Farassat -- P. Nystrom
JIAFS -- NASA/LaRC -- GWU

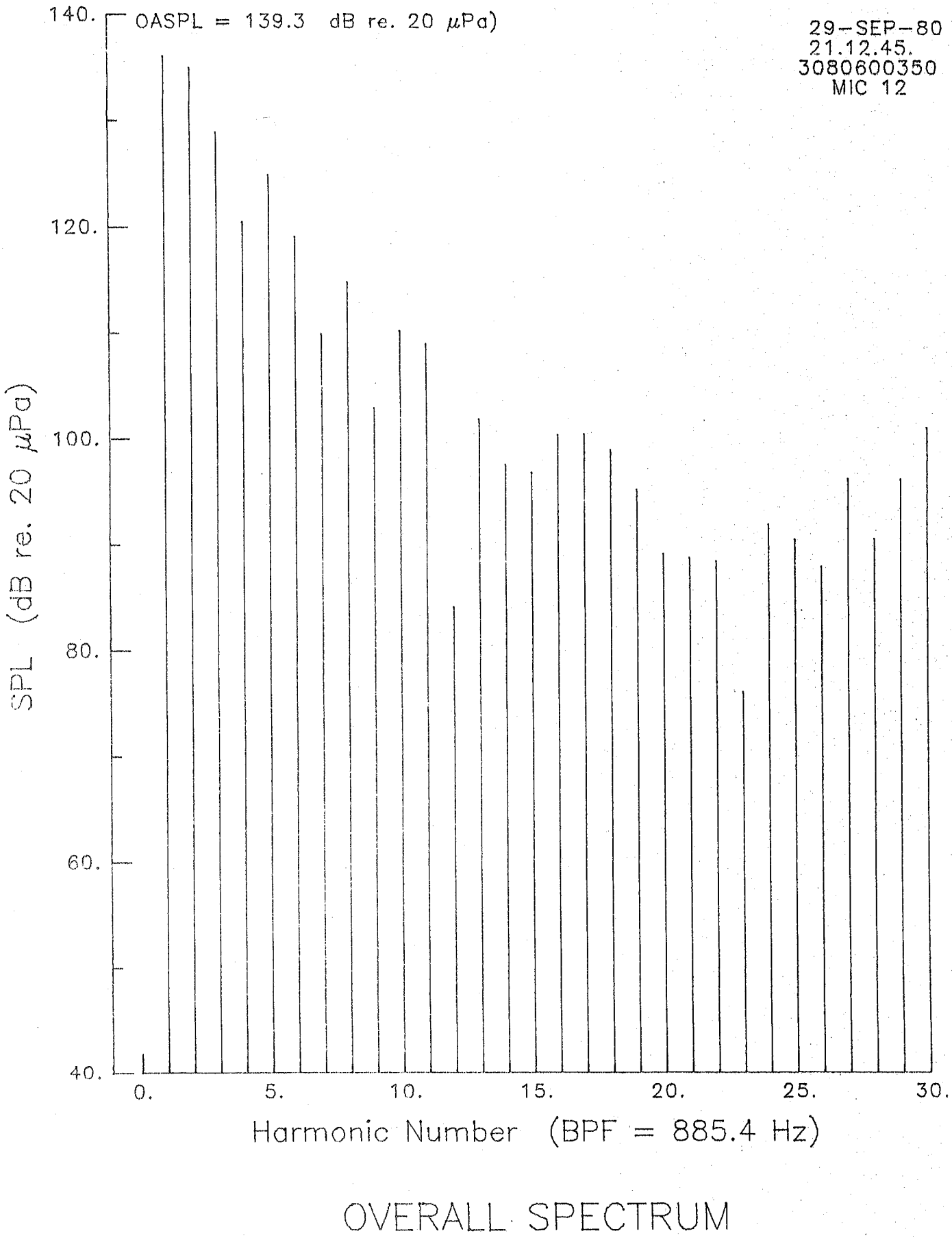

Figure 9(g).- Continued.

F. Farassat -- P. Nystrom
JIAFS -- NASA/LaRC -- GWU

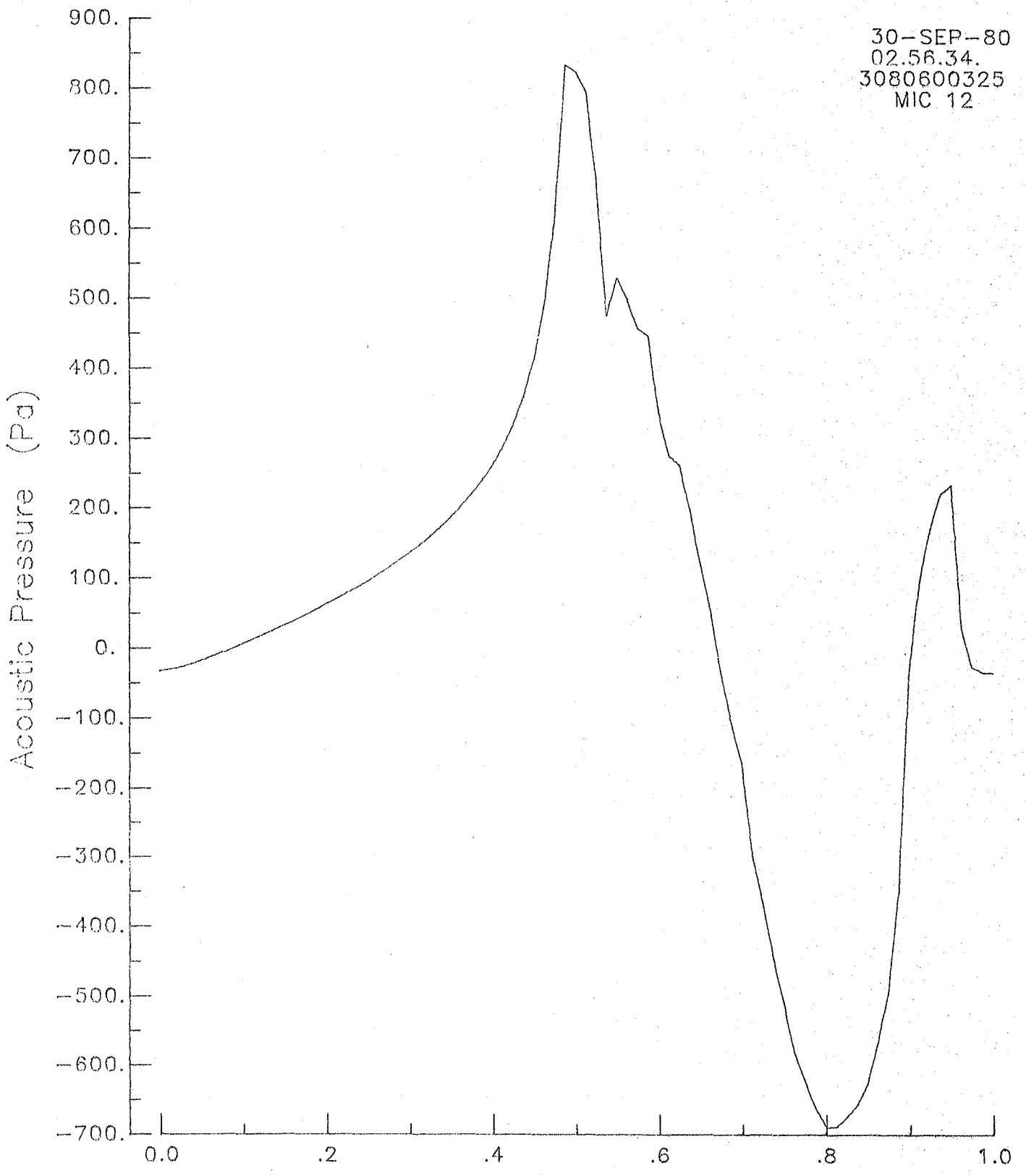

OVERALL PRESSURE

Figure 9(g).-Continued.

F. Farassat -- P. Nystrom
JIAFS -- NASA/LaRC -- GWU

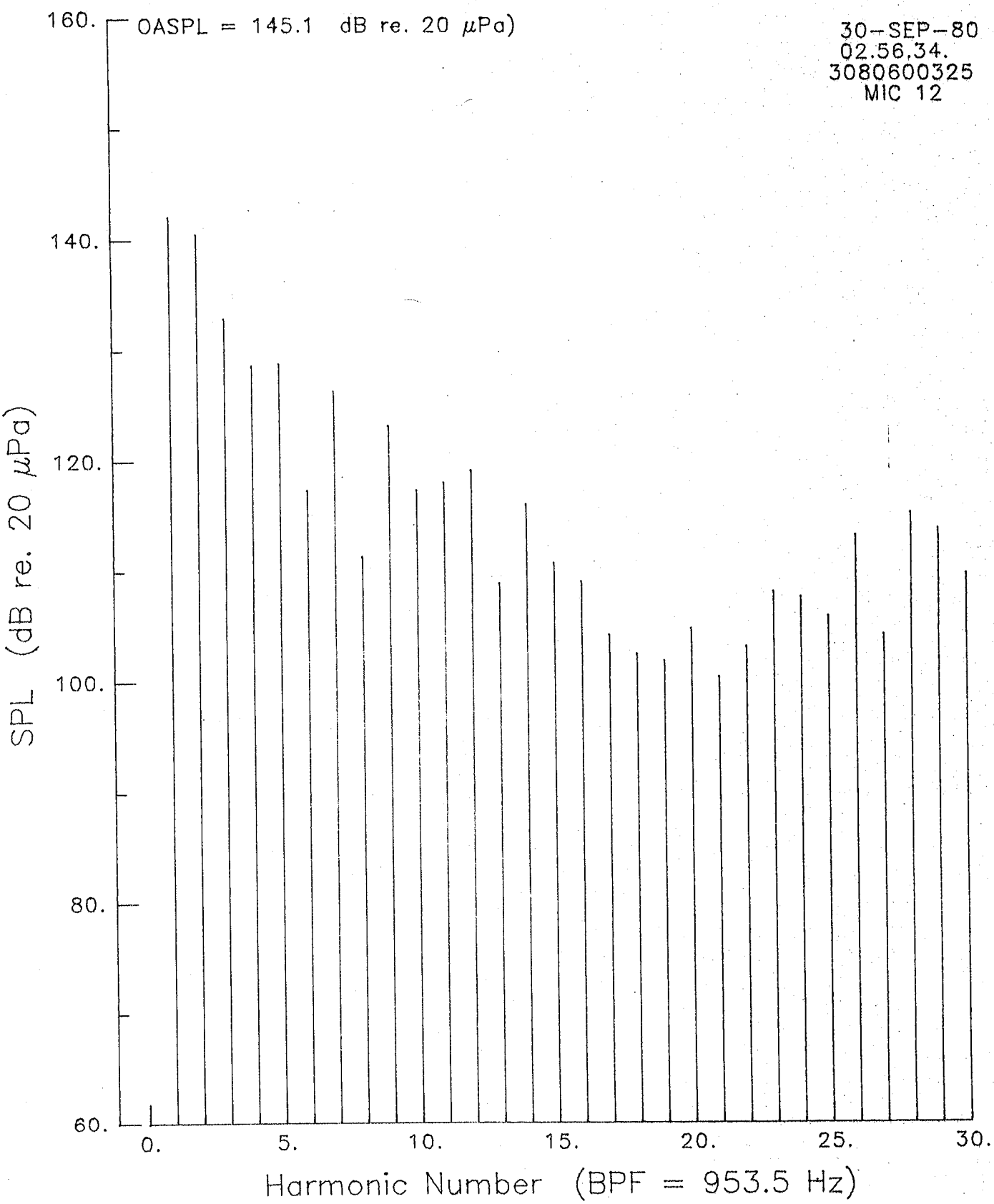

Figure 9(g).- Continued.

F. Farassat -- P. Nystrom
JIAFS -- NASA/LaRC -- GWU

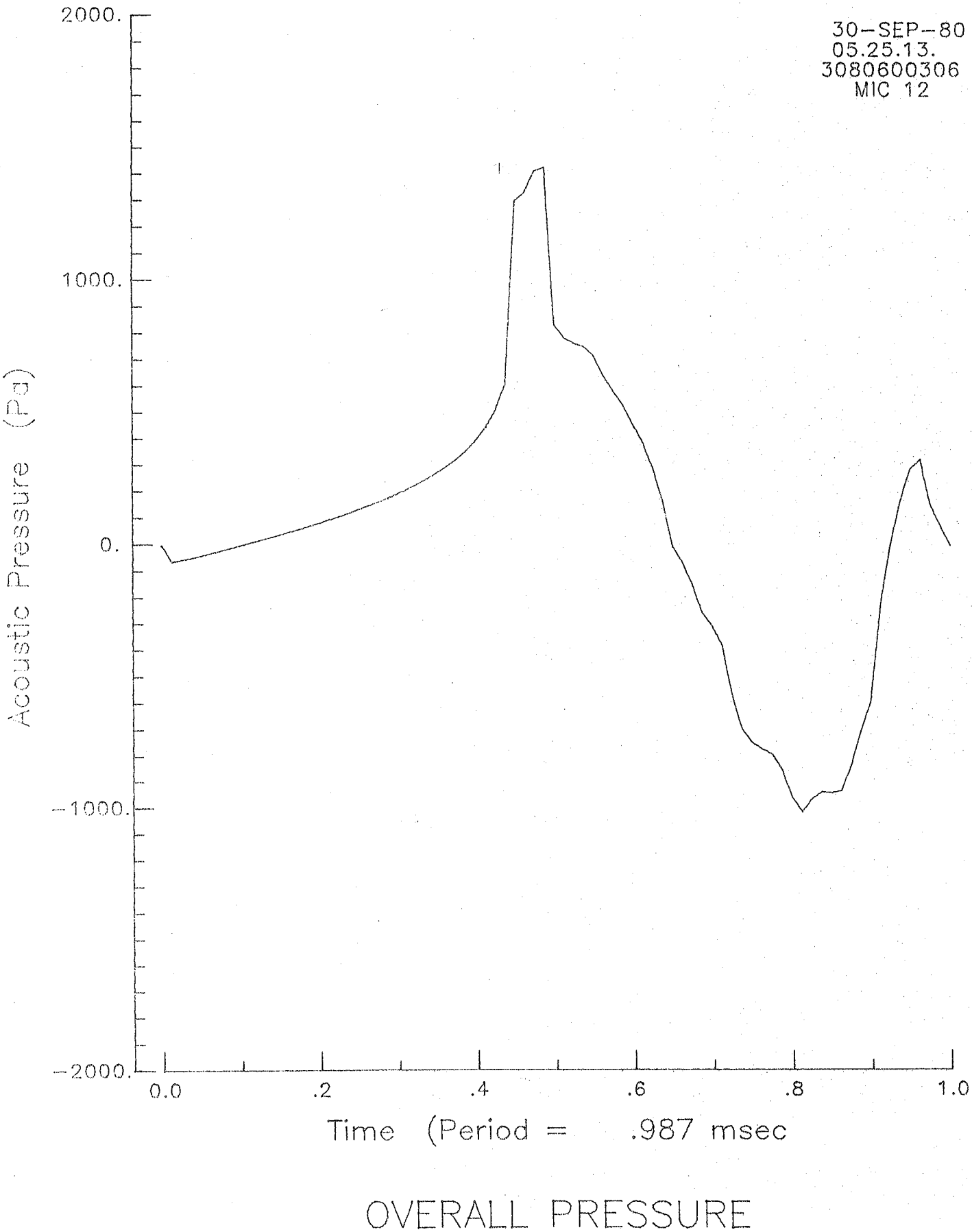

OVERALL PRESSURE

Figure 9(g).- Continued.

F. Farassat -- P. Nystrom
JIAFS -- NASA/LaRC -- GWU

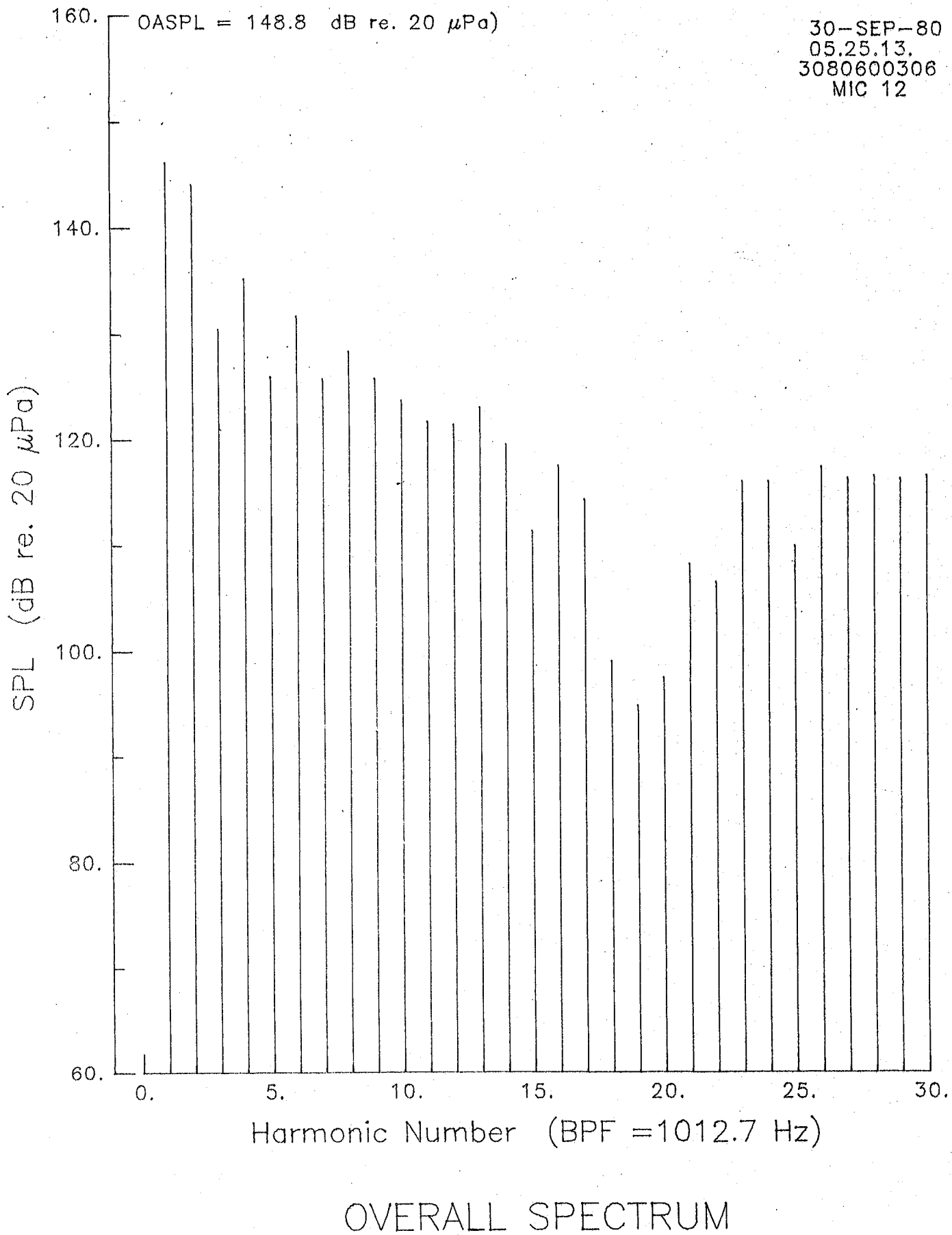

Figure 9(g).- Continued.

F. Farassat -- P. Nystrom
JIAFS -- NASA/LaRC -- GWU

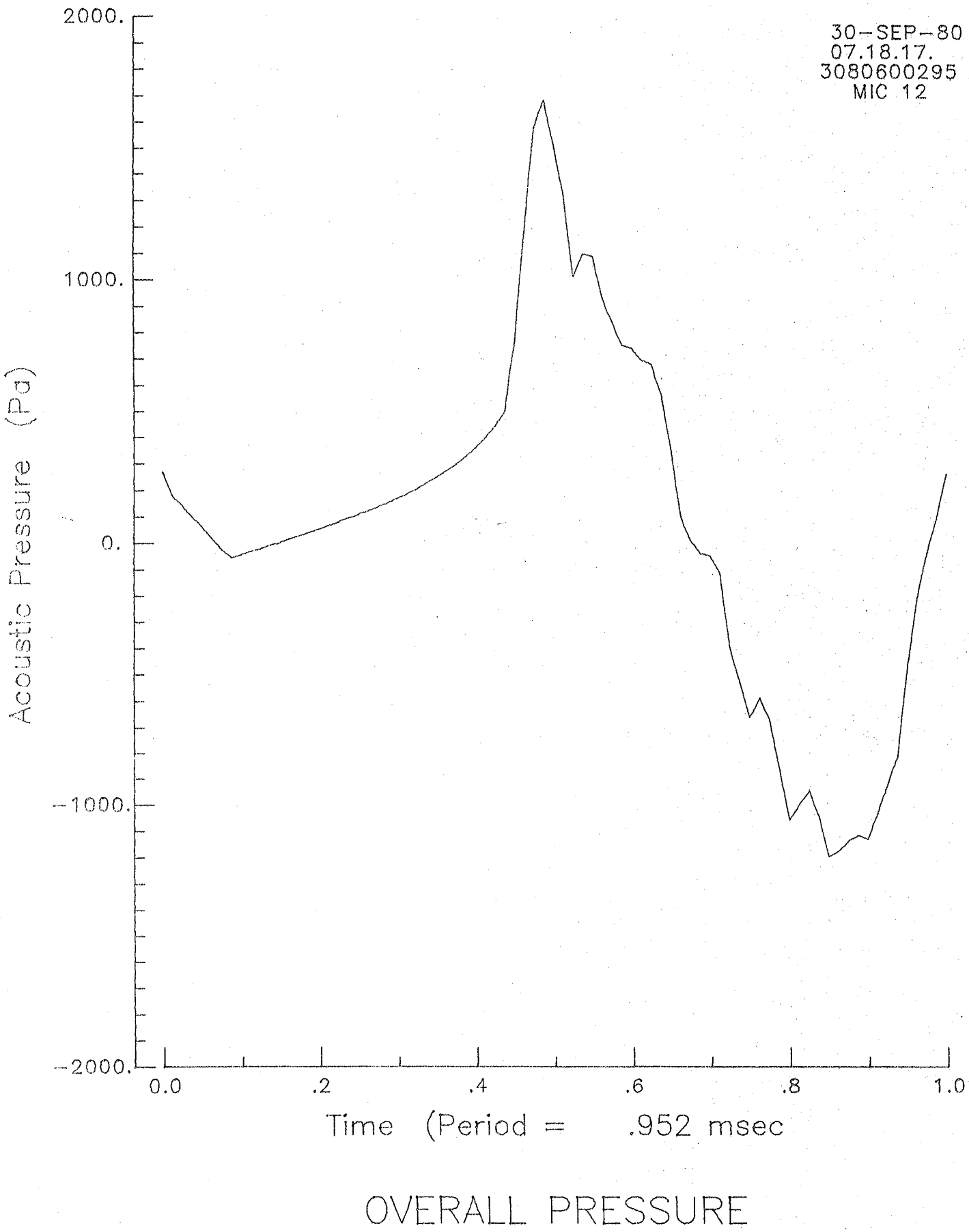

Figure 9(g).- Continued.

F. Farassat -- P. Nystrom
JIAFS -- NASA/LaRC -- GWU

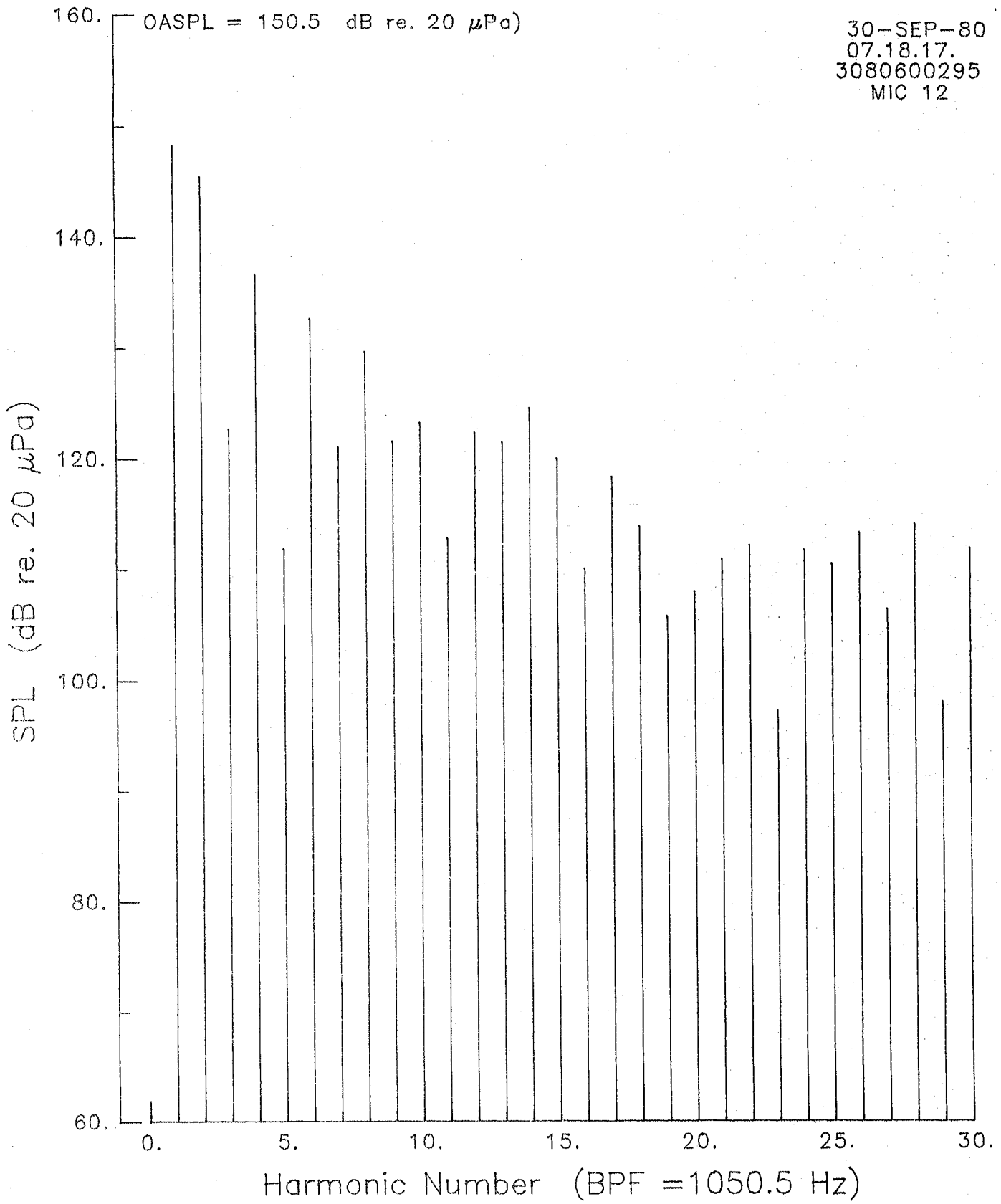

OVERALL SPECTRUM

Figure 9(g).- Concluded.

F. Farassat -- P. Nystrom
JIAFS -- NASA/LaRC -- GWU

SR-3 BLADE

FLIGHT ALTITUDE 6.10 km (20,000 ft)

FLIGHT MACH NUMBER 0.8

MICROPHONE 7

(ADVANCE RATIO VARIED)

Figure 10.- Free-field acoustic pressure signatures and spectra for SR-3 blade - Altitude 6.10 Km (20,000 ft), M=0.8, Microphone 7. Note the advance ratio is varied in these calculations.

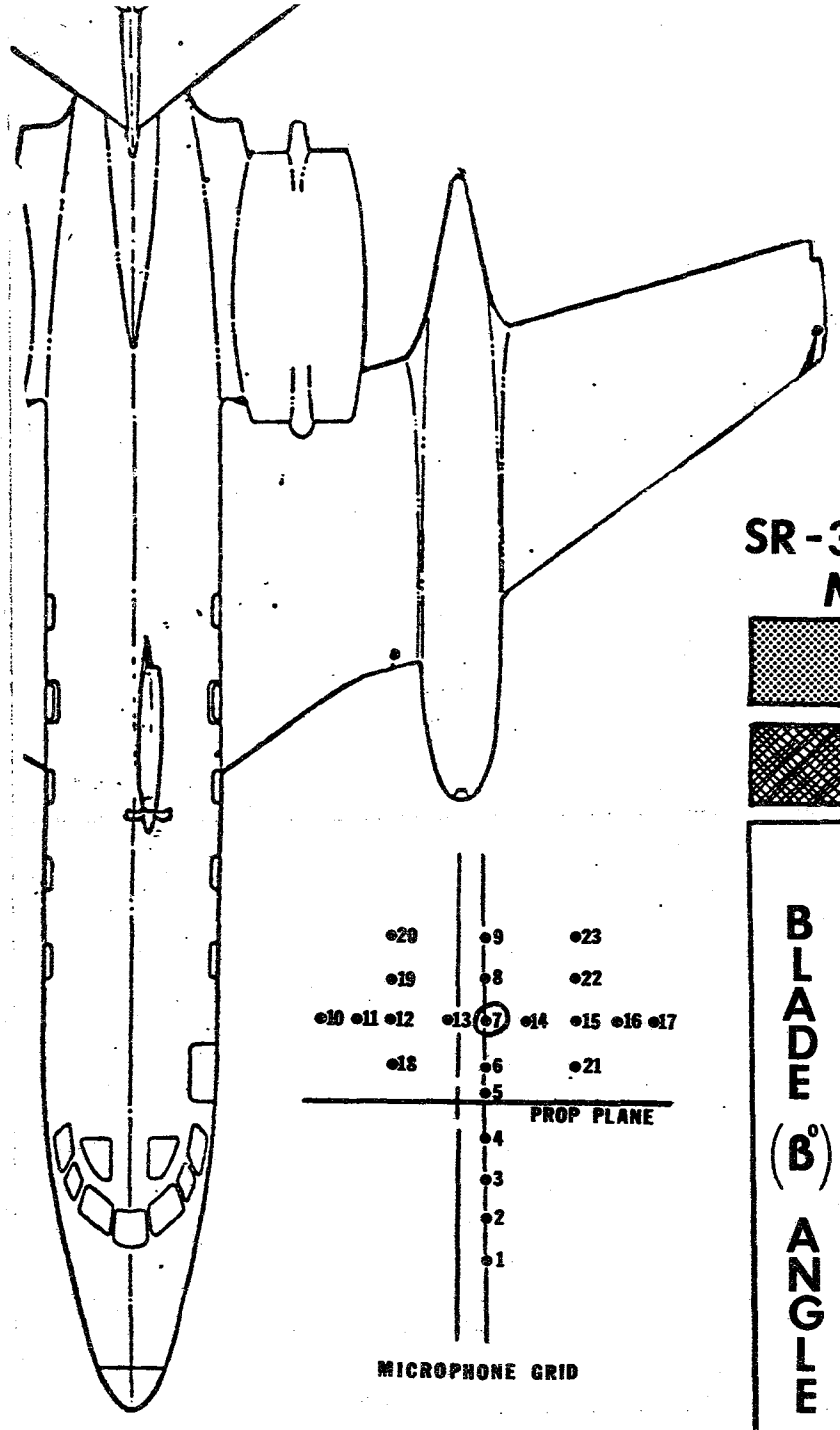

SR-3 TEST MATRIX

EXCEEDS BLEED SYS. POWER CAPACITY

BLADE CRITICAL SPEED

BLADE ANGLE (β°)	ADVANCE RATIO (J)	ALTITUDE (FT) 20,000						ALTITUDE (FT) 25,000						ALTITUDE (FT) 30,000					
		MACH # .50	.60	.65	.70	.75	.80	.50	.60	.65	.70	.75	.80	.50	.60	.65	.70	.75	.80
59.3	4.30																		
	3.50																		
	3.25																		
	3.06																		
	2.90																		
61.3	4.30						X												
	3.50						X												
	3.25				■		X				■						■		
	3.06						X						■						■
	2.95						X						■					■	■
63.3	4.30																		
	4.07																		
	3.50												■						■
	3.25						■						■						■

Figure 10.- Continued.

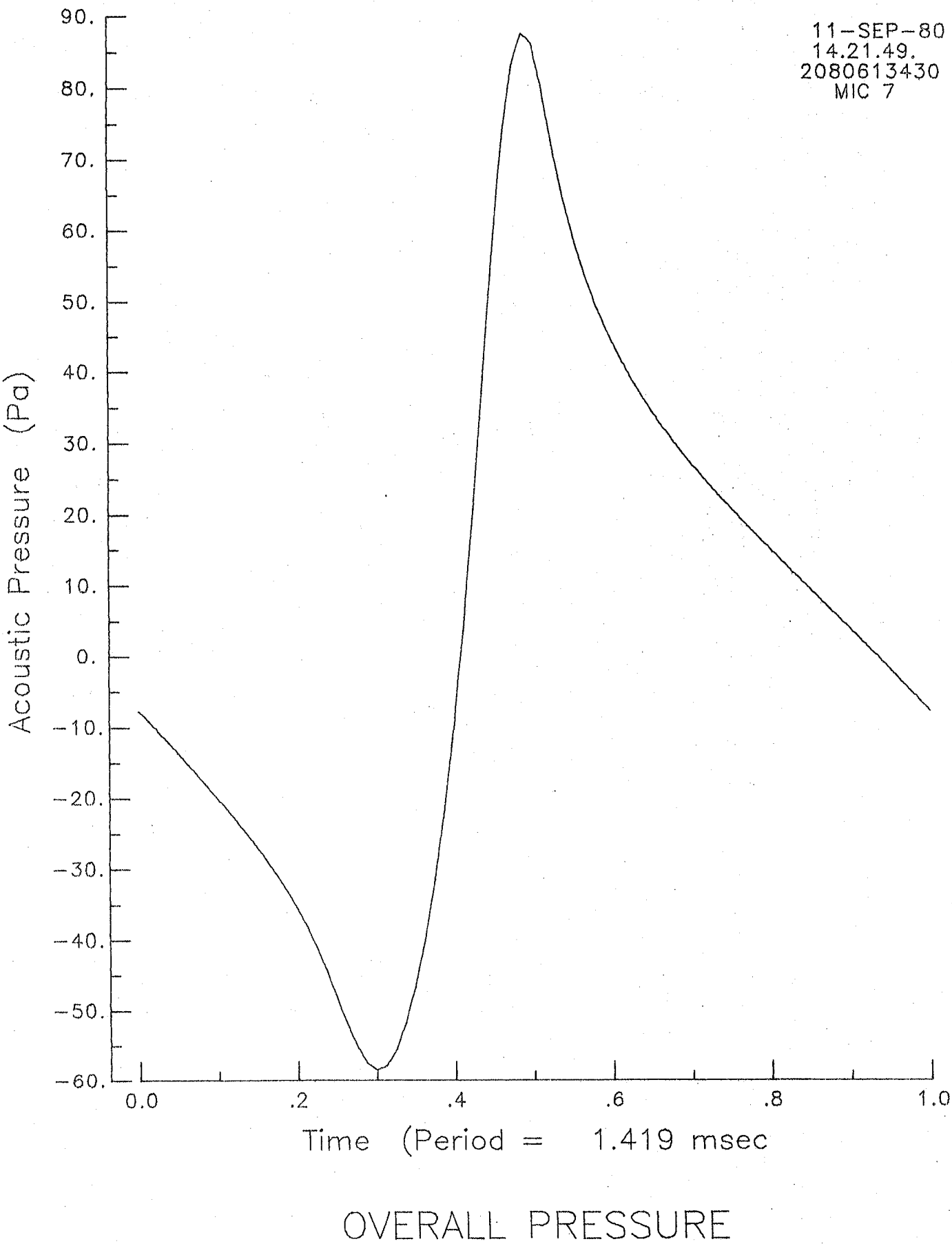

Figure 10.- Continued.

F. Farassat -- P. Nystrom
JIAFS -- NASA/LaRC -- GWU

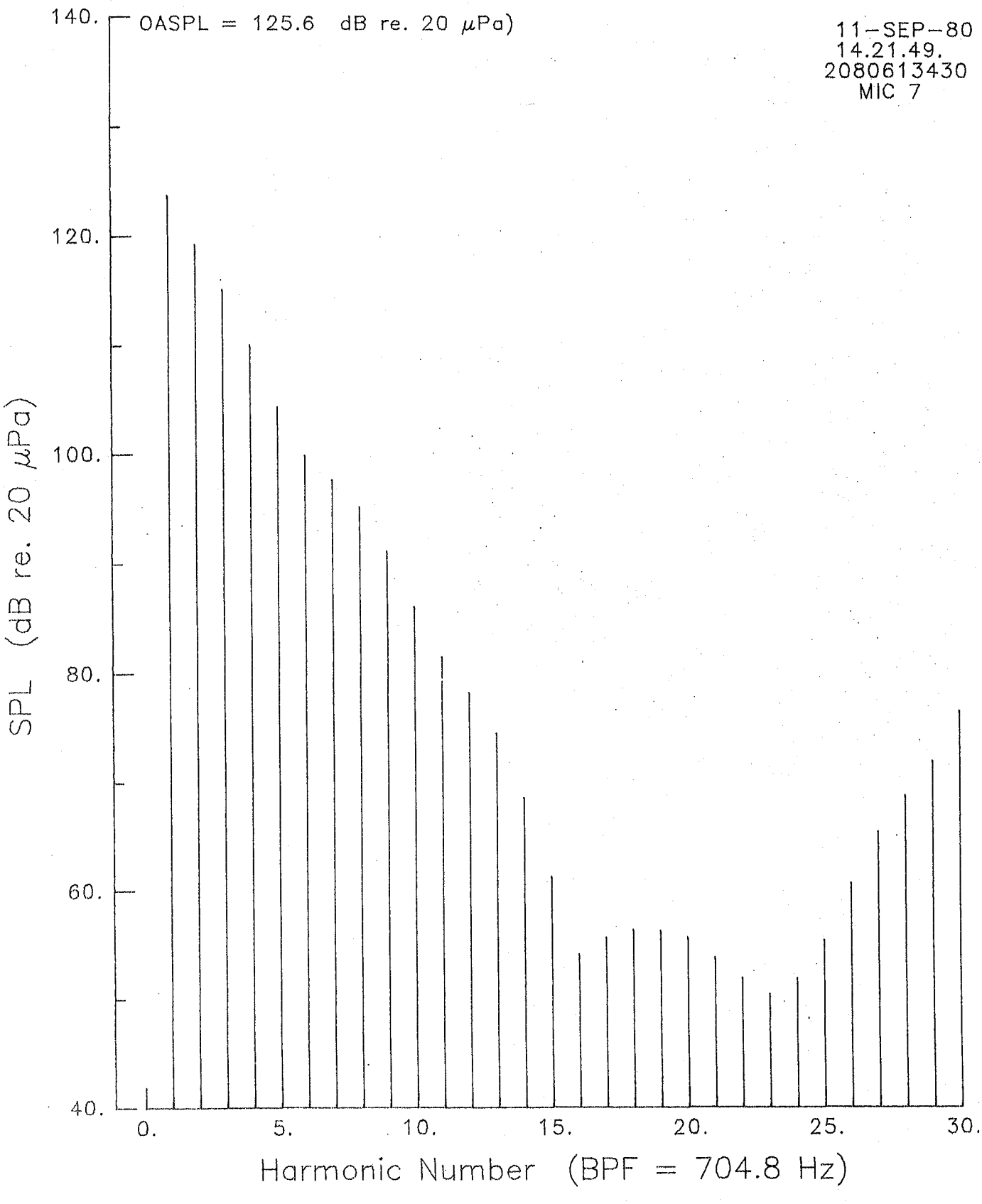

OVERALL SPECTRUM

Figure 10.- Continued.

F. Farassat -- P. Nystrom
JIAFS -- NASA/LaRC -- GWU

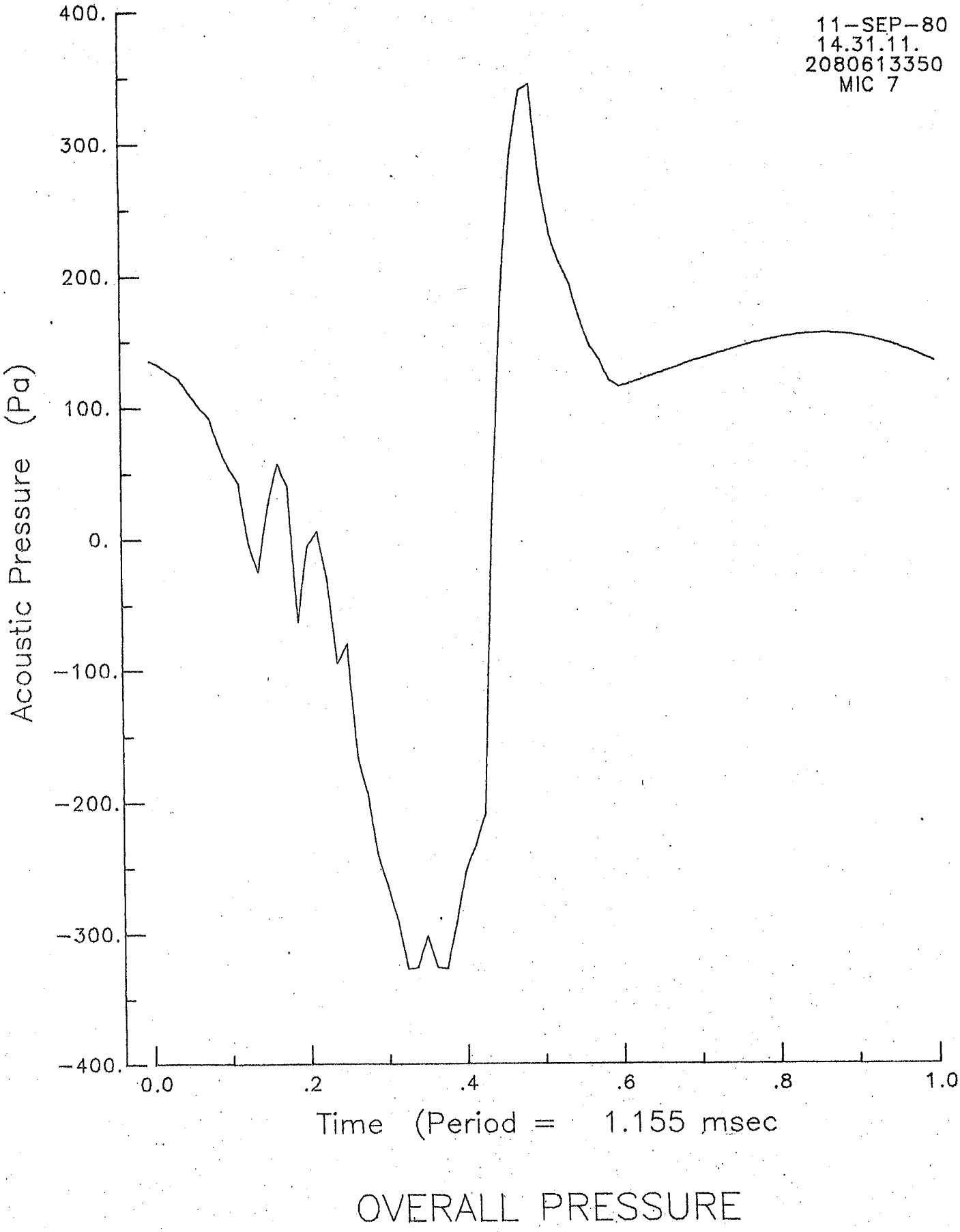

Figure 10.- Continued.

F. Farassat -- P. Nystrom
JIAFS -- NASA/LaRC -- GWU

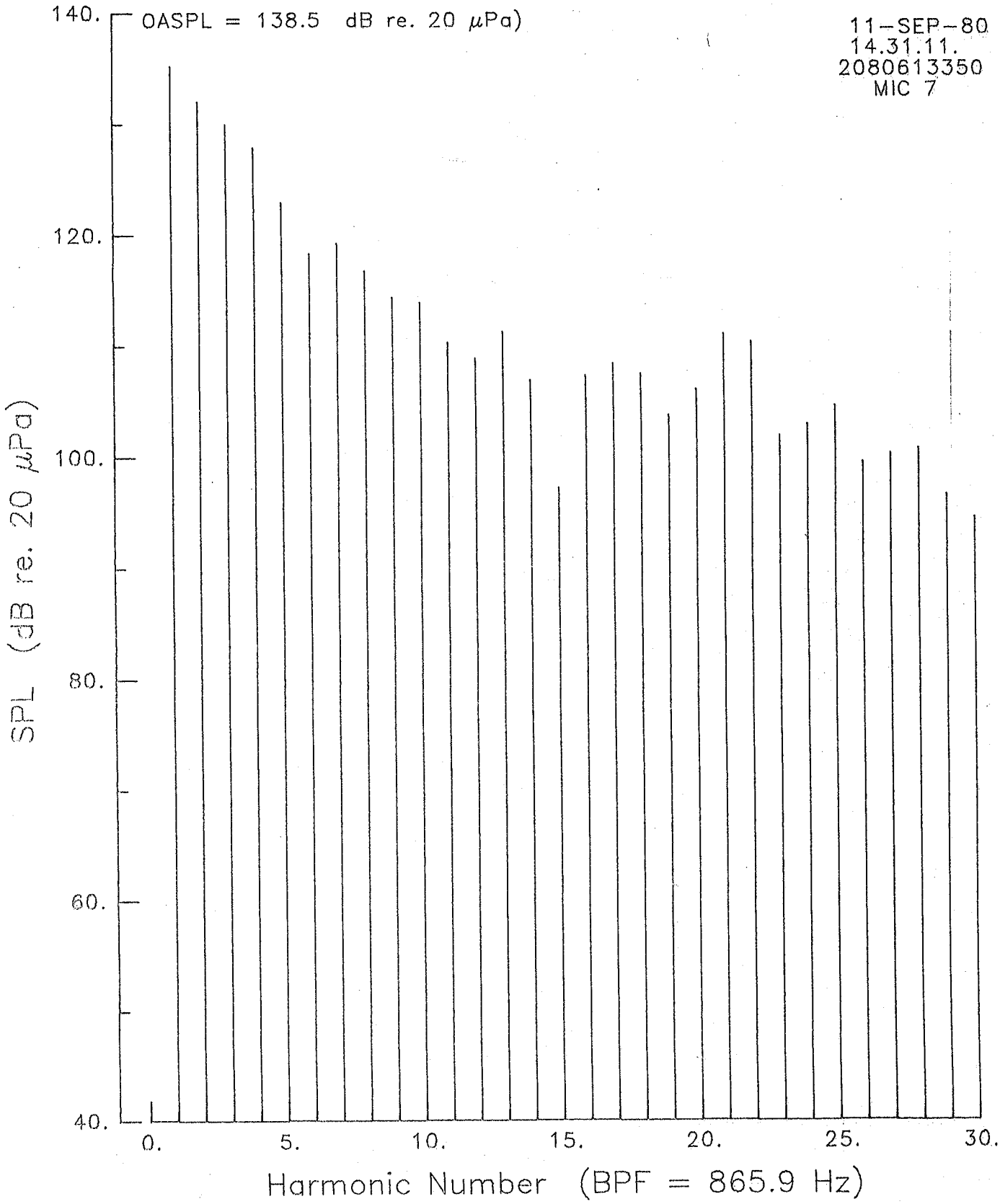

Figure 10.- Continued.

F. Farassat -- P. Nystrom
JIAFS -- NASA/LaRC -- GWU

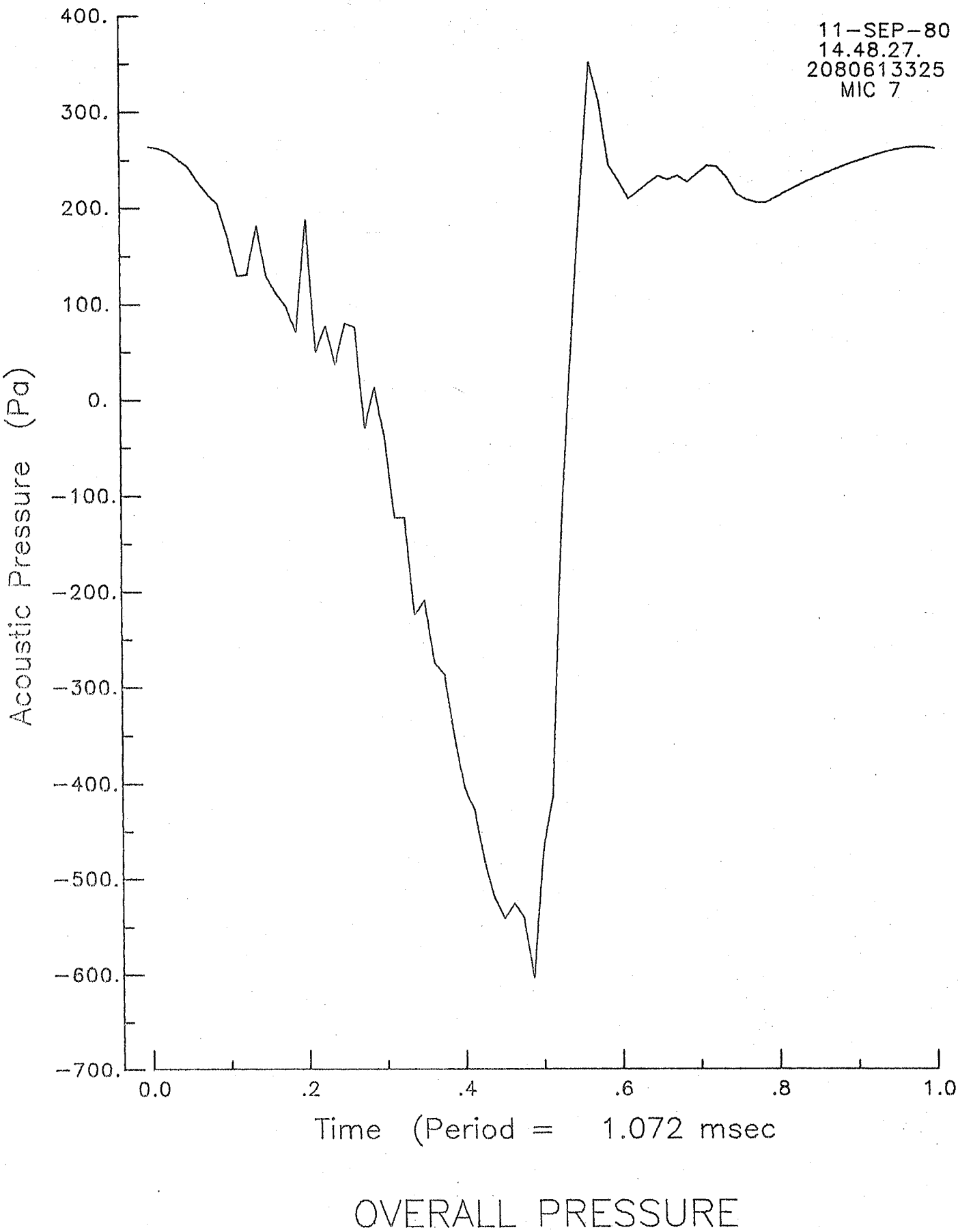

Figure 10.- Continued.

F. Farassat -- P. Nystrom
JIAFS -- NASA/LaRC -- GWU

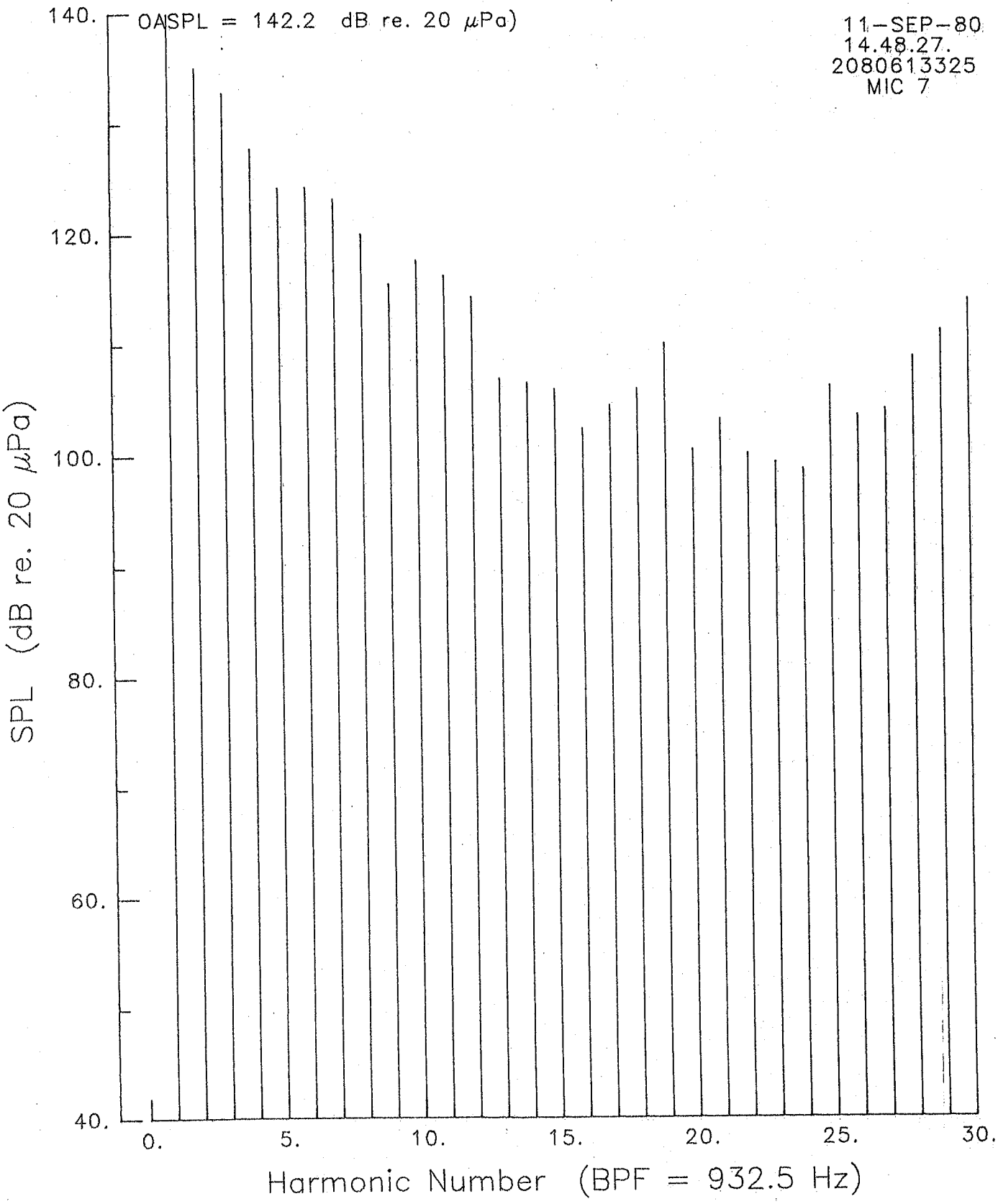

OVERALL SPECTRUM

Figure 10.- Continued.

F. Farassat -- P. Nystrom
JIAFS -- NASA/LaRC -- GWU

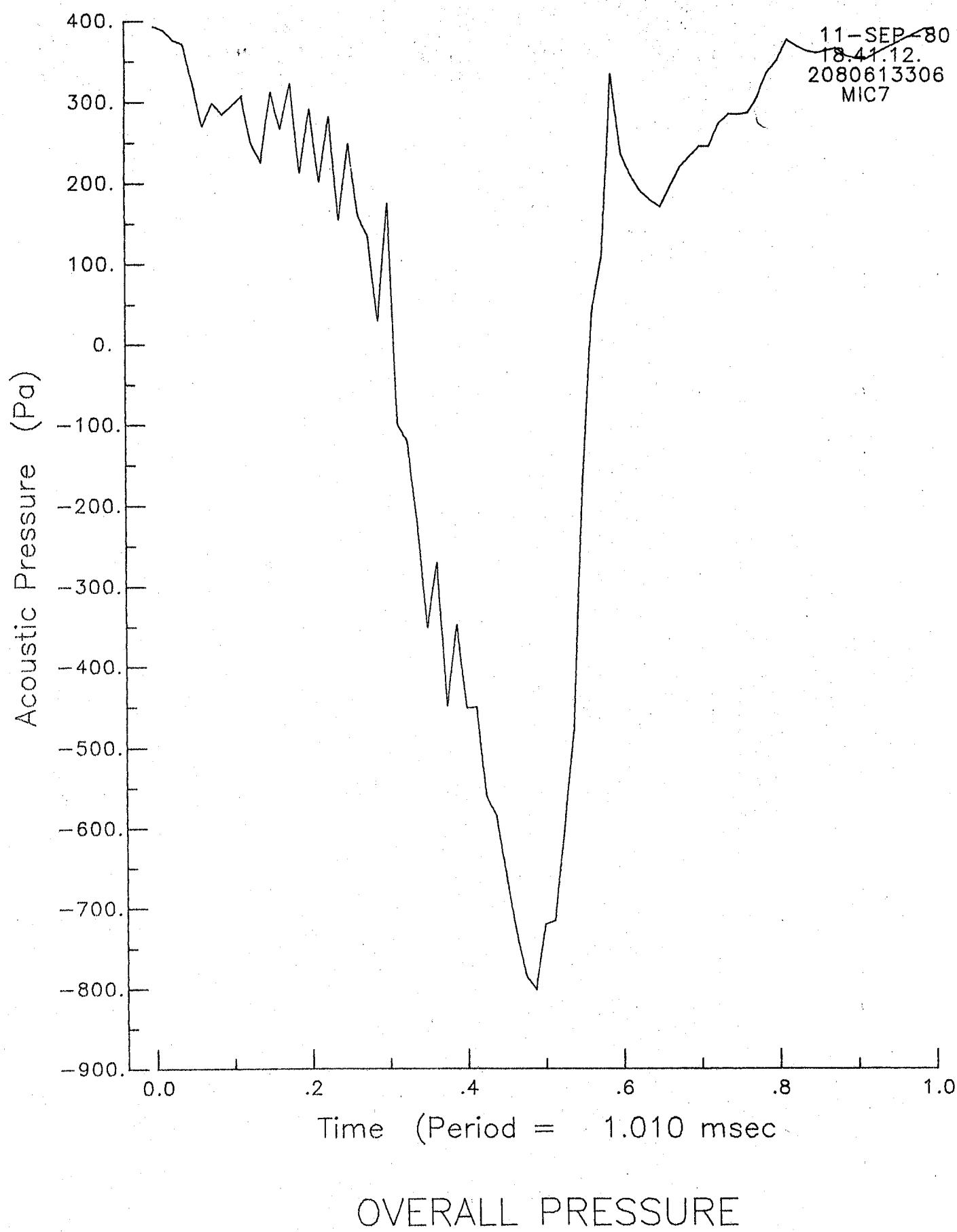

Figure 10.- Continued.

F. Farassat -- P. Nystrom
JIAFS -- NASA/LaRC -- GWU

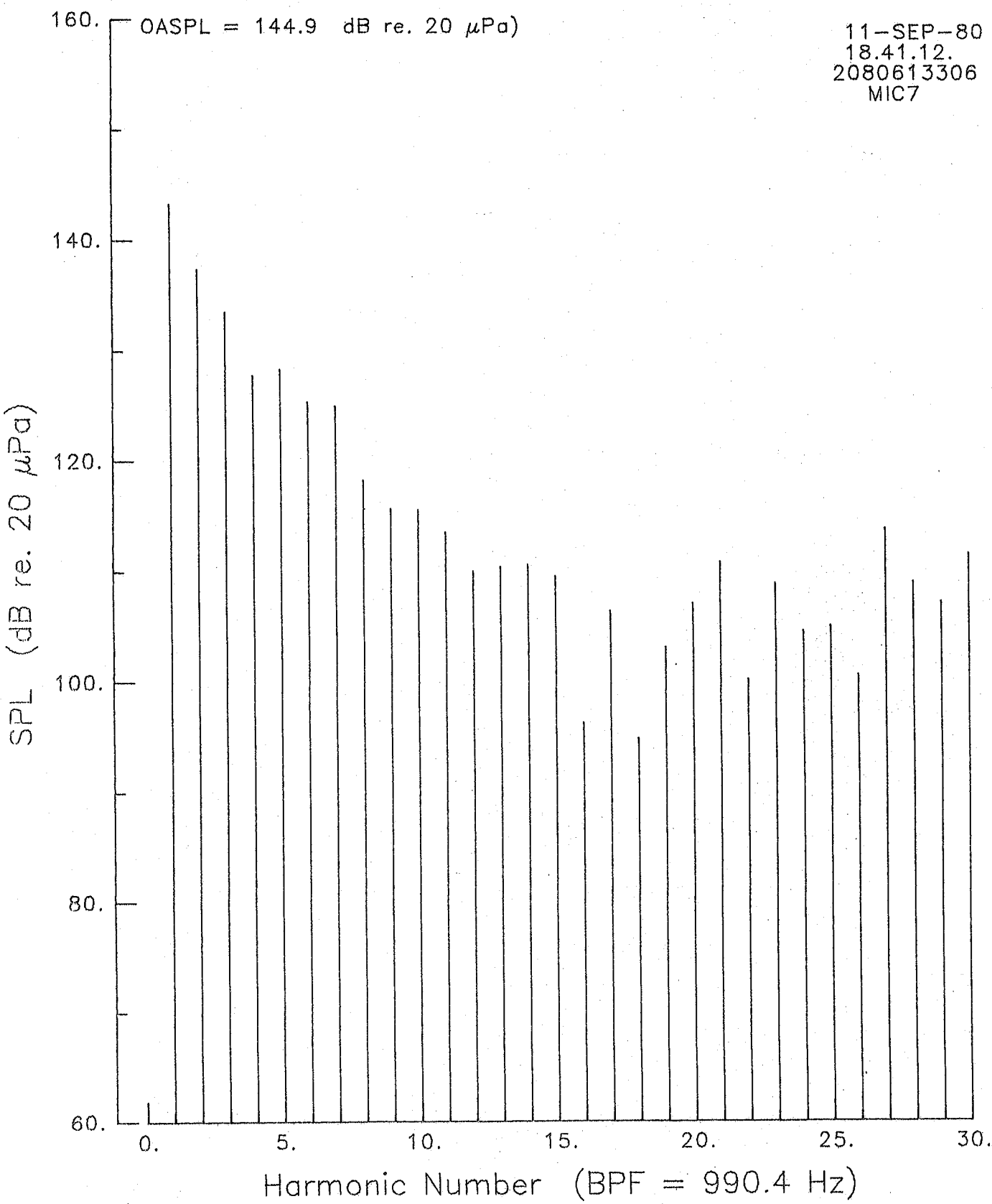

Figure 10.- Continued.

F. Farassat -- P. Nystrom
JIAFS -- NASA/LaRC -- GWU

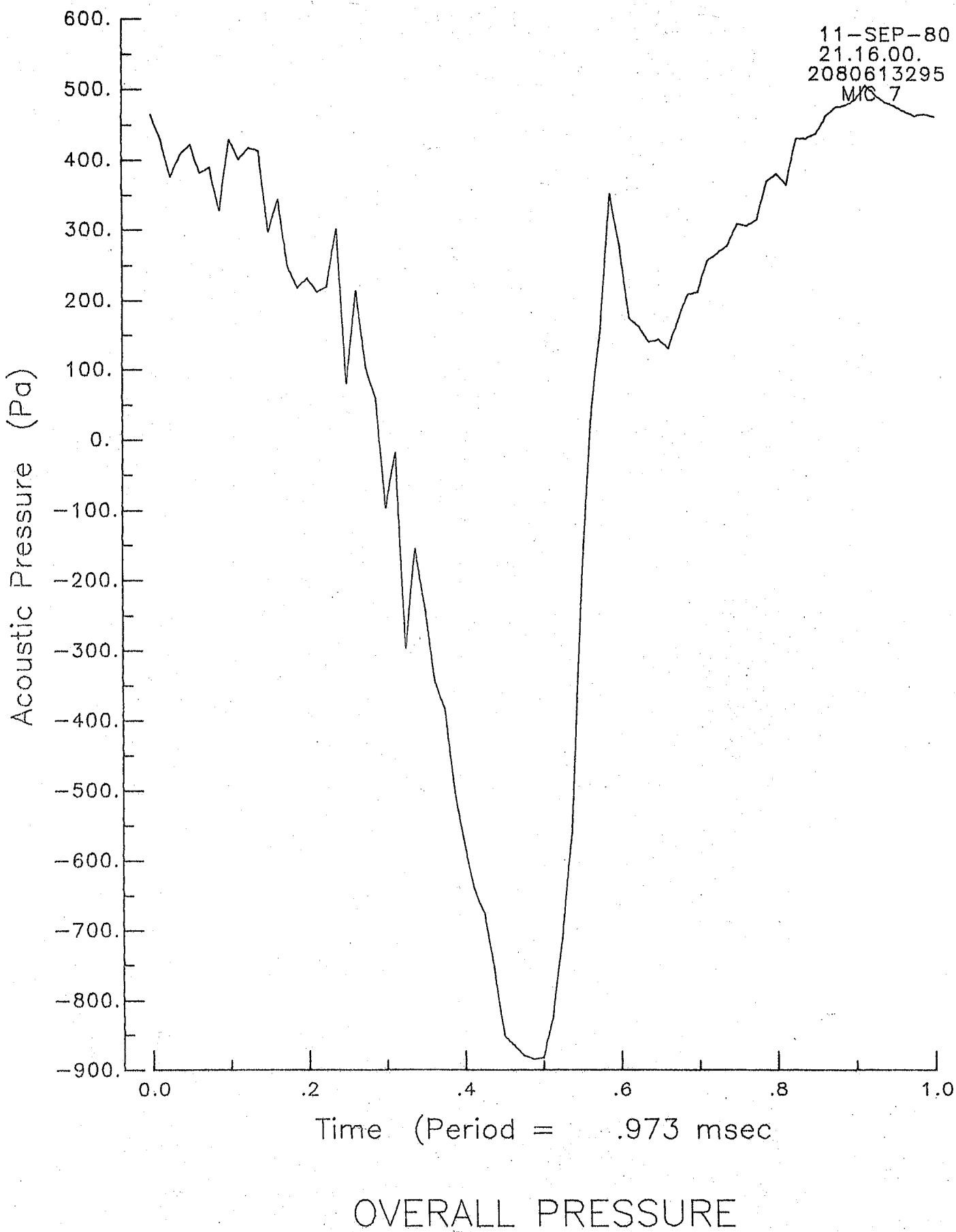

Figure 10.- Continued.

F. Farassat -- P. Nystrom
JIAFS -- NASA/LaRC -- GWU

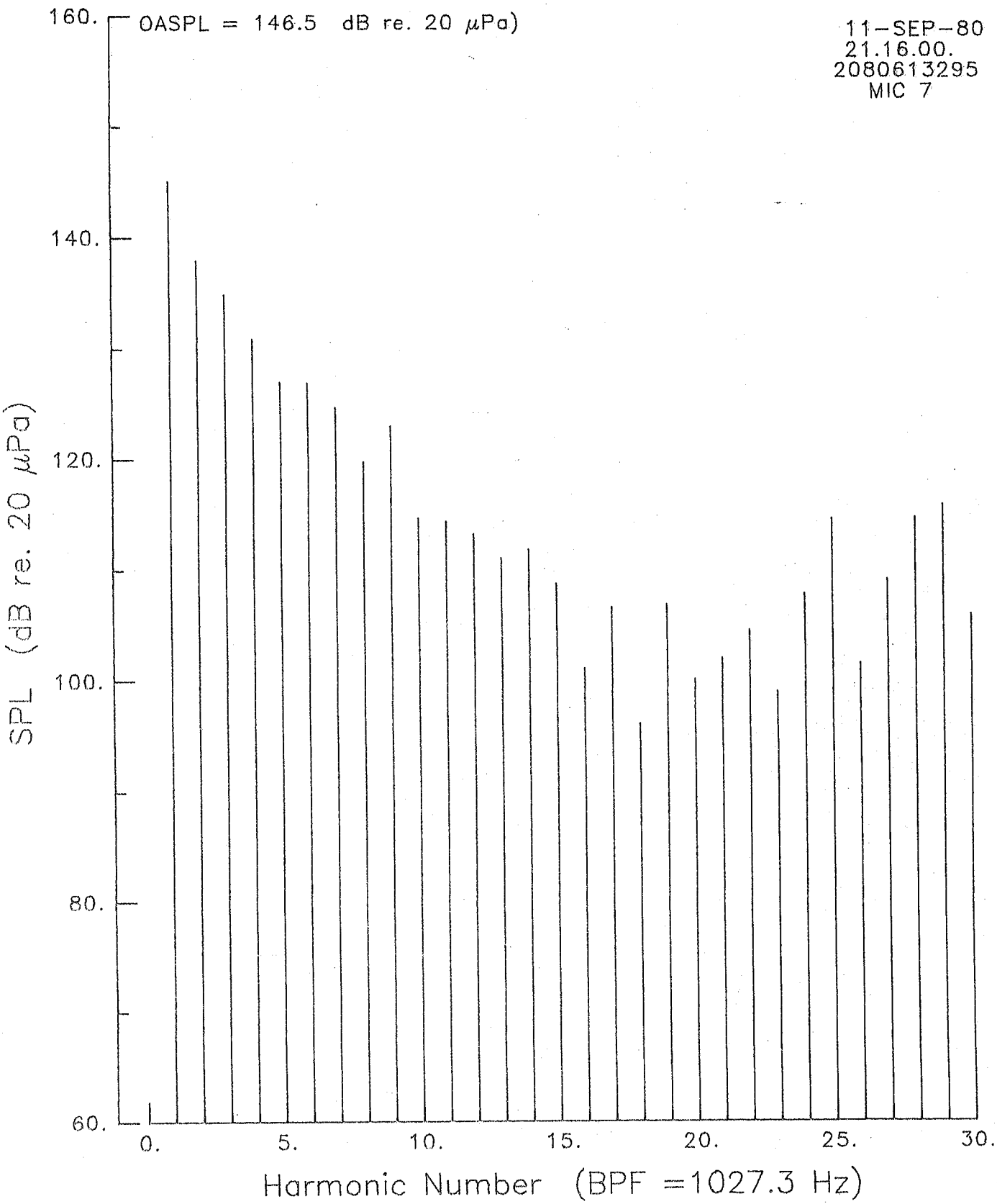

Figure 10.- Concluded.

F. Farassat -- P. Nystrom
JIAFS -- NASA/LaRC -- GWU

SR-3 BLADE

FLIGHT ALTITUDE 7.63 km (25,000 ft)

FLIGHT MACH NUMBER 0.8

MICROPHONE 7

(ADVANCE RATIO VARIED)

Figure 11.- Free-field acoustic pressure signatures and spectra for SR-3 blade - Altitude 7.63 Km (25,000 ft), M=0.8, Microphone 7. Note the advance ratio is varied in these calculations.

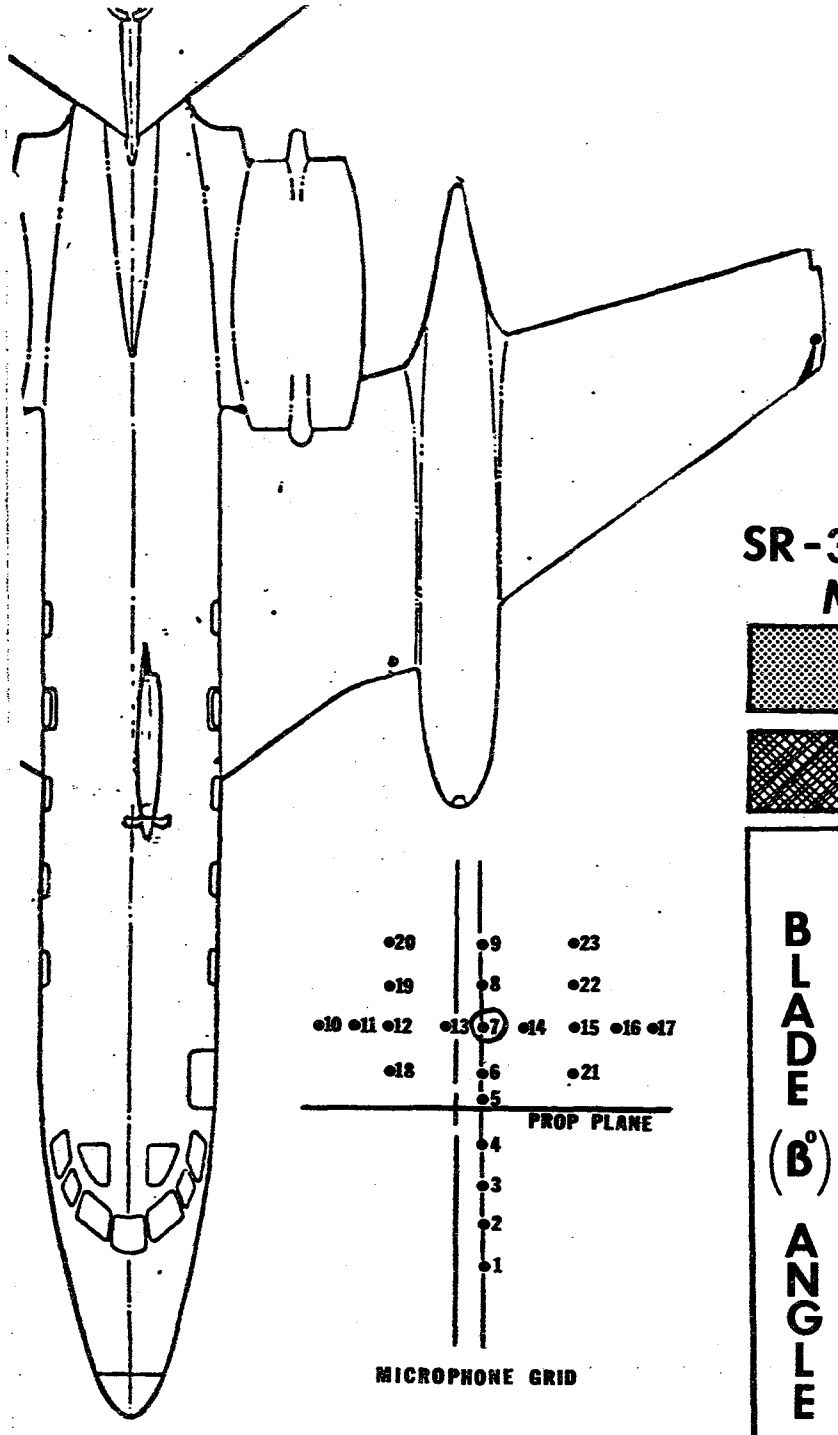

Figure 11.- Continued.

SR-3 TEST MATRIX

EXCEEDS BLEED SYS. POWER CAPACITY

BLADE CRITICAL SPEED

BLADE ANGLE (β°)	ADVANCE RATIO (J)	ALTITUDE (FT) 20,000						25,000						30,000					
		MACH # .50	.60	.65	.70	.75	.80	.50	.60	.65	.70	.75	.80	.50	.60	.65	.70	.75	.80
59.3	4.30												X						
	3.50												X						
	3.25				▨						▨		X				▨		
	3.06												▨						▨
	2.90						▨						▨					▨	▨
61.3	4.30												X						
	3.50												X						
	3.25				▨						▨		X				▨		
	3.06												▨						▨
	2.95						▨						▨					▨	▨
63.3	4.30																		
	4.07																		
	3.50																		
	3.25						▨						▨						▨

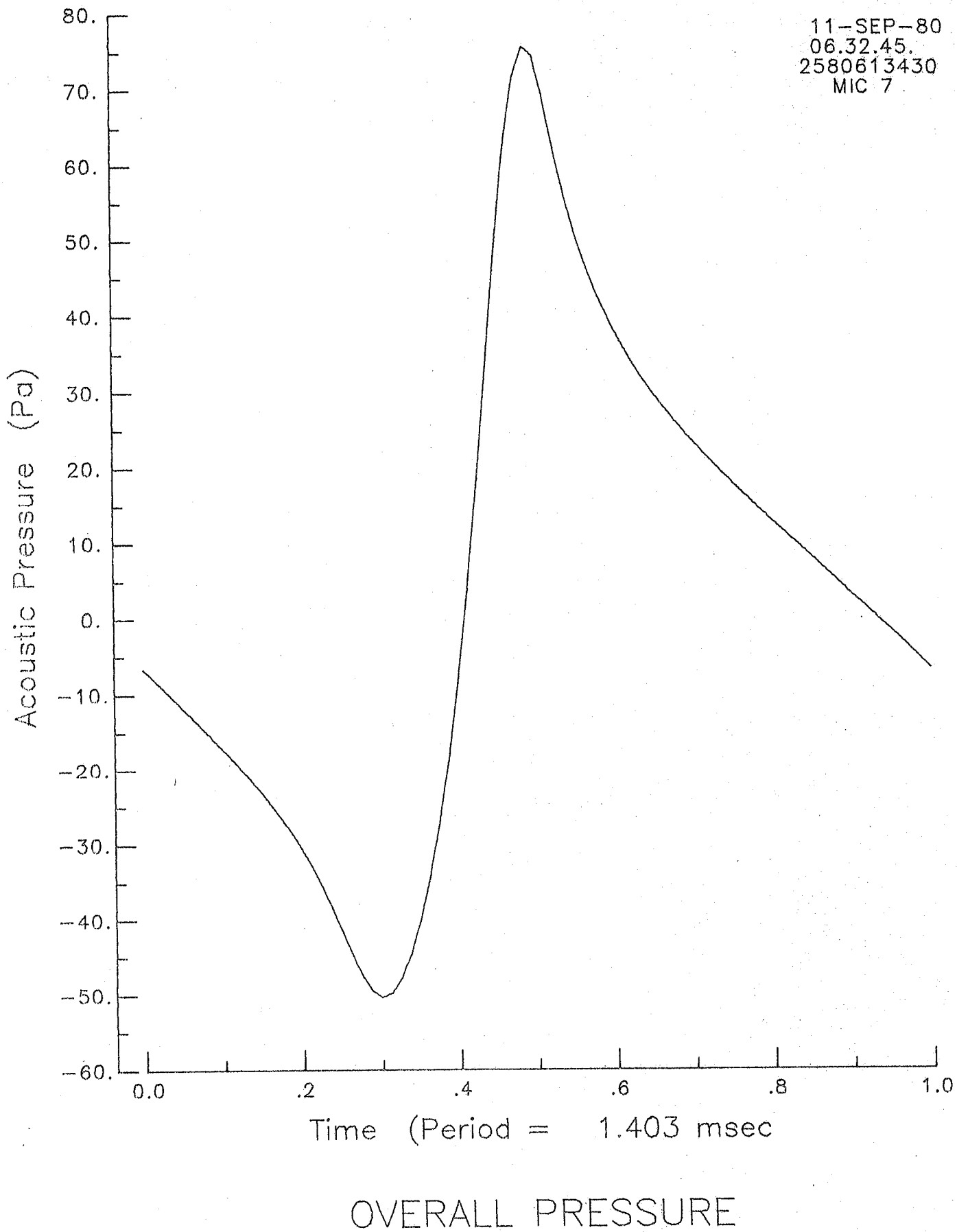

OVERALL PRESSURE

Figure 11.- Continued.

F. Farassat -- P. Nystrom
JIAFS -- NASA/LaRC -- GWU

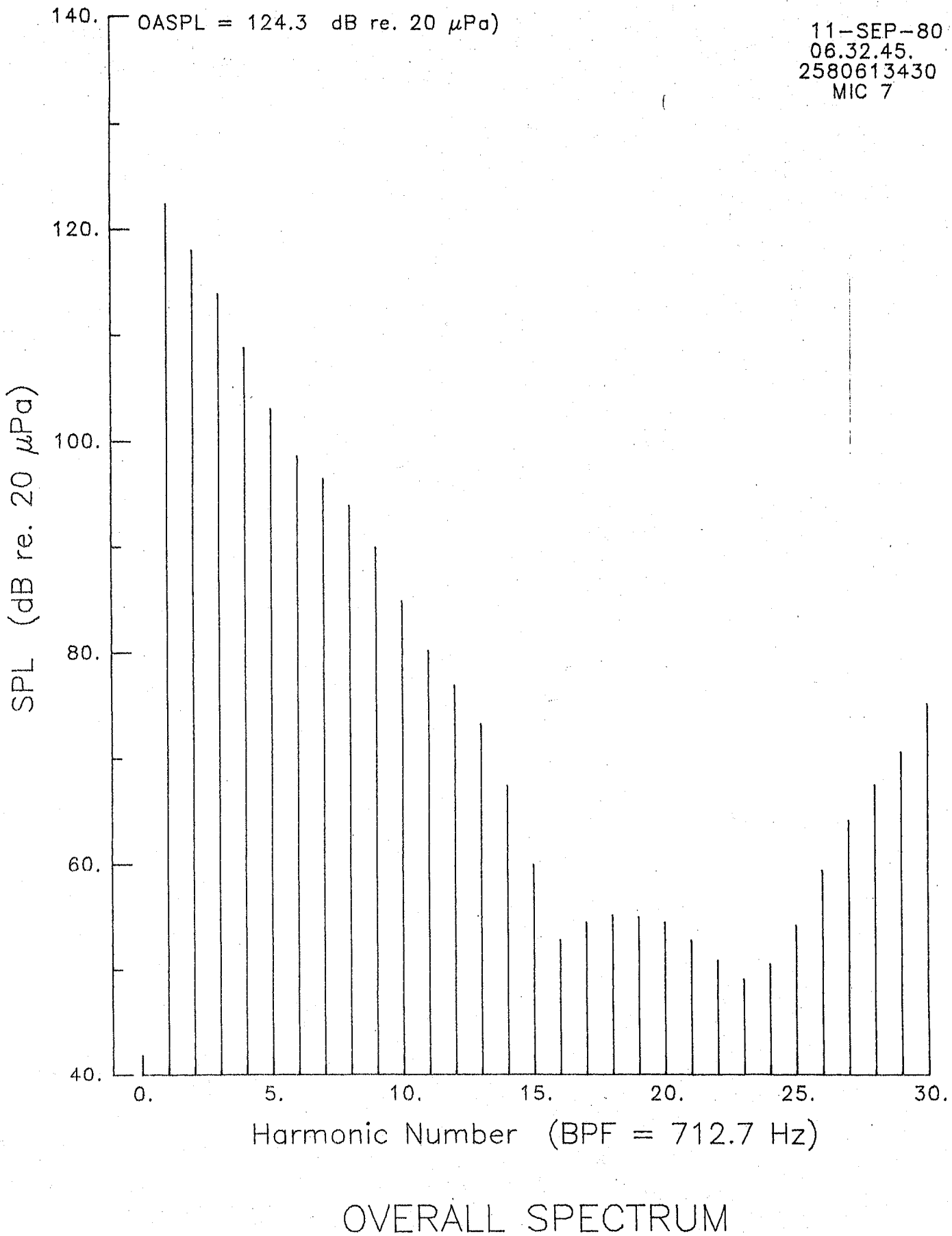

Figure 11.- Continued.

F. Farassat -- P. Nystrom
JIAFS -- NASA/LaRC -- GWU

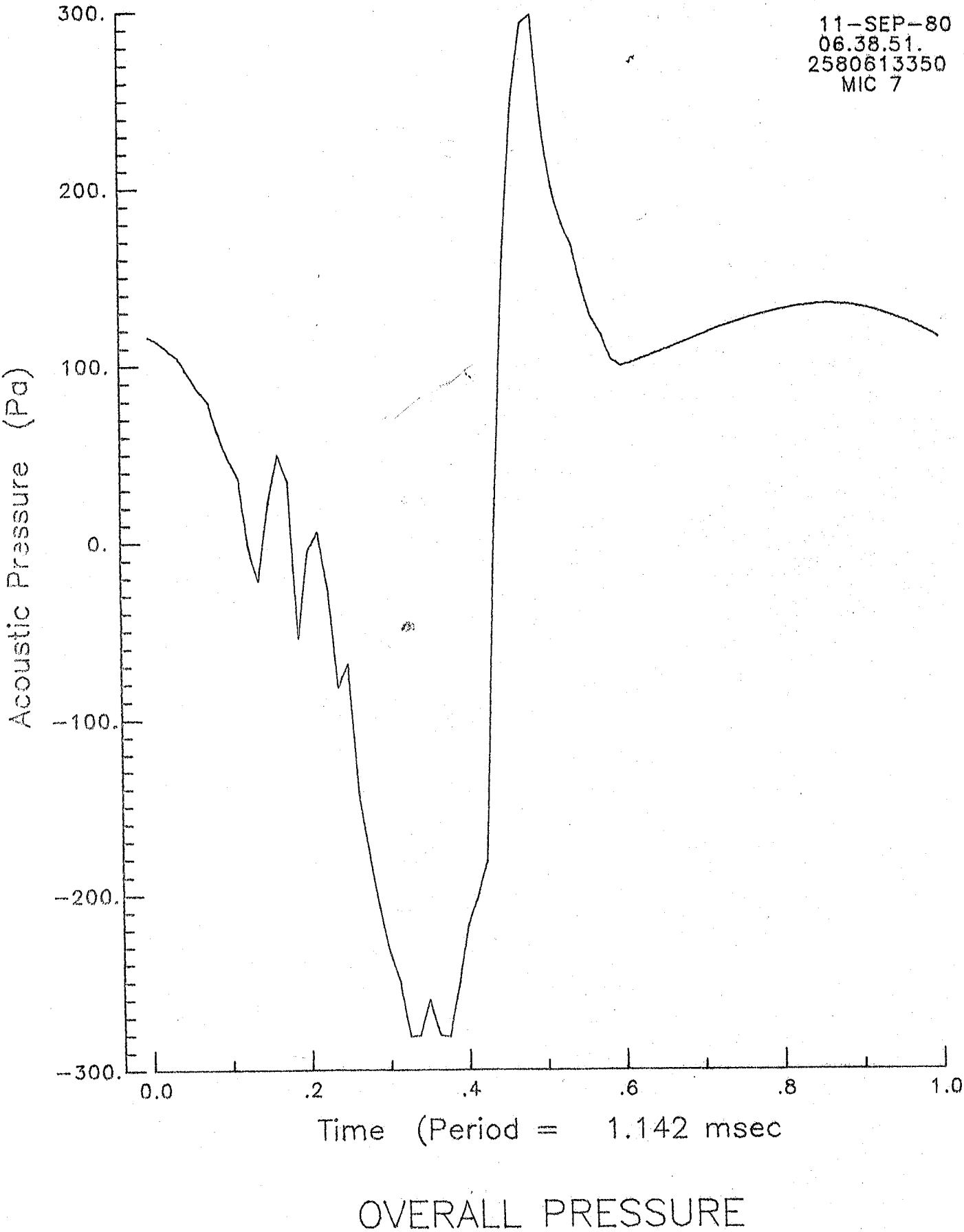

Figure 11.- Continued.

F. Farassat -- P. Nystrom
JIAFS -- NASA/LaRC -- GWU

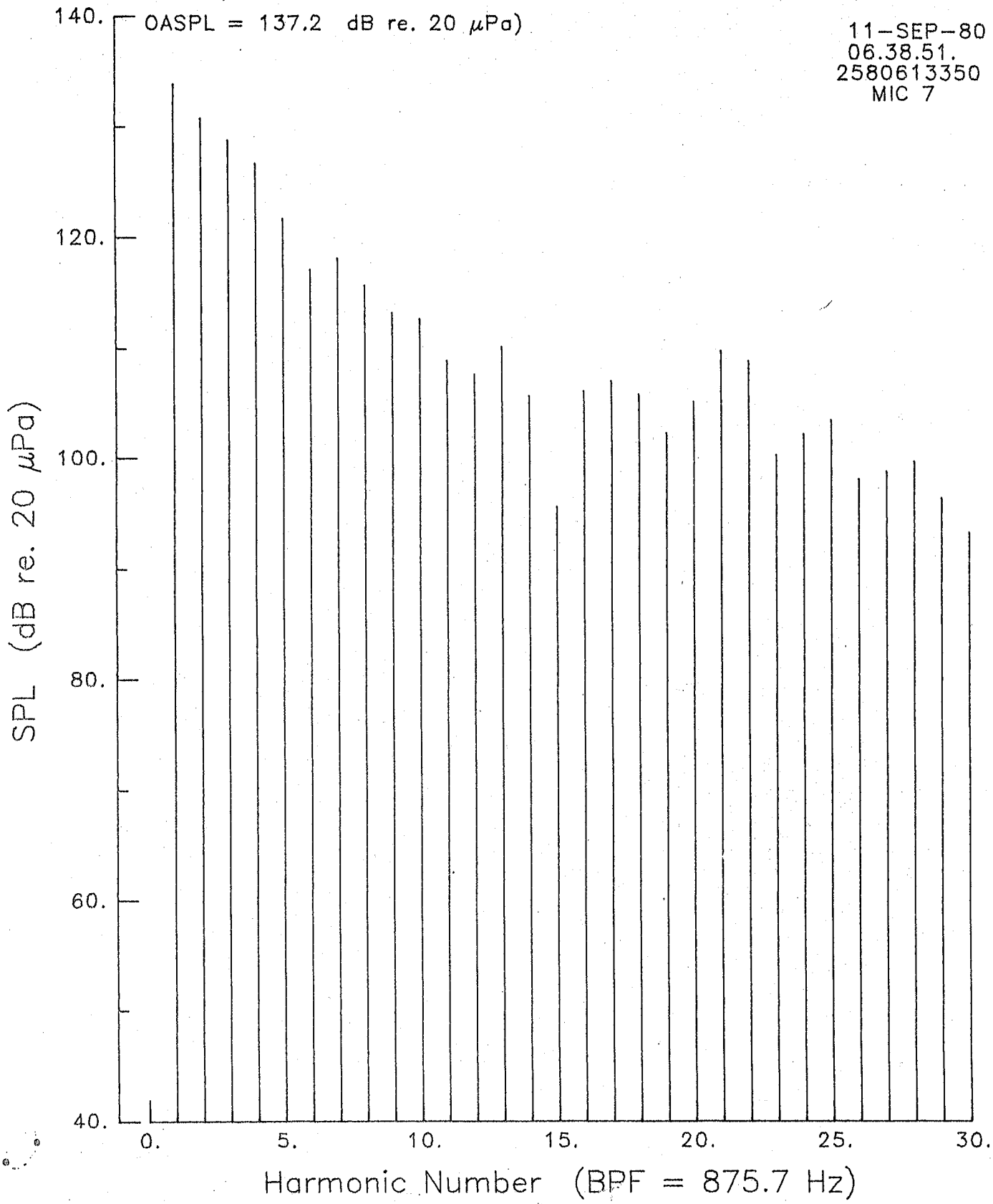

Figure 11.- Continued.

F. Farassat -- P. Nystrom
JIAFS -- NASA/LaRC -- GWU

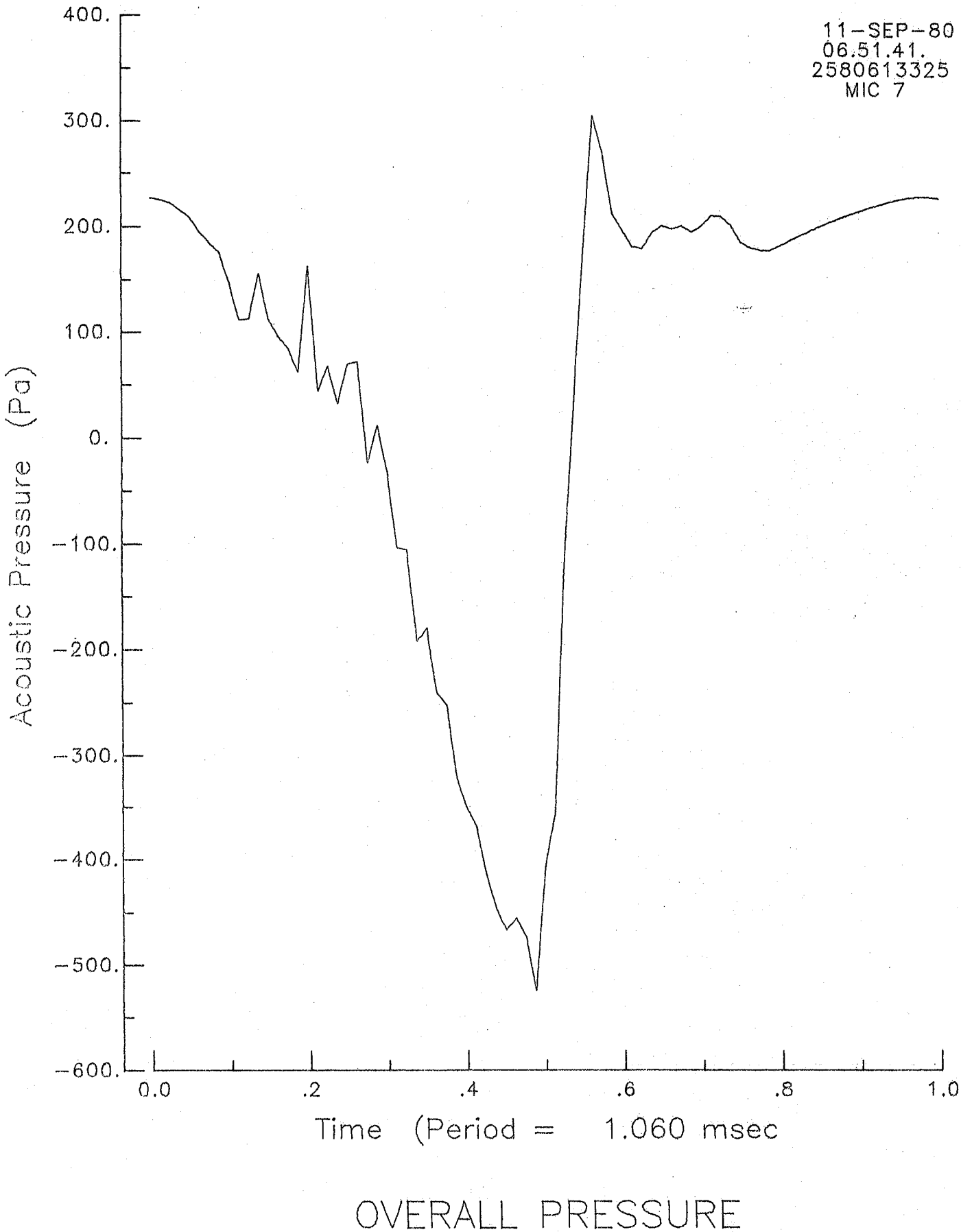

Figure 11.- Continued.

F. Farassat -- P. Nystrom
JIAFS -- NASA/LaRC -- GWU

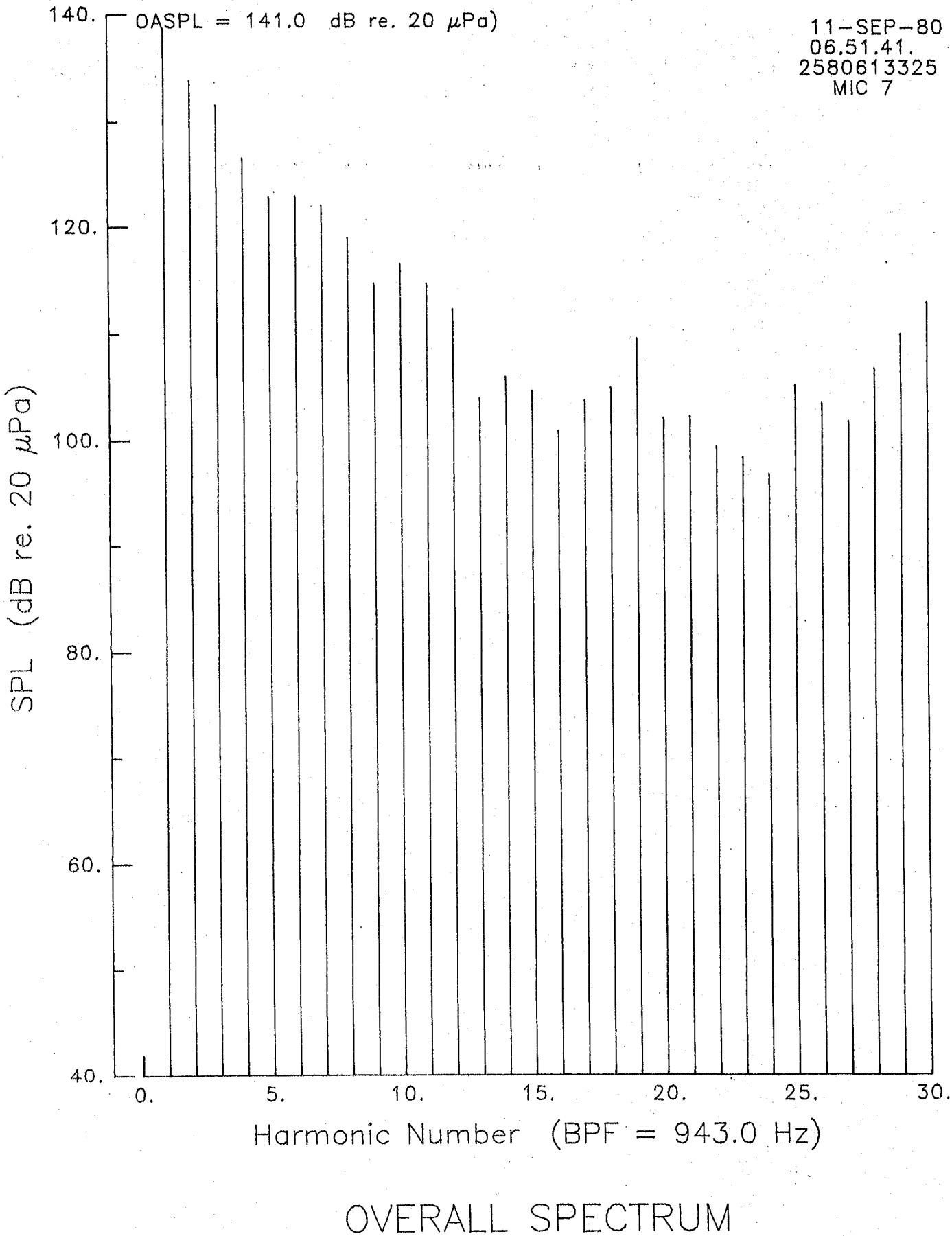

Figure 11.- Continued.

F. Farassat -- P. Nystrom
JIAFS -- NASA/LaRC -- GWU

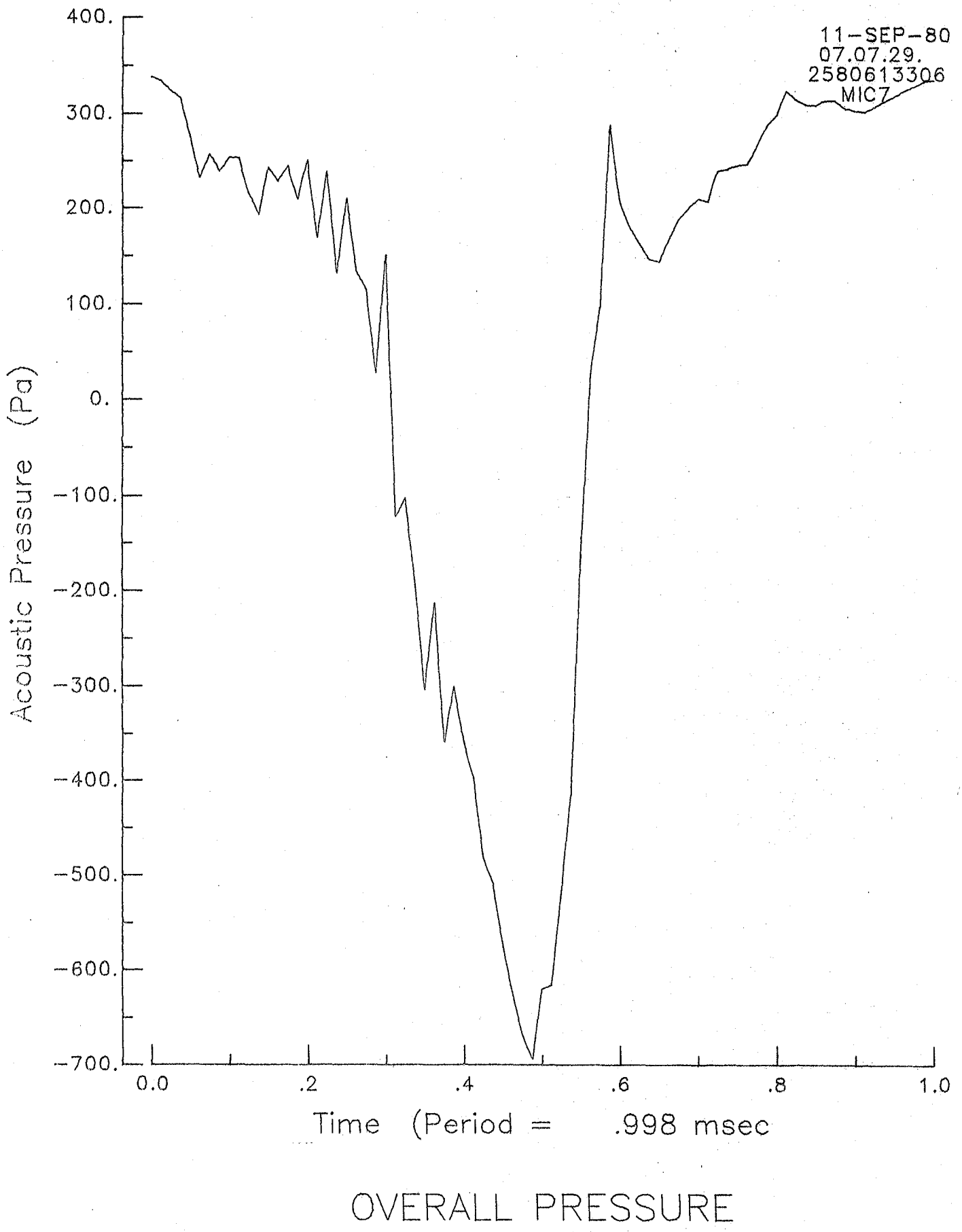

Figure 11.- Continued.

F. Farassat -- P. Nystrom
JIAFS -- NASA/LaRC -- GWU

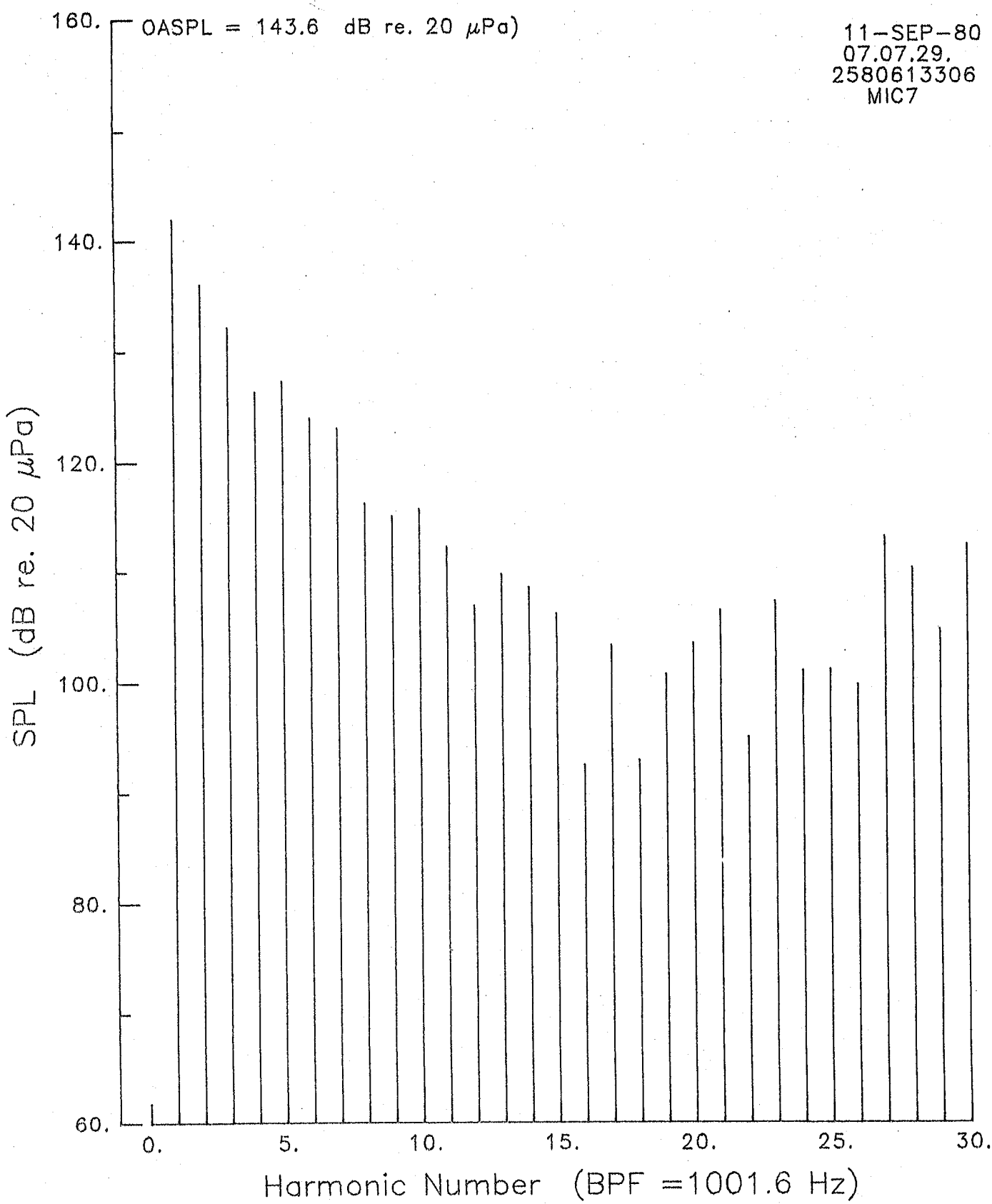

Figure 11.- Continued.

F. Farassat -- P. Nystrom
JIAFS -- NASA/LaRC -- GWU

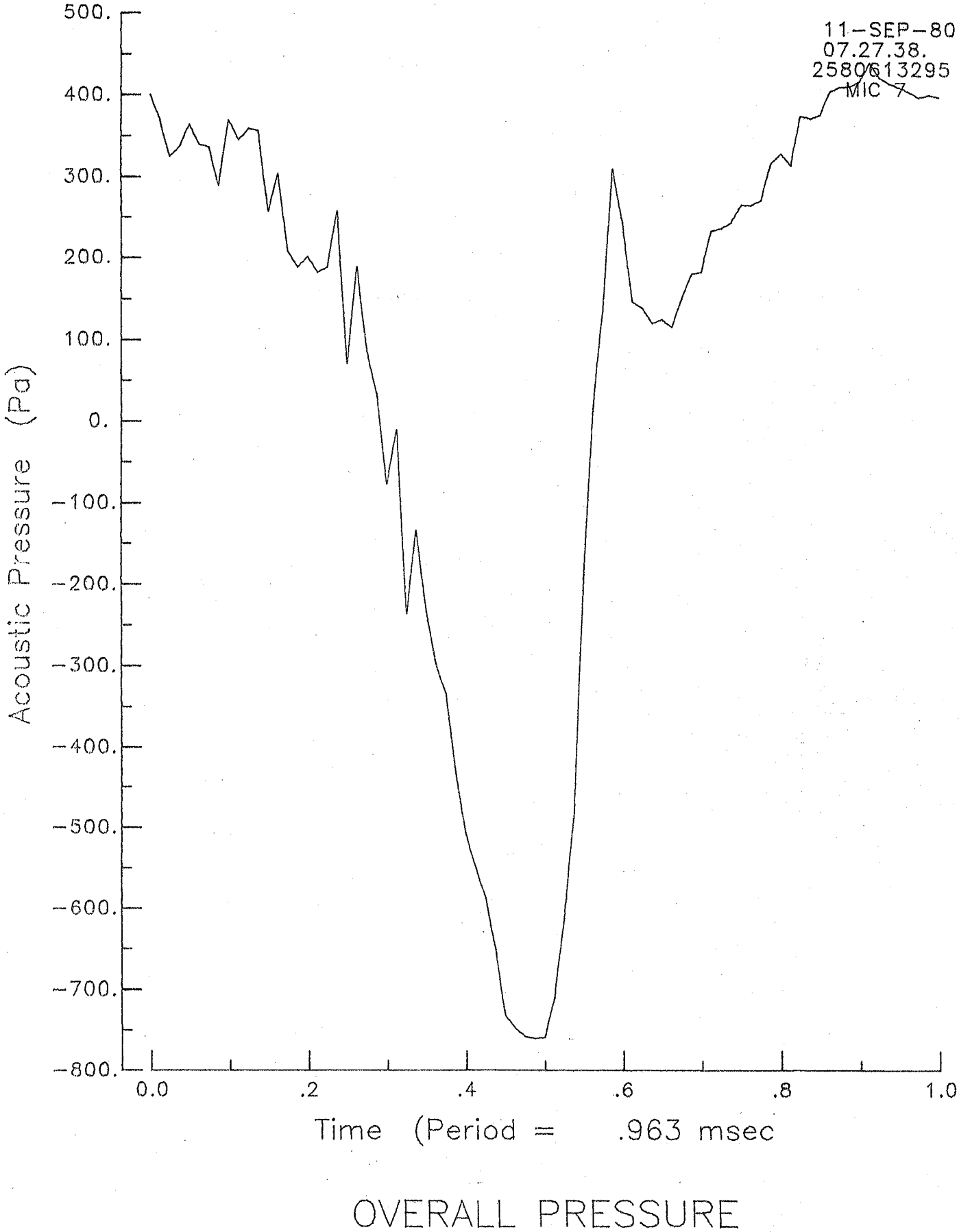

Figure 11.- Continued.

F. Farassat -- P. Nystrom
JIAFS -- NASA/LaRC -- GWU

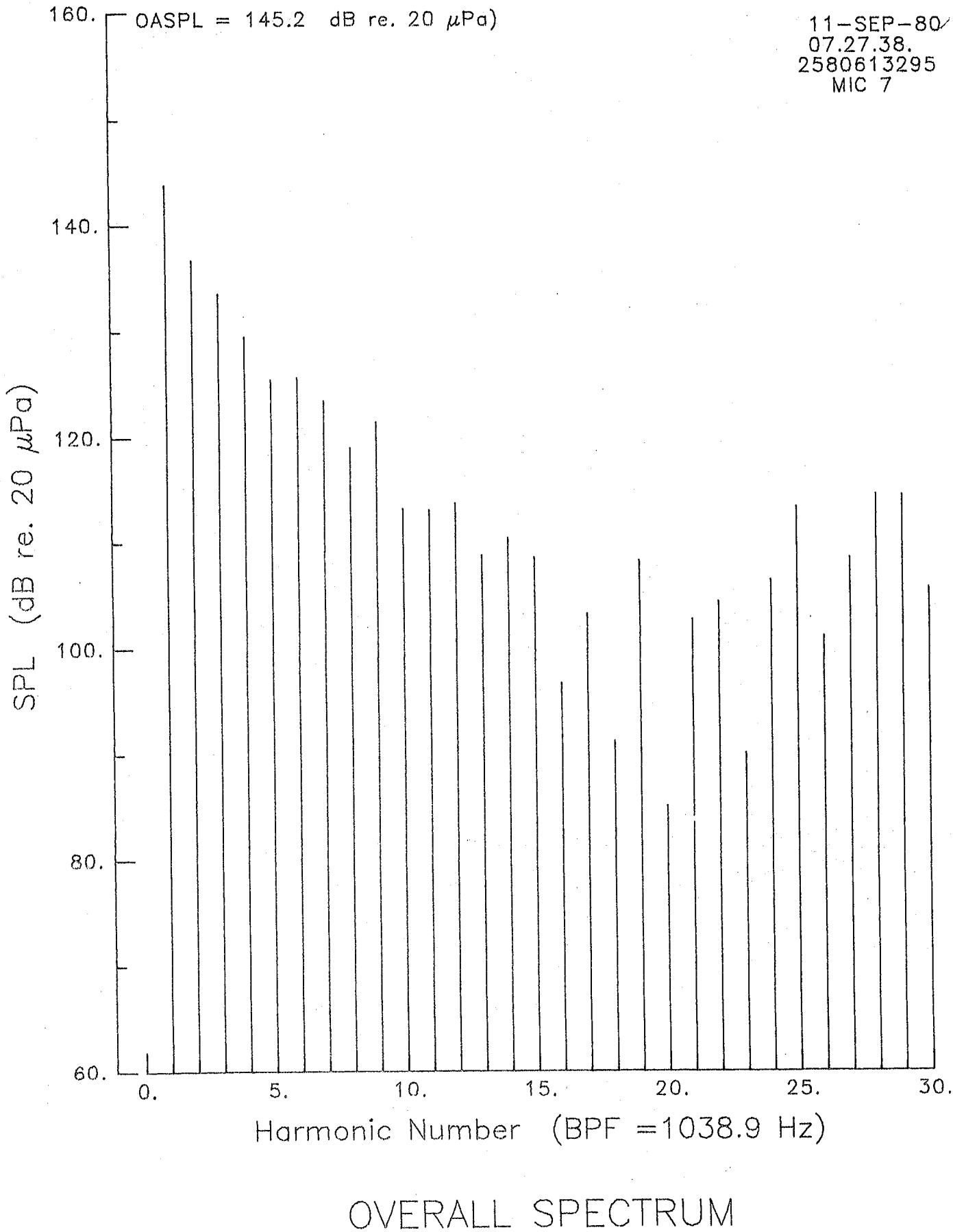

Figure 11.- Concluded.

F. Farassat -- P. Nystrom
JIAFS -- NASA/LaRC -- GWU

SR-3 BLADE

FLIGHT ALTITUDE 9.15 km (30,000 ft)

FLIGHT MACH NUMBER 0.6

MICROPHONE 7

(ADVANCE RATIO VARIED)

Figure 12.- Free-field acoustic pressure signatures and spectra for SR-3 blade - Altitude 9.15 Km (30,000 ft), M=0.6, Microphone 7. Note advance ratio is varied in these calculations.

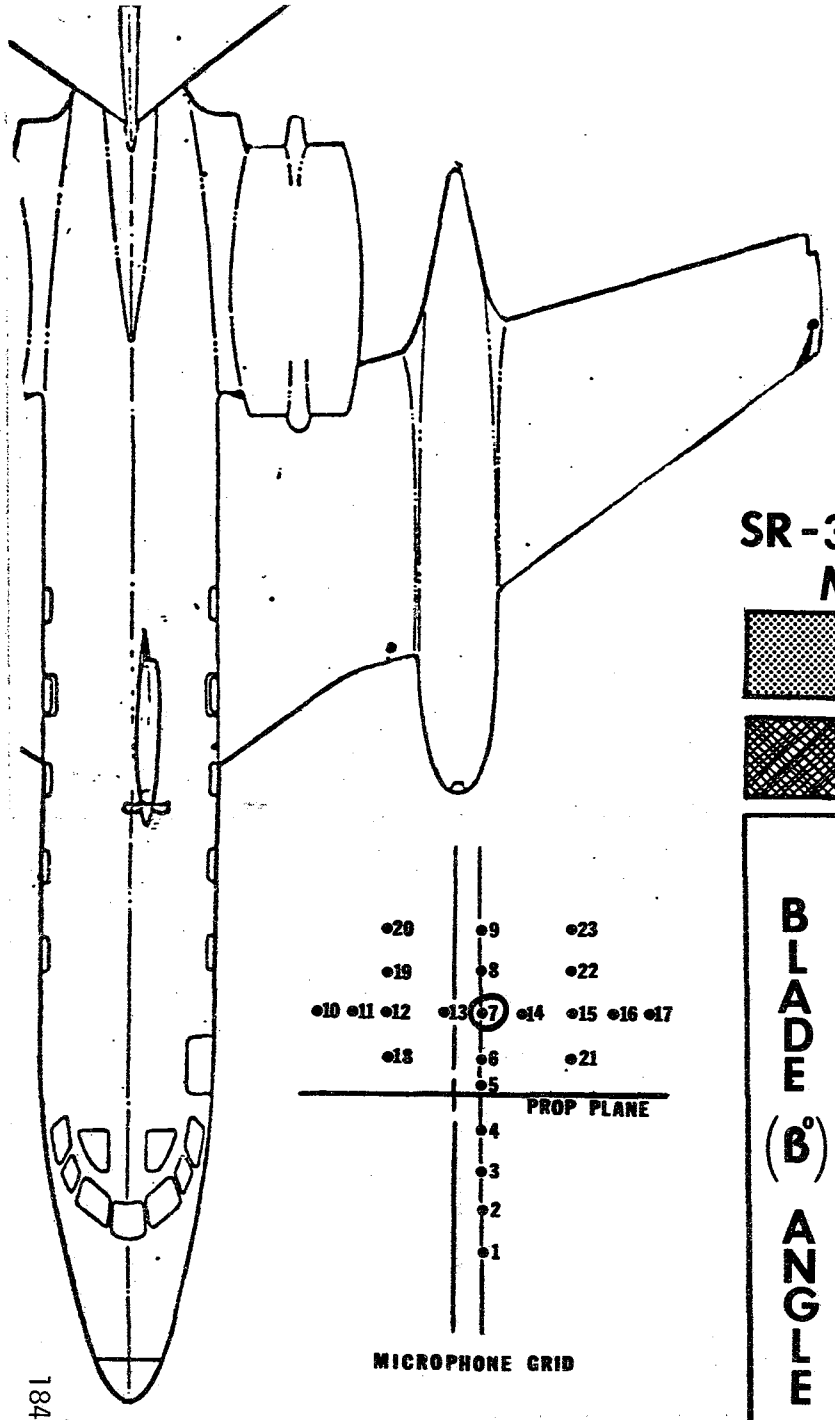

Figure 12.- Continued.

SR-3 TEST MATRIX

EXCEEDS BLEED SYS. POWER CAPACITY

BLADE CRITICAL SPEED

BLADE ANGLE (β°)	ADVANCE RATIO (J)	ALTITUDE (FT) 20,000						ALTITUDE (FT) 25,000						ALTITUDE (FT) 30,000					
		MACH # .50	.60	.65	.70	.75	.80	.50	.60	.65	.70	.75	.80	.50	.60	.65	.70	.75	.80
59.3	4.30																		
	3.50																		
	3.25																		
	3.06																		
	2.90																		
61.3	4.30														X				
	3.50														X				
	3.25														X				
	3.06														X				
	2.95														X				
63.3	4.30																		
	4.07																		
	3.50																		
	3.25																		

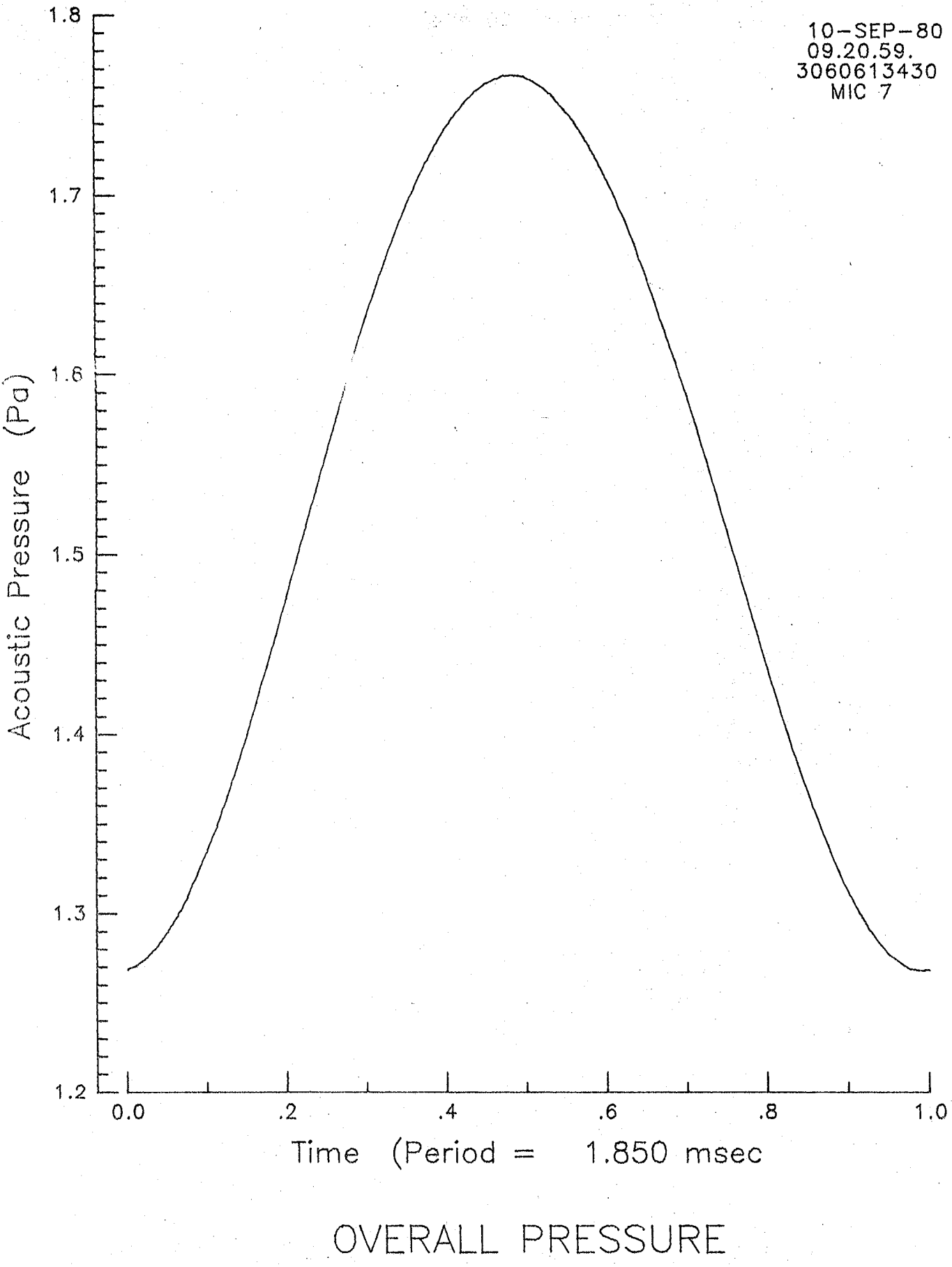

Figure 12.- Continued.

F. Farassat -- P. Nystrom
JIAFS -- NASA/LaRC -- GWU

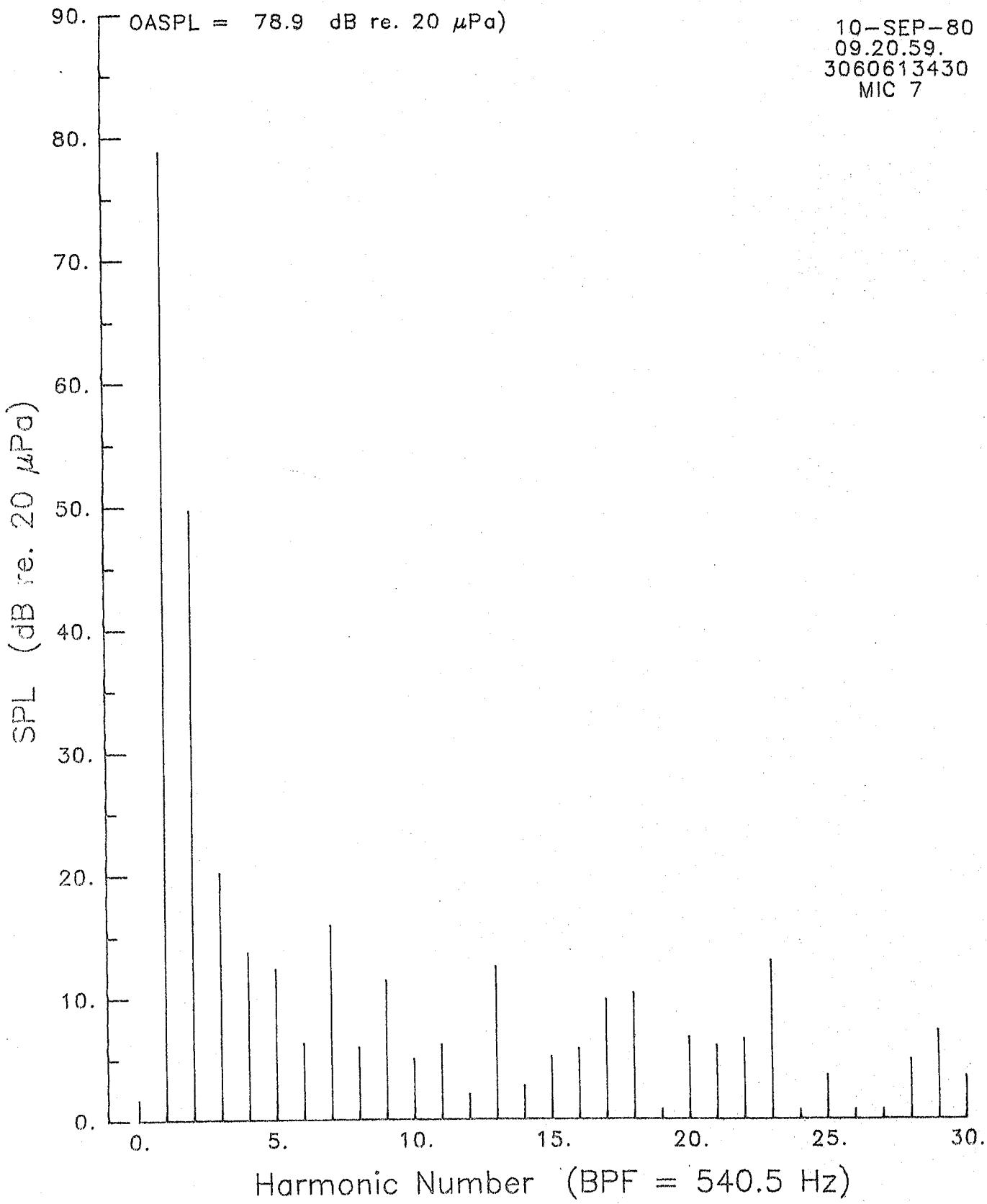

OVERALL SPECTRUM

Figure 12.- Continued.

F. Farassat -- P. Nystrom
JIAFS -- NASA/LaRC -- GWU

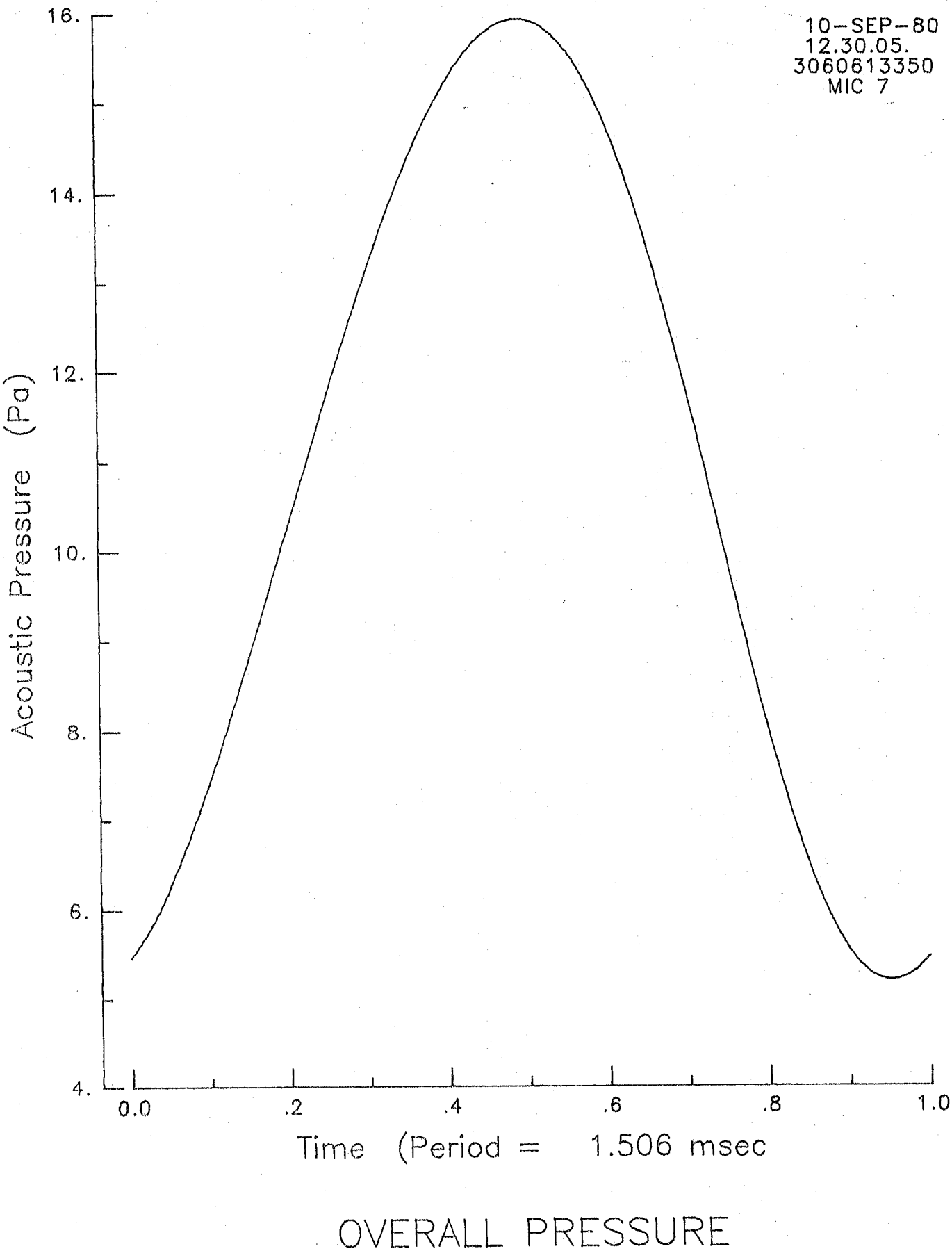

Figure 12.- Continued.

F. Farassat -- P. Nystrom
JIAFS -- NASA/LaRC -- GWU

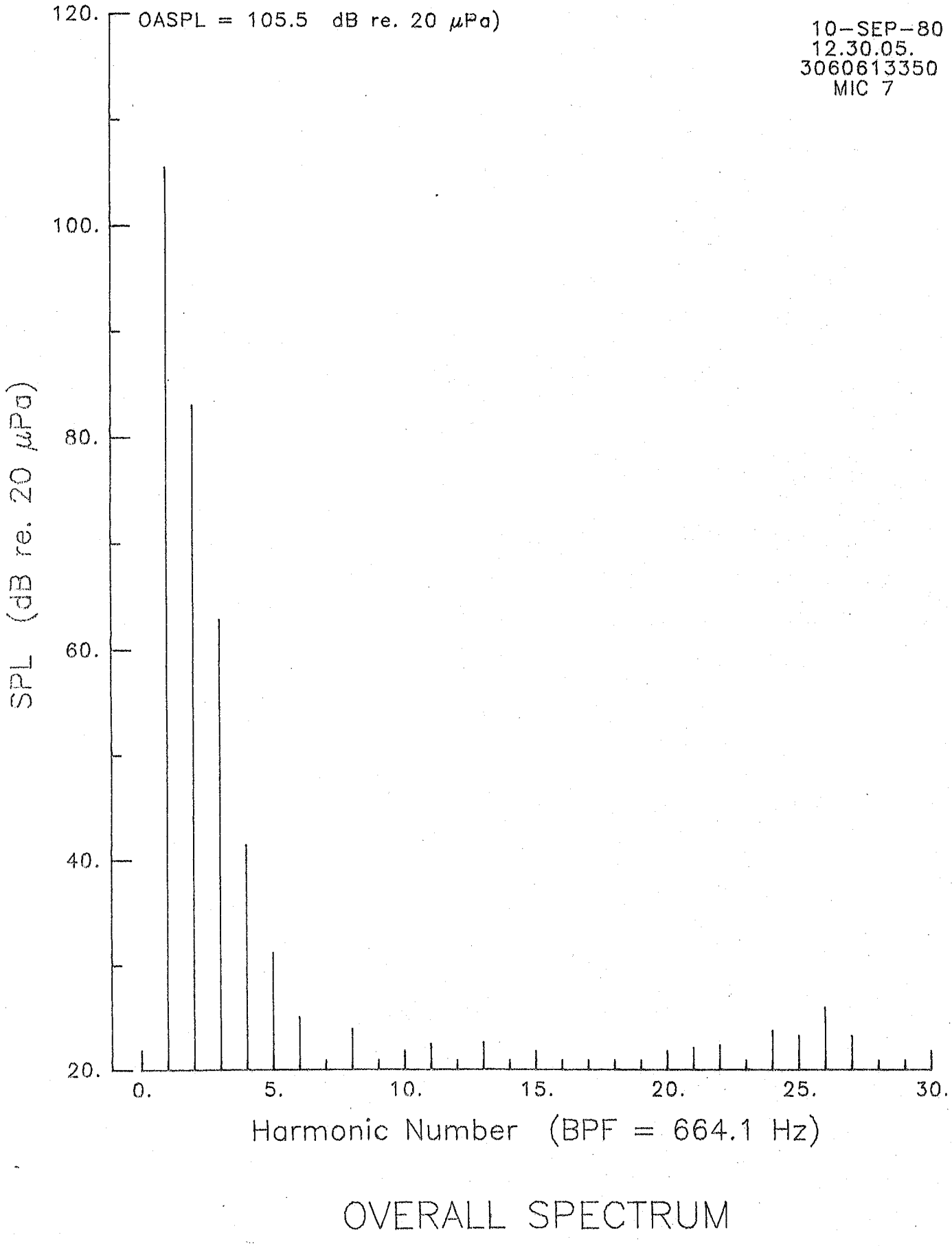

Figure 12.-Continued.

F. Farassat -- P. Nystrom
JIAFS -- NASA/LaRC -- GWU

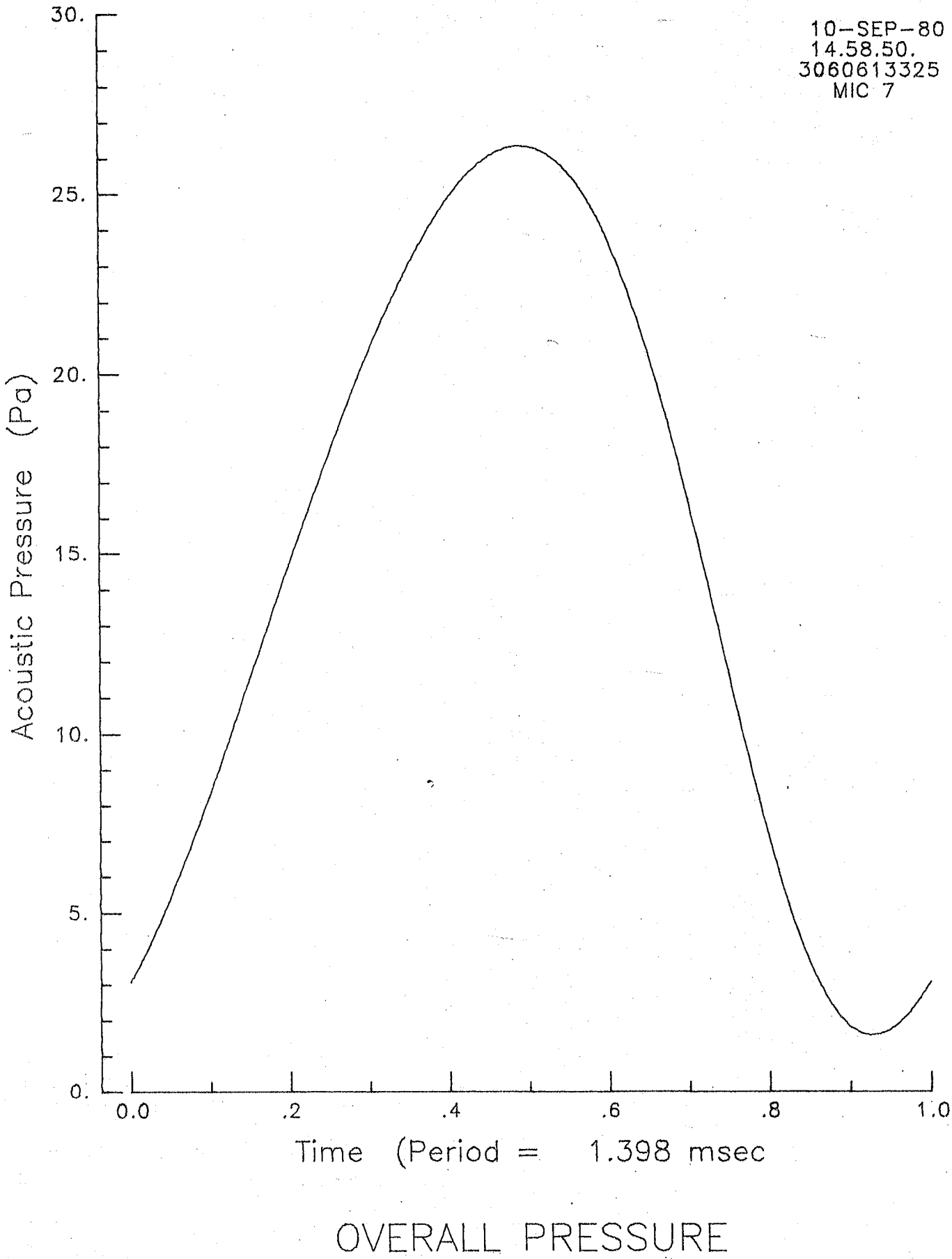

Figure 12.- Continued.

F. Farassat -- P. Nystrom
JIAFS -- NASA/LaRC -- GWU

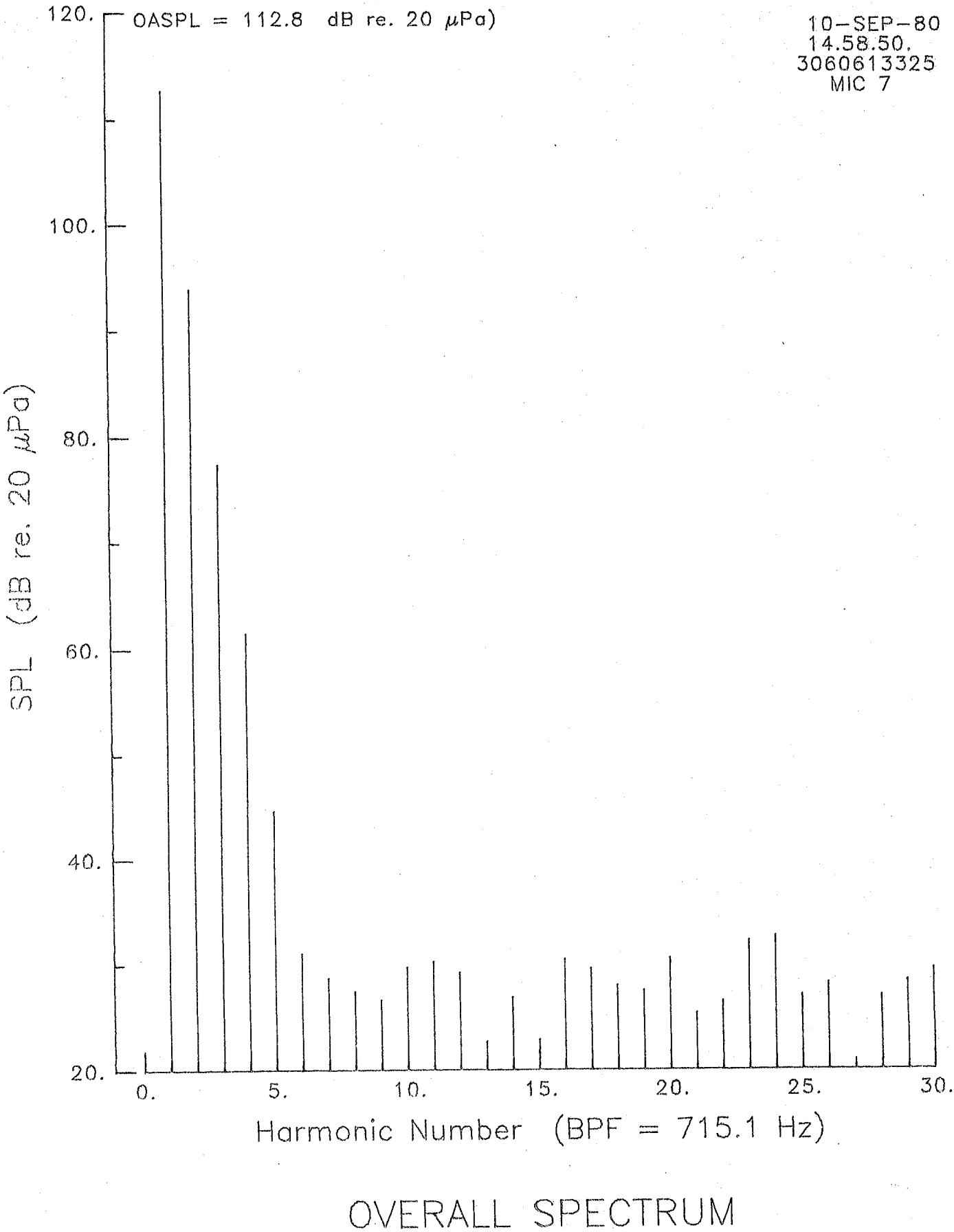

Figure 12.- Continued.

F. Farassat -- P. Nystrom
JIAFS -- NASA/LaRC -- GWU

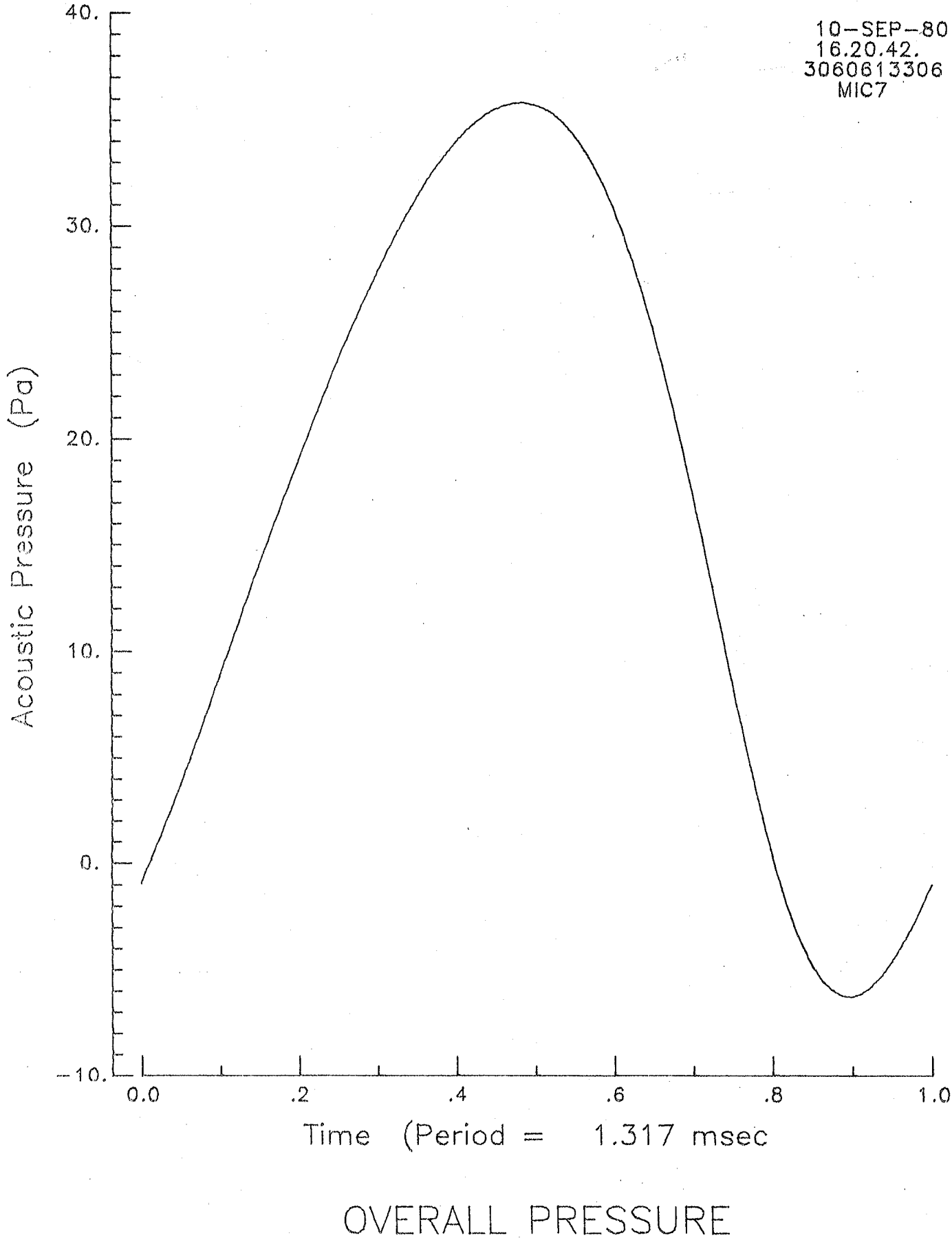

Figure 12.- Continued.

F. Farassat -- P. Nystrom
JIAFS -- NASA/LaRC -- GWU

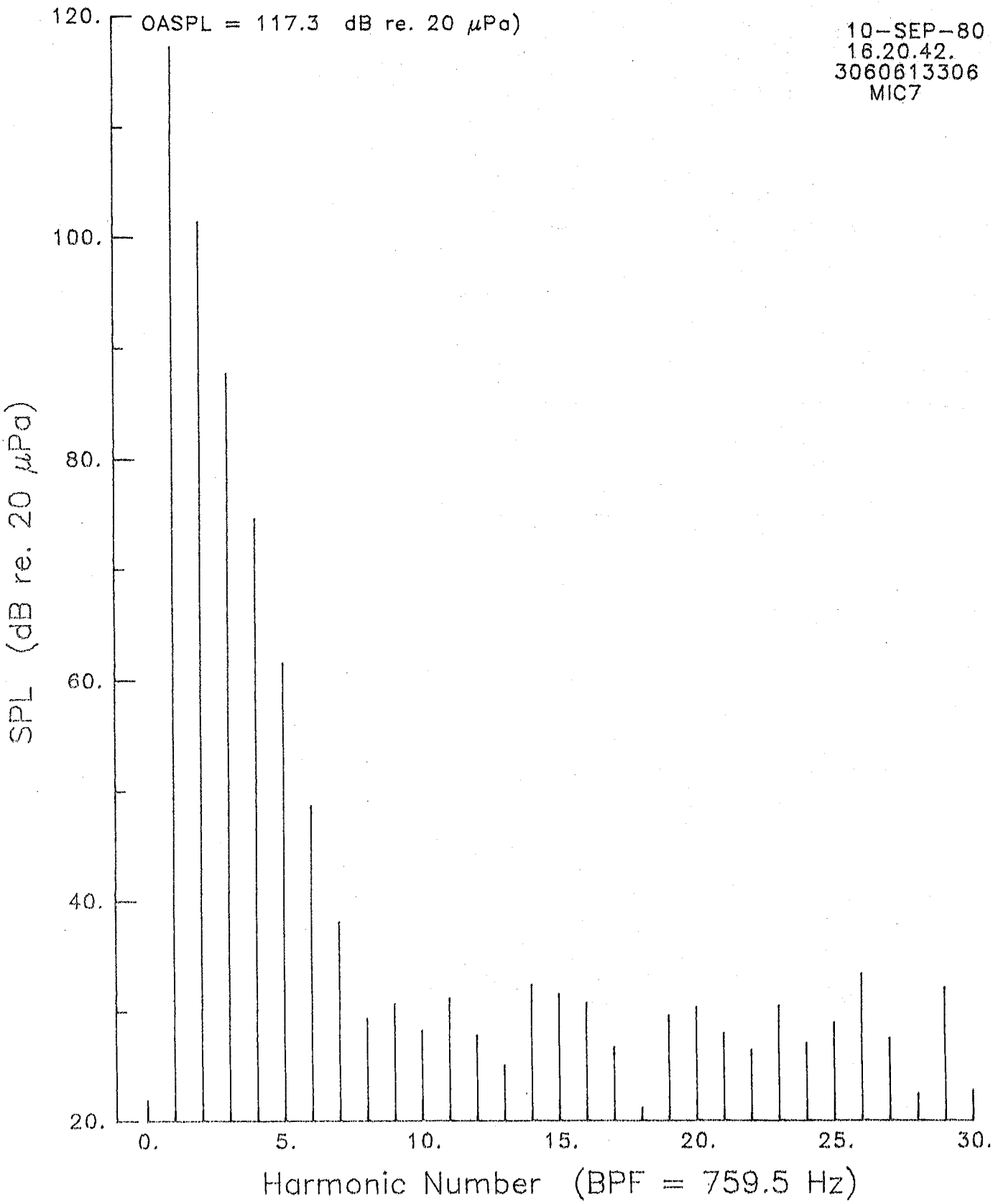

OVERALL SPECTRUM

Figure 12.- Continued.

F. Farassat -- P. Nystrom
JIAFS -- NASA/LaRC -- GWU

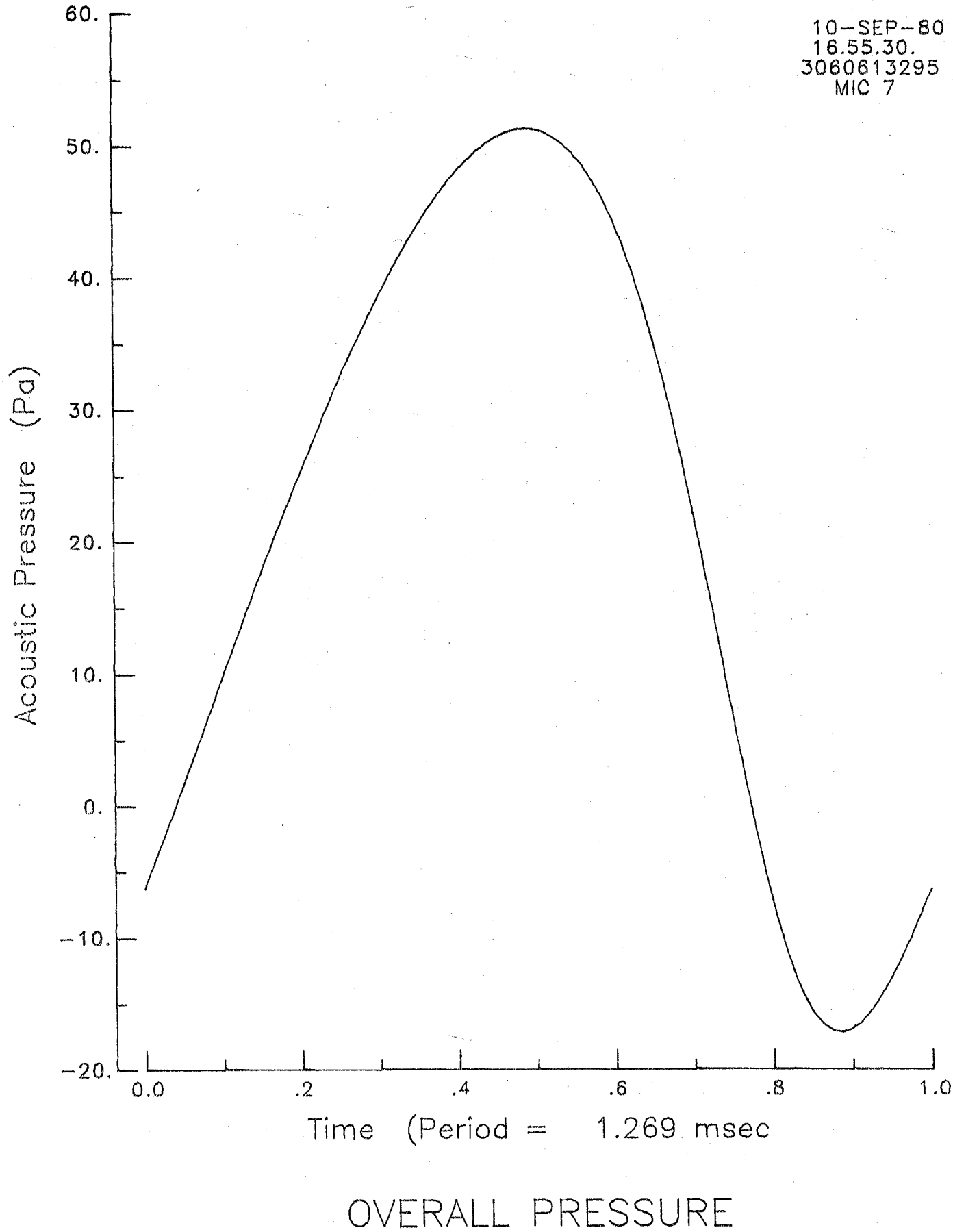

Figure 12.- Continued.

F. Farassat -- P. Nystrom
JIAFS -- NASA/LaRC -- GWU

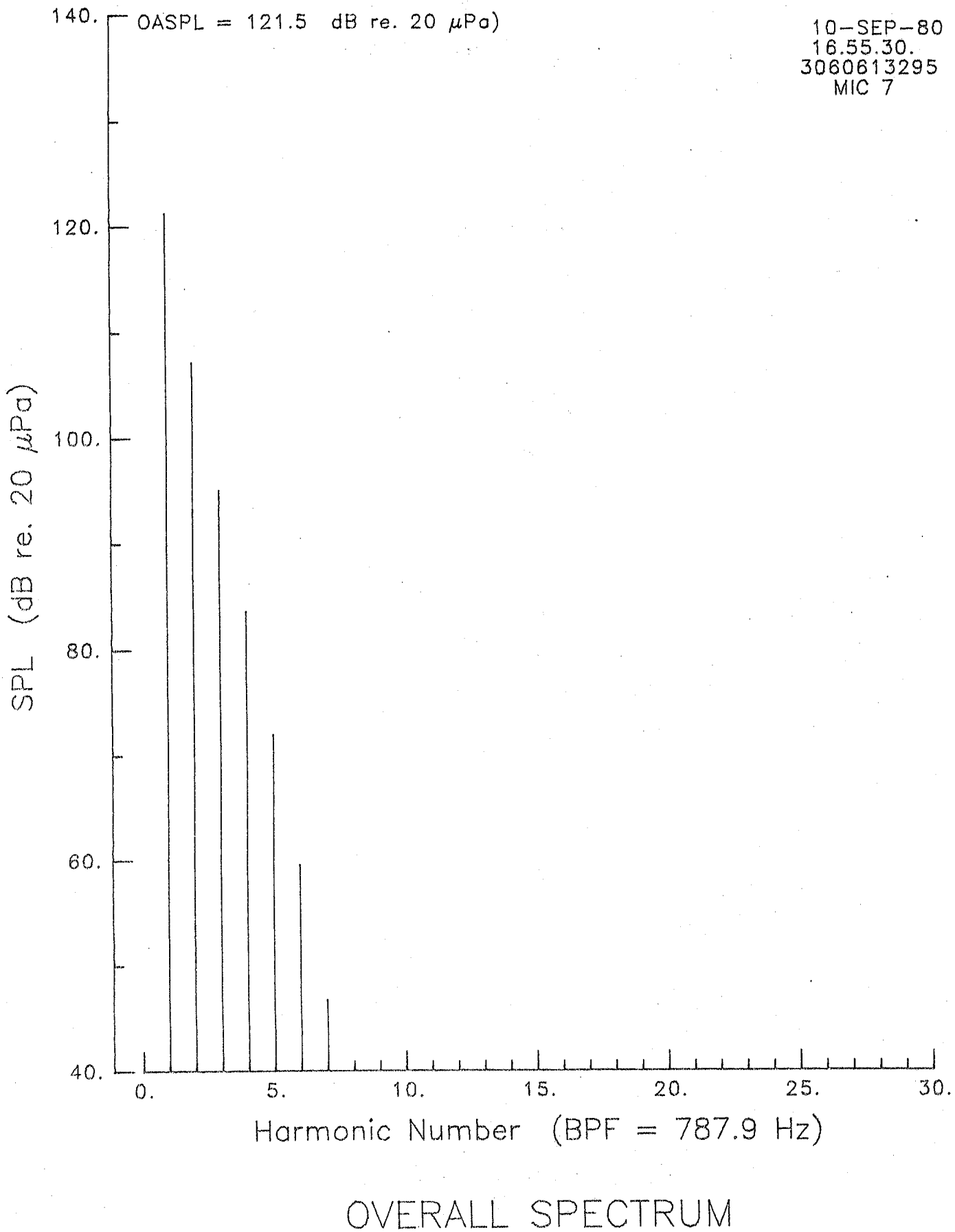

Figure 12.- Concluded.

F. Farassat -- P. Nystrom
JIAFS -- NASA/LaRC -- GWU

SR-3 BLADE

FLIGHT ALTITUDE 9.15 km (30,000 ft)

FLIGHT MACH NUMBER 0.7

MICROPHONE 7

(ADVANCE RATIO VARIED)

Figure 13.- Free-field acoustic pressure signatures and spectra for SR-3 blade - Altitude 9.15 Km (30,000 ft), M=0.7, Microphone 7. Note advance ratio is varied in these calculations.

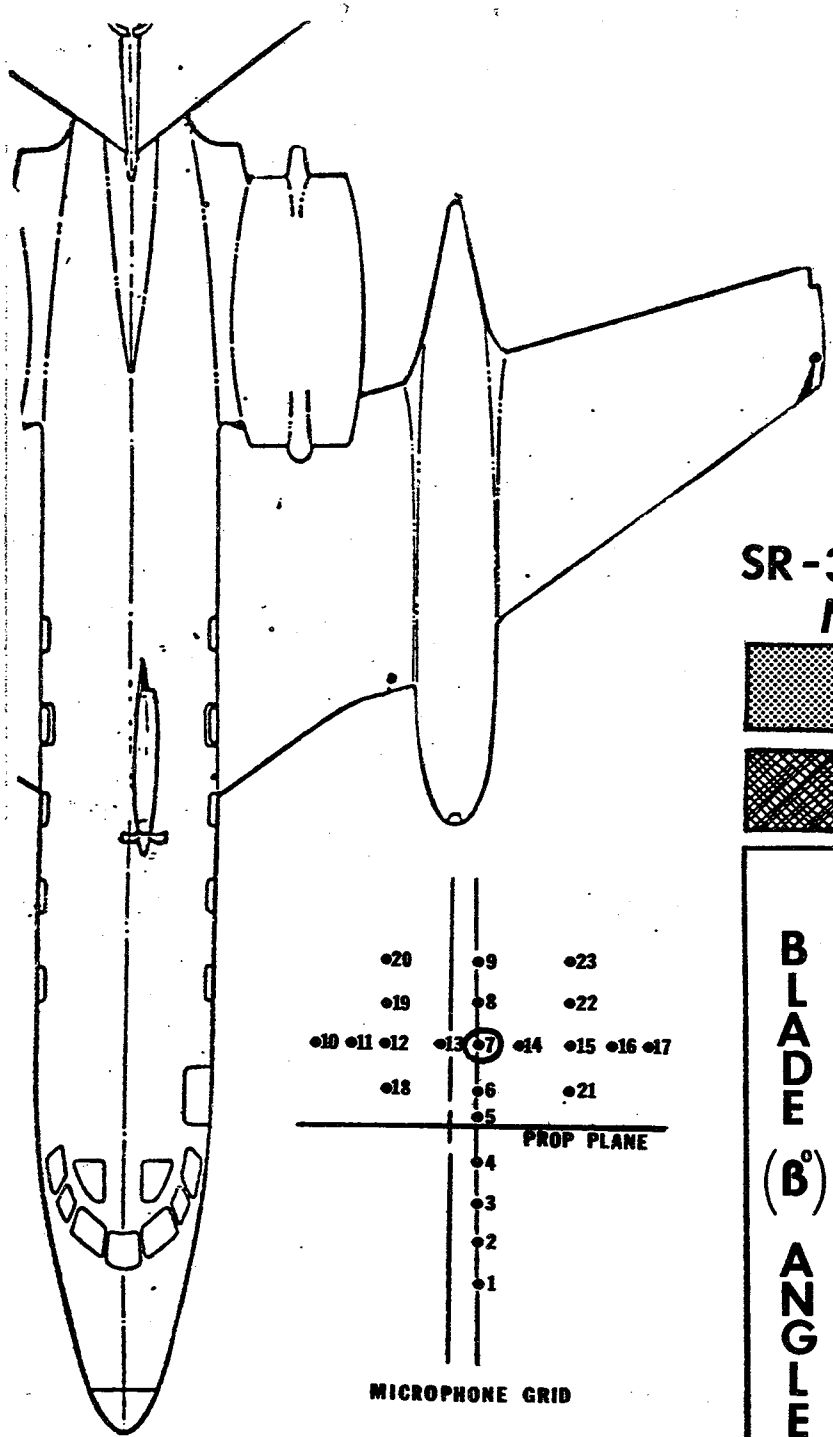

Figure 13.- Continued.

SR-3 TEST MATRIX

EXCEEDS BLEED SYS. POWER CAPACITY

BLADE CRITICAL SPEED

BLADE ANGLE (β°)	ADVANCE RATIO (J)	ALTITUDE (FT) 20,000 MACH # .50	.60	.65	.70	.75	.80	ALTITUDE (FT) 25,000 MACH # .50	.60	.65	.70	.75	.80	ALTITUDE (FT) 30,000 MACH # .50	.60	.65	.70	.75	.80
59.3	4.30																		
	3.50																		
	3.25																		
	3.06																		
	2.90																		
61.3	4.30																X		
	3.50																X		
	3.25				■						■						■		
	3.06												■				X		■
	2.95					■							■				X	■	■
63.3	4.30																		
	4.07																		
	3.50																		
	3.25					■							■						■

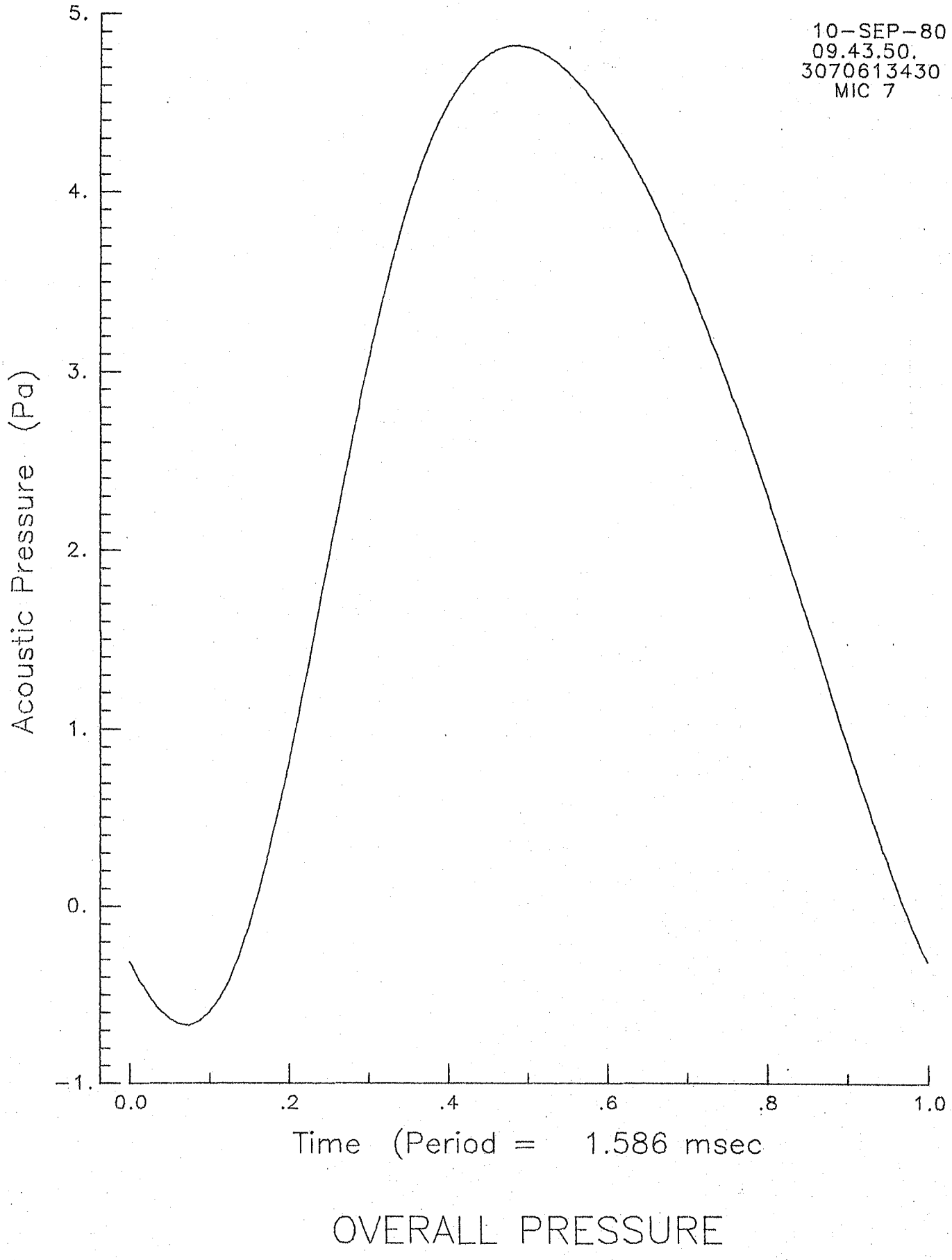

Figure 13.- Continued.

F. Farassat -- P. Nystrom
JIAFS -- NASA/LaRC -- GWU

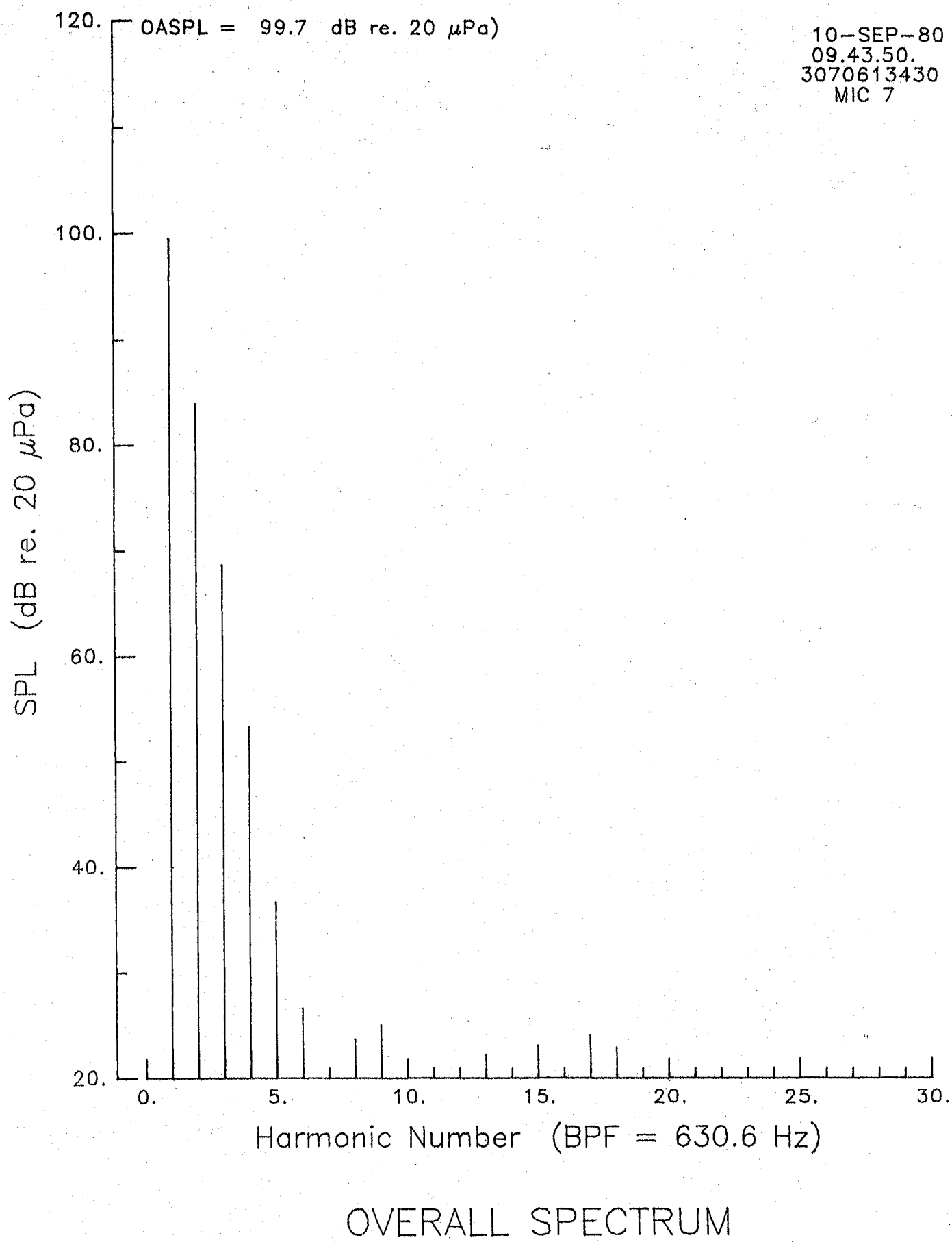

Figure 13.- Continued.

F. Farassat -- P. Nystrom
JIAFS -- NASA/LaRC -- GWU

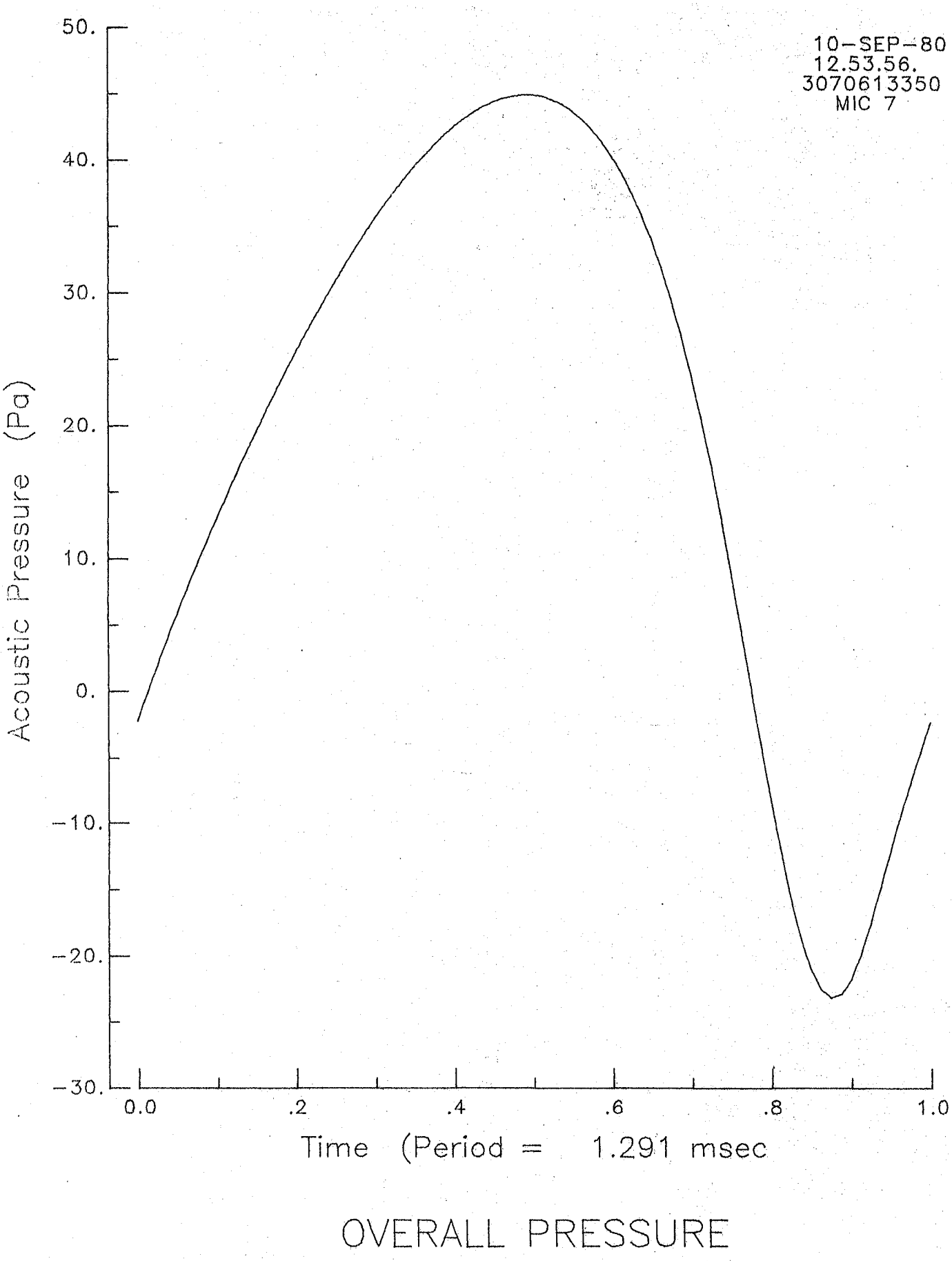

OVERALL PRESSURE

Figure 13.- Continued.

F. Farassat -- P. Nystrom
JIAFS -- NASA/LaRC -- GWU

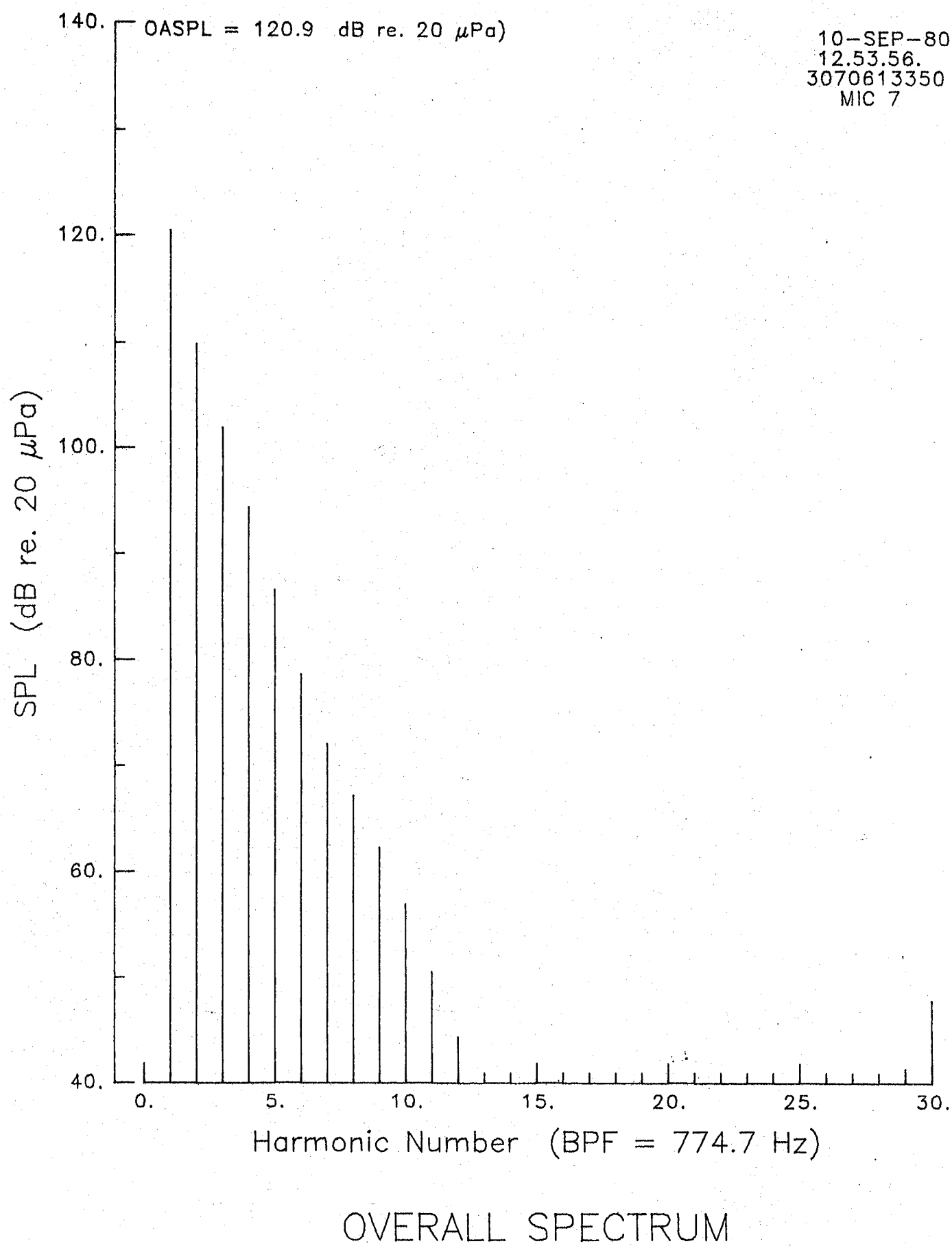

Figure 13.- Continued.

F. Farassat -- P. Nystrom
JIAFS -- NASA/LaRC -- GWU

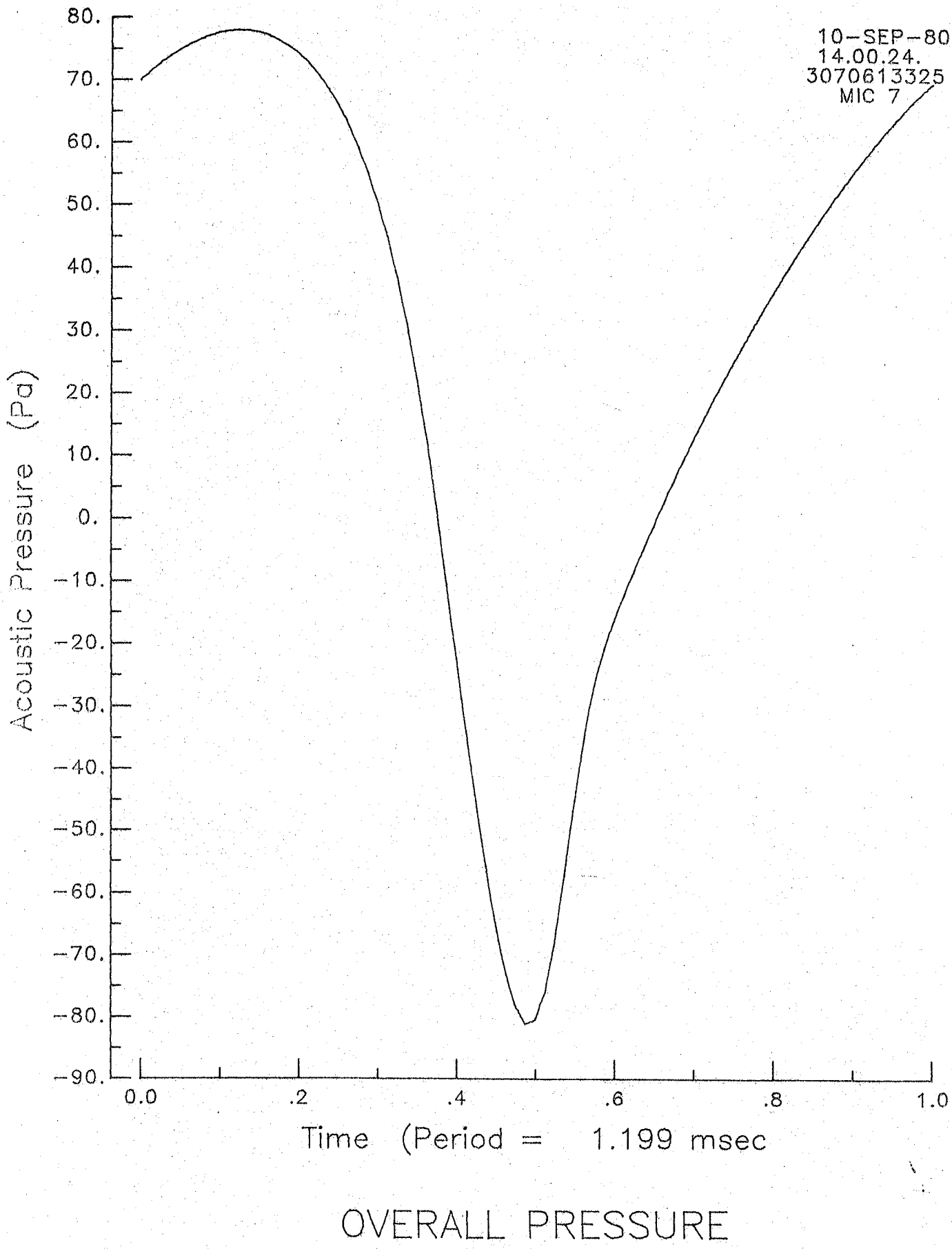

Figure 13.- Continued.

F. Farassat -- P. Nystrom
JIAFS -- NASA/LaRC -- GWU

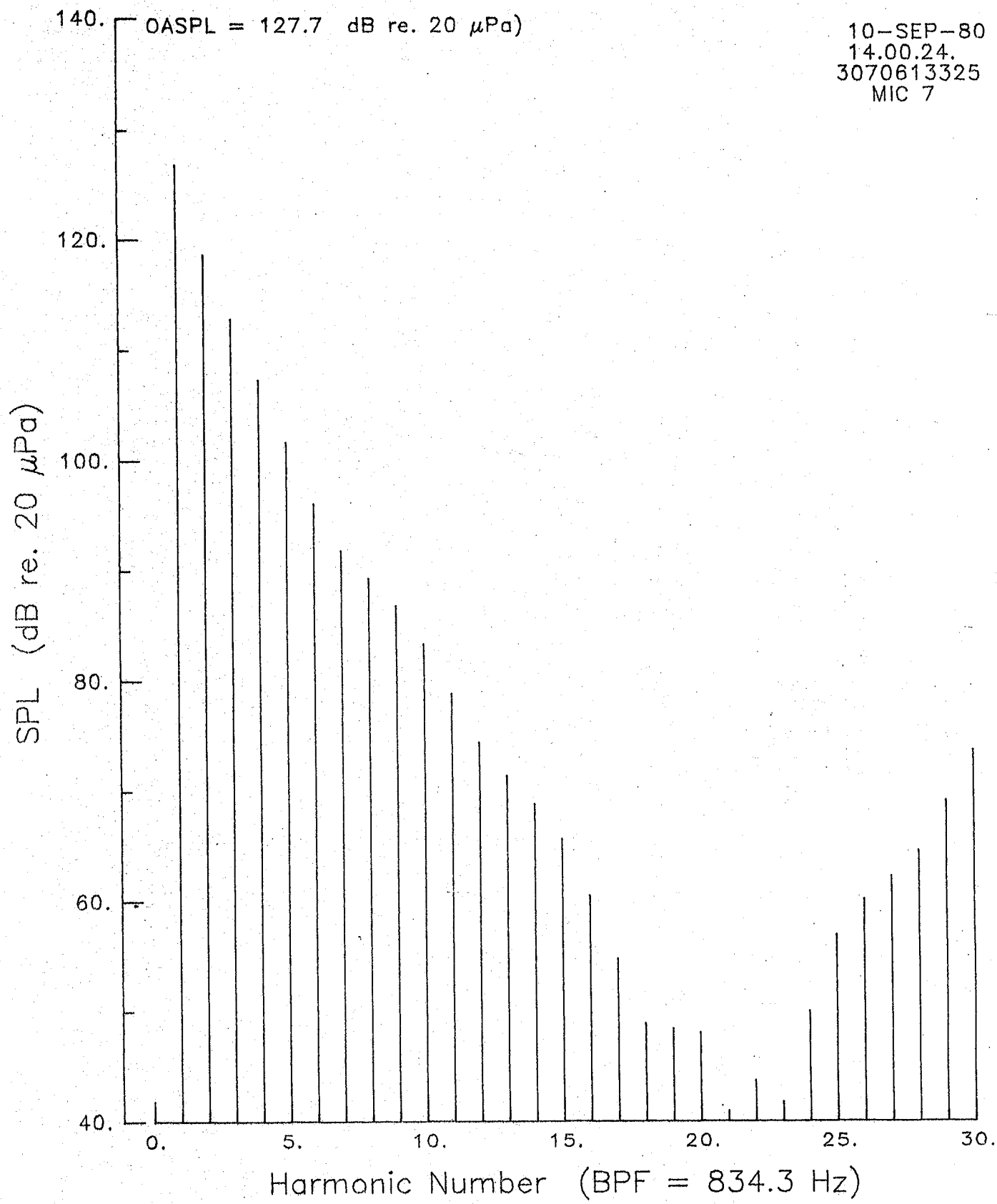

Figure 13.- Continued.

F. Farassat -- P. Nystrom
JIAFS -- NASA/LaRC -- GWU

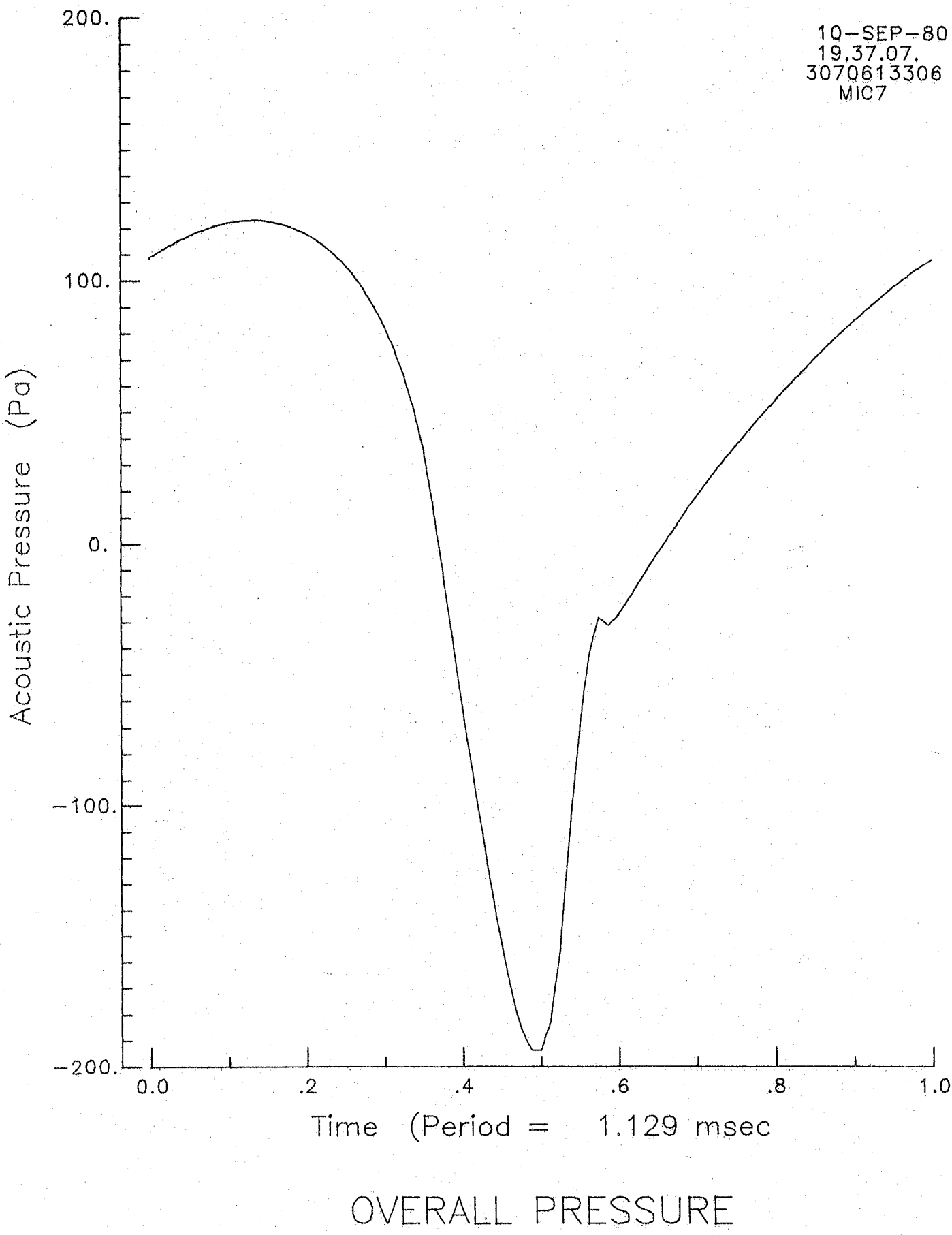

Figure 13.- Continued.

F. Farassat -- P. Nystrom
JIAFS -- NASA/LaRC -- GWU

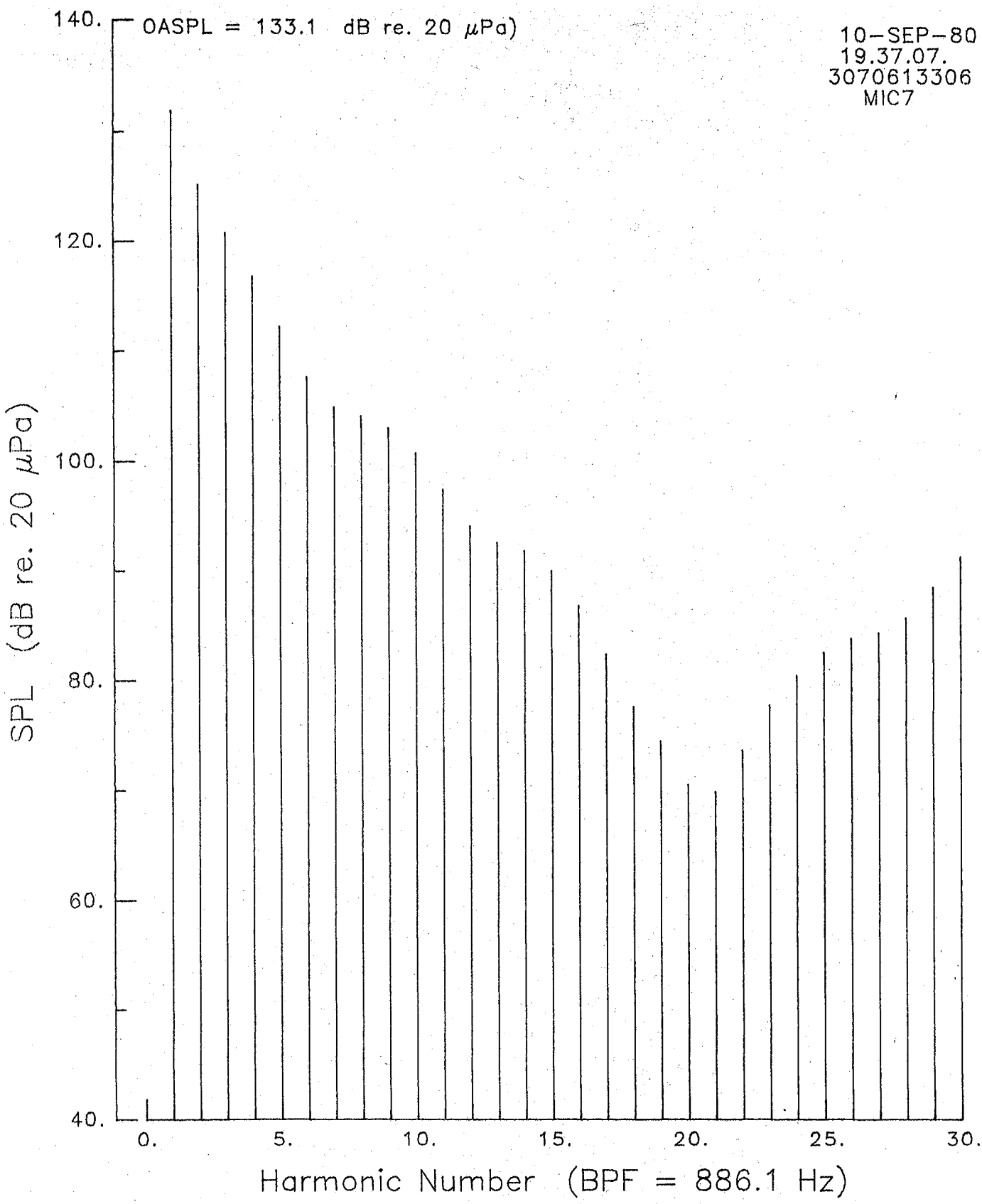

Figure 13.- Continued.

F. Farassat -- P. Nystrom
JIAFS -- NASA/LaRC -- GWU

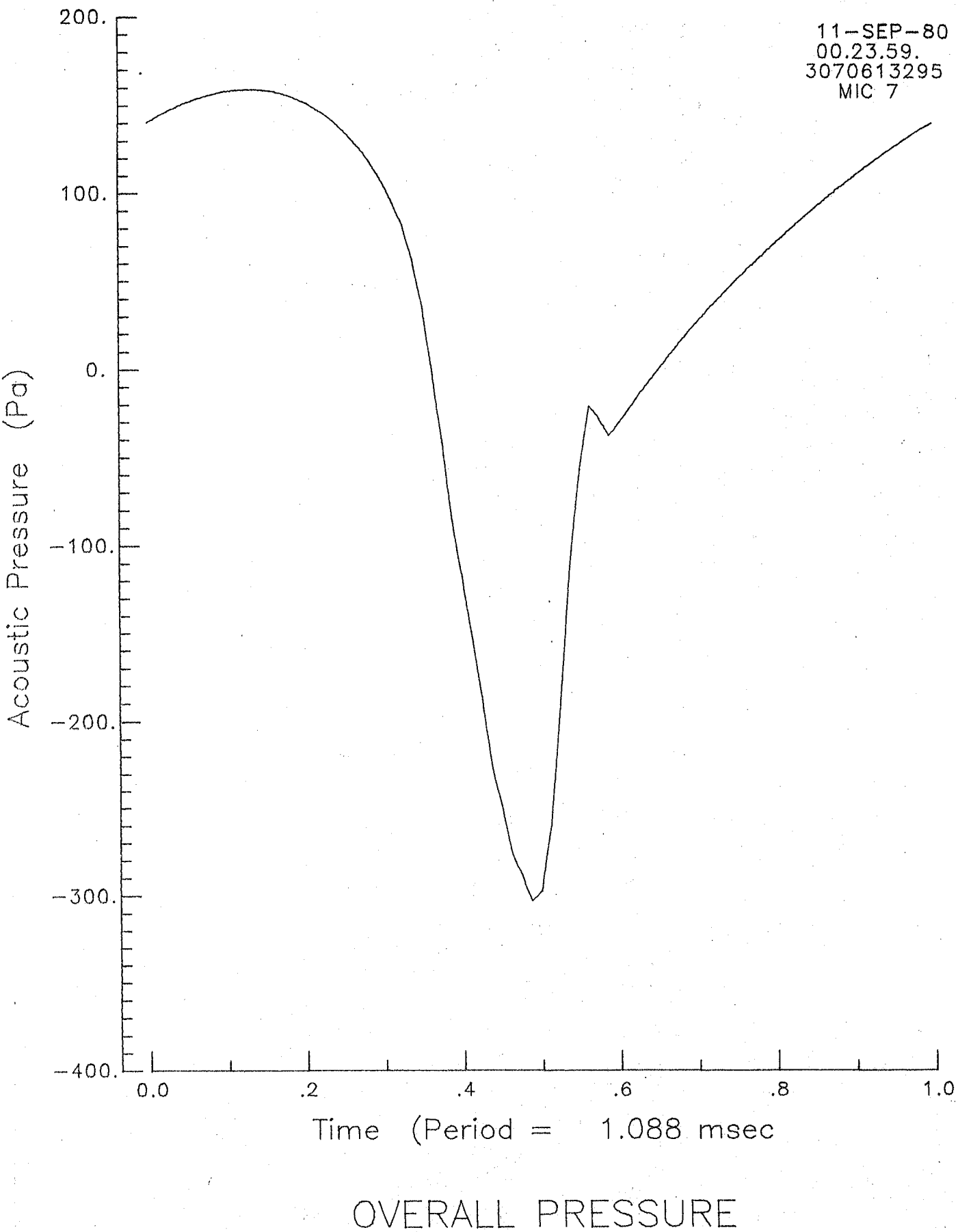

Figure 13.- Continued.

F. Farassat -- P. Nystrom
JIAFS -- NASA/LaRC -- GWU

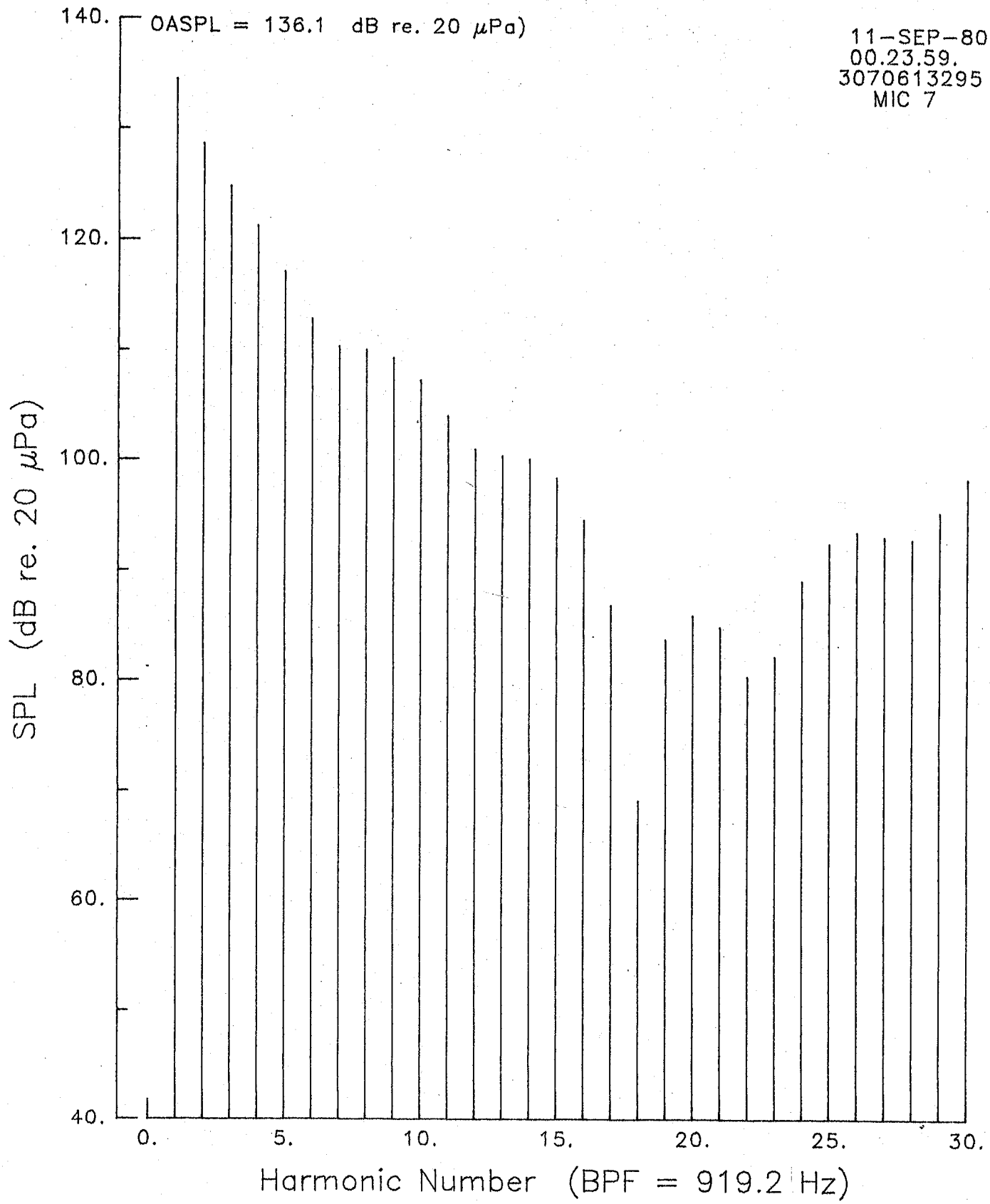

OVERALL SPECTRUM

Figure 13.- Concluded.

F. Farassat -- P. Nystrom
JIAFS -- NASA/LaRC -- GWU

SR-3 BLADE

FLIGHT ALTITUDE 9.15 km (30,000 ft)

FLIGHT MACH NUMBER 0.8

MICROPHONES 1, 4, 5, 7, 9, 10, 12

(ADVANCE RATIO VARIED)

Figure 14.- Free-field acoustic pressure signatures and spectra for SR-3 blade - Altitude 9.15 Km (30,000 ft), M=0.8, all microphone positions. Note advance ratio is varied in these calculations for each microphone position. The numbering of this figure is as follows:

Microphone 1 - Figure 14(a)
Microphone 4 - Figure 14(b)
Microphone 5 - Figure 14(c)
Microphone 7 - Figure 14(d)
Microphone 9 - Figure 14(e)
Microphone 10 - Figure 14(f)
Microphone 12 - Figure 14(g)

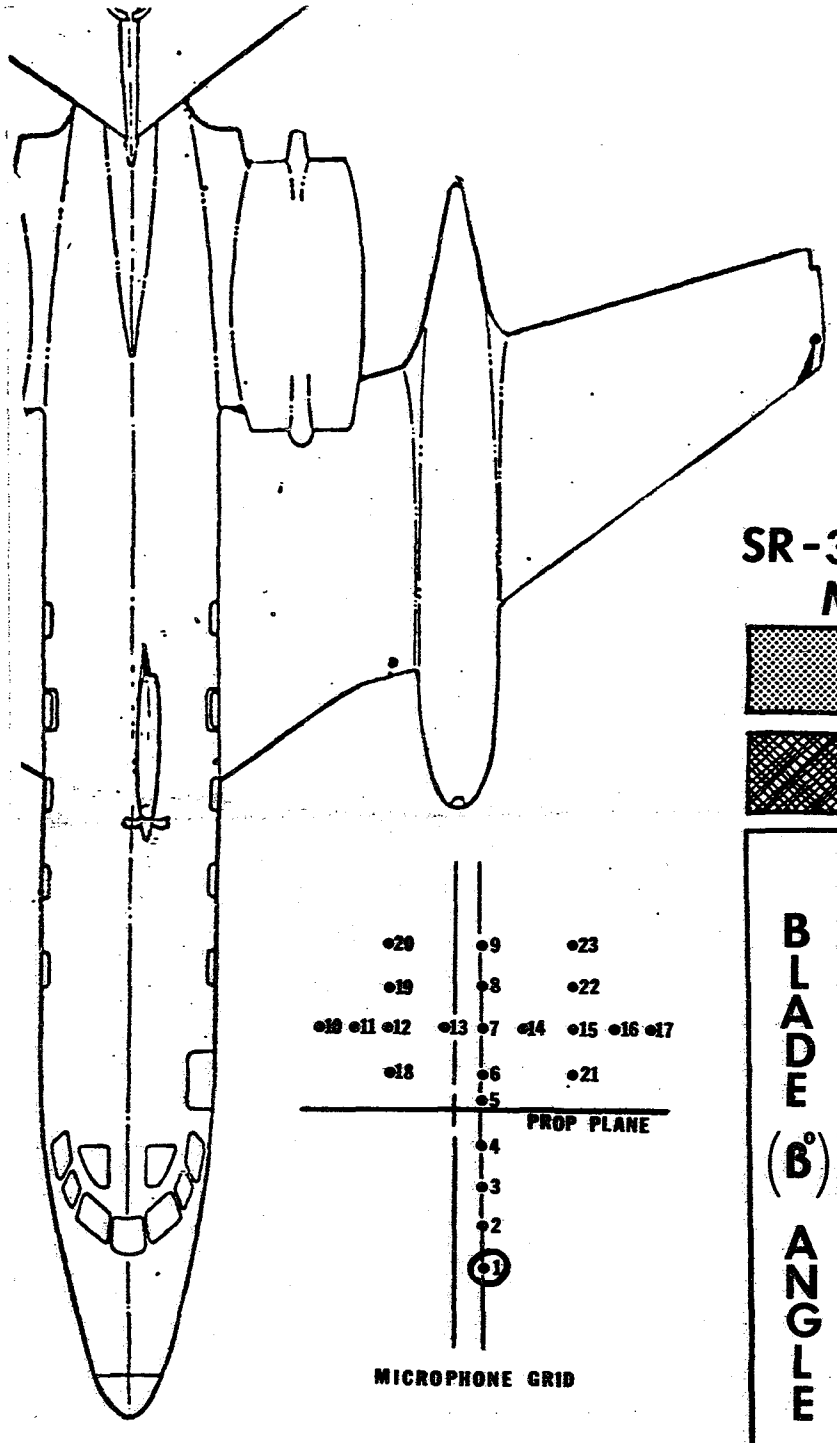

Figure 14(a).- Continued.

SR-3 TEST MATRIX

EXCEEDS BLEED SYS. POWER CAPACITY

BLADE CRITICAL SPEED

BLADE ANGLE (β°)	ADVANCE RATIO (J)	ALTITUDE (FT) 20,000						25,000						30,000					
		MACH # .50	.60	.65	.70	.75	.80	.50	.60	.65	.70	.75	.80	.50	.60	.65	.70	.75	.80
59.3	4.30																		X
	3.50																		X
	3.25																		X
	3.06																		X
	2.90																		X
61.3	4.30																		X
	3.50																		X
	3.25																		X
	3.06																		X
	2.95																		X
63.3	4.30																		
	4.07																		
	3.50																		
	3.25																		

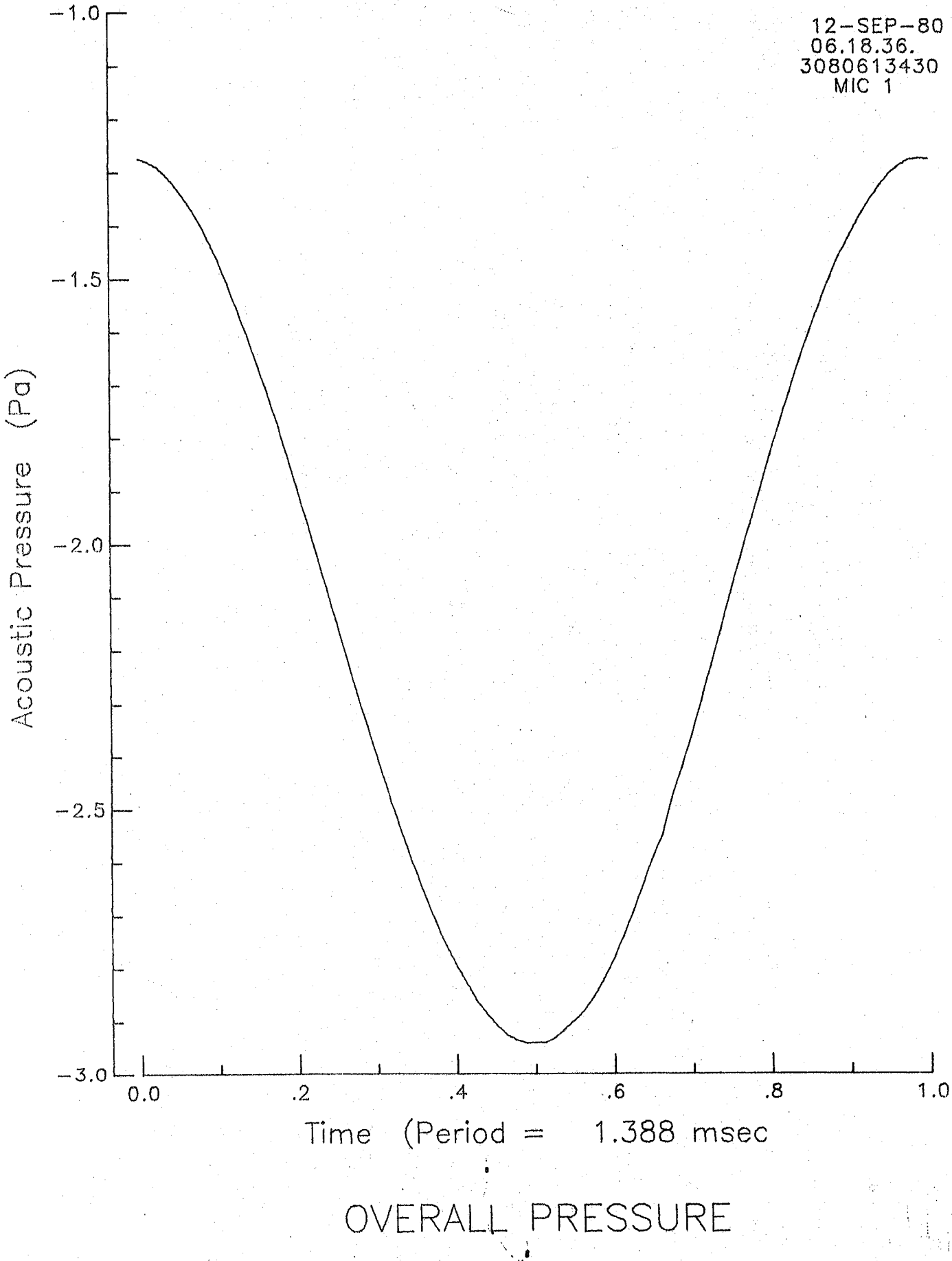

Figure 14(a).- Continued.

F. Farassat -- P. Nystrom
JIAFS -- NASA/LaRC -- GWU

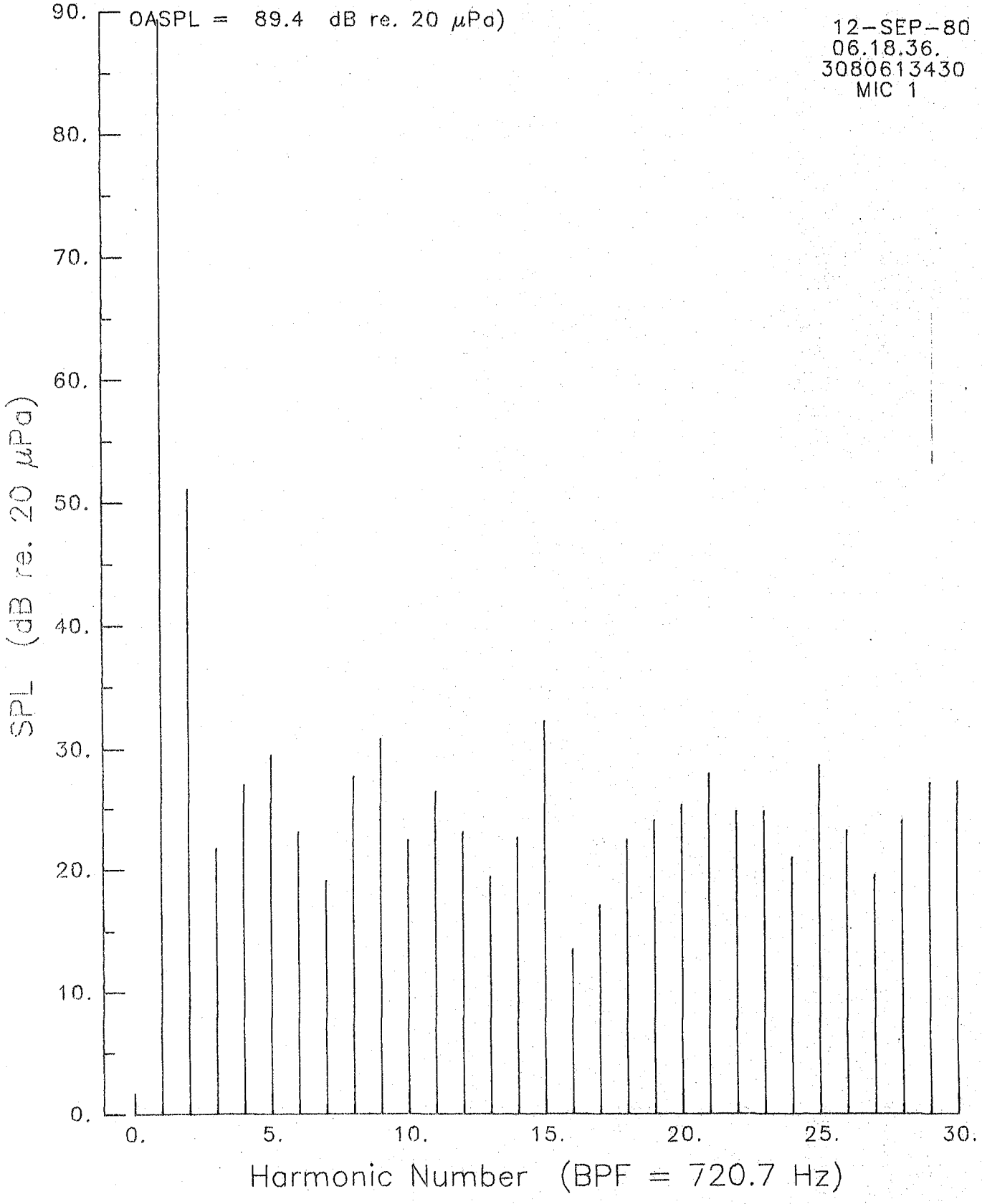

OVERALL SPECTRUM

Figure 14(a).- Continued.

F. Farassat -- P. Nystrom
JIAFS -- NASA/LaRC -- GWU

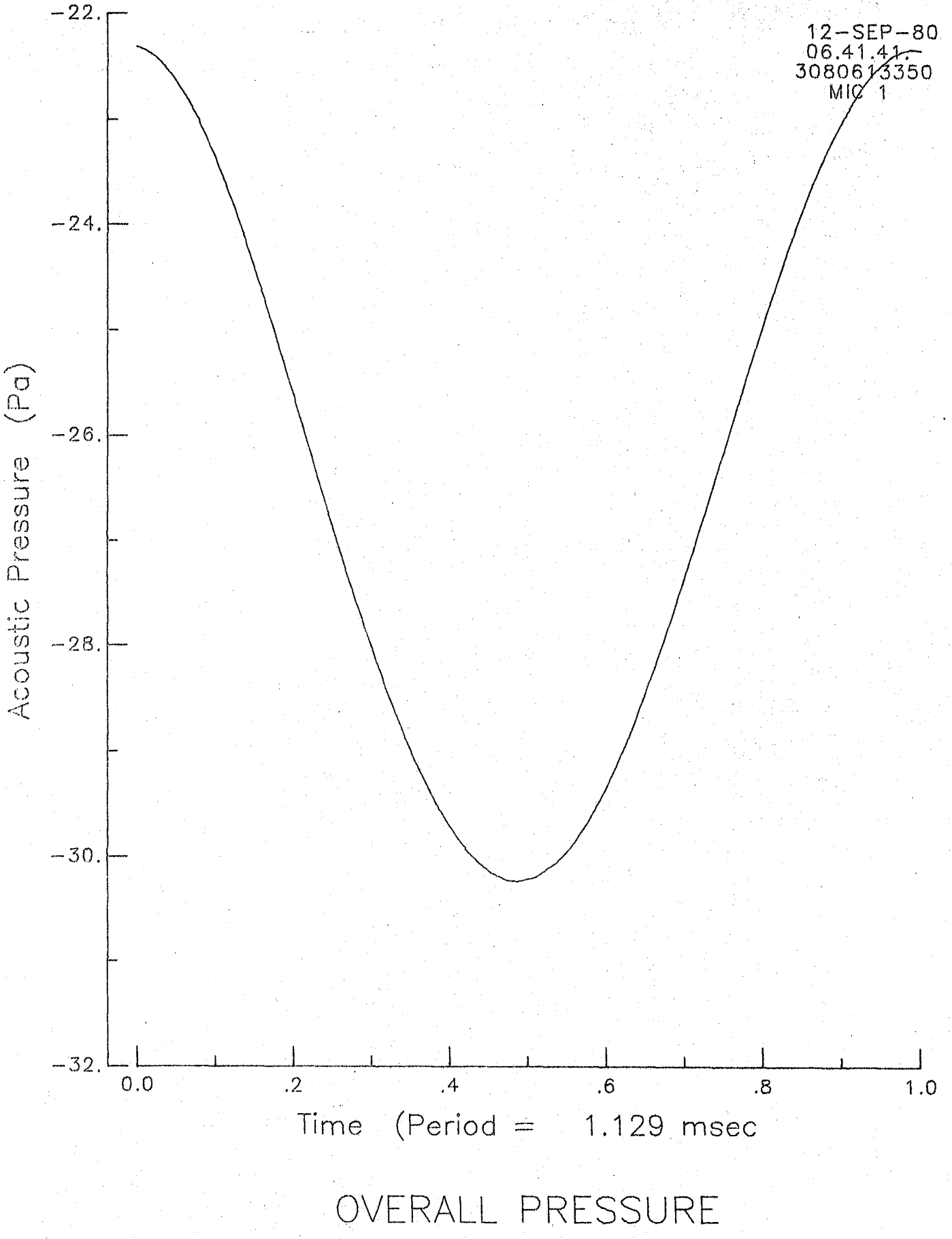

Figure 14(a).- Continued.

F. Farassat -- P. Nystrom
JIAFS -- NASA/LaRC -- GWU

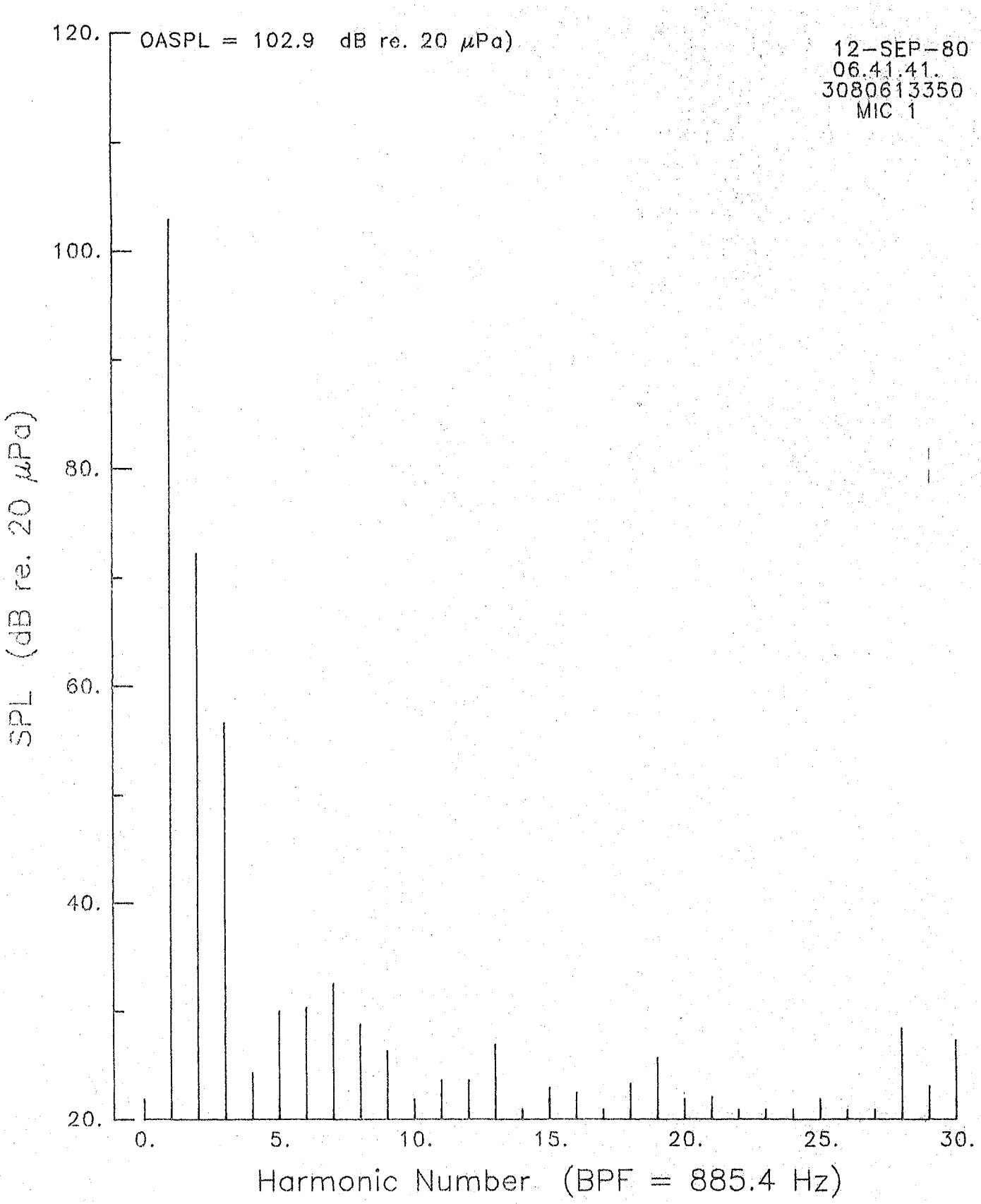

OVERALL SPECTRUM

Figure 14(a).- Continued.

F. Farassat -- P. Nystrom
JIAFS -- NASA/LaRC -- GWU

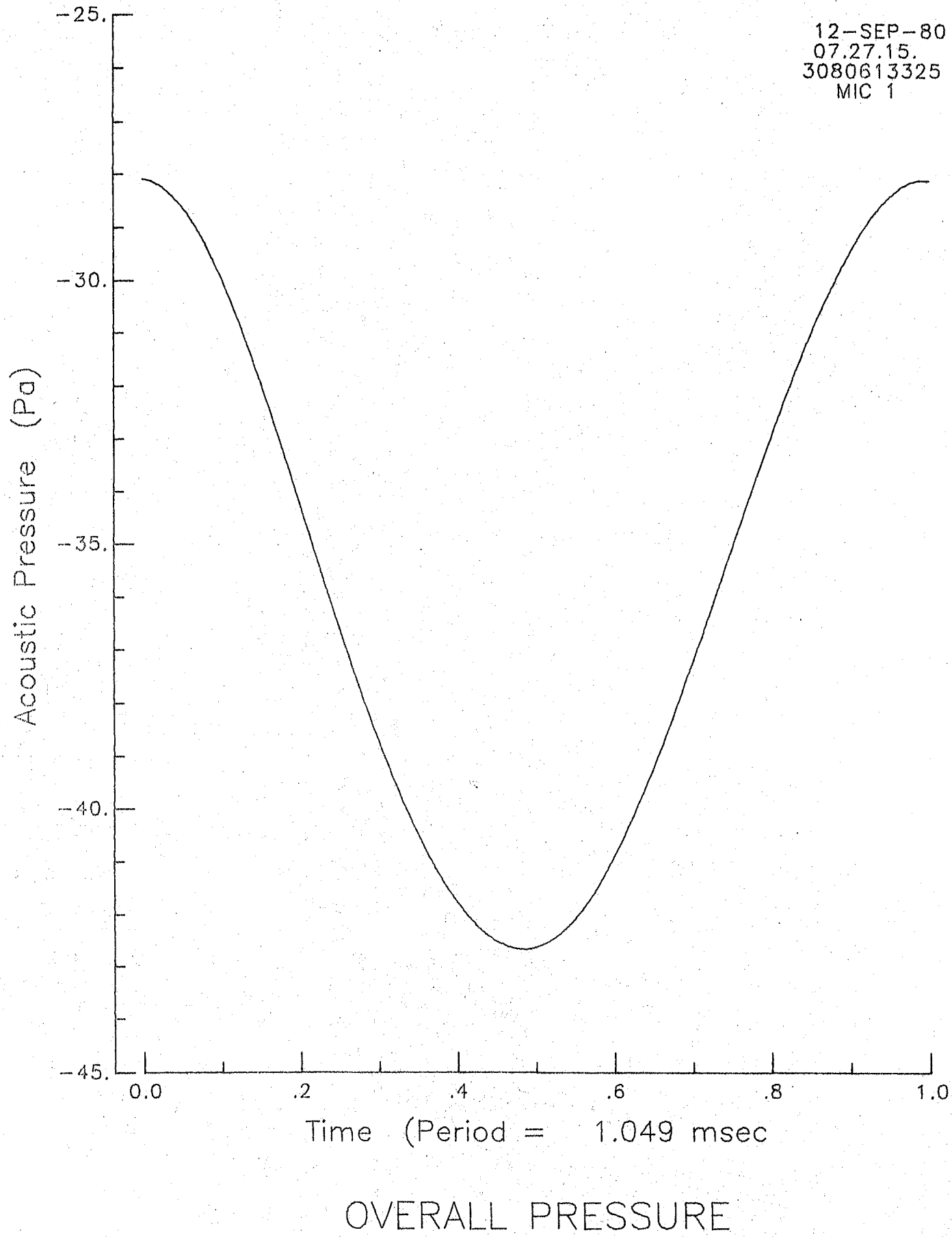

Figure 14(a).- Continued.

F. Farassat -- P. Nystrom
JIAFS -- NASA/LaRC -- GWU

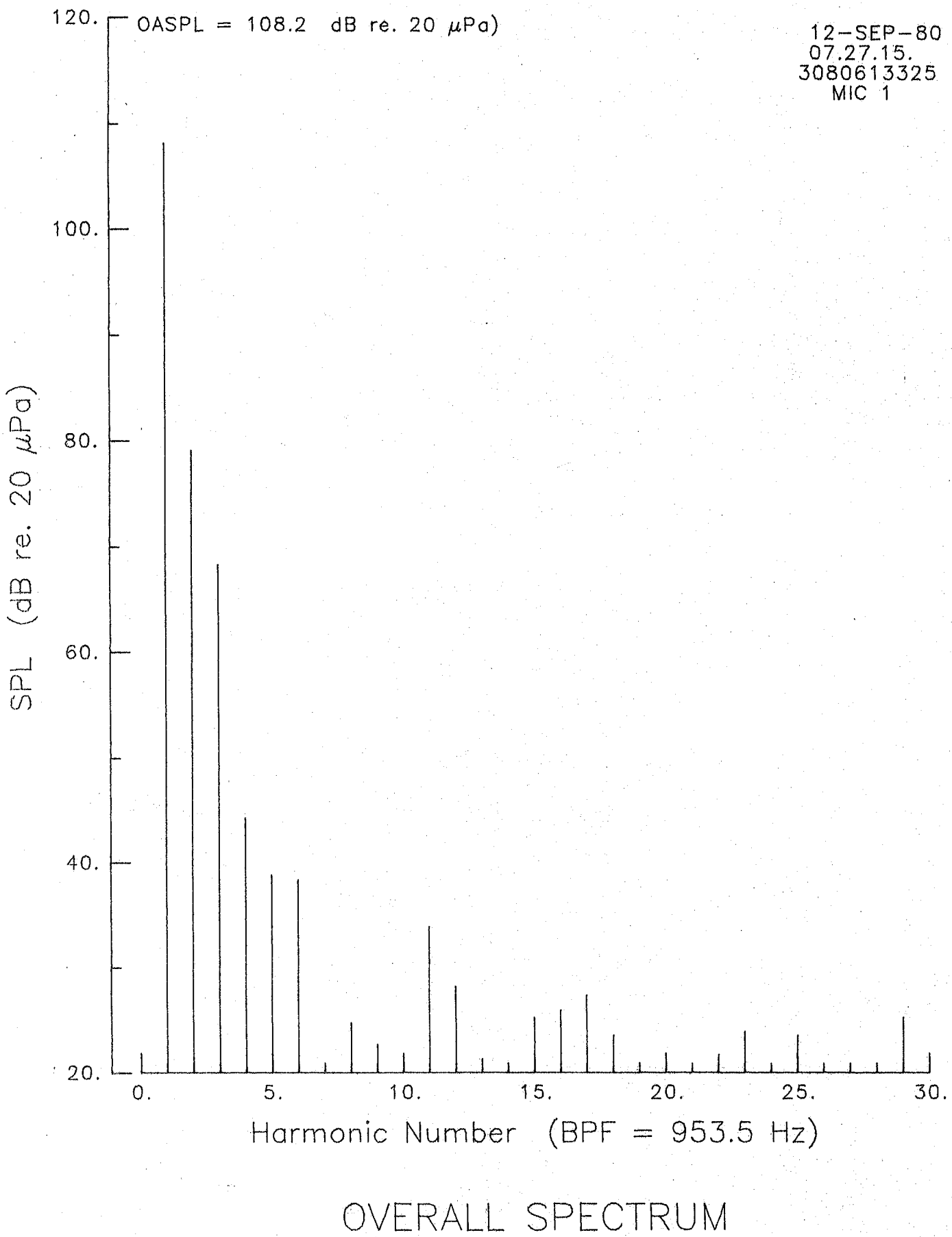

Figure 14(a).- Continued.

F. Farassat -- P. Nystrom
JIAFS -- NASA/LaRC -- GWU

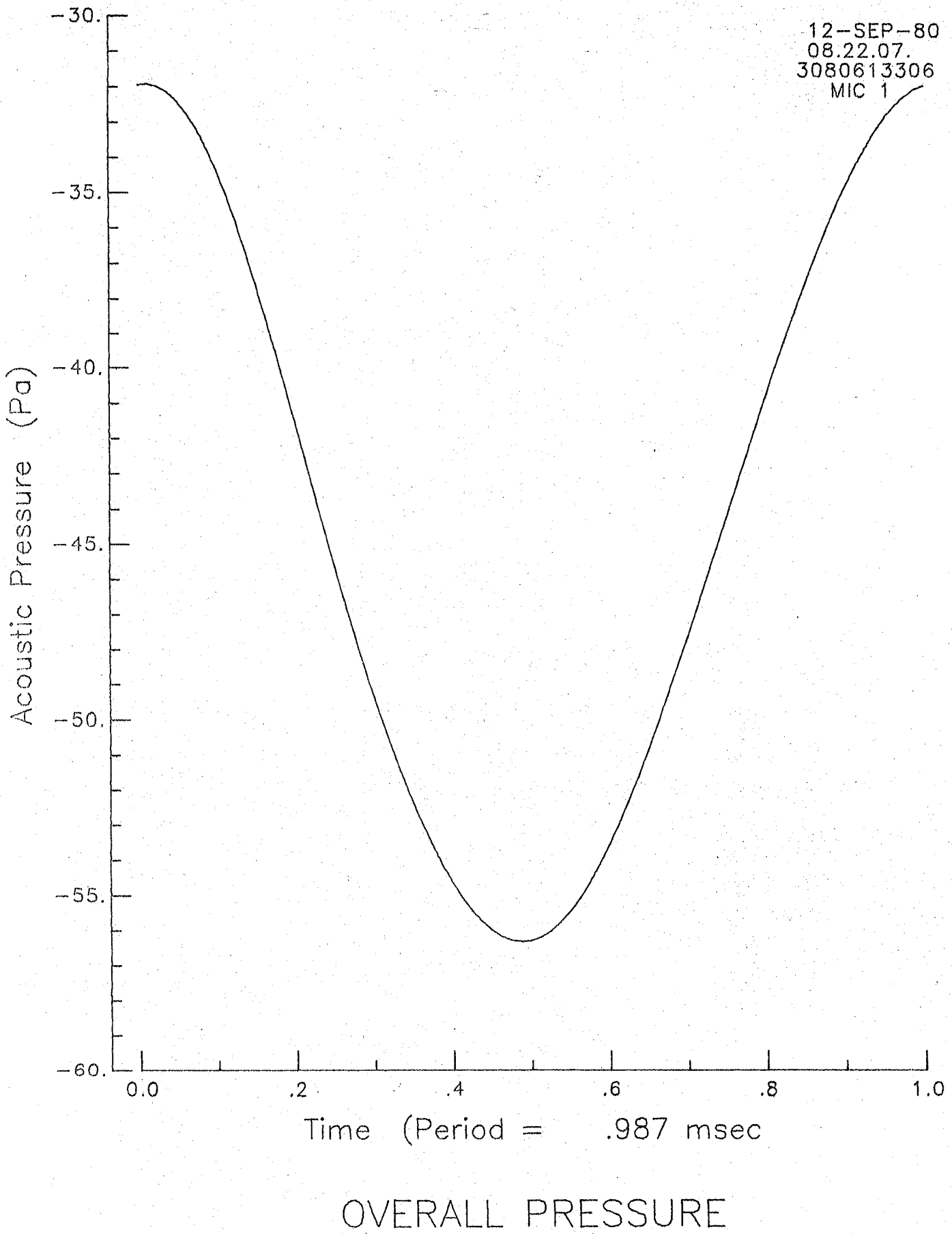

Figure 14(a).- Continued.

F. Farassat -- P. Nystrom
JIAFS -- NASA/LaRC -- GWU

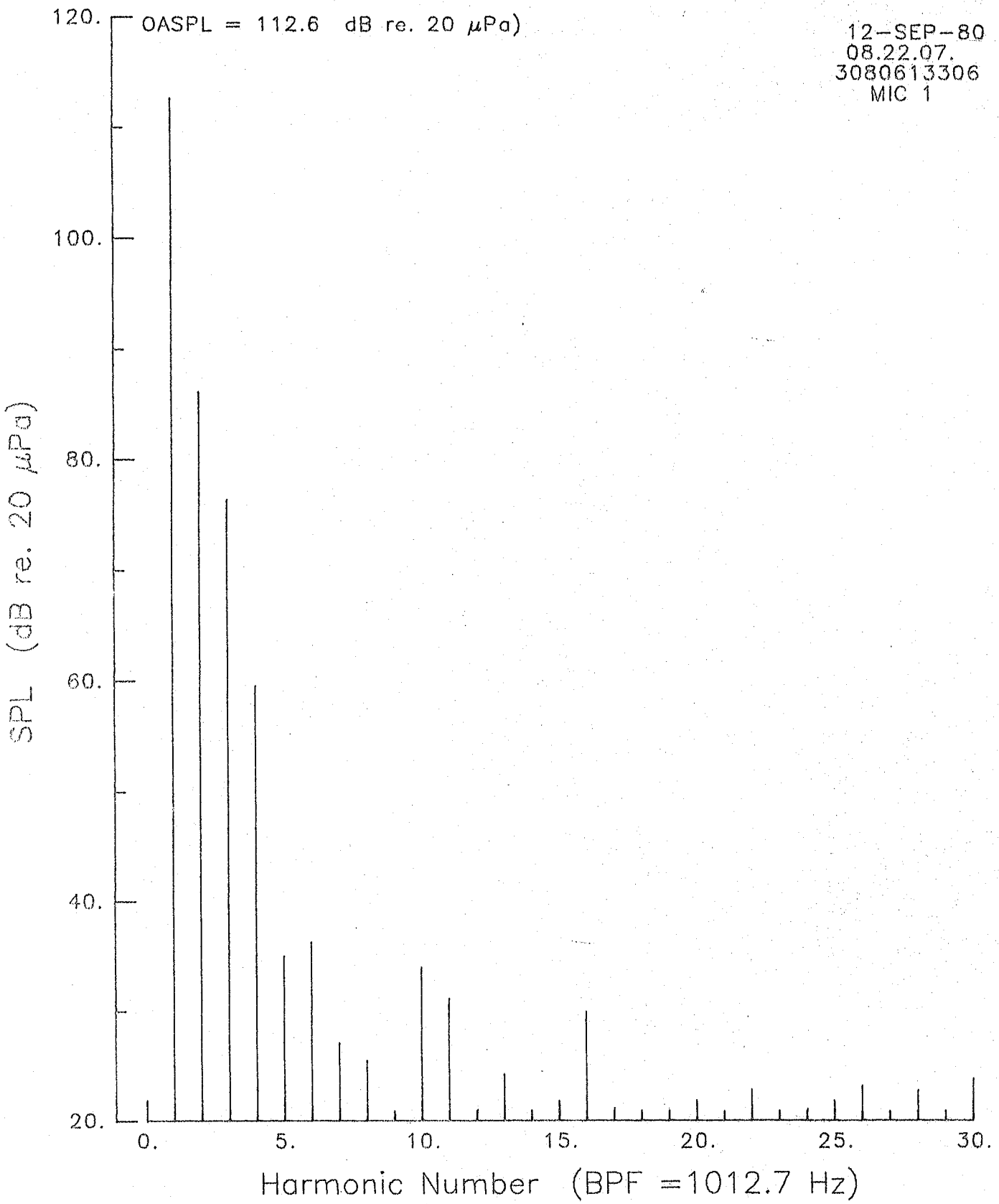

OVERALL SPECTRUM

Figure 14(a).- Continued.

F. Farassat -- P. Nystrom
JIAFS -- NASA/LaRC -- GWU

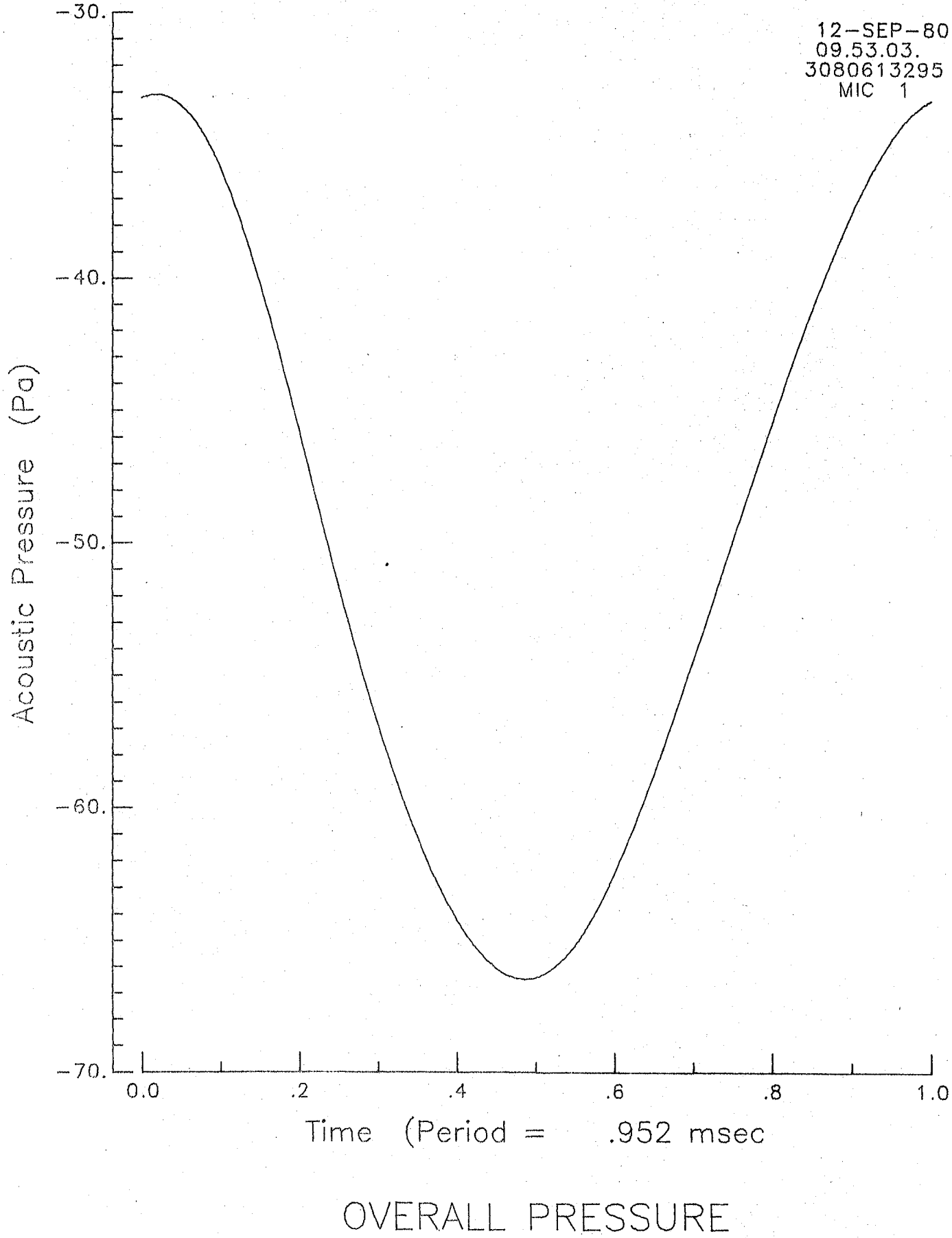

Figure 14(a).- Continued.

F. Farassat -- P. Nystrom
JIAFS -- NASA/LaRC -- GWU

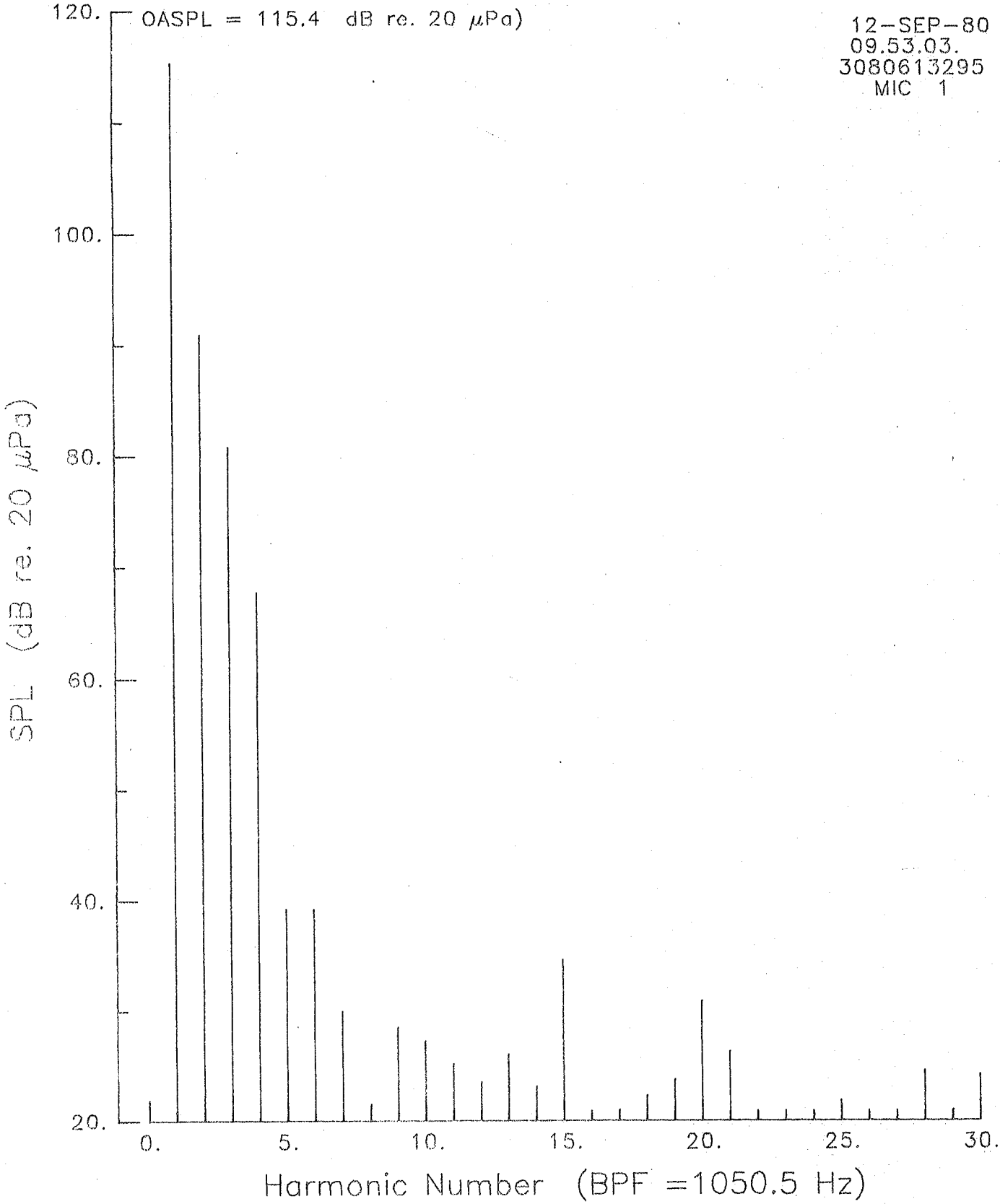

OVERALL SPECTRUM

Figure 14(a).- Concluded.

F. Farassat -- P. Nystrom
JIAFS -- NASA/LaRC -- GWU

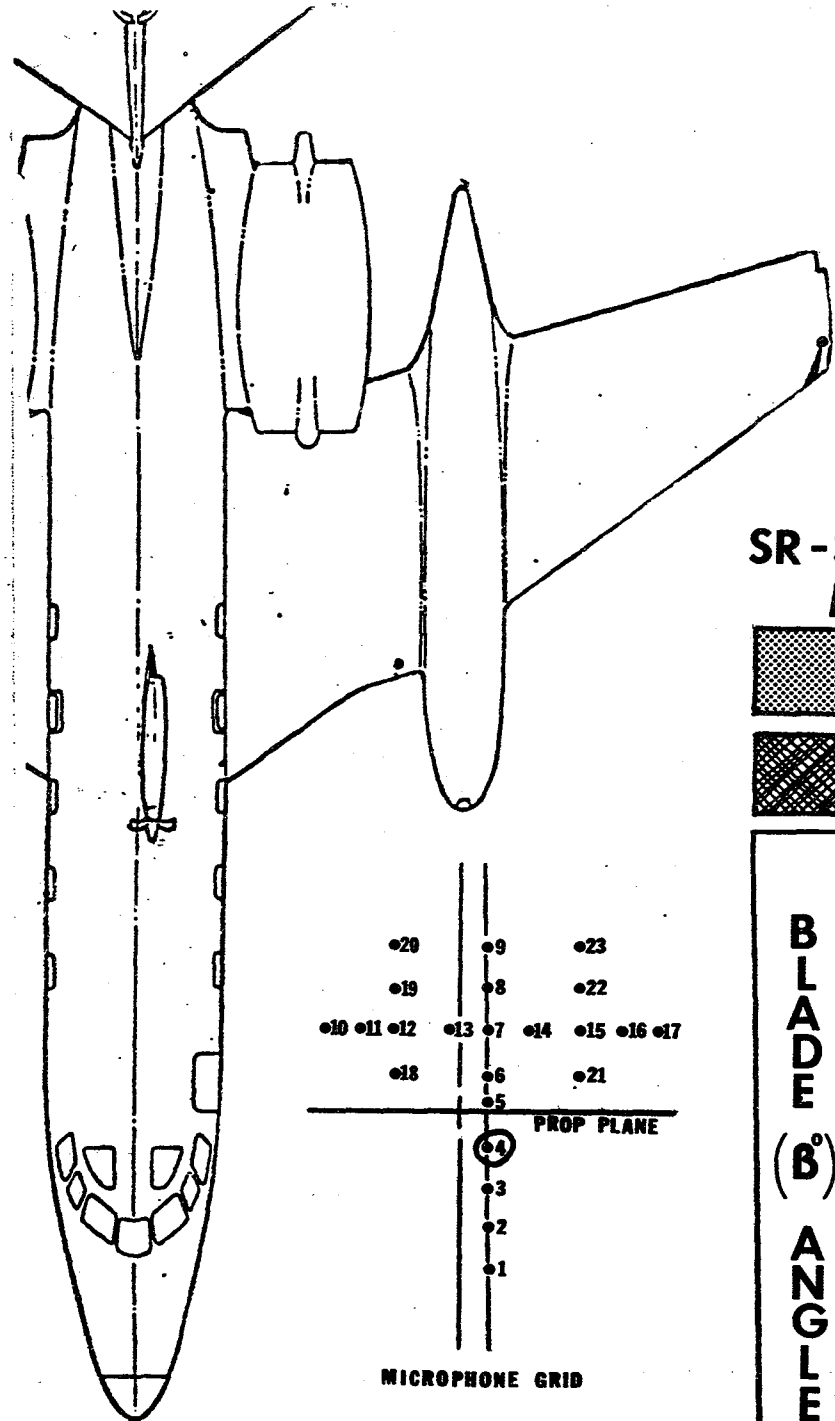

SR-3 TEST MATRIX

EXCEEDS BLEED SYS. POWER CAPACITY

BLADE CRITICAL SPEED

BLADE ANGLE (β°)	ADVANCE RATIO (J)	ALTITUDE (FT) 20,000						ALTITUDE (FT) 25,000						ALTITUDE (FT) 30,000			
		MACH # .50	.60	.65	.70	.75	.80	.50	.60	.65	.70	.75	.80	.50	.60	.65	.70	.75	.80
59.3	4.30																		
	3.50																		
	3.25																		
	3.06																		
	2.90																		
61.3	4.30																		X
	3.50																		X
	3.25																		X
	3.06																		X
	2.95																		X
63.3	4.30																		
	4.07																		
	3.50																		
	3.25																		

Figure 14(b).- Continued.

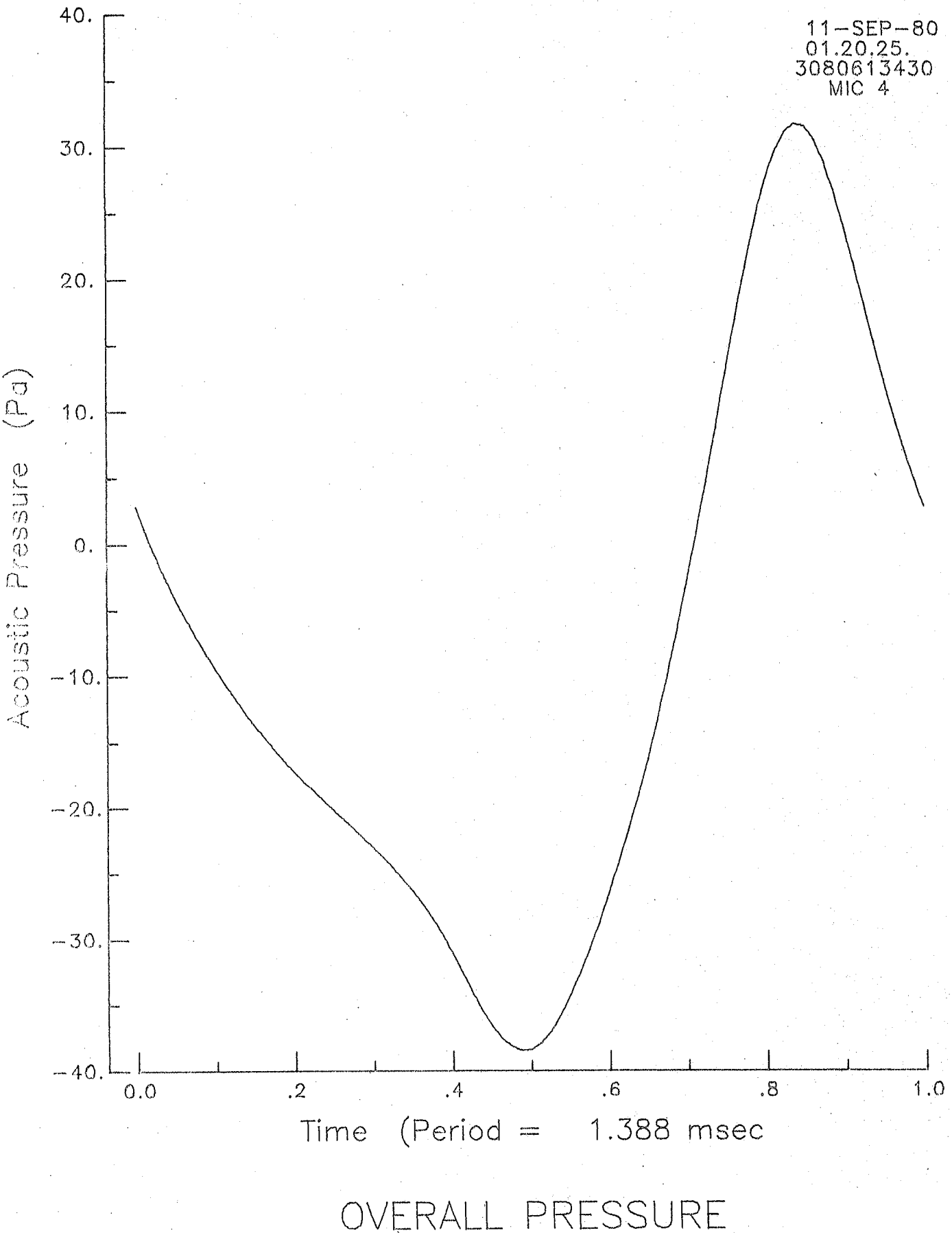

Figure 14(b).- Continued.

F. Farassat -- P. Nystrom
JIAFS -- NASA/LaRC -- GWU

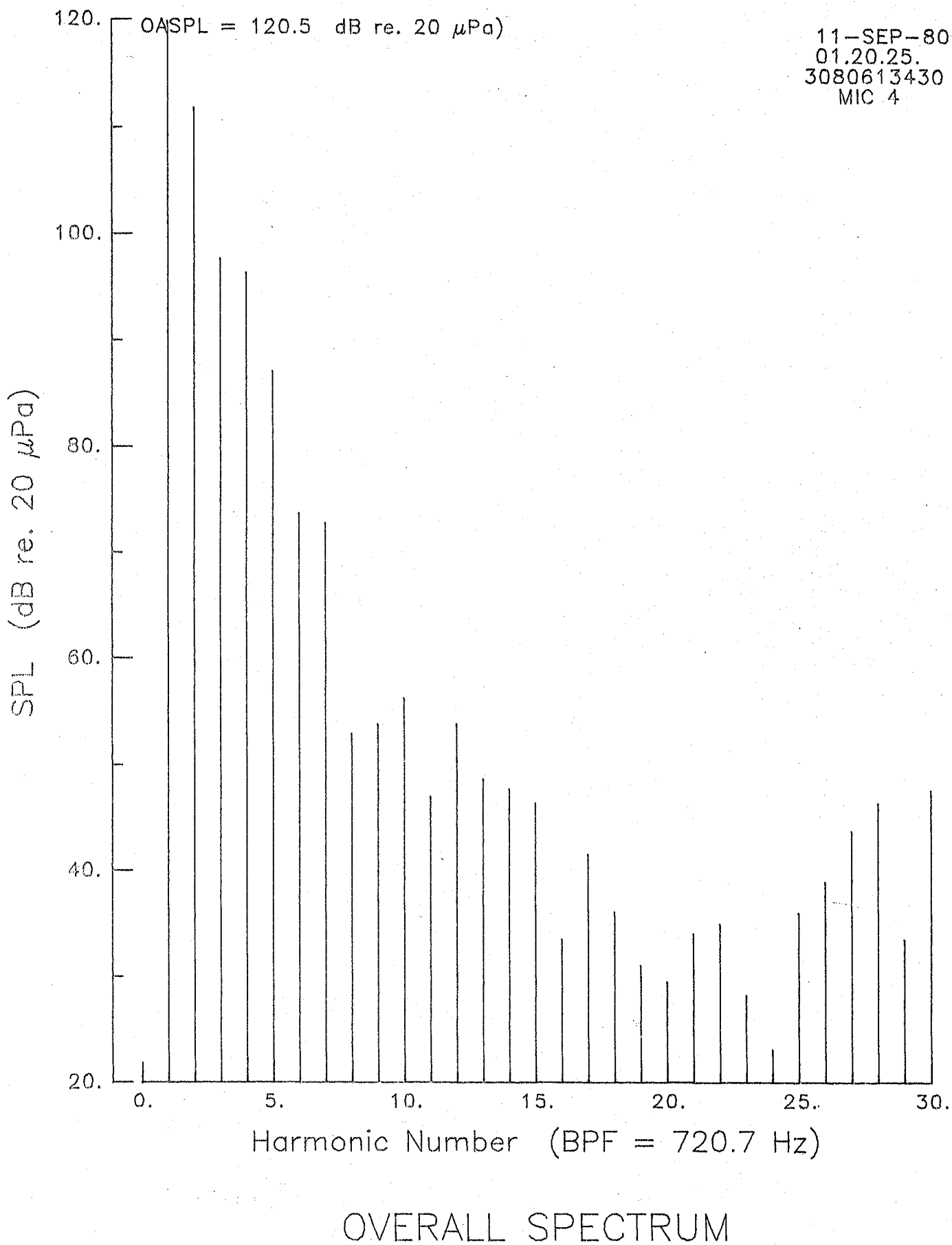

Figure 14(b).- Continued.

F. Farassat -- P. Nystrom
JIAFS -- NASA/LaRC -- GWU

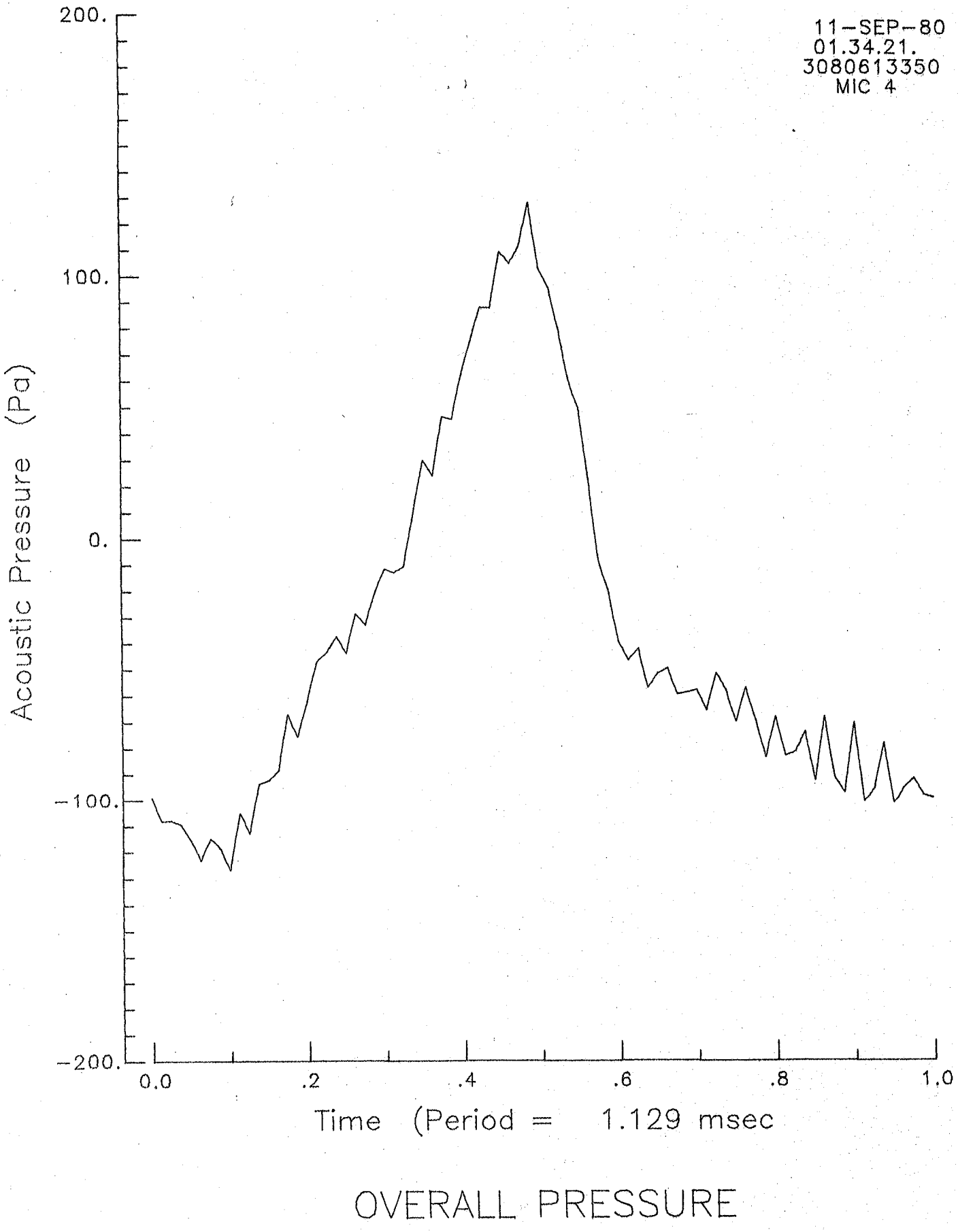

Figure 14(b).- Continued.

F. Farassat -- P. Nystrom
JIAFS -- NASA/LaRC -- GWU

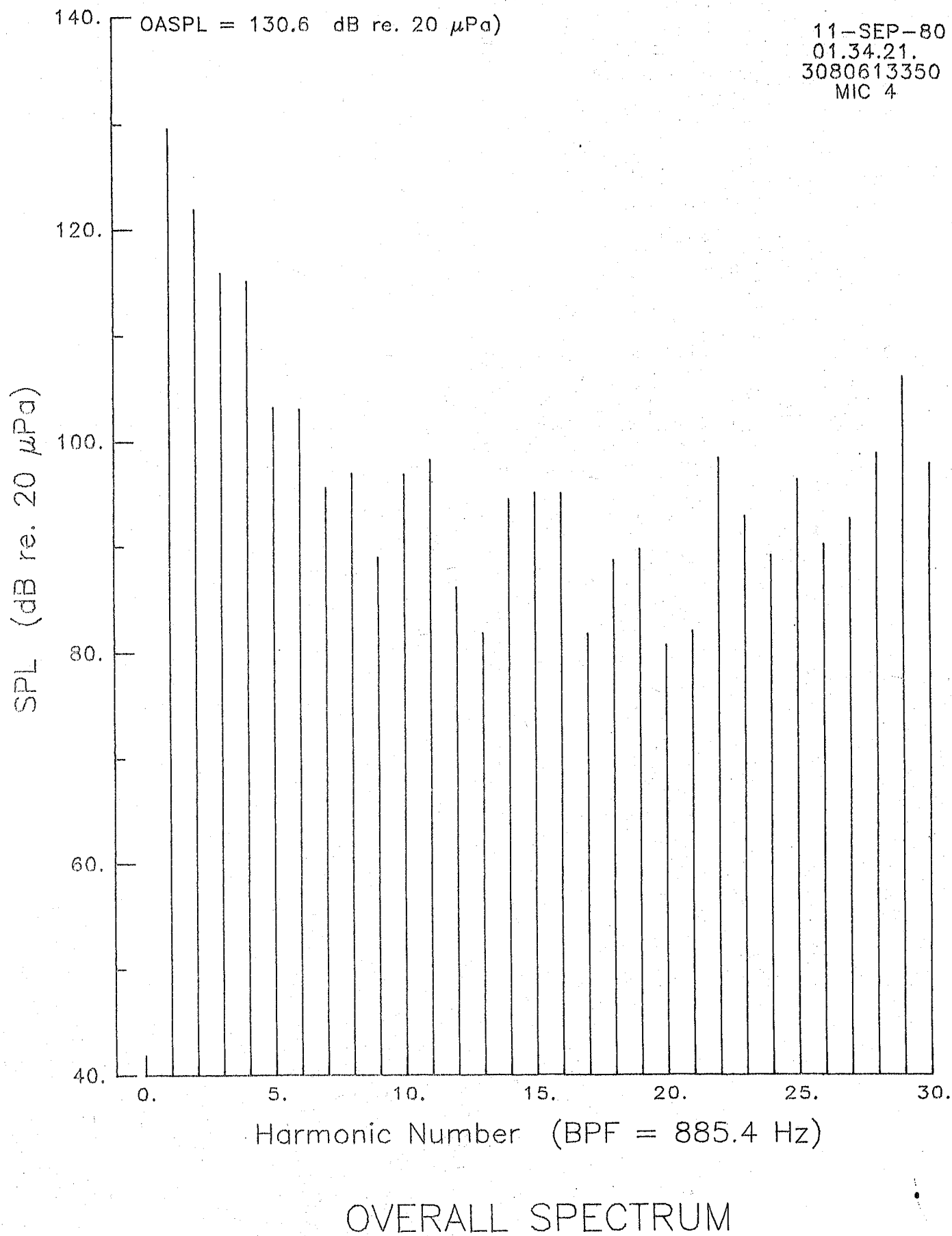

Figure 14(b).- Continued.

F. Farassat -- P. Nystrom
JIAFS -- NASA/LaRC -- GWU

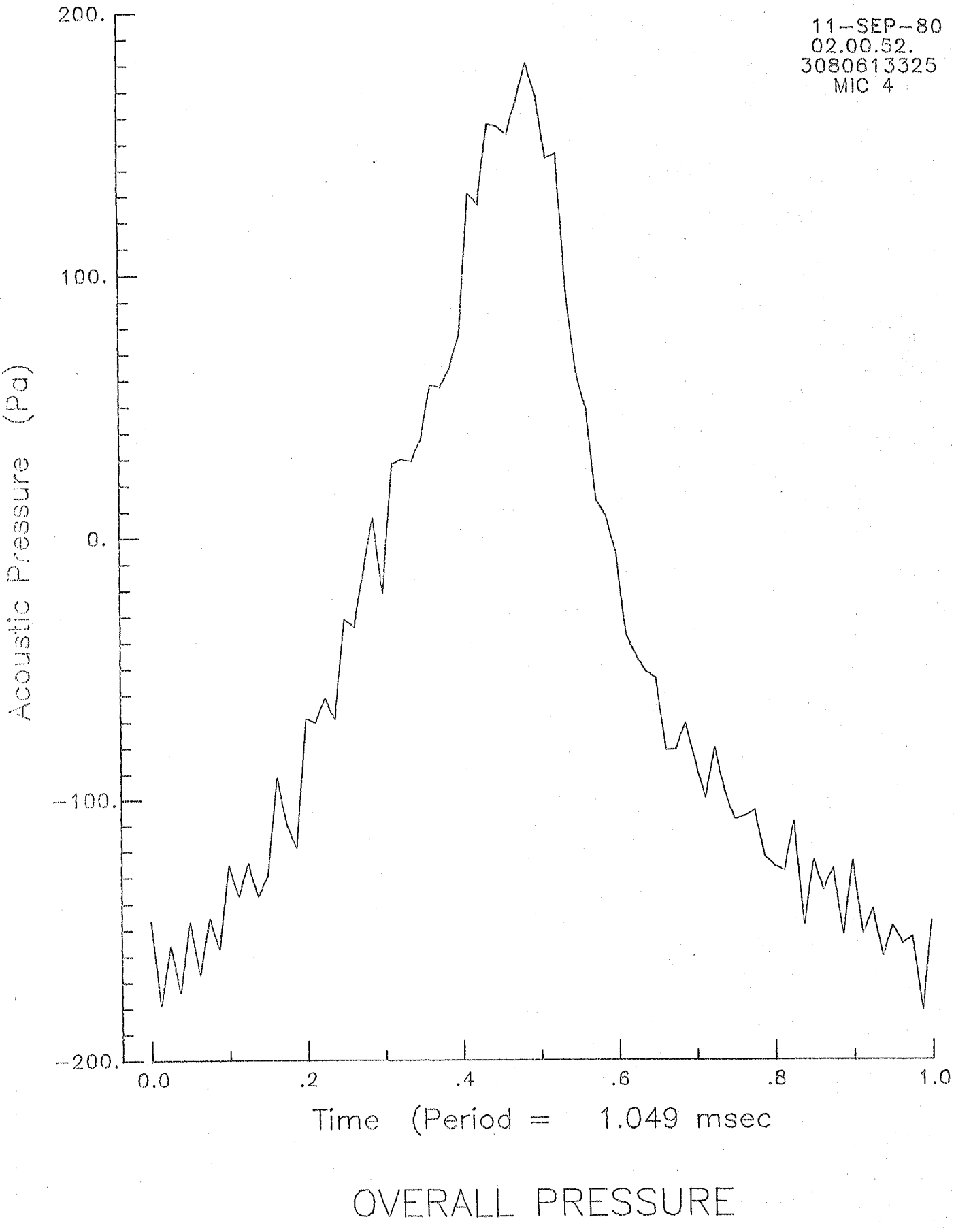

Figure 14(b).- Continued.

F. Farassat -- P. Nystrom
JIAFS -- NASA/LaRC -- GWU

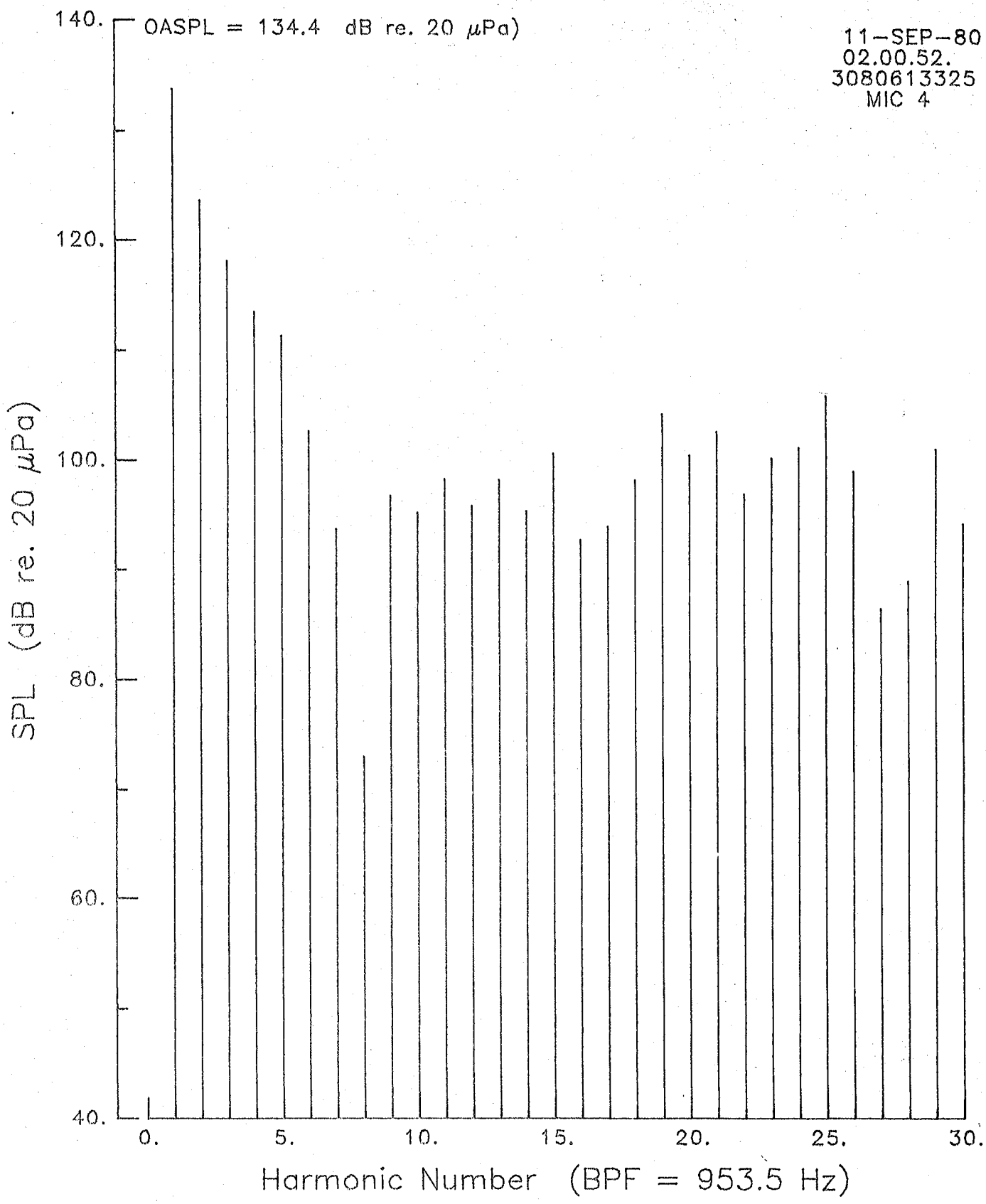

Figure 14(b).- Continued.

F. Farassat -- P. Nystrom
JIAFS -- NASA/LaRC -- GWU

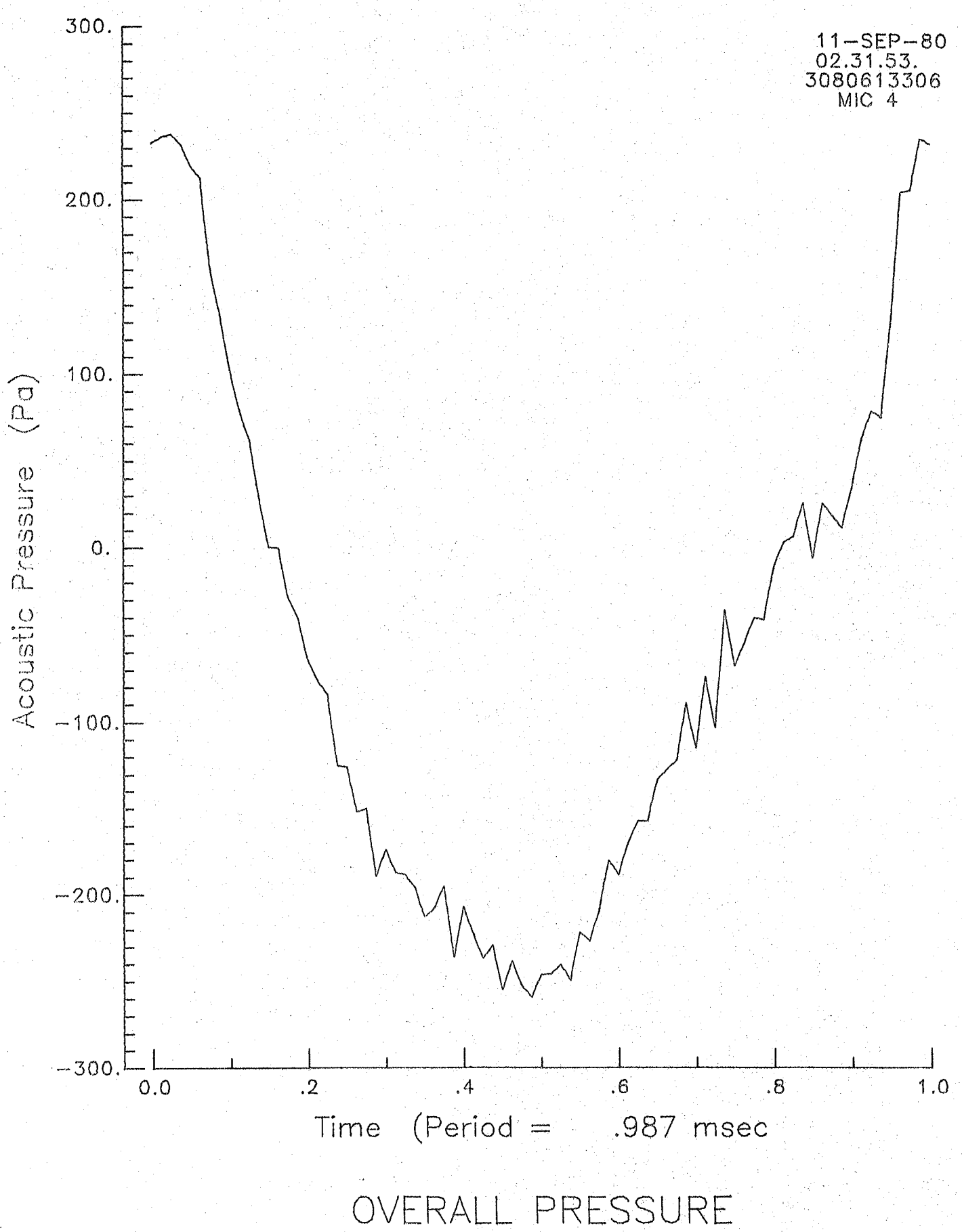

Figure 14(b).- Continued.

F. Farassat -- P. Nystrom
JIAFS -- NASA/LaRC -- GWU

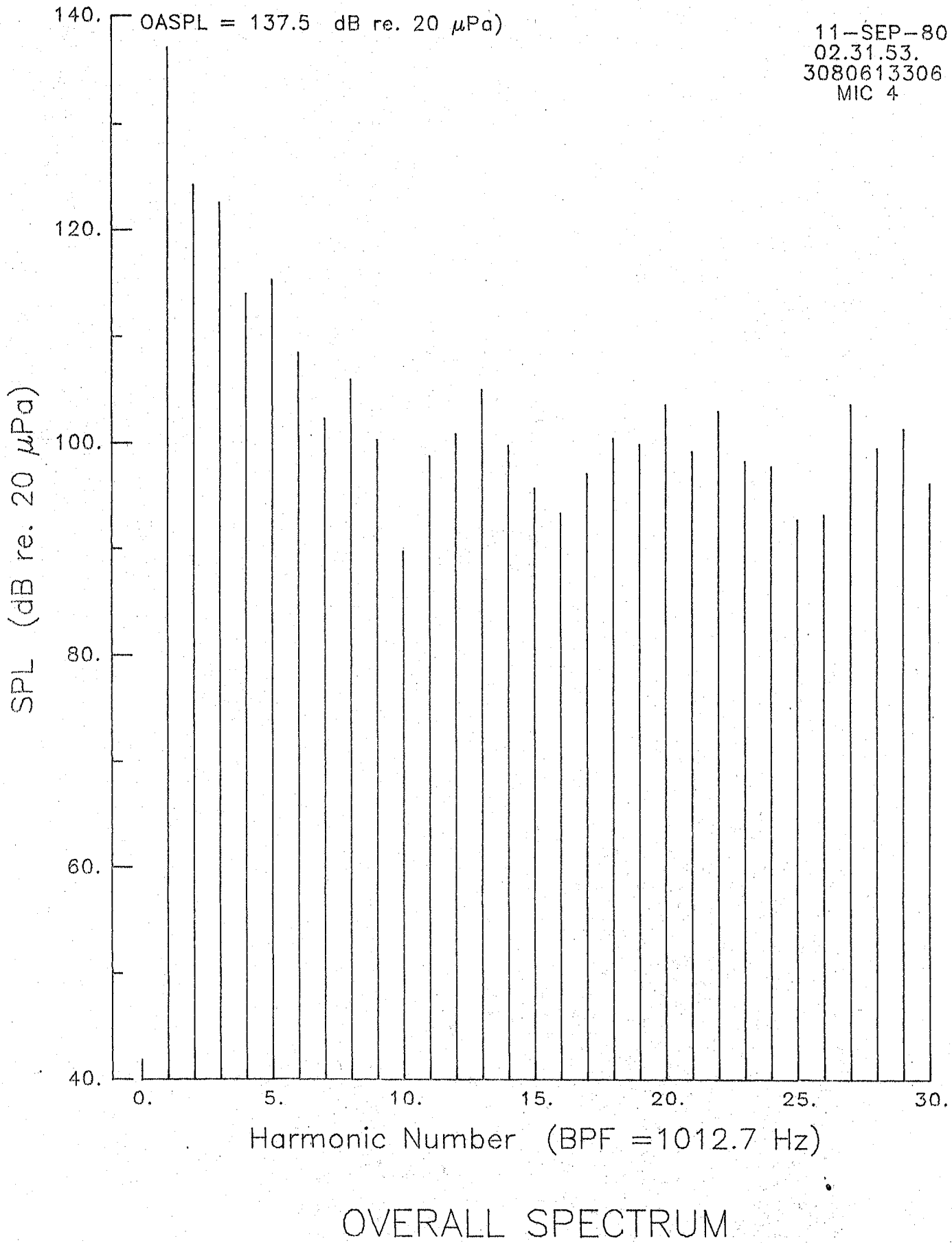

Figure 14(b).- Continued.

F. Farassat -- P. Nystrom
JIAFS -- NASA/LaRC -- GWU

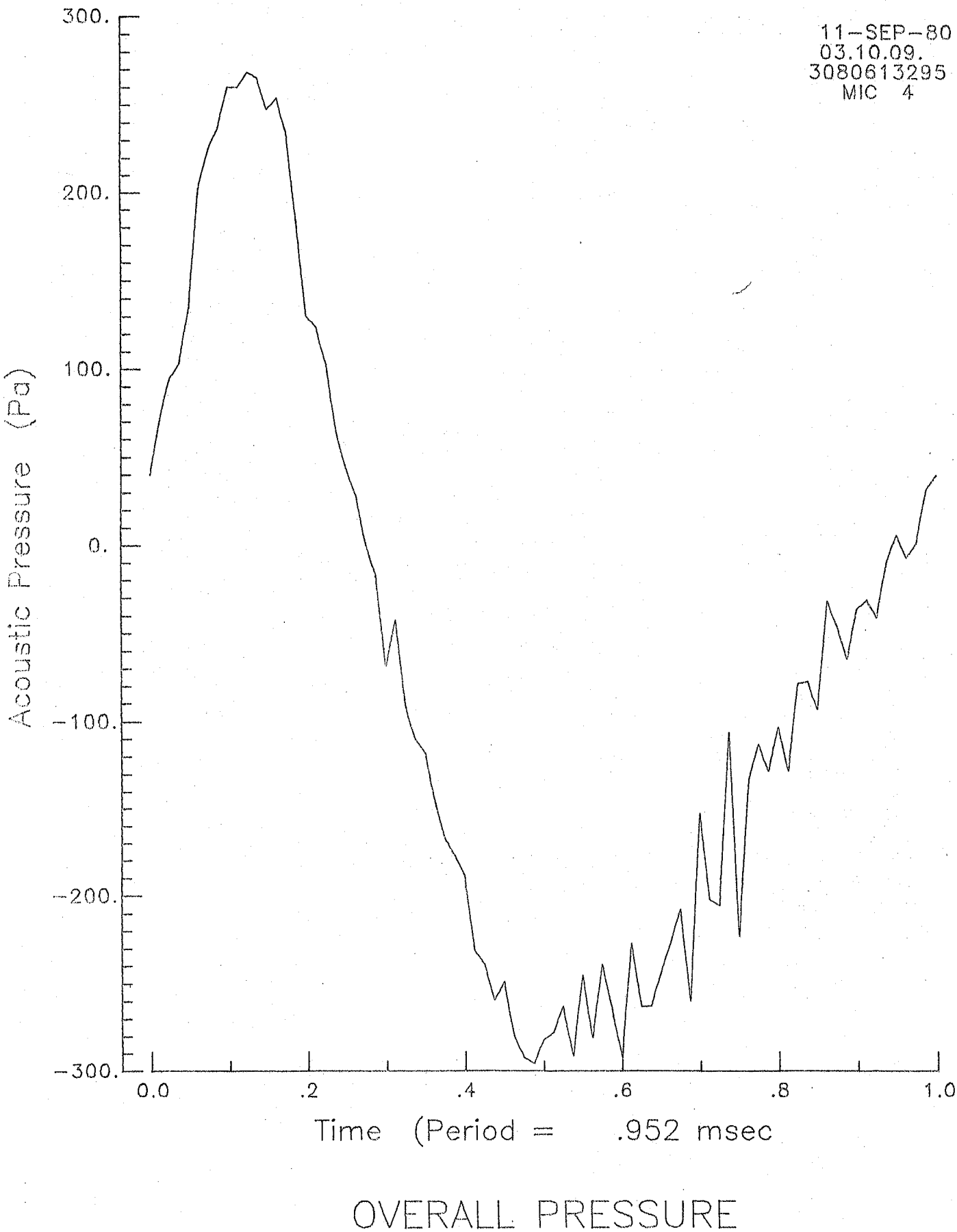

Figure 14(b).- Continued.

F. Farassat -- P. Nystrom
JIAFS -- NASA/LaRC -- GWU

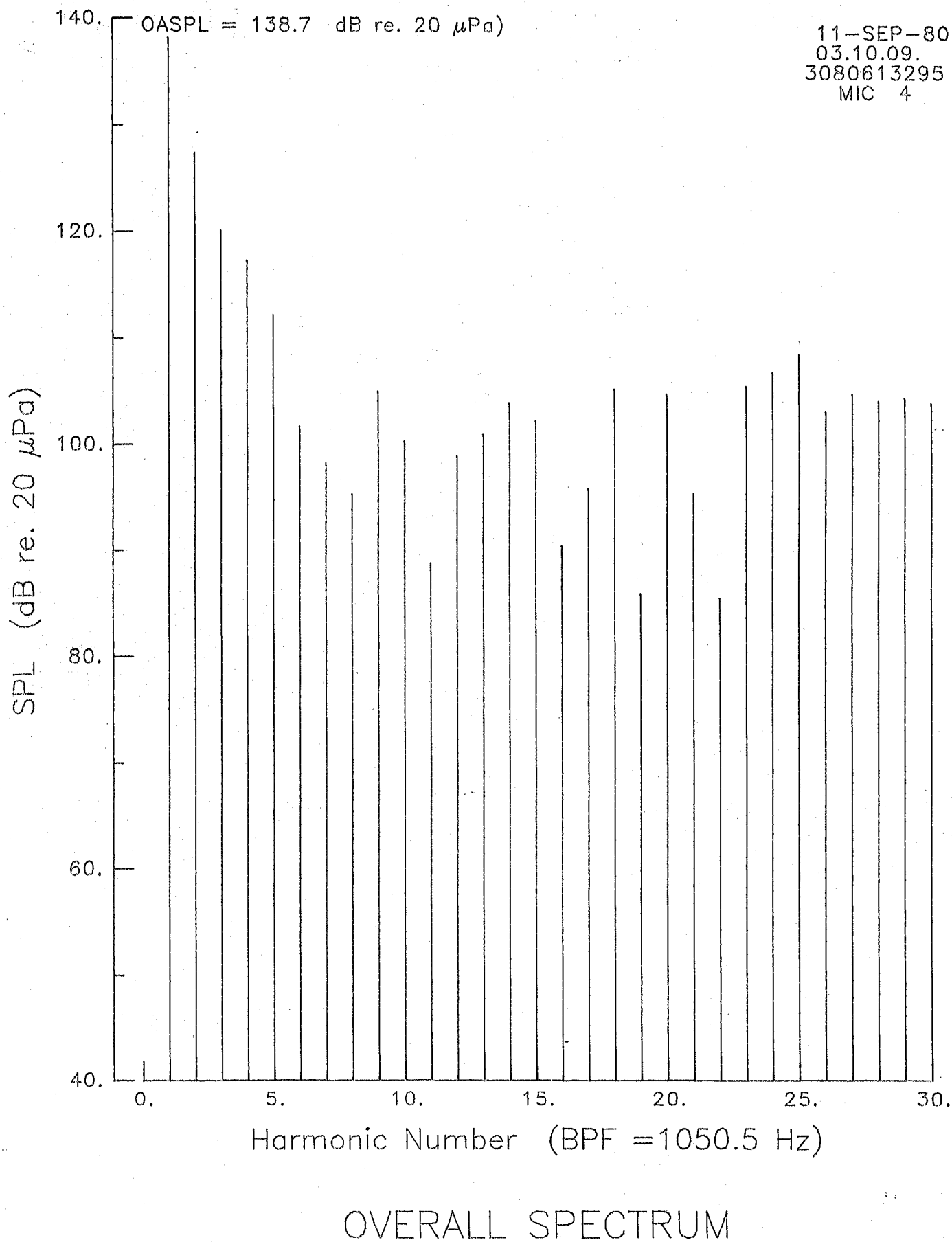

Figure 14(b).- Concluded.

F. Farassat -- P. Nystrom
JIAFS -- NASA/LaRC -- GWU

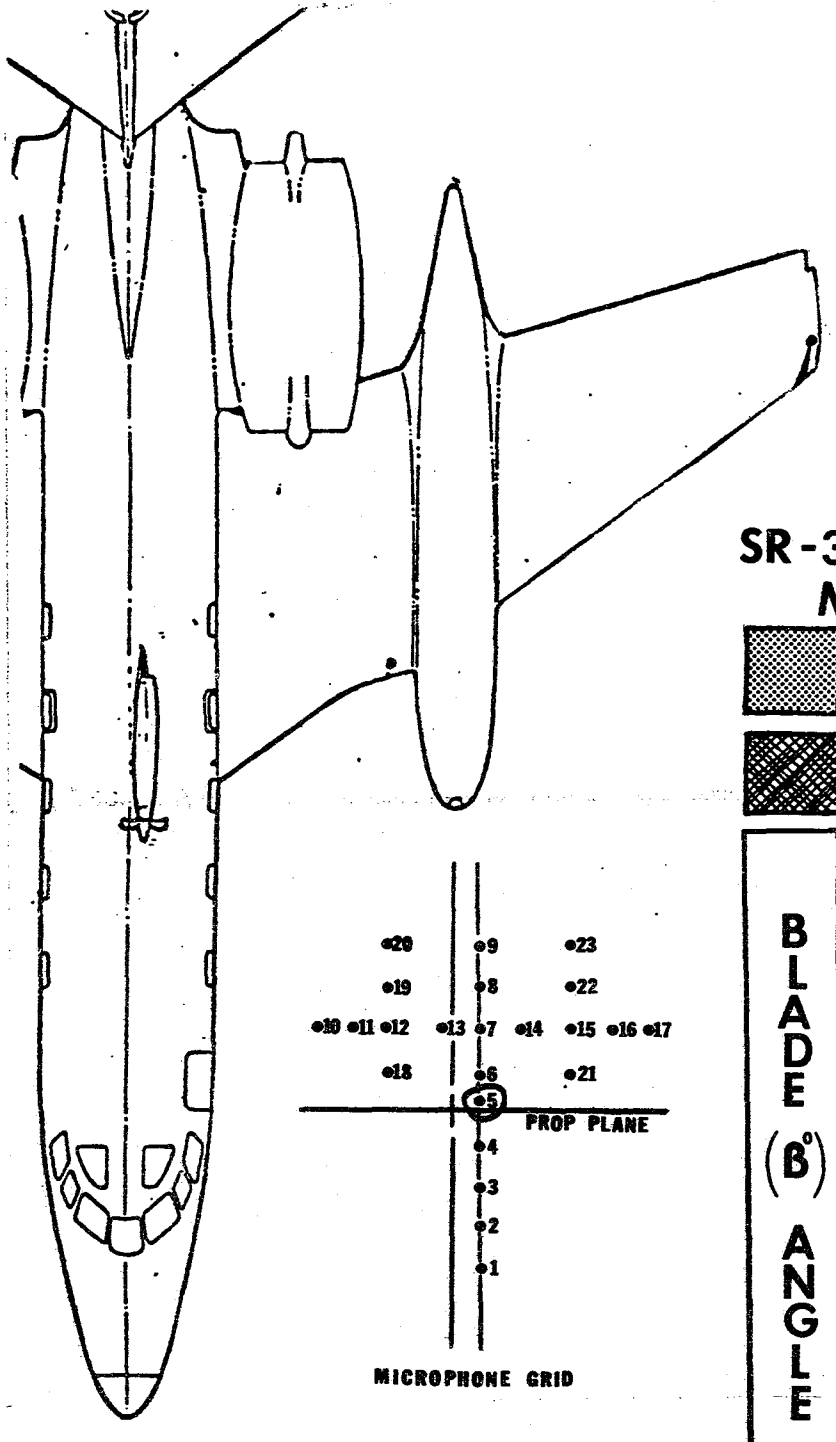

Figure 14(c).- Continued.

SR-3 TEST MATRIX

EXCEEDS BLEED SYS. POWER CAPACITY

BLADE CRITICAL SPEED

BLADE ANGLE (β°)	ADVANCE RATIO (J)	ALTITUDE (FT) 20,000						ALTITUDE (FT) 25,000						ALTITUDE (FT) 30,000			
		MACH # .50	.60	.65	.70	.75	.80	.50	.60	.65	.70	.75	.80	.50	.60	.65	.70	.75	.80
59.3	4.30																		
	3.50																		
	3.25																		
	3.06																		
	2.90																		
61.3	4.30																		X
	3.50																		X
	3.25				■						■						■		X
	3.06												■						X
	2.95						■											■	X
63.3	4.30																		
	4.07																		
	3.50																		
	3.25						■						■						■

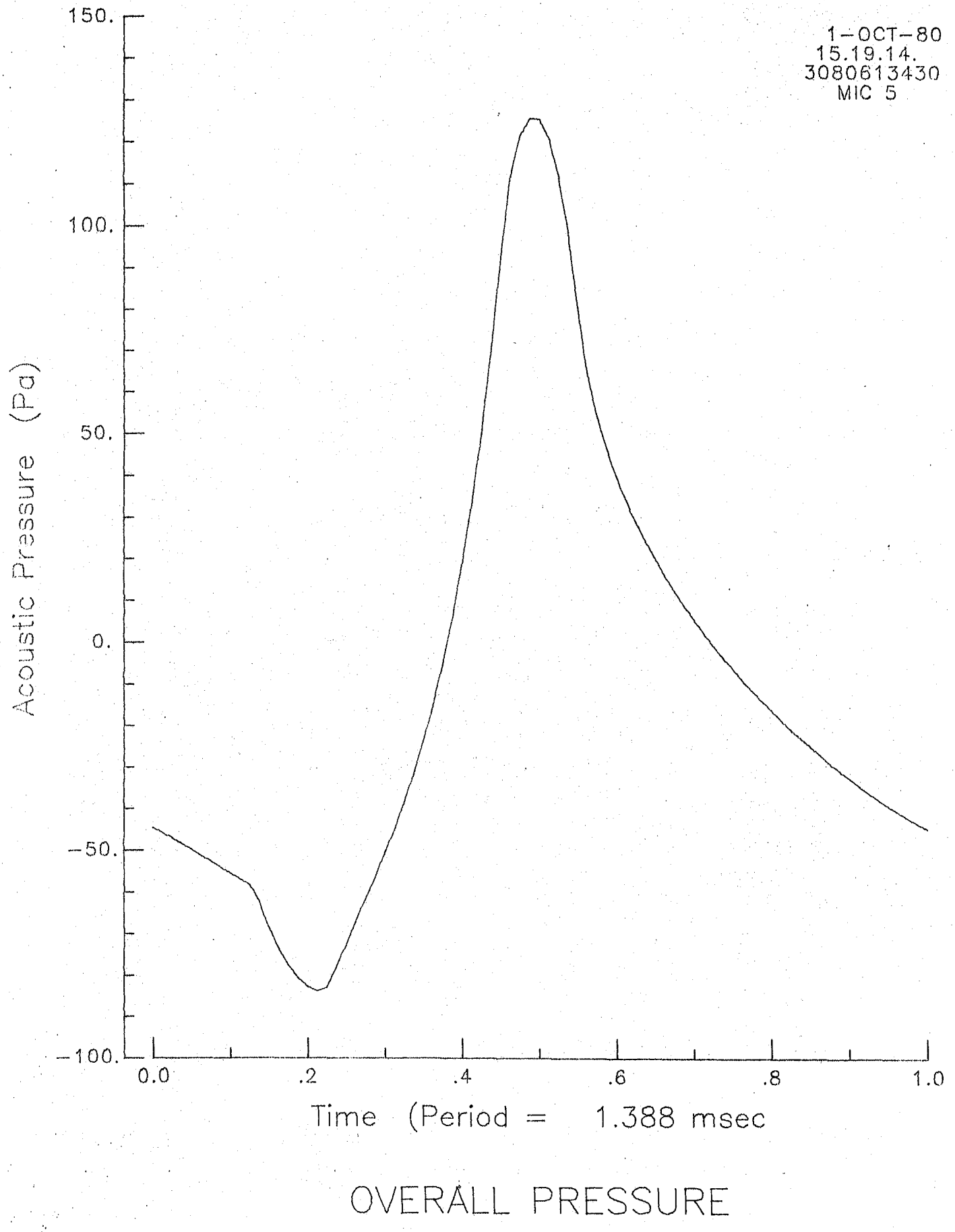

Figure 14(c).- Continued.

F. Farassat -- P. Nystrom
JIAFS -- NASA/LaRC -- GWU

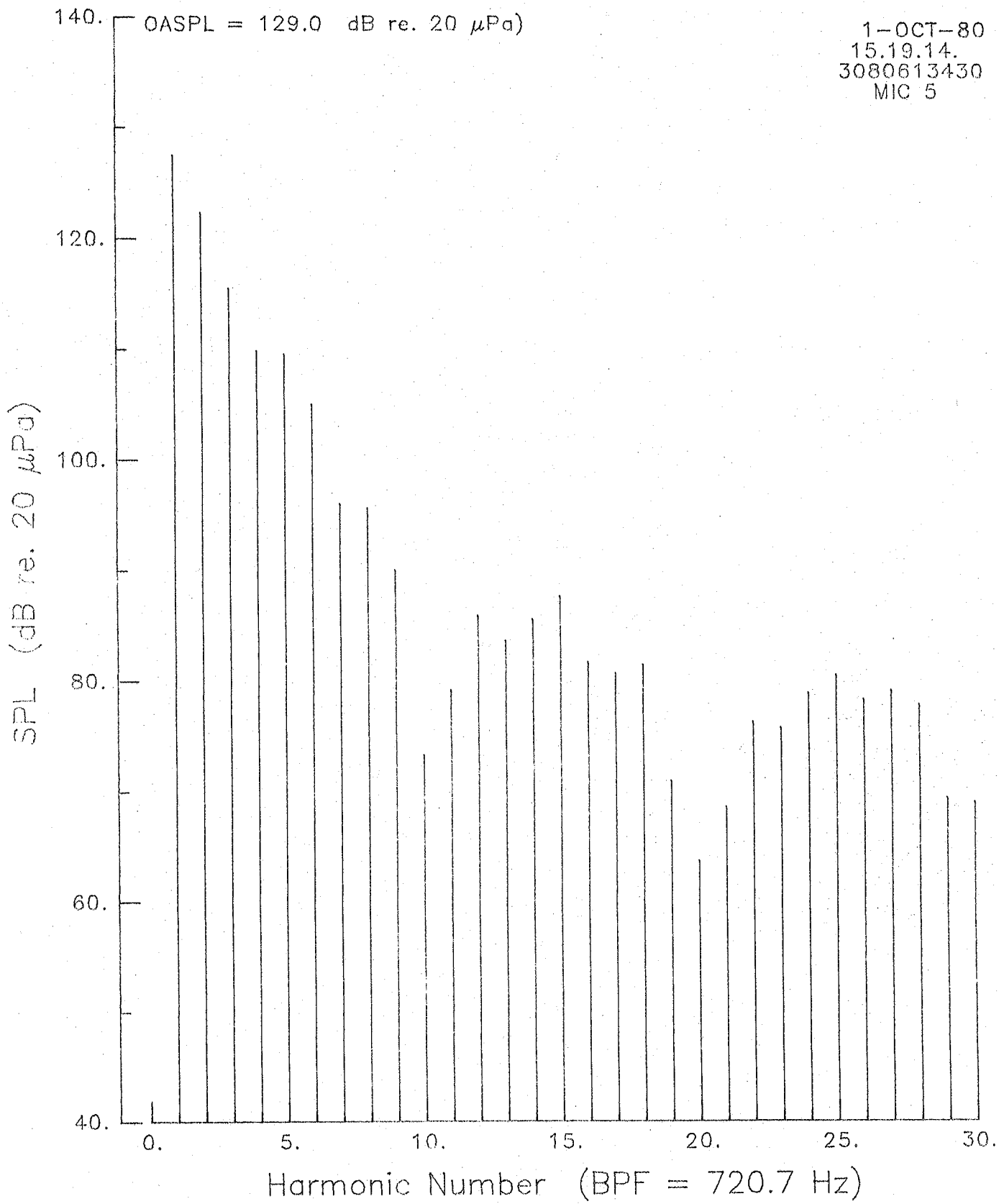

OVERALL SPECTRUM

Figure 14(c).- Continued.

F. Farassat -- P. Nystrom
JIAFS -- NASA/LaRC -- GWU

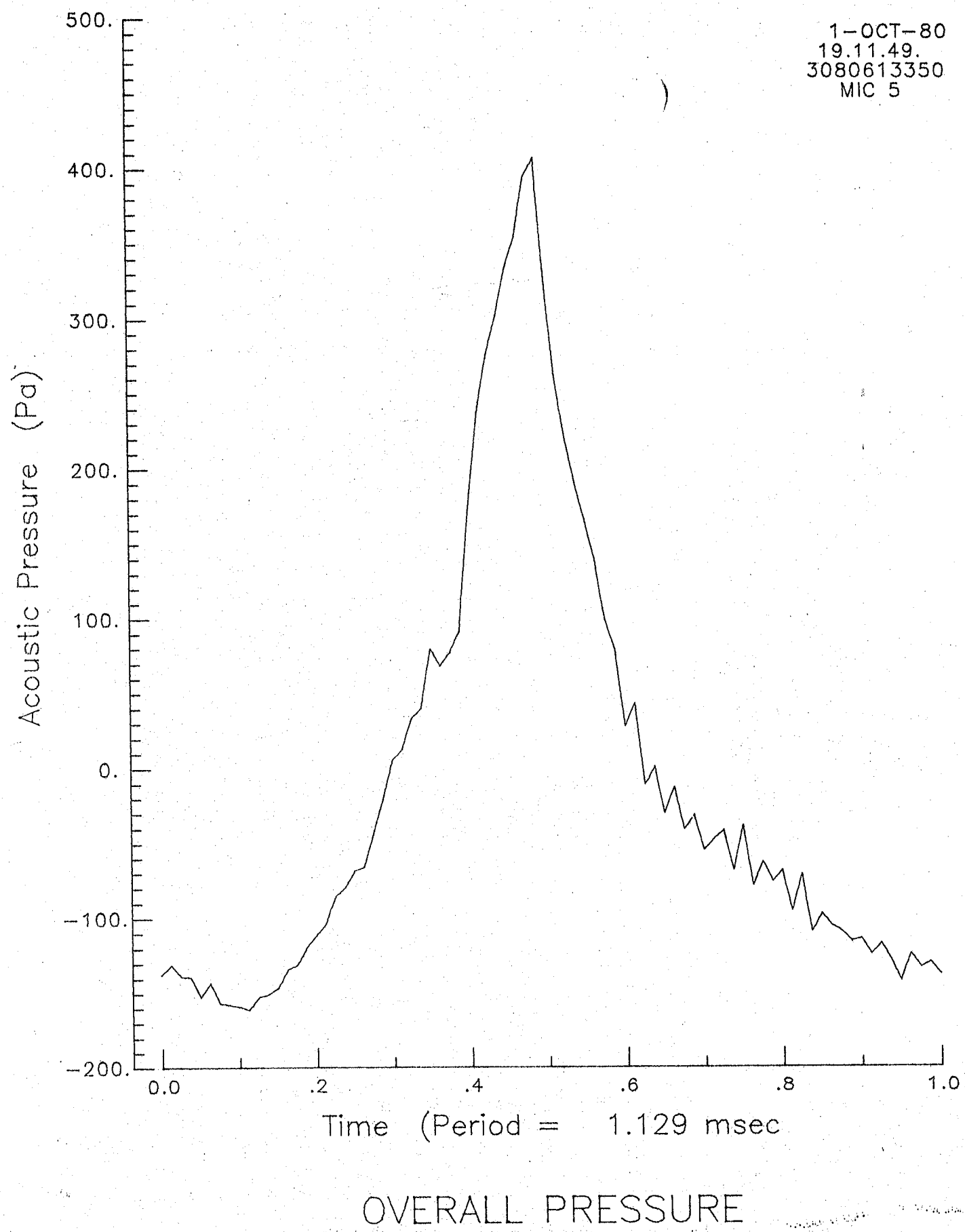

Figure 14(c).- Continued.

F. Farassat -- P. Nystrom
JIAFS -- NASA/LaRC -- GWU

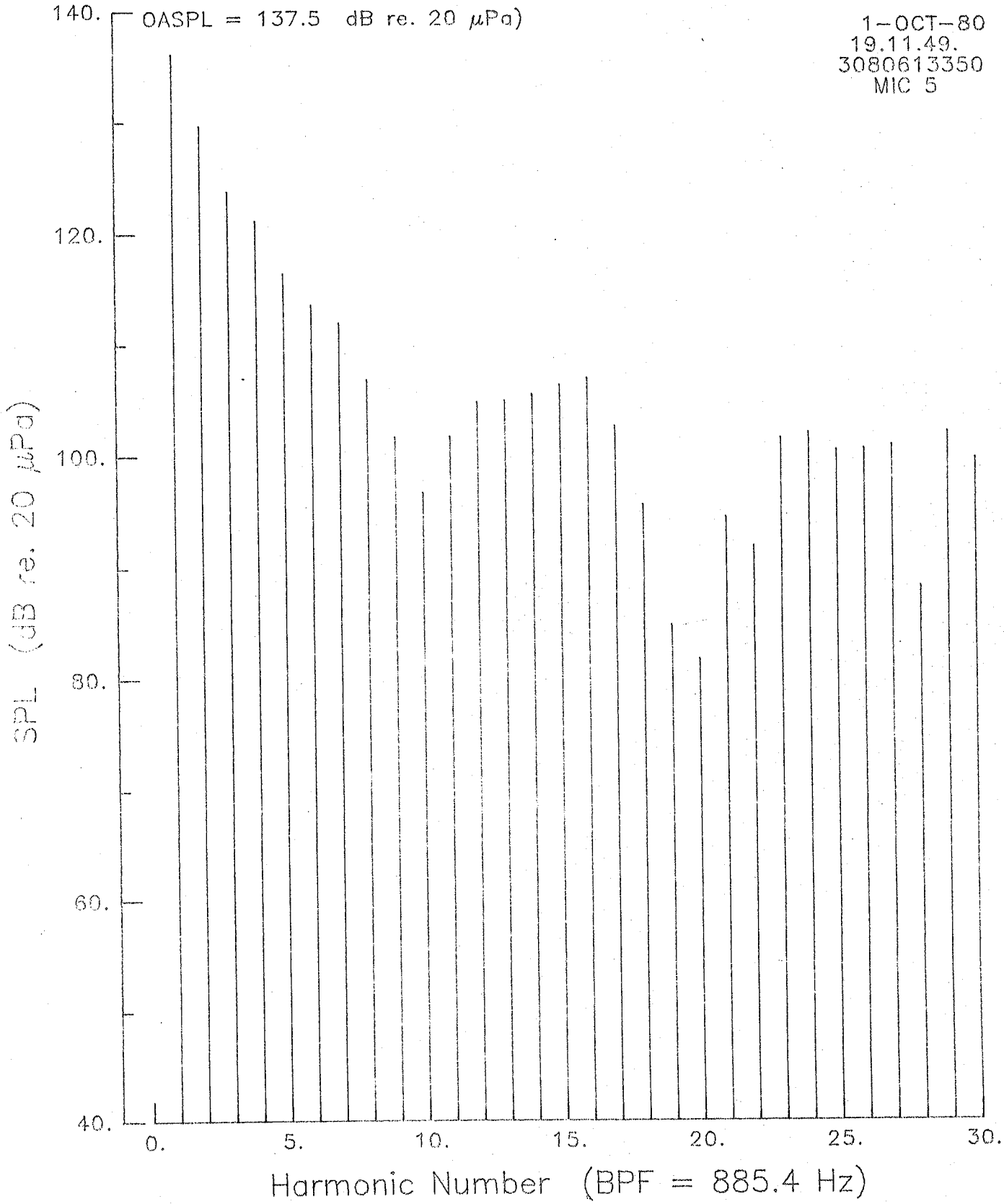

OVERALL SPECTRUM

Figure 14(c).- Continued.

F. Farassat -- P. Nystrom
JIAFS -- NASA/LaRC -- GWU

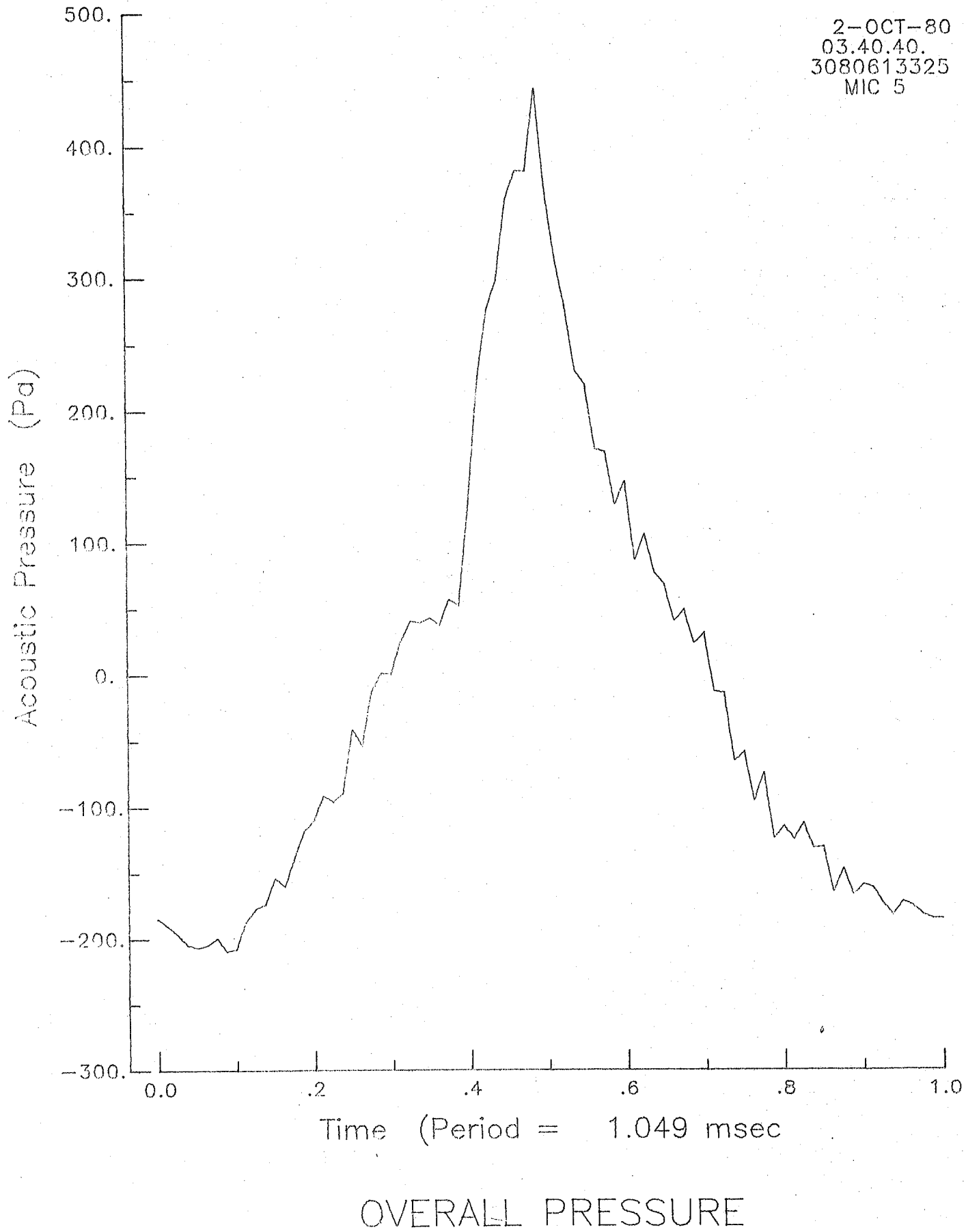

Figure 14(c).- Continued.

F. Farassat -- P. Nystrom
JIAFS -- NASA/LaRC -- GWU

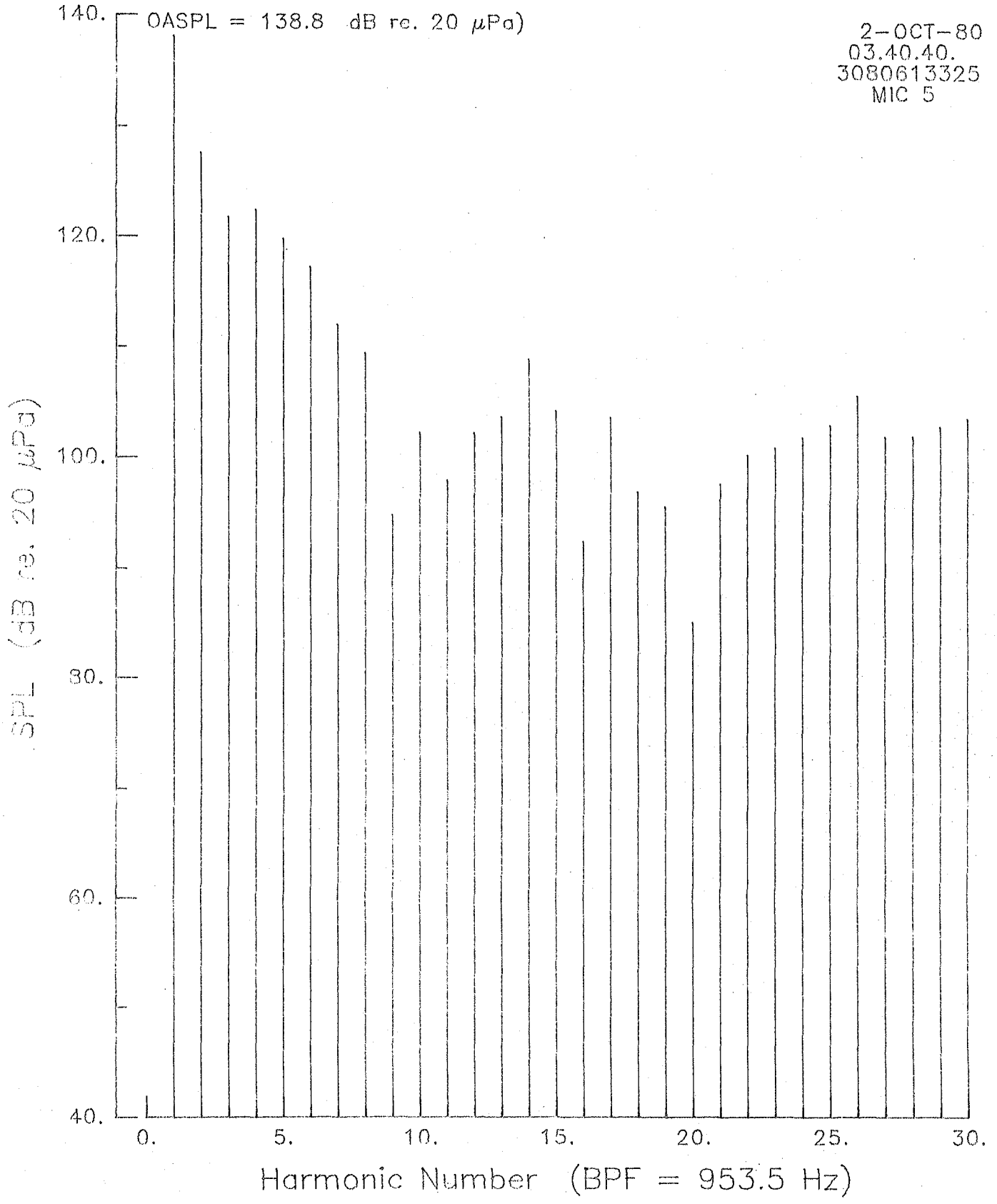

OVERALL SPECTRUM

Figure 14(c).- Continued.

F. Farassat -- P. Nystrom
JIAFS -- NASA/LaRC -- GWU

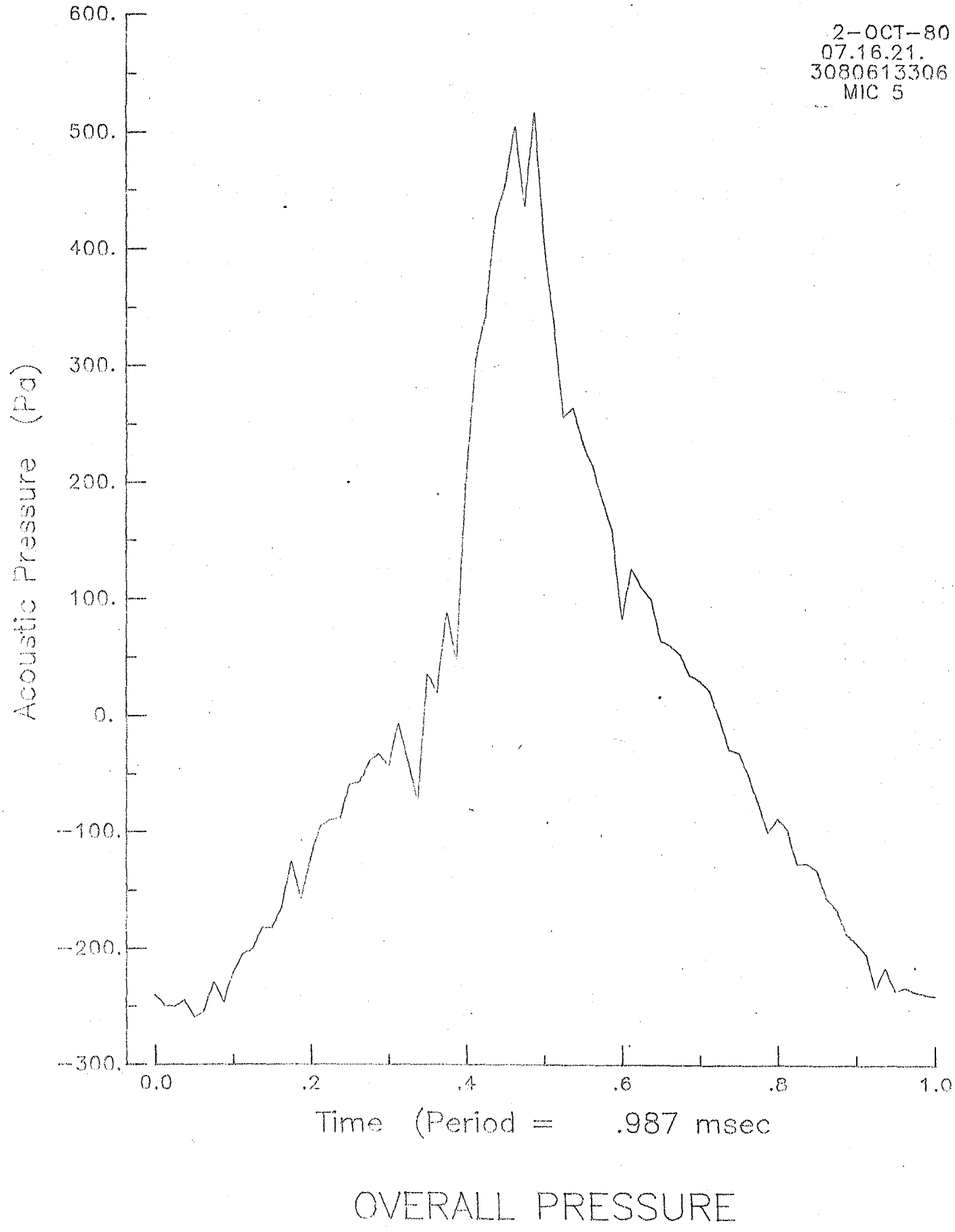

Figure 14(c).- Continued.

F. Farassat --- P. Nystrom
JIAFS --- NASA/LaRC --- GWU

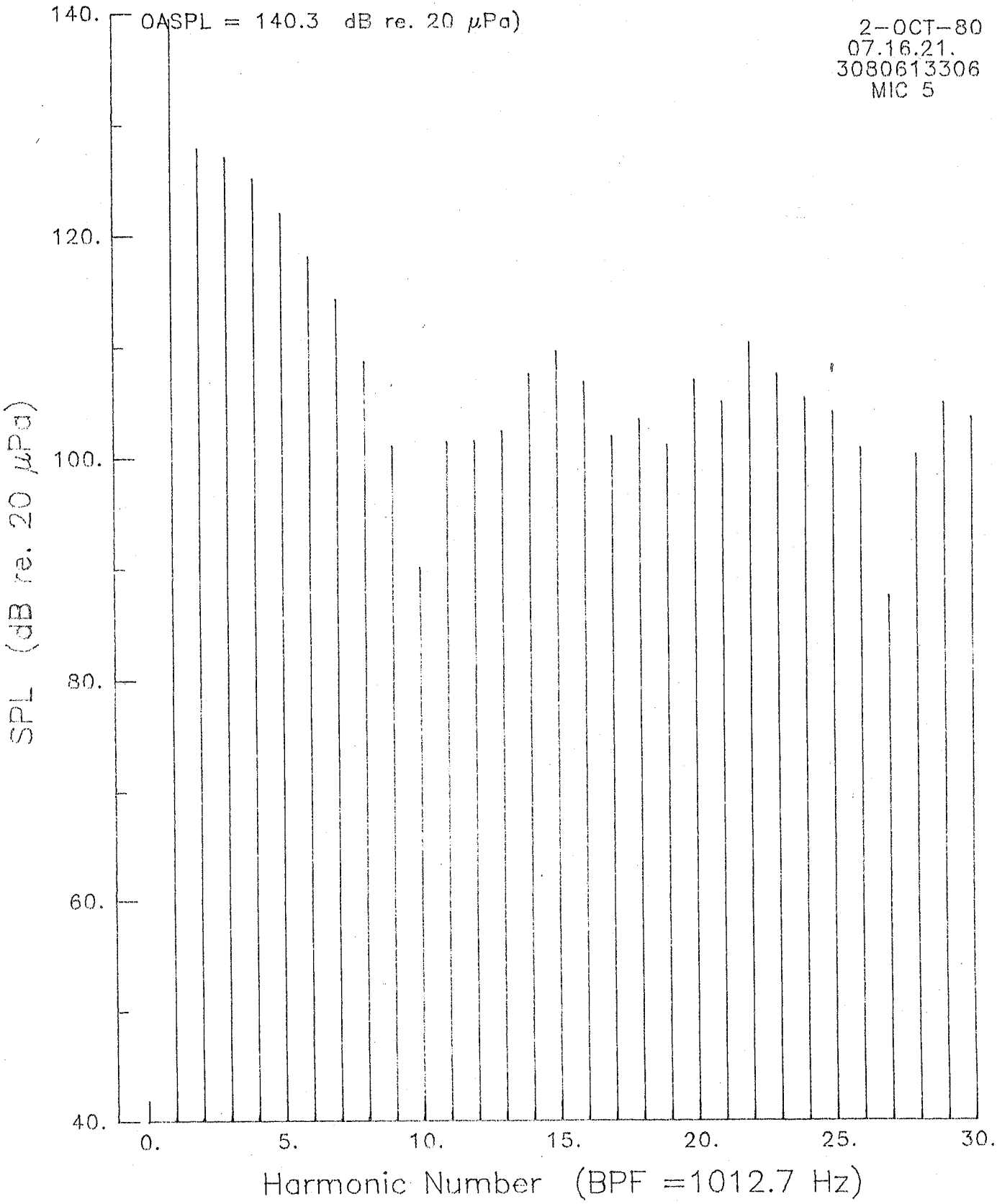

OVERALL SPECTRUM

Figure 14(c).- Continued.

F. Farassat -- P. Nystrom
JIAFS -- NASA/LaRC -- GWU

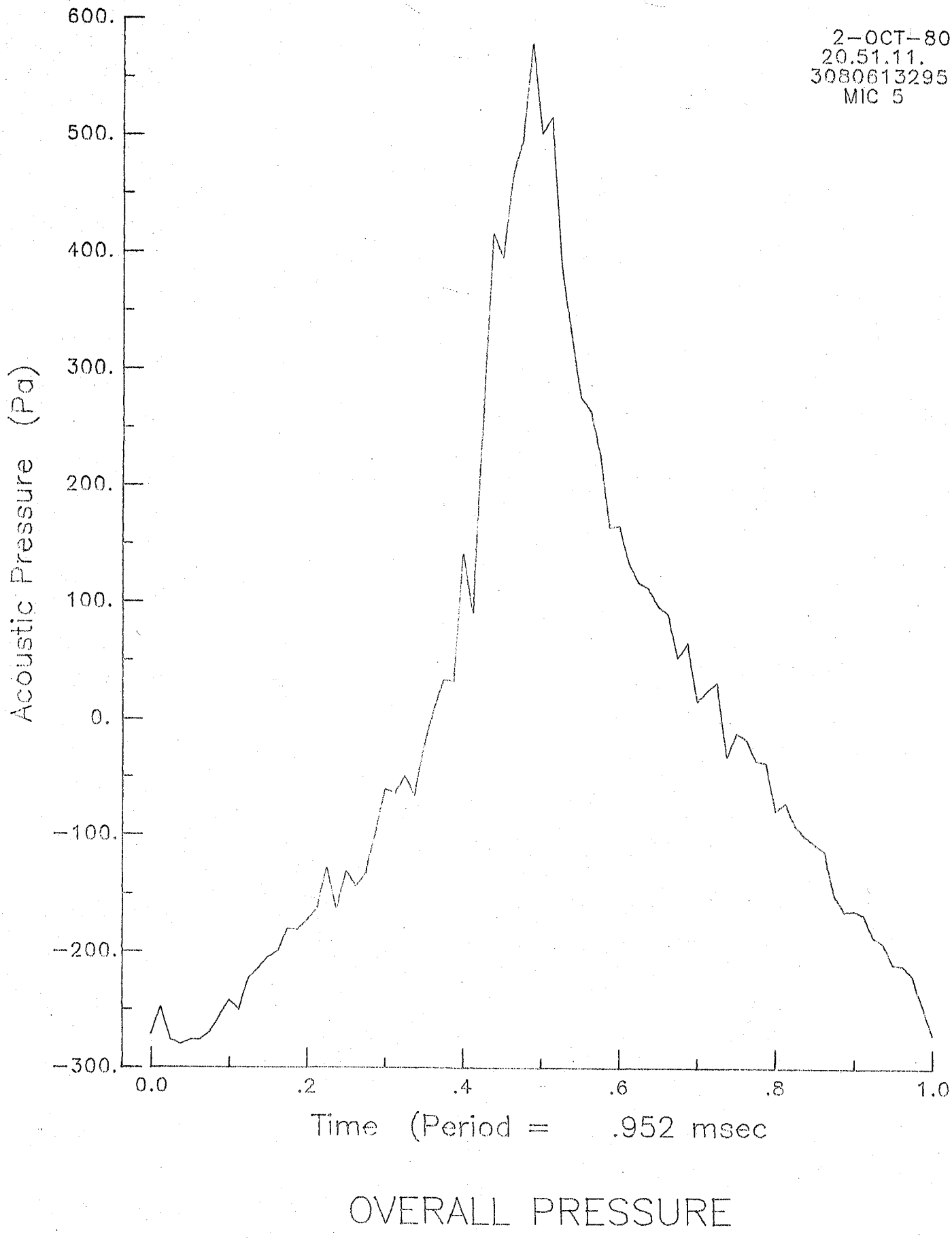

Figure 14(c).- Continued.

F. Farassat -- P. Nystrom
JIAFS -- NASA/LaRC -- GWU

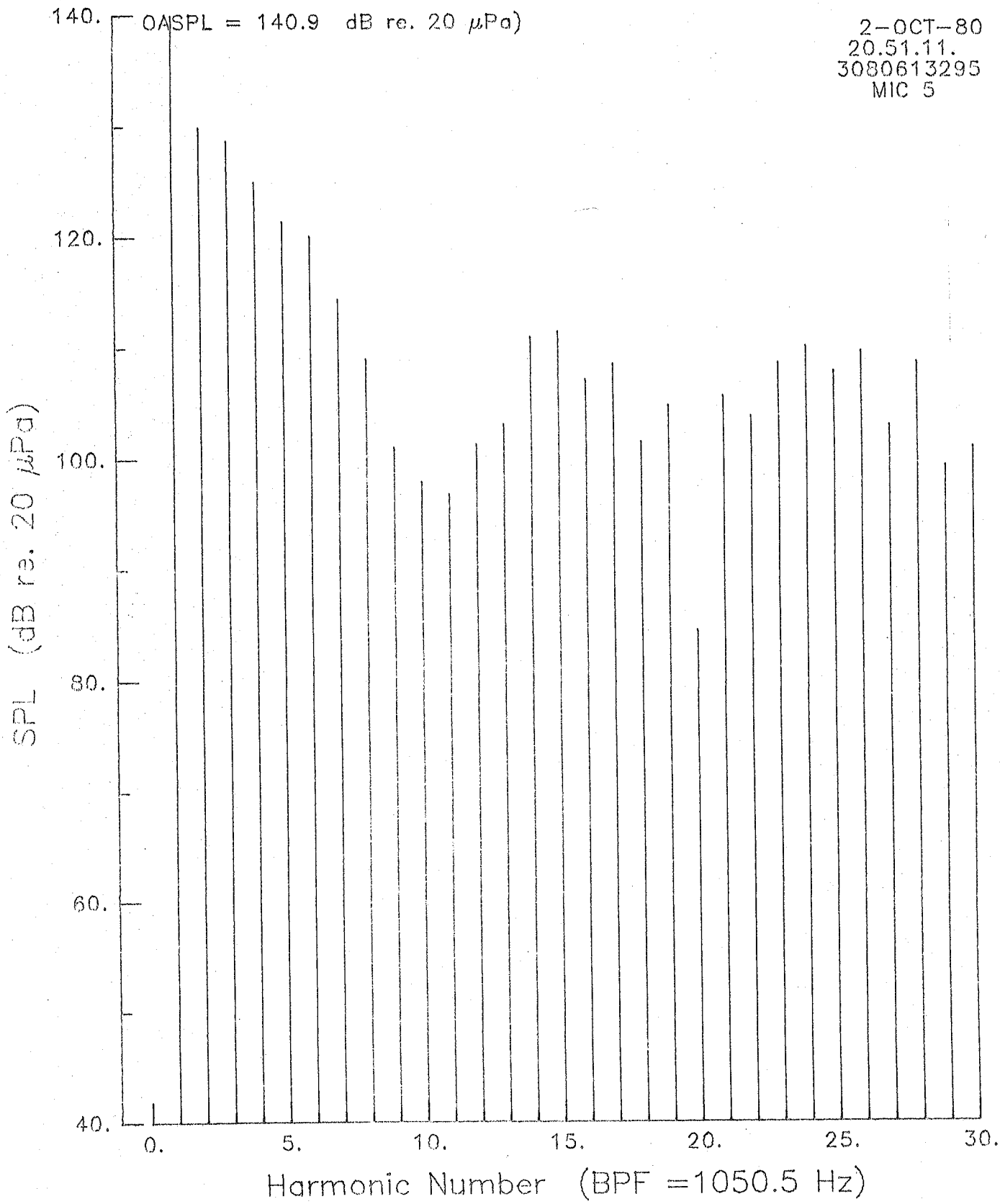

Figure 14(c).- Concluded.

F. Farassat -- P. Nystrom
JIAFS -- NASA/LaRC -- GWU

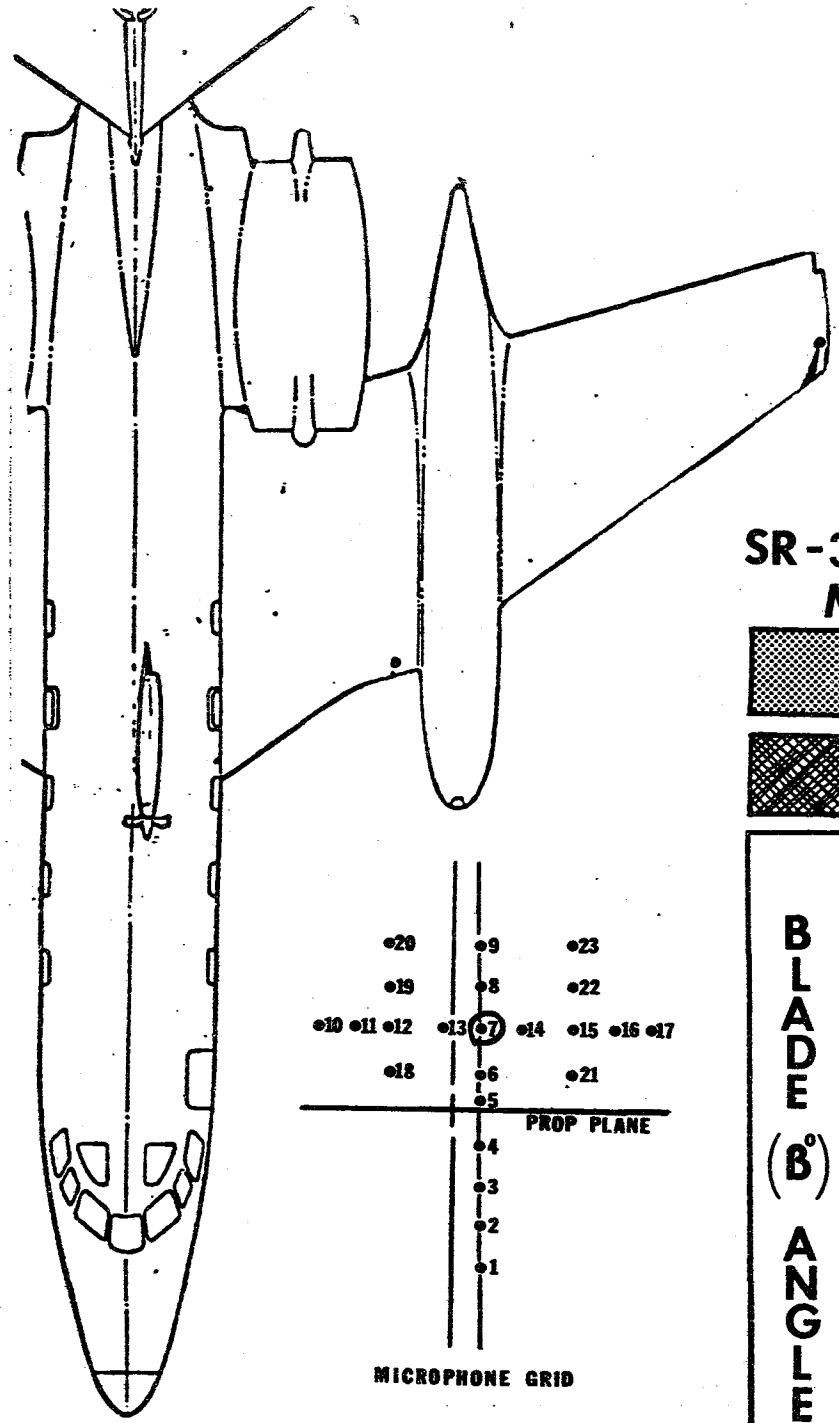

SR-3 TEST MATRIX

EXCEEDS BLEED SYS. POWER CAPACITY

BLADE CRITICAL SPEED

ALTITUDE (FT)	20,000						25,000						30,000					
MACH #	.50	.60	.65	.70	.75	.80	.50	.60	.65	.70	.75	.80	.50	.60	.65	.70	.75	.80
BLADE ANGLE (β°) 59.3 / ADVANCE RATIO (J) 4.30																		X
3.50																		X
3.25																		X
3.06																		X
2.90																		X
BLADE ANGLE (β°) 61.3 / ADVANCE RATIO (J) 4.30																		X
3.50																		X
3.25				■						■						■		
3.06												■						
2.95						■						■					■	
BLADE ANGLE (β°) 63.3 / ADVANCE RATIO (J) 4.30																		
4.07																		
3.50																		
3.25						■						■						■

Figure (d).- Continued.

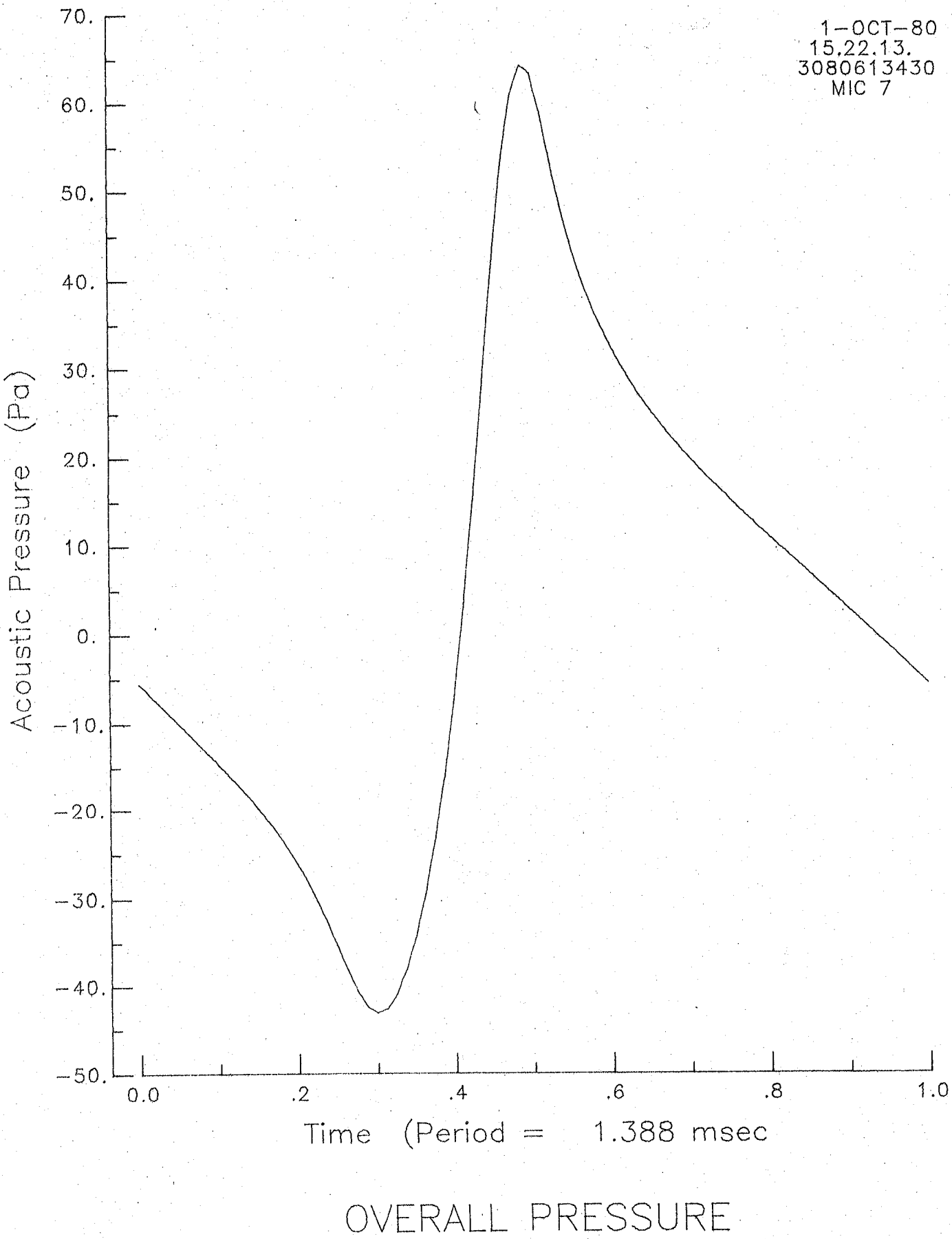

Figure 14(d).- Continued.

F. Farassat -- P. Nystrom
JIAFS -- NASA/LaRC -- GWU

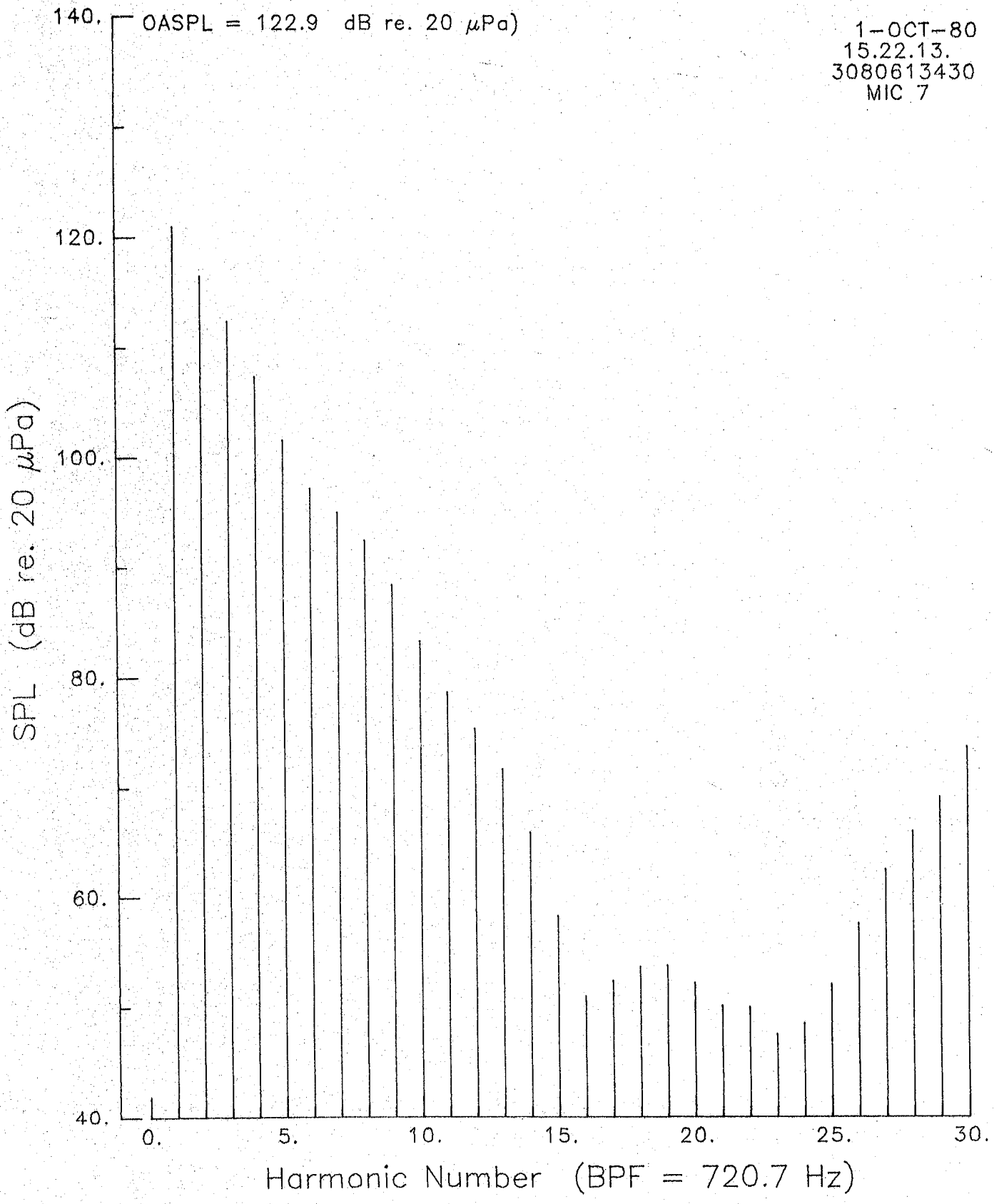

Figure 14(d).- Continued.

F. Farassat -- P. Nystrom
JIAFS -- NASA/LaRC -- GWU

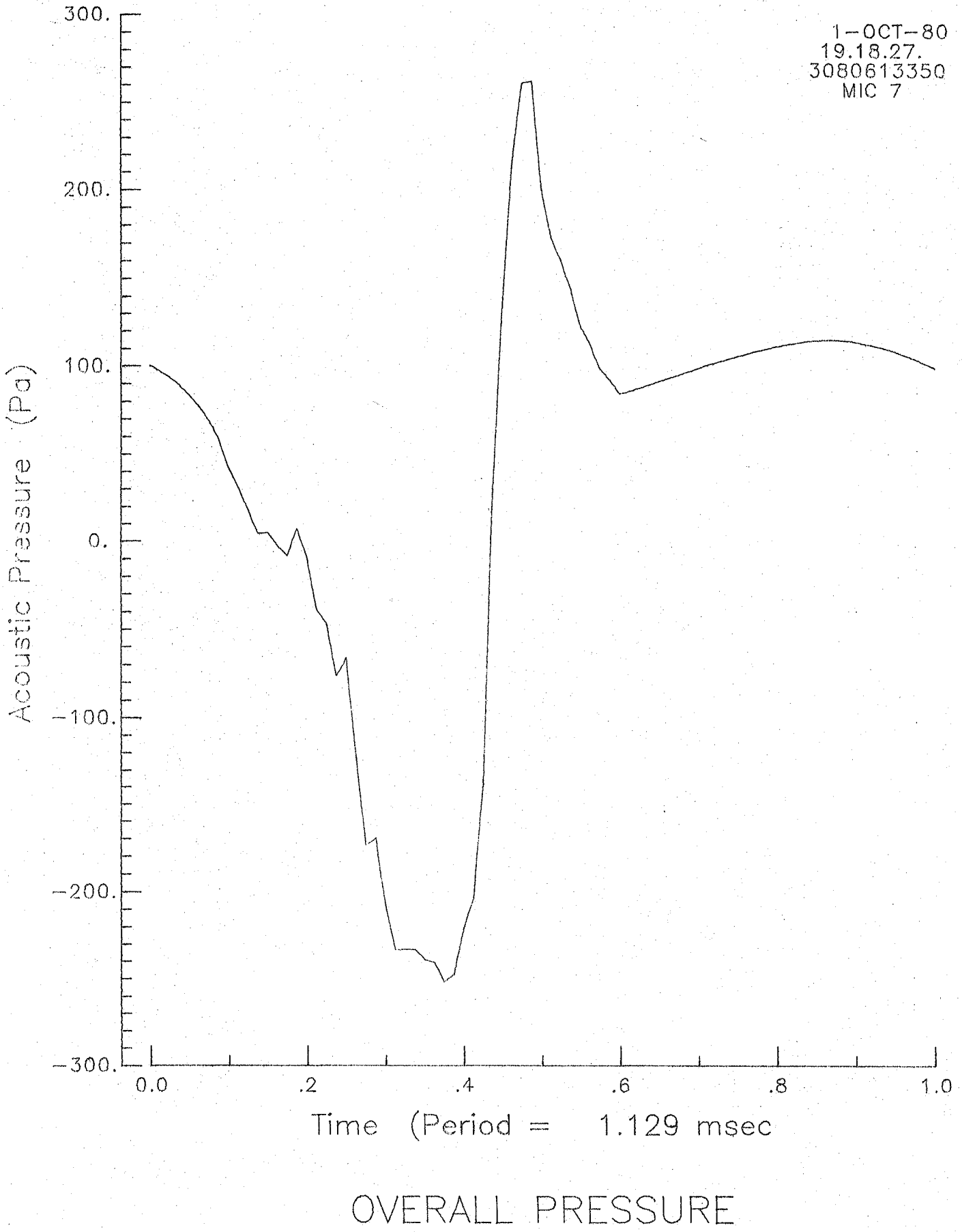

Figure 14(d).- Continued.

F. Farassat -- P. Nystrom
JIAFS -- NASA/LaRC -- GWU

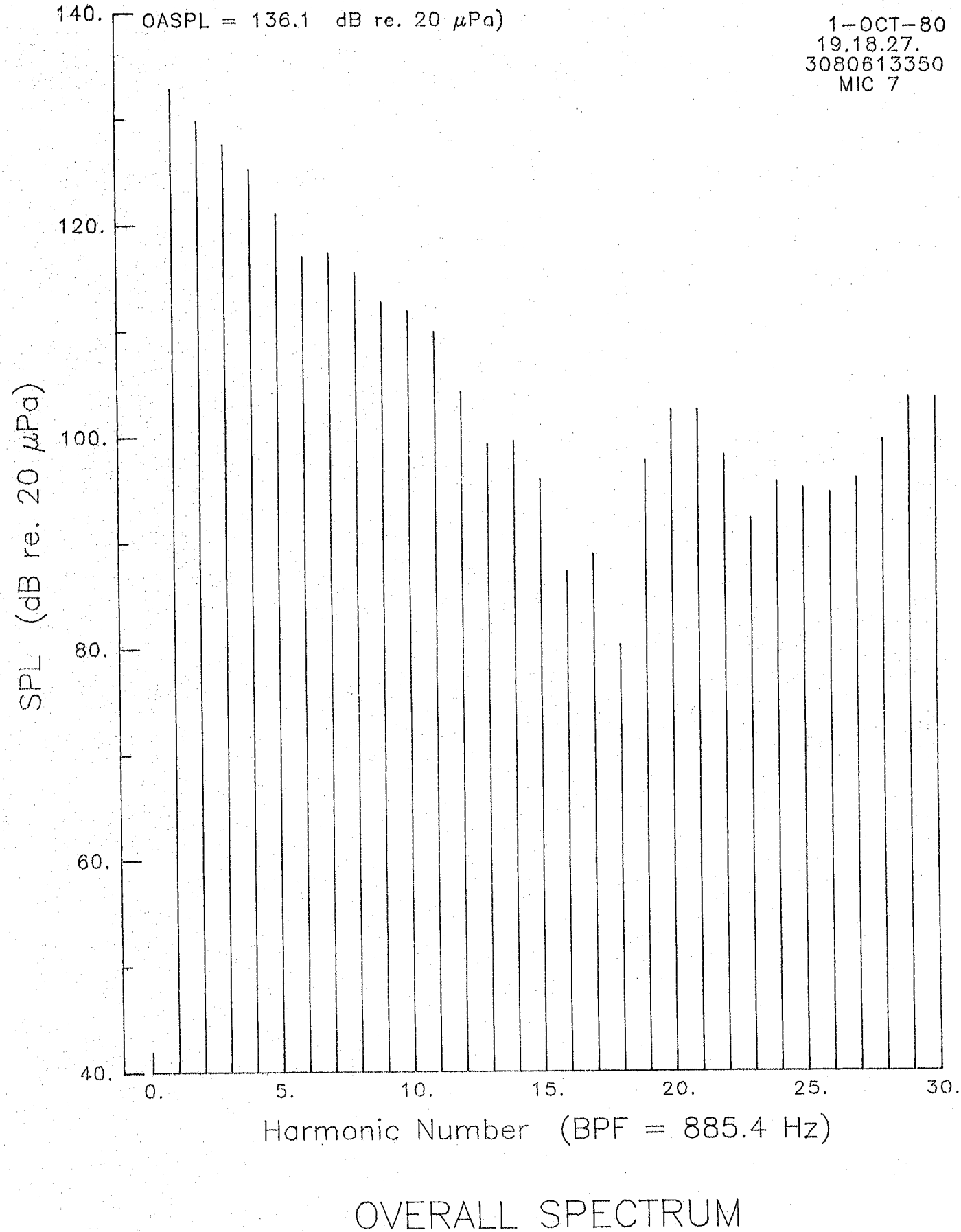

Figure 14(d).- Continued.

F. Farassat -- P. Nystrom
JIAFS -- NASA/LaRC -- GWU

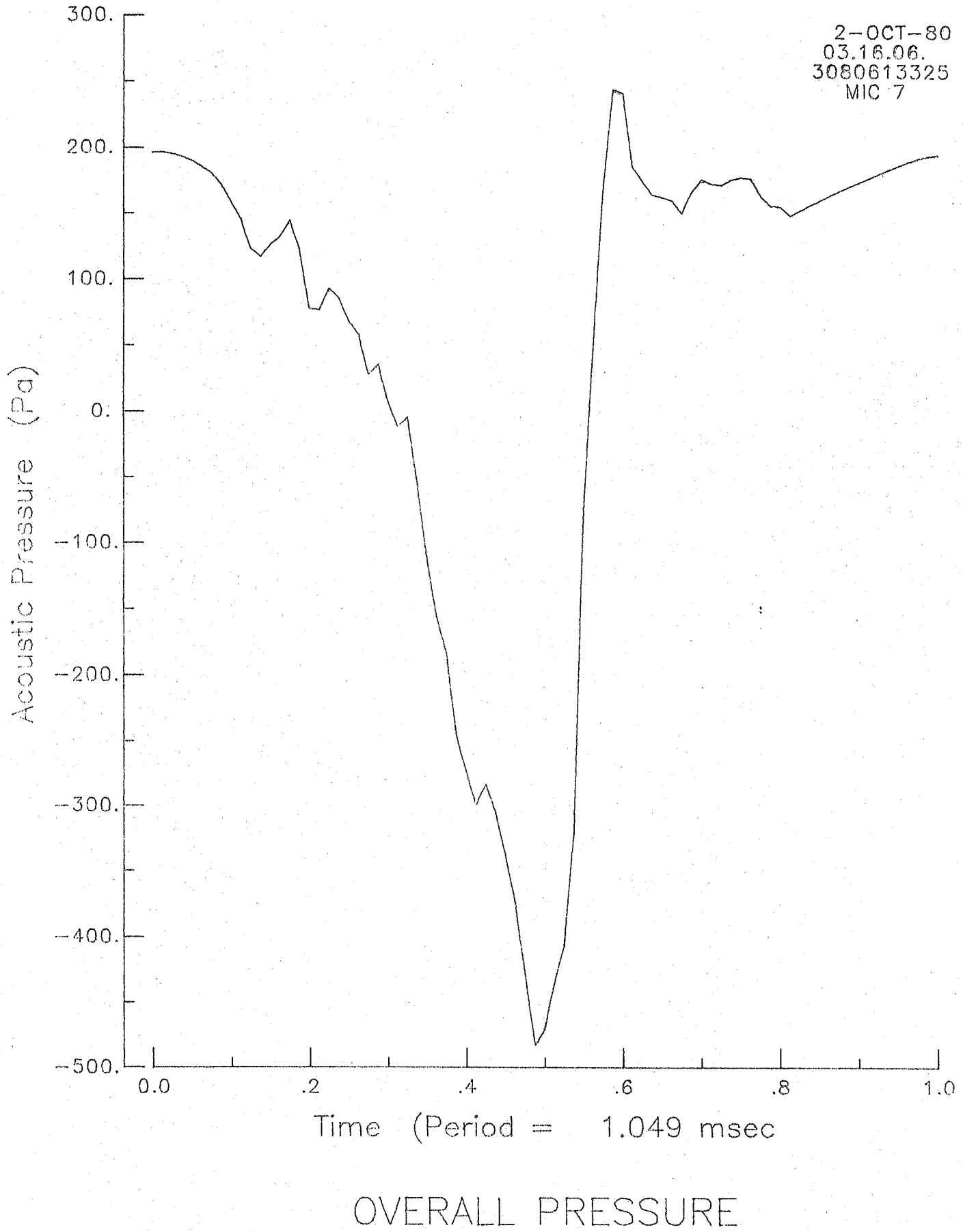

Figure 14(d).- Continued.

F. Farassat -- P. Nystrom
JIAFS -- NASA/LaRC -- GWU

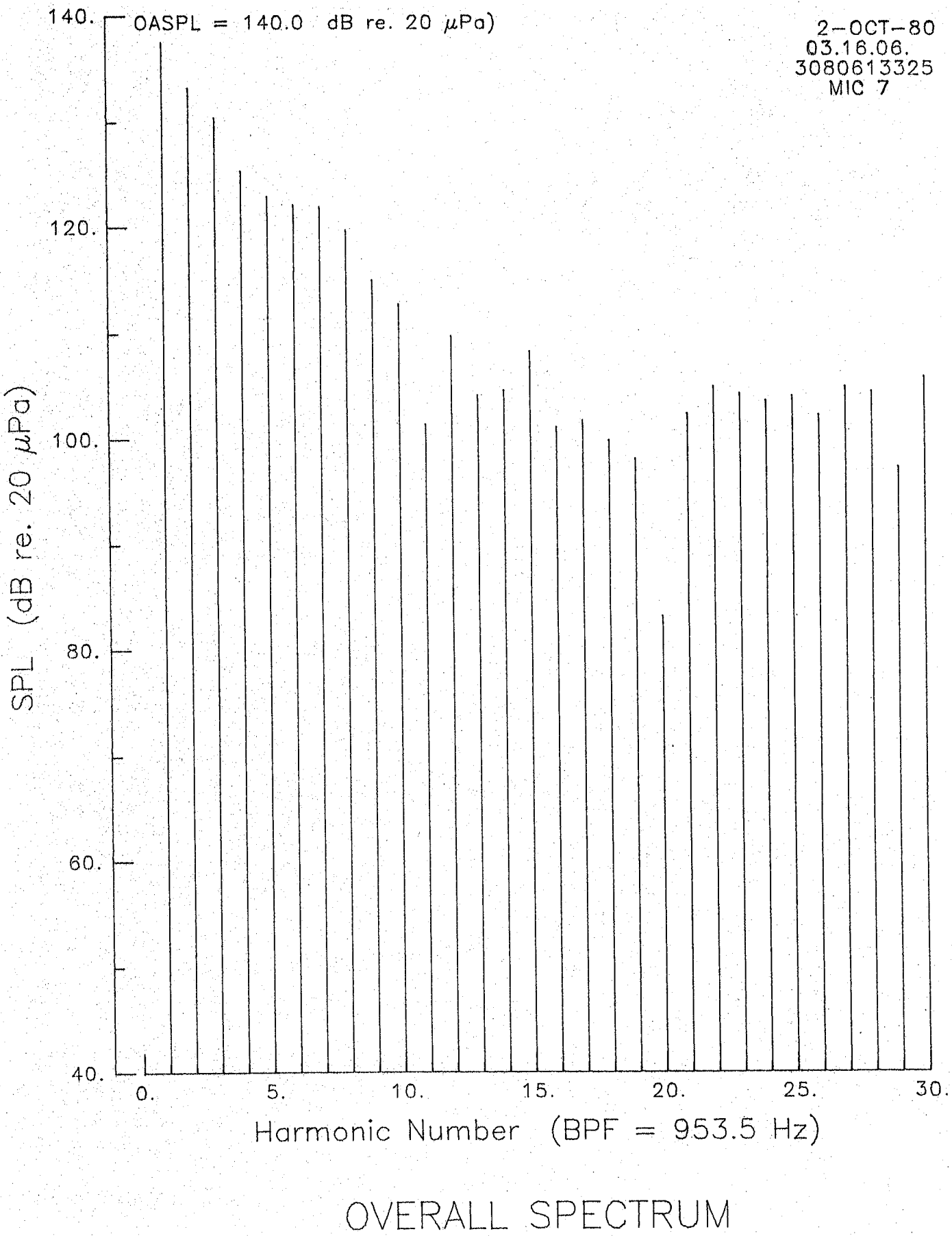

Figure 14(d).- Continued.

F. Farassat -- P. Nystrom
JIAFS -- NASA/LaRC -- GWU

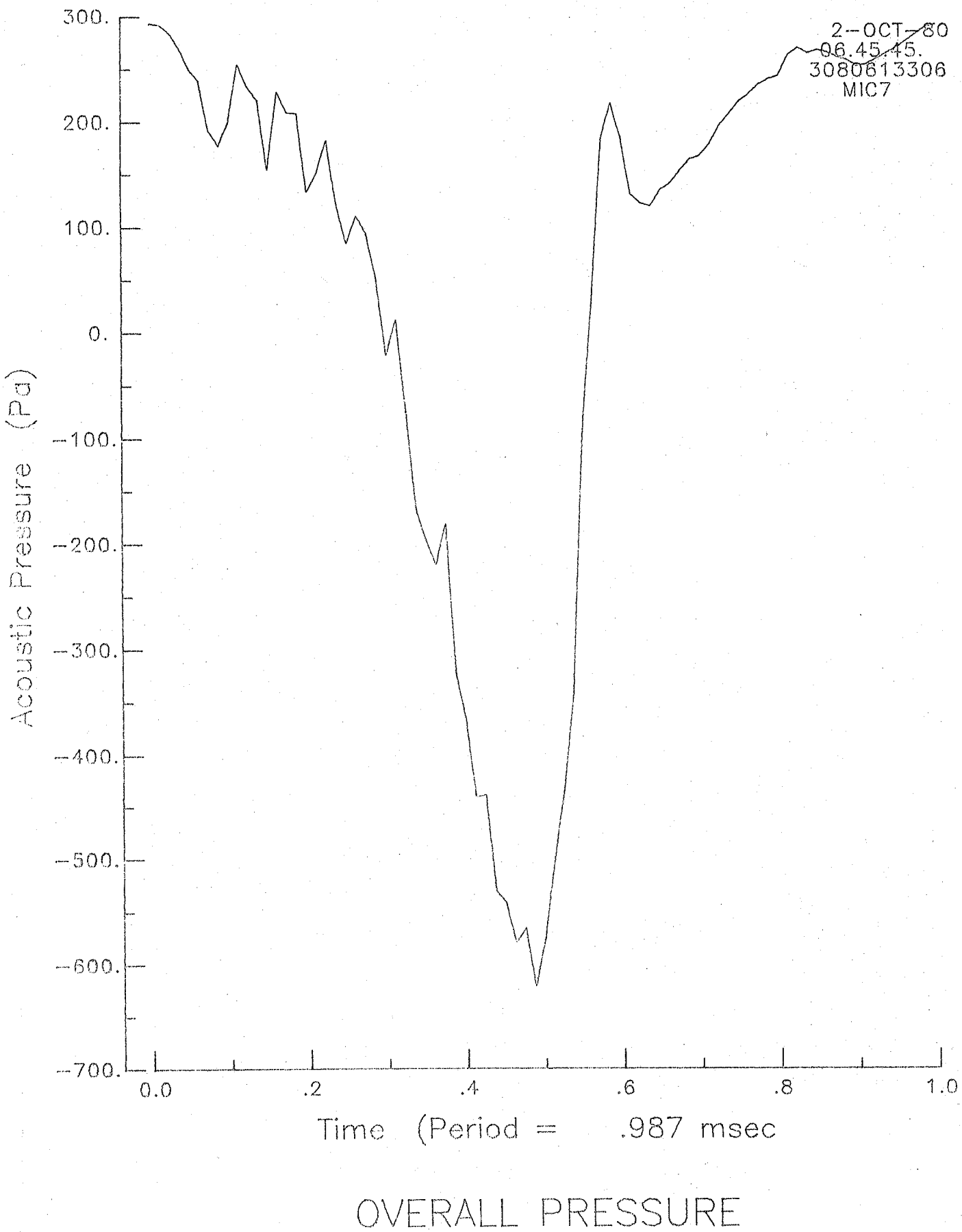

Figure 14(d).- Continued.

F. Farassat -- P. Nystrom
JIAFS -- NASA/LaRC -- GWU

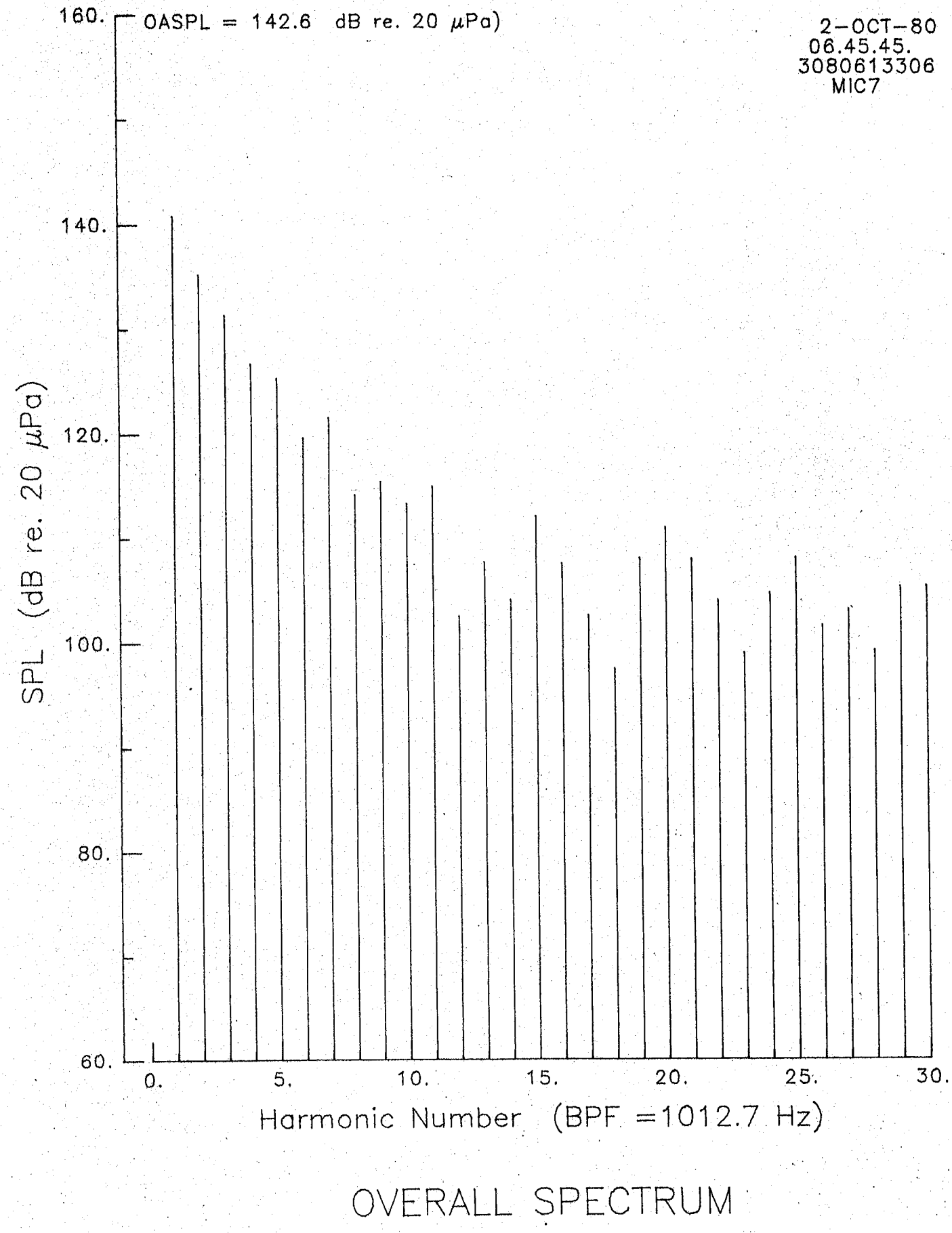

Figure 14(d).- Continued.

F. Farassat -- P. Nystrom
JIAFS -- NASA/LaRC -- GWU

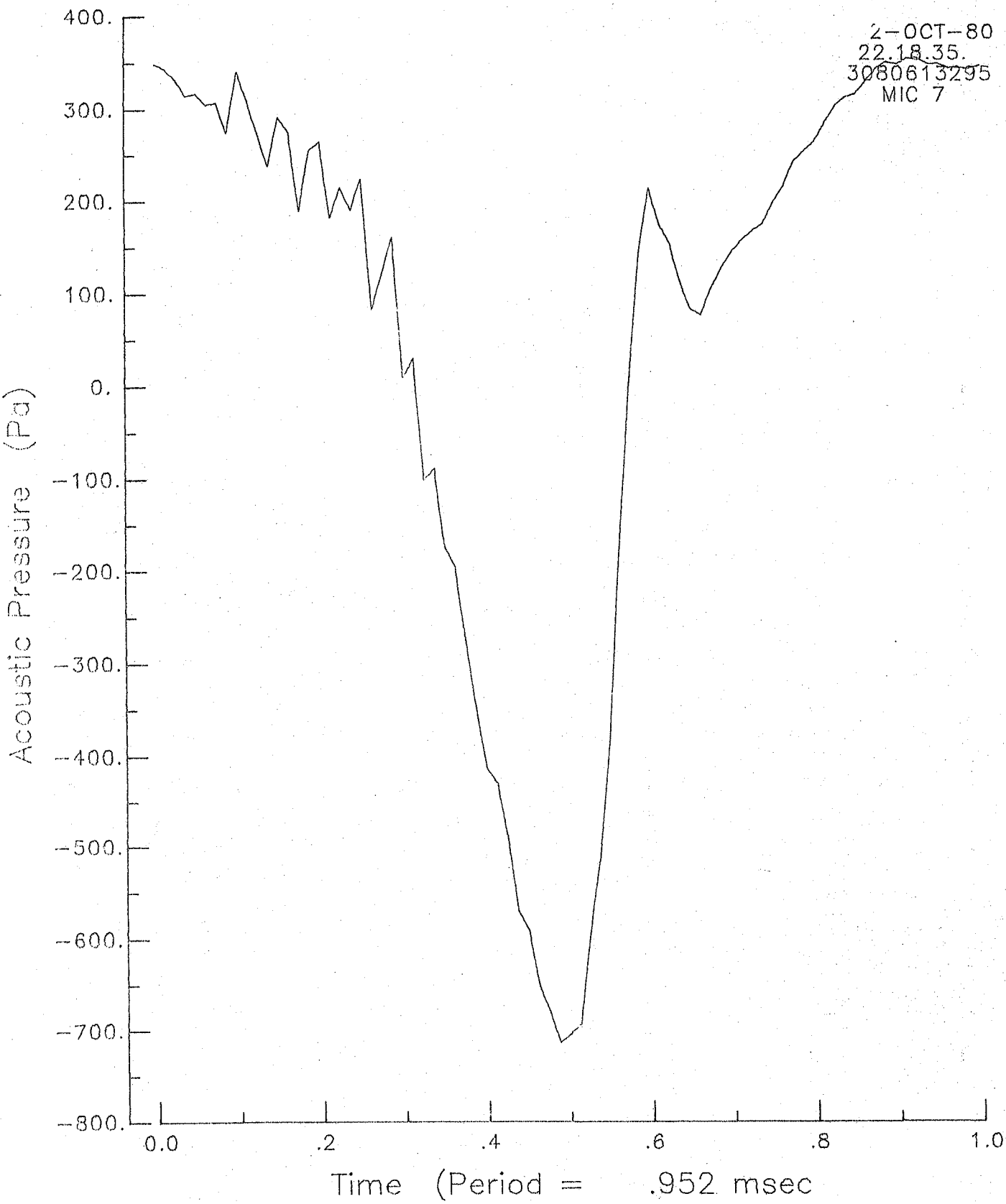

OVERALL PRESSURE

Figure 14(d).- Continued.

F. Farassat -- P. Nystrom
JIAFS -- NASA/LaRC -- GWU

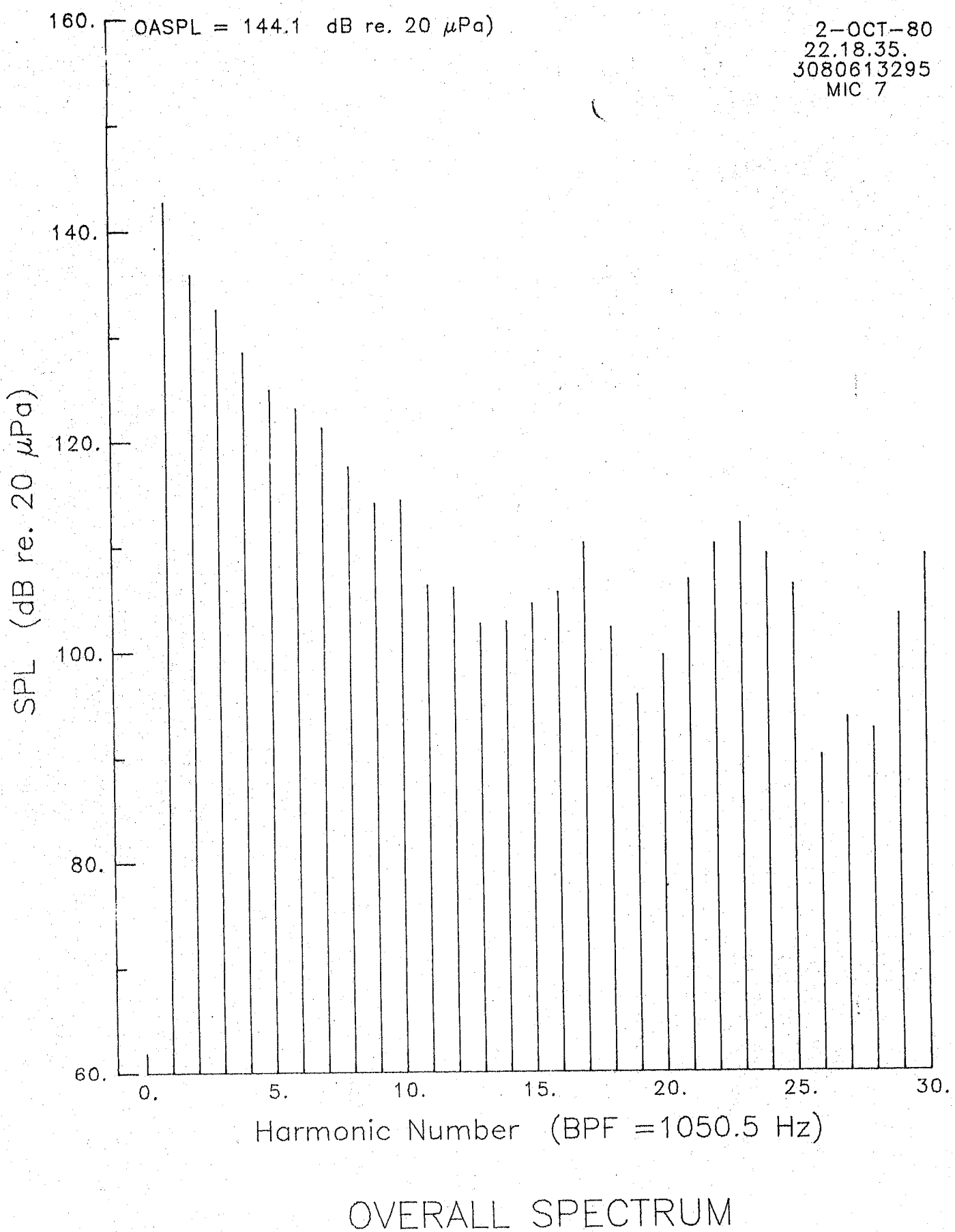

Figure 14(d).- Concluded.

F. Farassat -- P. Nystrom
JIAFS -- NASA/LaRC -- GWU

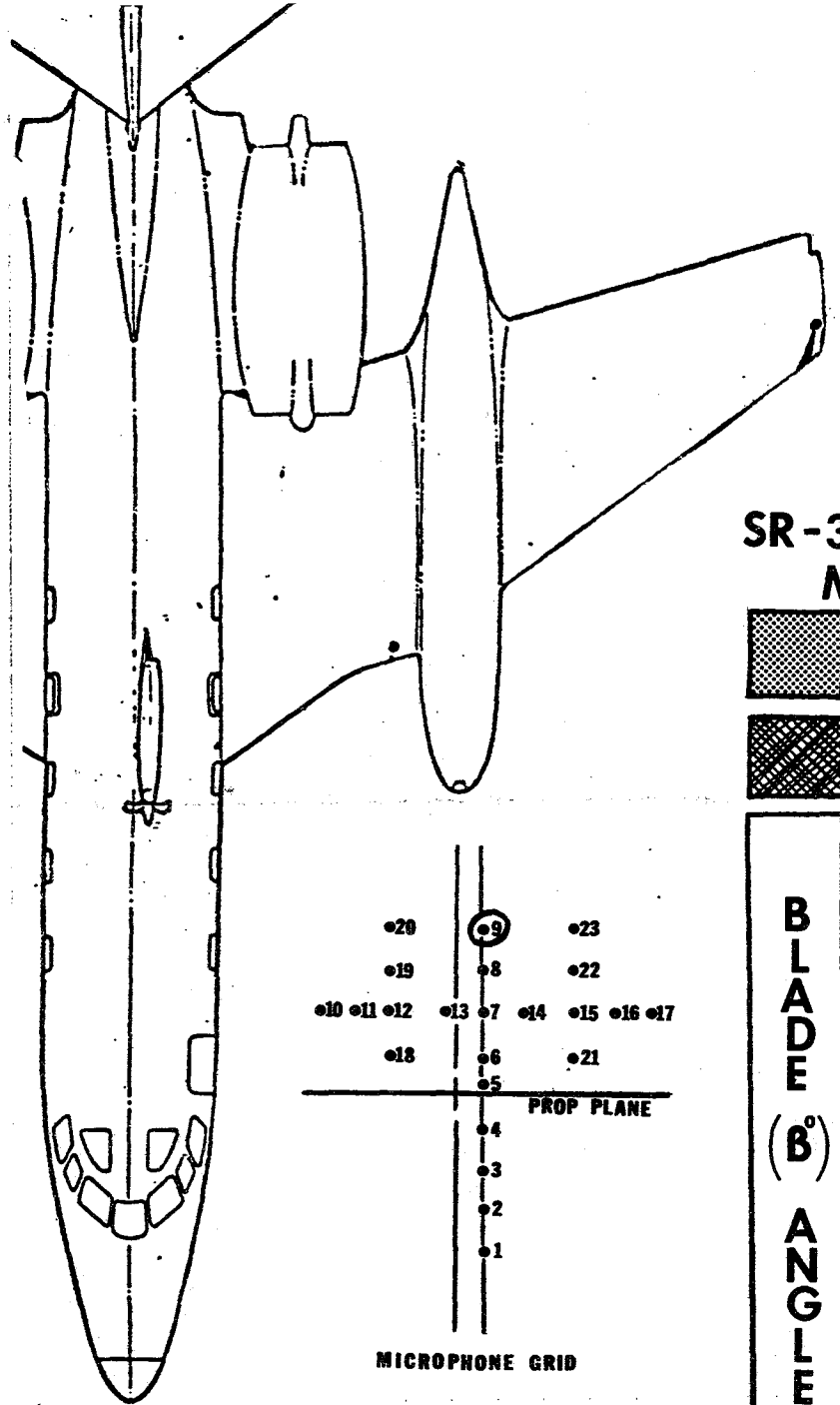

Figure 14(e).- Continued.

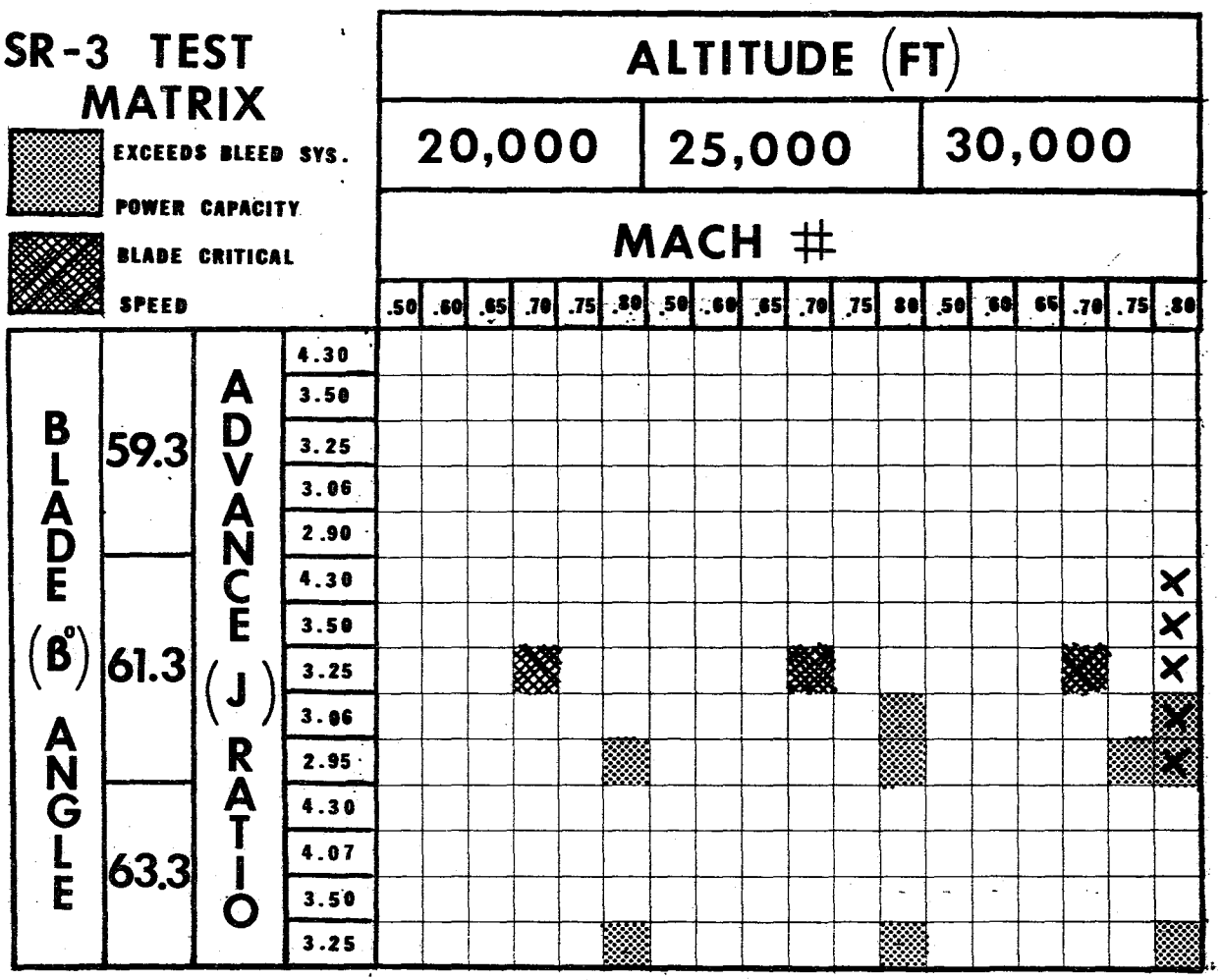

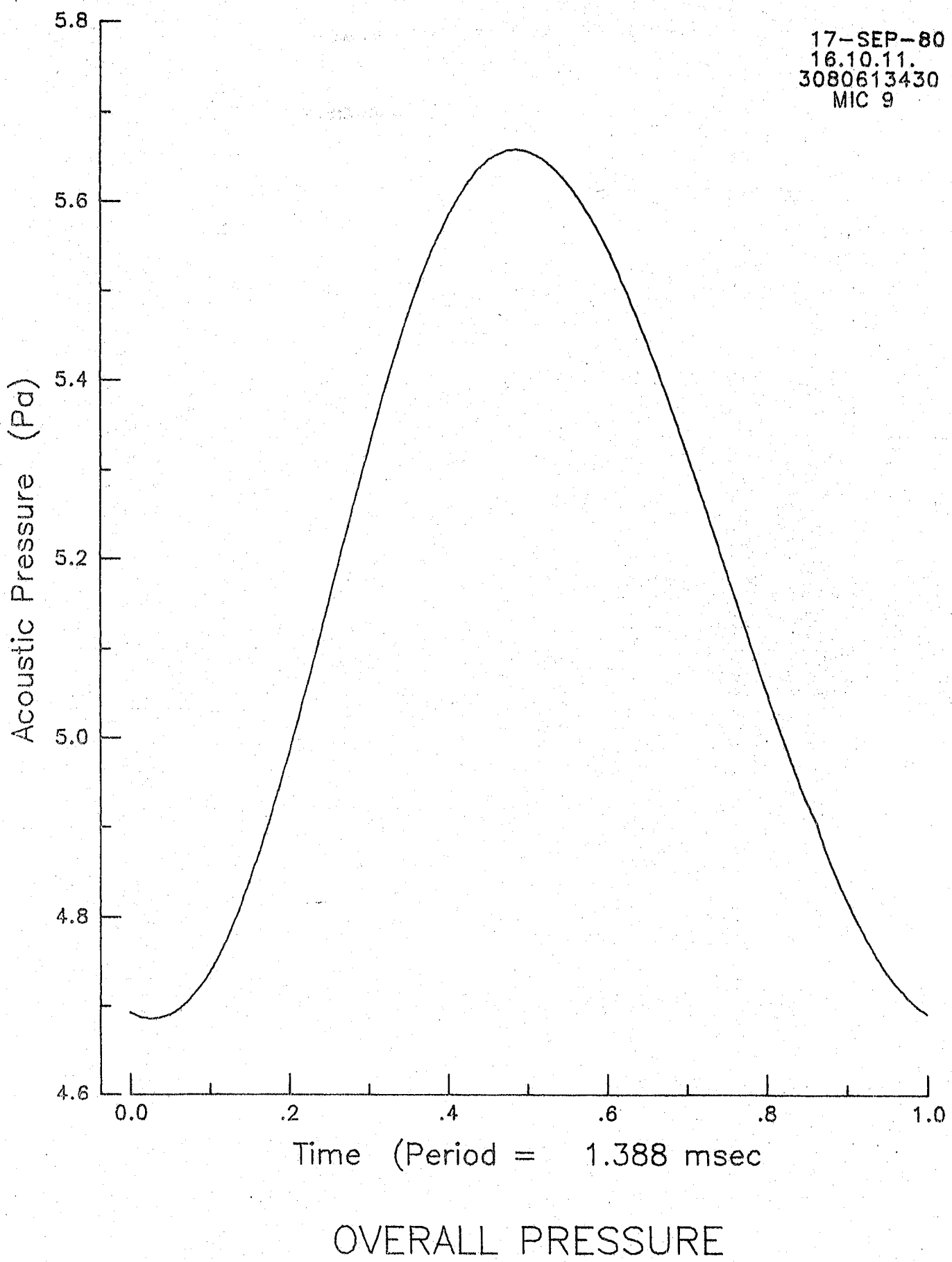

Figure 14(e).- Continued.

F. Farassat -- P. Nystrom
JIAFS -- NASA/LaRC -- GWU

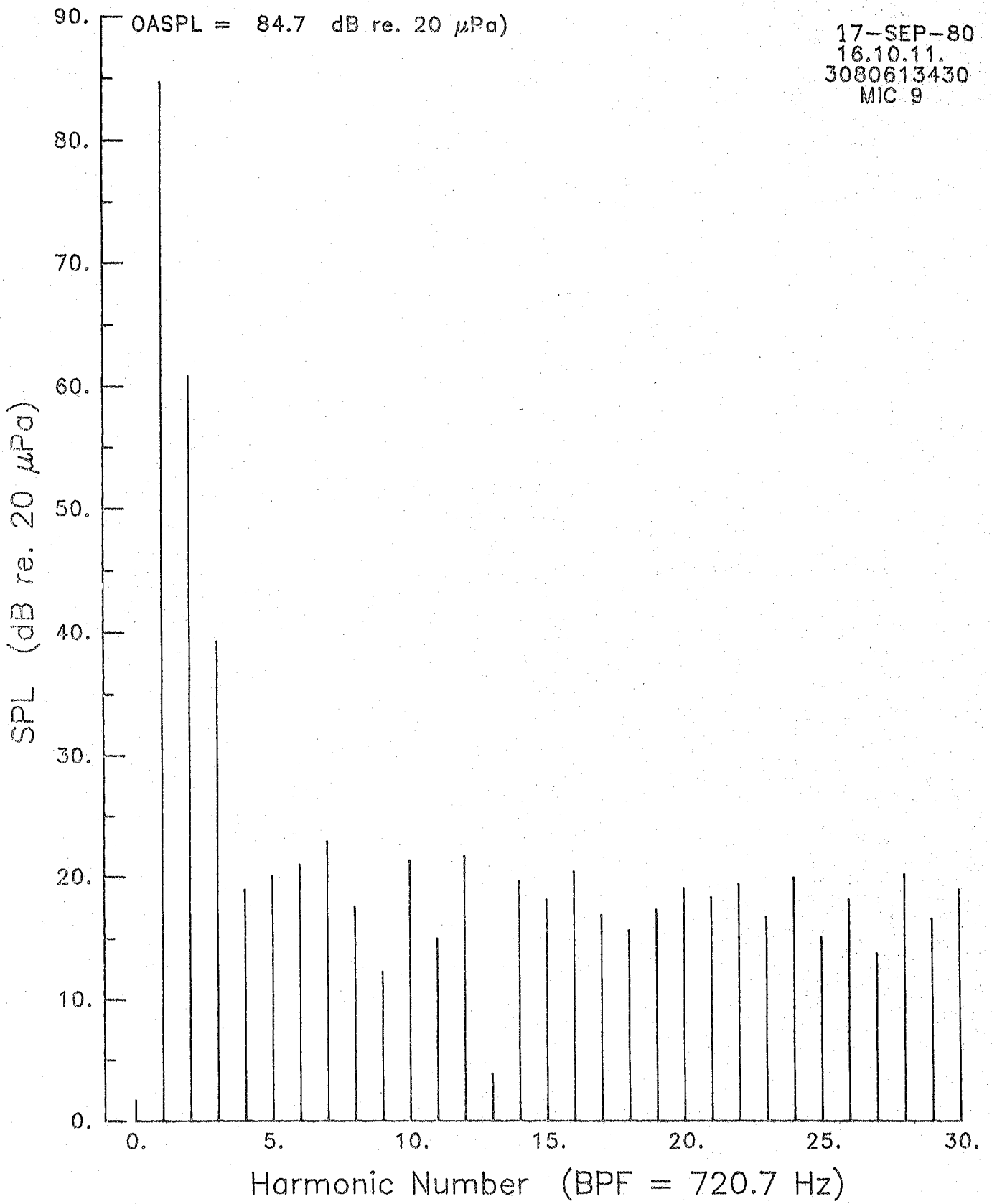

OVERALL SPECTRUM

Figure 14(e).- Continued.

F. Farassat -- P. Nystrom
JIAFS -- NASA/LaRC -- GWU

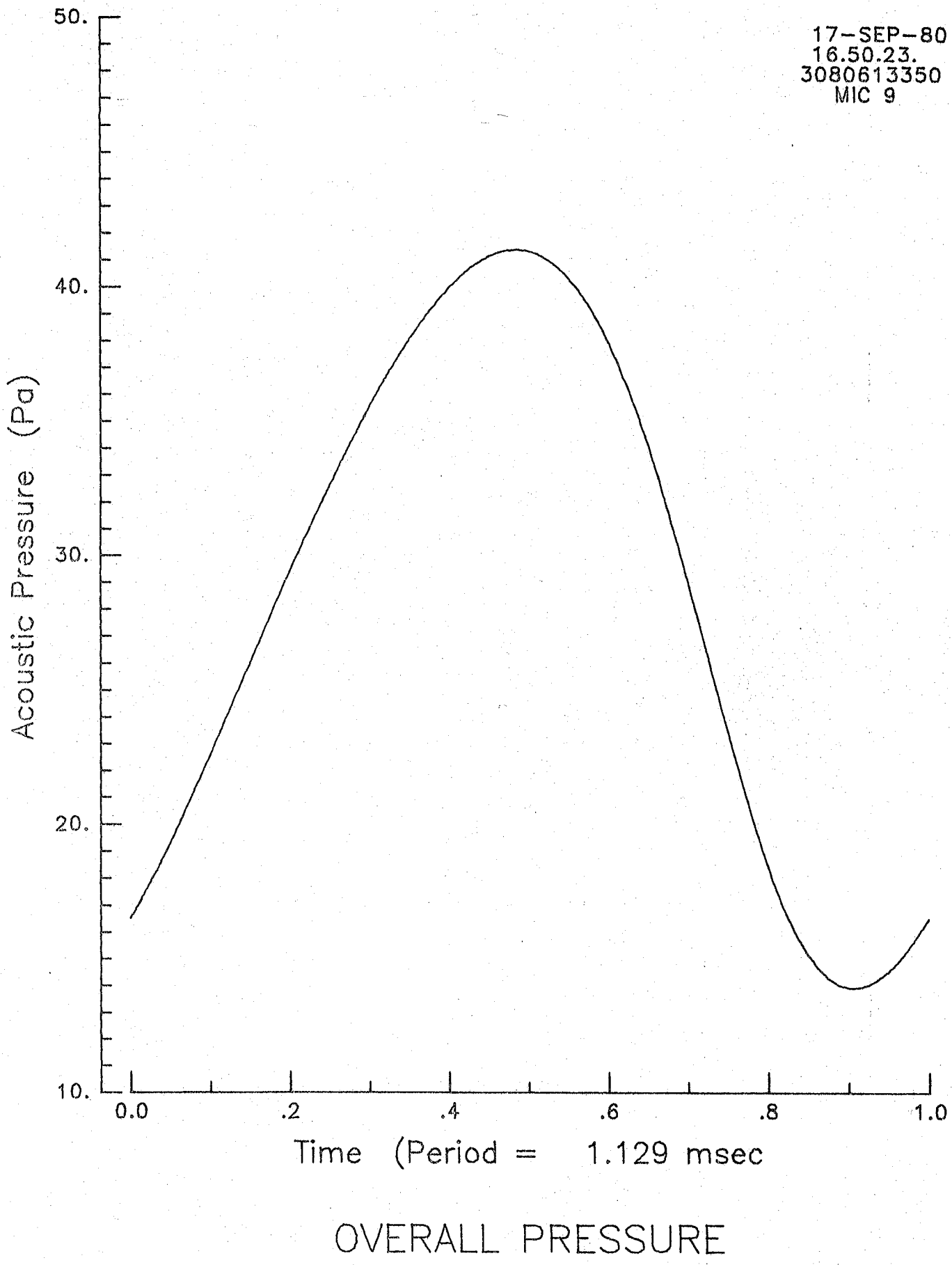

Figure 14(e).- Continued.

F. Farassat -- P. Nystrom
JIAFS -- NASA/LaRC -- GWU

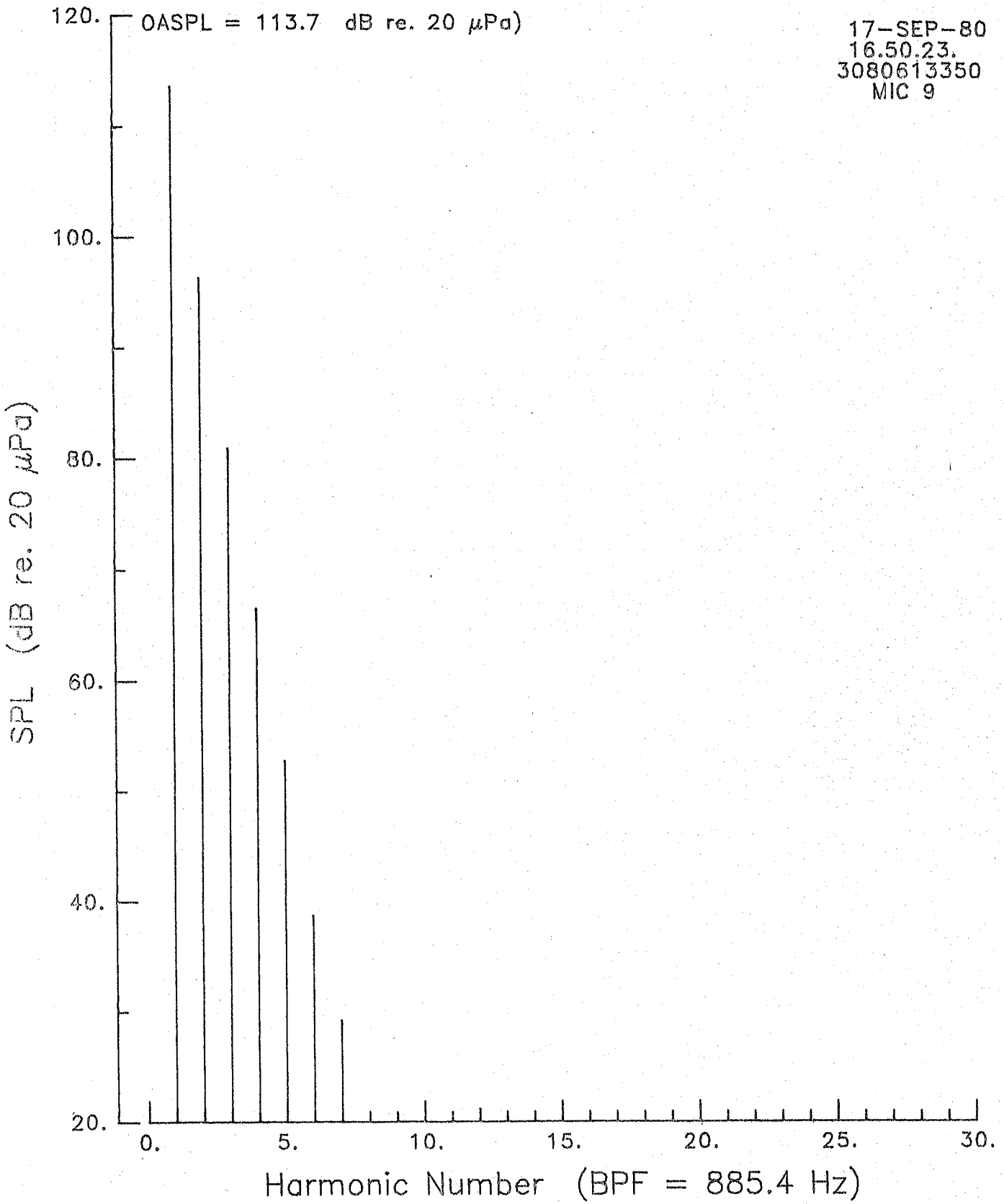

OVERALL SPECTRUM

Figure 14(e).- Continued.

F. Farassat -- P. Nystrom
JIAFS -- NASA/LaRC -- GWU

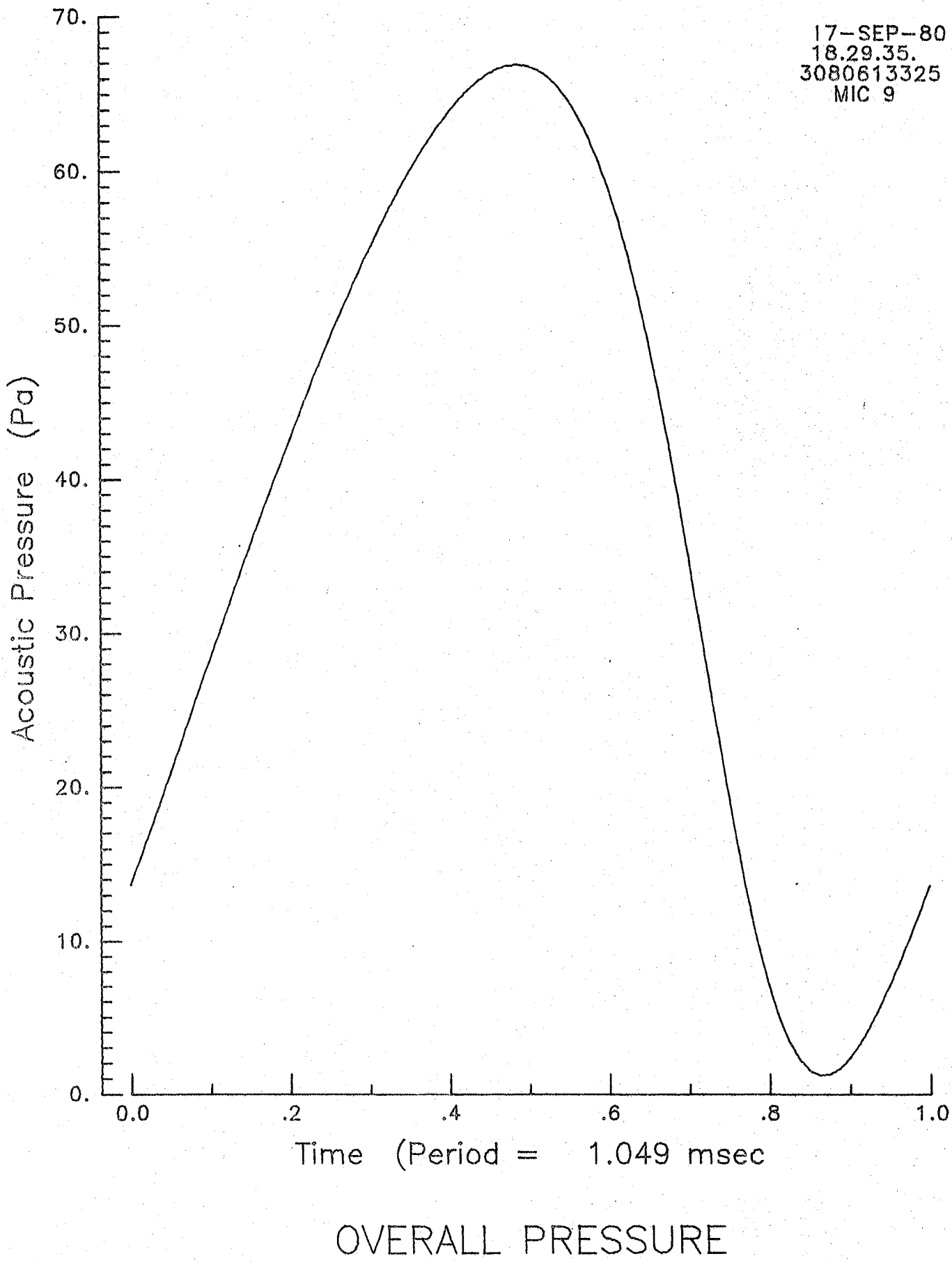

Figure 14(e).- Continued.

F. Farassat -- P. Nystrom
JIAFS -- NASA/LaRC -- GWU

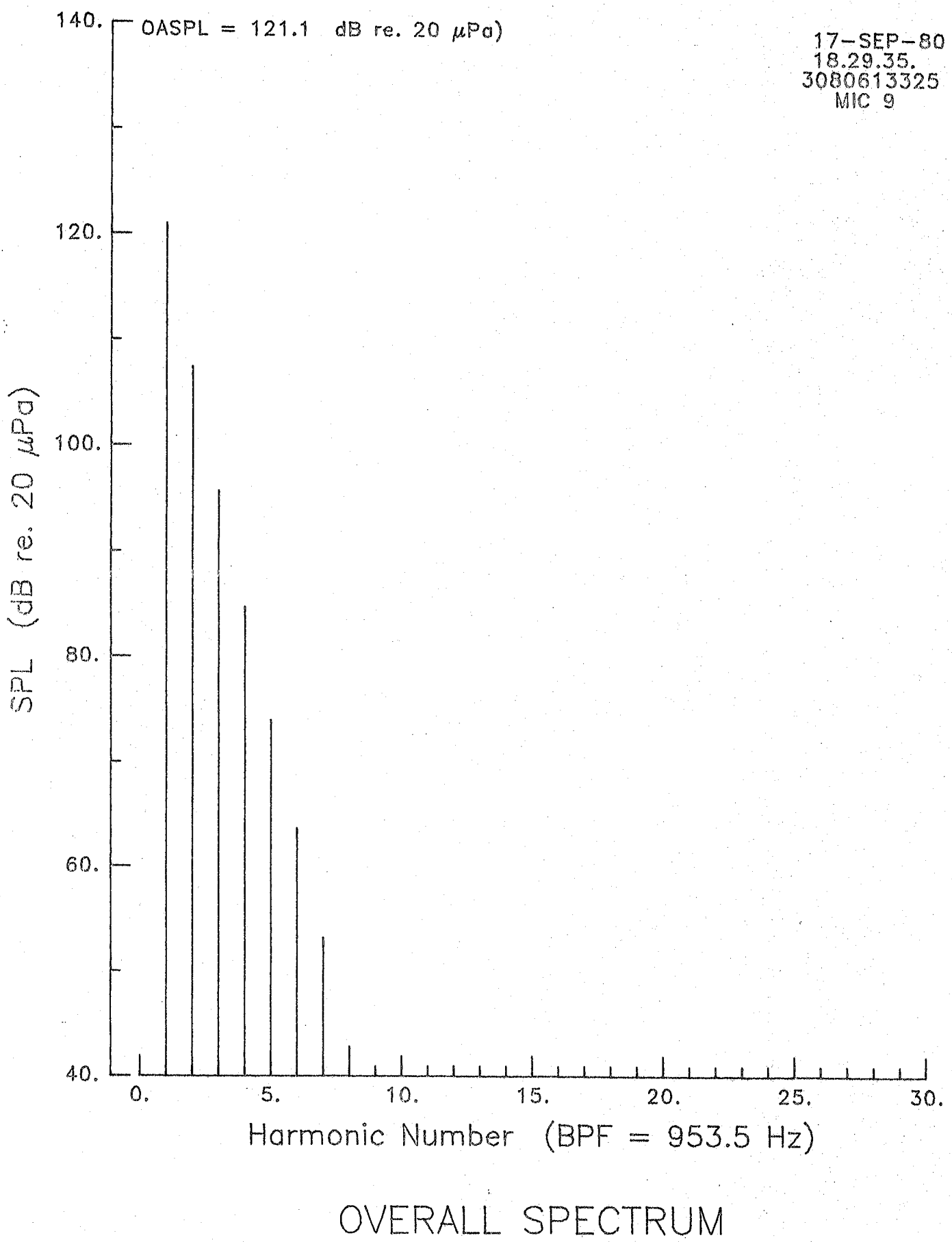

Figure 14(e).- Continued.

F. Farassat -- P. Nystrom
JIAFS -- NASA/LaRC -- GWU

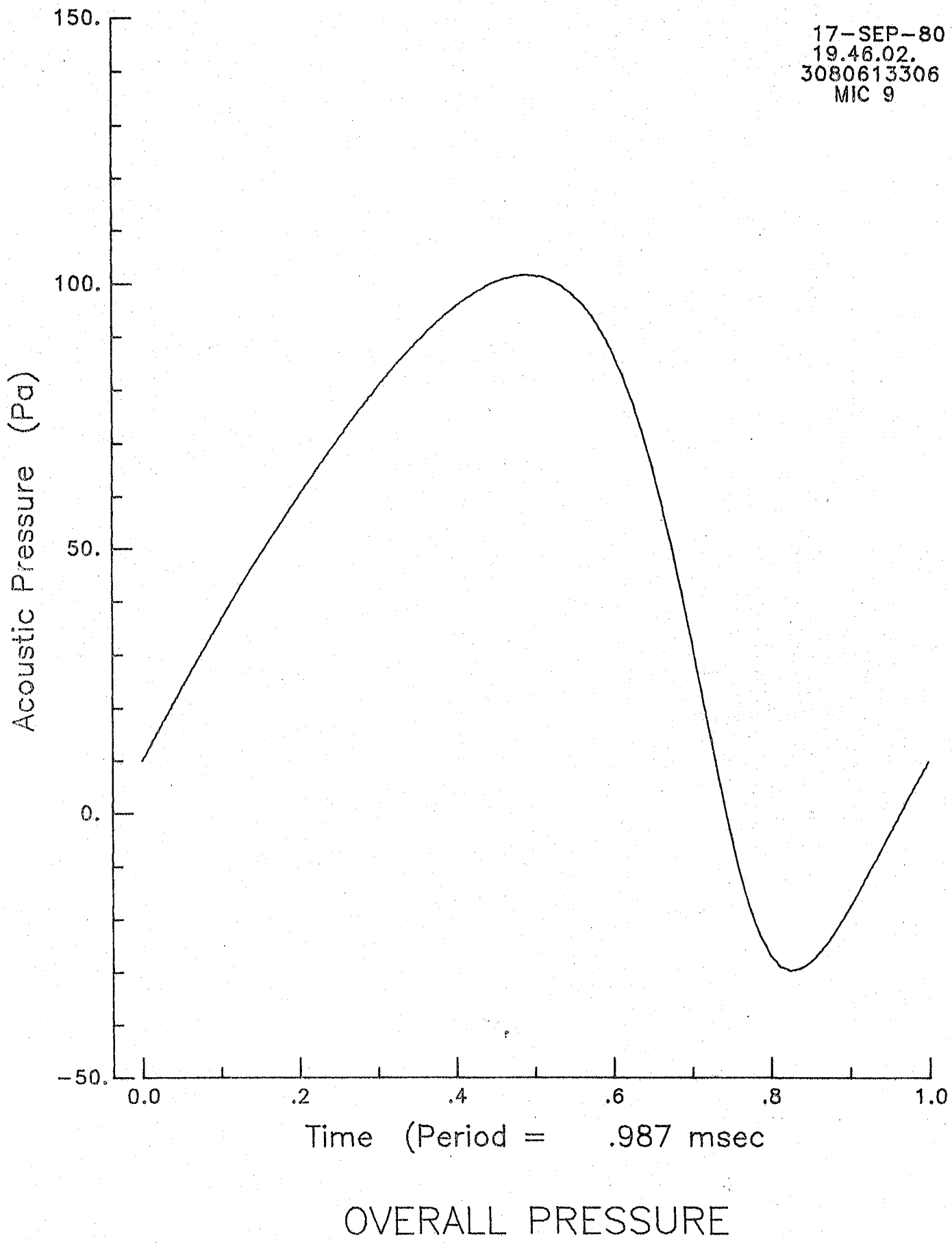

Figure 14(e).- Continued.

F. Farassat -- P. Nystrom
JIAFS -- NASA/LaRC -- GWU

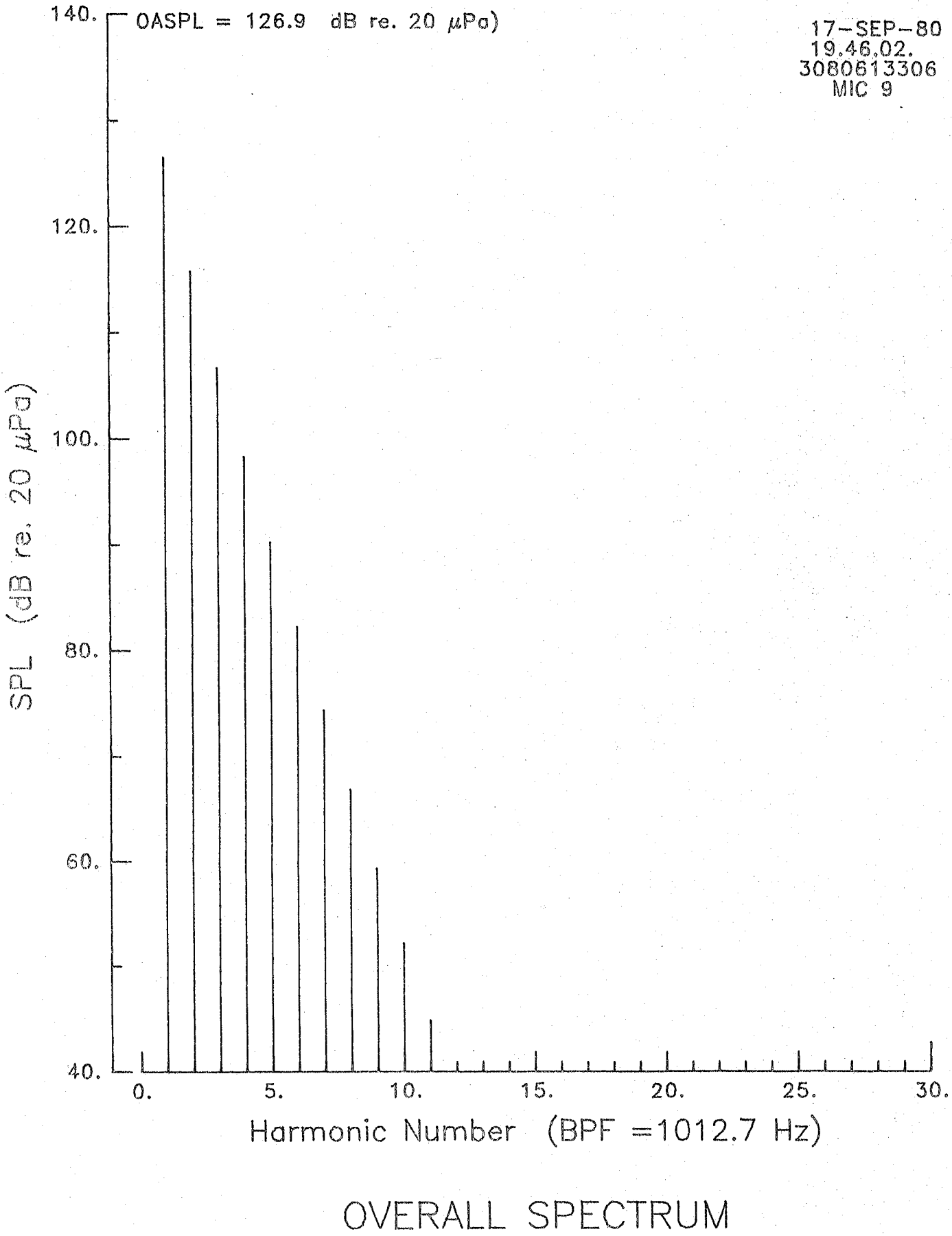

Figure 14(e).- Continued.

F. Farassat -- P. Nystrom
JIAFS -- NASA/LaRC -- GWU

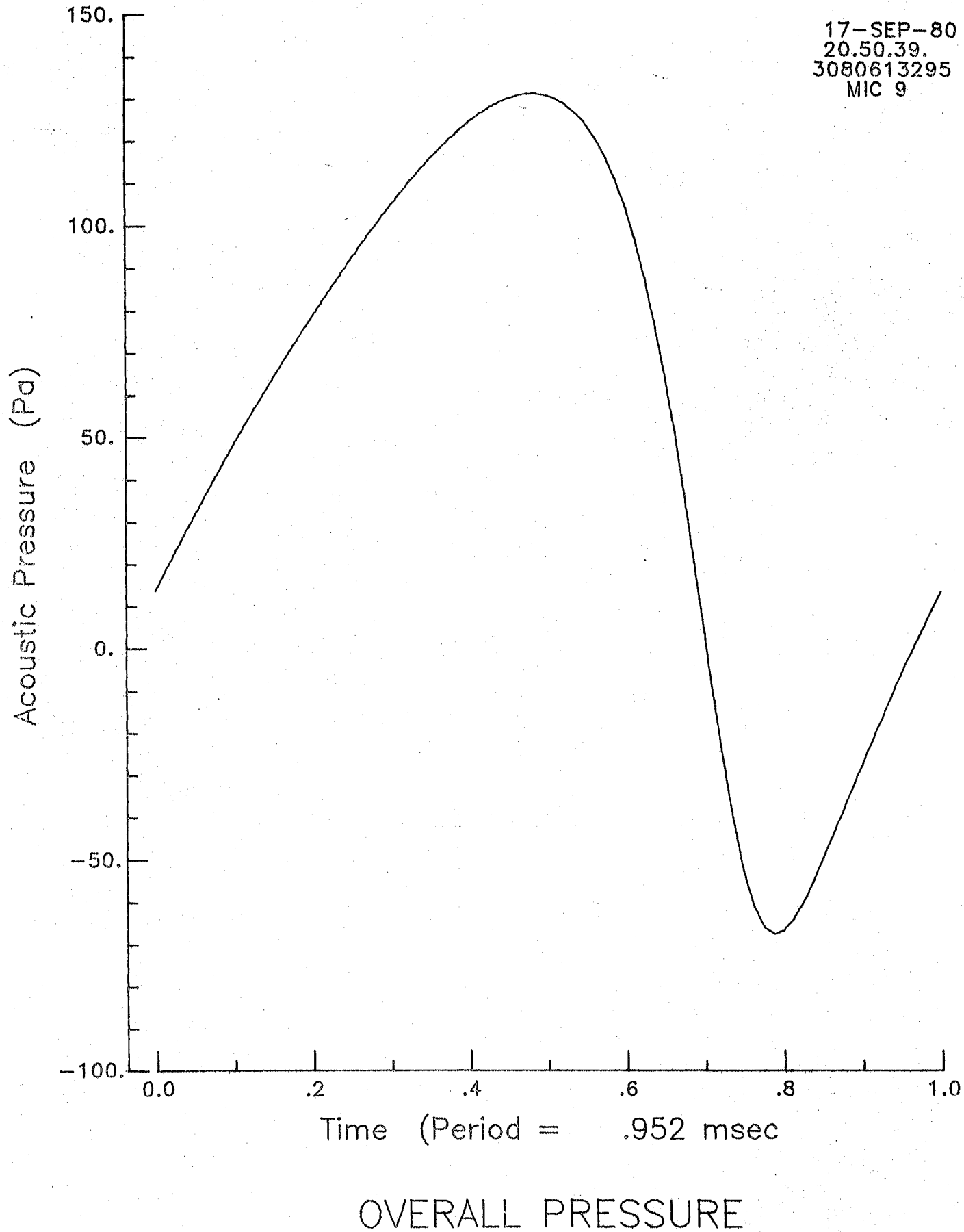

Figure 14(e).- Continued.

F. Farassat -- P. Nystrom
JIAFS -- NASA/LaRC -- GWU

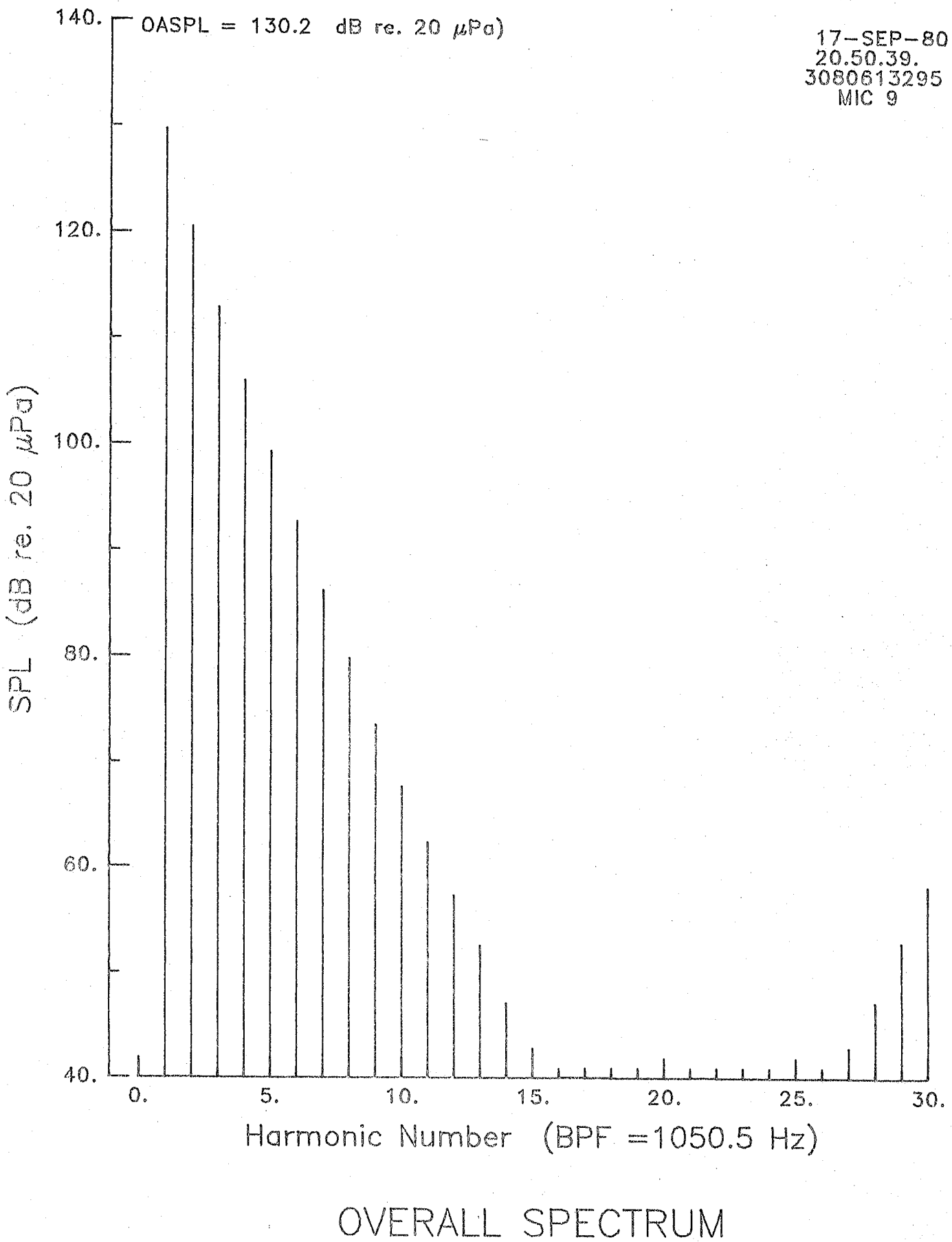

Figure 14(e).- Concluded.

F. Farassat -- P. Nystrom
JIAFS -- NASA/LaRC -- GWU

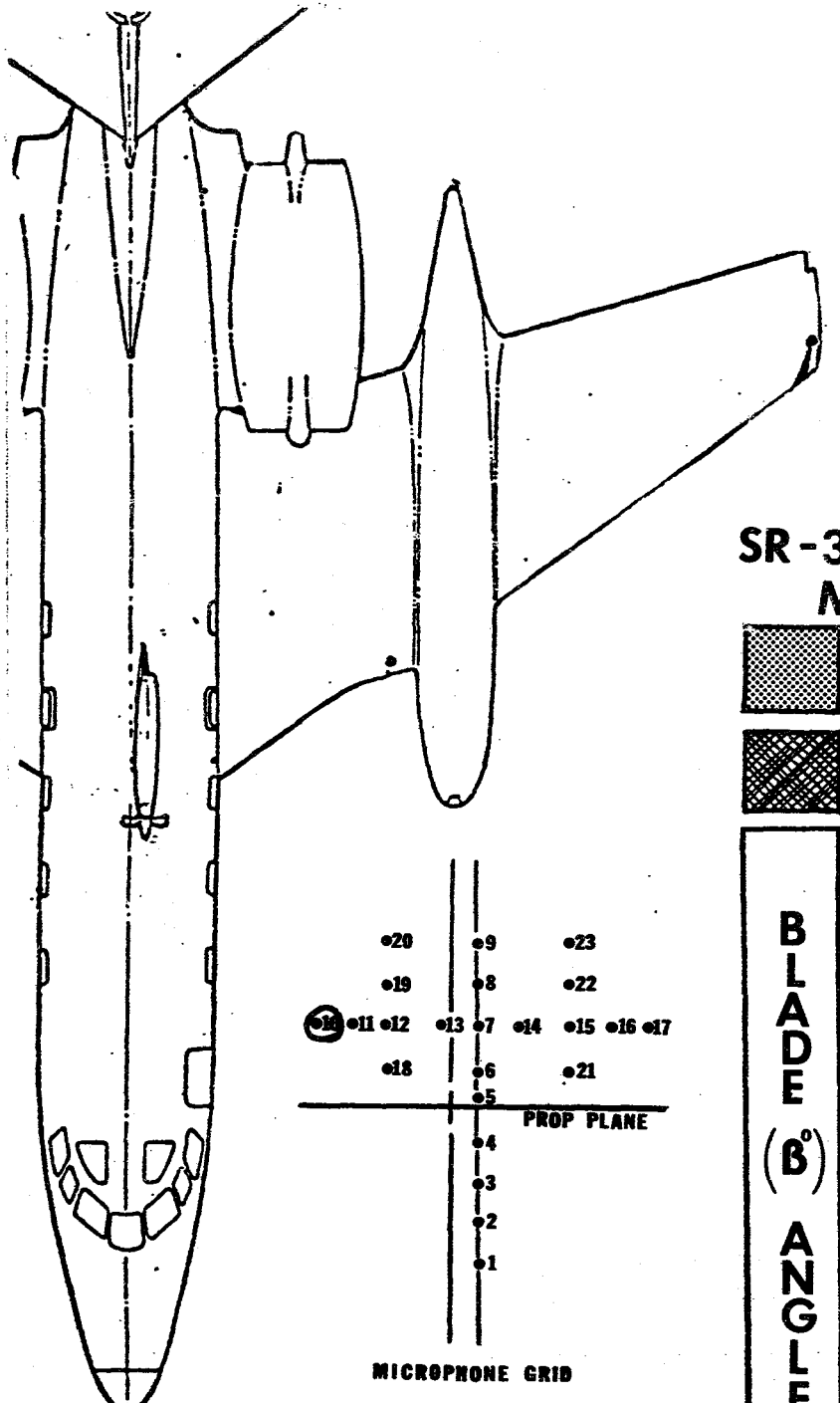

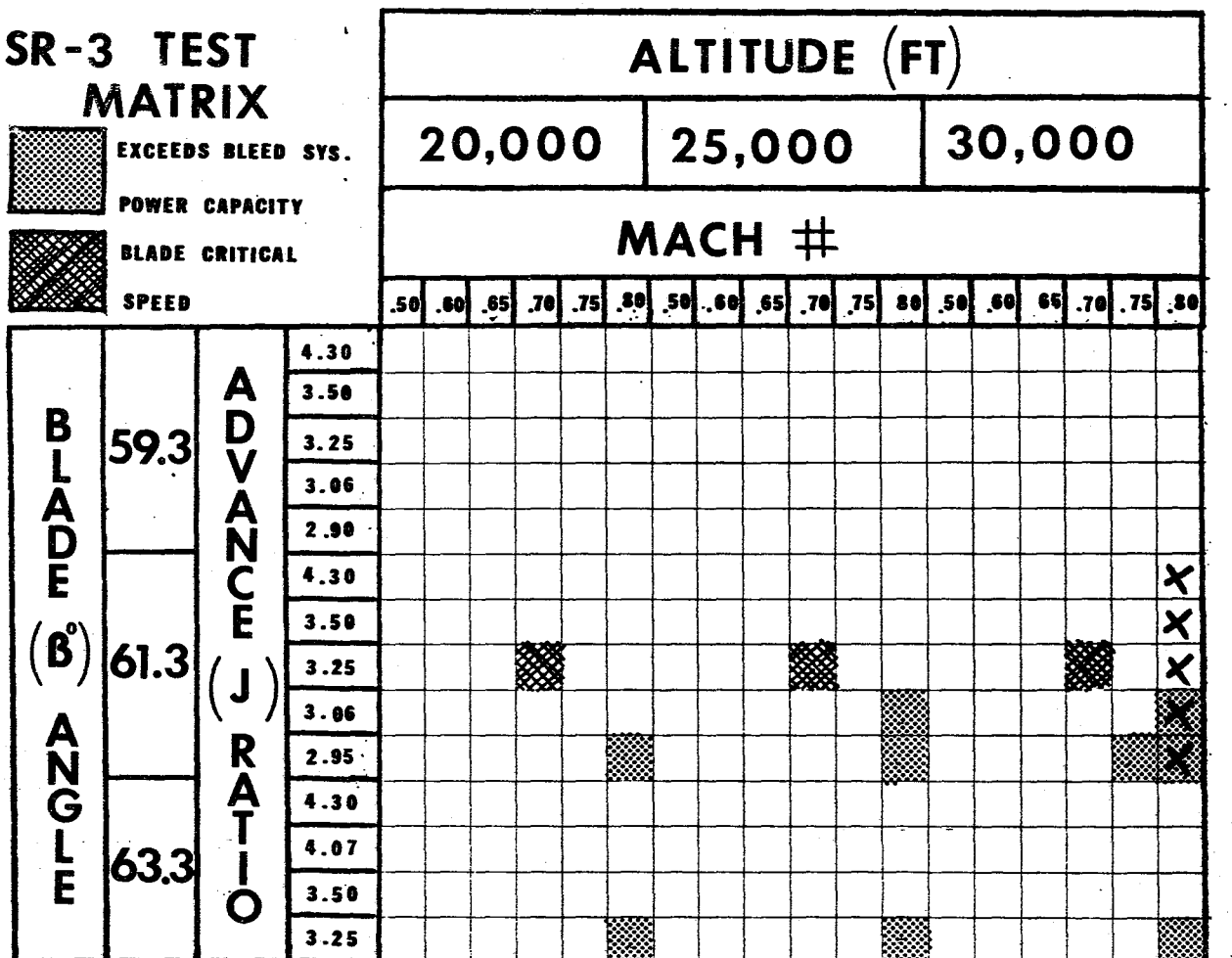

Figure 14(f).- Continued.

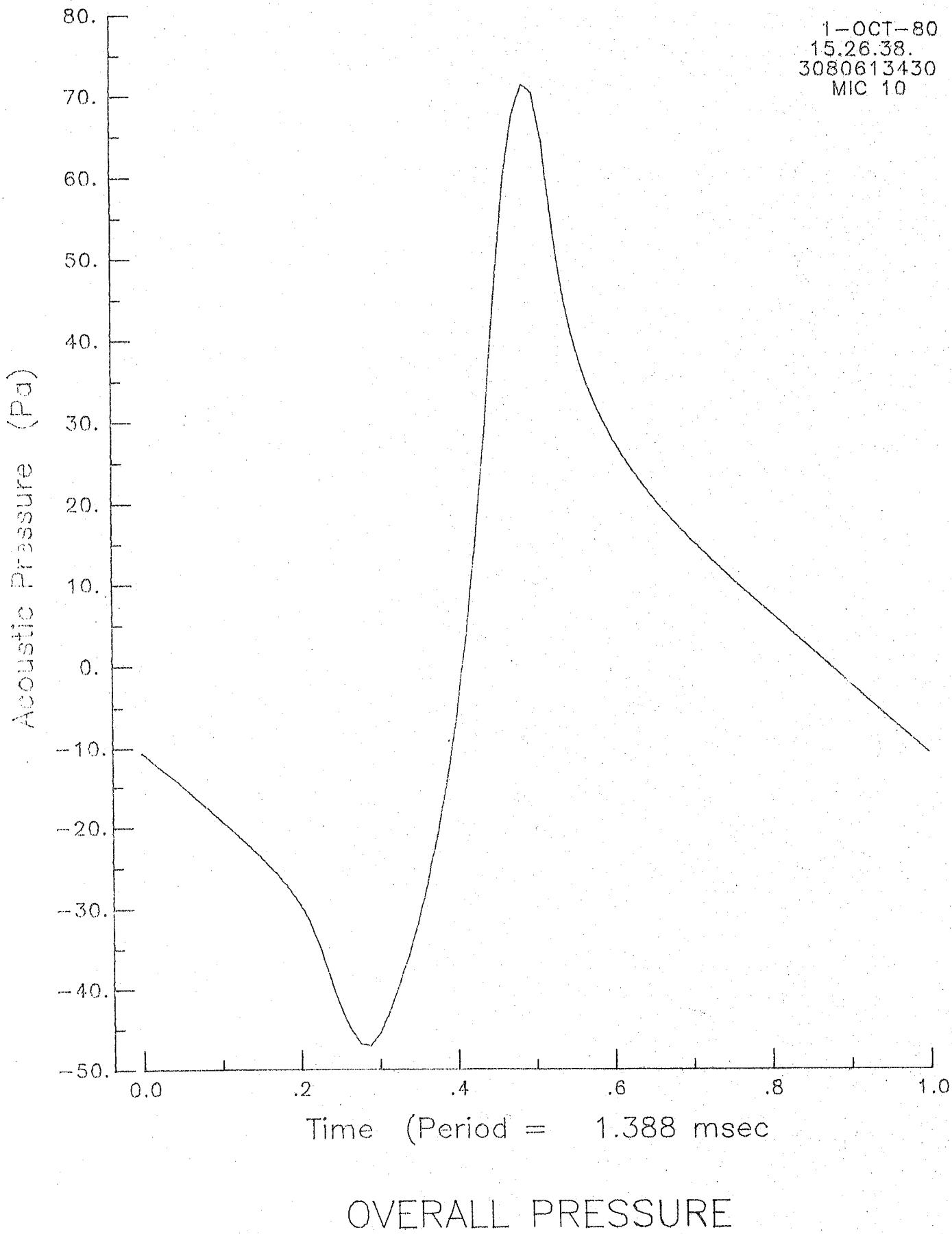

OVERALL PRESSURE

Figure 14(f).- Continued.

F. Farassat -- P. Nystrom
JIAFS -- NASA/LaRC -- GWU

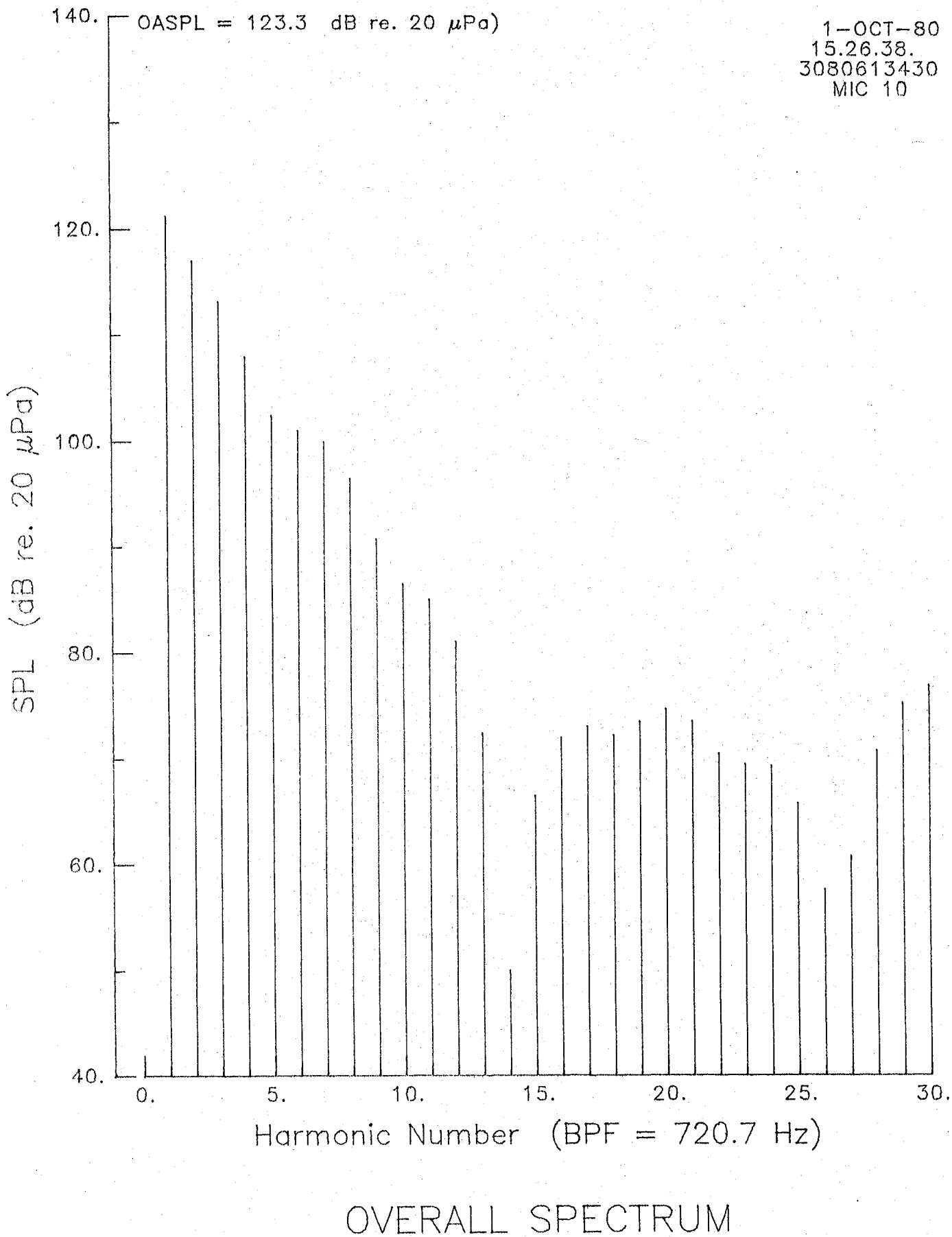

Figure 14(f).- Continued.

F. Farassat -- P. Nystrom
JIAFS -- NASA/LaRC -- GWU

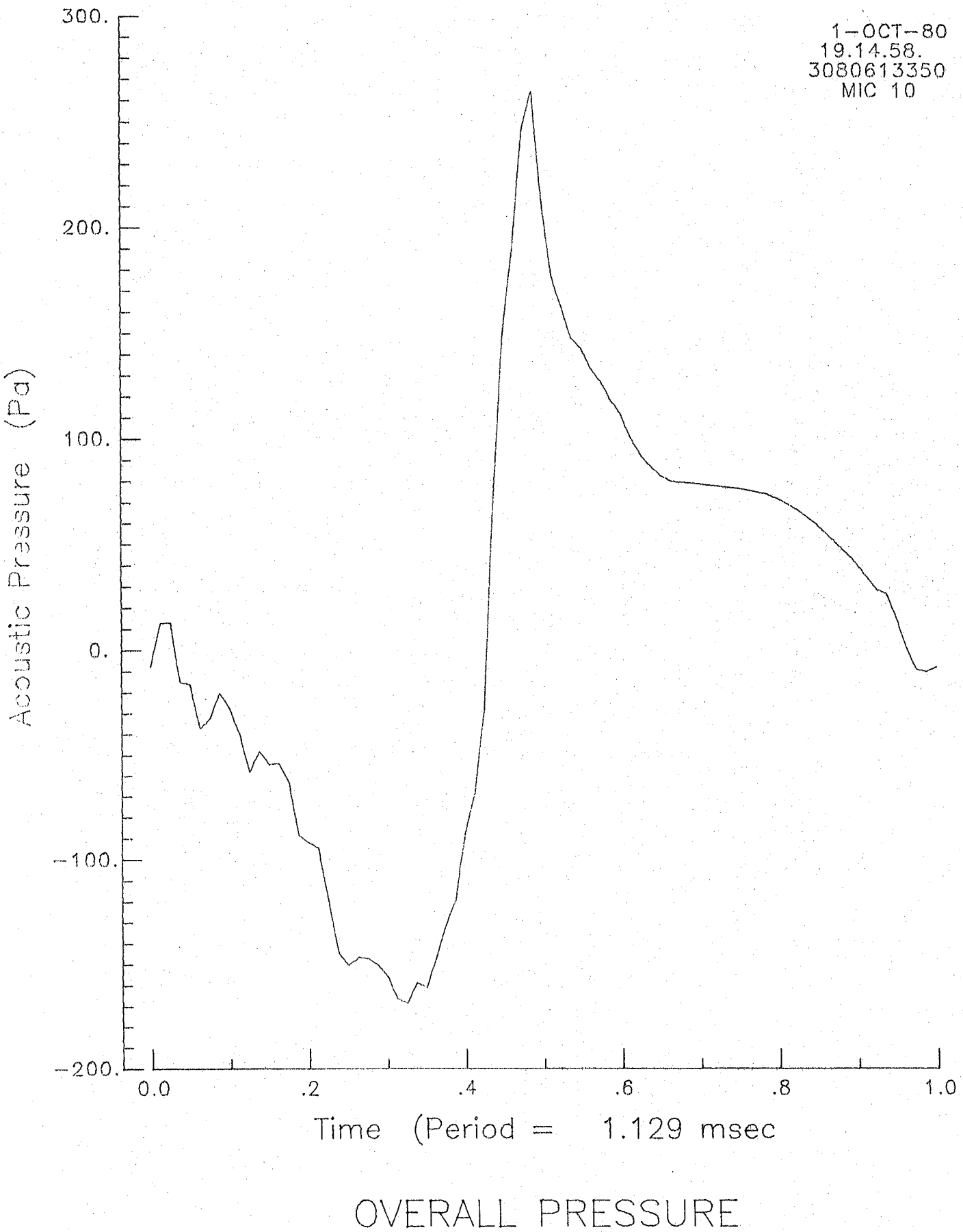

Figure 14(f).- Continued.

F. Farassat -- P. Nystrom
JIAFS -- NASA/LaRC -- GWU

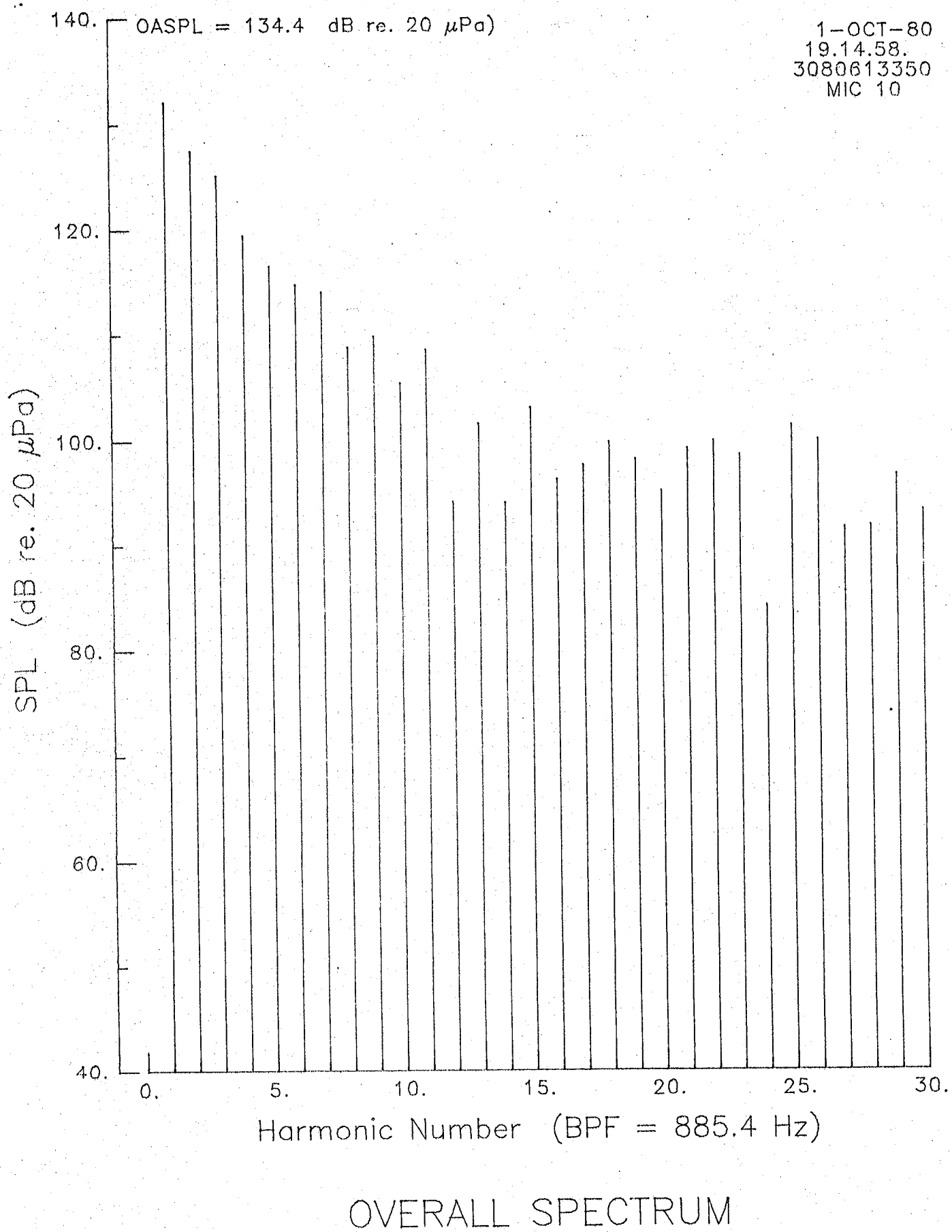

Figure 14(f).- Continued.

F. Farassat -- P. Nystrom
JIAFS -- NASA/LaRC -- GWU

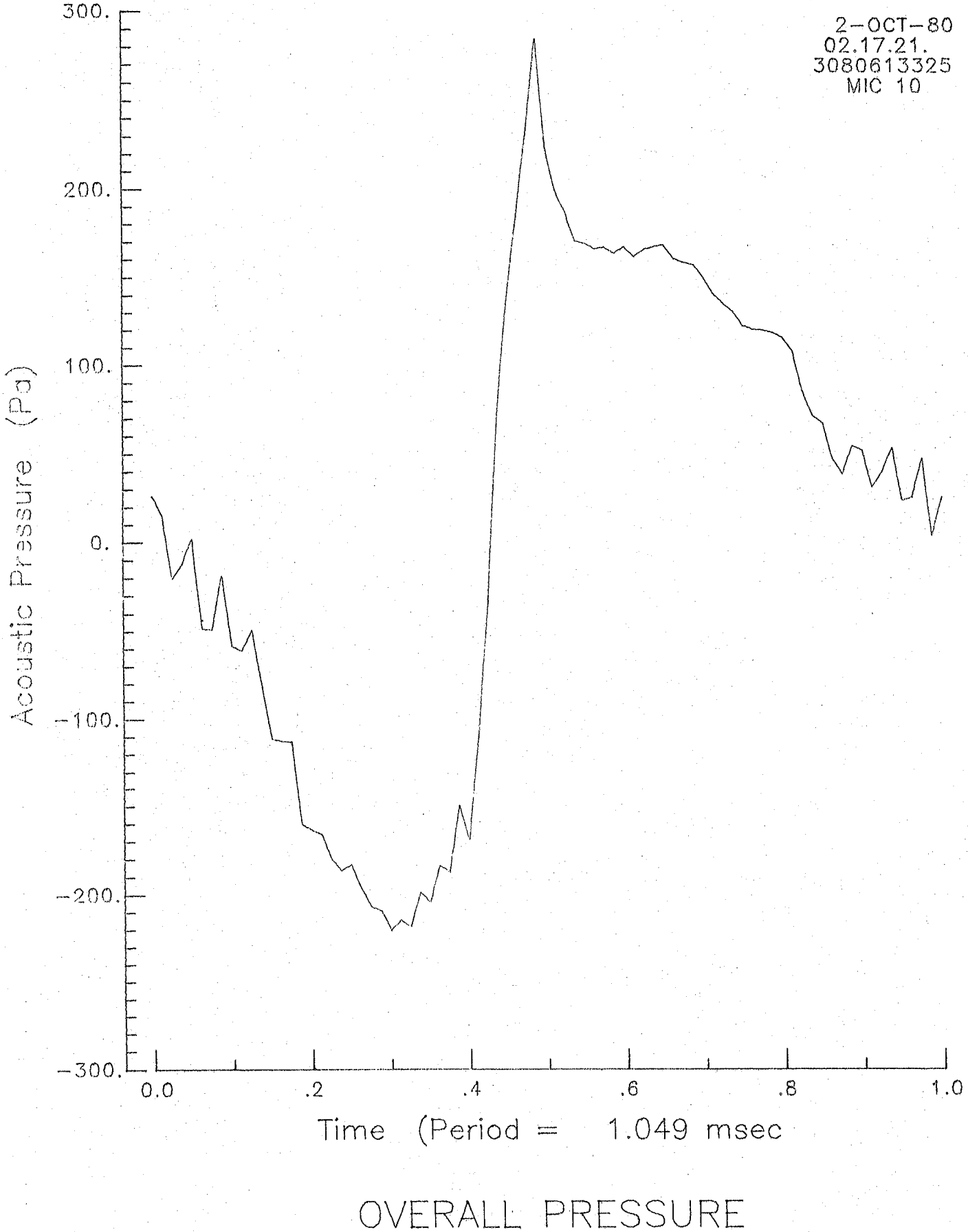

Figure 14(f).- Continued.

F. Farassat -- P. Nystrom
JIAFS -- NASA/LaRC -- GWU

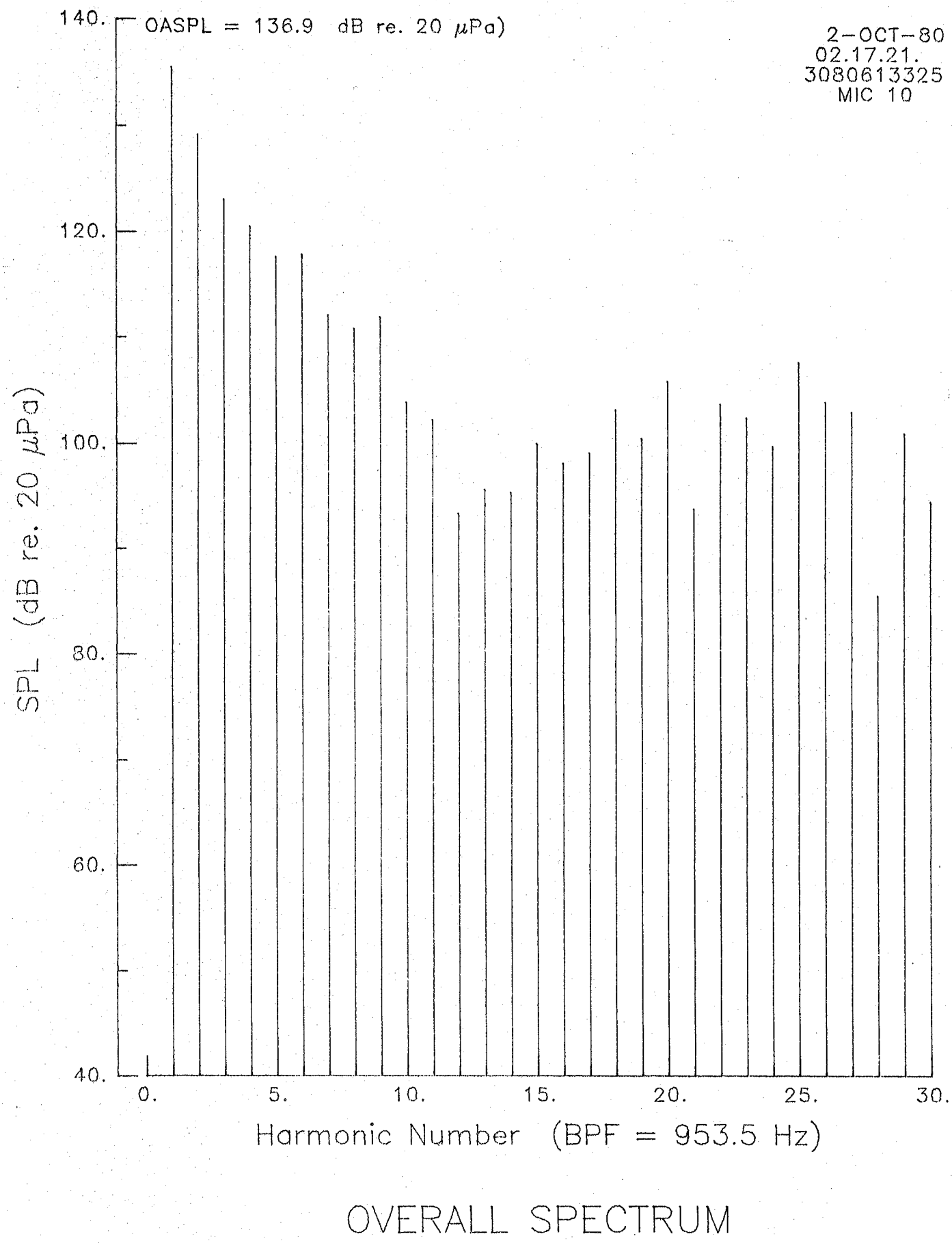

Figure 14(f).- Continued.

F. Farassat -- P. Nystrom
JIAFS -- NASA/LaRC -- GWU

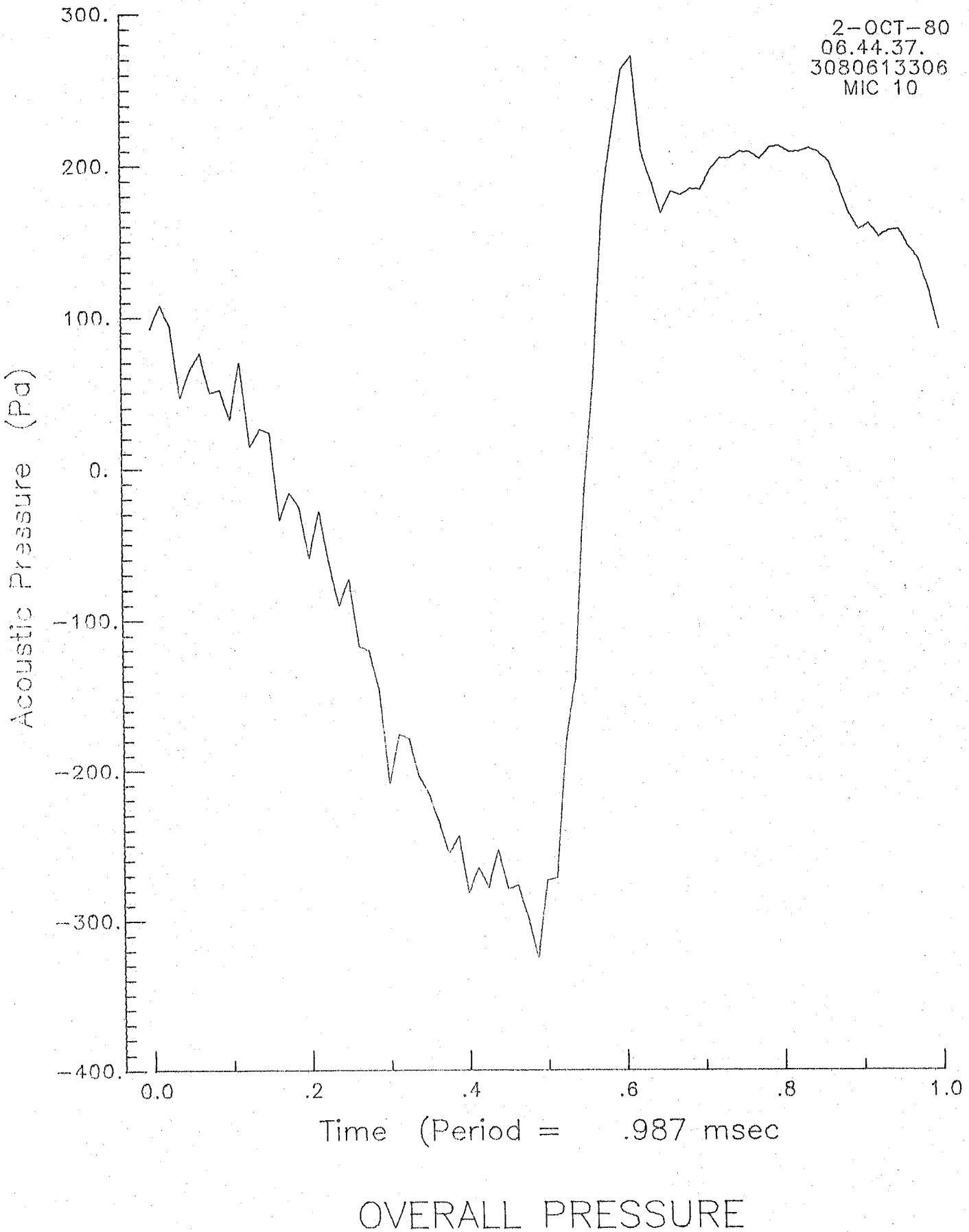

OVERALL PRESSURE

Figure 14(f).- Continued.

F. Farassat -- P. Nystrom
JIAFS -- NASA/LaRC -- GWU

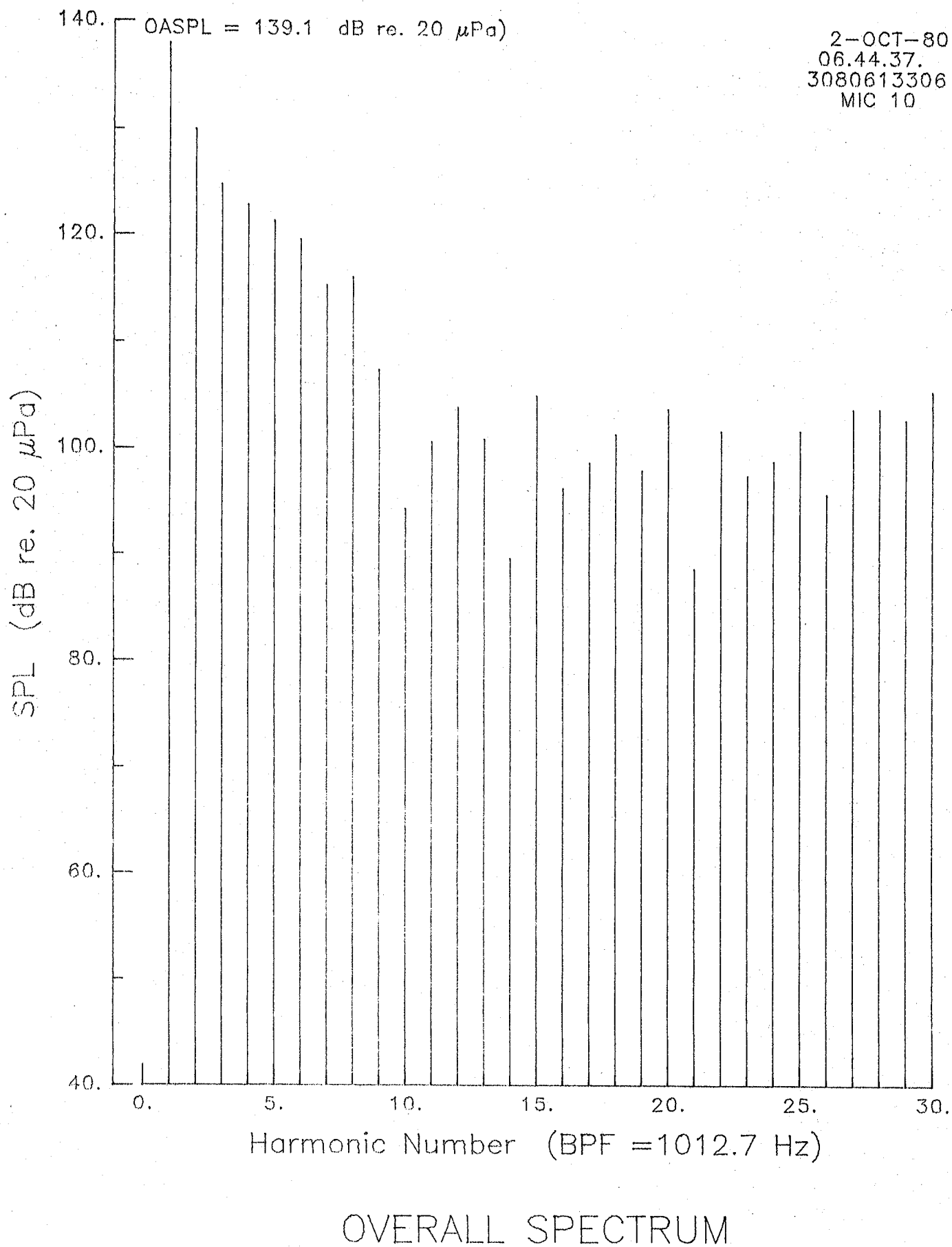

Figure 14(f).- Continued.

F. Farassat -- P. Nystrom
JIAFS -- NASA/LaRC -- GWU

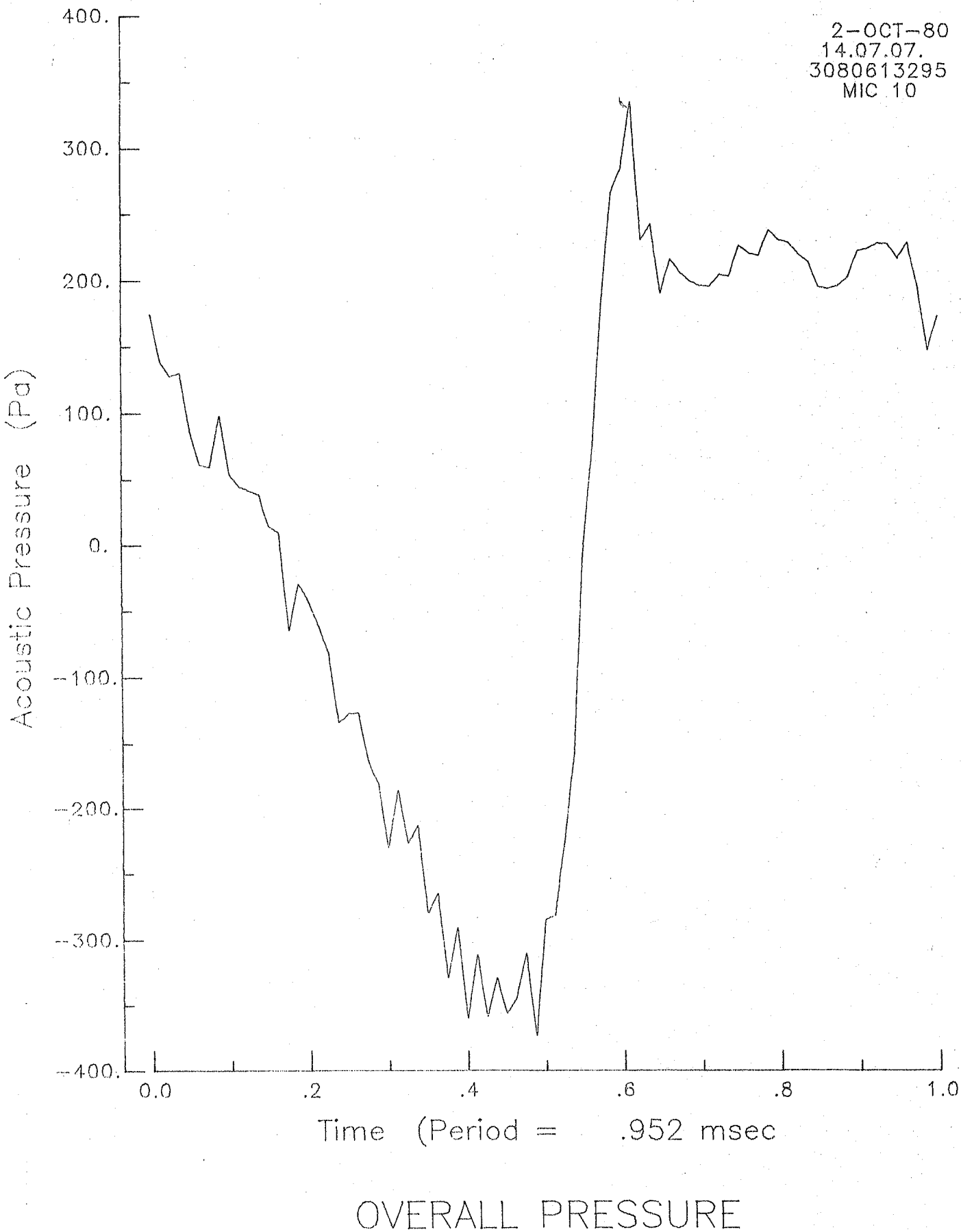

Figure 14(f).- Continued.

F. Farassat -- P. Nystrom
JIAFS -- NASA/LaRC -- GWU

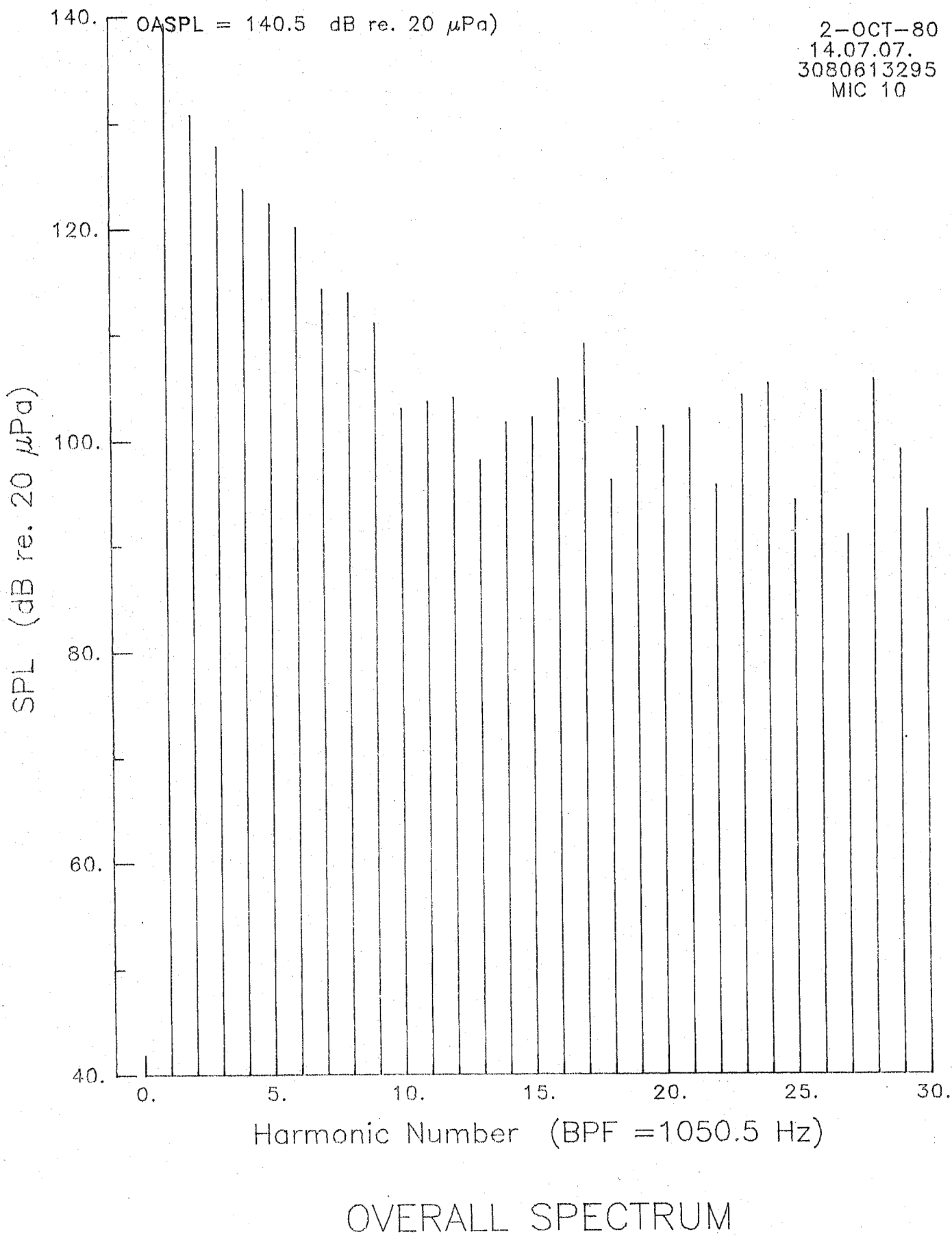

Figure 14(f).- Concluded.

F. Farassat -- P. Nystrom
JIAFS -- NASA/LaRC -- GWU

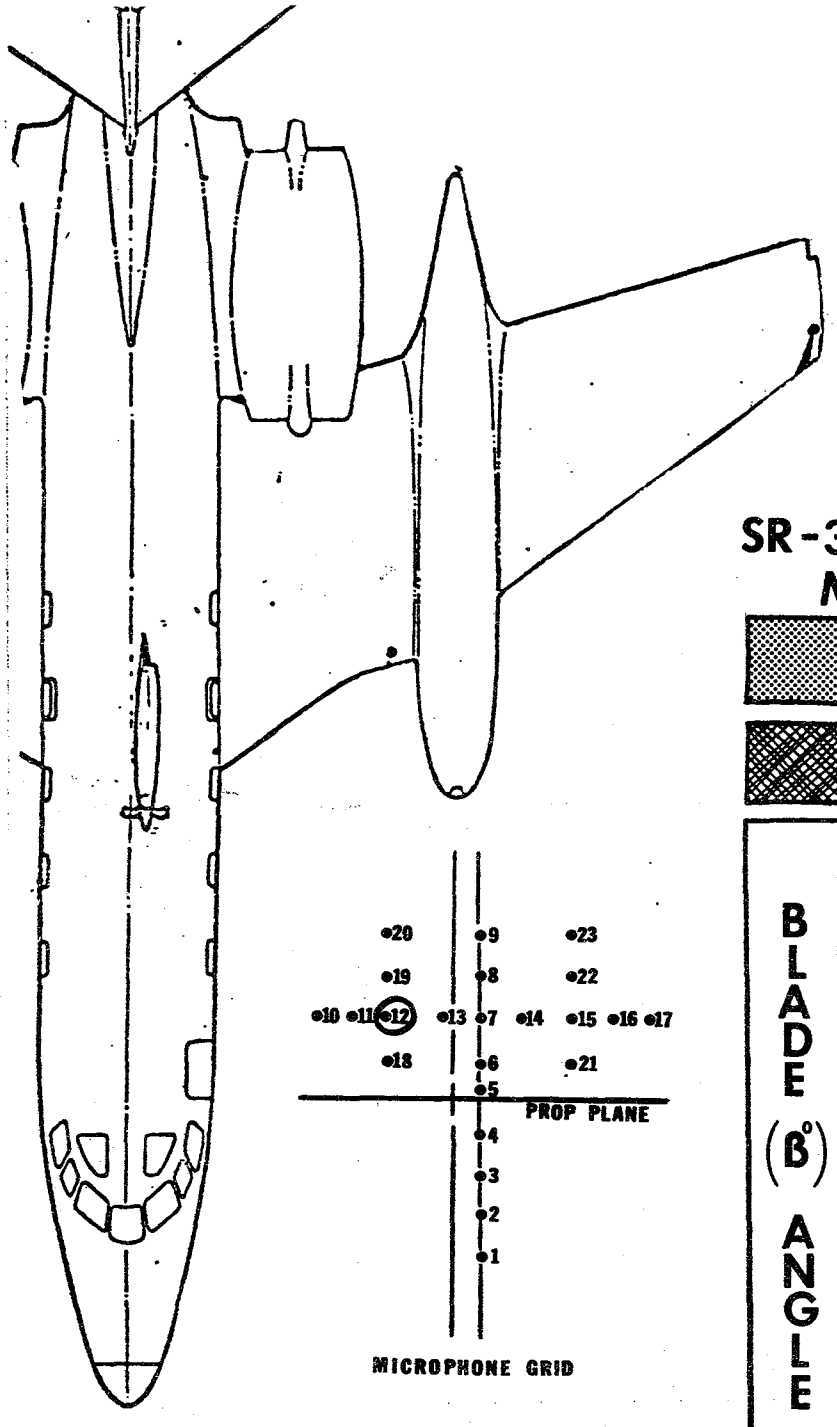

SR-3 TEST MATRIX

EXCEEDS BLEED SYS. POWER CAPACITY

BLADE CRITICAL SPEED

BLADE ANGLE (β°)	ADVANCE RATIO (J)	ALTITUDE (FT) 20,000 — MACH # .50	.60	.65	.70	.75	.80	ALTITUDE (FT) 25,000 — MACH # .50	.60	.65	.70	.75	.80	ALTITUDE (FT) 30,000 — MACH # .50	.60	.65	.70	.75	.80
59.3	4.30																		
	3.50																		
	3.25																		
	3.06																		
	2.90																		
61.3	4.30																		X
	3.50																		X
	3.25				X						X						X		X
	3.06												X						X
	2.95						X						X						X
63.3	4.30																		
	4.07																		
	3.50																		
	3.25						X						X						X

Figure 14(g).- Continued.

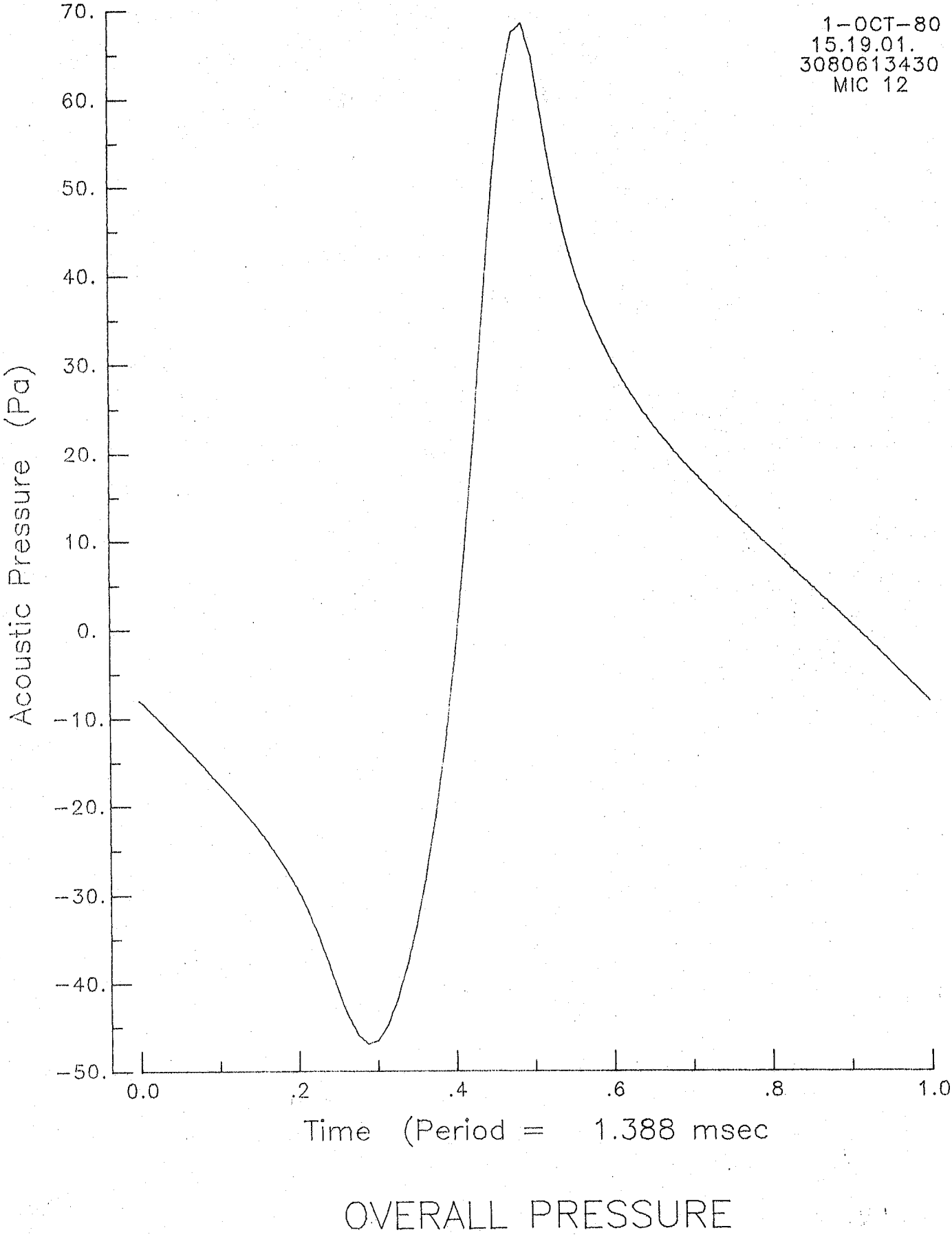

Figure 14(g).- Continued.

F. Farassat -- P. Nystrom
JIAFS -- NASA/LaRC -- GWU

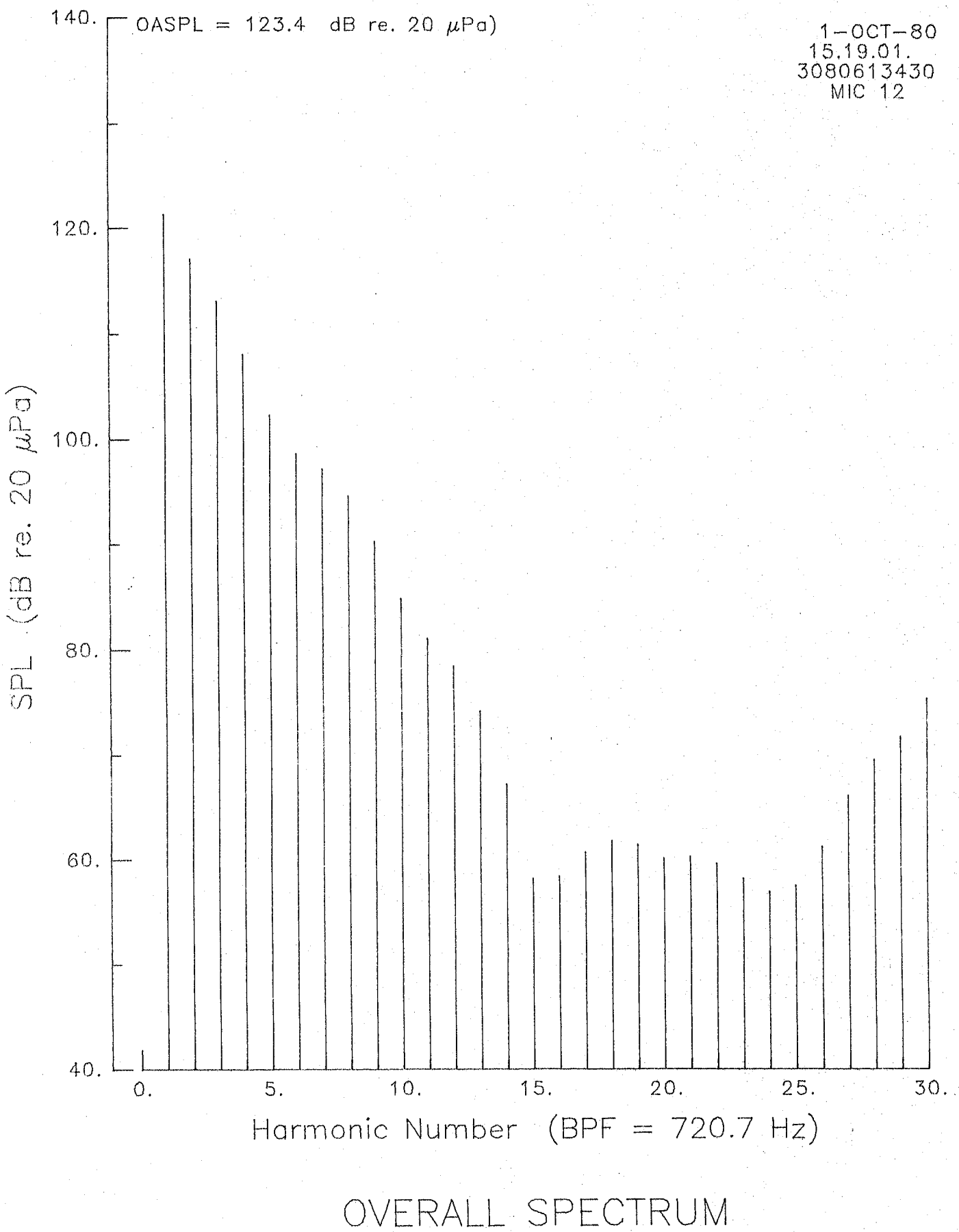

Figure 14(g).- Continued.

F. Farassat -- P. Nystrom
JIAFS -- NASA/LaRC -- GWU

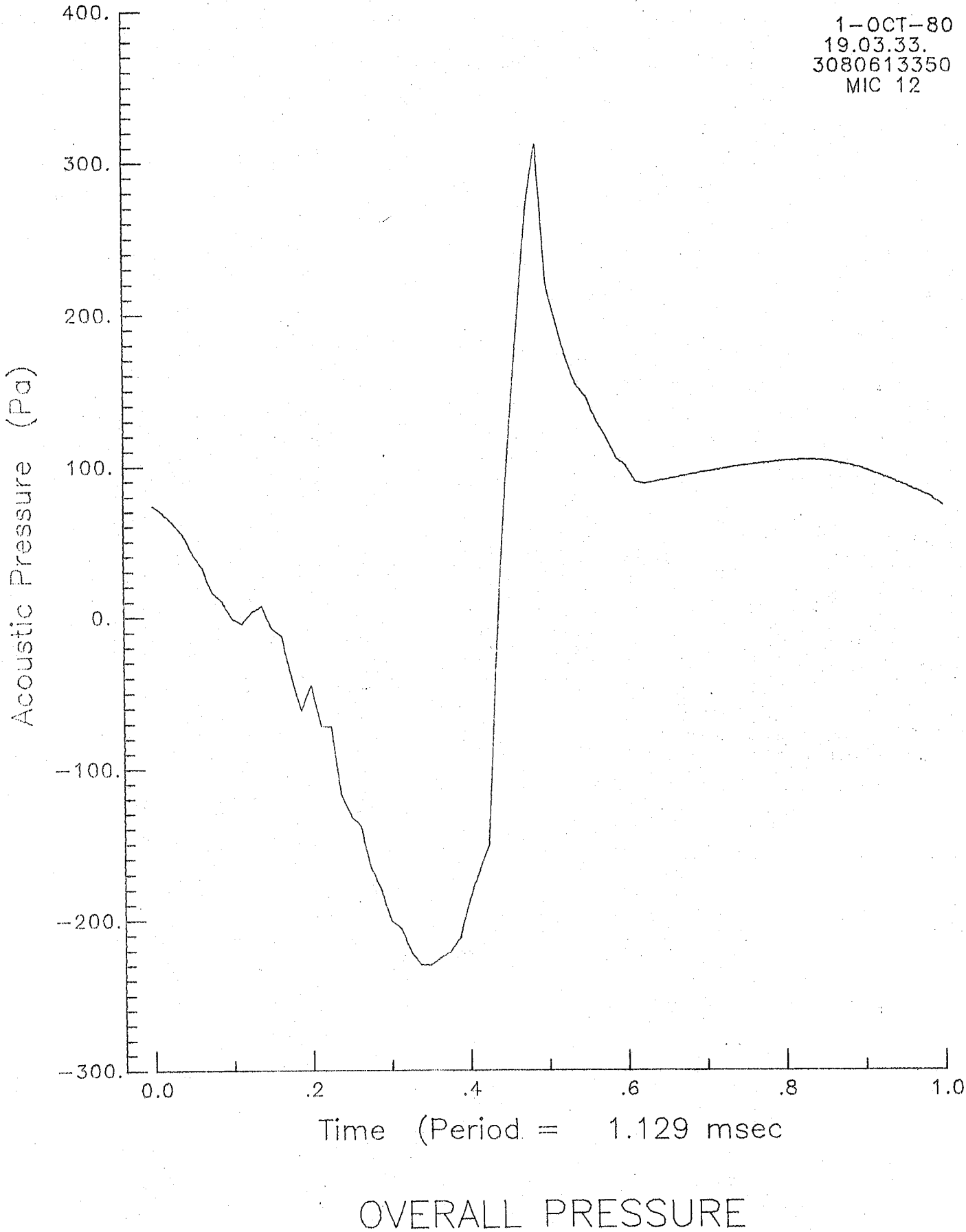

Figure 14(g).- Continued.

F. Farassat -- P. Nystrom
JIAFS -- NASA/LaRC -- GWU

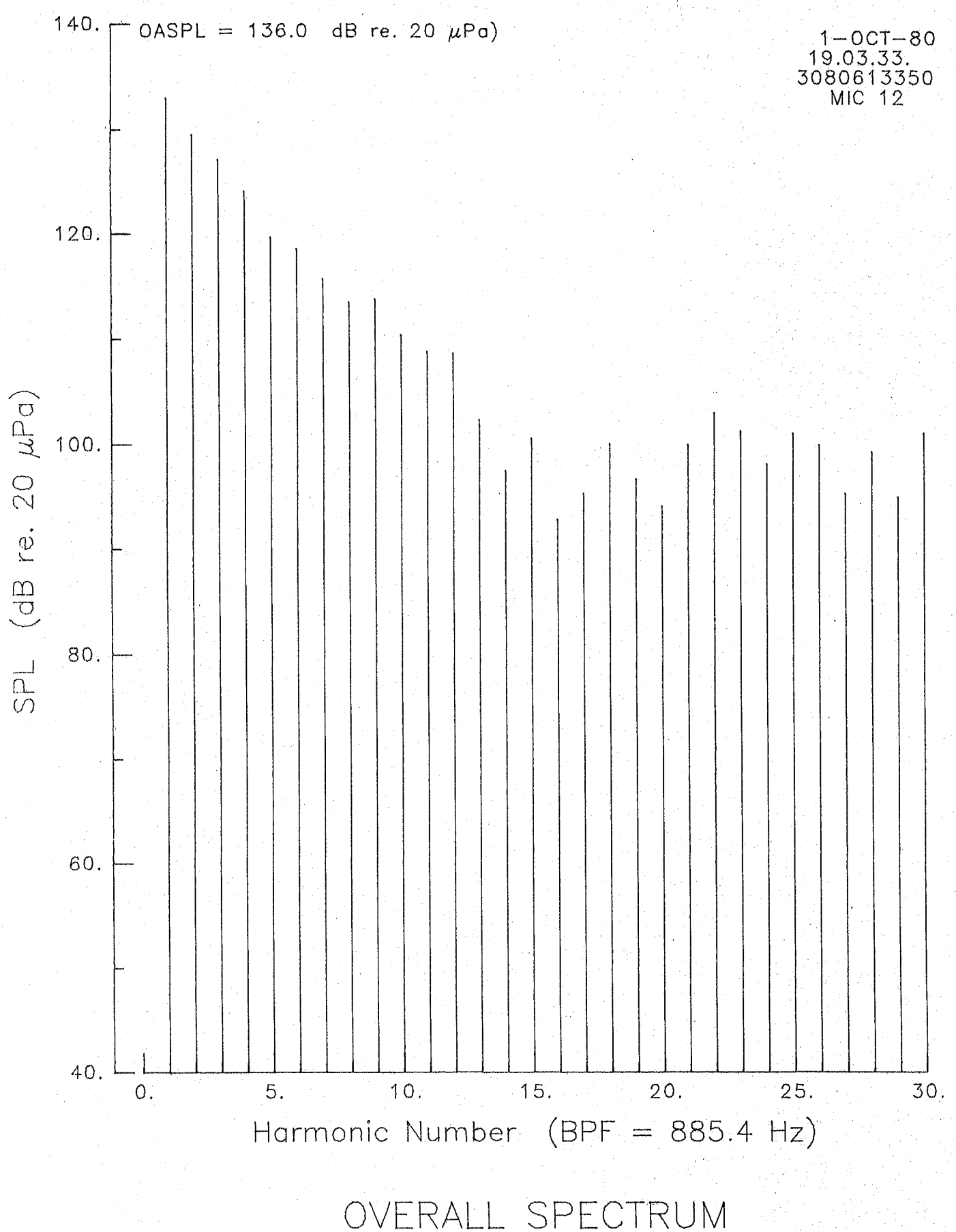

Figure 14(g).- Continued.

F. Farassat -- P. Nystrom
JIAFS -- NASA/LaRC -- GWU

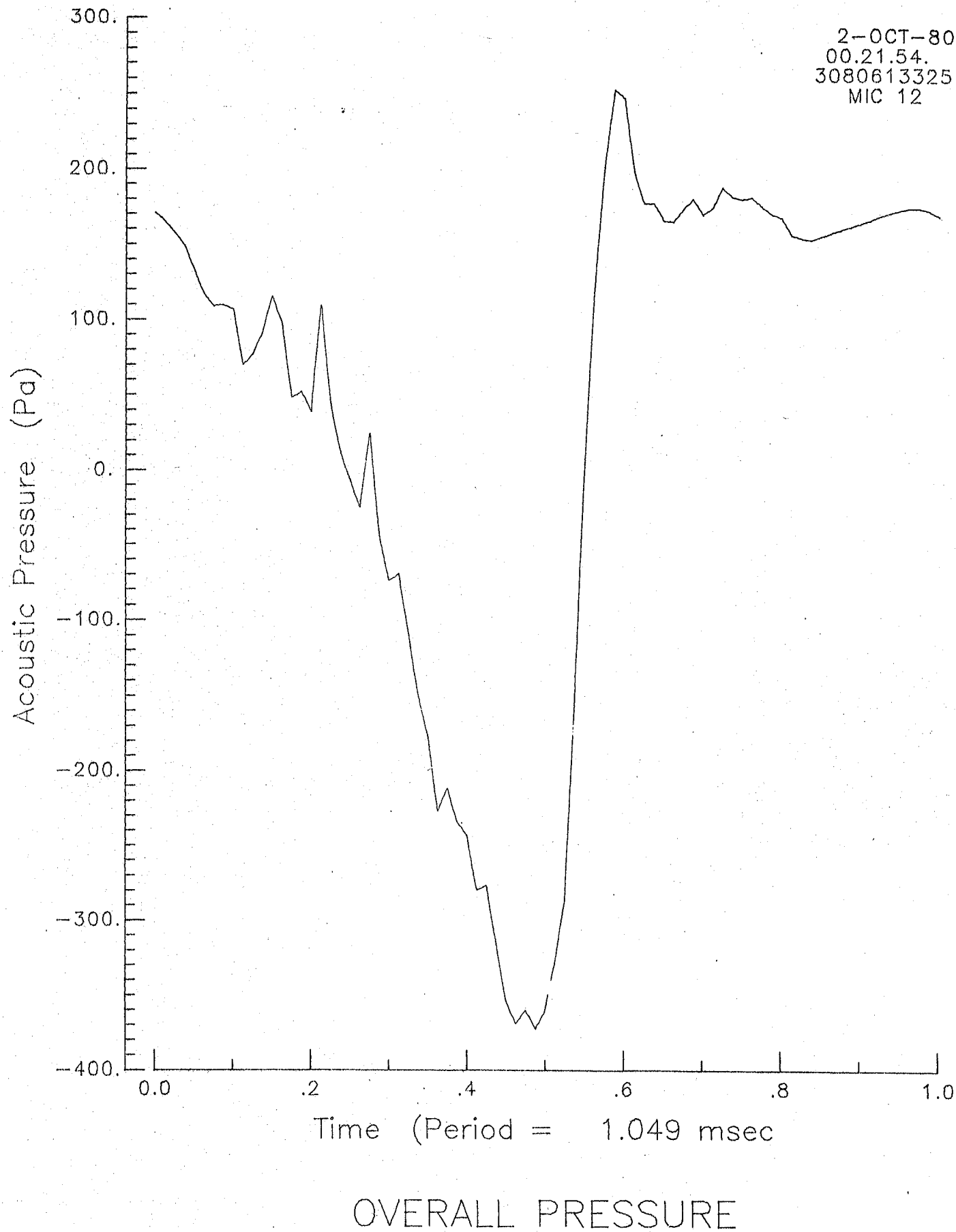

Figure 14(g).- Continued.

F. Farassat -- P. Nystrom
JIAFS -- NASA/LaRC -- GWU

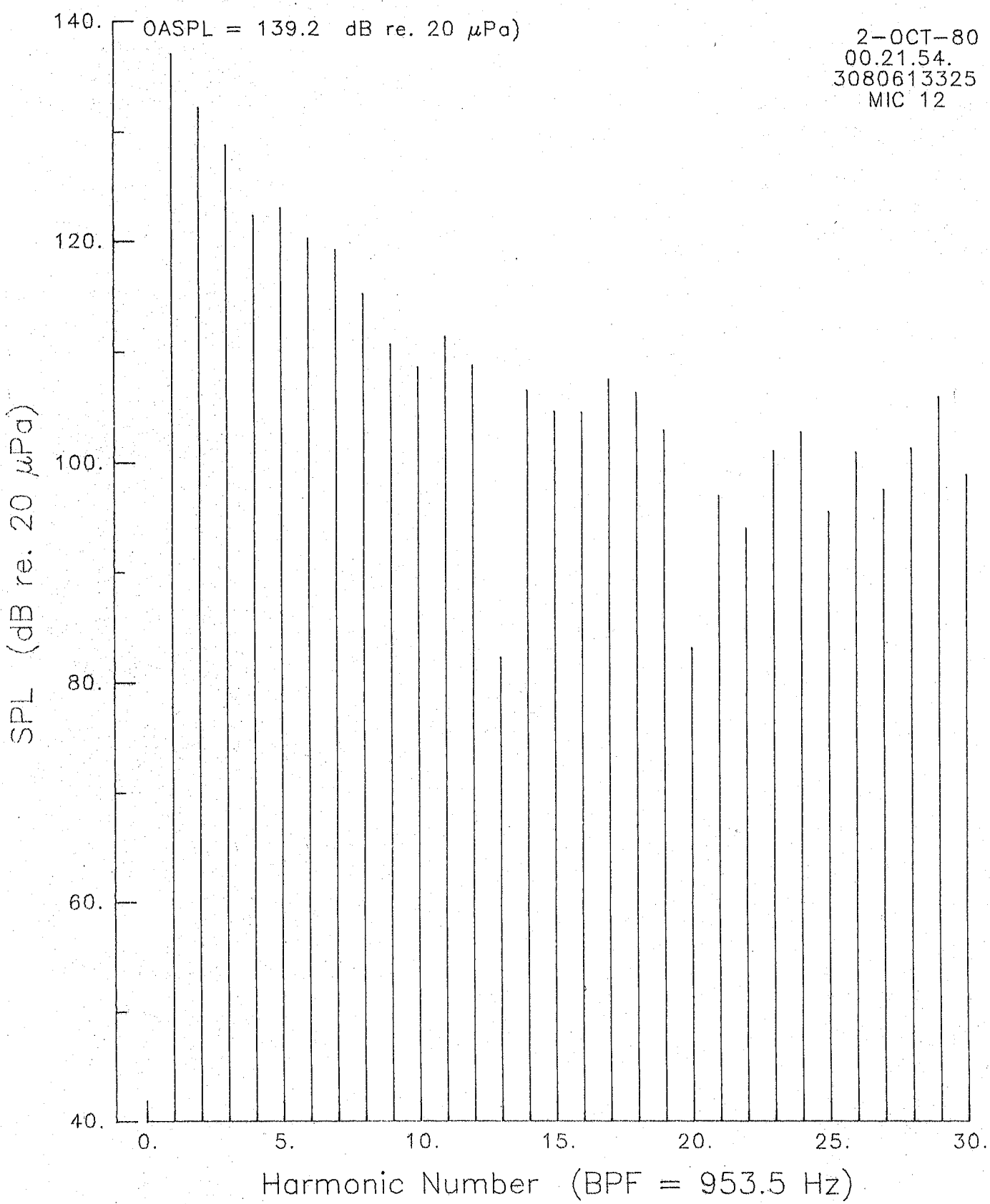

OVERALL SPECTRUM

Figure 14(g).- Continued.

F. Farassat -- P. Nystrom
JIAFS -- NASA/LaRC -- GWU

Figure 14(g).- Continued.

F. Farassat -- P. Nystrom
JIAFS -- NASA/LaRC -- GWU

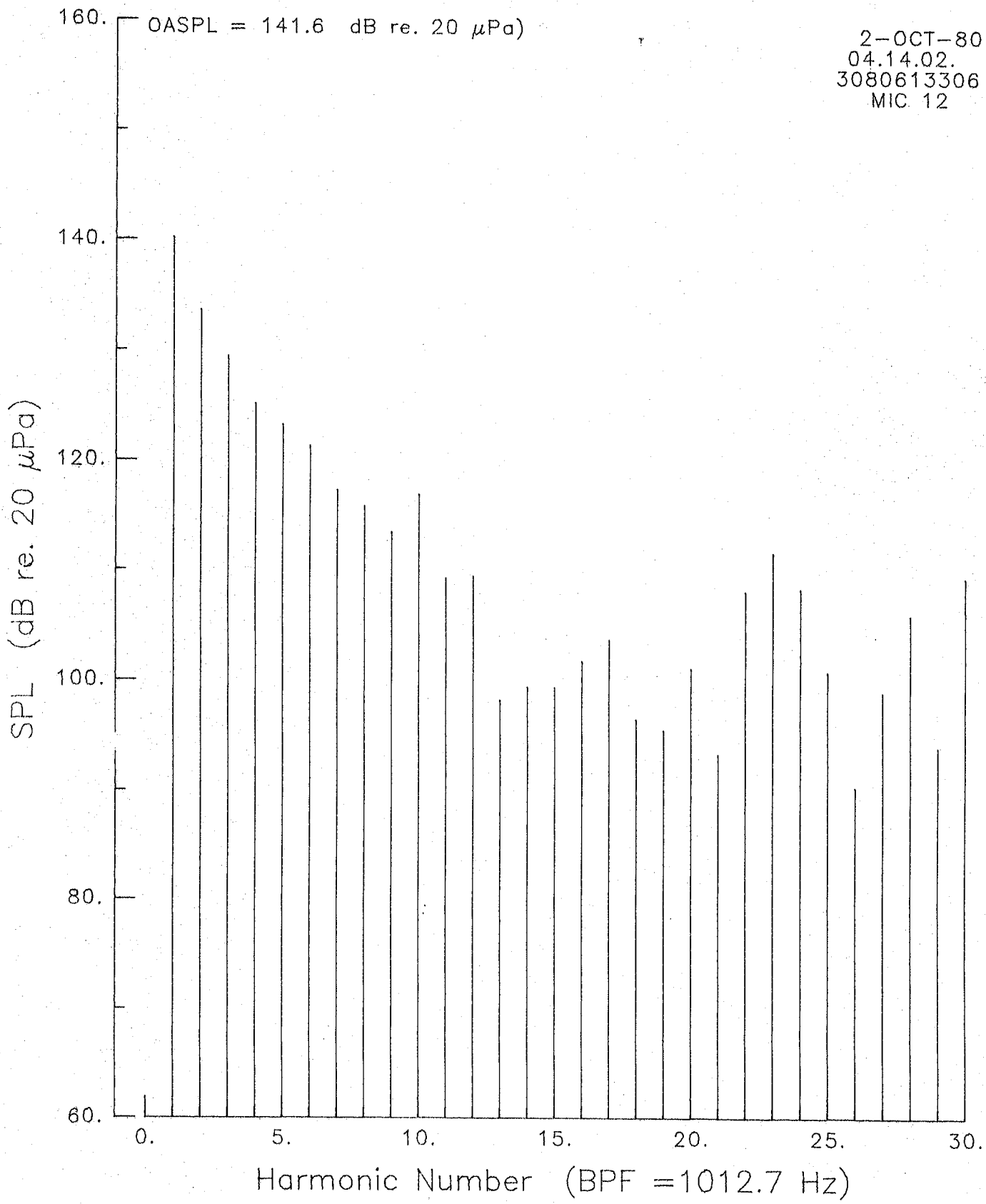

OVERALL SPECTRUM

Figure 14(g).- Continued.

F. Farassat -- P. Nystrom
JIAFS -- NASA/LaRC -- GWU

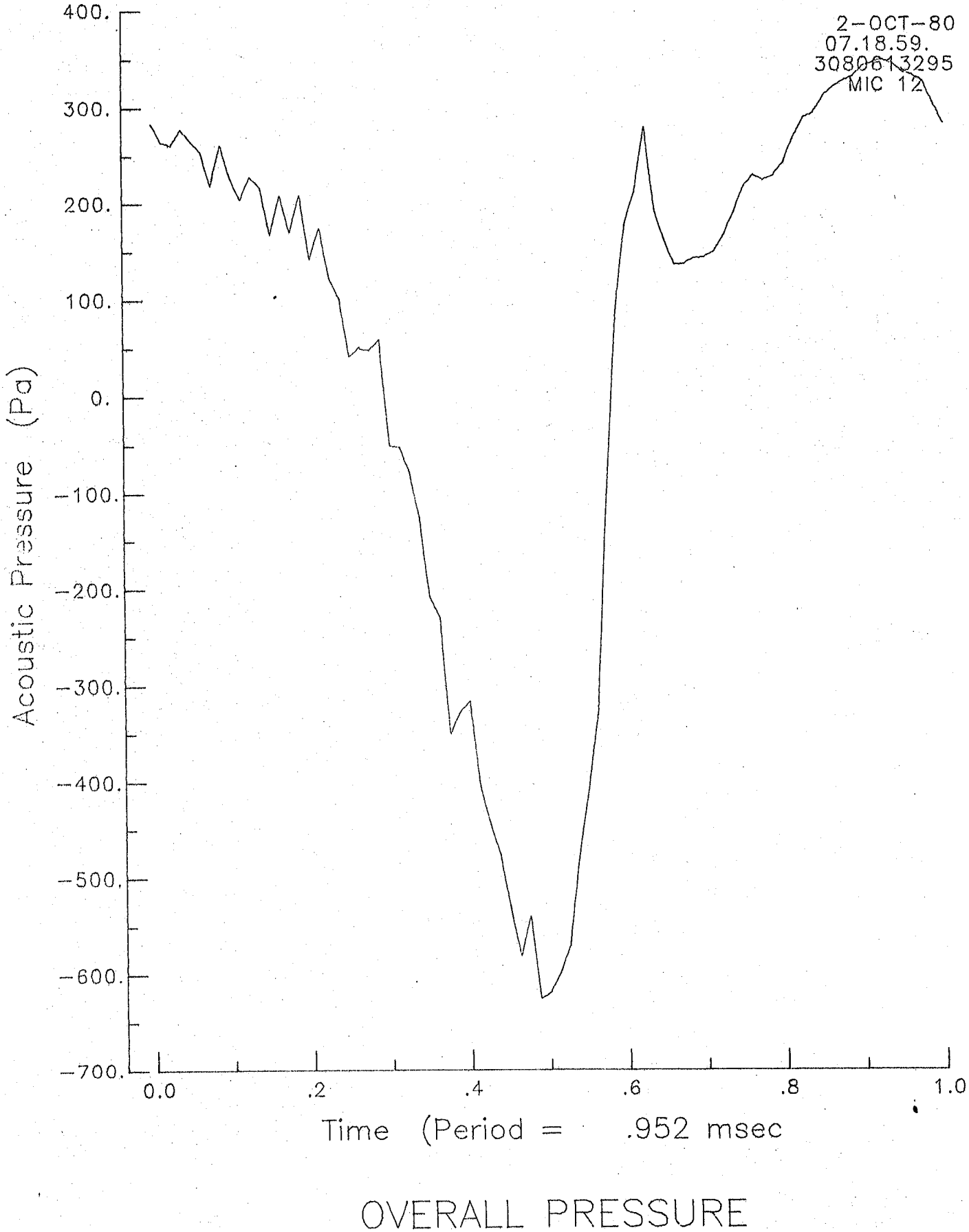

Figure 14(g).- Continued.

F. Farassat -- P. Nystrom
JIAFS -- NASA/LaRC -- GWU

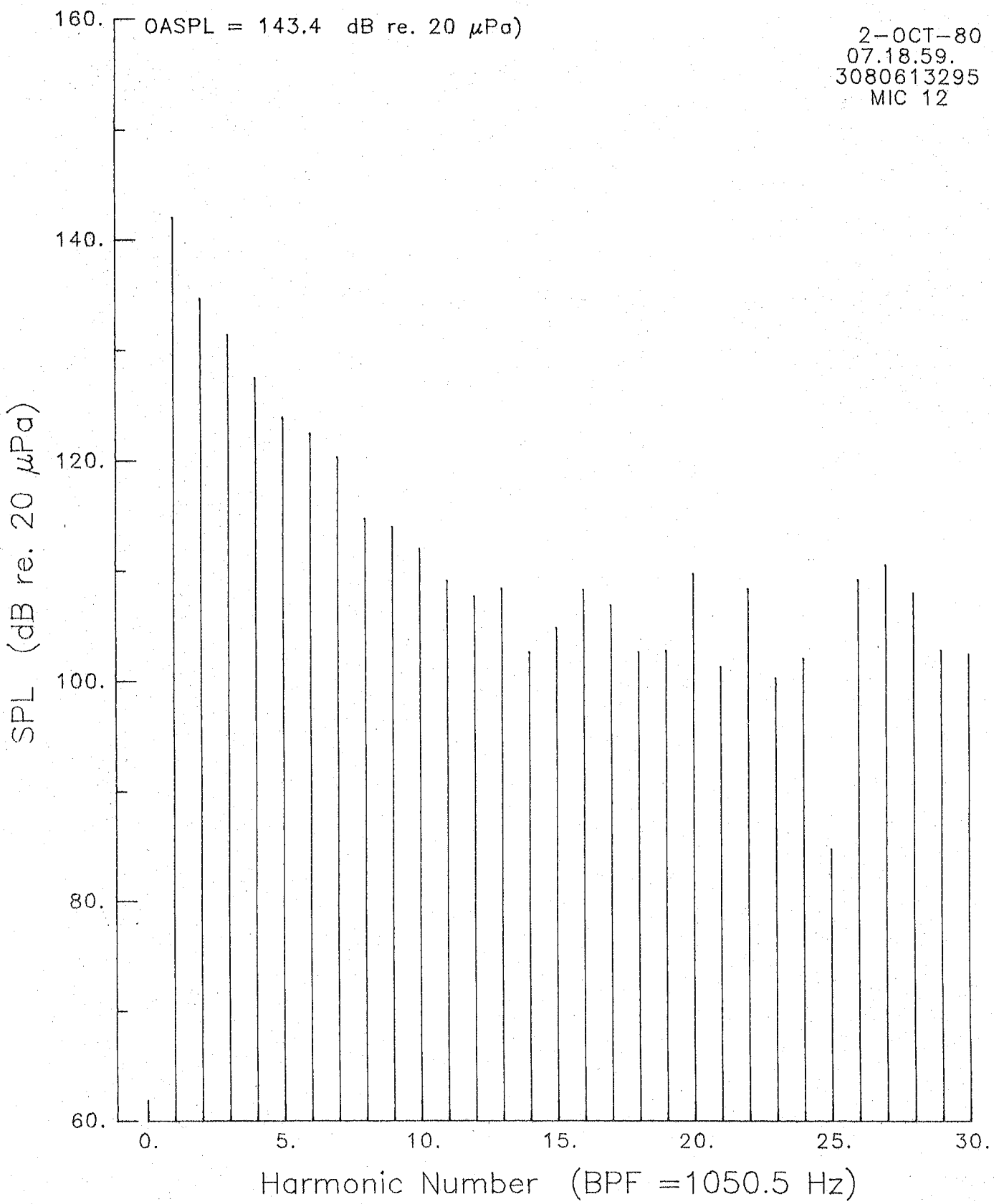

Figure 14(g).- Concluded.

F. Farassat -- P. Nystrom
JIAFS -- NASA/LaRC -- GWU

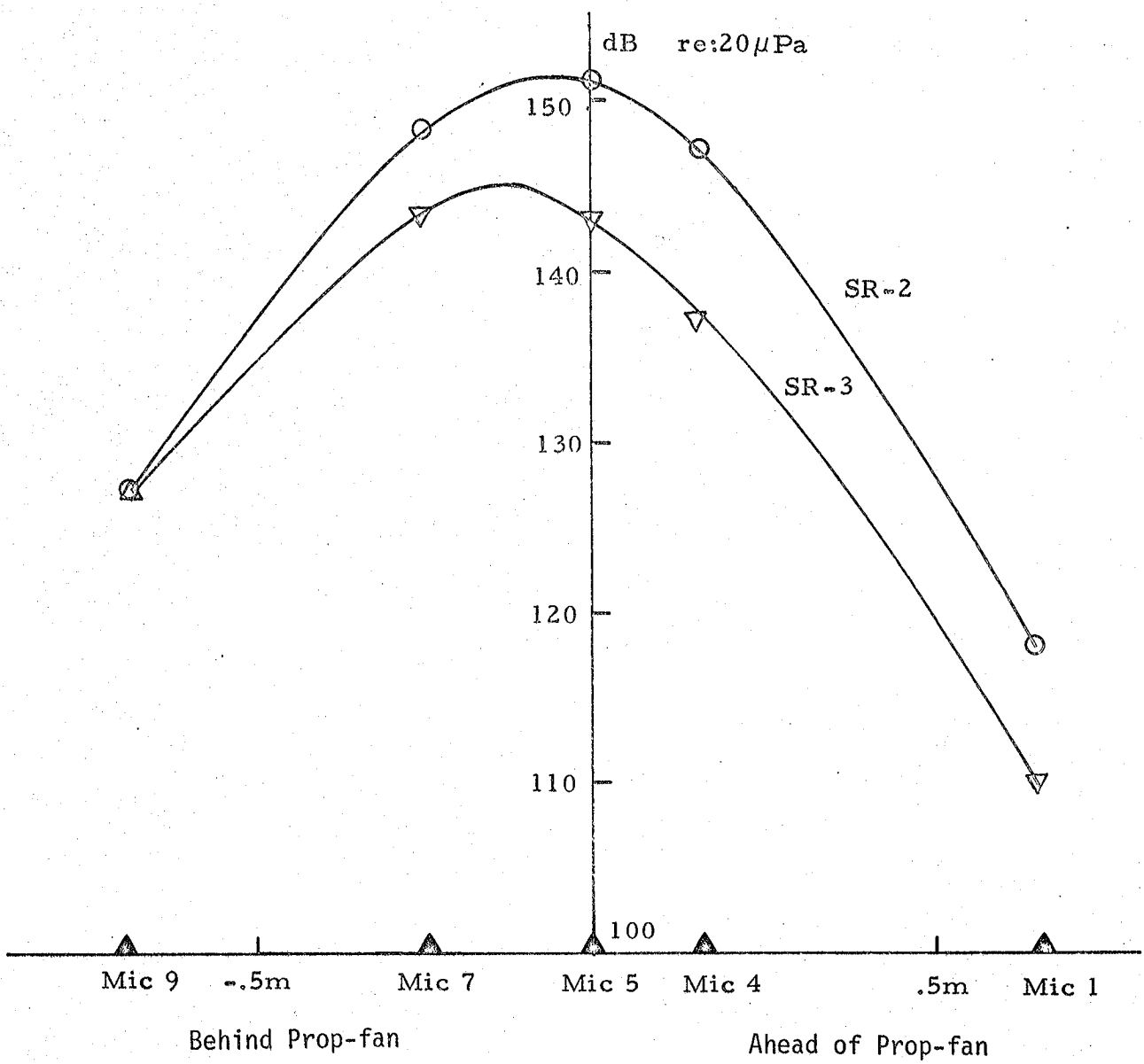

Figure 15.- Variation of the corrected levels of the blade passage frequency for SR-2 and SR-3 blades as a function of microphone position. Altitude 9.15 Km (30,000 ft), M=0.8, advance ratio 3.25. Microphones directly below prop-fan axis.

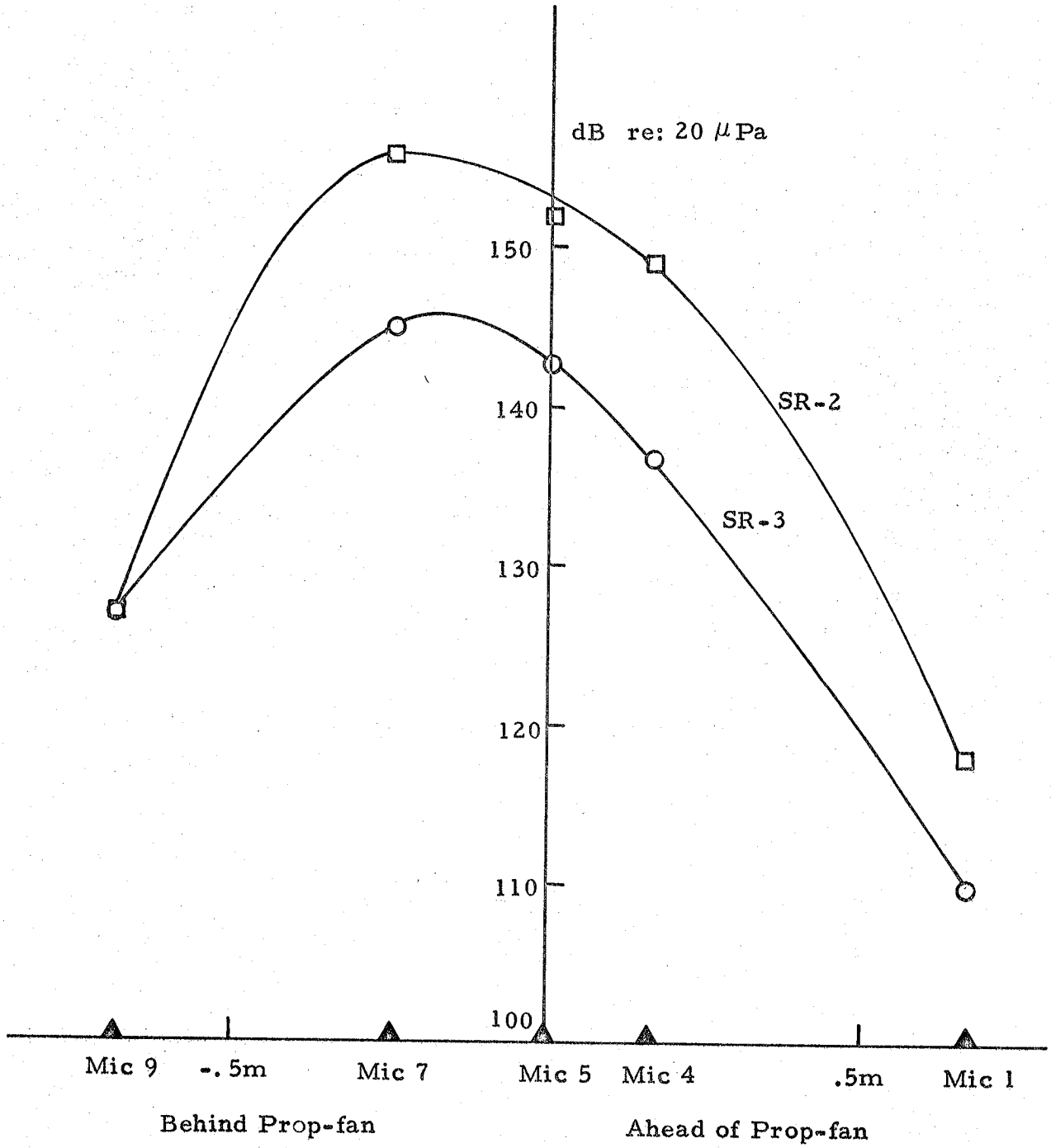

Figure 16.- Variation of the corrected overall sound pressure levels for SR-2 and SR-3 blades as a function of microphone position for constant advance ratio. Altitude 9.15 Km (30,000 ft), M=0.8, advance ratio 3.25.

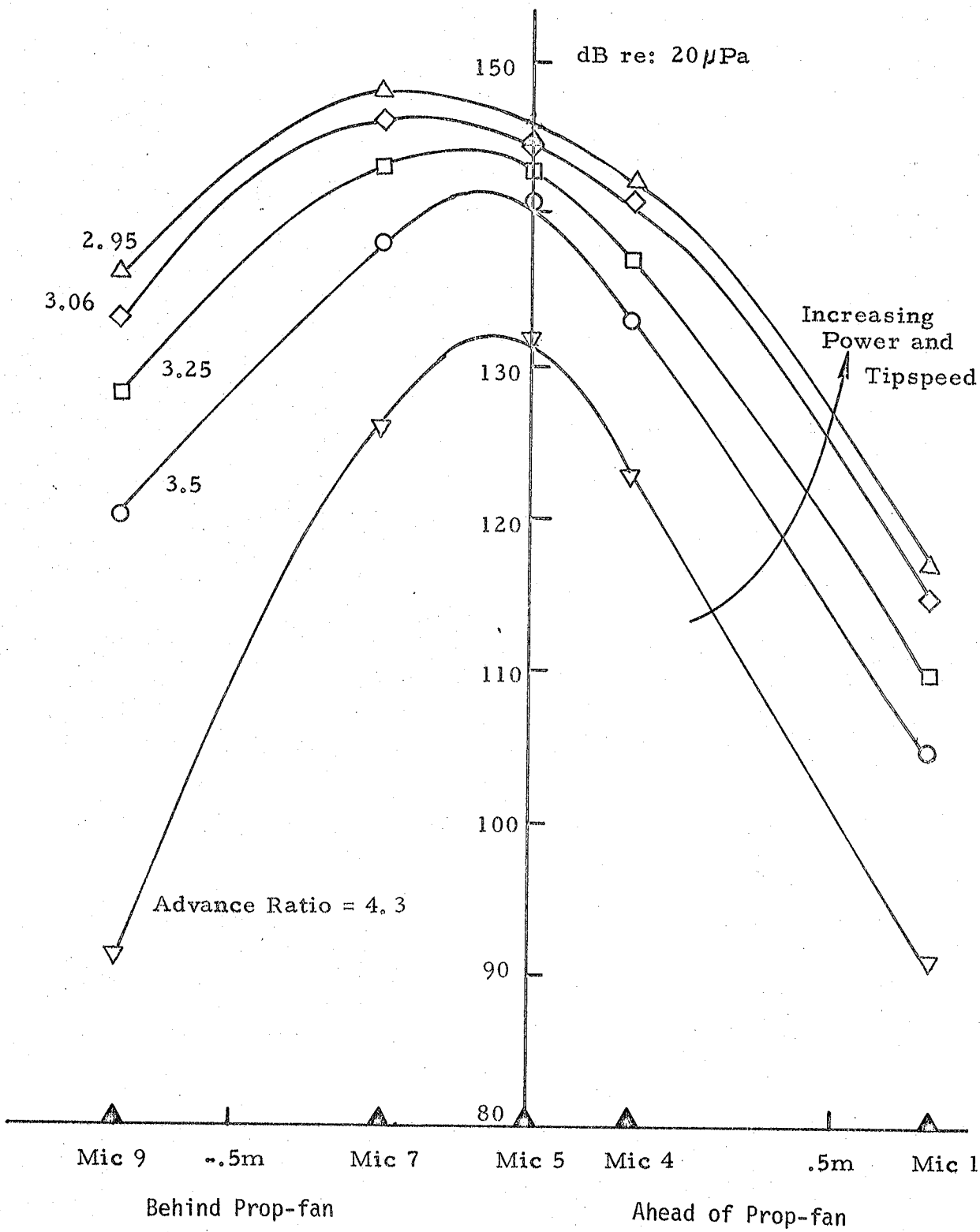

Figure 17.- Variation of the corrected levels of blade passage frequency for SR-3 blade as a function of microphone position for constant advance ratio. Altitude 9.15 Km (30,000 ft), M=0.8. Microphones directly below the prop-fan axis.

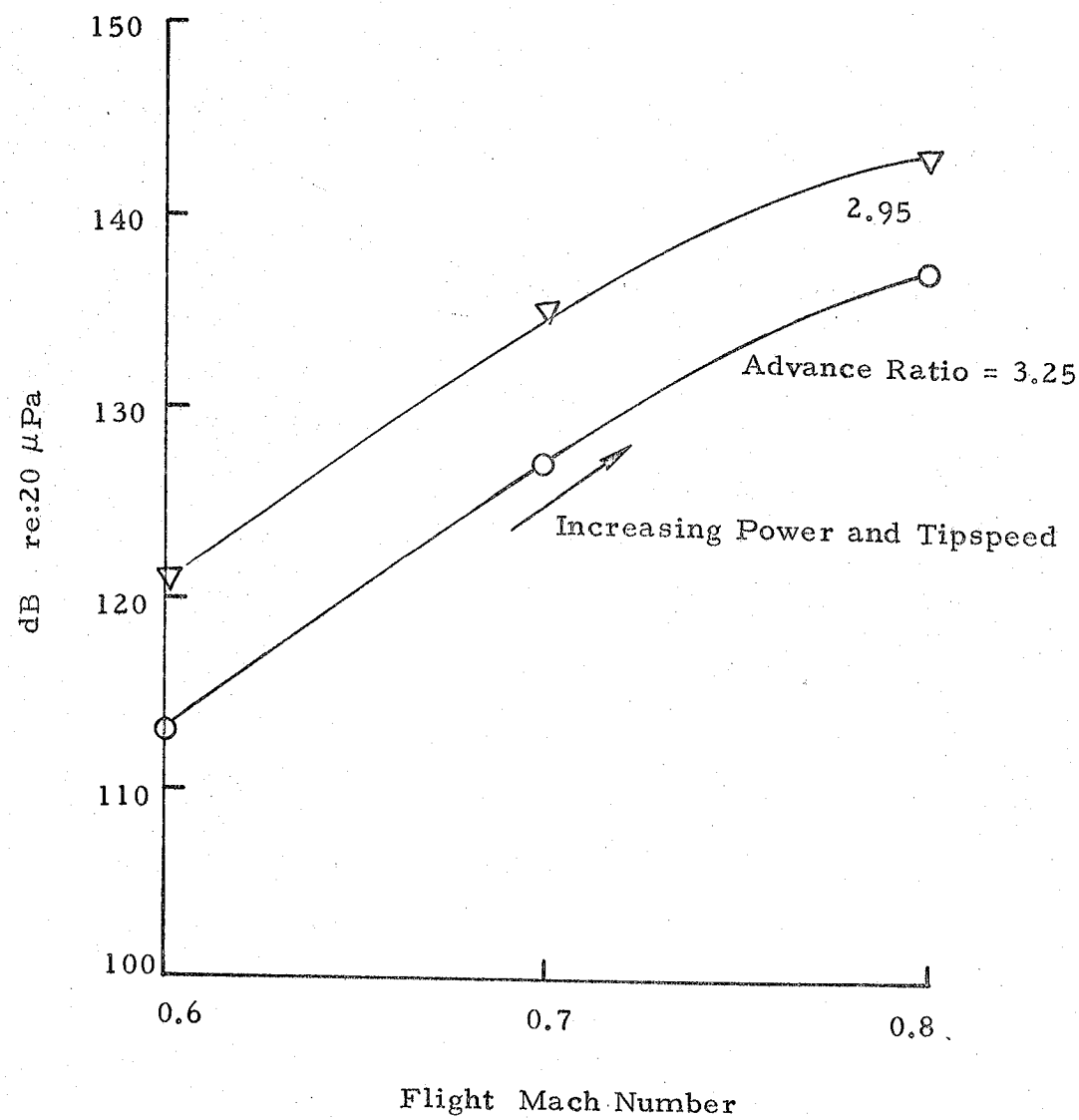

Figure 18.- Variation of the free-field levels of the blade passage frequency as a function of flight Mach number for constant advance ratio. Altitude 9.15 Km (30,000 ft), microphone 7, SR-3.

1. Report No.	2. Government Accession No.	3. Recipient's Catalog No.
NASA TM-81916		

4. Title and Subtitle	5. Report Date
Noise Prediction for Jetstar Prop-Fan Test	December 1980
	6. Performing Organization Code
7. Author(s)	8. Performing Organization Report No.
F. Farassat, R. M. Martin, and G. C. Greene	
	10. Work Unit No.
9. Performing Organization Name and Address	505-41-43-01
NASA Langley Research Center Hampton, VA 23665	11. Contract or Grant No.
	13. Type of Report and Period Covered
12. Sponsoring Agency Name and Address	Technical Memorandum
National Aeronautics and Space Administration Washington, DC 20546	14. Sponsoring Agency Code

15. Supplementary Notes

The authors gratefully acknowledge the technical assistance of Mr. C. V. Holbrook of Hampton Technical Center.

16. Abstract

The acoustic calculations reported in this memorandum are for two model prop-fan designs (SR-2 and SR-3 blades) scheduled for test on top of Jetstar aircraft. The predicted acoustic pressure signatures and spectra for selected microphone positions on the fuselage and operating conditions are presented here. The computer program used for these calculations were developed at NASA Langley by Farassat and Nystrom. A detailed presentation of the input data, the acoustic results and the corrections for microphone fuselage reflection are included in this report. The general trend observed in these calculations is that the acoustically optimized model (using SR-3 blades) is substantially quieter than the model with SR-2 blades. This latter design has conventional straight blades.

17. Key Words (Suggested by Author(s))	18. Distribution Statement
Aeroacoustics Advanced propellers	Unclassified - Unlimited Subject Category 71

19. Security Classif. (of this report)	20. Security Classif. (of this page)	21. No. of Pages	22. Price*
Unclassified	Unclassified	290	A13

* For sale by the National Technical Information Service, Springfield, Virginia 22161